



Nuclear Production of Hydrogen

Third Information
Exchange Meeting
Oarai, Japan
5-7 October 2005



Nuclear Production of Hydrogen

**Third Information Exchange Meeting
Oarai, Japan
5-7 October 2005**

**Including the
Second HTTR Workshop on
Hydrogen Production Technologies**

**Co-organised by the
Japan Atomic Energy Agency (JAEA)**

© OECD 2006
NEA No. 6122

ORGANISATION FOR ECONOMIC CO-OPERATION AND DEVELOPMENT

Pursuant to Article 1 of the Convention signed in Paris on 14th December 1960, and which came into force on 30th September 1961, the Organisation for Economic Co-operation and Development (OECD) shall promote policies designed:

- to achieve the highest sustainable economic growth and employment and a rising standard of living in member countries, while maintaining financial stability, and thus to contribute to the development of the world economy;
- to contribute to sound economic expansion in member as well as non-member countries in the process of economic development; and
- to contribute to the expansion of world trade on a multilateral, non-discriminatory basis in accordance with international obligations.

The original member countries of the OECD are Austria, Belgium, Canada, Denmark, France, Germany, Greece, Iceland, Ireland, Italy, Luxembourg, the Netherlands, Norway, Portugal, Spain, Sweden, Switzerland, Turkey, the United Kingdom and the United States. The following countries became members subsequently through accession at the dates indicated hereafter: Japan (28th April 1964), Finland (28th January 1969), Australia (7th June 1971), New Zealand (29th May 1973), Mexico (18th May 1994), the Czech Republic (21st December 1995), Hungary (7th May 1996), Poland (22nd November 1996), Korea (12th December 1996) and the Slovak Republic (14 December 2000). The Commission of the European Communities takes part in the work of the OECD (Article 13 of the OECD Convention).

NUCLEAR ENERGY AGENCY

The OECD Nuclear Energy Agency (NEA) was established on 1st February 1958 under the name of the OEEC European Nuclear Energy Agency. It received its present designation on 20th April 1972, when Japan became its first non-European full member. NEA membership today consists of 28 OECD member countries: Australia, Austria, Belgium, Canada, Czech Republic, Denmark, Finland, France, Germany, Greece, Hungary, Iceland, Ireland, Italy, Japan, Luxembourg, Mexico, the Netherlands, Norway, Portugal, Republic of Korea, Slovak Republic, Spain, Sweden, Switzerland, Turkey, the United Kingdom and the United States. The Commission of the European Communities also takes part in the work of the Agency.

The mission of the NEA is:

- to assist its member countries in maintaining and further developing, through international co-operation, the scientific, technological and legal bases required for a safe, environmentally friendly and economical use of nuclear energy for peaceful purposes, as well as
- to provide authoritative assessments and to forge common understandings on key issues, as input to government decisions on nuclear energy policy and to broader OECD policy analyses in areas such as energy and sustainable development.

Specific areas of competence of the NEA include safety and regulation of nuclear activities, radioactive waste management, radiological protection, nuclear science, economic and technical analyses of the nuclear fuel cycle, nuclear law and liability, and public information. The NEA Data Bank provides nuclear data and computer program services for participating countries.

In these and related tasks, the NEA works in close collaboration with the International Atomic Energy Agency in Vienna, with which it has a Cooperation Agreement, as well as with other international organisations in the nuclear field.

© OECD 2006

Permission to reproduce a portion of this work for non-commercial purposes or classroom use should be obtained through the Centre français d'exploitation du droit de copie (CCF), 20, rue des Grands-Augustins, 75006 Paris, France, Tel. (33-1) 44 07 47 70, Fax (33-1) 46 34 67 19, for every country except the United States. In the United States permission should be obtained through the Copyright Clearance Center, Customer Service, (508)750-8400, 222 Rosewood Drive, Danvers, MA 01923, USA, or CCC Online: <http://www.copyright.com/>. All other applications for permission to reproduce or translate all or part of this book should be made to OECD Publications, 2, rue André Pascal, 75775 Paris Cedex 16, France.

FOREWORD

As growing demand for energy has prompted an increasing use of fossil fuels, the resulting issue of climate change has in turn led to renewed interest in the use of hydrogen as an energy carrier. Currently, hydrogen is mainly manufactured by reforming fossil fuels, implying that greenhouse gas emission reduction benefits will not be significant unless a non-carbon-emitting hydrogen manufacturing route is developed. There is thus a resurgence of interest in using heat or surplus electricity from nuclear power plants to produce hydrogen through water cracking.

The NEA Nuclear Science Committee organised its Third Information Exchange Meeting on the Nuclear Production of Hydrogen on 5-7 October 2005 in Japan. The meeting was hosted by the Japan Atomic Energy Agency (JAEA) and co-sponsored by the International Atomic Energy Agency (IAEA). The JAEA Second High-temperature Engineering Test Reactor (HTTR) Workshop on Hydrogen Production Technologies was imbedded in the meeting.

The objectives of the meeting were to exchange information on current scientific and technical issues related to the nuclear production of hydrogen and to identify possible international collaboration. Thirty-five oral presentations were made on the following themes:

- The prospects for hydrogen in future energy structures and nuclear power's role.
- The status of nuclear hydrogen research and development efforts around the globe.
- Integrated nuclear hydrogen production systems.
- Nuclear hydrogen technologies and design concepts.
- Basic and applied science in support of nuclear hydrogen production.

The participants concluded that significant experimental progress had been made since 2003 in developing nuclear hydrogen production technology. Both the number of participants and presentations at the information exchange meetings have increased substantially. The first meeting in 2000 was attended by 40 participants; the second meeting in 2003 attracted 86 participants; 143 participants from nine countries and two international organisations attended this third meeting.

The participants recommended that the meeting series be continued as they found it to be the best forum for a focused examination of the scientific and technical issues related to nuclear hydrogen production, bringing together key researchers from around the world. The participants strongly endorsed further international co-operation on issues related to the nuclear production of hydrogen.

In light of the IAEA plan to organise an international conference on “Non-electric Applications of Nuclear Power: Seawater Desalination, Hydrogen Production and Other Nuclear Applications” in mid-2007, the participants recommended that the NEA Nuclear Science Committee organise its fourth meeting on the Nuclear Production of Hydrogen in 2008.

The present proceedings include all of the papers presented at the meeting, session summaries and the recommendations formulated by the meeting participants.

This page intentionally left blank

TABLE OF CONTENTS

FOREWORD	3
OPENING SESSION	9
<i>Thierry Dujardin</i>	
Welcome address	11
<i>Osamu Oyamada</i>	
Opening Remark.....	13
SESSION I	
The prospects for Hydrogen in Future Energy Structures and Nuclear Power’s Role	15
<i>Chair: M.C. Petri</i>	
<i>M. Hori, M. Numata, T. Amaya, Y. Fujimura</i>	
Synergy of Fossil Fuels and Nuclear Energy for the Energy Future	17
<i>G. Rothwell, E. Bertel, K. Williams</i>	
Can Nuclear Power Complete in the Hydrogen Economy?.....	27
<i>S. Shiozawa, M. Ogawa, R. Hino</i>	
Future Plan on Environmentally Friendly Hydrogen Production by Nuclear Energy	43
SESSION II	
The Status of Nuclear Hydrogen Research and Development Efforts around the Globe	53
<i>Chair: M. Methnani, W.A. Summers</i>	
<i>M. Hori, S. Shiozawa</i>	
Research and Development For Nuclear Production of Hydrogen in Japan	55
<i>A.D. Henderson, A. Taylor</i>	
The U.S. Department of Energy Research and Development Programme on Hydrogen Production Using Nuclear Energy	73
<i>F. Le Naour</i>	
An Overview of the CEA Roadmap for Hydrogen Production.....	79
<i>Y. Sun, J. Xu, Z. Zhang</i>	
R&D Effort on Nuclear Hydrogen Production Technology in China	85

<i>A.I. Miller</i> An Update on Canadian Activities on Hydrogen	93
<i>Y-J. Shin, J-H. Kim, J. Chang, W-S. Park, J. Park</i> Nuclear Hydrogen Production Project in Korea.....	101
<i>K. Verfondern, W. von Lensa</i> Michelangelo Network Recommendations on Nuclear Hydrogen production	107

SESSION III

Integrated Nuclear Hydrogen Production Systems	119
---	------------

Chairs: A. Miller, K. Verfondern

<i>X. Yan, K. Kunitomi, R. Hino and S. Shiozawa</i> GTHT300 Design Variants for Production of Electricity, Hydrogen or Both.....	121
<i>M. Richards, A. Shenoy, K. Schultz, L. Brown, E. Harvego, M. Mc Kellar, J.P. Coupey, S.M. Moshin Reza, F. Okamoto, N. Handa</i> H2-MHR Conceptual Designs Based on the SI Process and HTE	141
<i>P. Anzieu, P. Aujollet, D. Barbier, A. Bassi, F. Bertrand, A. Le Duigou, J. Leybros, G.Rodriguez</i> Coupling a Hydrogen Production Process to a Nuclear Reactor	155
<i>T. Iyoku, N. Sakaba, S. Nakagawa, Y. Tachibana, S. Kasahara, K. Kawasaki</i> HTTR Test Programme Towards Coupling with the IS Process.....	167
<i>H. Ohashi, Y. Inaba, T. Nishihara, T. Takeda, K. Hayashi Y. Inagaki</i> Current Status of Research and Development on System Integration Technology for Connection Between HTGR and Hydrogen Production System at JAEA	177

SESSION IV

Nuclear Hydrogen Technologies and Design Concepts	187
--	------------

Chairs: K. Kunitomi, J.S. Herring, Y.S. Shin, T. Takeda

<i>K. Onuki, S. Kubo, A. Terada, N. Sakaba, R. Hino</i> Study on Thermochemical Iodine-Sulfur Process at JAEA	189
<i>S. Kubo, S. Shimizu, H. Nakajima, K. Onuki</i> Studies on Continuous and Closed Cycle Hydrogen Production by a Thermochemical Water-Splitting Iodine-Sulfur Process	197
<i>A. Terada, Y. Imai, H. Noguchi, H. Ota, A. Kanagawa, S. Ishikura, S. Kubo, J.Iwatsuki, K. Onuki, R. Hino</i> Experimental and Analytical Results on H ₂ SO ₄ and SO ₃ Decomposers for IS Process Pilot Plant.....	205

<i>M.A. Lewis, M.C. Petri, J.G. Masin</i> A Scoping Flowsheet Methodology for Evaluating Alternative Thermochemical Cycles	219
<i>S. Suppiah, J. Li, R. Sadhankar, K.J. Kutchcoskie, M. Lewis</i> Study of the Hybrid Cu-Cl Cycle for Nuclear Hydrogen Production.....	231
<i>M. Arif Khan, Y. Chen,</i> Preliminary Process Analysis and Simulation of the Copper-Chlorine Thermochemical Cycle for Hydrogen Generation	239
<i>W.A. Summers, J.L. Steinke</i> Development of the Hybrid Sulfur Thermochemical Cycle	249
<i>P. Anzieu, P. Carles, A. Le Duigou, X. Vitart, F. Lemort</i> The Sulfur-Iodine and Others Thermochemical Processes Studies at CEA	259
<i>K-K. Bae, K-S. Kang, S-D. Hong, C-S. Park, C-H. Kim, S-H. Lee, G-J. Hwang</i> A Study on Hydrogen Production by Thermochemical Water-splitting IS (Iodine-Sulfur) Process	269
<i>P. Zhang, B. Yu, L. Zhang, J. Chen, J. Xu</i> Present Research Status and Development Plan of Nuclear Hydrogen Production Programme in INET	277
<i>T. Nakagiri, T. Kase, S. Kato, K. Aoto</i> Development of the Thermochemical and Electrolytic Hybrid Hydrogen Production Process for Sodium Cooled FBR.....	287
<i>J.S. Herring, J.E. O'Brien, C.M. Stoots, G.L. Hawkes, P. Lessing,</i> <i>W. Windes, D. Wendt, M. Mc Kellar, M. Sohal, J.J. Hartvigsen</i> Progress in High-temperature Electrolysis for Hydrogen Production.....	297
<i>Y. Kato</i> Possibility of a Chemical Hydrogen Carrier System Based on Nuclear Power	309

SESSION V

Basic and Applied Science in Support of Nuclear Hydrogen Production 319

Chairs: Y. Kato, P. Anzieu, Y. Sun

<i>C-H. Kim, B-K. Kim, K-S. Kang, C-S. Park, S-H. Lee, S-D. Hong, G-J. Hwang, K-K. Bae</i> A Study on the HI Concentration by Polymer Electrolyte Membrane Electrolysis.....	321
<i>H-S. Choi, G-J. Hwang, C-S. Park, H-J. Kim, K-K. Bae</i> The Preparation Characteristics of Hydrogen Permselective Membrane for Higher Performance in IS Process of Nuclear Hydrogen Production.....	329
<i>H. Karasawa, A. Sasahira, K. Hoshino</i> Thermal Decomposition of SO ₃	337

<i>S. Fukada, S. Suemori, K. Onoda</i> Direct Energy Conversion by Proton-conducting Ceramic Fuel Cell Supplied with CH ₄ and H ₂ O at 600-800°C	345
<i>M. Ozawa, R. Fujita, T. Suzuki, Y. Fujii</i> Separation and Utilisation of Rare Metal Fission Products in Nuclear Fuel Cycle as for Hydrogen Production Catalysts?.....	355
<i>H. Kawamura, M. Mori, S-Z. Chu, M. Uotani</i> Electrical Conductive Perovskite Anodes in Sulfur-based Hybrid Cycle	365
<i>Y. Izumizaki, K-C. Park, Y. Tachibana, H. Tomiyasu, Y. Fujii</i> Generation of H ₂ by Decomposition of Pulp in Supercritical Water with Ruthenium (IV) Oxide Catalyst.....	381
SESSION SUMMARIES	389
RECOMMENDATIONS	391
<i>Annex A: List of Participants</i>	393
<i>Annex B: Meeting Organisation</i>	411
<i>Annex C: Additional Presentations to the Second HTTR Workshop</i>	413

OPENING SESSION

This page intentionally left blank

WELCOME ADDRESS

Thierry Dujardin

Deputy Director, OECD/NEA

Good morning ladies and gentlemen,

It's a great pleasure for me to welcome you, on behalf of the OECD Nuclear Energy Agency (NEA), to this third Information Exchange Meeting on the Nuclear Production of Hydrogen. This meeting is co-organised with the Japan Atomic Energy Research Institute (JAERI), which very recently (a few days ago) merged with the Japan Nuclear Cycle Development Institute (JNC) to form a new organisation called the Japan Atomic Energy Agency (JAEA).

I am sure that you will all join me in offering our best wishes of success to this new Agency. I am also very pleased to note the collaboration between this third NEA information exchange meeting and the second High-Temperature Engineering Test Reactor (HTTR) workshop by the JAEA. These two meetings have been wisely combined and there will be a special session on the third day devoted mainly to HTTR related applications.

I would take this opportunity to thank the members of the Organising Committee and of the Scientific Advisory Board for all their efforts in preparing this meeting and also the IAEA for co-sponsoring the meeting which, I am sure, will be a successful one.

The NEA Nuclear Science Committee (NSC) has already organised two information exchange meetings on the Nuclear Production of Hydrogen. The first such meeting was held in Paris in October 2000 with 40 participants from 11 countries and international organisations. Its main conclusions were that the nuclear production of hydrogen has the potential to play a significant role in energy production in the 21st century but that a significant time period will be required for the R&D to establish high-temperature, reactor-driven, thermochemical water cracking on a commercial scale.

The second information exchange meeting was held at Argonne National Laboratory, US in October 2003, now with 86 participants from the nine different countries and international organisations. The participants concluded that substantial experimental progress had been made in developing nuclear hydrogen production technology. In considering the rapidly growing interest in hydrogen as an ecologically friendly energy carrier in combination with the carbon-free manufacturing route through nuclear energy, the participants proposed to the NEA that a third meeting on the subject be organised no later than 24 months following the second meeting.

This rapidly growing interest in nuclear production of hydrogen is reflected also in the fact that there are 35 papers will be presented at this third meeting, compared to 19 and 22 papers at the two previous meetings.

To illustrate the growing interest in nuclear production of hydrogen, let me tell you that the NEA Steering Committee, the governing body of my Agency, organised a policy debate on Nuclear Energy in the Hydrogen Economy at its meeting last October. During this debate, it was stressed that the nuclear sector should participate actively in the discussions on a hydrogen economy, and that international co-operation is essential to ensure the development of nuclear systems for efficient hydrogen production. In this context, undertakings like Generation IV International Forum can enhance the synergy between national programmes and the effectiveness of the overall efforts. As you are probably aware, the NEA is also providing technical Secretariat services to the Generation IV International Forum, this is a significant lever to develop these synergies.

Information exchange meetings such as the one we are organising today are among the best tools that the NEA may use to fulfil its mission of promoting international collaboration. They are very useful first, for building an overall picture of ongoing and planned research activities in a specific area, second, for providing opportunities to meet and to discuss common issues and possibly to establish international collaborations, either on a bilateral or on a multilateral basis.

I have seen in the programme that Dr. Mark Petri and Dr. Ryutaro Hino of the Organising Committee will co-chair a discussion at the end of this meeting. Although I will not be able to stay for this discussion, I look forward to getting feedback from it and especially to being informed of your recommendations. Indeed, the NEA Secretariat will be happy to forward such recommendations to the NEA Nuclear Science Committee, for their consideration in our future programme of work.

Finally, I would like to thank the Japan Atomic Energy Agency (JAEA) for co-organising this meeting and especially Dr. Shusaku Shiozawa and Dr. Takashi Nagata, the former and present Directors-General of the Oarai Establishment, for their support of this information exchange meeting and also more globally for their support to the NEA activities.

I wish you all a very interesting and fruitful meeting.

Thank you for your attention.

OPENING REMARK

Osamu Oyamada

Director of the Nuclear Science and Energy Directorate, Japan Atomic Energy Agency, Japan

Good morning ladies and gentlemen,

On behalf of the JAEA, I would like to extend a cordial welcome to all of you, gathering here for the 3rd OECD/NEA Information Exchange Meeting on the Nuclear Production of Hydrogen, including the 2nd HTTR Workshop on Hydrogen Production Technologies.

At the opening of this workshop, I would like to announce that the former organisation of JAERI and JNC was united to the new organisation “Japan Atomic Energy Agency”, JAEA for brevity, as of 1st October, just four days before. The Research & Development on the VHTR and Nuclear Process Heat Application will be continued in this newly established organisation, the JAEA .

I have been appointed to the position of Director of the Nuclear Science and Energy Directorate, which covers from the fundamental studies such as nuclear data, reactor physics, materials sciences as well as the research & development on VHTR and nuclear hydrogen research.

It is widely recognized that hydrogen is one of the solutions against the global environmental issues of the emission of greenhouse effect gases. Also it is widely recognised that nuclear energy would make a significant contribution to the production of the hydrogen without emitting the greenhouse gases.

Recently, research and development of hydrogen production technology by nuclear energy have been augmented in the world. We JAEA have developed the high temperature gas-cooled reactor technology by HTTR and also developed nuclear hydrogen production technology such as the thermochemical water splitting method by utilising the high temperature produced by HTGR. Also, we recently are developing new hydrogen production technology by the use of fast breeder reactor . We are very happy to discuss the recent results with the worldwide participants.

It is our great pleasure to have the 3rd OECD/NEA Information Exchange Meeting on the Nuclear Production of Hydrogen including the 2nd HTTR Workshop on Hydrogen Production Technologies organised by the OECD/NEA and the JAEA and co-sponsored by the IAEA.

We also prepare the special session of the 2nd HTTR Workshop in the evening of the 7 October and we will present recent results of the HTTR technologies.

We hope that all of the participants have interesting and fruitful meeting. Also please enjoy your stay at Oarai for three days. In Japan, autumn is the nice season to enjoy foods, you can taste variety of delicious fruits or fishes, mushrooms, and so on.

I hope you will be refreshed with the nice foods and atmosphere of Oarai.

Thank you very much.

This page intentionally left blank

SESSION I

**THE PROSPECTS FOR HYDROGEN IN FUTURE ENERGY STRUCTURES
AND NUCLEAR POWER'S ROLE**

Chair: M.C. Petri

This page intentionally left blank

SYNERGY OF FOSSIL FUELS AND NUCLEAR ENERGY FOR THE ENERGY FUTURE

Masao Hori

Nuclear Systems Association

Mamoru Numata

JGC Corporation

Takayuki Amaya

JGC Corporation

Yasushi Fujimura

JGC Corporation

Abstract

The paper reviews the methods of producing or upgrading the energy carriers utilizing fossil fuels and nuclear energy, individually or synergistically, for the 21st century when the best-mixed supplies of available primary energies are crucial.

Besides the individual process of primary energies to energy carriers, the synergistic process of primary energies to the energy carriers will become important with the features of resource saving, reducing CO₂ emissions and economic production, due to the higher conversion efficiency and low cost of nuclear heat.

A new synergistic process for bitumen upgrading is presented. There remain many possibilities of new, innovative, synergistic processes, which combine chemical and nuclear systems for efficient, clean and economical production of energy carriers.

1. Introduction

Fossil fuels, in general, have the environmental problem due to the CO₂ emission, and fossil fuels, except coal, have the resource problem for the future supply. Also, nuclear energy might have a supply stagnancy problem, if the demand for the nuclear energy increases as estimated by the World Energy Council (WEC), due to deficiency of fissile materials in the 21st century, though a timely introduction of Plutonium recycling with appropriate breeding setup could ease the problem.

To supply energy for the production of hydrogen and other energy carriers as well as electricity generation, it is essential to utilise both fossil fuels and nuclear energy in a manner to ensure the continuing supply of energy while reducing CO₂ emissions, so as to solve the global problems of resources and environment in the 21st century.

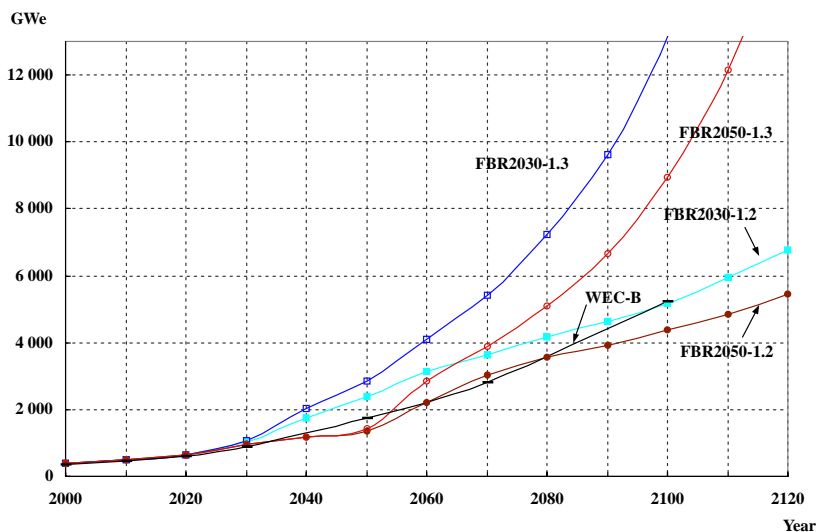
Synergistic utilisation of fossil fuels and nuclear energy has prospects of efficient conversion of primary energies into energy carriers and lower the cost of conversion as well as the favorable impacts on resources and environment.

The paper reviews the methods of producing or upgrading the energy carriers utilising fossil fuels and nuclear energy, individually or synergistically, for the 21st century when the best-mixed utilisation of available primary energies are crucial.

2. Supply capability of nuclear energy

According to the estimates of WEC (Ref. 1), the world primary energy demand in 2100 would be about 4 times that of 1990 in case of the middle course (B case) with nuclear energy expected to supply 24% of total primary energy for electricity production. This amount of nuclear supply corresponds to the capacity of about 5200 units of 1000 MWe plants. The supply of fissile fuel to these plants is feasible as shown in Figure 1, assuming the ultimate resources of natural uranium 16.3 Mton, by the NEA/IAEA Red Book (Ref. 2), and the recycling use of plutonium by fast breeder reactors (FBR) with breeding ratio of 1.2 ~ 1.3 introduced from 2030 ~ 2050 (Ref. 3).

Figure 1. Nuclear Supply Capacity as Projected by the Four Transition Strategies Comparison with the WEC-B Case



In order to reduce global greenhouse gas emissions and begin displacing fossil fuels, optimising the recycling use of plutonium in FBR could increase energy supply by nuclear energy to 1.5 times in 2050 and 2 times in 2100 of the WEC-B case estimates. By effectively utilising nuclear energy, this excess supply capacity of nuclear energy over the WEC-B Case could replace fossil fuels share as shown in the Table 1. (Ref. 3).

**Table 1. Primary energy supply for 1990-2100
WEC-B case R proactive nuclear deployment case
energy in gtoe [109 ton oil equivalent]**

	1990	2050	2100
Fossil	6.9	12.7 → 11.4	15.0 → 5.0
Nuclear	0.45	2.7 → 4.0	8.3 → 18.3
Hydro + Renewables	1.6	4.4	11.4
Total	9.0	19.8	34.7

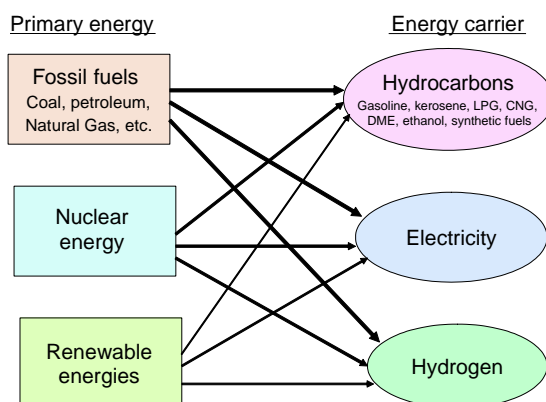
In such a scheme, the global supply quantity of fossil in 2100 would become smaller than it was in 1990, thus attaining stabilisation of atmospheric carbon dioxide concentration even in the face of global growth of energy use by a factor of four.

Either in the WEC-B case or in the Proactive Nuclear Deployment Case in Table 1, the world has to utilise concurrently all of these primary energies in the 21st century. Therefore, it would be worthwhile to investigate ‘synergistic’ energy conversion processes by which these primary energies work together to produce or upgrade energy carriers so as to obtain benefits from any combined effects to efficiency, cost, and/or so (Ref. 4). In this paper, synergy between fossil fuels and nuclear energy are reviewed and investigated.

3. Review of converting process from primary energy to energy carriers

Here, the energy carries are categorised into three as shown in Figure 2, namely hydrocarbons, electricity and hydrogen. As for the hydrocarbon energy carriers, gasoline, kerosene, liquefied petroleum gas, compressed natural gas and so on are used at present, while dimethyl ether, ethanol, synthetic fuels and so on will be used in the future.

Figure 2. Production of energy carriers from primary energies



In the production technologies, there are individual processes and synergistic processes. The individual process is a process where only one primary energy is used to supply energy for converting to an energy carrier. The synergistic process is a process where two or more primary energies (fossil fuels and nuclear energy in this paper) are used to supply energies for converting to an energy carrier.

At present, fossil fuels and nuclear energy are individually producing such energy carriers as hydrocarbons, electricity and hydrogen commercially, though some are still in developing stages. As for the hydrocarbon energy carriers, gasoline, kerosene, methane and other hydrocarbons produced from petroleum and natural gas are presently used, but in the future synthetic hydrocarbons produced or upgraded by nuclear energy will be used.

3.1 Individual process

Some of the examples of the individual processes for converting the primary energies to energy carriers are shown in Table 2.

In Table 2, the nuclear electricity generation is now commercially conducted, and nuclear hydrogen production is now under research and development. As for the nuclear hydrocarbon production, a nuclear synthetic methane recycling process is being developed by the Tokyo Institute of Technology for on-board steam-methane reforming with calcium oxide for CO₂ sorption (Ref. 5).

Table 2. Examples of individual process for converting primary energy to energy carrier

	Hydrocarbons	Electricity	Hydrogen
Fossil fuels	<ul style="list-style-type: none"> ➤ Petroleum refining ➤ Coal gasification 	<ul style="list-style-type: none"> ➤ Coal fired power plant ➤ Natural gas fired power plant 	<ul style="list-style-type: none"> ➤ Steam methane reforming ➤ Steam coal gasification
Nuclear energy	<ul style="list-style-type: none"> ➤ Nuclear synthetic methane recycling 	<ul style="list-style-type: none"> ➤ PWR ➤ BWR ➤ HWR 	<ul style="list-style-type: none"> ➤ Electrolysis ➤ Thermo-chemical water splitting

3.2 Synergistic Process

Examples of the synergistic processes using both fossil fuels and nuclear energy to produce or upgrade energy carriers are reviewed.

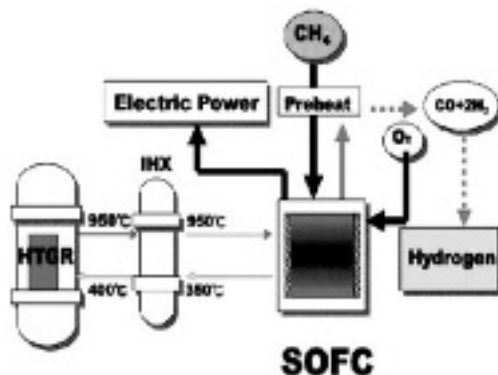
A. Synergistic hydrocarbon upgrading process

- Crude oil upgrading to the carbon saver fuels (C₁H₂+) by adding nuclear hydrogen (C. Forsberg – ORNL, Ref. 6)
- Oil sands upgrading to the synthetic crude by adding nuclear hydrogen produced by advanced CANDU reactor (J. Hopwood – AECL, Ref. 7).

B. Synergistic electricity generation process

- Fossil fuels superheated water reactors.
- Methane partial oxidation fuel cells with nuclear heat, called “Multi Power” Conversion System by HTGR (S. Ishiyama – JAERI, Figure 3, Ref. 8).

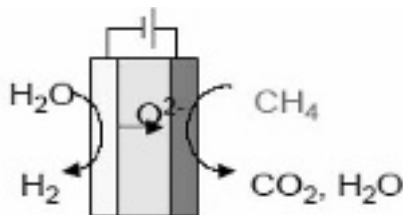
Figure 3. Concept of “multi power” conversion system by HTGR



C. Synergistic hydrogen production process

- Nuclear-heated steam-methane reforming (High temperature reforming, S. Shiozawa – JAERI, Ref. 9. Medium temperature reforming, M. Tashimo – ARTEC, Ref.10. Low temperature reforming of DME, Fukushima – Toshiba, Ref. 11)
- High temperature steam electrolysis with methane oxidation (L. Vance – LLNL, Figure 4, Ref. 12)
- Membrane reforming of synthetic natural gas from coal (M. Hori – NSA, Ref.13)

Figure 4. Natural gas assisted steam electrolyser total oxidation mode



4. Potential chemical processes and nuclear reactor for synergistic processes

As shown in the above examples, fossil fuels and nuclear energy can synergistically produce electricity and hydrogen, and can produce or upgrade hydrocarbons. The synergistic processes presently under study include such chemical reactions as steam reforming (both high temperature and medium temperature), hydrogasification (high temperature for coal), hydrocracking and hydrogenation (upgrading of hydrocarbons), methanation (coal to synthesised natural gas, CO₂ reduction), and electrochemical reactions using electrolysis cells and fuel cells.

For efficient conversion of primary energies to energy carriers, these processes are to be combined with suitable reactor types, such as high temperature reactors (VHTR, GFR, LMR, MSR) and medium temperature reactors (SFR, SCWR). These reactor systems are selected by the Generation IV International Forum as candidates of R&D co-operation (Ref. 14).

The high temperature reactors like VHTR holds the promise to be applied various chemical processes that need high temperature, especially for coal processes, to produce hydrocarbons and hydrogen. However, in high temperature reactors, due to material limitation at present, the pressure of chemical process should be in the same range as the primary coolant pressure, which may be a hindrance factor in some processes.

In the medium temperature reactors like SFR and SCWR, the pressure of chemical process can be different from the primary pressure. Usually, chemical equilibrium may be not favorable in medium temperature range for processing fossil fuels, but such technology as the membrane separation could alleviate the disadvantage.

It is expected that many promising processes with high efficiency and good economics could be developed in the future.

5. Expected features of synergistic process

The expected features of synergistic processes are:

- Saving resources of both fossil fuels and nuclear energy by processes of higher energy utilisation efficiency.
- Reducing CO₂ emissions by processes of higher energy utilisation efficiency.
- Lowering production costs by processes of higher energy utilization efficiency and by lower heat cost of nuclear energy.

Some considerations on the energy utilisation by synergistic processes are as follows:

- In the hydrogen production by nuclear heat, there is the limitation by thermodynamic law (the Carnot efficiency at the highest), because either the electrolysis or the thermochemical water splitting process has to go through the “heat engine” path.
- In the hydrogen production from fossil fuels, if it is chemical to chemical conversion such as by the steam-coal gasification reaction or by the steam-methane reforming reaction, there is no such thermodynamic limitation by the Carnot efficiency.
- In the hydrogen production from fossil fuels, either by the steam-coal gasification reaction or by the steam-methane reforming reaction, the endothermic heat of reaction is conventionally supplied by combustion of fossil fuels. If this endothermic heat is supplied from nuclear heat, full stoichiometric conversion of fossil fuels to hydrogen moles and effective conversion of nuclear heat to hydrogen heat can be achieved.
- In Table 3 are shown the heat conversion factor of producing hydrogen from nuclear energy, methane and the both (Ref. 15). Here, the heat conversion factor is defined as ratio of hydrogen heat to nuclear heat, ratio of hydrogen heat to methane heat, or ratio of hydrogen

heat to sum of nuclear heat and methane heat, all in the low heat value (LHV). The nuclear-heated steam methane reforming using the recirculation-type membrane reformer gives the ratio of 0.85 for hydrogen heat to sum of methane and nuclear heat.

Table 3. Heat conversion factor producing hydrogen from nuclear and fossil (low heat value)

Hydrogen production process	Energy source	Nuclear electricity (Elect./Heat =32~50 %)	Nuclear electricity & heat (High Temp)	Nuclear heat (High Temp)	Nuclear heat (Medium Temp*)	Natural gas heat (Combustion)
	Raw material	Water	Water	Water	Natural gas water	Natural gas water
	Production process	Electrolysis	Hot electrolysis	Thermo-chemical	Steam reforming	Steam reforming
Heat conversion factor [%]	H ₂ heat / nuclear heat	0.25~0.4	0.45	0.5	3.3 *	--
	H ₂ heat / methane heat	--	--	--	1.15 *	0.8

$$* (H_2 \text{ heat}) / (\text{nuclear heat} + \text{methane heat}) = 0.85$$

* In the case of recirculation-type membrane reformer, efficiency of reactor heat utilisation = 60%, yield of hydrogen from methane = 95%

6. Nuclear upgrading of bitumen to synthetic crude

The authors have investigated a process to upgrade the bitumen extracted from unconventional extra heavy oils (Oil sands in Canada, Orinoco tar sands in Venezuela, etc.) using nuclear energy.

AECL investigated the possibility of using the electricity, steam and hydrogen from ACR (advanced CANDU reactor) for extracting bitumen by the steam assisted gravity drainage from oil sands using nuclear steam and upgrading bitumen to synthetic crude oil using nuclear hydrogen (Ref. 7). In the AECL study, electrolysis by ACR-generated electricity is envisioned for producing hydrogen.

In our study, we envision that the hydrogen used for upgrading bitumen to synthetic crude is produced by nuclear-heated steam reforming of a part of the product (synthetic crude) as shown in the schematic flow diagram (Figure 5). The electricity and steam (heat) from the nuclear reactor would be supplied to all the processes through bitumen extraction to synthetic crude upgrading.

A typical composition of bitumen extracted from oil sands is : C = 83.2%, H = 10.4%, O = 0.94%, N = 0.36%, S = 4.8%. Ordinary crude oil contains H = 11~14%, so hydrogen is necessary for hydrocracking and hydrotreating (hydrogenation and desulfurisation) of bitumen for upgrading to synthetic crude.

Here, the composition of bitumen is assumed as C₁H_{1.5}S_{0.02} and that of synthetic crude oil as C₁H₂. Then, the hydrogen related reactions in the upgrading process from bitumen to synthetic crude oil are as follows;

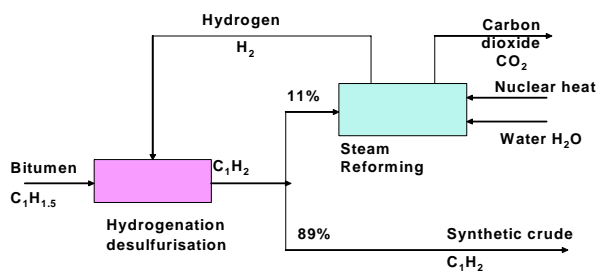
Hydrocracking and hydrogenation: $C_1H_{1.5} + 0.25 H_2 \rightarrow C_1H_2$

Desulfurisation: $S_{0.02} + 0.02 H_2 \rightarrow 0.02 H_2S$

Reforming: $C_1H_2 + 2H_2O + \text{nuclear heat} \rightarrow CO_2 + 3 H_2$

Assuming 90% efficiency for the above reactions, the mass balance of synthetic crude is shown in Figure 5. About 11% of product crude oil are used for producing hydrogen for hydrocracking and hydrotreating.

Figure 5. Schematic flow diagram of nuclear-heated steam reforming for upgrading bitumen to synthetic crude



As for the nuclear-heated steam reforming of synthetic crude, the medium temperature recirculation-type membrane reforming process (Ref. 10) can be applied, where either SFR (sodium fast reactor) or SCWR (supercritical water reactor) could be adopted as medium-temperature heat source.

As the medium temperature nuclear-heated steam methane reforming is assessed economically competitive with conventional natural gas based hydrogen production (Ref. 10), this kind of process for hydrocarbons upgrading will be promising as the feed of natural gas or combustion of bitumen/crude oil is not necessary for hydrogen production. Together with the nuclear supply of electricity and steam (heat) to the whole process, the nuclear hydrogen supply could eliminate the combustion of fossil fuels in the extraction and upgrading process of extra heavy oils.

7. Conclusion

- Hydrocarbons, electricity and hydrogen will be the energy carriers used mostly in the 21st century. Both fossil fuel and nuclear energy will be required to supply energy for producing these energy carriers, with the share of nuclear energy ever increasing for the future.
- As for nuclear energy, timely transition and appropriate breeder setup will be necessary before the middle of century. As for fossil fuels, from the supply/demand situation in the market, share of heavier (more carbon content, like oil sands, coal) fuels will increase for the future.
- Besides the individual process of primary energies to energy carriers, the synergistic process of primary energies to the energy carriers will become important with the features of resource saving, reducing CO₂ emissions and economic production, due to the higher conversion efficiency and low cost of nuclear heat.
- A new synergistic process for bitumen upgrading is presented. There remain many possibilities of new, innovative, synergistic processes, which combine chemical and nuclear systems for efficient, clean and economical production of energy carriers.

REFERENCES

- [1] N. Nakicenovic, *et al.*, “Global Energy Perspectives – A joint IIASA – WEC study”, Cambridge University Press ISBN 0-521-64569-7.
- [2] OECD/NEA & IAEA, “Joint Report on Uranium: Resources, Production and Demand” (1997).
- [3] M. Hori, “Role of Nuclear Energy in the Long-Term Global Energy Perspective”, Proceedings of OECD/NEA First Information Exchange Meeting on Nuclear Production of Hydrogen, Paris, France, 2-3, October 2000, p.25 (2001).
- [4] M. Tashimo *et al.* “Role of Nuclear Produced Hydrogen for Global Environment and Energy”, Proceedings of OECD/NEA Second Information Exchange Meeting on Nuclear Production of Hydrogen, Argonne USA, 2-3, October 2003, p.43 (2003).
- [5] Y. Kato *et al.*, “Zero Carbon Dioxide Release Hydrogen System Using Nuclear Powers” Transaction of The American Nuclear Society, 2005, Volume 92, p. 100 (ANS Annual Meeting, San Diego, June 2005)
- [6] C. Forsberg, *et al.*,”Hydrogen Production as a Major Nuclear Energy Application” Nuclear News p.41, (September 2001).
- [7] J. Hopwood1, *et al.*, “Advanced CANDU Reactor: An Optimized Energy Source of Oil Sands Application”, GENES4/ANP2003 Conference, Kyoto, JAPAN, Paper No. 1199, 15-19, September (2003).
- [8] S. Ishiyama, “Electricity and Hydrogen Multi Production Process with New Solid Electrolyte for HTGR, (1)” Transaction of Japan Atomic Energy Society (in Japanese), Vol. 2, No.1 p.14 (2003)
- [9] S. Shiozawa, *et al.*, “Present Status of JAERI’s R&D on Hydrogen Production Systems for HTGR”, Proceedings of OECD/NEA First Information Exchange Meeting on Nuclear Production of Hydrogen, Paris, France, 2-3, October 2000, p.57 (2001).
- [10] M. Tashimo, *et. al.*, “Advanced Design of Fast Reactor – Membrane Reformer”, Proceedings of OECD/NEA Second Information Exchange Meeting on Nuclear Production of Hydrogen, Argonne USA, 2-3, October 2003, p.267 (2003).
- [11] K. Fukushima *et al.*, “Conceptual design of low-temperature hydrogen production and high-efficiency nuclear reactor technology”, JSME Int. J. B, Fluids Therm. Eng. 47, 340 (2004)
- [12] L. Vance, *et al.*, “High-Efficiency Steam Electrolyze” DOE Hydrogen and Fuel Cells 2003 Annual Merit Review, May 20 (2003).

- [13] M. Hori, *et al.*, “Synergistic Production of Hydrogen Using Fossil Fuels and Nuclear Energy”, Proceedings of OECD/NEA Second Information Exchange Meeting on Nuclear Production of Hydrogen, Argonne USA, 2-3, October 2003, p.171 (2003).
- [14] Nuclear Energy Research Advisory Committee and Generation IV International Forum, “Generation IV Roadmap – R&D Scope Report for Water-Cooled Reactor Systems”, GIF -003-00 , (December 2002).
- [15] M. Hori, *et al.*, “Synergistic Hydrogen Production by Nuclear-Heated Steam Reforming of Fossil Fuels” COE-INES International Symposium, INES-1, Paper No. 43, 31 October - 4 November , (2004).

CAN NUCLEAR POWER COMPLETE IN THE HYDROGEN ECONOMY?

Geoffrey Rothwell*

Stanford University, Stanford, CA, USA

Evelyne Bertel

OECD/NEA, Issy-les-Moulineaux, France

Kent Williams

Oak Ridge National Laboratory, Oak Ridge, TN, USA

Abstract

Today, hydrogen is used primarily in the petroleum and petrochemical industries. The dominant technology to produce hydrogen is steam methane reforming (SMR), which uses natural gas as both feedstock and fuel. Hydrogen could become a major carrier of energy for distributed use, such as in fuel-cell vehicles. This paper compares the cost of hydrogen production using SMR technology with the cost of nuclear-powered hydrogen generation using a modular helium reactor (MHR). Natural gas prices between \$6 and \$8/GJ yield hydrogen from SMR with an average production cost between \$11.50 and \$14.50/GJ. The MHR shows a range of hydrogen production costs around \$15/GJ. Thus, the MHR might be competitive in the pipeline hydrogen market with natural gas prices above \$8/GJ. But high natural gas prices make the MHR extremely competitive with respect to Combined Cycle Gas Turbines. MHRs are likely to be more profitable in electricity markets than in hydrogen markets.

Keywords: hydrogen economics, electricity economics, nuclear power economics

*Send correspondence to Geoffrey Rothwell, Department of Economics, Stanford University, Stanford, California 94305-6072 USA or rothwell@stanford.edu

Acknowledgements

We are members of the Economic Modeling Working Group (EMWG) of the Generation IV International Forum (GIF). We thank C. Forsberg, R. Graber, R. Hagen, P. Peterson, W. Rasin, T. Resin, J-L Rouyer, members of the EMWG, participants at the “Third Information Exchange Meeting on the Nuclear Production of Hydrogen,” and seminar participants at EPFL for their encouragement, data, and comments. This paper reflects the views and conclusions of the authors and not those of the employers, sponsors, publishers, EMWG, or GIF.

Nuclear power in the hydrogen economy

Today, hydrogen is used in limited quantities, and mainly in petroleum refineries and the petrochemical industry. In the United States, for example, these uses represented 93% of hydrogen consumption in 2003. However, hydrogen is an attractive energy carrier that might play a major role in many energy systems in the long term. In the medium term, the most promising area for hydrogen might be substituting for gasoline in transportation. Hydrogen produced from non-fossil fuels might be a key option for transportation and other sectors as the prices of hydrocarbon resources soar or their consumption becomes restricted for environmental reasons [1].

The advantages of hydrogen-based energy systems will depend on the hydrogen production systems implemented. Hydrogen will be a clean, environmentally friendly and sustainable energy carrier only if its production is safe and sustainable, i.e., does not induce irreversible environmental damages or exhaust non-renewable natural resources. Nuclear-produced hydrogen offers unique characteristics in terms of environmental friendliness and energy efficiency.

The development of hydrogen-based energy systems will require building not only hydrogen production facilities and end-use devices, but also an infrastructure for the distribution of hydrogen. Such structural changes in production and use of energy will take time. This implementation lag could facilitate the penetration of nuclear energy in the hydrogen supply market. This penetration would prepare a foundation for the design and deployment of advanced nuclear energy systems (e.g., very high temperature reactors) that would be better adapted to hydrogen production than the current generation of nuclear power plants.

While nuclear energy has the potential to play a significant role in a hydrogen economy [2], there are uncertainties about when hydrogen demand will be large enough to justify deployment of nuclear plants dedicated to hydrogen production or dual-production units capable of generating electricity and producing hydrogen. Furthermore, many existing and advanced technologies will compete with nuclear energy for hydrogen production, and market competition will determine the best option.

Key issues to be addressed for assessing the future of nuclear-produced hydrogen include the size and evolution of the potential markets for hydrogen, and the economics of nuclear energy versus alternatives. This paper presents a reduced-form model of the hydrogen economy. It provides estimates of the average cost of hydrogen produced by steam methane reforming (SMR) as a function of the price of natural gas. It analyses cost estimates for electricity and pipeline hydrogen produced by an advanced nuclear energy system, the modular helium reactor (MHR) developed by General Atomics.¹ Finally, the competitiveness of the MHR in both electricity and hydrogen markets is discussed. The paper finds that for all prices of natural gas the MHR is more competitive in the electricity market than in the hydrogen market. (The models presented in the paper are applicable world-wide, but the illustrative examples developed below rely on economic data and conditions in the United States.)

¹ The MHR was chosen because it has been adapted for hydrogen production and because data supporting cost calculations are publicly available. There are other high-temperature nuclear power/thermo-chemical hydrogen systems that might have more favorable economics; however these more advanced systems are early in their development and have greater uncertainties. [3]

A model of the hydrogen economy

The demand for hydrogen has been growing and will continue to grow throughout the foreseeable future, whether the “hydrogen economy” emerges or not. According to the Chemical Market Reporter [4]: “The hydrogen market is getting stronger as the refining industry gears up to meet upcoming regulatory requirements in Europe, North America and other regions. In the longer term, hydrogen consumption should grow in Europe as refineries use the gas to reduce their production of heavy fuel oil. In North America, additional hydrogen demand is expected in conjunction with the use of heavier crudes that require incremental hydrotreating and hydrocracking capacity. The increased outsourcing of hydrogen supplies and the replacement of aging hydrogen production facilities in North America are also expected to encourage growth.”

There are two sectors of today’s hydrogen production economy: “captive capacity” owned by downstream users of hydrogen, e.g., oil refiners, and “merchant capacity” (outsourcing), where producers compete for business.² Throughout this decade, demand for hydrogen should continue to grow in the merchant sector: “Although aggregate hydrogen consumption is growing 4% annually, growth in the merchant hydrogen business is significantly higher, perhaps 10%” [5]. This implies adding 3-6 M m³/day of capacity each year.³ Can nuclear power capture a share of this pipeline hydrogen market?

Recent U.S. federal legislation points to the possibility of generating hydrogen with nuclear power. In July 2005, the U.S. Congress passed the Energy Policy Act of 2005 (PL 109-58), which addresses nuclear hydrogen production in Sections 641-645: “The Project shall consist of the research, development, design, construction, and operation of a prototype plant, including a nuclear reactor that – (1) is based on research and development activities supported by the Generation IV Nuclear Energy Systems Initiative under section 942(d); and (2) shall be used – (A) to generate electricity; (B) to produce hydrogen; or (C) both to generate electricity and to produce hydrogen. ... There is authorized to be appropriated to the Secretary for research and construction activities under this subtitle (including for transfer to the Nuclear Regulatory Commission for activities under section 644 as appropriate) – (1) \$1,250,000,000 for the period of fiscal years 2006 through 2015; and (2) such sums as are necessary for each of fiscal years 2016 through 2021.” (emphasis added)

To understand nuclear power in the hydrogen economy, Figure 1 represents a model of the hydrogen economy now being developed in association with the Economic Modeling Working Group (EMWG) of the Generation IV International Forum (GIF). Its primary purpose is to determine demand for central station (i.e., pipeline transmission) and distributed hydrogen (e.g., with electrolysis): (1) as crude oils become heavier; (2) as hydrogen fuel-cell vehicles compete with hybrid/internal combustion engines; and (3) as hydrogen infrastructure is built. This is the “Hydrogen Economy, Energy, Environment, and Transport” (HEEET) model.

² Ignoring the “cryogenic liquid” market (e.g., rocket fuel) that accounts for 7% of the merchant market, in 2003 the total U.S. merchant hydrogen gas capacity was about 1 500 M Standard Cubic Feet (SCF)/day. Most of this merchant production capacity (92%) was located in three states: Texas with 560 M SCF/day, Louisiana with 440 M SCF/day, and California with 380 M SCF/day [5,6]. Also, the Chemical Market Reporter [5] writes, “Another 3 billion SCF per day of captive hydrogen capacity exists at 145 locations in the US.” Therefore, in 2003 the U.S. had a total capacity of about 4 500 M SCF/day, or about 127 M m³/day.

³ Chemical Market Reporter [4] writes, “As reported, Air Products will raise hydrogen production at its plant in Baytown, Tex, to 3 million cubic meters per day to supply ExxonMobil’s nearby refinery, as well as other companies through a pipeline. Praxair Inc. has a 300-mile refinery hydrogen pipeline through Texas and Louisiana. The company expects hydrogen demand to grow by roughly 20 percent per year until at least 2012.”

In this model, energy is delivered to the hydrogen production sector through natural gas and electricity. The prices over time of natural gas and coal are econometric functions of exogenous, random oil prices. The cost of hydrogen production is described with cost-engineering models. The prices of distributed energy carriers (gasoline/diesel, electricity, and hydrogen) are determined in endogenous markets. The demand for vehicle type in the transportation sector is a function of fuel cost and vehicle investment dynamics. Our goal is to simulate probability distributions for costs, prices, and quantities of pipeline and distributed hydrogen to 2050 under various scenarios.

Figure 1. A Diagram of the hydrogen economy, energy, environment, and transport (HEEET) model

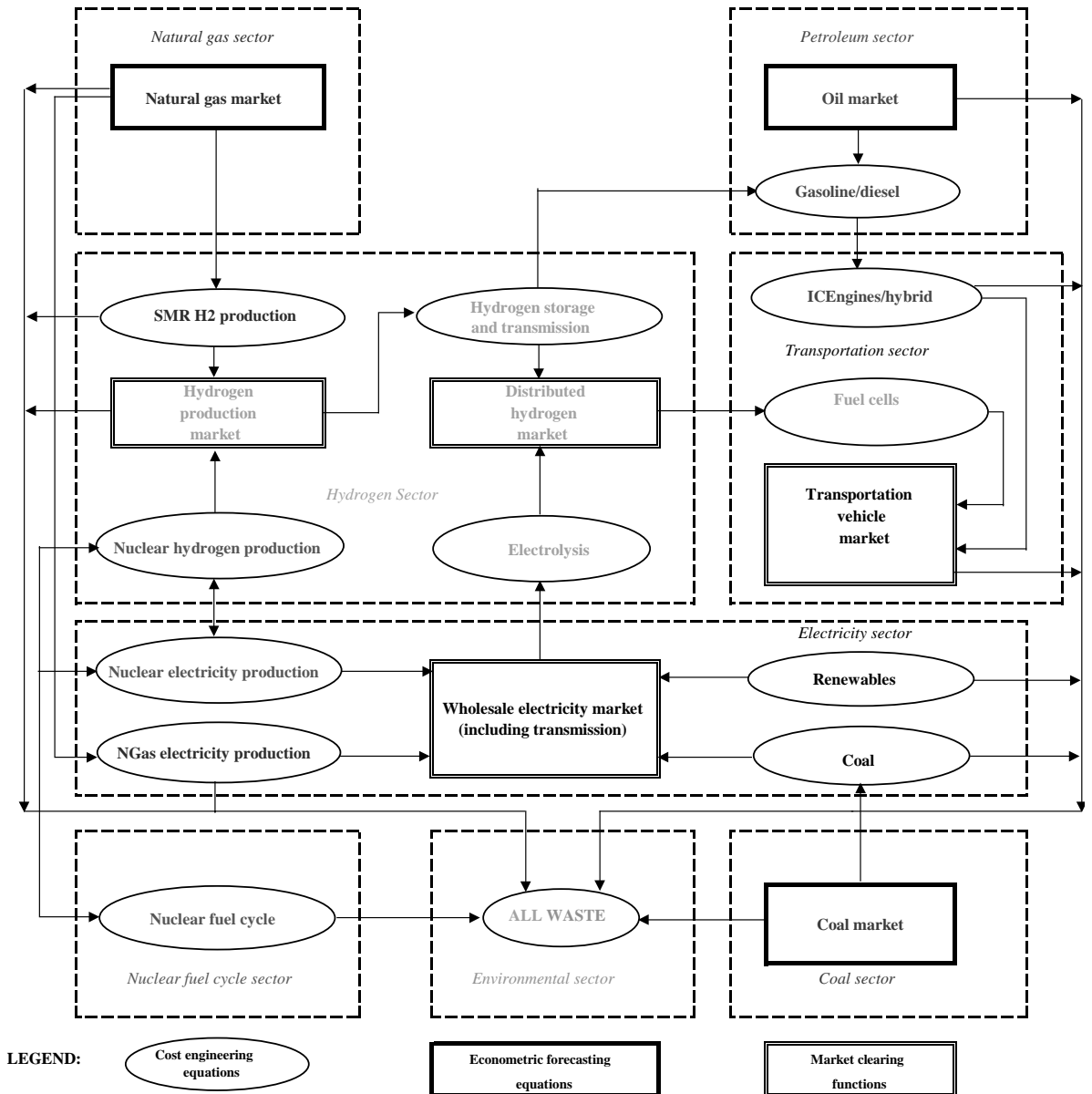
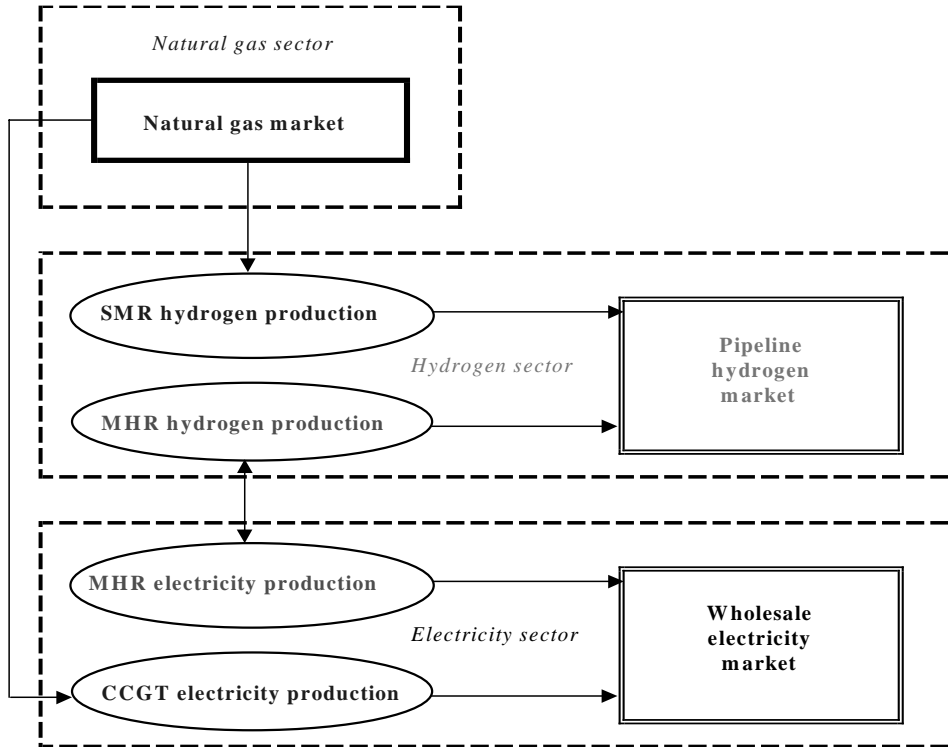


Figure 2 presents those sectors of the model discussed in this paper. These include (1) hydrogen produced with steam methane reforming (SMR) and with modular helium reactors (MHRs) and (2) electricity produced with combined-cycle gas turbines (CCGT) and with MHRs.

Figure 2. A reduced form of the HEEET Model



Average cost of hydrogen from steam methane reforming

Today most hydrogen is produced with SMR by chemically reacting natural gas and steam at high temperature [7]. SMR is described in [8] as: “*The conventional process occurs in a chemical reactor at temperatures of about 800-900° C. When fueled with fossil fuels it is the most economical method of producing hydrogen today [7]. The heat is generally supplied by burning an excess of the methane. This results in a loss of both the reactant, and some of the product hydrogen. Typical thermal efficiencies for steam reforming processes are about 70% [7].*”

Table 1. Costs of hydrogen produced by SMR [7]

Facility size (M Nm ³ /d)	Specific total capital investment (\$/GJ)	Hydrogen unit cost (\$/GJ)	Reference
Small facility			
0.27	27.46	11.22	Leiby 1994
Large facilities			
1.34	14.74	7.46	Leiby 1994
2.14	12.61	6.90	Leiby 1994
2.80	9.01	6.26	Kirk-Othmer 1991
6.75	10.00	5.44	Foster-Wheeler 1996

Table 1 reproduces a summary of hydrogen production cost using SMR as compiled in [7] where the price of natural gas was assumed to be \$2.96/GJ. “Specific Total Capital Investment” (Specific TCI) is TCI divided by annual output. “Hydrogen Unit Cost” is the Levelised Unit Energy Cost. Figure 3, reproduced from [5], illustrates the cost of hydrogen production by SMR as a function of natural gas prices and facility capacity. Economies of scale are nearly exhausted at 3 M m³/day.

Figure 3. Scale economies in SMR production of hydrogen (1998\$) [7]

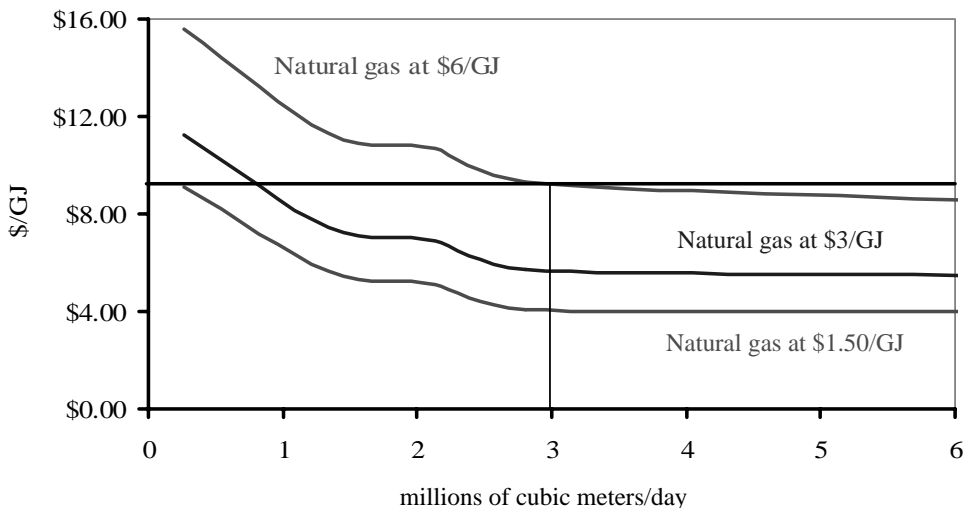


Table 2. A spreadsheet model of SMR average costs

Energy required for SMR (2 steps adding to CH ₄ +2H ₂ O >> CO ₂ + 4H ₂) [1500°F or ~815°C] endothermic reaction		Unit
Moles of CH ₄ to provide heat for reaction	420	KJ/g-mole of CH ₄ reactant
Total moles of CH ₄ to produce 4 moles of H ₂	0.495	moles at 100 % efficiency
Price of natural gas feedstock	1.708	moles at 70 % efficiency
	6	\$/GJ
Feedstock and fuel cost component	9.02	\$/GJ H₂
SMR plant construction cost	320	\$M
Typical large plant size (capacity)	6	M m ³ /day
Annual production at 80% capacity factor	1 752	M m ³ /yr
i.e.	4.8	M m ³ /day
Amortise at 10.23% per year capital recovery factor	18 710	\$/M m ³ H ₂
Capital cost component	1.72	\$/GJ H₂
Non-methane annual operations cost for SMR	15	\$/M m ³ /yr
Non-CH ₄ operations cost per unit	8 562	\$/M m ³ H ₂
O&M cost component	0.77	\$/GJ H₂
Levelised unit energy cost /GJ	11.50	\$/GJ H₂
Levelised unit energy cost /kg	1.39	\$/kg H₂

Table 2 depicts a simple cost-engineering model of SMR production of hydrogen using natural gas (assuming 100% methane). Average Cost is a function of facility size and the price of natural gas. Assuming a facility of 6 M m³ (~212 M SCF) per day, a capacity factor of 80%, a 70% thermal efficiency for SMR, and a natural gas price of \$6/GJ, the average cost of hydrogen would be about

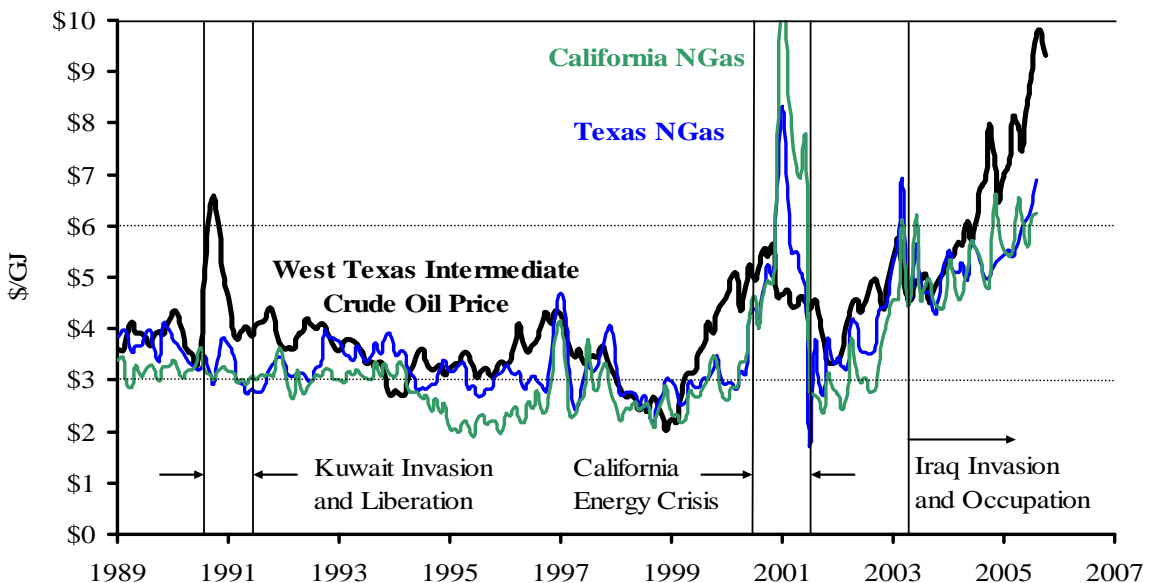
\$11.55/GJ in 2001 dollars (using the U.S. GDP implicit price deflator). The relationship between the average cost of H₂ and the price of natural gas at a facility of 6 M m³/day can be summarised as:

$$ACOST = \$2.55 + 1.50 \text{ PRICE} ,$$

where ACOST is the average cost of H₂ in \$/GJ and PRICE is the price of natural gas in \$/GJ (also, $1.50 = [(1.708 \text{ moles CH}_4)/(4 \text{ moles H}_2)] \cdot [(0.000849 \text{ GJ/g-mole CH}_4)/(0.000241 \text{ GJ/g-mole H}_2)]$). What is a reasonable price for natural gas?

Natural gas is sold in regional markets defined by pipeline capacity. Because of the importance of Texas and California in today's "hydrogen economy," Figure 4 presents the data for the West Texas Intermediate Crude Oil Spot Price and City Gate Natural Gas Prices in Texas and in California.⁴ By applying time-series econometric techniques to these data, one can conclude that the price of oil leads natural gas prices and that the price of oil does not follow changes in any other energy price [9,10].

Figure 4. WTI Crude and Natural Gas Prices in California and Texas, 1989-2005 (2001\$)



Average monthly natural gas prices since January 1, 2000, in Texas were \$4.60/GJ (in 2001 dollars) with a standard deviation of \$1.15/GJ, and \$4.70/GJ in California with a standard deviation of \$1.74/GJ. These are asymmetric distributions; for example, the mode monthly natural gas price in California was \$5.52/GJ. Therefore, prices of \$6-8/GJ are likely in the short run, given the price of crude oil (WTI) has averaged more than \$8/GJ throughout 2005, and natural gas prices follow oil prices. With these prices, the average cost of hydrogen would be between \$11.50/GJ and \$14.50/GJ. At a natural gas price of \$10/GJ, the average cost of hydrogen would be about \$17.50/GJ. This would represent a doubling of the price of natural gas in the U.S. since 2000, would increase the price of electricity, and would have profound effects on the economy generally and on the petrochemical industry specifically.

4 Data can be found at these web sites: (1) West Texas Intermediate Crude Oil Spot Price at <http://tonto.eia.doe.gov/dnav/pet/hist/rwtcM.htm> (2) City Gate Natural Gas Price in Texas at <http://tonto.eia.doe.gov/dnav/ng/hist/n3050tx3m.htm>, and (3) City Gate Natural Gas Price in California at <http://tonto.eia.doe.gov/dnav/ng/hist/n3050ca3m.htm>. These prices are converted to 2001 \$/GJ.

The demand for hydrogen in the petroleum and petrochemical sector should continue to grow. Although the merchant hydrogen market might not grow at 10% per year forever, new pipeline hydrogen production capacity could be fully employed in the foreseeable future as long it has an average cost of less than \$15/GJ. (This ignores the cost of a hydrogen pipeline and the cost of CO₂ emissions or sequestration from SMR, which must be addressed in a more complete analysis.)

Estimating the cost of electricity and hydrogen from a Modular Helium Reactor

Estimates of the cost of producing hydrogen with the MHR have been published previously [8,11,12,13]. The cost estimates were carried out assuming that the process adopted for hydrogen production is the sulphur-iodine (S-I) technology (a technology selected after an extensive search [9, 11]). S-I is a possible technology for producing hydrogen with high-temperature nuclear heat, but has not been demonstrated at an industrial scale. S-I hydrogen production involves a multi-phase, three-step process in which water, sulphur dioxide, and iodine are reacted to release hydrogen and oxygen, while recycling iodine and sulphur dioxide by decomposing sulphuric acid. The average cost of hydrogen calculated in those studies was as low as \$10/GJ.

However, estimating costs for future nuclear power technologies should adhere to a set of internationally agreed upon standards. In the following estimations, the methodology recommended by the EMWG/GIF is applied. A set of standards based on the International Atomic Energy Agency bid evaluation process has been developed by the EMWG: Cost Estimating Guidelines for Generation IV Nuclear Energy Systems. This document specifies a comprehensive set of cost estimating assumptions, such as the cost of capital and costs for each stage of the nuclear fuel cycle.⁵

Cost elements published previously [11,12,13], together with the characteristics of the MHR, have been used to estimate costs of hydrogen and electricity production by “Nth-of-a-Kind” units with the EMWG methodology. Table 3 presents the characteristics used in the EMWG spreadsheets to calculate costs for the GT-MHR producing electricity and the PH-MHR producing hydrogen; each plant is assumed to have 4 units. (The denomination PH-MHR refers to “Process Heat,” because hydrogen is produced by a high-temperature thermochemical process.)

Most of the operating data for the PH-MHR are the same as for the GT-MHR. GT-MHR has a capacity of 1.145 MWe. The “electricity-equivalent” size of the 4-unit plant is adjusted to reflect the lower efficiency of the PH-MHR: a 2.400 MWth plant operating at 42% efficiency would have an electric-equivalent rating of 1.008 MWe.

The S-I hydrogen facility was optimised for a heat source of 2.857 MWth. Because the 4-module MHR produces only 2.400 MWth, the facility size and costs are reduced linearly by 16%. Fuel costs are the same for the PH-MHR and the GT-MHR, but because of the lower electric-equivalent output, fuel costs per MWh-equivalent are higher for the PH-MHR.

Regarding reactor operating costs, “Assuming the O&M costs scale as the capital cost, the O&M cost is \$23,400,000 per year for the PH-MHR” [13, p. 3-37]. This cost has been converted to an all-staff equivalent of 292.5 persons at \$80,000 per person per year. (This technique overestimates staff sizes, but gives a rough evaluation of whether staff sizes are reasonable.) Also, the annual chemical facility O&M costs are estimated at \$48.775 M [13, Table 3-16], plus water costs of \$1.805M.

⁵ The EMWG Guidelines, developed within the GIF framework, will be released in the near future, together with software designed for estimating the economics of Generation IV nuclear energy systems.

Table 3. Characteristics of the GT-MHR and PH-MHR

Plant characteristics	GT-MHRx4	PH-MHRx4
Reactor type		
Net thermal capacity (MWth)	2 400	2 400
Net electric capacity (MWe/MWe equivalent)	1 145	1 008
Thermodynamic efficiency (%)	47.7	42
Capacity factor of the reactor (%)	90	90
Economic life (years)	40	40
Construction duration (years) for 4 units	5	5
*Contingency rate [from EMWG <i>Guidelines</i>] (%)	15	15
*Real discount rate for IDC & amortisation	10	10

Operation and Maintenance (O&M) costs		
On-site total O&M (without chemical facility costs, \$/year)	30.11	23.40
On-site staff count (all O&M expressed in persons per year)	376.4	292.5
On-site staffing cost, including benefits (\$/person)	80 000	80 000
Annual chemical facility costs (\$/year)	0	50.580

Fuel characteristics and costs		
*Enrichment level of feed (% U-235)	0.711	0.711
Enrichment plant tails assay (% U-235)	0.3	0.3
First core average enrichment level (% U-235)	15.5	15.5
Reload average enrichment level (% U-235)	15.5	15.5
Fuel elements in full core (number)	1 020	1 020
Fuel elements per reload (number)	510	510
Average time between refuelling (years)	1.5	1.5
*Cost of uranium ore (\$/lb)	12	12
*Cost of uranium ore (\$/kg)	31.2	31.2
*Cost of conversion from U ₃ O ₈ to UF ₆ (\$/kgU)	6	6
*Cost of enrichment (\$/SWU)	100	100
Cost of fuel fabrication (\$/kgHM) (implied from total fuel cost)	5 756	5 756
*Cost of once-through waste disposal (\$/MWh)	1	1

* *Data from the EMWG Guidelines*

Table 4 presents the direct construction costs for the two plants. Equipment costs must be adjusted to account for hydrogen production: these costs include the intermediate heat exchanger (\$56 M), reactor-process piping (\$38 M), primary helium circulator (\$33 M), and intermediate loop circulator (\$22 M) (for a total of \$149 M). These costs are added to Account 22. On the other hand, 84% of the “Fixed Capital Investment” of the S-I hydrogen production facility (\$571.531M x 0.84 = \$480 M) in account 23’ (Chemical Facility) replaces account 23 (Turbine-Generator). Also, the initial chemical inventory (primarily iodine) is equal to \$114.8 M x 0.84 = \$96 M. (Although there is an implicit assumption in [13] that all iodine is recycled, this assumption is challenged in [14].)

Table 4. Direct construction cost for 4-unit GT-MHR and PH-MHR (M\$) [13]

Account	GT-MHR	PH-MHR
21 Buildings, structures & improvements on site	132	132
22 Reactor plant equipment & HX equipment	443	403
23 Turbine-Generator	91	–
23' Chemical Facility	–	480
24 Electrical equipment	62	50
25 Water intake and heat rejection plant	33	–
26 Miscellaneous plant equipment	28	28
27 Special materials (including chemicals)	–	96
20 Capitalised direct costs	790	1 190

Adjustments made, compared to previous studies, include (1) contingency rate, (2) discount rate, and (3) decontamination and decommissioning (D&D) costs. Table 5 shows the total capital costs for both plants, highlighting adjustments made. First, the contingency rate is increased to 15% and applied to both the reactor and chemical facility.⁶ Given that the S-I process has not been proven at an industrial scale, a 15% contingency is less than what EPRI Technology Assessment Guidelines would suggest. (The contingency could be doubled to 30% given the state of S-I technology; see discussion in [15].) Second, the real amortisation and IDC rate is increased to 10% and applied to all initial capital costs, including the chemical facility, initial chemical inventory, and first fuel core. (Replacement fuel is levelized over the economic life of the plant.) Third, the D&D costs were estimated at \$263 M and \$204 M respectively for GT-MHR and PH-MHR for 4 units, following the EMWG Guidelines (assuming the S-I facility does not require decontamination).

Table 5. Nth-of-a-Kind total construction cost for 4-unit GT-MHR and PH-MHR (M\$)

Account	GT-MHR	GT-MHR adjusted	PH-MHR	PH-MHR adjusted
Capitalised Direct Costs (Account 20)	790	790	1 190	1 190
Indirects, Owners' costs (Accounts 30,40)	275	275	214	214
First Fuel Load (Account 56)	180	180	180	180
Total Contingency (Accounts 29,39,49,59)	53	187	41	237
<i>Contingency Rate</i>	<i>4%</i>	<i>15%</i>	<i>3%</i>	<i>15%</i>
Interest During Construction (Account 62) <i>5 years for 4 units, real IDC rate = 10%</i>	129	345	167	439
D&D costs (from EMWG Guidelines)	0	263	0	204
Total Capitalised Cost plus first fuel load	1 426	1 775	1 792	2 260
Specific Capital Cost for 4-unit plant (\$/kWe)	1 245	1 550	1 777	2 242

⁶ Although contingency appears to have been added to the “Fixed Capital Investment” in [13, Table 13-3] under the item “Contingency” and Fee, the contingency and fee are equal to 18% of the “Total Bare Module Cost with Adders”. This is nearly equal to the indirect rate (“Fee”) for reactor construction (17.3%). Therefore, contingency could be as low as 0.7%, if indirect costs for the chemical facility are equal to those for the reactor.

Table 6 presents the results of the levelised cost calculations for a 40-year economic life. The annual production of 201.982 tonnes of hydrogen per year (6.2 M m³/day) is from [13, Table 3-16]. The cost of hydrogen is \$12.58/GJ under the assumptions in [13], with a Capital Recovery Factor (CRF) of 10.5%. With the cost of the first fuel core and a real CRF of 10.23%, the cost is \$15.11/GJ (see last column, last line in Table 6).

Table 6. Levelised Cost for General Atomics 4-unit MHR

	GT-MHR	GT-MHR adjusted	PH-MHR*	PH-MHR* adjusted
Capital Recovery Factor	10.50%	10.23%	10.50%	10.23%
Capital Cost (\$/MWh)	16.15	20.10	21.29	29.08
Fuel Cycle Cost (\$/MWh)	7.40	7.40	8.27	8.27
O&M Cost (\$/MWh)	3.34	3.34	9.31	9.31
D&D Cost (\$/MWh)	0.00	0.07	0.00	0.06
Cost of electricity (\$/MWh)	26.89	30.91		
Cost of H2 (\$/kg)			1.53	1.84
Cost of H2 (\$/GJ)			12.58	15.11

* *The PH-MHR cost (\$/MWh) is expressed in MWh equivalence*

With the EMWG Guidelines' adjustments, the cost of hydrogen increases to \$15.11/GJ, which in [13] is between the values of \$13.90/GJ for a CRF of 12.5% and \$16.50/GJ for a CRF of 16.5%. A reasonable range of a state-of-the-art MHR with the S-I technology is \$12-\$16/GJ. Therefore, the PH-MHR might be able to compete in the pipeline hydrogen market with high natural gas prices. The next section calculates whether the GT-MHR or PH-MHR would be more competitive in their respective markets.

Cost comparison of GT-MR versus PH-MHR as function of the price of natural gas

As can be seen from Table 6, the projected cost of electricity for the GT-MHR is about \$31/MWh. This cost can be compared to the projected cost of electricity from an "Advanced Combustion Turbine" (Combined Cycle Gas Turbine, CCGT) [16, Table 38]. (The analysis in this section follows [17].)

The levelised unit electricity cost for CCGT using natural gas can be calculated following [18]. The USDOE-EIA Annual Energy Outlook 2005 [16] assumes an overnight construction cost of \$374/kWe (including a contingency of 5%) and a construction time of two years. With a real discount rate of 10% (i.e., a 10.23% CFR), a capacity factor of 80%, and a plant economic life of 40 years, the levelised capital cost is \$6/MWh. With variable O&M costs of \$2.80/MWh, fixed O&M costs of \$9.31/kWe, and an 80% capacity factor, O&M costs are \$4.13/MWh. Finally, with a heat rate of 8.550 Btu/kWh and a natural gas price of \$6/GJ (as assumed above), the levelised fuel costs are \$54.38/MWh. Without including dismantling or salvage value of the CCGT, the average levelised cost is about \$64.50/MWh, as shown in Table 7. (This is an average cost; it does not necessarily represent wholesale market prices; and it does not include transmission and distribution charges.)

Table 7. Levelised Cost for MHR, SMR, and CCGT with \$6/GJ natural gas

	Gas CCGT & SMR	Nuclear		Δ [Gas-Nuclear]
		GT-MHR adjusted	PH-MHR adjusted	
CCGT				
Capital Cost (\$/MWh)	6.00	20.10	29.08	
Fuel Cycle Cost (\$/MWh)	54.38	7.40	8.27	
O&M Cost (\$/MWh)	4.13	3.34	9.31	
D&D Cost (\$/MWh)	0.00	0.07	0.06	
Levelised electricity cost (\$/MWh)	64.51	30.91		+ 33.60
SMR				
Levelised H ₂ cost (\$/kg)	1.41		1.84	- 0.43
Levelised H₂ cost (\$/GJ)	11.55		15.11	- 3.56

In Table 7 the difference between the average cost of electricity for the GT-MHR and the CCGT is about \$33.60/MWh. If the CCGT sets the price of electricity, much of this cost difference represents profit potential to the GT-MHR owner. With an annual output of about 9,000 GWh per year, this represents a cost difference of about \$300 M per year. On the other hand, at \$6/GJ for natural gas, the cost of producing hydrogen with the PH-MHR is higher by \$3.56/GJ than the cost of producing hydrogen with SMR. (A carbon emission fee could be this high, allowing PH-MHR technology to compete with SMR.⁷ Further, at all positive values for the price of natural gas, the GT-MHR is more competitive than the PH-MHR. (This does not examine the carbon savings of each technology.)

Concluding Remarks

The market potential for nuclear technology grows as the price of natural gas rises following the increasing price of oil. World energy markets are calling for new energy sources faster than anyone imagined one year ago: who then would have forecast \$65 per barrel for crude oil in mid-2005? In addition, many countries are implementing or considering policy measures to address global climate change. This enhances the attractiveness of carbon-free options, such as nuclear energy.

Any economic analysis today comparing nuclear energy versus fossil fuels must be revisited if and when carbon values are added to the cost of technologies emitting greenhouse gases. However, the comparisons presented in the paper highlight significant differences between the competitiveness of nuclear energy for generating electricity and for producing hydrogen by thermochemical processes.

⁷ Future research will determine how carbon dioxide emission charges will influence both (1) hydrogen production using natural gas and SMR, and (2) electricity production using natural gas with CCGT. Other research will investigate how the cost of low and high temperature electrolysis and the cost of hydrogen storage, transmission, and distribution will influence the competitive balance between the GT-MHR and the PH-MHR.

Within the limitations of the analysis, this paper's calculations show that advanced nuclear energy systems are more likely to compete successfully in electricity markets than in hypothetical hydrogen markets. This finding is not surprising, recognising that the nuclear industry benefits from several decades of industrial experience and learning with nuclear power plants dedicated to electricity generation (and with direct-cycle turbine-generator technologies), while nuclear hydrogen production is at an early stage of technology preparedness.

Given the limited resources to develop new nuclear energy systems and given lead times and investments necessary to implement the hydrogen transmission and distribution infrastructure, the analysis here suggests that it might be wise to emphasise the design and development of advanced nuclear systems aimed at minimising the cost of electricity with commercial potential within one decade, i.e., to invest in the development of "Generation III+" technologies.

Research on high-temperature thermochemical hydrogen production techniques and very high temperature reactors should continue, while policy measures to encourage the implementation of hydrogen infrastructure would progressively lead to the development of hydrogen distribution networks, hydrogen end-use devices (e.g., fuel-cell vehicles), and the "hydrogen economy."

REFERENCES

- [1] Science, 13 August 2004. <http://www.sciencemag.org/content/vol305/issue5686/>
- [2] Rogner, H.H. and Scott, D.S. (2001), Building Sustainable Energy Systems: The role of Nuclear-derived Hydrogen, in Nuclear Production of Hydrogen, OECD/NEA, ISBN 92-64-18696-4
- [3] Forsberg, C.W., P.F. Peterson, and D.F. Williams (2005). "Liquid-Salt Cooling for Advanced High-Temperature Reactors," proceedings of ICAPP'05, Seoul, Korea (May 15-19).
- [4] Chemical Market Reporter (2005). "Hydrogen Market Strengthens as Demand Grows," (March 14): p. 18.
- [5] Chemical Market Reporter (2003). "Chemical Profile: Hydrogen," (Feb. 24): p. 43.
- [6] Chemical Market Reporter (2001). "Chemical Profile: Hydrogen," (Jan. 29): p. 37.
- [7] Padro, C.E.G. and V. Putsche (1999). Survey of the Economics of Hydrogen Technologies. National Renewable Energy Laboratory. <http://www.eere.energy.gov/hydrogenandfuelcells/pdfs/27079.pdf>
- [8] Crosbie, L.M. and D. Chapin (2003). "Hydrogen Production by Nuclear Heat." presented at GENES4/ANP2003, Kyoto, Japan (Sept. 15-19). http://www.mpr.com/pdf_files/hydrogen.pdf
- [9] Rothwell, G.S. (2004), "Texas Energy Price Variance," Texas Institute Advanced Chemical Technology and the U.S. Department of Energy (Nov.).
- [10] Rothwell, G.S. (2005), "Can the Modular Helium Reactor Compete in the Hydrogen Economy?" Stanford Institute for Economic Policy Research, Stanford University. <http://siepr.stanford.edu/home.html>
- [11] Brown, L.C., G.E. Besenbruch, K.R. Schultz, A.C. Marshall, S.K. Showalter, P.S. Pickard, J.F. Funk (2002), "Nuclear Production of Hydrogen Using Thermochemical Water-Splitting Cycles." presented at International Congress on Advanced Nuclear Power Plants (ICAPP), Embedded Topical Meeting, Hollywood, Florida (June 9-13).
- [12] Schultz, K.R. and General Atomics (2002), "High Efficiency Generation of Hydrogen Fuels Using Nuclear Energy," presented to Department of Energy, Nuclear Energy (Feb. 26). <http://www.eere.doe.gov/hydrogenandfuelcells/pdfs/32405d.pdf>
- [13] Brown, L.C., Gottfried E. Besenbruch, R.D. Lentsch, K.R. Schultz, J.E. Funk, P.S. Pickard, A.C. Marshall, and S.K. Showalter (2003). "High Efficiency Generation of Hydrogen Fuels Using Nuclear Power." GA-A24285. (General Atomics, June). <http://web.gat.com/pubs-ext/AnnSemiannETC/A24285.pdf>

- [14] Werkoff, F. (2003), "On the profitability of hydrogen production using nuclear power," presented at The First European Hydrogen Energy Conference, Grenoble, France (Sept. 2-5).
- [15] Rothwell, G.S. (2005), "Cost Contingency as the Standard Deviation of the Cost Estimate," *Cost Engineering* 47 (7): 22-25 (July). <http://www.aacei.org/resources/costengineering.shtml>
- [16] U.S. DOE-EIA (2005), *Assumptions to the Annual Energy Outlook 2005*. [http://www.eia.doe.gov/oiaf/aeo/assumption/pdf/0554\(2004\).pdf](http://www.eia.doe.gov/oiaf/aeo/assumption/pdf/0554(2004).pdf)
- [17] Stewart, J., A. Lamont, and G.S. Rothwell (2001), "The Economic Feasibility of Small Modular Reactors," Lawrence Livermore National Laboratory (Nov.).
- [18] Rothwell, G.S. (2005), "Contingency in Levelized Capital Cost Estimation," *AACE International Annual Meeting Transactions*, June 25-29, 2005. <http://www.aacei.org/annualmeeting/abstracts.shtml>

This page intentionally left blank

FUTURE PLAN ON ENVIRONMENTALLY FRIENDLY HYDROGEN PRODUCTION BY NUCLEAR ENERGY

Shusaku Shiozawa, Masuro Ogawa and Ryutaro Hino

Japan Atomic Energy Agency (JAEA),

Oarai, Ibaraki, 311-1394, Japan

Abstract

It is universally recognised that hydrogen is one of the best energy media and its demand will increase greatly in the near future. However, since little hydrogen exists naturally, it is necessary to develop suitable technology to produce hydrogen without CO₂ emission from the view point of global environmental protection. Hydrogen production from water using nuclear energy, especially a high-temperature gas-cooled reactor (HTGR), is one of the most attractive solutions for environmental issue, because HTGR hydrogen production by water splitting methods such as the IS process etc. has a high potential to produce hydrogen effectively and economically.

This paper reviews, first, HTGR position in uranium economy and HTGR demands corresponding to future fuel-cell vehicle (FCV) market in Japan, and then surveys a HTGR hydrogen cycle coupled with a fast breeder reactor (FBR) fuel cycle. As for current nuclear power plant, it is necessary for us to consider the demand of natural uranium as a resources issue and the management of the high-level radioactive waste (HLW) as an environmental issue. The management of HLW is one of the key issues because HLW contains long-lived hazardous nuclides such as minor actinides (MAs) and long-lived fission products (FPs) whose radio-toxicity lasts for millions of years. The HTGR hydrogen cycle coupled with the FBR fuel cycle is an appropriate solution to mitigate the above issue; HTGR could be operated with the MOx fuel using plutonium bred by FBR, and FBR could burn off MAs. Then, HTGR can supply high-temperature heat to the IS process. This coupling of the HTGR hydrogen cycle with the FBR fuel cycle could offer an effective synergy to accomplish an environmentally friendly fuel-hydrogen production by water splitting cycle.

Introduction

It is universally admitted that hydrogen is one of the best energy media and its demand will increase greatly in the near future. However, since little hydrogen exists naturally, it is necessary to develop suitable technology to produce hydrogen without CO₂ emission from the view point of global environmental protection. Hydrogen production from water using nuclear energy, especially a high-temperature gas-cooled reactor (HTGR), is one of the most attractive solutions for environmental issue, because HTGR hydrogen production by water splitting methods such as the IS process, has a high possibility to produce hydrogen effectively and economically.

This paper reviews HTGR demands corresponding to future fuel-cell vehicle (FCV) market in Japan, and surveys a HTGR hydrogen cycle coupled with a fast breeder reactor (FBR) fuel cycle. Also, this paper introduces our activity on the HTGR hydrogen production system conducted at the Japan Atomic Energy Agency (JAEA).

HTGR Demands for Hydrogen Production

Until now, hydrogen is being used as raw materials of chemical products such as nitrogenous fertiliser, but hardly used as an energy carrier like electricity. However, in the near future hydrogen will be used as clean energy carrier for fuel cells to generate electricity, because hydrogen can significantly contribute to reduce greenhouse gas emissions and fuel cells have been rapidly developed in the world. Research and development (R&D) of fuel cell vehicles and stationary power generators are being carried out all over the world as shown in Figure 1.

Figure 1. Hydrogen Economy

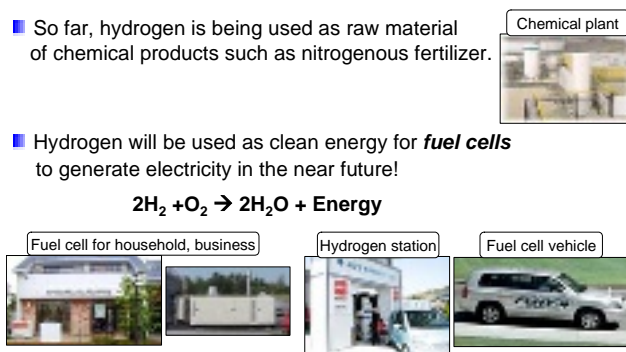
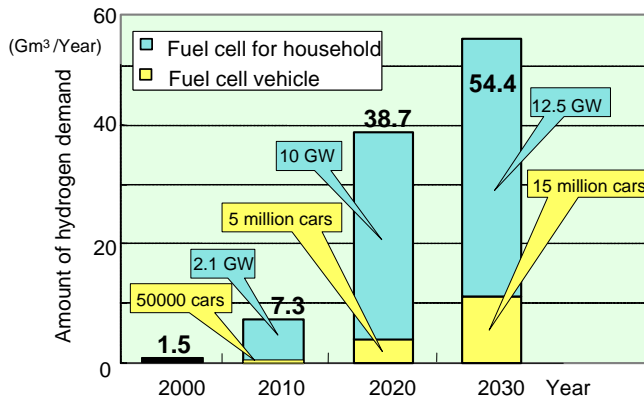


Figure 2 shows the introduction target of FCVs and HTGRs. The number of vehicles in Japan is about 75 million at present and there is not a substantial increase of vehicles in the future, considering the change of the population. Hydrogen demand was only 1.5 Gm³ in fiscal 2000 in Japan. The government of Japan is planning to introduce 5 million of fuel cell vehicles by 2020 and 15 million of fuel cell vehicles by 2030 (1).

Figure 2. Future Demands of Hydrogen



Hydrogen must be produced from raw materials and energy since hydrogen exists scarcely in the nature. Fossil resources of natural gas, oil and coal and water are used as the raw materials as shown in Figure 3. Combustion heat or electricity is used as the energy. A conventional and economical hydrogen production process in industry is mainly a steam reforming of methane (natural gas), which emits a large amount of carbon dioxide. On the other hand, by using nuclear energy or natural energy, hydrogen can be produced from water with electrolysis without emission of carbon dioxide. The cost of hydrogen produced with electrolysis greatly depends on the cost of electricity, which is generally not inexpensive because electricity is secondary energy so called energy carrier. A thermochemical water splitting method by using high temperature nuclear heat has a high potential to produce hydrogen effectively and economically.

Figure 3. Methods of Hydrogen Production

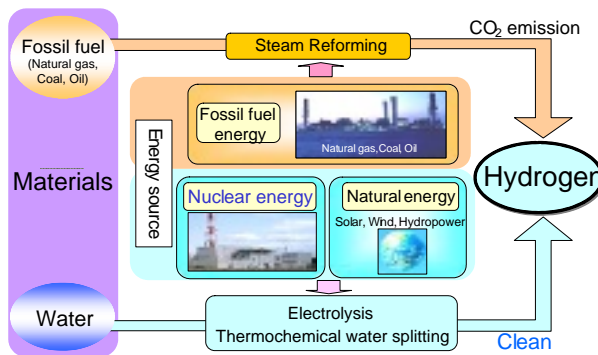


Figure 4 shows a site areas necessary for photovoltaic cell and windmill to supply electricity to one hydrogen station (2). Here, the hydrogen station produces hydrogen at a rate of $300\text{m}^3/\text{h}$ by using water electrolysis with electrolysis efficiency of 75%. Then the hydrogen station is necessary for 1 300kW of electricity and the site area of 0.1ha ($1\ 000\ \text{m}^2 = 40\text{m} \times 25\text{m}$).

Figure 4. Necessary Site Area for Supplying Hydrogen to One H₂-Station

Facility for energy conversion	Site area necessary to produce hydrogen of 300m ³ /h at one small H ₂ -station of 0.1ha (=40m x 25m)	
Photovoltaic cells	6-10 ha 60-100 times area of H ₂ -station	
Windmills Two large windmills (75-88 m blade-diameter)	30 ha 300 times area of H ₂ -station	
HTGR Thermal output of 600MW	6 ha for about 270 H ₂ -stations	

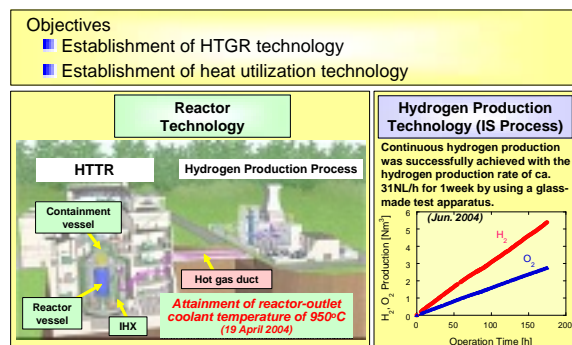
Height: 100 m

To generate 1 300kW of electricity, necessary area of photovoltaic cells is up to 10ha (100 000m²), and that of windmills with up to 88 m blade-diameter working under the wind speed of 5m/s to 7m/s is even greater than that of photovoltaic cells, up to 30ha. In contrast, atomic power, especially one HTGR with a thermal power of 600 MW, whose site area is about 6 ha, can provide electricity for about 270 H₂-stations.

HTTR Project

JAEA constructed a high-temperature gas cooled reactor named High-Temperature Engineering Test Reactor (HTTR) at the O-arai Research and Development Center. The HTTR is a graphite-moderated and helium gas-cooled reactor with 30 MW of thermal power, which is the first HTGR in Japan. We are proceeding the project using the HTTR. Figure 5 shows an overview of the HTTR project. The HTTR project mainly consists of following two objectives: establishments of HTGR technology and heat utilization technology.

Figure 5. Research and Development at JAEA



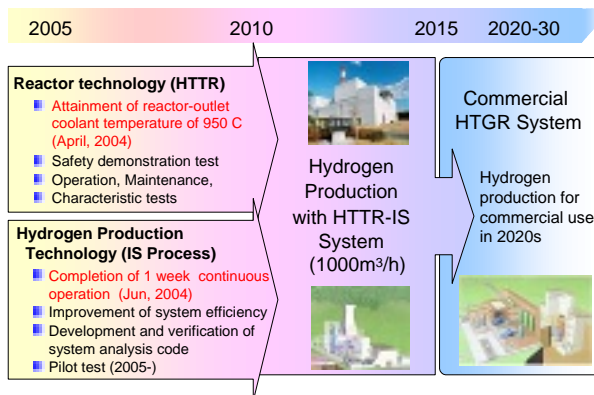
Under these objectives, JAEA is carrying out R&D on reactor technology by using the HTTR and on hydrogen production technology of the IS process.

Helium gas of the HTTR coolant is circulated under a pressure of 4 MPa, and through an intermediate heat exchanger, high temperature heat is transferred to the hydrogen production process as shown in Figure 5. The first criticality of the HTTR was achieved in 1998, and the full power operation of 30 MW was attained in 2001. Then, the reactor outlet temperature was 850°C. Safety demonstration tests have been conducted since 2002. In April 2004, we conducted first high-temperature operation of 950°C (3).

As for the hydrogen production technology, we have developed the IS process step by step. After verification of the theory of the IS process in 1997 with a lab-scale apparatus at a hydrogen production rate of 1 L/h (4), further tests have been conducted by using a bench-scale test apparatus made of glass. In June 2004, continuous hydrogen production was successfully achieved with a hydrogen production rate of about 31 L/h for 1 week (5) as shown in Figure 5.

Figure 6 shows our plan. According to the HTTR project, HTTR is being operated to accumulate the HTGR operation experience and to prepare the safety and maintenance database. Operational and test results obtained with the HTTR can contribute to the R&D programme of HTGR development in other countries: USA, France and others.

Figure 6. JAEA's Plan



R&D of hydrogen production is also successfully proceeded: improvement of system efficiency, and development, verification of system analysis code etc. Also, a pilot test program to produce hydrogen at a rate of 30m³/h by using the IS process (6) will be started in the 2nd half fiscal year of 2005.

We do hope that our activity shall lead to realising commercial HTGR system through the hydrogen production test with the HTTR-IS system (hydrogen production rate of 1000m³/h)

Future Plants for Hydrogen Production

It is said that hydrogen demand is gradually increasing at a primary stage by 2010, and would grow by 2020, then would widely and rapidly expand after 2020 (1) as shown in Figure 7. Until 2020 of the growth stage, hydrogen is produced with existing methods such as steam reforming from fossil fuels, purification of by-product gas generated in steel works and electrolysis at a hydrogen station. In order to meet a large demand of hydrogen at the matured stage after 2020, technologies of HTGR hydrogen and coal reforming hydrogen are expected to be developed. In the coal reforming, technology for carbon dioxide sequestration should be developed (1). In addition, renewable energy hydrogen would share specific demand of hydrogen. Thus, a hydrogen production system with a HTGR that can produce a large amount of hydrogen is one of most promising systems in the future hydrogen economy. (See Figure 1)

Figure 7. Future Plants for Hydrogen Production

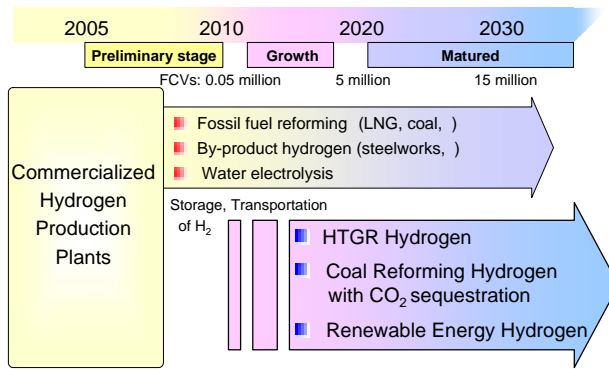
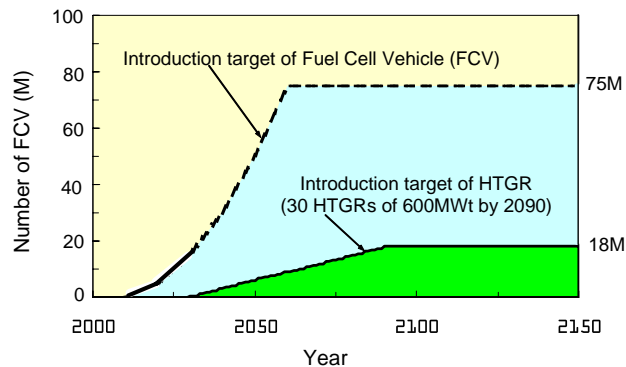


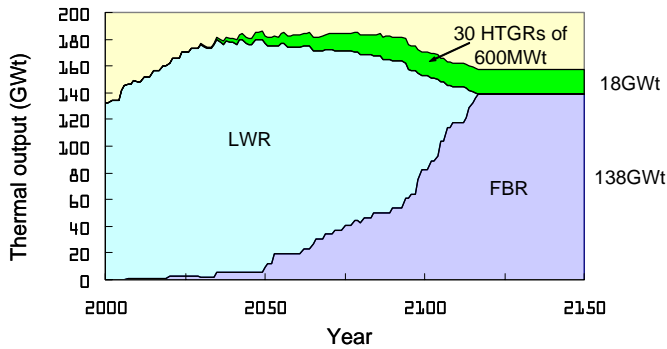
Figure 8 shows the introduction target of FCVs as shown in Figure 2, that is, 50,000 by 2010, 5 million by 2020 and 15 million by 2030 as shown by a solid and dotted lines. In this case, future introduction target of FCVs is set at in 75 million cars, which is present total number of cars in Japan. One 600 MW thermal HTGR can supply hydrogen for 0.6 million FCVs. Therefore 30 HTGRs can supply hydrogen for 18 million, that is about 24% of the total number of FCVs.

Figure 8. Introduction Target of FCV and HTGR



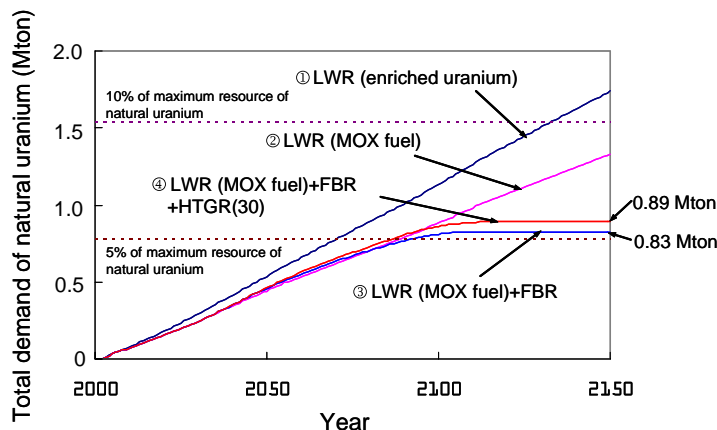
In Japan, commercial fast breeder reactors (FBRs) will be introduced from 2050 in earnest to replace light-water reactors (LWRs). Figure 9 shows the composition of the nuclear power plants in future, which assumes that the thermal output will be 138 GWt and then electricity demand 58 GWe, considering the change of the population and the growth of other power generation such as fuel cells. At around 2120, all the LWR power plants will be completely replaced by the FBR power plants. Commercial HTGRs of 600 MWt will be introduced from 2030 for supplying hydrogen to meet great demand of hydrogen. 30 HTGRs are assumed to be constructed for the hydrogen production as shown in Figure 8. Then, it is assumed to construct a new HTGR every 2 years until 2090.

Figure 9. Composition of Nuclear Plant on Thermal Output



The total demand of natural uranium from 2000 to 2150 is shown in Figure 10. Lines 1 and 2 shown in Figure 10 indicate the total demand of natural uranium necessary for LWRs using the enriched uranium fuel without fuel reprocessing and the reprocessed fuels (the MOX fuels), respectively. It is clear that the fuel reprocessing is effective for reducing the demand of natural uranium.

Figure 10. Total Demand of Natural Uranium by 2150

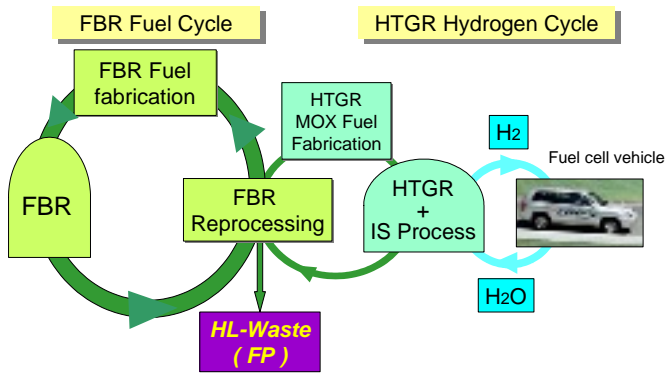


Line 3 is the case where FBRs are introduced from 2050. Then, LWRs are assumed to be operated with the MOX fuel, and to be replaced with FBR (a breeder factor of 1.16) after their life time of 60 years. As shown by line 3, we will need little natural uranium from around 2110, and the total demand of natural uranium from 2000 will be up to 0.83 million tons at the most.

Line 4 shows the case introducing HTGRs from 2030 into the case shown by line 3. After replaced all LWRs by FBRs, 30 HTGRs of 600 MW thermal output can be operated using the MOX fuel. It is assumed to construct a new HTGR every 2 years until 2090 as mentioned above. Then, HTGRs will use enriched uranium fuels by 2110 and use MOX fuels, so that the total demand will increase up to 0.89 million tons, which is only 7% increase compared with line 3.

Figure 11 shows the future status of the nuclear and the hydrogen production plants. The FBR fuel cycle is one of the best ways to mitigate the resources and the environmental issues. The issue of natural uranium can be solved by the FBR fuel cycle, and then HTGRs will be operated with the MOX fuel using plutonium bred by FBR. As for the high level radioactive waste, the load to environment can be significantly reduced by burning off the minor actinides with FBR.

Figure 11. FBR Fuel and HTGR Hydrogen



Hydrogen production from water using nuclear energy is one of the solutions promising for reducing CO₂ emission from the viewpoint of the global warming issue. Especially, HTGR has a possibility to effectively and economically produce hydrogen with water splitting methods such as the IS process, compared with other type nuclear reactors. In the future, we hope to realise the system on environmentally friendly hydrogen production by combination of FBR, HTGR and the IS process.

Concluding Remarks

Japan should have diverse resources to produce hydrogen for national energy security, because Japan has little domestic resources. HTGR hydrogen production plant is one of the most promising systems in the near future around 2020 or later. JAEA welcome you for joining HTTR Project to realise the HTGR hydrogen production.

REFERENCES

- [1] NEDO, Research on Scenario towards Hydrogen Society (FY2003-FY2004) Final Report, March, 2005.
- [2] M. Oagwa and S. Shiozawa, Evaluation of Hydrogen Production System with High Temperature Gas-cooled Reactor, GENES4/ANP2003, Paper 1055 (2003).
- [3] T. Iyoku, *et al.*, HTTR Test Program towards Coupling with the IS Process, 3rd Information Exchange Meeting on the Nuclear Production of Hydrogen, October 5-7, 2005, Oarai, JAEA.
- [4] H. Nakajima, *et al.*, A study on a closed-cycle hydrogen production by thermochemical water-splitting IS process, Proc. 7th Int. Conf. Nucl. Eng. (ICONE-7), ICONE-7104 (1999).
- [5] S. Kubo, *et al.*, A demonstration study on a closed-cycle hydrogen production by thermochemical water-splitting Iodine-Sulfur process, Nucl. Eng. Des., Vol.233, pp.347-354 (2004).
- [6] A. Terada, *et al.*, Development program of hydrogen production by thermochemical water splitting IS process, Proc. 13th Int. Conf. Nucl. Eng. (ICONE-13), ICONE13-50183 (2005).

This page intentionally left blank

SESSION II

THE STATUS OF NUCLEAR HYDROGEN RESEARCH AND DEVELOPMENT EFFORTS AROUND THE GLOBE

Chairs: M. Methnani, W.A. Summers

This page intentionally left blank

RESEARCH AND DEVELOPMENT FOR NUCLEAR PRODUCTION OF HYDROGEN IN JAPAN

Masao Hori

Nuclear Systems Association, Japan

Shusaku Shiozawa

Japan Atomic Energy Research Institute*

Abstract

The measures toward Hydrogen Energy Society are described in the “Basic Energy Plan” (October 2003), in which nuclear hydrogen production is expected as a process which suppresses carbon dioxide emission to the utmost and is independent from fossil fuels expenditure. Producing hydrogen using nuclear energy has the merits of sustainable bulk supply capability and high energy density leading to energy security, as well as the advantageous environmental effect.

For nuclear hydrogen production, Japan Atomic Energy Research Institute has been developing both the high temperature gas-cooled reactor and the iodine-sulfur thermochemical process. Various other processes for nuclear hydrogen production are being proposed, evaluated or studied by many organizations in Japan.

The research and development being conducted in Japan for nuclear hydrogen production are reviewed and summarised.

* The Japan Atomic energy Research Institute (JAERI) merged with the Japan Nuclear Cycle Development Institute (JNC) into the Japan Atomic Energy Agency (JAEA), on 1 October 2005, after submission of this paper.

1. Introduction

At present, hydrogen is mostly used for industrial processes and its production corresponds to about 2% of total final energy of the world. The demand for hydrogen will become an order of magnitude larger by the middle of the century as the use of hydrogen expands – not only for industrial processes but also to transportation. Eventually, hydrogen is expected to become one of the major energy carriers.

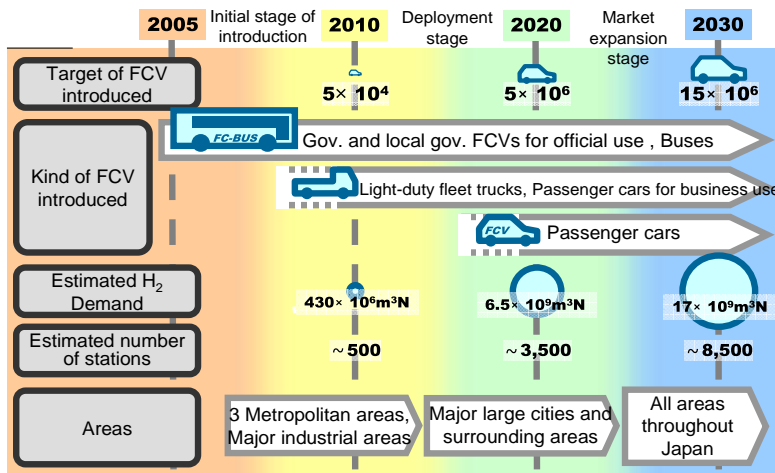
About 40% of the primary energy is currently converted to electricity in Japan. The ratio to be used for electricity production is forecasted to increase to more than half of total primary energy in the middle of century. Hydrogen is considered to be the most promising energy carrier for the non-electric purposes, which will use the remaining half of primary energy, because of its cleanliness and efficiency during conversion to power.

In Japan, the “WE-NET” hydrogen energy R&D project was conducted from 1993 to 2002 and the “Hydrogen Infra-Technology Program” is being conducted from 2003 to 2007, both supported by the Ministry of Economy, Trade and Industry (METI, former MITI).

The measures toward Hydrogen Energy Society are described in the “Basic Energy Plan” which was issued in October 2003 based on the Basic Energy Policy Bill. In the Plan, nuclear hydrogen production is expected as a process which suppresses CO₂ emission to the utmost and is independent from fossil fuels expenditure.

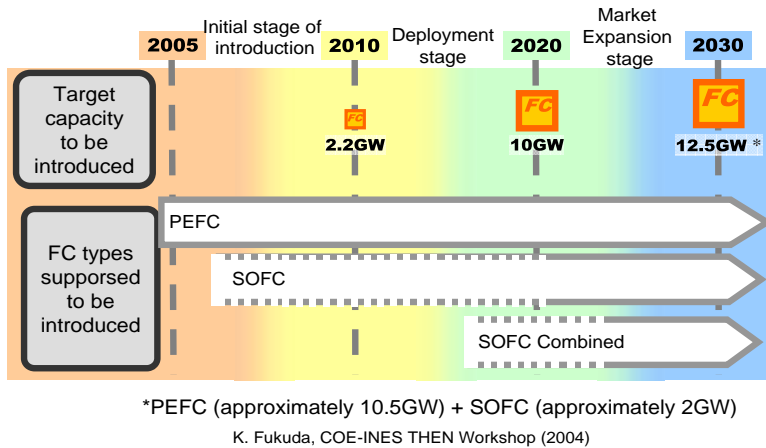
The scenarios on introduction of fuel cell vehicles (FCV) and stationary fuel cells were issued from the Advisory Panel of Agency for Natural Resource and Energy (ANRE) of METI, which are shown in Figure 1 and Figure 2.

Figure 1. Scenario of FCV Introduction and H₂ Infrastructure Construction
(ANRE Advisory Panel, March 2004, Supporting data provided by IAE)



K. Fukuda, COE-INES THEN Workshop (2004)

Figure 2. Scenario of Stationary FC Introduction
 (ANRE Advisory Panel, March 2004, Supporting data provided by IAE)

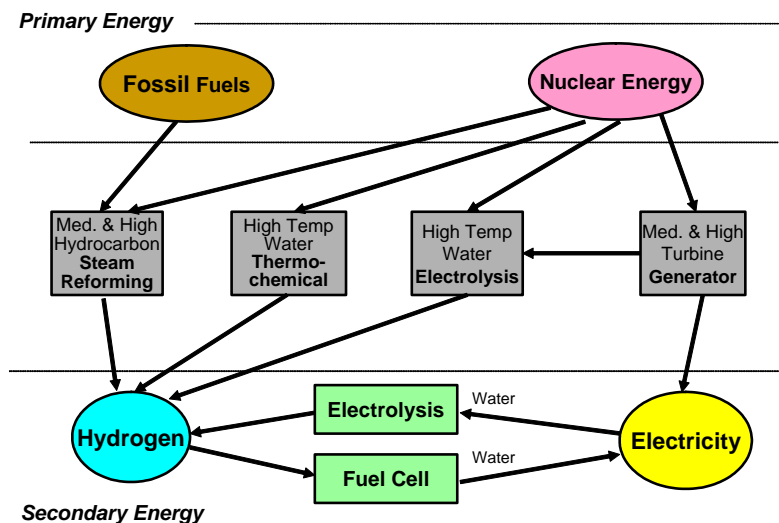


When producing hydrogen, as well as electricity, nuclear energy has the merits of sustainable bulk supply capability, advantageous environmental effects for minimising carbon dioxide emissions, and high energy density leading to energy security.

Nuclear energy will surely play an important role in Japan for the sustainable energy supply by producing hydrogen as well as generating electricity.

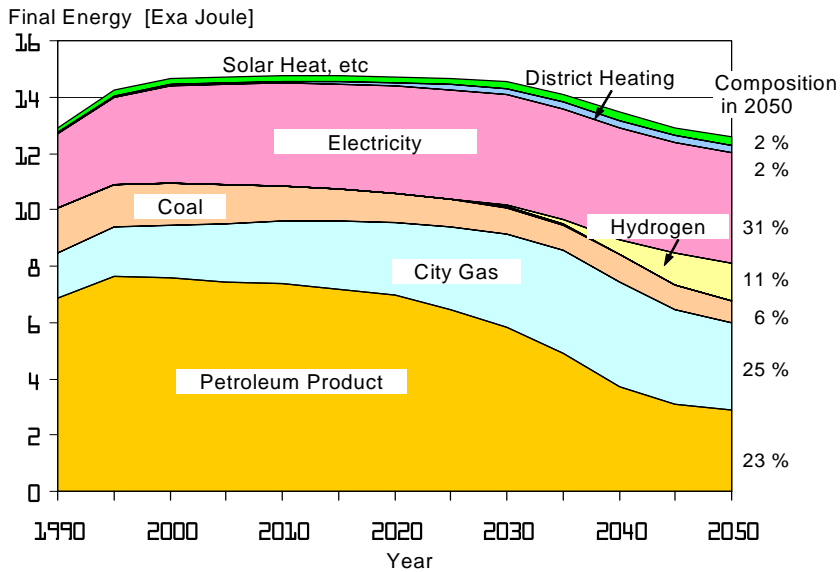
For the production of hydrogen using nuclear energy, many processes have been proposed. The leading processes now under research and development are electrolysis of water by nuclear electricity, high temperature electrolysis of steam by nuclear electricity and heat, thermochemical splitting of water by nuclear heat, and steam reforming of natural gas or other hydrocarbons by nuclear heat (Figure 3)

Figure 3. Methods for Hydrogen Production by Nuclear Energy



A recent report [1] from Japan Atomic Industrial Forum (JAIF) estimated that percentage of hydrogen energy carrier in the final energy in Japan in 2050 would be 11% as shown in Figure 4. About 2/3 of that hydrogen would be produced by the nuclear-heated steam methane reforming, because of its lowest production cost.

Figure 4. JAIF Estimate of Final Energy Consumption in Japan



The “zero-CO₂ emission” thermochemical process using nuclear heat would have sufficient possibilities to be adopted, if it becomes cost-competitive either by technical progress of the process development or by price rise of natural gas.

In the JAIF report, nuclear energy will supply 33% of primary energy in 2050, as compared to 13% of that in 2000.

2. Outline of Nuclear Hydrogen R&D Works in Japan

Varieties of research and development work on nuclear hydrogen production have been conducted in institutes, industries and universities in Japan. These works are classified in Table 1 by hydrogen production method, raw materials to be fed, types of energy used for the hydrogen production, types of typical nuclear reactor supplying energy for the hydrogen production, organizations working on the related subject.

Some of the recent R&D works in this table are described in the following sections, categorised by the working organisation.

Table 1 Nuclear Hydrogen Research and Development Works in Japan

Production method	Raw materials	Types of Energy Used For Producing Hydrogen	Types of Nuclear Reactor (Typical)	Organization working on related subjects
Electrolysis of water	Water	Electricity	LWR	CRIEPI Hitachi
High temp. electrolysis of steam	Water	Electricity + Heat (High temp.) or + Heat (Medium temp.)	VHTR SFR, SCWR	Toshiba
Thermochemical splitting of water	Water	Heat (High temp.)	VHTR	JAERI
Thermochemical splitting of water [Hybrid]	Water	Heat (High temp.) or Heat (Medium temp) + Electricity	VHTR SFR, SCWR	CRIEPI JNC
Steam reforming of methane	Natural gas + Water	Heat (High temp.)	VHTR	JAERI
Steam reforming of methane	Natural gas + Water	Heat (Medium temp.) [Membrane or sorption enhanced reaction]]	SFR, SCWR	MHI-ARTEC- TGC-NSA Tokyo Tech
Steam reforming of methane [On-board, sorption enhanced]	Synthesized Methane + water	Heat (High temp) [Regeneration of absorber] [Recycling of carbon]	VHTR	Tokyo Tech
Steam reforming of DME	Dimethyl ether + Water	Heat (Low temp.)	LWR	Toshiba
Radiocatalysis of water	Water	Gamma ray	Spent fuels	CRIEPI

Note: FES is working on VHTR development for hydrogen production.

Reactor type: LWR (Light Water Reactor), VHTR (Very High Temperature Gas Reactor), SFR (Sodium Fast Reactor), SCWR (Supercritical Water Reactor).

Organisation: CRIEPI (Central Research Institute of Electric Power Industry), Hitachi (Hitachi Ltd), Toshiba (Toshiba Corporation), FES (Fuji Electric Systems Co.), JNC (Japan Nuclear Cycle Development Institute), JAERI (Japan Atomic Energy Research Institute), MHI (Mitsubishi Heavy Industries, Ltd), ARTEC (Advanced Reactor Technology Co.), TGC (Tokyo Gas Co.), NSA (Nuclear Systems Association), Tokyo Tech (Tokyo Institute of Technology).

3. R&D in Japan Atomic Energy Research Institute

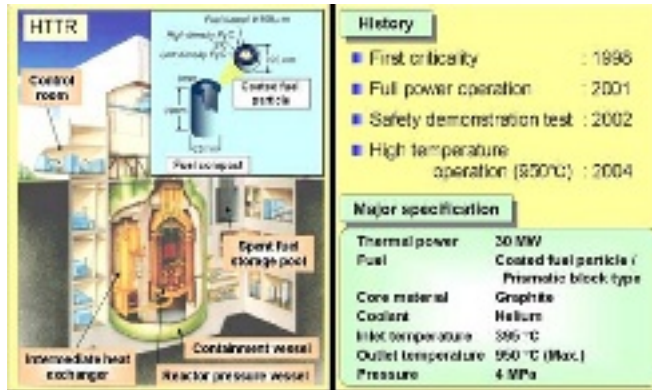
The Japan Atomic Energy Research Institute (JAERI) constructed a high-temperature gas cooled reactor named High-Temperature Engineering Test Reactor (HTTR) at the Oarai Research Establishment. JAERI has been conducting the HTTR project aiming to establish HTGR technology and the heat utilisation technology. To accomplish these goals, R&D on the following subjects has been carried out: (1) HTGR technology using the HTTR, (2) system integration technology for connecting hydrogen production processes to HTGR, and (3) thermochemical IS process for hydrogen production.

HTGR technology

Figure 5 shows the structure and history of the HTTR. The HTTR, the first HTGR in Japan, is a graphite-moderated and helium gas-cooled reactor with 30 MW of thermal power. The core is composed of graphite prismatic blocks, and the fuel element of the HTTR is a so-called pin-in-block type. Fuel is cylindrical graphite compact. Tri-isotropic (TRISO)-coated fuel particles with UO₂ kernel are dispersed in the graphite compact. Enrichment of ²³⁵U is 3-10 (average 6) wt%. Helium gas is

circulated under the pressure of 4 MPa, and through the intermediate heat exchanger, high temperature heat is to be transferred to the hydrogen production process.

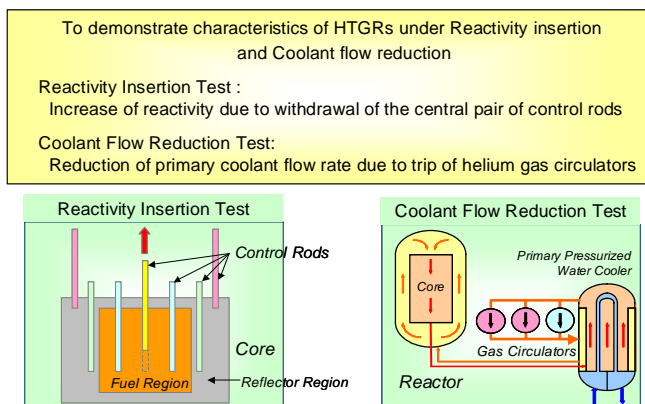
Figure 5. Overview and History of HTTR



The HTTR achieved the first criticality in 1998, and the full power operation was attained with reactor outlet helium temperature of 850°C in 2001. The first high-temperature operation of 950°C was conducted in April 2004. Since 2002, safety demonstration tests have been carried out to demonstrate the inherent safety of the HTGR. [2]

The safety demonstration tests in the HTTR are conducted to demonstrate an inherent safety feature, that is an excellent feature in “Shutdown” of the HTGRs, as well as to obtain the core and plant transient data for validation of safety analysis codes and for establishment of safety design and evaluation technologies of the HTGRs. The safety demonstration tests consist of “Reactivity insertion test – control rod withdrawal test” and “Coolant flow reduction test” as shown in Figure 6. In the control rod withdrawal test, a central pair of control rods is withdrawn and a reactivity insertion event is simulated. In the gas-circulators trip test, primary coolant flow rate is reduced to 67% and 33% of rated flow rate by running down one and two out of three gas-circulators at the Primary Pressurized Water Cooler without a reactor scram, respectively.

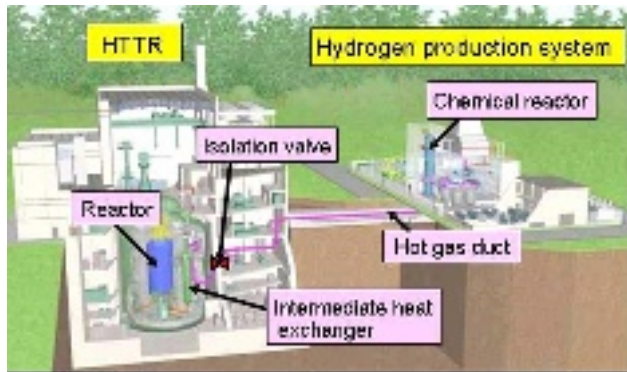
Figure 6. Safety Demonstration Tests by Using HTTR



(2) System integration technology

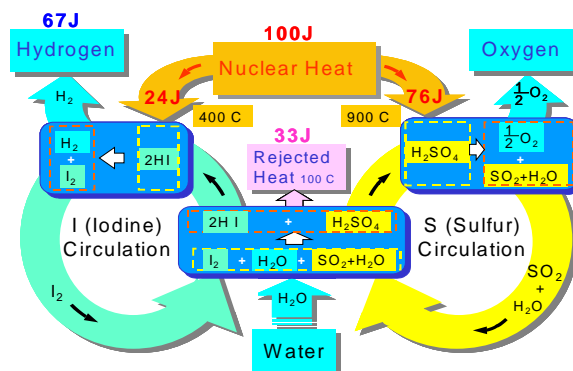
The system integration technology has been developed for the safe and economical connection between HTGR and the hydrogen production system. [3] Figure 7 shows an overview of the HTTR hydrogen production system. The heat generated in the reactor core is transferred to the secondary helium gas through the intermediate heat exchanger (IHX), and the secondary one is transported to the hydrogen production system passing through the hot gas duct. The R&D items of the system integration technology are as follows: a) the control technology to keep reactor operation against thermal disturbance caused by the hydrogen production system, b) estimation of tritium permeation from the reactor to produced hydrogen, c) the safety design against explosion of combustible gas and d) development of a high temperature isolation valve to separate reactor and hydrogen production systems in accidents.

Figure 7. Overview of HTTR Hydrogen Production System



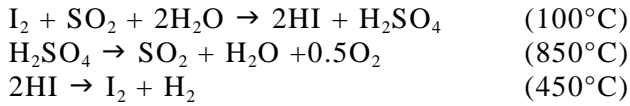
As for the control technology, JAERI proposed to use a steam generator (SG) as the thermal absorber, which is installed downstream the chemical reactor in the secondary helium gas loop, to mitigate temperature fluctuation of the secondary helium gas within an allowable value. By the simulation test with the mock-up test facility, it was confirmed that the SG could be used as the thermal absorber. The research of tritium permeation and the safety design against explosion for the IS process are under way. As for the high temperature isolation valve, a new coating material of the valve seat used over 900°C was developed and the seal performance of the angle type valve was confirmed to satisfy the design target with the 1/2 scale model of the HTTR hydrogen production system. However, the work to fit the valve seat was necessary to keep the seal performance after several times closing at a high temperature. The improvement of durability of the valve seat is the next target.

Figure 8. Reaction Scheme of IS Process



(3) Thermochemical IS process

Thermochemical water-splitting cycle is a method to make an effective use of the high temperature nuclear heat for hydrogen production. It works like a chemical engine to produce hydrogen from water by combining high temperature endothermic chemical reactions and low temperature exothermic chemical reactions, and the process accomplishes “zero-CO₂ emission”. JAERI has been conducting R&D on thermochemical hydrogen production by using an Iodine-Sulfur cycle (IS process). The IS process was proposed and has been actively studied by General Atomic Co, [4] and is composed of the following chemical reactions. Figure 8 shows the reaction scheme of the process.



JAERI has developed the IS process step by step. The theory of the IS process was verified in 1997 with a lab-scale apparatus at the hydrogen production rate of 1NL/h. Since 2000, engineering basic studies have been carried out as follows.

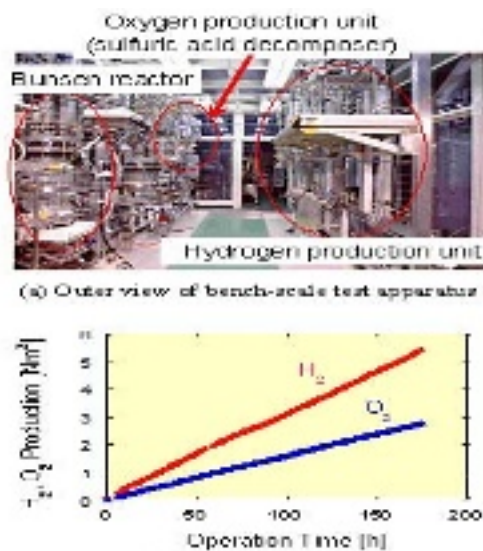
Closed-cycle continuous hydrogen production test using a bench-scale test apparatus made of glass. [5]

Study on alternative processing methods for the HI decomposition section.

Selection of corrosion-resistant materials and development of the concept for key components such as the H₂SO₄ vaporizer.

Figure 9 shows the bench-scale test apparatus and the test results. Continuous hydrogen production for one week was demonstrated with an automatic reaction control system, where the hydrogen production rate was about 31 NL/h [6].

Figure 9. Bench Scale Test Apparatus of IS Process and the Test Results



Based on the achievements, JAERI is planning to proceed to the next stage of IS process development, i.e. pilot test (Table 2). The pilot test will be carried out in the following fields, and is followed by HTTR-IS test to demonstrate nuclear hydrogen production.

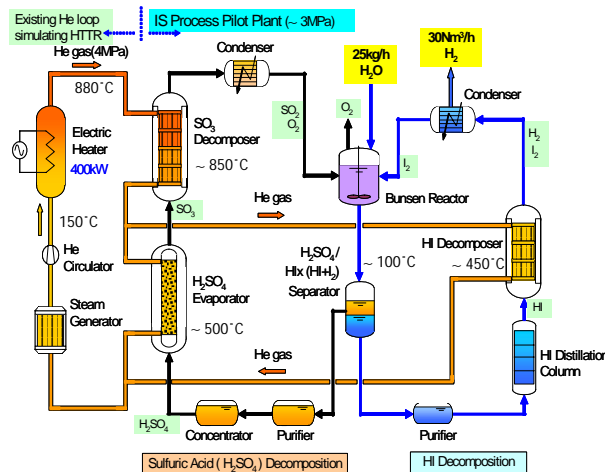
Table 2. Development Stages of IS Process

	Bench-scaled Test	Pilot Test	HTTR Test <i>nuclear demonstration</i>
Hydrogen production rate	~ 0.05 m ³ /h	~ 30 m ³ /h	~ 1000 m ³ /h
Heat supply	Electrical heater	Heat exchanger with helium gas (Electrical heater 0.4MW)	Heat exchanger with helium gas (Nuclear heat 10MW)
Material of chemical reactors	Glass	Industrial material (SiC, coated)	Industrial material
Pressure of chemical process	Atmospheric pressure	High pressure (up to 3MPa)	High pressure (up to 3MPa)
Time	FY 1999 -2004	FY2005 2010 (under planning)	FY 2009 2014 (under planning)

Pilot-scale hydrogen production test

A pilot test plant with hydrogen production capacity of about 30 Nm³/h is being designed. The pilot test plant will be made of industrial materials and operated using an electrically heated high-pressure helium gas as the heat source. Figure 10 shows a tentative scheme of the pilot test facility, which consists of the IS process pilot test plant and a helium gas circulation facility (He loop)

Figure 10. Flow Diagram Pilot Test Plant



Design and construction of the pilot test plant is planned to be carried out from FY2005 till FY2008, and the operation tests will be performed in the following two years.

Process improvement

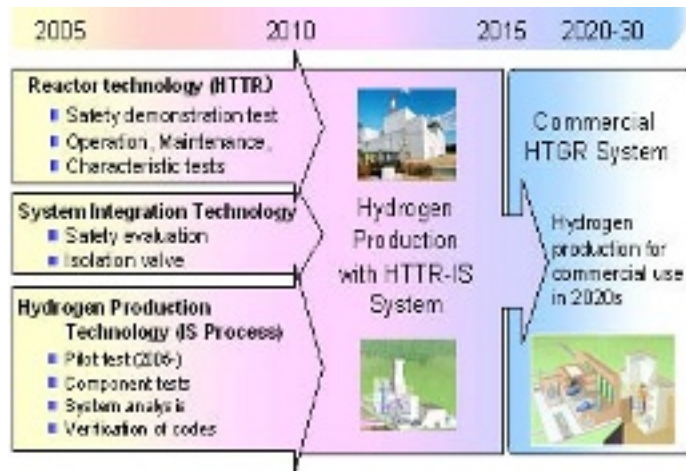
In order to develop IS process that exhibits competitive performance with other hydrogen production processes, R&D will be carried out in the fields of efficiency, materials, catalysts, etc.

Analytical code system for the IS process will be developed, which is to be used for designing a nuclear hydrogen production system using the HTTR (HTTR-IS process).

(4) Summary

Figure 11 summarises the JAERI's plan for the development of HTGR hydrogen production technology. JAERI are proceeding the HTTR project on reactor technology, system integration technology and hydrogen production technology to realise commercial HTGR system through the nuclear hydrogen production test with the HTTR-IS system.

Figure 11. JAERI's Plan for Development of HTGR Hydrogen Production Technology



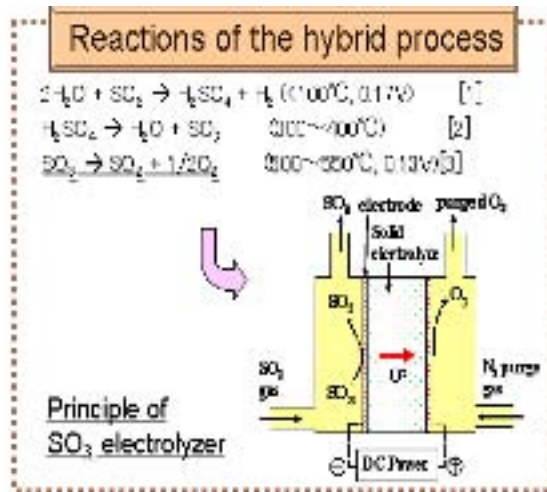
4. R&D in Other Organisations

4.1 Japan Nuclear Cycle Development Institute

A new thermochemical and electrolytic hybrid hydrogen production system in lower temperature range has been developed by the Japan Nuclear Cycle Development Institute (JNC) to achieve the hydrogen production from water by using the heat from a sodium cooled fast reactor (SFR) [7].

The system (Figure 12) is based on sulfuric acid (H_2SO_4) synthesis and decomposition process (the Westinghouse process) developed earlier. The sulfur trioxide (SO_3) decomposition process is facilitated by electrolysis with ionic oxygen conductive solid electrolyte to reduce the operation temperature $200^{\circ}C$ - $300^{\circ}C$ lower than the Westinghouse process.

Figure 12. Principles of JNC's Hybrid Process



The SO₃ splitting with the voltage lower than 0.5 V was confirmed at about 500°C, and theoretical thermal efficiency of the system based on chemical reactions was evaluated within the range of 35%~55% depending on the H₂SO₄ concentration and heat recovery.

A series of hydrogen production experiments to demonstrate the whole process were performed. Stable hydrogen and oxygen production was observed in the experiments, and maximum duration of the experiments was about 5 hours.

Furthermore, a hydrogen production plant with the thermochemical and electrolytic hybrid cycle has been designed and the hydrogen production efficiency has been evaluated. In this design, components in hydrogen production system are designed to be made of steels such as high Si cast iron which has good toughness against sulfuric acid. High hydrogen production efficiency of 42% (HHV) is achieved assuming development of high efficiency electrolysis.

4.2 Tokyo Institute of Technology

A new hydrogen carrier system for fuel cell vehicles, using on-board steam-methane reforming with calcium oxide for hydrogen production and regenerating/recycling of the reaction products by nuclear energy thus enabling zero CO₂ emission from the system, is being developed by Tokyo Institute of Technology (Tokyo Tech) [8].

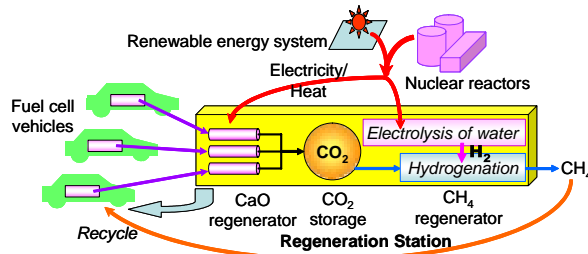
The adsorption enhanced reforming reaction is;



CO₂ generated from steam reforming is removed from the gas phase by CaO carbonation, thus producing H₂ gas without CO₂. CaCO₃ is de-carbonated and regenerated into CaO by nuclear heat around 800°C. Released CO₂ is recovered in a storage vessel, and is hydrogenated into methane using hydrogen produced by nuclear energy.

The system (Figure 13) consists of fuel cell vehicles using packages containing reforming materials of methane, CaO, and water, and a centralized package regeneration/recycling station using a nuclear reactor for energy input.

Figure 13. Concept of Nuclear Regenerating / Recycling of Hydrocarbon for Hydrogen Carrier System



Tokyo Tech also conducted a conceptual design study on a long-life multipurpose small-size fast reactor with a medium-temperature hydrogen production system using the sorption-enhanced steam-methane reforming reaction [9].

4.3 Central Research Institute of Electric Power Industries

A feasibility study on hydrogen production by PEM electrolysis with off-peak electricity was conducted in Central Research Institute of Electric Power Industries (CRIEPI) to evaluate the effect of availability and electric power transmission. [10]

The aim of using off-peak electricity is to reduce the electricity cost and to make the power plant investment more effective. However, in the case of off-peak electricity, the hydrogen production plant has a disadvantage of low availability. In the CRIEPI study, the hydrogen price at hydrogen stations for fuel-cell vehicles was assessed with a simple model. The model can take the plant size, plant availability and cost of electricity into account.

The results showed that hydrogen prices at hydrogen stations, produced at both on-site and off-site production plants, were approximately 64 yen/Nm³. In the case of off-peak electricity, the hydrogen price, produced at off-site production plants, can be decreased. On the other hand, it is difficult to decrease the hydrogen price, produced at on-site production plants, because of low availability.

Another study was conducted in CRIEPI on hydrogen cost at a hydrogen station in the introduction phase of hydrogen energy. The hydrogen stations in the introduction phase of hydrogen cars would be smaller than the present gasoline stations. Therefore, the hydrogen supply cost will be higher than the estimated price in the similar scale to the present gasoline stations. The hydrogen station assumed in the study deals with 450 Nm³ of hydrogen and 15 hydrogen cars in a day.

Hydrogen supply systems evaluated are COG (By-product hydrogen from cokes oven gas), on-site natural gas reforming, on-site PEM electrolysis and on-site alkaline electrolysis. The lowest hydrogen supply cost will be available at on-site natural gas reforming in the reference case. The hydrogen supply cost of each system will varies with the price of natural gas and electricity, the amount of hydrogen demand, the cost reduction of a production unit and hydrogen production efficiency. For making the electrolysis a main supplier of hydrogen, it is necessary to reduce the price of off-peak electricity and the cot of electrolysis units.

Also, CRIEPI has conducted to develop anode materials in the sulfur-based hybrid cycle (SHC) using high temperature gas-cooled reactors as a large-scale hydrogen production. [11] This SHC process consists of two main processes, i.e., the electrolysis of $\text{H}_2\text{SO}_3 + \text{H}_2\text{O} \rightarrow \text{H}_2 + \text{H}_2\text{SO}_4$ at

approximately 353K and the thermal decomposition of $\text{H}_2\text{SO}_4 \rightarrow \text{H}_2\text{O} + \text{SO}_2 + 1/2\text{O}_2$ at approximately 1123K. To realise the SHC process, it is necessary to develop inexpensive and high performance anode materials, which have the high corrosion resistance in the H_2SO_4 solution, the high electronic conductivity at 353K and the low anodic overpotential for the electrochemical reaction ($\text{H}_2\text{SO}_3 + \text{H}_2\text{O} \rightarrow \text{H}_2 + \text{H}_2\text{SO}_4$).

CRIEPI research group points out that there are some possibilities; Ti-based pyrochlores (chemical formula: $\text{A}_2\text{B}_2\text{O}_7$) and perovskites (chemical formula: ABO_3) are candidates as the anode materials because of their high corrosion resistance in the 50 weight% H_2SO_4 solution at 353K. Also, improvement techniques of electronic conductivity for the pyrochlores and perovskites have been developed.

CRIEPI also has been developing water splitting (hydrogen production) method by radiocatalysis, namely the radiation induced surface activation (RISA) phenomenon [12]. Gamma ray from spent fuels could be used as the energy source.

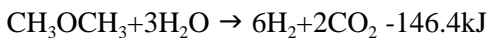
4.4 Toshiba Corporation

Toshiba proposed a hydrogen production method by nuclear-heated steam reforming of dimethyl ether (DME, CH_3OCH_3) for possible utilisation of low temperature nuclear heat from LWR, SCWR and SFR [13].

DME is usually synthesized by the partial oxidation of methane as follows;

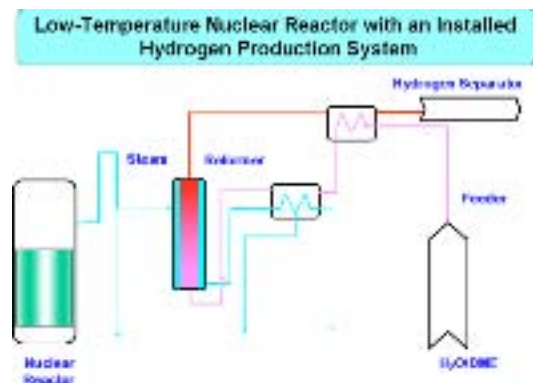


(DME has a future possibility to be synthesized from biomass without additional CO_2 emission.) The steam reforming reaction of DME is expressed by the following formulae;



This reforming reaction proceeds in the temperature range of 250~300°C, so the heat from LWR could be used for the reaction (Figure 14). It is suggested that, by combining this reforming process with turbine generator, the overall energy utilization efficiency of 75%~76% could be attained in the application to SFR and SCWR.

Figure 14. Toshiba's Concept of DME Steam Reforming



As for electrolytic hydrogen production using nuclear energy, Toshiba is engaged in research and development of high temperature steam electrolysis[14]. Some tubular electrolysis cell, which consists of Ni-YSZ cathode, YSZ electrolyte and LSC anode, is fabricated and electrolysis performance of those cells is tested and analyzed in cooperation with National Institute of Advanced Industrial Science and Technology (AIST). Toshiba is also developing the “cell stack”, which produces 1 Nm³H₂/hr or more, toward 2006.

4.4 Mitsubishi Heavy Industries

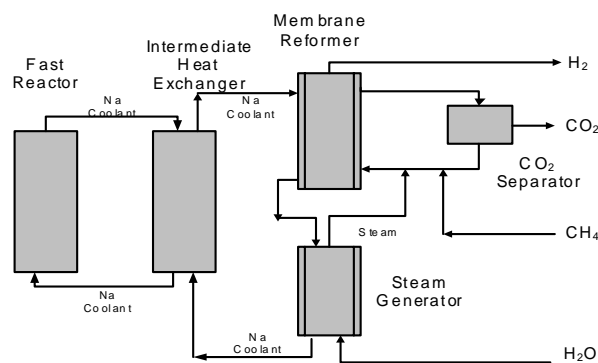
A concept for nuclear production of hydrogen, “FR-MR”, which combines sodium cooled fast reactors (SFR) with the membrane reformer technology, has been studied jointly by MHI, ARTEC, TGC and NSA [15].

The conventional steam methane reforming (SMR) requires high temperature around 800°C in the reforming process. The membrane reforming has only one stage of process under a non-equilibrium condition by removing hydrogen selectively through a palladium-alloy membrane tube. The steam reforming temperature can be decreased from 800°C to 550°C.

TGC has demonstrated the operation of membrane reformer at a hydrogen fueling station for FCV in downtown Tokyo in 2004-2005. The system performance, efficiency and long-term durability/reliability were confirmed by producing >99.99% hydrogen at 40 Nm³/h for more than 3 000 hours with hydrogen production efficiency of about 80% (HHV).

In the conceptual design, the nuclear plant is a type of SFR, mixed oxide fuel, sodium cooled with power output of 240 MWt for producing 200 000 Nm³/h. The schematic diagram of nuclear-heated recirculation-type membrane reformer is shown in Figure 15. The hydrogen production cost of this process is assessed to be competitive with those of the conventional, natural gas burning, steam methane reformer plants.

Figure 15. Concept of Fast Reactor Membrane Reformer

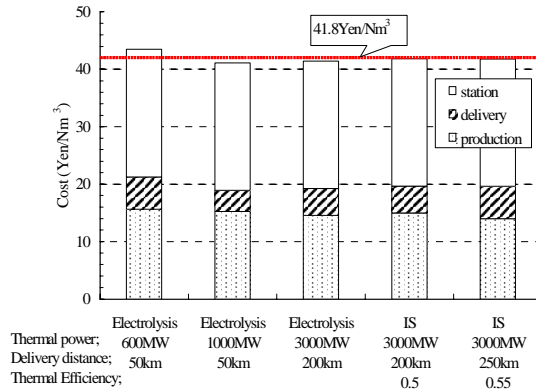


4.5 Hitachi

The cost of nuclear hydrogen supply for transportation usage, by thermochemical and electrical decomposition methods, was evaluated in order to compete with gasoline. The total cost for a centralized hydrogen production consists of production cost, delivery cost, and station cost [16].

Hydrogen production cost for the steam reforming of natural gas was evaluated to be 15.8 Yen/Nm³ including the CO₂ fixation cost. To meet this cost target, the heat cost of nuclear plants should be less than 1.29 Yen/kW_{th} assuming the corresponding power generation cost of 3 Yen/kW_h and the thermal efficiency of 0.43. The minimum conditions to meet the cost target were the thermal efficiency of 0.5 and the thermal nuclear power of 3 000 MW_t for the IS method, and the thermal nuclear power of 600 MW_t for the water electrolysis.

Figure 16. Hydrogen supply cost for the IS method and the water electrolysis



The target cost at the station to meet gasoline was calculated to be 41.8 Yen/Nm³ assuming a tax for volatile oil, gasoline cost of 100 Yen/L, and fuel cell vehicles with 2.5 times higher efficiency than gasoline cars. For the 3 000 MW_t nuclear plant, both the IS method and the water electrolysis method could provide hydrogen at the station when the transportation distance was less than 200 km. For the water electrolysis, hydrogen was economically provided under conditions where the thermal power of 1 000 MW_t and the transportation distance of 50 km were met. In any case, the reduction of the station costs is necessary to compete with gasoline because station costs make up more than 50% of the hydrogen supply cost. Higher operation temperature of nuclear plants is necessary to reduce the power generation cost and increase the power generation efficiency.

4.6 Fuji Electric Systems

VHTR (very high temperature gas cooled reactor) is essential for the high efficiency nuclear hydrogen production such as the thermochemical splitting of water and/or high temperature electrolysis of steam. Fuji Electric Systems (FES) is developing the VHTR system, with General Atomics (GA), based on the MHR (Modular Helium Reactor with the outlet gas temperature of 850°C for the gas-turbine electricity production) shown in Figure 17 [17].

Figure 17 Gas turbine modular helium reactor



Several potential modifications to the thermal hydraulic design of MHR core have been studied in order to produce helium at temperature up to 1 000°C while maintaining acceptable fuel performance and operating temperature for the reactor vessel and other component. These modifications include using lateral restraint and sealing mechanism to reduce the amount of coolant flow that bypass the fuel block cooling holes, alternative paths for routing the inlet flow to the top of the reactor vessel, and optimizing the flow distribution to increase the amount of coolant flow in the hotter channels.

Preliminary results show it should be possible to operate the MHR with a coolant outlet temperature of up to 1 000°C using nuclear-grade graphite fuel blocks, carbon-carbon composite materials for control rods and other internal reactor components, and existing coated-particle fuel technology with silicon carbide (SiC) and pyrolytic carbon coatings.

5. Research Forum on Nuclear Hydrogen Production

A research forum on nuclear hydrogen production, which is called “Nuclear Hydrogen Society”, was established in January 2001 in Japan. Presently, 47 members from 35 organisations are registered. The members are from such diversified fields as electric and gas utilities, nuclear plant design and manufacture, petroleum, iron making, chemical engineering, construction, merchandising, research institutes, and universities.

Research meetings are being held every 1.5 months for information exchange and discussion on nuclear hydrogen related progresses in Japan and worldwide. A review report (in Japanese) covering key issues on nuclear production of hydrogen was published in 2002.

Acknowledgement

The authors would like to express their appreciation to the following experts for compiling the nuclear hydrogen related activities conducted at various organisations in Japan; Ryutaro Hino (JAERI), Toshio Nakagiri and Yoshitaka Chikazawa (JNC), Hisashi Ninokata and Yukitaka Kato (Tokyo Tech), Yoshiyuki Asaoka and Masahiro Furuya (CRIEPI), Kimichika Fukushima and Shigeo Kasai (Toshiba), Shouji Uchida (ARTEC), Hidetoshi Karasawa (Hitachi), and Futoshi Okamoto (FES).

REFERENCES

- [1] Nuclear Reactor Development Committee, “Nuclear Vision 2050 – Vision and Roadmap” (in Japanese), Japan Atomic Industrial Forum (November, 2004).
- [2] S. Fujikawa, *et al.*, “Achievement of Reactor-Outlet Coolant Temperature of 950°C in HTTR,” *J. Nucl. Sci. Technol.*, 41[12], 1245 (2004).
- [3] Y. Inagaki, *et al.*, “Research and Development Program on HTTR Hydrogen Production System”, Proc. GENES4/ANP2003, Kyoto, Japan, Sep. 15-19, 2003, No.1062 (2003).
- [4] J.H. Norman *et al.*, “Thermochemical Water-Splitting Cycle, Bench-Scale Investigations, and Process Engineering”, General Atomic Report, GA-A 16713 (1982).
- [5] S. Kubo *et al.*, “A demonstration study on a closed-cycle hydrogen production by the thermochemical water-splitting iodine-sulfur process,” *Nucl. Eng. Des.*, 233, 347 (2004).
- [6] A. Terada *et al.*, “Development program of hydrogen production by thermochemical water splitting IS process,” Proc. 13th Int. Conf. Nucl. Eng. (ICONE13), Beijing, China, May 16-20, 2005, ICONE13-50183.
- [7] T. Nakagiri *et al.*, “Development of a New Thermochemical and Electrolytic Hybrid Hydrogen Production System for Sodium Cooled FBR”, ICONE13-50147, 13th International Conference on Nuclear Engineering, Beijing (May 2005).
- Y. Chikazawa *et al.*, “Conceptual Design of Hydrogen Production Plant with Thermochemical and Electrolytic Hybrid Method Using a Sodium Cooled Reactor”, ICAPP’05-5084, 2005 International Congress on Advances in Nuclear Power Plants, Seoul (May 2005).
- [8] Y. Kato, *et al.*, “Carbon dioxide zero-emission hydrogen carrier system for fuel cell vehicle”, *Chem. Eng. Res. Design*, 83(A7), pp. 900-904 (2005).
- [9] H. Ninokata *et al.*, “Long life Multipurpose Small Size Fast Reactor with Liquid Metallic-fueled Core”, *Progress in Nuclear Energy*, 37, No. 1-4, 299-306 (2000).
- A. Netchaev, *et al.*, “Safety Characteristics of the Multipurpose Fast Reactor (MPFR)”, *Annals of Nuclear Energy*, 28, 1717-1732 (2001).
- [10] Y. Asaoka., “Feasibility Study on Hydrogen Production with Off-Peak Electricity - Evaluation of the effects of availability and electric power transmission” CRIEPI Komae Research Laboratory Report (In Japanese) No. T02039 (April 2003).
- Y. Asaoka, “Hydrogen Station Model in the Introduction Phase of Hydrogen Energy and its Cost Assessment – Role of Hydrogen Production by Electrolysis” CRIEPI Komae Research Laboratory Report (In Japanese) No. T03070 (April 2004).

- [11] H. Kawamura, *et al.*, “Sulfur-based hybrid cycle for hydrogen production (Part 1) – Electrical conductivity and corrosion resistance of reduced $Gd_{2-x}Ti_2-yMyO_{7-\delta}$ (M=Cr,Mn,Fe,Co,Ni) anode by B-site doping”, Proceedings of 15th World Hydrogen Energy Conference, June (2004).
- M. Mori, *et al.*, “Sulfur-based hybrid cycle for hydrogen production (Part 2) - Electrical conductivity and corrosion resistance of reduced $Gd_{2-x}Ti_2-yMyO_{7-\delta}$ (M=Cr,Mn,Fe,Co,Ni) anode by B-site doping”, Proceedings of 15th World Hydrogen Energy Conference, June (2004).
- H. Kawamura, *et al.*, “Electrical Conductive Ceramic Anodes in Sulfur-based Hybrid Cycle for Hydrogen Production”, 1st Proceedings International Hydrogen Energy Congress and Exhibition IHEC 2005.
- [12] M. Furuya, “High Efficiency Hydrogen Production Technology Using Radiation Induced Surface Activation” (In Japanese) Nuclear Eye January 2003 (Nikkan Kogyo Shuppan).
- M. Furuya, *et al.*, “Development of High Efficiency Hybrid Hydrogen Production Method Using Radiocatalysis” (In Japanese) Proceedings of Atomic Energy Society of Japan, p.So-10, (2002).
- [13] K. Fukushima *et al.*, “Conceptual design of low-temperature hydrogen production and high-efficiency nuclear reactor technology”, JSME Int. J. B, Fluids Therm. Eng. 47, 340 (2004).
- K. Yamada, *et al.*, “Hydrogen Production with Steam Reforming of Dimethyl Ether at the Temperature Less Than 573 K”, in Proceedings of International Congress on Advances in Nuclear Power Plants, No. 5138 (2005).
- [14] A. Ozaki *et al.* “Nuclear Hydrogen Production Systems” (In Japanese) Toshiba Review Vol. 60, No. 2 p. 27 (2005).
- [15] M. Tashimo, *et al.*, “Advanced Design of Fast Reactor-Membrane Reformer (FR-MR)”, Proceedings of Second Information Exchange Meeting on Nuclear Production of Hydrogen, Argonne USA (2003).
- S. Uchida, *et al.*, “Concept of Advanced FR-MR”, 15th World Hydrogen Energy Conference, Paper No. 30D-08, Yokohama Japan (2004).
- [16] H. Karasawa, “Cost Evaluation for Centralized Hydrogen Production”, The First COE-INES International Symposium, INES-1, Tokyo, No. 35 (October 2004).
- [17] M. Richards, *et al.*, “Thermal Hydraulic Design of a Modular Helium Reactor core operating at 1000? Coolant Outlet Temperature”, Proceedings of NUTHOS-6 (2004).
- M. Richards, *et al.*, “The H2-MHR: Nuclear Hydrogen Production Using Modular Helium Reactor”, Proceedings of ICAPP05 (2005).

THE U.S. DEPARTMENT OF ENERGY RESEARCH AND DEVELOPMENT PROGRAMME ON HYDROGEN PRODUCTION USING NUCLEAR ENERGY

A. David Henderson and Amy Taylor
United States Department of Energy

Abstract

As part of the Hydrogen Fuel Initiative proposed by President George W. Bush in 2003, the Nuclear Hydrogen Initiative is developing technologies to provide large amounts of hydrogen without pollution or greenhouse gases. The Nuclear Hydrogen Initiative is a research and development program within the Department of Energy's Office of Nuclear Energy, Science and Technology that is using a series of successively larger-scale experiments to demonstrate the commercial-scale, economically-feasible production of hydrogen using nuclear energy.

Programme Organisation

The Department of Energy's (DOE) Office of Nuclear Energy, Science and Technology, under the leadership of Office of Energy Efficiency and Renewable Energy (EERE), is working with the other DOE Offices, Fossil Energy and Science, involved in the hydrogen fuel initiative to meet the President's hydrogen fuel goal. An integrated *Hydrogen Posture Plan* was issued by these offices, which outlines the roles of the various organisations as well as the hydrogen research being conducted within the various DOE offices.

The Nuclear Hydrogen Initiative (NHI) funds research and development activities to demonstrate nuclear-based hydrogen producing technologies, to study potential hydrogen production schemes, and to develop deployment alternatives to meet future needs for increased hydrogen consumption. The program collaborates with the Generation IV Nuclear Energy Systems Initiative (Gen IV) to study potential nuclear energy configurations and evaluate deployment scenarios to meet future needs for increased hydrogen consumption. High operating temperatures and improved efficiencies make several Gen IV systems ideal for producing hydrogen, particularly the very-high-temperature reactor (VHTR) because of its passive safety and high temperatures.

The research funded by NHI is conducted primarily at the national laboratories because of its pre-commercial nature; specifically at Argonne National Laboratory (ANL), Idaho National Laboratory (INL), Oak Ridge National Laboratory (ORNL), Sandia National Laboratories (SNL), and Savannah River National Laboratory (SRNL). To the maximum extent possible, DOE also works directly with industry. However, given the current state of the technology, industrial involvement has been limited. Extensive research on high-temperature materials and heat exchangers is being conducted at the University of Nevada, Las Vegas Research Foundation (UNLVRF) in conjunction with other program partners.

Hydrogen Production Methods

Hydrogen can be produced by splitting water into hydrogen and oxygen. However, the feasibility of emission-free, large-scale production of hydrogen from water is as yet unproven. There are four major technologies that can utilize nuclear energy to make hydrogen:

- **Steam Reforming.** Steam reformation of methane currently produces most (about 95%) of the hydrogen produced in the United States. This process is efficient but has the environmental draw back of producing large quantities of carbon dioxide as a by-product. In addition, valuable primary energy sources are consumed in this process thus doing little to reduce the United States' dependence on foreign energy sources. As a result, the NHI is not investigating any steam reforming applications associated with nuclear power.
- **Conventional Electrolysis.** The maximum environmental benefits of electrolysis are realised when a non-emitting technology, such as nuclear energy, is used to produce the electricity. However, there are inherent inefficiencies in producing hydrogen using electricity alone. DOE hopes to gain substantial increases in efficiency by directly using the heat from a nuclear reactor to produce hydrogen using steam electrolysis or thermochemical cycles.
- **Thermochemical water-splitting cycles (TC).** These processes offer the potential for high efficiency hydrogen production at large-scale production rates, but the technology is relatively immature. The NHI is dedicating a substantial portion of its funding to develop and

demonstrate the feasibility of high-temperature thermochemical water-splitting cycles. The highest priority cycles are the sulfur-based cycles (sulfur-iodine and hybrid sulfur).

- **High-temperature electrolysis (HTE).** HTE, or steam electrolysis, promises higher efficiencies than standard electrolysis, which is employed commercially today. The new high-temperature design involves many technical challenges, including the development of high-temperature materials and membranes. NHI will address these issues and demonstrate the feasibility of the high-temperature electrolysis of steam.

Current Research on Nuclear Methods

Research and development under the NHI focuses on the development of the high-temperature water splitting technologies that can be driven by advanced nuclear systems and on the underlying science supporting these advanced technologies. Investigating and demonstrating these nuclear-based systems will require advances in materials and systems technology to produce hydrogen using thermochemical cycles and high-temperature electrolysis such as high-temperature and corrosive resistant materials development and advanced chemical systems analysis. This programme will move through successively larger-scale experiments, namely laboratory-, pilot-, and engineering-scale.

Thermochemical Cycles

The NHI approach for developing high-temperature thermochemical cycles is to develop baseline cycles while also determining the feasibility of alternate cycles. The baseline thermochemical cycles being considered are the sulfur-iodine and hybrid sulfur cycles. Laboratory-scale experiments will be developed for these technologies, as will any additional cycles that are identified and show enough potential to justify that level of investment. The sulfur-iodine and hybrid sulfur cycles are both baseline cycles because they are the most promising mature cycles and potentially have different failure mechanisms.

Sulfur-iodine Cycle

The U.S. DOE research and development on the sulfur-iodine (S-I) Cycle is being done primarily in collaboration with the French Commissariat à l'Énergie Atomique (CEA) under an International Nuclear Energy Research Initiative (I-NERI) agreement. There is close coordination between the project participants in developing the three component reaction sections – the H_2SO_4 decomposition section, the HI decomposition section, and the Bunsen reaction. Each participant is designing and constructing their respective section, and is working to integrate them in a Sulfur-Iodine Integrated Laboratory-Scale Experiment. This experiment will be located at SNL and is expected to begin operation in late 2007 or early 2008.

Currently, the sulfuric acid boiler and decomposition components in preparation for integrated laboratory-scale experiments are being demonstrated. In 2005 the ambient pressure H_2SO_4 decomposer test bed experiments were completed, the flash distillation concentrator was designed, and high-pressure components for the component reaction tests were developed. At the same time laboratory-scale demonstrations of extractive and reactive distillation options for the HIx decomposition section were developed, enabling a decision on the best HI distillation process to use in the integrated laboratory-scale experiment. In France, the CEA has completed construction of the Bunsen reactor and supporting equipment and plans to begin testing it before it is integrated with the other two sections in 2007.

High-temperature inorganic membranes are being developed for use in the separation of SO₂ and O₂ from other chemical species in the high-temperature decomposition of H₂SO₄. This separation has the potential to shift the equilibrium of the reaction resulting in a potentially lower reaction temperature or increased process efficiency. This work leverages existing membrane technology and high-temperature materials expertise.

The S-I cycle requires numerous other chemical separations. Currently, liquid-liquid extraction and distillation are the primary processes being used. To make the S-I process economically feasible, and reduce recycle of water and iodine in the cycle, better separations processes are required. The use of membranes for dewatering process streams is being investigated. Most importantly, the removal of water from a mixture of water, elemental iodine, and hydriodic acid (HI) will be studied. Additional studies exploring the use of a membrane to concentrate sulfuric acid will be initiated in fiscal year 2006. Catalysts are also being developed that will be highly-active and stable in the harsh acidic environments and high temperatures encountered in the S-I cycle.

Hybrid Sulfur Cycle

The Hybrid Sulfur (HyS) thermochemical cycle task addresses the key technology issues involved in the development of a hybrid sulfur hydrogen production system – including the SO₂ – H₂O electrolyzer design, SO₂/O₂ separation, and the unique materials and process issues associated with the acid decomposition section. An electrolyser is being developed that can be used in conjunction with the sulfuric acid decomposition section being developed for the S-I cycle in a Hybrid Sulfur Integrated Laboratory-Scale Experiment.

Calcium-Bromine Cycle

The potential of the Calcium-Bromine (Ca-Br) cycle for hydrogen production is also being investigated. First, key technical issues must be addressed to determine the viability of calcium bromine cycles for nuclear hydrogen production. Two areas of research are currently under investigation: examination of cold plasma or electrolytic steps for the hydrogen generation step instead of the iron bromide/oxide reaction beds in the UT-3 cycle, and investigation of the feasibility of a continuous molten spray reactor approach for the HBr generation step.

Alternative Thermochemical Cycles

The Nuclear Hydrogen R&D Plan identifies several thermochemical cycles that have potential for either high efficiencies or operation at lower temperatures, but were not sufficiently investigated or documented to determine their applicability for NHI. It is anticipated that additional thermochemical cycles may also be identified as promising by NHI, EERE, or other research efforts. The intent of this task is to provide focus for the investigation of potentially promising thermochemical cycles for nuclear energy systems and determine whether further research or development is warranted. After the most promising cycles are identified, the NHI will coordinate with the private sector and DOE ultra-high temperature (solar) thermochemical cycle efforts to analyze and evaluate the potential application of those cycles with nuclear heat sources, including flowsheet analysis of selected cycles as an initial screening assessment of alternatives.

High-temperature Electrolysis

High-temperature electrolysis (HTE) is being developed as one of the baseline processes for nuclear hydrogen production. All HTE activities are coordinated with other DOE research activities on solid oxide fuel cell materials and technology development. HTE has the potential for higher efficiency than conventional electrolysis. The current focus of HTE R&D is on providing a technical basis for estimating efficiency improvements and on the development of an HTE design to provide the basis for cost projections.

Computational Fluid Dynamics (CFD) analyses of individual flow channels in a solid oxide electrolyzer cell are being used to model temperature, current density, and local hydrogen production. In 2004, the integrated performance of an HTE plant and the thermal optimisation of the plant through various component arrangements were modeled. In addition, solid oxide electrolyser cell electrode materials with improved durability in the variable environment of the electrolyser cell are currently being developed.

The programme is investigating key technical issues for the development of HTE for nuclear application and developing plans for experimental demonstration at the various scaling levels. Components for laboratory-scale experiments have been fabricated and button cell and stack experiments conducted to evaluate candidate electrolyser characteristics and performance.

Building on previous work, a high-temperature inorganic membrane for the separation of hydrogen from steam at the outlet conditions of the solid oxide electrolyser cells is being developed to improve the overall thermal optimisation of the plant. Current work includes the use of existing experimental data and steam hydrogen separations at temperatures and pressures that will permit extrapolation to HTE operating conditions.

Systems Interface and Support Systems

The NHI is developing hydrogen production technologies to be coupled with an advanced nuclear energy system being developed in parallel as part of the Generation IV Nuclear Energy Systems Initiative. The key research currently underway in this area is the analysis of the S-I and HTE heat exchanger requirements and analysis of the heat transfer medium. Analysis efforts in both interface areas are coordinated extensively with the efforts conducted by universities, national laboratories, industry, and other Federal programs.

A partnership between universities, private industry and national laboratories has been established to identify and test high temperature materials and designs for NHI heat exchangers and other system interface components. The work performed by this partnership will identify candidate materials, and perform corrosion and physical property tests necessary for NHI heat exchangers and process equipment needed for thermochemical cycles and high temperature electrolysis.

Path Forward

The NHI has defined an aggressive path to demonstrate hydrogen production from nuclear energy by 2017. The technical challenges to achieving this goal are significant, but the development of emission-free hydrogen production technologies is essential to the long-term viability of a hydrogen economy. Nuclear energy has the potential to play a major role in assuring a secure and environmentally sound source of transportation fuels. The fundamental challenge is to focus finite

research resources on those processes which have the highest probability of producing hydrogen at costs that are competitive with gasoline. Both thermochemical and high-temperature electrolysis methods have the potential to achieve this objective, and the small-scale experimental precursors to the integrated laboratory-scale experiments have operated successfully to date and continue to show promise for larger-scale systems.

Initially, a broader research effort involving laboratory-scale demonstrations and analytical evaluations is needed to provide a more consistent and complete assessment on which to base future R&D funding and scaling decisions. The NHI program will perform consistent and independent analyses of performance and costs to support the comparative assessments required for technology selection and scaling decisions, and establish effective interfaces with industry and international partners. The development of a portfolio of hydrogen production technologies, including nuclear energy technologies, is vital to strengthen the United States' energy, economic, and national security.

AN OVERVIEW OF THE CEA ROADMAP FOR HYDROGEN PRODUCTION

F. Le Naour
CEA, France

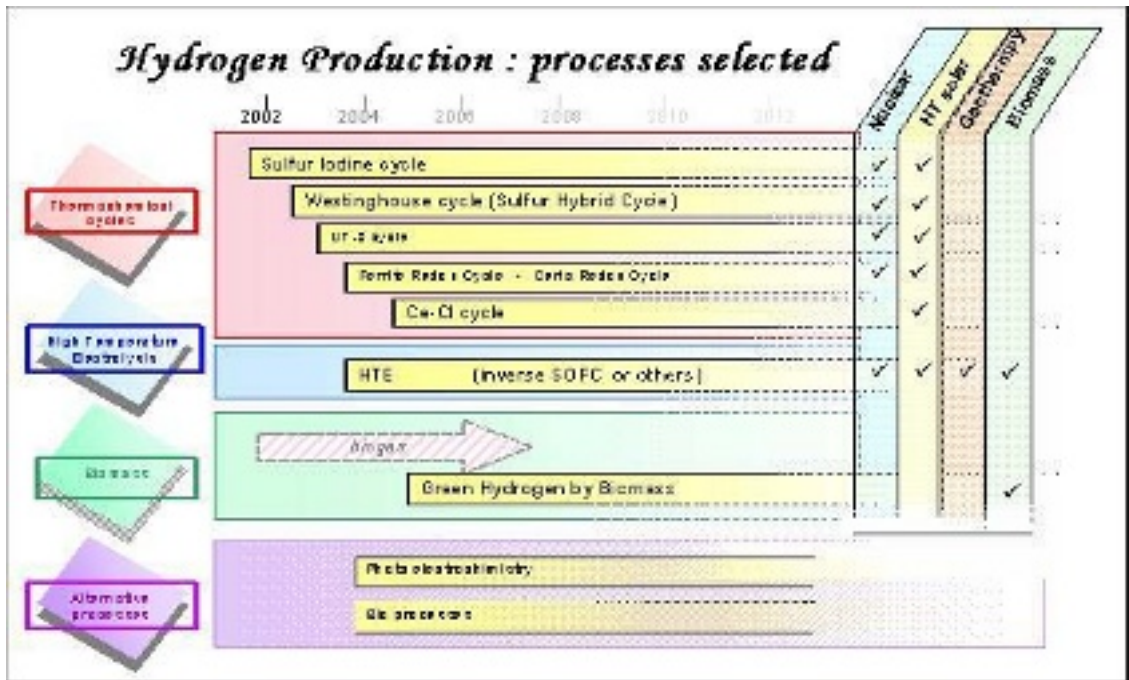
Abstract

Hydrogen is a most promising energy carrier to replace hydrocarbons as fuel sources, in particular for transport, with respect to lower greenhouse gases emissions. To provide massive hydrogen in a sustainable manner, the CEA has worked on high temperature free CO₂ processes, biomass decomposition and bioprocesses. This paper presents the status and future plan of research on CO₂ free processes, i.e. water splitting by high temperature electrolysis (HTE) or by thermochemical processes. Techno-economic analysis has been also performed to evaluate the feasibility of these technologies and partial conclusions are presented in this paper.

Introduction

To meet ever-increasing energy requirements and reduce emission of greenhouse gases (GHG), fuel sources to replace hydrocarbons have to be found. Hydrogen is currently the best way to reach this challenge. France profits from a clean electricity production in regards with the GHG emissions due to a strong nuclear policy. But transport is a very important polluting field and we have to develop solutions for cars, trucks and heavy transport. To provide hydrogen in urban areas, we need to find new technologies of massive production which are both non-polluting and sustainable.

In this context, the CEA has chosen to work on biomass decomposition, free CO₂ processes and bioprocesses. In this paper, we focus only on CO₂ free processes, i.e. on the splitting of water by high-temperature electrolysis or by thermochemical processes. These processes do rely on a high-temperature nuclear reactor, but can also be studied in relation with geothermic or solar sources of energy.



The main difficulty is to perform work necessary to choose the most promising processes without spreading the efforts too much. A roadmap with milestones needs to be established in order to assign the available resources onto a minimum number of processes. Before concluding the roadmap, work performed so far by CEA on thermochemical cycles and HTE, as well as on a techno-economic analysis, is presented.

Thermochemical Cycles

This is a large family of processes (over 1 300 cycles are listed) and our efforts should focus on the most promising ones and those it seems valid to couple with the nuclear reactors of the future.

The first subfamily is made up of the sulphur-based cycles, the two main ones being sulphur-iodine and Westinghouse (hybrid sulphur cycle).

The sulphur-iodine cycle, which consists of three chemical reactions, is currently the most frequently studied one and CEA research is mainly carried out in the framework of the international programme Generation IV, but also in the framework of the European STREP HYTECH. The teams from the Nuclear Energy Department are mainly in charge of studying and performing the Bunsen reaction (recomposition of HI and H₂SO₄), one of the bolts of this technology.

So many results were obtained up to 2005 that they cannot all be mentioned. We shall carry a particular lighting on the synthesis work on the efficiency criterion. This is a key parameter with a direct impact on the final cost of hydrogen and is therefore of prime importance in the comparative analysis of processes. The project team had to define 4 efficiency measurements taking account of progress in knowledge of the process. This is important because the choice of process is governed by prior comparison using values whose reliability depends on how far the work has progressed.

The two last years was marked by working diagram, the initial benchmark flowsheet. This result will enable the technological teams (chemical engineering at Marcoule, energy at Cadarache and materials at Saclay and Grenoble) to start working in on the optimisation of systems and components.

Alternative cycles are being evaluated for exploratory purposes at Marcoule and Saclay. Laboratory validation trials have been run, in particular on the UT3 cycle, which did not match the expectations announced in the literature, the ferrite redox cycle and, above all, the ceria-chloride cycle which, from the initial results, seems to promise good output. It is important to keep an activities of basic researches on these processes because we are not sure to be able to pass all the technological blockages on major cycles.

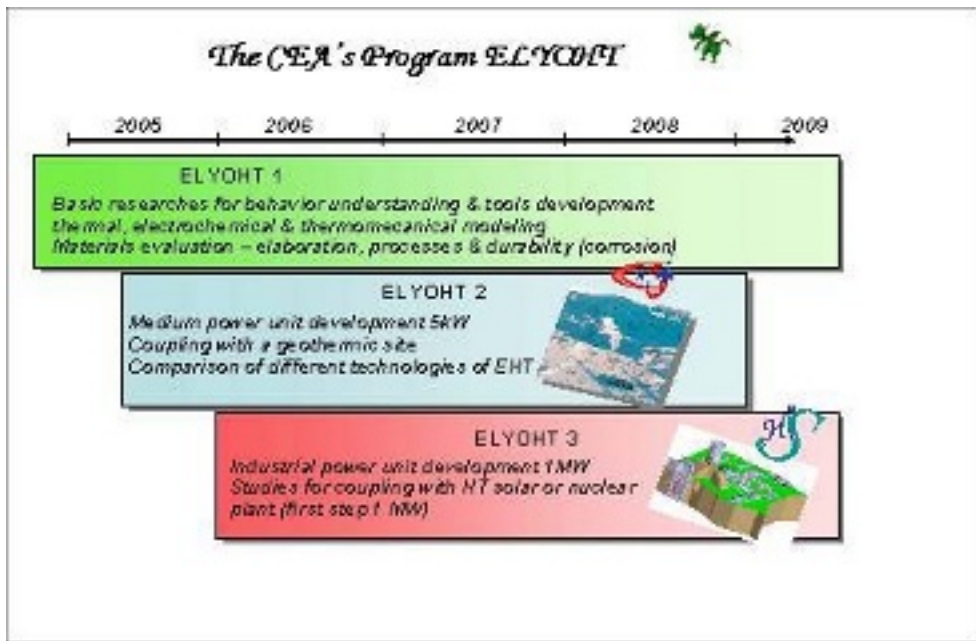
High-temperature Electrolysis (HTE)

Another process, derived from alkaline electrolysis widely used in industry, is high-temperature electrolysis. The efficiency of this process is increased by minimising ohmic losses. The source of heat can be a high-temperature nuclear reactor, a solar concentrator or a geothermic source.

The most widely researched technology today is that of the inverted SOFC cell, which is why most laboratories working on the topic use work done on SOFC. But research performed by Julich and at Dornier in Germany in the 1990s shows that the thermomechanical problems related to the use of ceramics will confine this technology to low power applications (<100kW).

The HTE problematic is now well formulated and give rise to an ambitious programme projected for the coming years. A group of SOFC experts met several times to evaluate the synergies and differences between the H T E and SOFC technologies and their discussions resulted in a ELYHOT programme, made up of three facets:

- ELYOHT 1 involves generic actions on technological models, measurements and building blocks (materials, architectures, test benches).
- ELYOHT 2 covers the design and production of a low power electrolyser (5kW) coupled, for example, with a geothermic source.
- ELYOHT 3, which should begin in 2006, covers the design and production of a high power electrolyser (1MW or more) which can be coupled to the HELITE high-temperature helium loop programmed by the Cadarache Nuclear Energy Department.



Techno-economic Analysis

For mass production of hydrogen, the most cost-effective and widely used process is currently the reforming of natural gas by water vapour. A production method using nuclear power, by high-temperature electrolysis or thermochemical cycles, would meet the requirements of sustainable development, both in resources and in polluting gas emissions. The technical feasibility of these solutions remains to be demonstrated, as does their economic feasibility.

To evaluate this feasibility, the techno-economic laboratory is working in collaboration with other CEA units in the framework of R&D projects, notably by using the operation draws they provide. It is highly involved in European projects: HyWays and its French version HyFrance, HYTECH and INNOHYP-CA and, with Iceland, in the Jules Verne project which is part of a collaboration between the CEA, the University of Iceland and the Icelandic New Energy Company.

Analysis performed up to now has led to the following partial conclusions:

- For high-temperature electrolysis, the operating method for the best energy yield does not seem to be the most cost-effective. The cost of the electrolyser could be a big amount of the cost of Hydrogen.
- For the sulphur-iodine cycle, the solutions for decomposition of sulphuric acid are satisfactory from an economic point of view but the current solutions of iodhydric acid decomposition require a very high power consumption in proportion. The conservation of iodine throughout its recirculation also seems a critical point in the process.

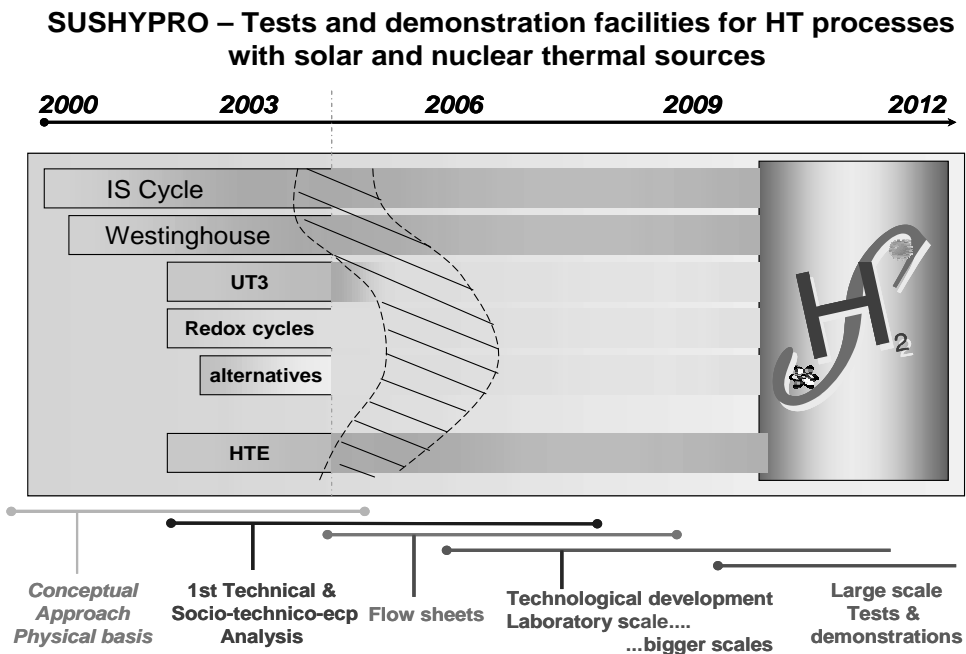
Proposed Roadmap

The level of knowledge on these different processes is not homogeneous. A strong effort has been done on IS cycle to be able to produce a small scale pilot for Bunsen loop in 2008. So we have now acquired a good vision of what could be a IS chemical plant and we are able to focus our researches on main technological blockages.

The results obtained today shows that we have to develop a parallel way on Westinghouse cycle (sulphur hybrid cycle). Some difficulties concerning the iodine loop justify that we engage works on this alternative process.

We have also to increase quickly the effort on HTE during the 3 or 5 next year in order to be able to compare and analyse these two or three major processes with the same level of knowledge. An interest of HTE compared with Thermochemical cycle is that we can begin by low power prototype (Some kW) and upgrade the technology up to 50 MW. Starting from SOFC technologies we can study very quickly the behaviour of new materials for HTE and proposed thermomechanical analysis in order to suggest different design able to be used at different level of power.

CEA is now associated in Europe with other famous research organisms CIEMAT in Spain and ENEA in Italy to built a R&D platform for massive H₂ production by HT processes. Named SUSHYPRO (sustainable hydrogen production), this platform aims to concentrate High Temperature facilities (HT solar, nuclear simulated loop). Associated with the main laboratories in charge of development of the different processes, this platform represents the convergent point for all the major processes in 2012. We will be able to test sub-systems or systems with a power of 1 to 10 thermal MW (100 kg H₂/h).



This page intentionally left blank

R&D EFFORT ON NUCLEAR HYDROGEN PRODUCTION TECHNOLOGY IN CHINA

Yuliang Sun, Jingming Xu, Zuoyi Zhang

Institute of Nuclear and New Energy Technology, Tsinghua University, Beijing, China

Abstract

To meet the target of social-economic development in China, both nuclear energy and secured supply of oil or its substitutes are of vital important roles in the Chinese primary energy supply mix from mid and long term point of view. A very active programme of developing high temperature gas-cooled reactors is being executed in China. A 10 MWth test reactor with spherical fuel elements was constructed in 2000 and is now under operation. A number of safety related experiments have been conducted with the test reactor facility. Research and development of direct cycle helium turbine technology is being carried out, and coupling a helium turbine system to the existing 10 MWth test reactor is foreseen. The industrial scale demonstration plant of modular HTGR design is being promoted. The overall hydrogen energy programmes are being discussed and defined. Regarding nuclear hydrogen R&D, laboratory scale research and experiments are being performed to study the process technologies of hydrogen production using nuclear process heat from HTGRs. Proposals of nuclear hydrogen R&D programme have been made to the central government and the programme is expected to start in the next Five-Year-Plan of China which begins from 2006.

Introduction

China has been experiencing continuously rapid social-economic development since 1980s. Continuing economical growth is expected for the coming decades. Secured increasing energy supply is one of the pre-conditions to support the continuing growth. There are a few key challenges in China's energy sector. Two of them are the environmental impact of energy production and consumption including the green-house gas emission issue, and the supply of sufficient, environmentally sound energy carriers to meet the dramatically increasing demand from the transportation sector and from the urbanisation process. To address and meet these challenges, a number of effective measures have to be taken. Among these measures, considerably increasing the application of nuclear energy is seen as practical and effective to substitute, on a large scale, for coal, on which there has been an over-dependency in China's primary energy mix. To find a substitute form of energy carrier for oil is, from mid and long terms point of view, of strategic importance to meet the energy demand of the transportation sector. Hydrogen is a promising energy carrier which could possibly help to address a number of key challenges such as environmental concern and secured energy supply. In such context, China is taking a very active approach to address the nuclear application issues and is starting a systematic approach to address the hydrogen issue.

In addition to the capacity installation of large scale water reactor based nuclear power plants, which is currently taking place and will continue to take place in the coming decades, a very active programme of developing high temperature gas-cooled reactors (HTGR) is being executed in China. A 10 MWth test reactor (HTR-10) with spherical fuel elements was constructed in 2000 and is now under operation. A number of safety related experiments have been conducted with the test reactor facility. Research and development of direct cycle helium turbine technology is being carried out, and coupling a helium turbine system to the existing 10 MWth test reactor is foreseen. The industrial scale demonstration plant of modular HTGR design is being promoted. The overall hydrogen energy programs are being discussed and defined. Regarding nuclear hydrogen R&D, laboratory scale research and experiments are being performed to study the process technologies of hydrogen production using nuclear process heat from HTGRs. Proposals of nuclear hydrogen R&D program have been made to the central government and the program is expected to start in the next Five-Year-Plan of China which begins from 2006.

Development programme of high temperature gas-cooled reactors

The current development programme of high temperature gas cooled reactors in China includes the following main items:

- Operation of the erected HTR-10 and operation-associated research and development including safety experiments.
- Research and development of direct cycle helium turbine technologies including coupling a helium turbine system to the current HTR-10 reactor configuration.
- Promotion of the first industrial scale modular HTGR demonstration plant based on steam turbine power generating technology.
- Research and development on process heat application HTGRs.

The above items are described below respectively.

The 10 MW high temperature gas-cooled test reactor (HTR-10)

China launched its national high technology research and development programme in March 1986 (therefore the so-called “863” Program). It was, in this program, proposed and approved to build a test reactor which would have a thermal power rating of 10MW. It is expected that the following objectives would be met through the HTR-10 reactor and its related R&D programme:

- to acquire know-how to design, construct and operate the HTGRs;
- to establish an irradiation and experimental facility;
- to demonstrate the inherent safety features of modular HTGR designs;
- to test power generation coupling technology with HTGR;
- to demonstrate process heat utilization technologies of HTGR.

The HTR-10 is designed for co-generation of electricity and district heating, using steam turbine cycle, for its first project implementation phase. Spherical fuel elements are used in HTR-10. The important features of the modular HTGR designs are applied to the HTR-10. Figure 1 shows the primary systems of the HTR-10. The design parameters are listed in Table 1.

Figure 1. HTR-10 Primary System

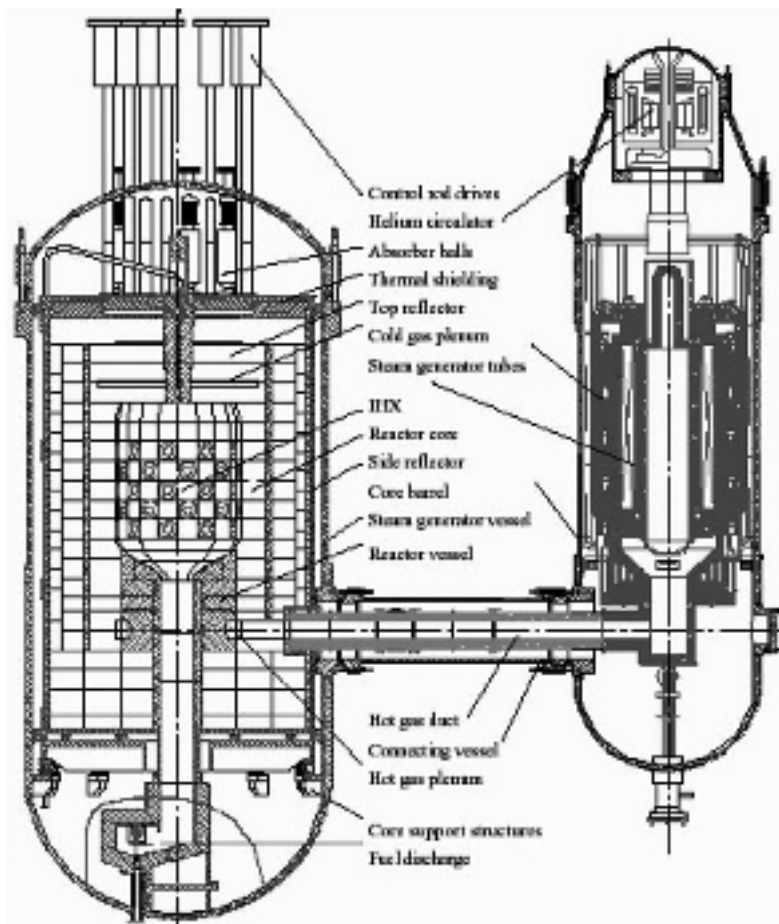


Table 1 Key Design Parameters of HTR-10 (Equilibrium Core)

Thermal power	MW	10
Reactor core diameter	cm	180
Average core height	cm	197
Primary helium pressure	MPa	3.0
Average helium temperature at reactor inlet/outlet	°C	250/700
Helium mass flow rate at full power	kg/s	4.3
Average core power density	MW/m ³	2
Power peaking factor		1.54
Number of control rods in side reflector		10
Number of absorber ball units in side reflector		7
Nuclear fuel		UO ₂
Heavy metal loading per fuel element	g	5
Enrichment of fresh fuel element	%	17
Number of fuel elements in core		27,000
Fuel loading mode	multi-pass	
Average residence time of fuel elements in core	EFPD	1,080
Max. power rating of fuel element	kW	0.57
Max. fuel temperature at normal operation	°C	919
Max. burn-up	MWd/tHM	87,072
Average burn-up	MWd/tHM	80,000
Max. thermal flux in core (E>1.86ev)	n/cm ² s	3.43x10 ¹³
Max. fast flux in core (E>1Mev)	n/cm ² s	2.77x10 ¹³

The HTR-10 test reactor was erected in 2000. First criticality was achieved in December 2000. Full power operation was achieved in January 2003. Since then, the HTR-10 has been under operation. Valuable operational experience is under accumulation. Important safety experiments have been performed with HTR-10. Overall, the construction and operation of HTR-10 has been very successful so far. Table 2 shows the comparison of key design and operation data.

Table 2. Comparison Between the Key Operation and Design Data at Full Power

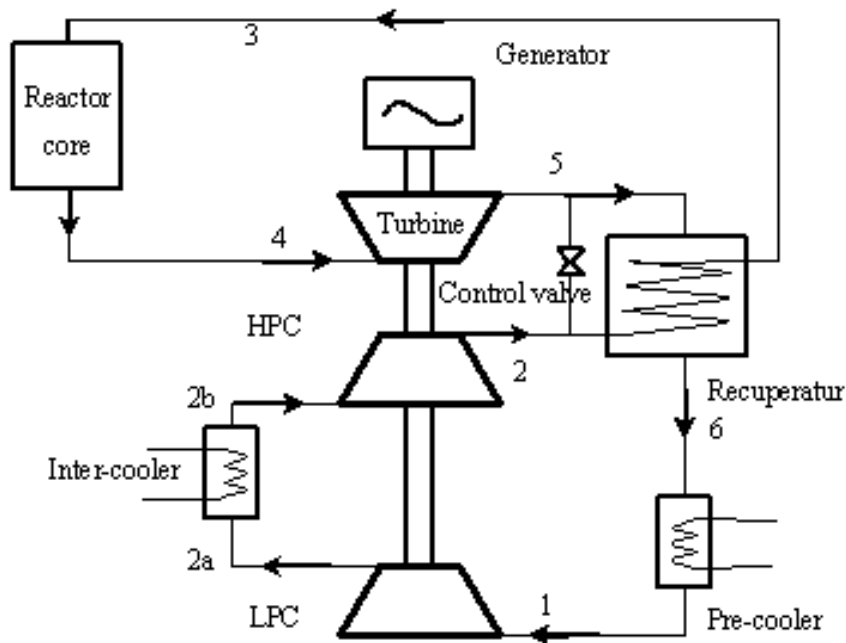
		Design	Operation
Reactor thermal power	MW	10	10.22
Electrical power	MW	2.5	2.49
Primary helium pressure	MPa	3.0	2.93
Helium temperature at core outlet	°C	700	700.1
Helium temperature at core inlet	°C	250	236.2
Primary helium flow rate	kg/s	4.3	3.99
Main steam pressure	MPa	3.5	3.45
Main steam temperature	°C	435	430
Feed water temperature	°C	104	100
Feed water flow rate	kg/s	3.49	3.56

Research and development of direct cycle helium turbine technologies

INET is carrying out research and development of direct cycle helium turbine technologies. It is planned, as the second phase of the HTR-10 project, to couple a direct helium turbine cycle to the existing HTR-10 reactor, called the HTR-10GT project. This project uses a direct gas turbine cycle to convert the nuclear energy into electricity. The power conversion part includes turbo-machines consisting of a turbine, two compressors and a generator, all of which will be installed in a primary boundary pressure vessel. At full power condition, the temperatures at reactor inlet and outlet are designed to be 330°C and 750°C respectively while the core pressure is designed to be 1.56 MPa with a helium flow rate of 4.56 kg/s. The design of turbo-compressor is based on above described conditions. The compromise of material strength and the turbo-compressor features gives a rotary speed of 250 s^{-1} (15,000 r/min). All other features of the power conversion components are based on these basic parameters.

The HTR-10GT project is featured by a closed recuperated and inter-cooled Brayton Cycle consisting of the reactor core, a helium turbine, a recuperator, a pre-cooler, a low pressure compressor, an inter-cooler and a high pressure compressor, as shown in Figure 2.

Figure 2. Schematic Diagram of HTR10GT



The nuclear energy is first converted to thermal energy carried by helium in the reactor. The heated helium from the reactor comes to the turbine inlet, expands to do work in turbine and then passes through the recuperator – lower pressure side where it transfers heat to the high pressure side helium. Then helium from the recuperator comes to the pre-cooler where it is cooled. After cooling, helium comes to the low pressure compressor inlet, where it is compressed and comes to the inter-cooler for further cooling to increase compressor efficiency, then after cooling it flows to the inlet of high pressure compressor. After compression, helium passes through the recuperator – high pressure side where it is pre-heated and then enters into the reactor core. Helium passes the reactor core, is heated again, thus closing the cycle.

The key components like turbo-machineries for HTR-10GT are under fabrication. When all the components are manufactured, an ex-core integral test will be made. After the confirmation of performances through the integral test, the helium turbine cycle is planned to be coupled to the HTR-10 reactor.

Promotion of the first industrial scale modular HTGR demonstration plant (HTR-PM)

The high temperature gas cooled reactor – pebble bed module (HTR-PM) is a modular high temperature gas cooled reactor (HTGR) plant, which is designed by the Institute of Nuclear and New Energy Technology, Tsinghua University of China. The HTR-PM design is now at the stage of concept design optimisation. The current HTR-PM design features 160 MW electrical output per module.

The HTR-PM is being promoted for an industrial demonstration plant. The HTR-PM design intends to reflect as much as possible the past experience and lessons learned from HTGR development worldwide, and to use the proven methodologies and technologies of the HTR-10 test reactor. Now that there is the real project background, the mature steam turbine cycle has been chosen for power generation in order to avoid too much R&D items and to shorten the overall duration of the demonstration project. The HTR-PM design has the following key technical features:

- Spherical fuel elements with TRISO coated particles are used, which have proven capability of fission product retention under 1 600°C in accidents.
- A two-zone core design is adopted, with one central movable column of graphite spheres surrounded by pebble fuel elements. The purpose of using the two-zone core design is to increase the power output of a single reactor module while maintaining the passive decay heat removal capability.
- Ceramic materials, graphite and carbon bricks which are high temperature resistant surround the reactor core.
- Decay heat in fuel elements is assumed to be dissipated by means of heat conduction and radiation to the outside of the reactor pressure vessel, and then taken away to the ultimate heat sink by water cooling panels on the surface of the primary concrete cell. Therefore, no coolant flow through the reactor core would be necessary for the decay heat removal in loss of coolant flow or loss of pressure accidents. The maximum temperature of fuel in accidents shall be limited to 1 600°C.
- Spherical fuel elements are charged and discharged continuously in a so-called “multi-pass” mode, which means fuel elements pass through the reactor core several times before reaching the discharge burn-up.
- Two independent reactor shutdown systems are foreseen. Both systems are assumed to be located in the graphite blocks of the side reflector. When called upon, the neutron absorber elements are assumed to fall into the designated channels located in the side reflectors, driven by gravity.
- The reactor core and the steam generator are housed in two steel pressure vessels, which are connected by a connecting vessel. Inside the connecting vessel, the hot gas duct is mounted. All pressure-retaining components, which comprise the primary pressure boundary, are in touch with the cold helium of the reactor inlet temperature.

- Under an accident with complete loss of pressure, the primary helium inventory is allowed to be released into the atmosphere. Then the helium release channel is assumed to be closed, and the reactor building is vented and serves as the last barrier to radioactivity release.
- Several HTR-PM modules could be built at one site to satisfy the power capacity demand of a utility. Some auxiliary systems and facilities could be shared among the modules.

The HTR-PM project is strongly supported by the Chinese government. Electrical power industries and nuclear industries are taking active part in the promotion of the demonstration project. The China Huaneng Group (one of the largest power companies in China), the China Nuclear Engineering Group Co. and INET/Tsinghua University have agreed to cooperate on the project. Other institutions are being involved for siting evaluation and plant design.

Research and development on process heat application HTGRs

Research work on HTGR applications started in the early 1980s. Investigations were performed with the oil and petrochemical industries and with the coal industry to define the application potential of HTGR on power-heat co-generation basis. The goal was to use HTGR as a substitute of fossil fuel plants to generate a large amount of process heat to be used in these industries, thus saving a lot of fossil fuels and resulting in less environmental pollution. Feasibility studies were carried out together with the Shengli Oil Field and Yanshan Petrochemical Complex to use HTGR process heat for the heavy oil recovery in oil fields and for petrochemical plants. Later on, basic research was performed on hydrogen production processes through methane reforming. Computer code development was made to simulate the chemical processes. Preliminary laboratory scale experiments were performed to experimentally study hydrogen production under simulated nuclear heating conditions.

Currently, in parallel to the execution of engineering projects including HTR-10, HTR-10GT and HTR-PM, studies have been continuously underway on advanced HTGR concepts (Process-heat HTR, or PHTR) including advanced concepts for hydrogen production purposes. Recently, a proposal has been made to considerably increase the efforts of R&D on PHTR designs suitable for hydrogen production. It is expected that remarkably increased funding will be made available starting from 2006 to support the R&D in this direction. The PHTR R&D programme during the 2006-2010 will focus on strategic routing exploration, plant design studies and identification of key technologies yet to be developed. It is currently foreseen to spend 10 years from 2011-2020 to bring the PHTR technology together with the application technology to a status of being able to be demonstrated on industrial scale after 2020.

It is believed that the reactor technology development through real projects like HTR-10 and HTR-PM provides the soundest basis for the research and development of advanced modular high temperature gas-cooled reactor designs for nuclear hydrogen production.

Research and development of hydrogen production technology

Among all the nuclear power technologies, high temperature gas cooled reactor is the most promising technology suitable for hydrogen production due to its potential of high efficiency power generation and providing high temperature process heat.

INET has constructed the HTR-10 test reactor, providing a real nuclear facility for future nuclear hydrogen technology research and development.

INET is conducting preliminary studies on hydrogen production technologies using I-S chemical splitting process and high temperature electrolysis process. A proposal is being made to the Ministry of Science and Technology of the central government to start a nuclear hydrogen program starting from 2006. The main components of the proposal include the following:

- Process R&D of I-S splitting process and high temperature electrolysis (2006-2008).
- Erection of laboratory scale test rig aiming at a hydrogen production rate of about 100 l/h (2008-2010).
- Experiments using the erected test-rig and design of a prototype facility, coupled to HTR-10 (2010-2015).
- Construction and operation of the prototype facility. Preparation of a demonstration plant project (2015-2020).
- Industrial scale demonstration of nuclear hydrogen production (2020 and after).

China's government pays great attention and attaches considerable importance to the development of a possible up-coming hydrogen economy. Early 2005, a workshop was called to discuss related issues of a hydrogen economy. The INET proposal for a nuclear hydrogen R&D programme is expected to be very likely supported.

AN UPDATE ON CANADIAN ACTIVITIES ON HYDROGEN

Alistair I. Miller

Atomic Energy of Canada Limited

Abstract

While Canada is one of the charter signatories of the International Partnership for the Hydrogen Economy, its national programme of R&D is still being defined. With awareness of what the national program will likely include and on the premise that nuclear energy will be the main primary source of energy, Atomic Energy of Canada Limited has evolved a vision of the way forward.

AECL's perspective is based on Canada's existing strengths in hydrogen technology and on the vital importance of significant deployment of hydrogen as a fuel ahead of the commercialisation of Gen IV reactors. Based on Canada's strong position in technology for fuel cells, low-temperature electrolysis, hydrogen storage, and relatively inexpensive electricity, we are promoting phase-out of coal-fired electricity generation between 2010 and 2030 and phase-out of oil-fuelled vehicles between 2020 and 2040. The electricity generation and the initial launch of hydrogen for vehicles will largely depend on Gen III+ reactors. Hydrogen production based on a mix of nuclear and wind generation looks interesting. Distributed generation using low-temperature electrolysis is particularly suited to early deployment of hydrogen fuelling when demand is small.

For hydrogen production after about 2030, AECL is evolving a Gen IV SCWR reactor from its Gen III+ Advanced CANDU® Reactor (ACR®). In the context of our SCWR design, we plan to collaborate with the USDOE's Argonne Laboratory in the development of the relatively low-temperature (~515°C) Cu-Cl thermochemical cycle. We are also working on ways to apply electrical heating to provide higher temperatures for high-temperature electrolysis and I/S technologies.

AECL, in partnership with others, is also developing several existing technical strengths:

- 1) heterogeneous catalysis for PEM fuel cells.
- 2) low-temperature electrolysis cells adapted for variable current loads; and is considering resumption of work on.
- 3) plasmolysis of hydrogen sulphide.

Introduction

The key question is “How do we severely curtail CO₂ emissions, worldwide?” If what we propose does not accomplish this, failing to address the key question becomes part of the problem. The envisaged role for hydrogen is as a non-polluting energy carrier for the transport sector. Its use would avoid both local pollution – with the possible exception of some NO_x if it were utilised in internal combustion engines (ICEs) – and CO₂ emissions. The reduction in CO₂ emissions is, of course, only accomplished if the hydrogen production process emits little or no CO₂. Hydrogen production by steam-methane reforming (SMR) would not accomplish this unless the co-produced CO₂ were to be effectively sequestered.

Atomic Energy of Canada Limited’s (AECL) vision of hydrogen production has two phases and a variation:

- 1) For the early stages of hydrogen fueling of the transport sector, hydrogen would be produced by low-temperature electrolysis (LTE) close to the point of fueling. The electricity would be produced from sources that emitted little or no CO₂.
- 2) When the hydrogen fueling market has grown large enough, centralised hydrogen production will become economic, either using thermochemical processes (such as sulfur-iodine (S/I)), high-temperature electrolysis (HTE), or SMR with sequestration.
- 3) The variation on Phase 2 is the continuing use of LTE for centralised production including AECL’s NuWind© concept in which electricity from nuclear reactors and wind turbines is combined.

The Nadir of SMR-Produced Hydrogen

Unlike oil, where prices are unified worldwide, the price of natural gas has always shown large regional variations. Recently, North American prices have been in the 10 to 14 \$ⁱ/GJ. At 60 \$/bbl, the energy content of oil is valued at about 11 \$/GJ. So it appears that oil and natural gas are now being priced in North America as interchangeable energy sources – not unreasonably given the growing extent of capacity for dual-fuelling that now exists in industry. Given the limited availability of new supplies of natural gas within North America, one can reasonably assume that this link will continue.

The market for natural gas in North America is tied together by pipelines. Beyond the reach of this pipeline network, markets for natural gas outside North America have lower, usually much lower, prices. It has often been argued that liquefied natural gas (LNG) would effectively cap the natural gas price in gas-deficient markets like North America at around 5 \$/GJ. So far, this has not happened because of the limited capacity of the handful of LNG terminals in North America. However, in a world of inexorable growth in demand for oil from emerging economies, oil prices seem quite likely to remain closer to 60 \$/bbl than to 40 \$/bbl or less. Note that the actual cost of production in the Middle East, which is as little as 1 or 2 \$/bbl, is irrelevant. So it is our judgment that growth in North America’s capacity to import LNG is likely to bring the value of LNG into line with that of oil, worldwide, rather than to bring down the price of natural gas in North America.

ⁱ All dollars are U.S.

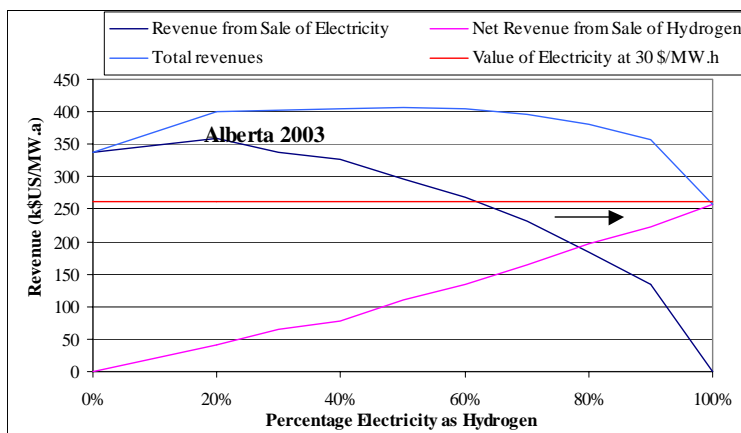
The developers of new projects for oilsands extraction in the northern part of Alberta, Canada appear to agree with our expectation of high natural gas prices since they are contemplating use of substitute energy sources to natural gas for their considerable energy needs and for hydrogen to upgrade the bitumen that is produced to synthetic crude. This is totally reasonable: at 12.5 \$/GJ for natural gas, SMR hydrogen costs about 2 300 \$/tonne H₂ or 2 700 \$/tonne if a realistic cost of sequestrationⁱⁱ is included. *One concludes that higher prices for natural gas mean that hydrogen produced by SMR is no longer the low-cost process of choice.* This is true today in North America and is likely to become the case in other markets.

The New Competitiveness of Electrolytic Hydrogen

The cost of hydrogen production by both electrolysis and SMR is dominated by the cost of their energy inputs. Around 300 \$/t H₂ is associated with capital costs and operation of an SMR while electrolysis cells costing 300 \$/kW require produce capital costs of about 400 \$/t H₂. Electricity from Generation III+ nuclear reactors (such as Westinghouse’s AP-1000, AECL’s ACR-1000©, or the European EPR) is expected to cost 3 to 5 ¢/kW.h – 1 500 to 2 500 \$/t H₂. This is without credits for co-production of oxygen (300 \$/t H₂) and heavy water (120 \$/t H₂ net of production costs). On this basis, the total cost of electrolytic hydrogen would be comparable to that from an SMR.

These costs are for continuous production of hydrogen by electrolysis. Studies by AECL [1] have shown that the economics for electrolytic hydrogen production are substantially improved if they are operated intermittently when the price of electricity to the grid is relatively low. While this increases the cost of the electrolysis installation and introduces costs for hydrogen storage, the savings in electricity costs easily offset these. Figure 1 gives an example of the revenues that would have occurred with varying levels of electricity conversion using actual hourly prices paid for electricity in Alberta in 2003 and valuing hydrogen at 2 000 \$/t. There is more revenue from sale of any mixture of electricity and hydrogen than from sale of only electricity or from total conversion of the electricity to hydrogen and sale of that hydrogen.

Figure 1. Value of revenue from sales of hydrogen and electricity, Alberta 2003



ii. 400 \$/t H₂ for CO₂ sequestration occurs with a cost for separation, transport and sequestration of 50 \$/t CO₂. (About 7.5 tonnes of CO₂ is produced for every tonne of H₂.) Including the effects of collateral CO₂ releases from the energy used in CO₂ sequestration, we calculate that the likely cost may be closer to 70 \$/t CO₂.

If one were to assume 50% conversion of electricity to hydrogen, a 1 000-MW(e) reactor would provide hydrogen fuel for around 400 000 cars with PEM fuel cells operating a typical (for North America) 20 000 km/a. The balance of the electrical output would be sold to the electricity grid at times of highest demand. Not only does this extend the nuclear power market beyond electricity but it also opens up nuclear's share of the electricity market beyond their normal base-loaded part.

Adding Wind Turbines alongside Nuclear-Generated Electricity

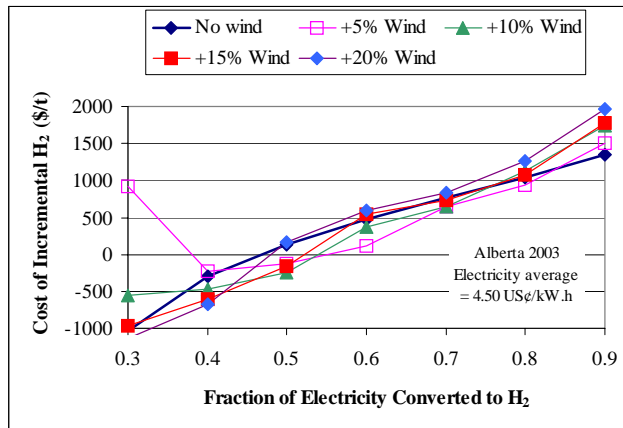
The main drawback to generating electricity from wind and other fickle sources is their intermittency and the need to provide a back-up source of electricity generation. This is a major problem and many studies of actual and proposed wind deployment have examined it. One excellent study by the national electricity generator (ESB) in Ireland examines this problem in detail [2]. The study's conclusion is that wind generation has little scope for reducing CO₂ emissions from the current or future Irish electricity-generating mix. A solution often proposed to address wind's intermittency is to convert the electricity generated into hydrogen using electrolysis. But a simple examination of the economics of electrolysis shows that this is not economically competitive.

In favourable locations, wind turbines can average around 33% of nameplate capacity and produce electricity at about 4 ¢/kW.h – comparable to that from Generation III+ nuclear. This would lead to a capital cost of 1 200 \$/t H₂ (allowing for three-fold oversizing to match wind's low capacity factor) and an electricity cost of 2 000 \$/t H₂. The hydrogen storage cost is hard to calculate because wind (in middle latitudes) has large seasonal variability – as much as three-fold more in peak winter months compared to summer lows. However, underground cavern storage (similar to that used for natural gas) does not introduce a large cost element. Even so, the costs of electricity and capital do not lead to a competitive price for hydrogen produced in this way.

Because the electrolysis installation is already so large when all wind-generated power is converted to hydrogen, the concept of adding yet more electrolysis capacity to allow sale of a mixture of electricity and hydrogen is also unattractive.

To deal with this, AECL has developed the NuWind© concept. In this concept, a mix of electricity from nuclear and wind sources is either sold into the high-value peaks of the electricity market or converted to hydrogen. When the price of electricity is low, any wind-produced electricity is used for electrolysis alongside the electricity generated from the nuclear source. Crucially, the electrolysis installation is designed to handle a about a 40% range of current densities – which is estimated to increase the capital cost by 10%. This also leads to a modest increase in electricity consumption per tonne of hydrogen. Details can be found elsewhere [1]. Figure 2, which combines electricity price data from Alberta in 2003 with actual wind data from a typical mid-latitude site shows that the cost of additional hydrogen coming from the wind source is indistinguishable from that of the nuclear-based hydrogen over a broad range of fractional conversion of the electricity and up to 20% of the electricity being generated by wind (i.e. a wind farm with a nameplate capacity 60% of that of the nuclear).

Figure 2. Cost of hydrogen generation with nuclear alone and incremental cost of additional hydrogen generation from wind, Alberta 2003



Competitiveness of Hydrogen from Conventional Electrolysis with Advanced Concepts

The most important aspects of hydrogen production by LTE are (1) that it is currently competitive with SMRs using natural gas in the North American context; (2) that it can be deployed immediately; and (3) that it is a near-zero CO₂-emission technology.

Even before the cost of CO₂ capture and storage is included, intermittency of hydrogen generation gives LTE cost superiority over SMR-generation at today's natural gas prices where electricity prices float with market demand. Contrary to the intuitive expectation that electrolysis can only compete where electricity prices are low, it is important to realise that high average electricity prices favour this approach. High prices lead to higher revenues from the electricity product without affecting the cost of electricity generation.

In about twenty years time, new high-temperature production processes may be ready for deployment. This, however, is about as early as their widespread deployment will be possible *and it is probably ten years after hydrogen-fueled vehicles will begin to come into widespread use*. So, with its immediate availability and intrinsic scalability, LTE is the natural forerunner of either HTE or thermochemical processes. A typical 2 000 MW(th) reactor operating with 50% conversion efficiency to hydrogen would fuel 1.1 million vehicles using PEM fuel cells. Though some high-temperature reactor technologies envisage building reactors an order of magnitude smaller, these high-temperature processes are definitely large-scale technologies and multiple sources will presumably be linked by a network of hydrogen pipelines. Their economic competitiveness – currently unknowable – will determine whether they will ultimately displace LTE though it seems plausible that LTE will persist in places where the demand is smaller and pipelines are unavailable. Nonetheless, LTE using off-peak electricity sets a fairly demanding target for HTE and thermochemical processes. If the latter's conversion efficiencies are found to fall much below 50%, LTE will probably offer superior economics through production of electricity (at around 50% conversion efficiency from 950°C reactors) and conversion to hydrogen using LTE.

Canadian Work on Technology Associated with Hydrogen Production

With financial support from Natural Resources Canada, AECL is carrying out a modest program of R&D on high-temperature hydrogen-production processes. The main focus is on the copper-chlorine system, which is principally being studied by the USDOE's Argonne National Laboratory (ANL) [3]. AECL is assembling a consortium of Canadian university researchers to develop the electrochemical step in this cycle in which cuprous chloride is disproportionated into copper and cupric chloride. A particular attraction of this cycle is the relative low temperature (530°C) required for heat input, a temperature that is within reach of AECL's Mark 2 SuperCritical-Water Reactor (SCWR). SCWRs are envisaged as the next stage in the incremental development of CANDU reactors after the ACR.

AECL also has a small program examining SO₃ decomposition using resistance heating of catalysed surfaces. This is a common step of a group of hydrogen-production processes including S/I and the Westinghouse process.

PEM Fuel Cell Development

For many years, Canada has been a notable leader in the development of PEM fuel cells. Sharing of intellectual property among Canadian fuel-cell developers in the last few years has led to a surge in progress. Ballard, who are leading developers of PEM fuel cells and have numerous collaborative agreements with major automobile manufacturers, can now achieve repeated cold starts from -20°C, retain 95% of the original power output after 2 000 hours of operation, and achieve a cost of 100 \$/kW (assuming mass production). Ballard is now forecasting competitive PEM-engined vehicles by 2010.

AECL is working with several Canadian PEM developers to apply its heterogeneous catalyst expertise (developed for processes to produce and purify heavy water) to PEM technology. Early work suggests that a significant reduction in platinum loading may be achievable.

Other Routes to Hydrogen Production

With large natural gas production, Canada must dispose of large amounts of hydrogen sulfide (H₂S). The Claus Process is the standard technology used to convert H₂S to sulfur and water. This is wasteful since a small energy input (10% of that needed to dissociate water) is required to dissociate H₂S into sulfur and hydrogen.

In the early 1990s, AECL and Shell Canada collaborated to develop technology originating in the Russian Kurchatov Institute to apply an RF plasma to dissociate H₂S. Proof-of-principle was achieved and AECL is now considering resumption of development since it has potential for significant hydrogen production from much smaller inputs of electrical energy than is needed for electrolysis.

CO₂ Abatement is Urgent

A massive reduction in CO₂ emissions associated with energy supplies is the World's Number One environmental priority. The capacity for CO₂ (assisted by other greenhouse gases) to cause climate change worldwide cannot be quantified precisely though overwhelming qualitative evidence of warming is accumulating in, for example, the melting of previously permanent Arctic sea-ice cover.

If the complex effect of CO₂ on global warming was not bad enough, its direct effect in acidifying the surface waters of the world's oceans is more definite and more clearly deleterious[4] a doubling

of pre-industrial CO₂ levels (from 280 to 560 ppm) will lower pH by around 0.4 units. Lower acidity does its most obvious damage through conversion of carbonate ion (CO₃²⁺) to bicarbonate (HCO₃⁻) thus:



The dissolved carbonate ion is essential to the building and retention of exoskeletons of corals and phytoplankton, key components of ocean food chains. By 560 ppm CO₂ in the atmosphere, reduction of carbonate is expected to lead to huge disruption of these food chains. (Previous, naturally occurring excursions of CO₂ concentration have been counterbalanced by the higher acidity causing carbonate rock to dissolve. However, this is a slow mechanism dependent on the turnover of ocean water and it has no chance of keeping up with the speed with which atmospheric CO₂ is currently rising – about 100 times faster than past naturally occurring changes.) The rise of atmospheric CO₂ concentration is well-documented and the mechanisms of its accumulation in the atmosphere quite well understood with about half the CO₂ added to the atmosphere quickly dissolving in the well-mixed surface layer of the oceans.

From the ocean's surface layer, a small amount of CO₂ migrates to deeper layers, partly in the form of calcium carbonate in the shells of dead organisms raining down to deeper depths and partly through sinking of dense, highly-saline water in the Thermohaline Circulation. Injections of CO₂ to the atmosphere beyond the capacity of these removal mechanisms accumulate and the CO₂ concentration rises continuously, currently at almost 2 ppm per annum. The removal mechanisms would be in balance with CO₂ addition rate if the addition rate were about 40% of the rate in the year 2000. To place the challenge of stabilisation in context, while CO₂ emissions are stabilizing in many industrially developed countries, large emerging economies are becoming significant contributors as they industrialise rapidly. (In their defence, the per-capita emissions of countries such as China and India are still far below those of developed countries.) Consequently, the overall rate of increase continues to rise.

Atmospheric CO₂ concentration will finally stabilise – either by collective human action, by exhaustion of carbon sources (around an atmospheric CO₂ level of ~2000 ppm), or by the collapse of our technological society. If it is to be stopped by collective human action, the stabilized level will depend on the speed and vigour with which low-carbon energy sources are deployed. Delay raises the ultimate level of stabilisation.

A concentration of 450 ppm CO₂ has recently gained favour as a level with a fair chance of avoiding severe disruptions of the biosphere and the global economy. Given that this is only 70 ppm or about 35 years at current rates above the current level, stabilization at this level is a remote possibility. Most large energy-producing facilities committed today will not have reached the end of their planned lives in 35 years.

Whether 450 ppm is really a “safe” level is unknowable but it should be appreciated that yet higher levels carry ever-greater threats of disruption, possibly including the triggering of runaway feedback mechanisms that would surpass current anthropogenic emissions. Hence the need for urgency in adopting policies that will stop the rise of atmospheric CO₂ at the lowest possible level. Because global energy use is going to at least double as emerging economies industrialise and transportation represents almost 30% of current global energy use and the proportion is rising, energy for transportation must move substantially away from hydrocarbons if we are to stabilise atmospheric CO₂ levels. Currently, hydrogen is the only practicable CO₂-free alternative fuel. That is the simple case for the “Hydrogen Economy”.

It is possible that battery storage may ultimately improve to a point where it can make a significant contribution but we simply cannot afford to wait for breakthroughs in battery technology to occur.

REFERENCES

- [1] Miller, A.I. and Duffey, R.B., “Co-production of hydrogen and electricity from wind and nuclear sources (NuWind©) using cavern storage for hydrogen”, paper presented at ICENES 2005, the 12th International Conference on Emerging Nuclear Energy Systems, Brussels, Belgium, 2005 August 21-26.
- [2] “Impact of Wind Power Generation in Ireland on the Operation of Conventional Plant and the Economic Implications”, ESB, 2004 February.
<http://www.eirgrid.com/EirGridPortal/uploads/Publications/Wind%20Impact%20Study%20-%20main%20report.pdf>.
- [3] Serban, M., Lewis, M.A. and Basco, J.K., “Source Kinetic study of the hydrogen and oxygen production reactions in the copper-chloride thermochemical cycle”, 2004 AIChE Spring National Meeting, Conference Proceedings, 2004, pp 2690-2698.
- [4] “Ocean acidification due to increasing atmospheric carbon dioxide”, The Royal Society, Policy Document 12/05, 2005 June, ISBN 0 85403 617 2.
<http://www.pml.ac.uk/pml/news/RS%20ocean%20acidification%20report.pdf>.

NUCLEAR HYDROGEN PRODUCTION PROJECT IN KOREA

Young-Joon Shin, Jong-ho Kim, Jonghwa Chang, Won-seok Park, Jongkuen Park

Korea Atomic Energy Research Institute

150 Dukjin-dong, Yuseong-gu, Daejeon, Korea 305-600

Tel; +82 42 868 2795, Fax; +82 42 868 2636, E-mail; nyjshin@kaeri.re.kr

Abstract

In 2004, the Korea Atomic Energy Research Institute(KAERI) received a contract from the Ministry of Science and Technology(MOST) to launch the Project “Nuclear Hydrogen Development and Demonstration(NHDD)”. The team selected the SI process connected to a high temperature gas cooled reactor for further development and a demonstration. Under the current NHDD schedule a lab-scale SI process is being developed and then the integrated test operation will be completed in 2009. The lab-scale process will be demonstrated at prototypical temperatures and pressures for metallic and ceramic equipment. In the next phase, a pilot plant will be constructed and operated by 2013. This process will also be demonstrated at prototypical temperatures and pressures, too. Upon a successful completion of the pilot-scale integrated loop demonstration, a Demo Plant will require an installing and it will be tied to a VHTR in the 1st half of 2019. After a successful demonstration of the Demo Plant, the technology will be ready to be commercialised in the 2020s in Korea.

Introduction

The new worldwide task presented to us since the Kyoto Protocol for the UN Framework Convention on Climate Change in December 1997 is how to overcome the energy imbalance for the future well-being of humans. It has been suggested that hydrogen should partially replace gasoline for fueling automobiles within the next decade and its economical competitiveness should be obtained by the 2020s. A very high temperature gas-cooled reactor (VHTR) can be effectively used for hydrogen production through several CO₂-free alternative technologies, such as the Sulfur-Iodine (SI) cycle, the High Temperature Electrolysis of Steam (HTES), and others.

JAERI has carried out a significant development effort on the SI cycle, culminating in the operation of a bench-scale unit that produced hydrogen at a rate of 30 L/h for 180 hours continuously. However, the system was an all-glass system that operated at an atmospheric pressure. The commercial hydrogen production system will be running at pressures from 10 to 50 bar for metallic or ceramic equipment. Therefore a significant development effort is still needed for the SI cycle.

General Atomics' efforts in the nuclear production of hydrogen began before the "oil crisis" in the early 1970s. In USA, an i-NERI project was initiated by DOE in 2003. The Department of Physico-Chemistry in the Nuclear Energy Directorate of the French Commissariat à l'Énergie Atomique (CEA), SNL, and GA have joined together for this international effort. SNL has the responsibility for the coordination of the project and is building and testing the front-end sulfuric acid decomposition system. CEA is designing and building the Bunsen reactor, and the GA team is designing and building the HI decomposition system. Under the current i-NERI schedule the different sections of the SI process are being developed as stand alone laboratory demonstrations and they will be completed in 2006. Upon a successful demonstration of the individual sections, a fully integrated, closed loop will be assembled and operated at a production rate of 1,000 L/hr. The process will be demonstrated at prototypical temperatures and pressures in prototypical (metallic) equipment. Upon a successful completion of the integrated loop demonstration, the scale up will be in three steps: Pilot Plant (1 MW_{th}) by 2011, Engineering Demo Plant (50 MW_{th}) by 2017, and Commercial Production Facilities (500 ~ 2 400 MW_{th}) beyond 2021.

In 2004, the KAERI together with the Korean Institute of Energy Research (KIER) and the Korean Institute of Science and Technology (KIST), received a contract from the MOST to launch the Project "Nuclear Hydrogen Production Technology Development and Demonstration (NHDD)". The team selected the S-I process connected to a high temperature gas cooled reactor for further development and a demonstration.

Under the KAERI's NHDD schedule, the SI process of ~1 000 L/hr is being developed as stand alone laboratory demonstrations by the KIER and KIST, and then the integrated test operation will be completed in 2009. The lab-scale process will be demonstrated at prototypical temperatures and pressures for metallic and ceramic equipment.

Upon a successful demonstration of the individual sections and a fully integrated loop, the pilot plant will be constructed and operated at a production rate of 30~100 m³/hr (23.5~78.2 metric tons/yr of H₂) by 2013. This process will also be demonstrated at prototypical temperatures and pressures for prototypical equipment, too.

Upon a successful completion of the pilot-scale integrated loop demonstration, the Demo Plant will require an installing in a 70 MW plant, capable of producing 7 821 metric tons/yr of H₂. This unit will be tied to the VHTR of 100 MW_{th} in the 1st half of 2019. After a successful demonstration of the

Demo Plant, the technology will be ready to be commercialized, covering 20% of the total vehicle fuel demand in Korea for the 2020s.

NHDD Project Option and Target

The NHDD project includes the development of an advanced SI cycle and a VHTR for a future hydrogen production based on domestic resources, free from a greenhouse gas release, and cost-competitive as hydrogen production options. From the aspects of an energy demand and a current energy supply system, a simple expansion of the current system for a sustainable development in Korea is not possible because of a limitation of fossil energy resources, a global environment campaign due to climate change, and energy securities.

Among the primary energy options, high temperature nuclear energy would offer a significant potential for a sustainable development to satisfy the three hydrogen production options. Based on the thermodynamic analysis, a SI cycle can effectively produce hydrogen at a high temperature (> 850°C) through a series of chemical reactions resulting in the production of hydrogen from water.

However thermochemical technologies including the SI cycle technology are at an early stage of development and not well known to commit to a closed loop test by a prototypical process. This higher risk should be investigated to solve the future sustainable energy problem, and the final targets of the NHDD project for a hydrogen economy have to be completed by 2021.

Development Strategy and Management Processes

R&D for a nuclear hydrogen production technology development focuses on the development of an advanced SI thermochemical cycle as a baseline cycle and the evaluation of alternative cycles such as a high temperature electrolysis and the new technologies to be introduced continuously. Alternative cycles could be identified which have potential advantages in efficiency, cost, and process simplicity.

In order to commercialize the developed technologies as soon as possible, the industries are required to participate from an early development stage. The industries will lead the construction and operation of the demonstration facilities while the Government will lead the programme in the design stages. In order to assure a cost-effective research, international collaboration will be expanded and promoted continuously. Cooperation through the GIF-VHTR/HP and the on-going bilateral collaboration will be fostered.

The MOST provides a Request for Proposal(RFP) guidance to the national and private research institutes and universities based on their technical capabilities and manpowers at each phase which consists of a several years term. According to the RFP guidance, each institute or university develops draft proposals that include R&D cost, schedule, and scope by a work breakdown system. The review groups evaluate the draft proposals according to their review guidelines, such as budget, completeness, etc. On the other hand, the review groups monitor the project performance against an established baseline each year and control a new years research budget according to their rules.

The system-type project like the NHDD is composed of a main project and several sub-group projects. The main project manages the R&D activities of the sub-group projects including the development of research plans and the direction of the tasks. The main project also integrates the intersection of the programmatic and technical processes required for a programme coordination.

Technical Integration and R&D Activities

The technical integration of the sub-groups' projects is performed and managed by the main project. The technical integration functions are to 1) coordinate and implement a technical direction, 2) develop a nuclear hydrogen R&D plan, 3) ensure that the scope and schedule including the milestones are met. In the 1st phase(2004-2005), the NHDD project has a main project and 4 sub-group projects, and the number of the sub-group projects in the 2nd phase(2006-2009) will be expanded.

The R&D activities are and will be performed under several work packages, such as a basic chemistry, an evaluation of alternatives, a process development, an equipment development, a material database, a catalyst development and database, and a hydrogen process coupling technology.

The R&D activities for the basic chemistry focus on the development of the main technologies for an advanced SI process, such as a Busen reaction, a mutual separation of the heavy-/light-phases, electro dialysis to concentrate the HI_x solution, a membrane separation to recover the hydrogen from the HI-H₂-I₂ gas mixtures, and a decomposition of SO₃ at an atmospheric condition.

A high temperature electrolysis and a methane-methanol-iodomethane cycle to produce hydrogen as alternative cycles have been evaluated from the aspects of an overall thermal efficiency and their technological feasibilities. New technologies to be introduced in the future will be continuously evaluated.

The R&D activities for the process and equipment developments will be performed at prototypical conditions based on a high pressure and temperature and metallic-based equipment. On the other hand, a dynamic simulation computer code to analyse the transient state of an advanced SI process will be developed by 2009. This computer code will be applied for the dynamic analysis of the pilot and demo scale SI facilities.

Catalysts for the decomposition of sulfuric acid and sulfur trioxides have been developed and their engineering performance tests are being conducted at present.

In order to develop a ceramic membrane material for a hydrogen separation, experimental efforts are being made. The development of an adsorbent for a separation of oxygen from the SO₃-SO₂-O₂ mixture will be initiated in 2006.

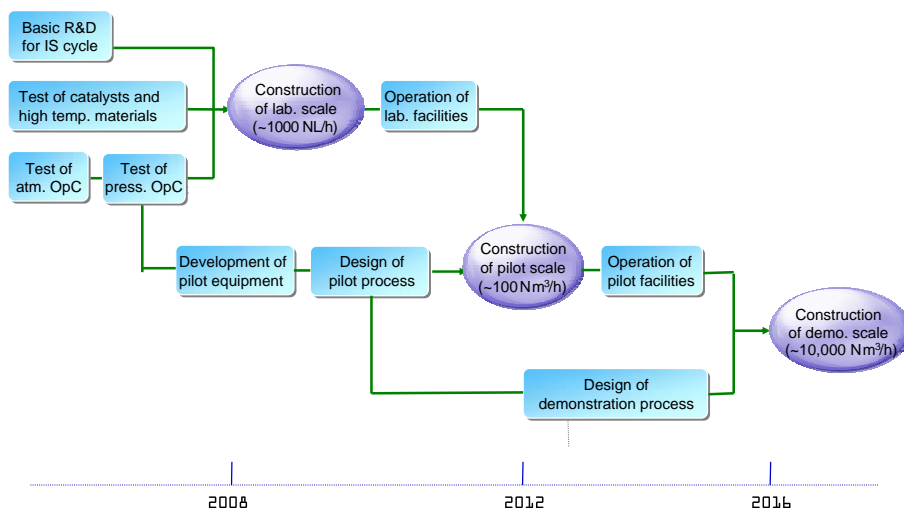
Coupon and autoclave corrosion tests to screen equipment materials for the advanced SI process are being carried out and their experimental data is being continuously logged. The database of merchantable catalysts for a HI decomposition is being constructed through experimental activities.

In order to develop an evaluation methodology of the coupling process efficiency, a methodology and the requirements for the safety aspects, and a methodology for the system integration, flow sheet, mass & thermal balances for the coupling process for an intermediate circuit of the coupling process will be conducted by MARS-GCR and HyPEP computer codes. A probabilistic safety assessment of a hydrogen production system which will address the interfacing events between nuclear and non-nuclear will be performed.

Project Schedule and Research Phases

Based on a systematic project, the development of a SI nuclear hydrogen production process will be carried out through the 5 research phases from 2004 to 2021 as shown in Figure 1.

Figure 1. R&D schedule of a SI nuclear hydrogen production project.



The R&D activities in the 1st phase (2004-2005) focus on the development of the main technologies for an advanced SI process, such as a Busen reaction, a mutual separation of the heavy-/light-phases, electro dialysis to concentrate the HIx solution, a membrane separation to recover the hydrogen from the HI-H₂-I₂ gas mixtures, and a decomposition of SO₃ at an atmospheric condition.

The 2nd phase (2006-2009) R&D activities undertake a SI process optimization and the performance tests of various chemical reactors selected for the SI cycle. The 2nd phase research covers a dynamic code development for the SI process, a construction of a lab. scale (~1 000 NL/h) SI process, and integrated operations of the process at prototypical pressures. On the other hand, conceptual and basic designs of a pilot scale (~100 Nm³/h) SI process and its equipment will also be carried out according to the optimized process established from the theoretical evaluation using a commercial-base computer code and the experiences of the lab. scale construction and operations. Preliminary performance tests of the equipment, mechanical devices, and accessories for the pilot scale SI process should be carried out to obtain the design basis. Not only the several catalysts based on non-noble metals required for section II in the SI cycle but also a membrane for the separation of the hydrogen required for section III will be developed during the 2nd phase research period.

In the 3rd phase (2010-2012), most of the design bases for the engineering approaches including the process controls will be acquired by constructing and operating a pilot scale SI process. Dynamic studies on the start-up, shut-down, and arbitrary transient motions of the pilot scale SI facilities will be performed theoretically to verify the process viability and safety by using the dynamic computer codes developed in the 2nd phase. Pilot scale experiments will be carried out with non-nuclear heat sources based on prototypical process technology and operating conditions.

As a result of a successful operation of the pilot scale facility, technological spin-offs to the industries can be anticipated. It means therefore that the next phase will involve a partnership with the industry to construct and operate an engineering scale demonstration facility.

In the 4th phase (2013-2017) and 5th phase (2018-2021), the engineering scale demonstration facility (~10,000 Nm³/h) will be designed and constructed in partnership with the industry. In the first half of 2019, the facility will be coupled to the VHTR system. After a completion of the safety check for the coupling system between the VHTR and the engineering scale SI facility, a full power hydrogen generation test by the VHTR will be conducted finally in 2020.

Conclusions

Korea has selected an advanced SI thermochemical cycle as a baseline cycle for a nuclear hydrogen production and it is evaluating the alternative cycles such as a high temperature electrolysis and new technologies to identify their potential advantages in efficiency, cost, and process simplicity.

The advanced SI process for a commercial-base nuclear hydrogen production is at an early stage and it still has a technical uncertainty. Therefore step-by-step approaches from a lab-scale test to an engineering-scale test are required to diminish this technical uncertainty.

In order to assure a cost-effective research, international collaboration will be expanded and promoted continuously. Cooperation through the GIF-VHTR/HP and the on-going bilateral collaboration will be fostered.

Successful operation of the engineering scale demonstration facility will not only provide a commercial facility but also offer the first step for a hydrogen economy and a cleaner world.

Acknowledgements

This work has been done under “Nuclear Hydrogen Development and Demonstration(NHDD) Project” and we are grateful to MOST for financial help.

MICHELANGELO NETWORK RECOMMENDATIONS ON NUCLEAR HYDROGEN PRODUCTION

Karl Verfondern, Werner von Lensa
Research Center Jülich, 52425 Jülich, Germany

Abstract

The MICHELANGELO Network (MICANET) was started within the 5th EURATOM Framework Programme (FP5) with the objective to elaborate a general European R&D strategy for the further development of the nuclear industry both in short, medium, and long term. To broaden the application range of nuclear power beyond dedicated electricity generation, the network proposed an orientation for future EURATOM R&D programmes including new industrial aspects of nuclear energy like Combined Heat and Power (CHP) and particularly the production of hydrogen or other fuels as a link to CO₂-free energy sources. MICANET is acting as the European counterpart and partner to the Generation IV International Forum (GIF). The MICANET project is in its final phase and will be terminated by the end of this year. Goals achieved related to nuclear hydrogen production and other non-electrical nuclear applications will be outlined.

Introduction

The European Union comprises highly industrialised countries with extended urban agglomerations, and therefore needs to rely on a secure and economic supply with energy. In addition, there is the interest to increase the supply security by diversification of the primary energy carriers and, at the same time, limit the effects of energy consumption on the environment. The situation in the European Union as predicted for the next 30 years is characterized by a growing demand for energy and, at the same time (after 2010), a decreasing domestic energy production. While in 2000, 48% of the energy demand had to be covered by imports, this share will increase to 70% in 2030, if no additional measures are taken. In addition, this development will push CO₂ emissions to a plus of 14% compared to the 1990 level, far off the Kyoto commitment of an 8% reduction. Although aware of the major risks of a rapid increase in energy demand worldwide, particularly in emerging economies, and of the uncertainty about how long oil and gas reserves will last, the discussion in the EU on the structure of its future energy economy has not yet reached the top of the political agenda. Main reasons are the diversity in national energy policies and the tendency among the EU member states to consider their energy strategies as a matter of national security. Therefore a closer collaboration among the EU countries is required. Another important point is the fact that a competition of the different energy carriers is not really given. Market is distorted by the existing questionable automatism of a coupling in the price fluctuations for all energy carriers. There is no rational reason of increasing prices for abundantly available primary energies such as coal or gas, when the oil price is escalating due to resource shortage. A decoupling, however, is necessary for future energy alternatives to keep them affordable.

Nuclear power is one of the major energy sources in Western Europe covering more than a third of its total electricity demand. The nuclear share, however, varies significantly between countries: while some countries completely refrain from nuclear, in other countries the nuclear shares range between ~3% for the Netherlands to ~78% for France. On the European level, there exists long-term intensive cooperation among the nuclear vendors, utilities and research organizations, not only aiming at an evolutionary development of existing nuclear technology, but also searching for innovative concepts of power plants and components with different and improved safety characteristics. It was the main incentive for the foundation of the MICHELANGELO Network to move away from the fragmentation and isolation of national research efforts and elaborate a common European position on the priorities of future R&D for a sustainable use of nuclear energy within the worldwide activities in this area.

With the recent worldwide increased interest in hydrogen as a clean fuel of the future, Europe has also embarked on comprehensive research, development, and demonstration activities with the main objective of the transition from a fossil towards a CO₂ emission free energy structure as the ultimate goal. The near and medium term, however, due to the growing demand for hydrogen in the petrochemical and refining industries, will be characterized by a coexistence between the energy carriers hydrogen and hydrocarbons. Due to the increasing share of “dirty fuels” such as heavy oils, oil shale, tar sands entering the market, the need for both process heat and hydrogen will also increase significantly [1].

The Michelangelo Network – MICANET

In 1997, the European initiative MICHELANGELO, conducted as a Concerted Action within the 4th Framework Programme (FP4) of the European Commission (1997-2000) was created by 19 European partners to define a general European R&D strategy for the further development of the nuclear industry. It was shown that there is a high potential for innovative nuclear techniques, systems,

and concepts which can offer socially acceptable, environmentally benign and competitive solutions, which are, however, only realisable with international cooperation as is the case, e.g., in the Generation IV International Forum (GIF).

In 2001, the former SINTER (Sustainable & Innovative Nuclear Technology R&D) Network and the MICHELANGELO Initiative were merged into a European platform in form of a network, the MICHELANGELO Network or short: MICANET with the main objective to elaborate and propose to the EC an R&D strategy on how to keep the option of nuclear fission energy for Europe open in the future. MICANET also proposed under the EU FP5 was finally contracted with a duration of 48 months until end of 2005. MICANET is subdivided into different work packages concentrating on innovative nuclear reactor designs, criteria for future systems, and non-electricity applications. The latter includes the issue of the production of hydrogen by nuclear power and will be described in more detail.

The principal result of the work of MICHELANGELO Network is the establishment of a consistent strategy of the European nuclear R&D including specific proposals for future key projects, some guidelines for establishing international cooperation, in particular with Generation IV initiative, a set of criteria to be satisfied by future nuclear systems. The desired consequence of the project is expected to be the beginning of a dynamic, long-term R&D partnership between the main European organisations of the nuclear industry and research in the form of a stable network in an international frame.

In order to achieve the goal of a European roadmap for nuclear energy, it is necessary to pursue innovative approaches of nuclear designs which may be the only ones to obtain – apart from technical and economical issues – also political and social acceptability. Another essential requirement is the establishment of a long-term stable partnership not only among the European projects dealing with innovative nuclear fission energy systems, but also between Europe and the nuclear industries worldwide. It includes the careful watch and evaluation of the work done in other parts of the world with similar prospects. In particular, a strong European partnership to the U.S. initiative “Generation IV” was developed in order to obtain a benefit for Europe. But this holds also for other international initiatives like INPRO (IAEA) or the Three Agency Study (IAEA, IEA, OECD/NEA) or the US-DOE Nuclear Energy Research Initiative NERI, and in addition, respective national programs like the HTTR project in Japan or the HTR-10 in China.

While GIF is concentrating on reactor design to be ready for commercial deployment by the year 2030, MICANET has been looking also on the role of nuclear energy in near and medium term missions, i.e., the transition phase from the present fossil era to CO₂ emission free technologies in the future. Due to the fact that fossil fuels will still be used for a longer time, it is highly recommended to follow also the more pragmatic way of a CO₂-reduced economy by providing nuclear primary energy to cogeneration and crude oil processing including evolution in present industrial practice like steam reforming of natural gas in a transition phase. The network is offering a platform for information exchange, to create points of synthesis and to align methodologies. Furthermore, the MICHELANGELO Network will identify cooperation options for the execution of the projects. This will certainly contribute to reinforce the competence of the European Union in nuclear technologies with regard to increasing efforts in Canada, China, Japan, Korea, Russia, South Africa, or the United States.

Up to now, nuclear energy has served only as a generator of electricity. However, in the decades to come, nuclear may be called upon to play a significant role in other energy sectors with the most promising to be hydrogen, high temperature process heat for other industrial applications, desalination to produce fresh water, and district heating. Therefore the network has made proposals of orientation

for future EURATOM R&D Framework Programmes including new aspects of nuclear energy like Combined Heat and Power (CHP), desalination, and hydrogen or other fuel production as a complement to other CO₂-free energy sources.

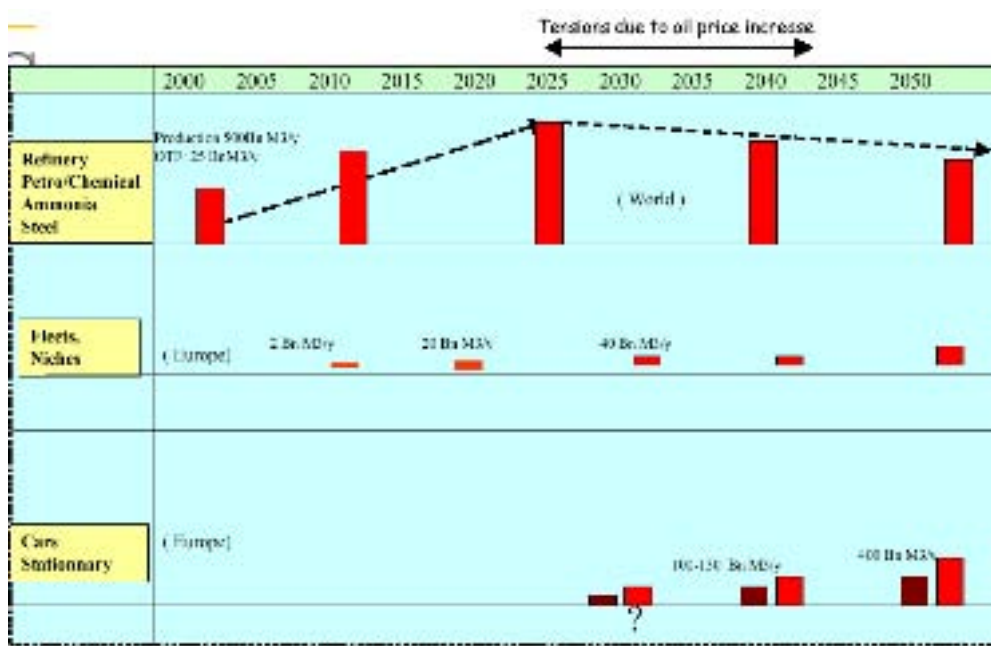
General Recommendations of MICANET on the Use of Nuclear Power for H₂ Production

Market for Hydrogen

As a matter of fact, a major hydrogen economy is already existing. Significant amounts of hydrogen are currently produced in the fertilizer industry for the manufacture of anhydrous ammonia. Hydrogen also plays a large and growing role in the refining of petroleum products, where the reserves of high quality light sweet crude oils are declining and the available crude stocks are becoming progressively heavier. These heavier crudes require larger amounts of hydrogen to produce cleaner burning end-point fuels with a higher hydrogen-to-carbon ratio. As to the United States, assuming 50% efficiency, current hydrogen production would soon require the equivalent of the output of all 103 existing nuclear power plants. Hydrogen demand is expected to grow at a rate of 4-10% per year.

For the future, a significant additional potential of hydrogen is foreseen especially in two areas: in the transportation sector and as a distributed electrical energy source through the use of fuel cells. In developed countries, primary energy is about evenly distributed among electricity generation, transportation, and industrial uses. If hydrogen is started to be utilized as a transportation fuel, the demand for and the capability to produce the hydrogen will accelerate rapidly. A projection of the hydrogen market in Europe is shown in Figure 1.

Figure 1. Projection of hydrogen market as assessed by EC High Level Group



Electricity (electrons) and hydrogen (protons) form complementary and synergetic options for transferring and storing energy for different end-uses. They are in a certain way inter-changeable (“hydricity”) although conversion losses occur. Both together are also complementary to each other in that either one is superior to the other in certain aspects offering much more flexibility in optimising

energy structures on a macro-scale (e.g. substitution of natural gas fired peaking plants by hydrogen). H₂ combined with a re-use of abundantly available CO₂ to produce liquid synthetic fuels may also contribute to a reduction of CO₂ emission. Hydrogen or hydrogen-rich liquid fuel (e.g. methanol) can be converted to electricity for transport purposes via fuel cells. Decentralised hydrogen production systems can be established via electrolysis if cheap (CO₂-free) electricity is available (e.g. off-peak nuclear power). A new hydrogen market may be at first introduced and prepared via the electricity sector. However, one main obstacle for the storage of electricity by intermediate hydrogen production is the cost of part-time operation of the chain (electrolyser, turbine plant) intended for avoidance of part time operation of the nuclear plant.

As the non-electric use of nuclear grows in the hydrogen economy, issues of uranium reserves will become important. For this reason, fast breeder reactors would need to play a bigger role in either providing new nuclear fuel for thermal reactors and high temperature process heat for thermochemical water splitting systems. In addition, thorium represents an option for an intermediate stage expanding the availability of nuclear fuel. This will help in optimal use of nuclear fuels in closed cycles, which will result in a more sustainable transition. The transition technologies should be introduced in a step-wise fashion that matches supply and demand as the hydrogen economy develops in a growing market. Correspondingly H₂ cost reduction can be expected due to economies of scale and further improvements in hydrogen related systems. The objectives of a step by step to mass market are as follows:

Validate technical and economic viability;

- Receive feedback from real environment.
- Guide further R&D activities.
- Overcome main legal and political barriers.
- Define codes and standards well in advance.
- Get public and industry buy-in and that of other critical stakeholders early on.

Medium and long-term strategies for introducing nuclear hydrogen production into the market will start from the present use of hydrogen and the present methods. Technologies with reduced CO₂ emissions and those substituting natural oil and gas resources will have to be included in addition to the puristic CO₂ emission free approaches. Centralized large scale hydrogen production systems will have to be assessed together with decentralised systems using electricity and electrolysers at the client site.

Conventional Hydrogen Production

Hydrogen represents – like electricity – a secondary energy carrier to be converted from other primary energy resources. Conventional hydrogen production is mainly based on the conversion of fossil fuels; only a small share of about 4% of the world's H₂ production is from electrolysis. The future for hydrogen and the potential for nuclear generated H₂ will be driven by major factors such as production rates of oil and natural gas, societal and governmental decisions about global climate change gases and CO₂ emissions, and the economics of hydrogen production and transmission.

The most widely applied process for hydrogen production at present is steam reforming of natural gas or other light hydrocarbons. The necessary process heat can be substituted by nuclear process heat

from HTGRs, as has been successfully demonstrated in pilot plants under nuclear conditions in both Germany and Japan. The process is not CO₂ free but allows savings of natural gas of up to 30%, thus representing an important transition technology. The ultimate test for large-scale penetration of the energy market by hydrogen will be determined by the economics of production and end use. Consumer perceptions regarding availability and convenience of use will be important as well. Steam reforming of methane is used extensively by refineries. This approach may also allow opportunities for much nearer term utilization of nuclear power for hydrogen production. In addition, research is underway using membrane techniques that can re-circulate reaction product gases and can further reduce the CO₂ from steam reforming. Nuclear-assisted steam reforming of methane could constitute a strategy for a successful continuum towards other CO₂-free production approaches.

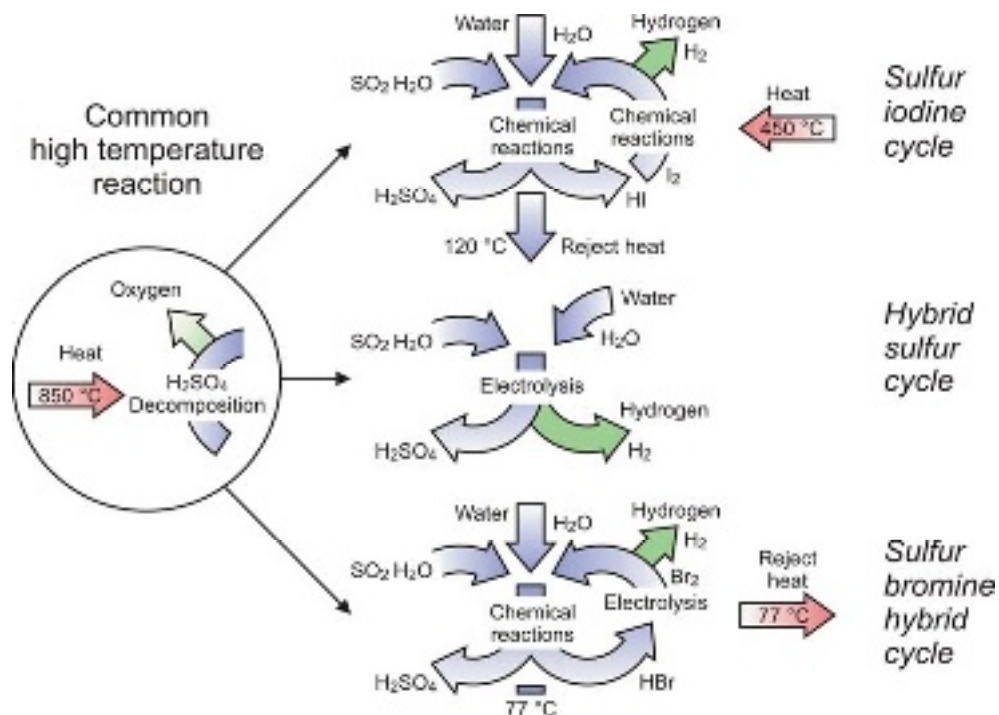
The other short-term option (next 5-15 years) is the production of hydrogen by electrolysis. Currently efficiencies are in the range of 60% to 80% and they may reach 90%. In addition, electrolyzers can be very attractive to serve as remote and decentralized production sites for H₂. The availability of cheap electricity, e.g., from hydropower is an essential prerequisite. In principle, off-peak electricity from existing LWRs can also be converted to hydrogen. H₂ from electrolysis is about 3 times more expensive than from petrochemical processes. The overall demand is balanced by the park of different power plant types: NPPs are operated for base load, using the advantage of low fuel costs and distribution of capital costs over continuous operation. Short temporary demand is supplied by plant with low investment/high fuel cost shares meaning that there is no off-peak situation for NPPs, unless there is a large share of NPPs in the plant park. A decision for deploying nuclear power for off-peak operation has to compare cost of NPPs and the flexible fossil fired plants. As fossil fuel becomes more expensive, the use of nuclear energy outside the base load region becomes more attractive and can be supplemented by hydricity approaches.

Nuclear Hydrogen Production in High Temperature Processes

High temperature processes are key technologies as hydrogen production efficiencies principally depend on (modified) Carnot laws. The efficiency of electrolysis can be enhanced by increasing the operational temperatures and considerably reducing the electricity needs. High temperature electrolysis (HTE) has to be built on high efficient electricity generation either on Brayton, Rankine or combined cycles. Benefits for the HTE development can also be taken from ongoing SOFC research efforts. HTE at moderate temperatures (< 850-900°C) would allow for less ambitious reactor coolant temperatures. The power size of the production units, availability requirements and necessary redundancies by modularization has to be assessed.

Thermal water-splitting requires temperatures of more than 4 000°C in the direct process but can also be done by successive chemical reactions on lower temperatures. The focus is on the candidate thermochemical processes based on the sulfur family including the Westinhouse hybrid cycle (see Figure 2) and here particularly on the common reaction process of sulfuric acid splitting. Another candidate process is the calcium-bromine or UT-3 cycle. Different coolants (e.g. molten salt, gas, liquid metals) in the intermediate circuit for coupling the nuclear with the chemical facility should also be studied. High temperature heat pumps may help to reach sufficient temperature levels without increasing the coolant gas temperature of the nuclear heat source beyond actual metallic materials limits. “Nuclear driven” steam reforming or coal gasification may well serve as a bridge to the water splitting processes.

Figure 2. Various thermochemical processes of the sulfur family to generate hydrogen



If the nuclear source is a very high temperature reactor (VHTR), the high temperature processes could be either thermochemical cycles or high temperature electrolysis. In both cases the complexity of the processes implies that capital and maintenance costs would be higher than for alkaline electrolysis and even further increased, because they are non-proven processes. The efficiency of the production of electricity by a VHTR can be estimated in the range $0.45 \leq \eta_{el} \leq 0.5$ the global efficiency of high temperature process for the production of hydrogen will have to be greater than 33% but preferably 36.5 % or more. This has a direct impact on the choice of technical options:

Operational process temperatures and heat source should be as high as technically feasible;

Thermochemical processes or electricity generation at lower temperatures will always be inferior with regard to the thermal efficiency η .

Since the dissociation temperature is extremely high, water splitting always needs several successive processes to provide the dissociation energy i.e. electricity generation plus electrolysis (plus heat) or a follow-up of different endothermic and exothermic VCH processes at lower temperatures.

As a result, it can be stated that a high temperature level is an absolute necessity and the final conversion efficiency is fundamentally independent of any route of conversion technology based on the assumption of the same conditions for input and output.

Safety of Combined Nuclear and Chemical Facilities

The coupling of a nuclear reactor to a hydrogen production plant located in a chemical complex requires special attention with regard to safety, regulatory aspects, and licensing. There is a need for nuclear process heat reactors to have a common approach, within the EU and the GIF, respectively, of

safety issues related with hydrogen such as explosions and fires, confinement and limits of contaminants (e.g., tritium), as well as reliable isolation of both nuclear and chemical plants. Current safety requirements, basically oriented to LWR nuclear plants, must be modified to Gen-IV and new reactors prone for hydrogen production which are inherently safe, reliable, and simple to operate. It also includes a set of new EU codes and standards applicable to the design, materials, fabrication, inspection, and quality of nuclear and hydrogen systems and components operating under these new conditions. This common EU regulatory frame work and standards will help the industrial deployment, coordinate licensing process, and reduce the uncertainties to obtain agreement by national and local authorities of the hydrogen/nuclear facilities.

European Activities on Nuclear Power and Hydrogen Production

In the European Union, there are no explicit research activities dedicated to nuclear hydrogen production. Respective research programs are either concentrating on the nuclear or on the hydrogen aspects. There is, however, a little overlap of both areas in such a way that research on innovative nuclear reactor designs also takes into consideration one of their most pronounced features, which is the possibility of penetration of the non-electricity market with H₂ production as a major issue. On the other hand, research projects which deal with large-scale H₂ production methods of the future, may also include the option of nuclear power to provide the required primary energy.

The Michelangelo Network has been with a strong focus on innovative nuclear reactor designs. As was mentioned already, MICANET was and still is involved in the initiation, preparation, and conduction of various EU research projects, mainly on the nuclear side, but also with some connection to the hydrogen side. Among the current nuclear projects with a certain relationship to hydrogen, the most important is the “Integrated Project” (IP) RAPHAEL, acronym for “Reactor for Process Heat, Hydrogen, and Electricity Generation”. The IP consisting of 35 partners started in April 2005 and has a duration of 48 months. Its main objectives are on the one hand a study of advanced gas-cooled reactor technologies, which are needed for industrial reference designs, but also taking benefit from the existing demonstrator projects in Japan and China. On the other hand, it will explore options for the new nuclear generation with “very high temperature” applications, i.e., at coolant exit temperatures of 1000°C and above. The proposal comprises efforts in all VHTR sections including reactor physics and thermodynamics, fuel, back-end, materials and components development, and safety.

In the European Union, it has been recognised in the meantime that for the introduction of hydrogen energy into the future energy market, political support, e.g., by public funding of research projects, is essential to stay competitive and a key to long-term success. Hydrogen production technologies are strongly focusing on CO₂-neutral or CO₂-free methods as represented by, e.g., biomass conversion or thermochemical water splitting processes or reforming of fossil fuels plus CO₂ sequestration. Primary energy sources include nuclear and renewable energies.

What MICANET represents on the nuclear side, this is the Hydrogen Network HYPNET on the hydrogen side. HYPNET was established in 1999 and created in 2002 as a “Thematic Network” within FP5 with initially 12 partners. It is working on the development of strategies for the introduction of a European hydrogen fuel infrastructure.

In 2002, a so-called “High Level Group on Hydrogen and Fuel Cells (HLG)” has been established by the European Commission (EC). Its principal task was to initiate strategic discussions for the development of a European consensus on the introduction of hydrogen energy. The group strongly recommended the development of an integrated European strategy on hydrogen energy by the creation of a political framework consisting of a partnership of major private and public hydrogen stakeholders.

The International Partnership for a Hydrogen Economy (IPHE) was launched in 2003 representing 15 countries and the European Union. Work is done here on governmental level to foster international collaboration on policy and research programs and thus to accelerate the transition to a hydrogen economy with the H₂ to come from multiple sources: renewables, nuclear, fossil plus sequestration. In 2004, the EC started another policy group, the “European Hydrogen and Fuel Cell Technology Platform”. Key elements of the integrated European strategy to be deployed include a strategic research agenda with performance targets, timelines, lighthouse demonstration projects, and a deployment strategy or roadmap for Europe. A “Quick Start” initiative launched by the EC resulted in 16 contracts (as of March 2004) after the first call covering various technologies of hydrogen (10) and fuel cells (6) with approx. 100 million Euro of EU funding within the actual FP6 to be matched by corresponding private funding [2].

Three of the awarded contracts are dealing with the production of hydrogen. HYTHEC is a specific targeted research project (STREP) with the objective to evaluate the potential of thermochemical processes, focusing on the sulfur-iodine cycle and on the Westinghouse hybrid cycle. Nuclear and solar will be considered as the primary energy sources with a maximum temperature of the process limited to 950°C. In particular, a large scale solar furnace will be used as an experimental tool to study the high temperature reactions. The Integrated Project CHRISGAS will develop and optimize an energy-efficient and cost-efficient method to produce hydrogen-rich gases from biomass. This gas can then be upgraded to commercial quality hydrogen or to synthesis gas for liquid fuels production. New process equipment will be developed and tested, and implemented in a pilot facility to produce hydrogen-enriched gas. In the Hi2H₂ STREP, it is proposed to develop a high temperature water electrolyzer with very high electrical efficiencies. The project will make use of technological developments that have been made in the field of high temperature fuel cells and evaluate a planar solid oxide water electrolyser.

HYWAYS is an IP proposed by HYPNET to elaborate a fully validated European Hydrogen Energy Roadmap as a synthesis of national roadmaps from the participating member states. It will comprise a comparative analysis of regional hydrogen supply options and energy scenarios including renewable energies. Technical, socio-economic and emission challenges and impacts of realistic hydrogen supply paths as well as technological and economical needs will be investigated. Starting in Phase 1 with a preliminary analysis for the six countries France, Germany, Greece, Italy, the Netherlands, and Norway, it will be extended by 5-7 more countries joining the project partnership.

HYSAFE is conceived as a Network of Excellence. The main objective will be to strengthen, integrate and concentrate existing capacities and fragmented research efforts aiming at the removal of safety-related barriers to the large-scale introduction of hydrogen as an energy carrier. By harmonising methodologies for safety assessment, the focus is on studies of fire and explosion safety, mitigating techniques, and detection devices. In this way, the network contributes to promoting public awareness and trust in hydrogen technology. Its specific objectives include:

- improve common understanding and approaches for addressing hydrogen safety issues;
- integrate experience and knowledge on hydrogen safety in Europe;
- contribute to EU safety requirements, standards and codes of practice;
- promote public acceptance of hydrogen technologies.

Conclusion

The main challenge at present is to include the production of hydrogen and combined heat and power applications by means of nuclear energy into the general strategies and to establish transition technologies from present industrial practice or emerging new resources (“dirty fuels”) in order to stabilize the cost for energy.

Acknowledgements

The work was conducted under the MICHELANGELO network funded by the European Commission (FIKW-CT-2001-20180).

REFERENCES

- [1] C.W. Forsberg, What is the Initial Market for Hydrogen from Nuclear Energy? Nuclear News, January 2005, 24-26.
- [2] European Commission,, Hydrogen Economy: New EU Hydrogen and Fuel Cell Quick Start Initiative, Press Release March 18, 2004,
<http://europa.eu.int/rapid/pressReleasesAction.do?reference=IP/04/363&format=HTML&aged=0&language=EN&guiLanguage=en>

This page intentionally left blank

SESSION III

INTEGRATED NUCLEAR HYDROGEN PRODUCTION SYSTEMS

Chairs: A. Miller, K. Verfonden

This page intentionally left blank

GTHTR300 DESIGN VARIANTS FOR PRODUCTION OF ELECTRICITY, HYDROGEN OR BOTH

X. Yan, K. Kunitomi, R. Hino and S. Shiozawa

Nuclear Applied Heat Technology Division
Nuclear Science and Energy Directorate
Japan Atomic Energy Agency
Oarai-Machi, Ibaraki-ken 311-1394, Japan

Abstract

Japan Atomic Energy Agency has undertaken an extensive design study of gas turbine high temperature reactor, named the GTHTR300. A design philosophy of system simplicity, economical competitiveness, and originality has enabled the evolution of a family of GTHTR300 plant design variants with production ranging from electricity to hydrogen or both. The key elements of this design philosophy are sharing of common system technologies, incorporating original design simplification, and focused research and development in quest for a strong and practical plant economy.

Common to all design variants is a block reactor of top rated power 600 MWt with passive safety and highest coolant outlet temperature 950°C by existing fuel and material. The reactor is combined, when appropriate, with an iodine-sulfur thermochemical process for hydrogen production and with a mechanically and aerodynamically similar line of direct cycle helium gas turbines for electricity generation. The generated electricity supplies reactor and hydrogen plant operations in addition to grid output. In all design variants the gas turbine circulates reactor coolant directly, obviating need for a dedicated primary coolant circulator. Comprehensive research and development programs have been carried out for enabling technologies, with the aim of supporting commercial readiness around 2015.

This paper discusses the family of GTHTR300 plant variants, their underlying system designs and associated research and development programs.

turbine power cogeneration. Thermochemical cracking of water molecules taking place in the IS process yields hydrogen gas product. Figure 1 shows the coupling arrangement of the IS hydrogen plant to the reactor gas turbine power plant. Added finally in this year is the GTHTTR300H, a self-reliant hydrogen production system that uses a major share of reactor thermal power for process heat input with the balance used by gas turbine to circulate primary coolant while still co-generating the significant electricity needed by hydrogen production as well as by reactor operations.

The overall goal of the commercial plant design study is to provide a family of system options capable of producing competitive electricity, hydrogen or a mix of both and yet deployable in the near term. The development of the multiple systems simultaneously does not necessarily suggest to have investment and risk multiplied. Rather, the development requirement is minimised thanks to a design philosophy of system simplicity, economical competitiveness and originality, namely the SECO philosophy. There are three major elements to this design philosophy.

The first element is technology simplification. All design variants are built on the premise that they share common system technologies to maximum extent possible. As a result, the design variants share a unified reactor and primary coolant circuit, an aerodynamically and mechanically similar line of helium gas turbines used for electricity production, and the IS process selected to produce hydrogen. This paper shows that the helium gas turbine and the IS process are compatible application systems with the high temperature reactor heat source to enable economically competitive energy production.

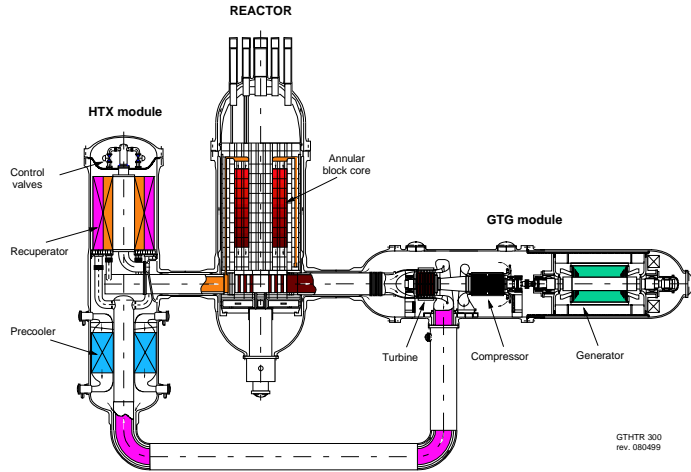
The second element of the SECO design philosophy has been incorporating unique design attributes that are less demanding on the system technologies required. The efforts in this area have resulted in such original design simplification as conventional steel reactor pressure vessel construction, horizontal gas turbine installation, system modular arrangement among others. Sections two and three of this paper discuss the technical design features of the GTHTTR300 plant variants in greater detail.

The third element that has been made possible by constant pursuit of technology and design simplification is a focused technological development scope that comes with low risk and investment of overall development. Furthermore, since the technologies to be developed are shared by several systems, the benefit of investing in any one development is increased. On the site where the HTTR is constructed for acquiring the reactor technology, JAEA has also been carrying out research and development on the helium gas turbine and the IS process. Section four of this paper describes the underlying systems and associated research and development activities.

2. GTHTTR300 & GTHTTR300+: Design variants for electricity production

In addition to being one of the two electric power generation options, the GTHTTR300 provides the baseline plant design upon whose reactor and system arrangement all other design variants, including those of hydrogen plants to be described in the next section, are based. As seen in Table 1, the reactor outlet coolant temperature is selected to be 850°C. While the selected temperature is modest comparing with the capability of the present fuel, it is intended to avoid turbine blade cooling with use of conventional blade materials.

Figure 2. Reactor system arrangement in GTHTR300 and GTHTR300+



The GTHTR300+ is a growth system that achieves growth in performance by advancing operational parameters with no change to be made in integrated system design. The reactor outlet temperature is raised to 950°C, matching the top coolant temperature of the HTTR. To retain similar reactor core physics design, fuel burnup period is shortened by half a year from that of the baseline design. Because of the higher reactor outlet temperature the turbine blade is now cooled by compressor bleed cold helium. The blade cooling need may be minimised by adopting advanced heat resistant alloys developed for advanced combustion gas turbines with trace of activating elements removed to suit nuclear service. The growth system also relies on reasonable advancement to be made in gas turbine aerodynamic efficiencies and recuperator effectiveness as indicated in Table 1.

Table 1. GTHTR300 and GTHTR300+ design parameters

	GTHTR300 — baseline design —	GTHTR300+ — growth system —
Reactor thermal power	4 x 600 MWt	4 x 600 MWt
Net electric generation	1096 MWe	1200 MWe
Net generating efficiency	45.6%	50%
Plant capacity factor	>90%	90%
Reactor type	graphite moderated, helium-cooled, prismatic block fuel	graphite moderated, helium-cooled, prismatic block fuel
Reactor pressure vessel	SA533 (Mn-Mo) steel	SA533 (Mn-Mo) steel
Core inlet temperature	587 °C	663 °C
Core outlet temperature	850 °C	950 °C
Coolant inlet pressure	6.92 MPa	6.42 MPa
Coolant flow	439 kg/s	401 kg/s
Core power density	5.4 W/cc	5.4 W/cc
Average fuel burnup	120 GWd/ton	120 GWd/ton
Refueling interval	24 months	18 (24) months
Gas turbine cycle type	recuperated, non-intercooled, direct Brayton cycle	recuperated, non-intercooled, direct Brayton cycle
Gas turbine pressure ratio	2.0	2.0
Gas turbine inlet temperature	850 °C	950 °C
Turbine polytropic efficiency	92.8%	93.8%
Compressor polytropic efficiency	90.5%	91.5%
Recuperator effectiveness	95%	96%

As shown in Figure 2, the reactor system is made up of three modular pressure vessel units containing the reactor core assembly, the gas turbine generator, and the heat exchangers, respectively. The units are housed in separate buildings in construction. Partitioning the primary system into properly sized modules and arranging them separately facilitate cost-effective shop construction and parallel site construction. These functionally-oriented modular units are independently accessible in maintenance. The GTHTR300 and GTHTR300+ are characteristic of following design features:

- Fully passive reactor safety.
- High fuel burnup based upon the HTTR type fuel.
- Conventional steel reactor pressure vessel construction.
- Non-intercooled, direct Brayton cycle power conversion.
- Horizontal, single-shaft gas turbine and direct drive of synchronous electric generator.
- Odular system arrangement.

Figure 3 shows a schematic of the direct Brayton cycle employed. Cycle intercooling is ruled out, even though it yields two-percentage points higher efficiency, because the added complexities and costs in construction and operations offset the marginal efficiency gain, resulting in no net benefit in cost of electricity [4]. On the other hand, cycle recuperation, that recovers significant turbine exhaust heat, offers substantial efficiency gain and thus a compelling economical case for design choice. A 95-96% effective recuperator is feasible by employing compact plate heat exchangers operating in high pressure benign helium gas streams.

Figure 3. Recuperative direct Brayton cycle

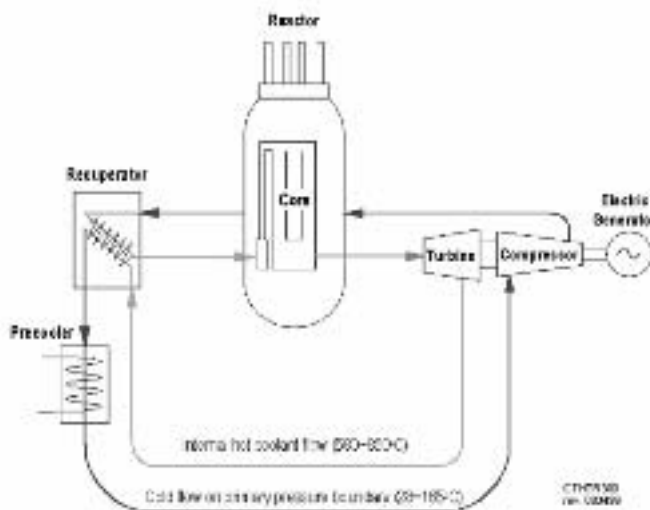
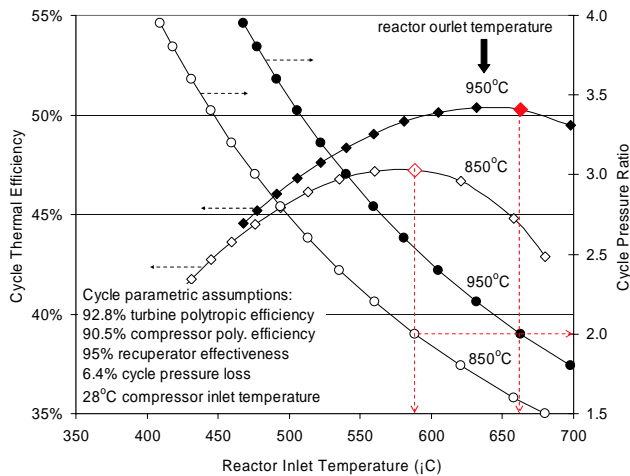


Figure 4 helps explain methodical selection of several other important cycle parameters. As stated earlier, the reactor outlet coolant temperature is set to 850°C for the GTHTTR300 cycle and increased to 950°C in the GTHTTR300+ cycle due in part to whether the turbine blade cooling is warranted. For each of these given core outlet temperatures, core inlet coolant temperature has been selected as appropriate for arriving at peak cycle thermal efficiency. As seen, the core inlet temperature is 587°C for the 850°C core outlet temperature cycle and 663°C for the 950°C cycle. The resulting relatively high core inlet temperatures in both cycles offer design benefit important to reactor core, which is a topic of more detailed discussion in Section 4 of this paper.

Figure 4. Brayton cycle characteristics



The gas turbine cycle pressure ratio corresponding to peak thermal efficiency remains nearly identical at around 2.0 for both the 850°C and 950°C core outlet temperature cycles. This is the basis for the baseline and growth cycles to employ a similar line of gas turbines, which is another topic to be discussed later in Section 4.

A commercial plant will consist of four reactor primary system units (4 x 600 MWt) operating in parallel, each of which is housed in its own underground confinement structure, but shares most other operations and maintenance facilities and functions. The power plant rating is 1 096-1 200 MWe busbar output at a net efficiency of 45-50%. The estimated cost of electricity is less than 3.5¢/kWh, about 30% below the cost of existing LWRs in Japan.

3. GTHTR300C & GTHTR300H: Design variants for hydrogen production

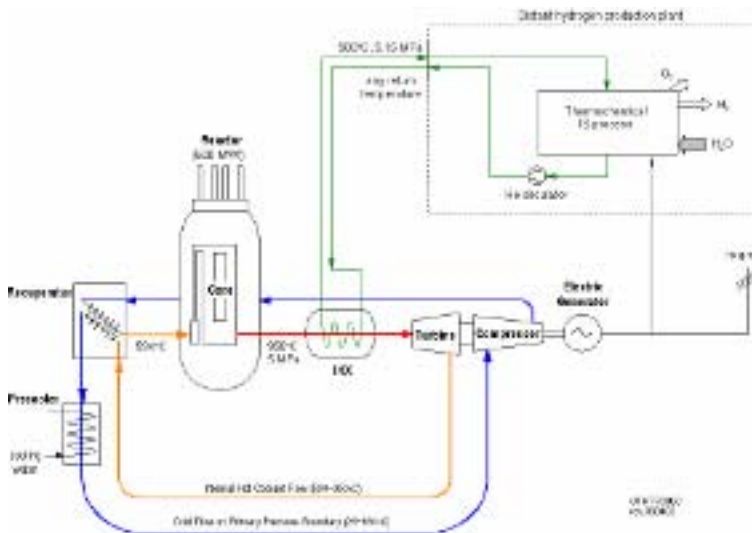
The two design variants, GTHTR300C and GTHTR300H, add variable hydrogen production capability in the GTHTR300 plant family. Like the power plant design variants, the hydrogen production plants are based on identical integrated system design and the variable hydrogen production is met by adjusting operating parameters only. The GTHTR300C produces hydrogen using effectively one-third of reactor thermal power with the balance of the reactor power going to electric power production. The GTHTR300H is designed to be a self-reliant hydrogen production system. Not only it yields massive hydrogen production using effectively 85% of reactor thermal power but also it has the ability to co-generate the significant electric power needed to support hydrogen production and reactor operations. In all GTHTR300 plant variants, the direct cycle gas turbine circulates reactor coolant directly, thereby obviating development need for a dedicated coolant circulation system.

The cogeneration cycle shown in Figure 5 evolves from the power-only production cycle, shown previously in Figure 3, by adding an intermediate heat exchanger (IHX) in serial between reactor and gas turbine. The particular serial arrangement makes the logarithmic mean temperature difference as large as 150°C between the primary and secondary fluids, creating a design condition for compact IHX. A secondary loop circulates hot helium from IHX to the distant hydrogen plant and completes necessary environmental separation between the nuclear facility from the chemical plant [5].

In GTHTR300C a nominal 170 MWt of the total 600 MWt per reactor thermal power, is extracted through the IHX as process heat input to the hydrogen process and the balance of reactor thermal power is used for gas turbine electric power generation. The reactor outlet helium gas of 950°C enters the shell

side of the IHX and heats the tube-side secondary helium to 900°C. The helium gas of 850°C exiting the shell side of the IHX enters the gas turbine power conversion cycle. A gross of 202MWe electricity is generated at an estimated 46.8% efficiency. About 12% of the electricity generated is used in hydrogen plant operations to power electrolyzers, circulators, pumps and other utilities. Combining the process heat and the thermal equivalence of electricity gives a 219 MWt effective thermal input to hydrogen production.

Figure 5. Electricity and hydrogen cogeneration cycle of GTHTR300C and GTHTR300H



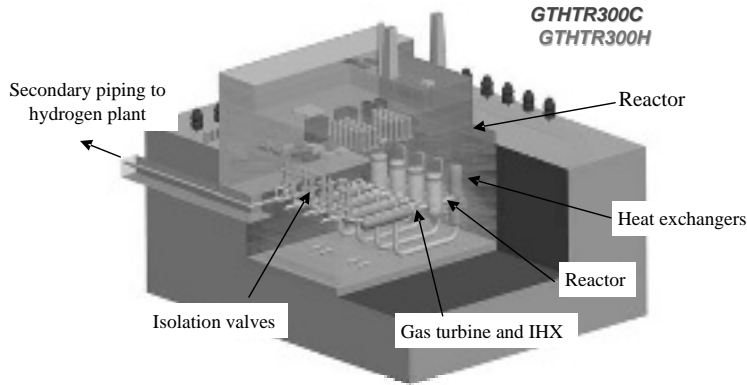
In the case of GTHTR300H, a major fraction of the total reactor thermal power, 371 MWt, is extracted from the IHX. The reactor outlet helium gas of 950°C enters the shell side of the IHX and heats the tube-side secondary helium to 900°C. Due to the significant IHX heat extraction, the primary helium gas that leaves the shell side of the IHX is now at 730°C. This temperature is still high enough to power the highly-recuperative gas turbine to generate 87.6 MWe at 38.3% cycle efficiency in addition to circulating reactor coolant. A majority of the generated electricity is used to meet the electricity demand in hydrogen production. Combining the process heat and thermal equivalence of electricity consumption gives 505 MWt effective thermal input to hydrogen production process.

The primary coolant pressure is lowered to 5 MPa from 7 MPa for the power-only reactor for two design considerations. The first is to reduce the design pressure loads on a host of high temperature heat exchangers, including IHX and chemical reactors, to secure sufficient life of these usually costly components. The second consideration is to maintain design and performance similarity of the gas turbines to the baseline unit of the GTHTR300. The gas turbine design approach will be revisited in detail in the next section. Although the lowered primary pressure increases specific cost of gas turbine equipment, the benefits gained in the heat exchanger life cost saving and for gas turbine technology simplification offer more compelling design advantage.

The commercial plants of the GTHTR300C and GTHTR300H are depicted in Figure 6 to each consist of four reactors operating in parallel, adapting the same system arrangement described earlier for the electricity-only generating plants. Table 5 provides the design parameters and the rated electricity and hydrogen product rates from the four-reactor commercial plants. The nuclear produced heat is transported by the secondary helium circulation loop over a safe distance to the hydrogen plant inside a coaxial hot gas piping, which is a proven component of the HTTR.

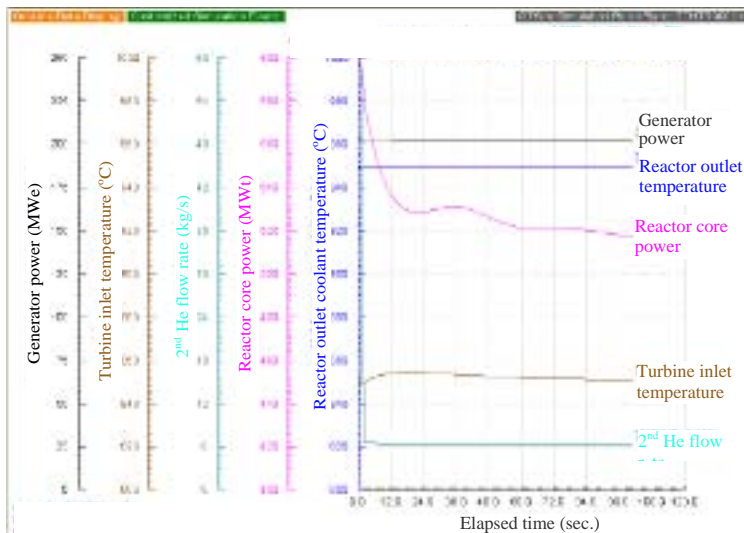
The layout for a commercial plant is depicted in Figure 6 to consist of four reactors operating in parallel, adapting the same system arrangement described earlier for the electricity-only generating plants. The nuclear produced heat is transported by the 2nd helium circulation loop over a safe distance to the hydrogen plant inside a coaxial hot gas piping, which is a proven component of the HTTR. Table 5 provides the design and production specification of the four-reactor commercial plants.

Figure 6. GTHTR300C and GTHTR300H commercial plant arrangement



Although a cogeneration system, the GTHTR300C may operate with one production in partial or full absence of the other, ensuring operational flexibility and stability in scheduled or forced outage. A simulated response to a hydrogen plant load upset is shown in Figure 7. Reactor operating parameters are shown to undergo orderly transient while maintaining stable production of electricity. The reactor outlet coolant temperature remains essentially constant due to large thermal capacity of the graphite core whereas the reactor power is brought down by the negative temperature coefficient of reactivity of the inherent core design. The turbine inlet temperature is returned, following a modest rise, to the rated value, by bypassing 10% compressor discharged cold gas to the fore of turbine to mix with the rising temperature gas there. Though not explicitly shown in Figure 7, the water cooled pre-cooler acts as a passive thermal shock absorber that prevents thermal excursion from occurring anywhere in primary coolant circuit. Should the hydrogen plant load remains off in extended time, core outlet temperature would be brought down gradually from 950°C to 850°C by insertion of reactor power control rods.

Figure 7. GTHTR300C plant response to 100% to 10% loss of IS hydrogen plant heat load



Likewise, the simulation of the cogeneration system to a loss of electricity load showed that stable production of hydrogen could be maintained in the IS process plant.

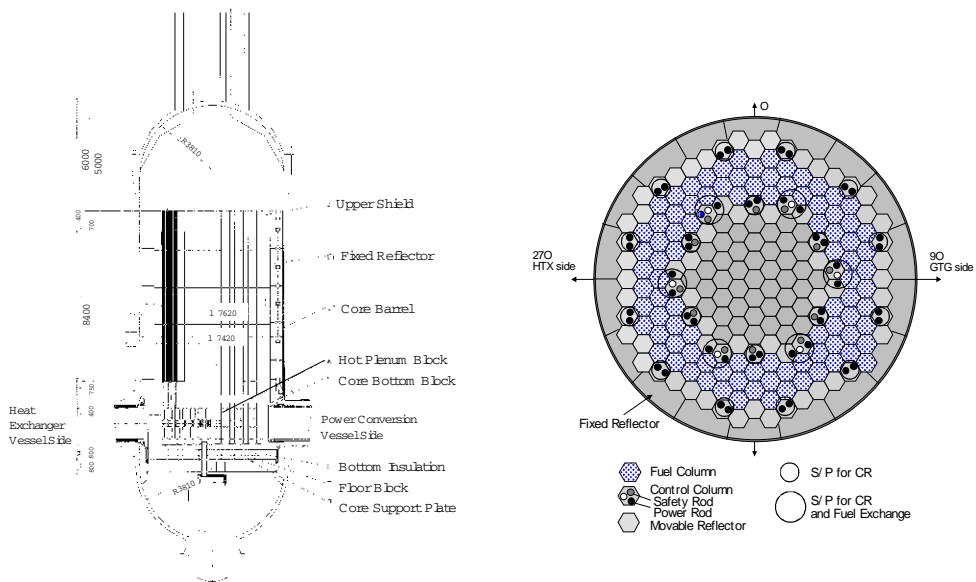
4. Systems and related R&D

The family of the GTHTR300 plant variants are based on three shared system technologies including reactor, helium gas turbine and, in the case of hydrogen production, the IS process system. This section discusses the underlying system designs and related research and development activities.

4.1 Reactor system

A unified reactor system design, including structural, thermal and physics designs, is employed by the GTHTR300 design variants. Table 2 summarises the overall reactor design parameters. As shown in Figure 8, a steel reactor pressure vessel (RPV) contains the graphite-moderated, helium-cooled prismatic core assembly. A unique reactor coolant circuit incorporates a pair of horizontal coaxial ducts providing the inner passage to channel hot helium gas into and out of the central core and the outer passage for cold helium gas to envelope the inner surface of the RPV. As a result, the RPV is maintained without active cooling in an operating temperature range that qualifies the 371°C design limit of conventional steel (SA533/508) for reactor pressure vessel construction. Details of this intrinsic RPV cooling scheme has been reported elsewhere [4].

Figure 8. The reactor design



The reactor active core consists of an annular ring of fuel columns surrounded by inner and outer replaceable reflector columns that partly contain control rod insertion channels. The core is embraced by outer permanent graphite reflector and enclosed in a steel core barrel. Each fuel column is stacked of eight hexagonal fuel blocks high and capped at top and bottom with reflector blocks. Dowels are used to align fuel blocks securely in a column. The fuel rods are located in the coolant holes of a fuel block. Burnable poisons are stored in three full-length holes. As shown in Figure 8, the coolant gas enters the reactor via the inner pipe of the horizontal coaxial duct on the left and travels upwards the gas channels embedded in the side reflector, turns in the top gas plenum to flow downward in the active core, and exits through the inner pipe of the horizontal coaxial duct on the right.

Table 2. Reactor design parameters

	GTHT300 - power plant - simple design	GTHT300+ - power plant - simple design	GTHT300C - power plant - GTHT300H - simple design
Reactor rating	600(MW) @ 850°C	600(MW) @ 950°C	600(MW) @ 950°C
Reactor design	Pressure vessel		0 - 0000
Fuel design	60 TRISO particles		0 - 0000
Reactor pressure vessel size	2.6x3.0x3.0 (m)		0 - 0000
Reactor fuel cycle	24h		0 - 0000
Refueling method	2 fuel rods/cycle		0 - 0000
Core physics design			
Fuel volume	30		0 - 0000
Inner reflector volume	25		0 - 0000
Outer reflector volume	45		0 - 0000
Core height (m)	3.0		0 - 0000
Average power density (W/m ³)	5.4		0 - 0000
Average burnup (GWd/t)	23		0 - 0000
Peak power factor	22		0 - 0000
Peak fuel density (g/cc)	1.6		0 - 0000
Enrichment (wt%)	8	7	0 - 0000
Average enrichment (wt%)	14.5	14.2	0 - 0000
Reactor pressure (MPa)	4	4	0 - 0000
DP (m/s)	4.0	7.6	0 - 0000
Reactivity margin (beta)	2-	1.8	0 - 0000
Reactor power scale factor	1.15	1.10	0 - 0000
Core thermal design			
Outlet (inlet) flow rate (kg/s)	429	405	322
Core inlet temperature (°C)	557	605	594
Core outlet temperature (°C)	850	950	950
Core inlet pressure (MPa)	1.6	1.6	1.6
Core outlet pressure (MPa)	28	28	28
Min. fuel element flow factor	1.32	1.20	1.20
Max. fuel temperature (inlet) (°C)	1108	1202	1244
Max. fuel temperature (outlet) (°C)	1546	1594	1635

The fuel burnup averages 120GWd/ton. Several enrichment zones averaging about 14% enrichment are chosen to make as less as possible power peaking factors, which are limited to less than 1.16 through a burnup period. This in combination with large coolant flow checks fuel operating temperatures in a range expected to result in low fission product activity in the primary circuit to ease equipment maintenance.

The GTHT300 reactor system has been designed based on the technologies and design codes developed and validated on the test reactor HTTR shown in Figure 9 and with further technical base for high burnup fuel [6] to allow specification of a modified TRISO coated particle fuel to meet commercial system objectives [7].

Figure 9. The HTTR test reactor



The characteristic design of low power density and peaking factor limits the maximum fuel temperature that could be reached during passive conduction cooldown following accidents. Figure 10

shows the transient temperatures of fuel and RPV in a loss of coolant accident (LOCA), in which decay heat is conducted from the central graphite core to the reactor pressure vessel and then removed by thermal radiation off the external wall of pressure vessel to surrounding reactor cavity cooling panels. The maximum temperatures reached in this as well as other bounding safety events satisfy the design limits of the fuel and pressure vessel

The IHX is a critical barrier component of the reactor pressure boundary. The present design selects a helical tube and shell heat exchanger because the same type is used in constructing the HTTR as shown in Figure 11. The Ni-base Hastelloy-XR was developed for this application as heat-resistant helium-service tubing material. A high temperature structural guide was established in design and licensing. The IHX structural integrity and thermal performance are demonstrated in operations at 950°C in the HTTR. Figure 11 compares the IHX designs for the GTHTTR300C and HTTR. Similar operating conditions are observed and the same tubing material and similar stress limits are followed in both designs. Because of GTHTTR300C IHX having a large LMTD, a rather compact tube bundle is sized and placed within the cylindrical envelope provided by the gas turbine horizontal pressure vessel (refer to Figure 6). Further study of the placement will be in order to optimise installation, including consideration for alternative arrangement following the HTTR IHX installation practice [8] and new designs such as the one under independent industrial study on plate IHX to develop fabrication, ISI methods and a design standard for gas reactors [9]. A proven plate IHX would make it simpler to integrate IHX into the gas turbine vessel unit.

Figure 10. Reactor maximum temperatures in LOCA passive conduction cooldown

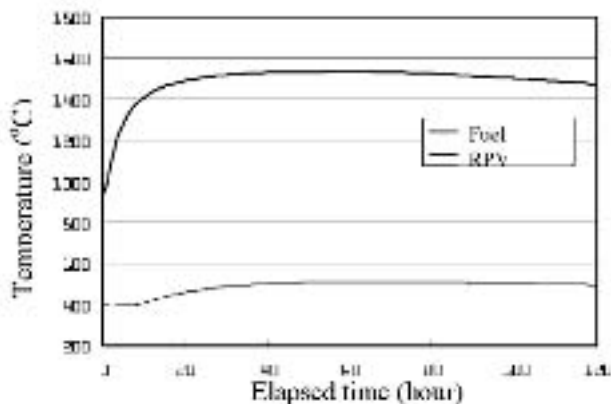
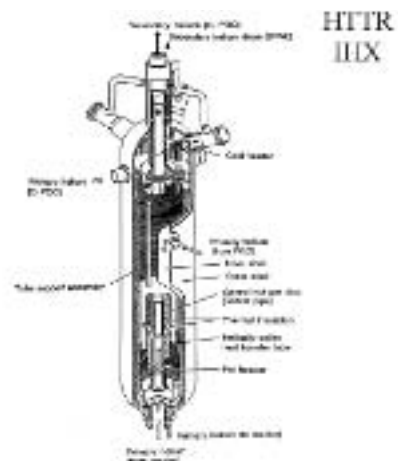


Figure 11. The IHX design comparison

	GTHTR300C	HTTR
	IHX	IHX
Thermal rating (MWt)	168	10
Primary inlet/outlet temperature (°C)	950/850	950/389
Secondary inlet/outlet temperature (°C)	500/900	237/868
Primary side pressure (MPa)	5.02	4.06
Secondary side pressure (MPa)	5.15	4.21
LMTD (°C)	154	113
Heat transfer tubing	Hastelloy XR	
OD x t (mm)	45 x 5	31.8 x 3.5
Ave. length (m)	14	22
Tube number	724	96
Helical tube bundle sizing		
OD x L (m)	4.57 x 2.97	1.31 x 4.87
Weight (ton)	51	5.4
Design lifetime (yr)	20	20

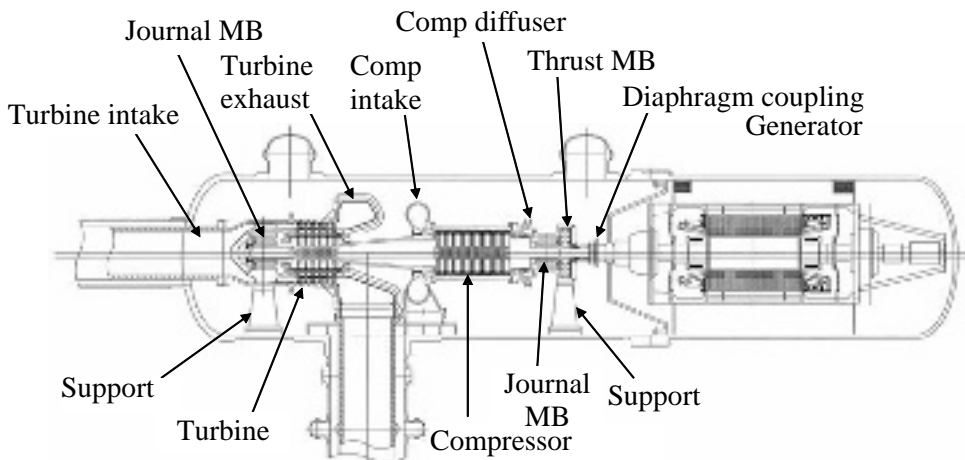


4.2 Helium gas turbine

High aerodynamic efficiency, reliability and serviceability are key performance requirements for helium gas turbine to qualify for nuclear power generation service. Besides little practical experience exists in the area, development of helium gas turbine to meet these performance goals presents a technical challenge, the extent of which proves to depend heavily on design choices made. The design approach for the GTHTR300 helium gas turbine has been to take advantage of successful experience in combustion gas turbines, while incorporating new design elements when must [4].

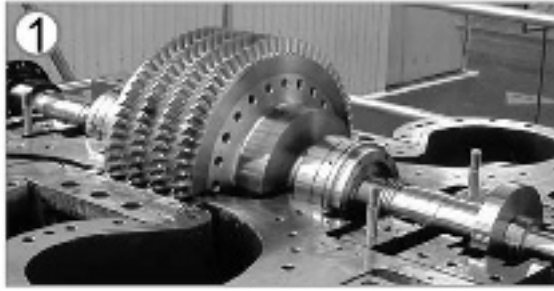
As shown in Figure 12, the baseline design of helium gas turbine is a single-shaft, axial-flow design having six turbine stages and twenty non-intercooled compressor stages. The gas turbine rated at 300 MWe and 3 600 rpm drives a synchronous generator from shaft cold end by a diaphragm coupling. The machine is placed horizontally to minimise bearing loads. These design features have been chosen in consistence with the established industrial practice in combustion gas turbines. The new gas turbine elements incorporated in the baseline unit are the narrow compressor flowpath, which is the result of working in helium, and the use of rotor magnetic bearings (MB) to avoid large pressure boundary penetration or potential lubricant contamination to reactor system. The development and test programs have been carried out to validate the new technology components uniquely present in this application.

Figure 12. Baseline design of GTHTR300 horizontal helium gas turbine in pressure vessel



Shown in Figure 13 is a model test compressor consisting of four axial stages in one third dimensional scale of the full size compressor stages. The test compressor was modeled after the aerodynamic features, including alternative sets of airfoils, under design consideration for the GTHTR300 baseline gas turbine compressor. It was put in a dedicated helium loop for aerodynamic development testing. The data obtained in test are concerned with aerodynamic losses particularly near end walls and growth through multiple rotating blade rows, surge predictability, clearance loss and inlet and outlet performance effects, all to be correlated closely to the full-scale design conditions.

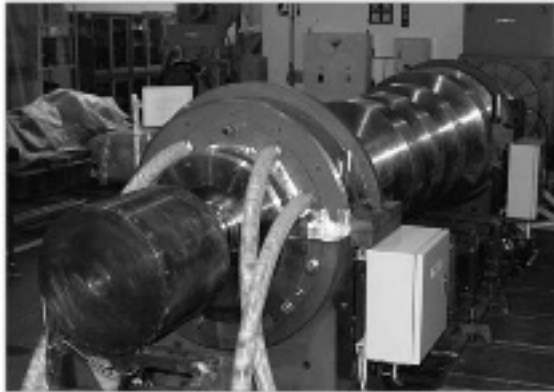
Figure 13. Test compressor of 1/3 full scale



The multi-year compressor development and test programme has just been concluded. The programme has achieved the intended goals of exploring basic helium compressor aerodynamics, relative to those of air compressors, and establishing the analytical tools qualified to design and evaluate the full scale compressor. With the qualified tools, the full scale compressor is predicated to over-achieve the design target of 90.5% flange-to-flange polytropic efficiency at design flow and surge margin. The level of performance matches those found in modern air gas turbine compressors. The helium compressor aerodynamics has well been advanced to proceed to prototype demonstration.

A magnetic bearing development and test programme is focused on evaluating optimal rotor-bearing clearance control method and developing magnetic bearing control algorithm to operate rotor above the 2nd bending critical speed. A test rig has been constructed and is presently undergoing commissioning. As shown in Figure 14, the test rig is a one-third scale mockup for the generator rotor of the GTHTR300 and has further built-in capability to test the multi-span and multi-bearing rotor configuration modeled after the GTHTR300 turbine-generator rotor drive train. Existing and new analytical techniques of rotordynamics and control will be test calibrated.

Figure 14. MB rotor test rig of 1/3 full scale



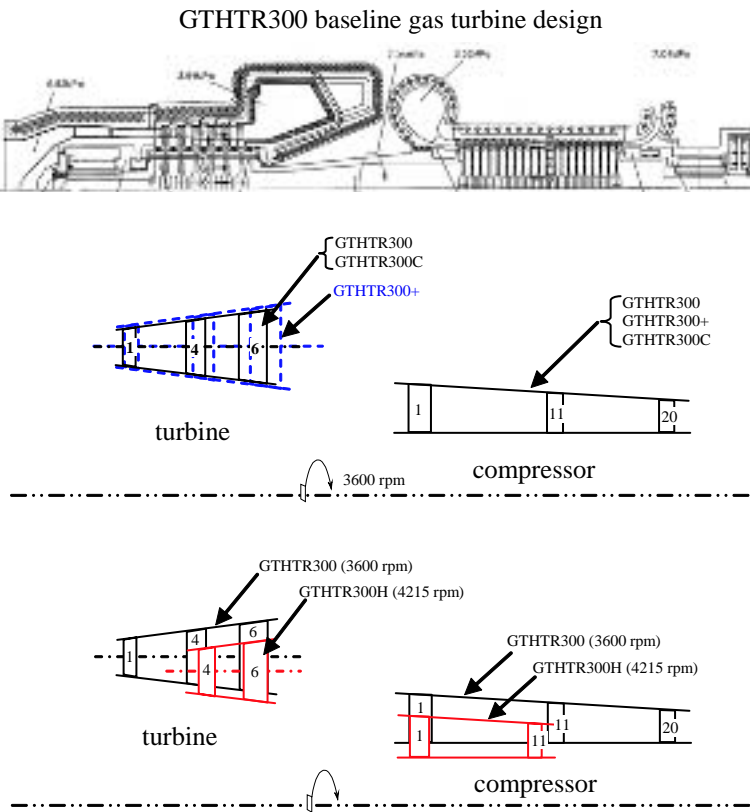
The baseline helium gas turbine design with its component development described so far is the unit in use in the power plant design variant, the GTHTR300. For the units used in other plant variants, geometric scaling from the baseline design has been applied to achieve design and technology simplification in accordance with the SECO design philosophy.

The scaling method is based on the principle that one can increase or decrease system pressure and alternatively or simultaneously increase or decrease the rotor diameter while holding the speed constant to produce aerodynamically and mechanically similar gas turbines of larger or smaller unit capacity. The complex blade airfoils, such as those obtained in the helium compressor development, become simply scalable from one machine to the other and the resulting aerodynamic working

conditions and efficiencies are unchanged. The centrifugal stresses remain also unchanged in discs and blades. This makes the technologies developed for the baseline unit also applicable in other units.

Figure 15 depicts the scaling method and Table 3 lists the base scaling parameters used. Starting from the GTHTR300 baseline gas turbine design, the compressors of GTHTR300+ and GTHTR300C retain the baseline flowpath and airfoils by a reduction in compressor inlet pressure to adjust to their respective through flow capacity. The reduction in compressor inlet pressure also achieves the corresponding effect of invariable basic geometry for the turbines of GTHTR300+ and GTHTR300C. Because the GTHTR300+ turbine operates in 100°C higher than the 850°C baseline turbine inlet temperature, its flowpath is widened by 9% around the mean pitch line. The number of compressor and turbine blade rows is the same due to the same pressure ratio specified in the underlying cycles.

Figure 15. Gas turbine scaling for the family of GTHTR300 plants



Relative to the GTHTR300 baseline gas turbine unit, the GTHTR300H unit has 1.47, instead of 2.0, compressor pressure ratio and 730°C, rather than 850°C, turbine inlet gas temperature. Because of the lower pressure ratio, the number of turbine and compressor stages necessary for the GTHTR300H is reduced. The GTHTR300H turbine adopts the rear three stages (4-6 stages) and the compressor the front eleven stages (1-11 stages) from the GTHTR300 baseline turbine and compressor, respectively. Furthermore, the diameter is reduced while holding rotor speed constant, to adjust to the reduced through flow of the GTHTR300H gas turbine while retaining similar aerodynamic conditions and mechanical stresses. The diameter reduction calls for increase in rotational speed from 3 600 to 4 215 rpm for the GTHTR300H. The asynchronous speed is acceptable because the generated electric power, 85 MWe, is meant mainly for in house consumption by hydrogen plant to power helium circulators, variable speed pumps, and to convert to direct current power source for use in process electrolyzers. The GTHTR300H gas turbine is significantly shorter and more compact. So is the

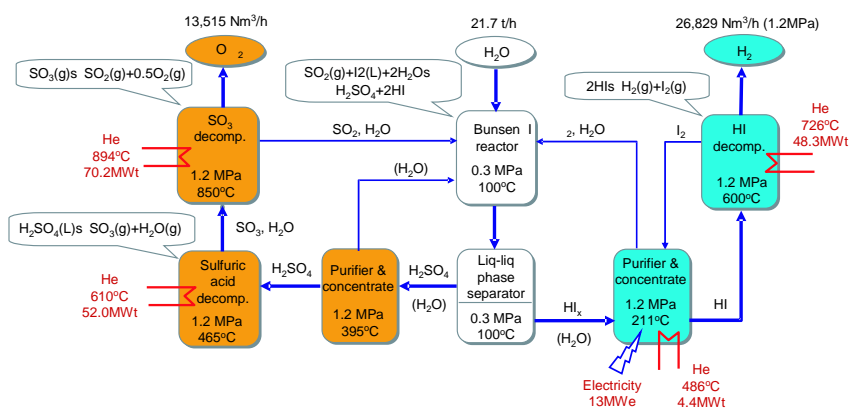
downsized electric generator of a reduced duty. The entire rotor train becomes considerably stiffened, making magnetic bearing suspension less challenged.

Table 3. Gas turbine scaling parameters

Unit	Gas turbine			Compressor section				Turbine section			
	Rotation speed [rpm]	pressure ratio	Mass flow [kg/s]	Inlet temperature [°C]	Inlet pressure [MPa]	rim speed [m/s]	Number of stages	Inlet temperature	Inlet pressure [MPa]	mean speed [m/s]	Number of stages
GTHTR300	3,600	2.00	445	28.0	3.5	282	20	850	6.8	377	6
GTHTR300+	3,600	2.00	408	28.0	3.2	282	20	950	6.2	377	6
GTHTR300C	3,600	2.00	327	26.2	2.6	282	20	850	5.0	377	6
GTHTR300H	4,215	1.47	327	26.2	3.5	282	11	730	5.0	377	3

4.3 IS process system

Figure 16. IS process heat and mass balance

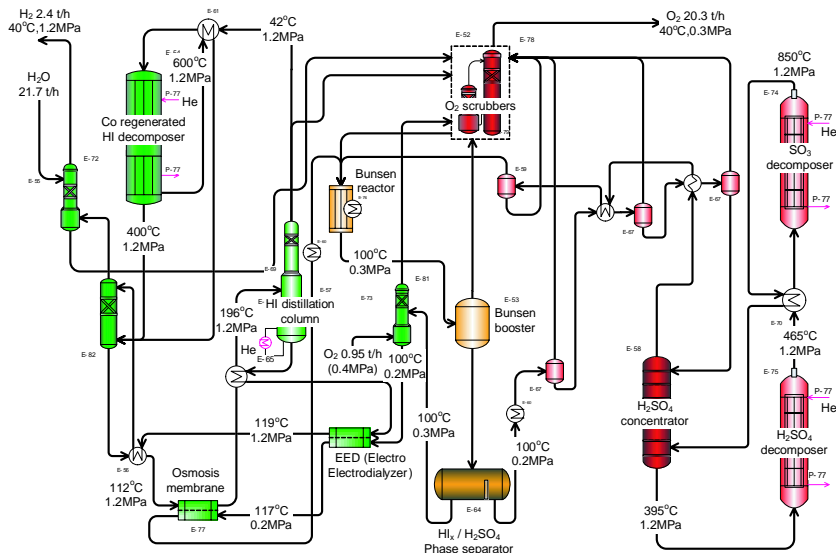


The IS process shown in Figure 16 involves three inter-cyclic thermochemical reactions to dissociate water molecules into hydrogen and oxygen gas products with heat and minor electricity as required energy input and with water as the only material feed. All process materials other than water are reagents. The nuclear generated heat in form of hot helium gas is used in various steps of process stream concentration and decomposition. The electric energy is used to power process electrolysers, gas circulators, pumps and other utilities. The energy and material balance provided in Figure 16 is representative of the GTHTR300C IS process corresponding to a nominal thermal input of 175MWt from the secondary helium circulation loop. For the GTHTR300H, the balance of energy and materials needs to be adjusted to the actual thermal rate while the marked process temperature and pressure conditions remain applicable to both systems.

The process flowsheet as presently developed is shown in Figure 17. The exothermic Bunsen reaction produces two aqueous solutions of sulfuric acid and hydriodic acid from material feeds of water, sulfur dioxide and iodine. The reaction favors presence of excess water and iodine to make it spontaneous and with iodine rich hydriodic acid (HI_x) formed to facilitate subsequent phase separation. The excess of water and iodide, however, imposes heavy process stream loads upon subsequent reactions, particularly so in the HI reaction steps. Though not yet reflected in the present flowsheet, improved reaction conditions are being studied with the goal of significantly reducing excessive reactants in order to simplify overall process and production cost.

In the endothermic sulfur reaction, sulfuric acid H_2SO_4 from Bunsen reaction is purified and concentrated before being decomposed in steps into H_2O and SO_3 and then to SO_2 and byproduct oxygen gas, involving heat temperatures up to $850^\circ C$. The sulfur reaction is relatively well established and the main technical issues are concerned with having decomposers that are sufficiently heat and corrosion resistant. These practical problems are being tackled in industrial trial fabrication of the key component elements completed with strength and performance evaluation.

Figure 17. GTHTR300C IS process flowsheet



In the endothermic HI reaction, hydriodic acid HI_x from Bunsen reaction is concentrated in a number of steps and the resulting hydrogen iodide concentrate is decomposed into reagent iodine and product hydrogen gas. The HI reaction steps appear to have the largest room for process improvement, for which several innovative process techniques have been incorporated in the present flowsheet. The HI concentration steps combine electro-electrodialysis cell and carbonized osmosis membrane to reduce excess iodine and water prior to final distillation. An iodine absorber is integrated into the HI decomposer to improve decomposition ratio in a newly proposed Co-regenerated process:

- (1) $2HI \rightarrow H_2 + I_2$ ($400^\circ C$)
- (2) $Co + I_2 \rightarrow CoI_2$ ($400^\circ C$)
- (3) $CoI_2 \rightarrow Co + I_2$ ($600^\circ C$)

- (4) $2HI \rightarrow H_2 + I_2$

Table 4. GTHTR300C IS process efficiency

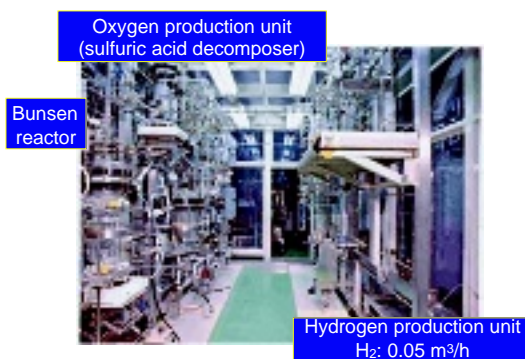
Thermal heat (MWt)	Electricity consumed (MWe)	Electricity cogeneration efficiency	IS plant net efficiency (HHV)
170.0	21.7	40	42.4%
		45%	43.6%
		50%	44.6%

By absorbing product I_2 from reaction (1) in the presence of reaction (2), as high as 80% once-through HI decomposition ratio is achievable in net reaction (4) as has experimentally been observed. The cobalt and iodine are regenerated in endothermic reaction (3).

The IS process efficiency has been estimated from a detailed flowsheet and best known process database. An overall process efficiency is defined as high heating value of total hydrogen produced against total thermal energy consumed. The total thermal energy consumption includes both the heat input and the thermal equivalent of electricity input needed to sustain hydrogen production operations. As presented in Table 4, the GTHTR300C delivers 170 MWt heat through IHX, which is distributed to several endothermic reactions (refer to Figure 16), and supplies additionally 21.7 MWe electricity mostly consumed by the process electrolyser (about 13MWe), and next by helium circulator (about 5MWe). The electricity supplied is co-generated in house by gas turbine at 47% gross efficiency. The overall efficiency is about 44% net with a hydrogen production rate of 26,829 Nm^3/h or 2.4 ton/h.

JAEA continues long-term basic studies to identify heat and corrosion resistant materials suited for constructing demanding acid reactors, propose innovative process techniques to improve efficiency [10], and develop techniques of closed-cycle operations and automation [11]. Figure 18 shows a bench scale test apparatus used in process automation study. The results of the basic studies have allowed the efforts now being made to address practical issues in appropriate scales. A pilot plant to test 30 m^3/h hydrogen production is being implemented. The technical and engineering data bases to be acquired in the pilot plant will enable JAEA to move forward with the final R&D goal of demonstrating nuclear production of hydrogen at 1000 m^3/h in an HTTR coupled test plant.

Figure 18. Bench scale IS process test apparatus



5. Summary

The SECO design philosophy of system technology sharing, design simplification, and focused R&D has enabled evolution of the GTHTR300 design variants that allow a flexible range of electricity and hydrogen products per reactor as indicated in Figure 19. Table 5 provides product ratings of commercial plants combining four reactors per plant. The ability to produce or co-produce hydrogen and electricity in a range of system options makes the GTHTR300 plant family strongly adaptable to market needs.

Moreover, the commonality of the technologies used in the family of the GTHTR300 plants makes any one of the plants suited to prototypical demonstration and initial deployment. The GTHTR300C being a substantial cogeneration system may be best suited in this role because it covers a full spectrum of the technologies used in the GTHTR300 plant family. The demonstration using the GTHTR300C may be phased to focus on electricity generation first and, once the reactor and gas

turbine system is confirmed, proceed to second phase of overall cogeneration system demonstration by coupling with the hydrogen plant.

Figure 19. Electricity and hydrogen products per reactor

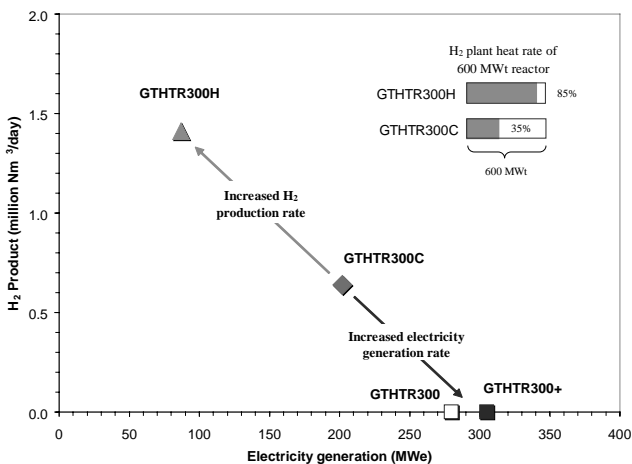


Table 5. GTHTR300 commercial production rates

		GTHTR300 - power plant -	GTHTR300+ - power plant -	GTHTR300C - cogen. plant -	GTHTR300H - H ₂ plant -
Reactor thermal power	MWt	4 x 600	4 x 600	4 x 600	4 x 600
Net electricity rate	MWe	1096	1200	697	137
Hydrogen production	Mm ³ /d	—	—	2.6	5.6
Plant net efficiency	%	46	50	45	40
Reactor outlet temperature	°C	850	950	950	950
Reactor inlet temperature	°C	587	663	594	594
Reactor coolant flow	kg/s	440	401	327	327
Reactor coolant pressure	MPa	7.0	6.4	5.0	5.0
Gas turbine heat rate per reactor	MWt	600	600	430	229
Turbine inlet temperature	°C	850	950	850	730
Gas turbine pressure ratio	=	2	2	2	1.5
Gross electricity generation	MWe	280	305	202	87
Generating efficiency	%	47	51	47	38
IS process heat rate per reactor	MWt	=	=	170	371
IS process effective heat rate	MWt	=	=	219	505
IS process top temperature	°C	=	=	850	850
IS process efficiency	%	=	=	43	41

The government of Japan plans to introduce five million fuel cell vehicles (FCVs) by 2020 and fifteen millions by 2030, against a backdrop of seventy five million total cars on road today. The plan envisions 100% FCVs in the later half of the century. The GTHTR300 plant family has the potential to play a significant role in supplying both emerging and matured hydrogen economy in Japan. Six GTHTR300C plants consisting of four reactors per plant, can fuel 7.5 million FCVs accounting 10% of the total number of cars. If deployed in time, these plants can simultaneously provide replacement power for the as many LWRs expected to retire by the year 2030 while co-producing the new hydrogen fuel on the existing sites. In longer term, adding either ten more plants of GTHTR300C or five plants of GTHTR300H could meet more than a quarter of the hydrogen fuel demand from a transportation sector that would become wholly hydrogen driven in a full-fledged hydrogen economy. In Japan, sustainability of HTGR energy production is being addressed by alternative fuel cycle and waste schemes such as the one outlined recently for an HTGR and FBR (fast breeder reactor) synergy to solve long-term issues of resources and wastes [12].

Acknowledgement

The authors wish to acknowledge the significant contributions to this work by a larger number of their colleagues in JAEA and domestic industries.

REFERENCES

- [1] Saito, S., *et al.*, (1994), Design of High Temperature Engineering Test Reactor (HTTR), JAERI 1332
- [2] Shiozawa, S., *et al.*, (2004), Overview of HTTR design features. Nucl. Eng. Des. 233, 11-21
- [3] Yan, X., *et al.*, (2000), Design innovations in GTHTTR300 gas turbine high temperature reactor, Proc. ICONE8, Baltimore, MD, USA, 2-6 April .
- [4] Yan, X., *et al.*, (2003b), Cost and performance design approach for GTHTTR300 power conversion system. Nucl. Eng. Des. 226, 351-373.
- [5] Nishihara, T., *et al.*, (2004), Development of high temperature isolation valve for the HTTR hydrogen production system. AESJ Transaction. (2004) Vol. 3, No. 4.
- [6] Sawa, K., *et al.*, (2002), Investigation of irradiation behavior of SiC-coated fuel particle at extended burnup. J. of Nucl.Tech. 142, 250-259.
- [7] Nakada, T., *et al.*, (2002), Nuclear design of the gas turbine high temperature reactor (GTHTTR300). JAERI-Tech 2002-066.
- [8] Kunitomi, K., *et al.*, (2004), Deployment of GTHTTR300 cogeneration for hydrogen and electric generation. Proc. ICAPP '04, Pittsburgh, PA, USA, 13-17 June .
- [9] Tokunaga, K., *et al.*, (2005), Technology development of high efficiency and high capacity gas to gas heat exchanger which is necessary to practical application of gas-cooled reactor. To appear in Proc. Global 2005, Tsukuba, Japan, 9-13 Oct .
- [10] Onuki, K., *et al.*, (2001), Electro-electrodialysis of hydriodic acid in the presence of iodine at elevated temperature, J. of Membrane Society, 192, 193-199.
- [11] Kubo, S., *et al.*, (2004), A demonstration study on a closed-cycle hydrogen production by thermochemical water-splitting iodine-sulfur process," Nucl. Eng. Des. 233, 347-354.
- [12] Shiozawa, S., (2005), Future plan on environmentally friendly hydrogen production by nuclear energy, Proc. of this meeting.

This page intentionally left blank

H2-MHR CONCEPTUAL DESIGNS BASED ON THE SI PROCESS AND HTE

Matt Richards, Arkal Shenoy, Ken Schultz, and Lloyd Brown
General Atomics

Ed Harvego and Michael McKellar
Idaho National Laboratory

Jean-Phillippe-Coupey and S.M. Moshin Reza
Texas A&M University

Futoshi Okamoto
Fuji Electric Systems

Norihiko Handa
Toshiba Corporation

Abstract

For electricity and hydrogen production, the advanced reactor technology receiving the most international interest is a modular, passively-safe version of the high-temperature, helium-cooled reactor referred to in the United States as the modular helium reactor (MHR). Because of its ability to produce high-temperature helium, the MHR is well suited for a number of process-heat applications, including hydrogen production. Two hydrogen-production technologies have emerged as leading candidates for coupling to the MHR: (1) thermochemical water splitting using the sulfur-iodine (SI) process and (2) high-temperature electrolysis (HTE). In this paper, we provide an update on conceptual designs being developed for coupling the MHR to the SI process and HTE. These concepts are referred to as the SI-based H2-MHR and the HTE-based H2-MHR, respectively.

INTRODUCTION

Hydrogen and electricity are expected to dominate the world energy system in the long term. The world currently consumes about 50 million metric tons of hydrogen per year, with the bulk of it being consumed by the chemical and refining industries. The demand for hydrogen is expected to increase, especially if the U.S. and other countries shift their energy usage towards a hydrogen economy, with hydrogen consumed as an energy commodity by the transportation, residential, and commercial sectors. Currently, steam reforming of methane is used to produce the vast majority of hydrogen consumed in the world. Eventually, an alternative source of hydrogen will be needed because the demand for natural gas is outpacing its production. In addition, there is strong motivation to not use fossil fuels in the future as a feedstock for hydrogen production, since the greenhouse gas carbon dioxide is a byproduct.

For the reasons given above, there is increased interest in using nuclear energy to produce hydrogen. In principle, nuclear electricity can be used to split water using conventional low-temperature electrolyzers. For a conventional light-water reactor that produces electricity with approximately 33% thermal efficiency and current generation electrolyzers operating with an efficiency of about 75% to convert electricity to high-pressure hydrogen, the overall efficiency for hydrogen production is approximately 25%. If a gas-turbine modular helium reactor (GT-MHR) is used to produce the electricity with 48% thermal efficiency, the overall efficiency for hydrogen production improves to 36%. However, even with high-efficiency electricity production, economic evaluations of coupling nuclear energy to low-temperature electrolysis have generally not been favorable when compared to steam reforming of methane [1].

Recent evaluations have shown hydrogen can be produced with high efficiency, safely, economically, and without the emission of greenhouse gases using the modular helium reactor (MHR) coupled to the SI thermochemical water splitting process and HTE [2]. These concepts are referred to as the SI-based H₂-MHR and the HTE-based H₂-MHR, respectively, and are described in this paper.

THE MODULAR HELIUM REACTOR

The high-temperature process heat required to drive both the SI process and HTE will be provided by the hot helium exiting the MHR reactor core. The reactor system design is based on that developed for the GT-MHR. As shown in Figure 1, the GT-MHR couples the MHR directly to a Brayton-cycle power conversion system (PCS). A GT-MHR module operates with a power level of 600 MW(t) and can produce electricity with thermal efficiencies ranging from 48% to 52% for core outlet temperatures ranging from 850°C to 950°C. For the HTE-based H₂-MHR, approximately 68 MW of heat is transferred through an intermediate heat exchanger (IHX) to generate superheated steam and the remaining heat is used to generate electricity. For the SI-based H₂-MHR, nearly all of the heat is transferred through an IHX to a secondary helium loop that supplies heat to the SI process. High temperature operation of the MHR with passive safety is enabled through the use of graphite fuel elements containing ceramic, TRISO-coated fuel (see Figure 2). Reference 3 provides additional information on the MHR design and its technology background.

Figure 1. The Gas Turbine Modular Helium Reactor

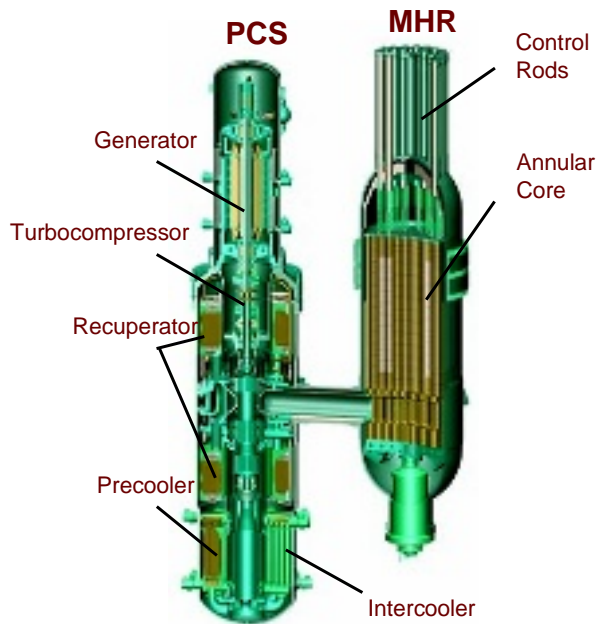
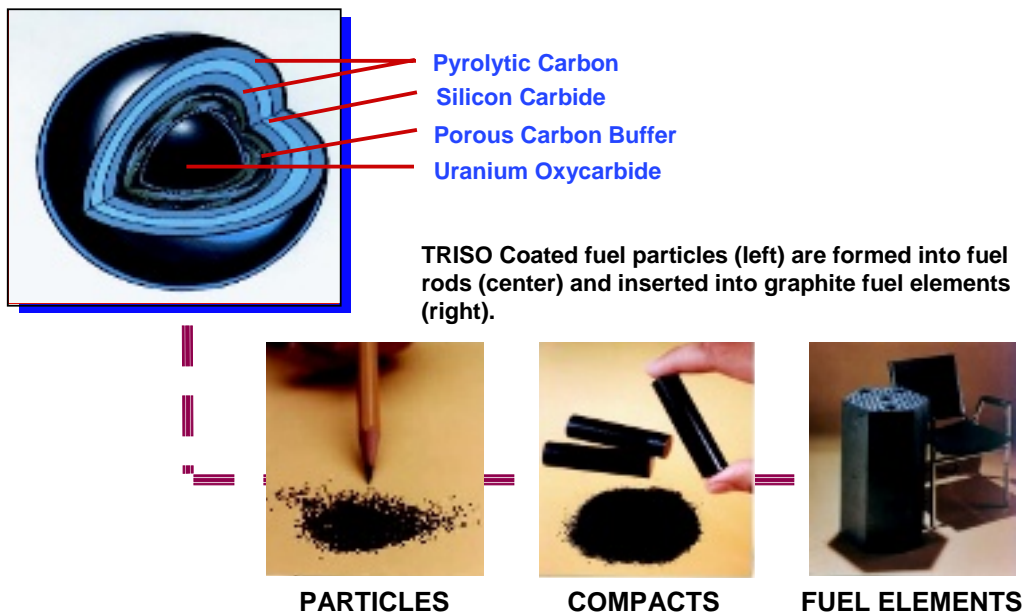


Figure 2. MHR Fuel Element Components



The GT-MHR was designed to operate with coolant inlet and outlet temperatures of 490°C and 850°C, respectively. As indicated in Table 1, the coolant inlet and outlet temperatures are increased to 590°C and 950°C respectively, for the H₂-MHR core. The outlet temperature was increased in order to improve the efficiency and economics of hydrogen production, but was limited to 950°C to avoid any potential adverse impacts on fuel performance during normal operation. Also, a higher coolant outlet temperature could require significant advances in technology to develop a viable IHX design. The coolant inlet temperature was also increased in order to maintain the same coolant flow and convective heat-transfer rates within the core as that for the GT-MHR. As discussed in References. 2 and 4, peak fuel temperatures during normal operation are maintained below 1 250°C as the result of design

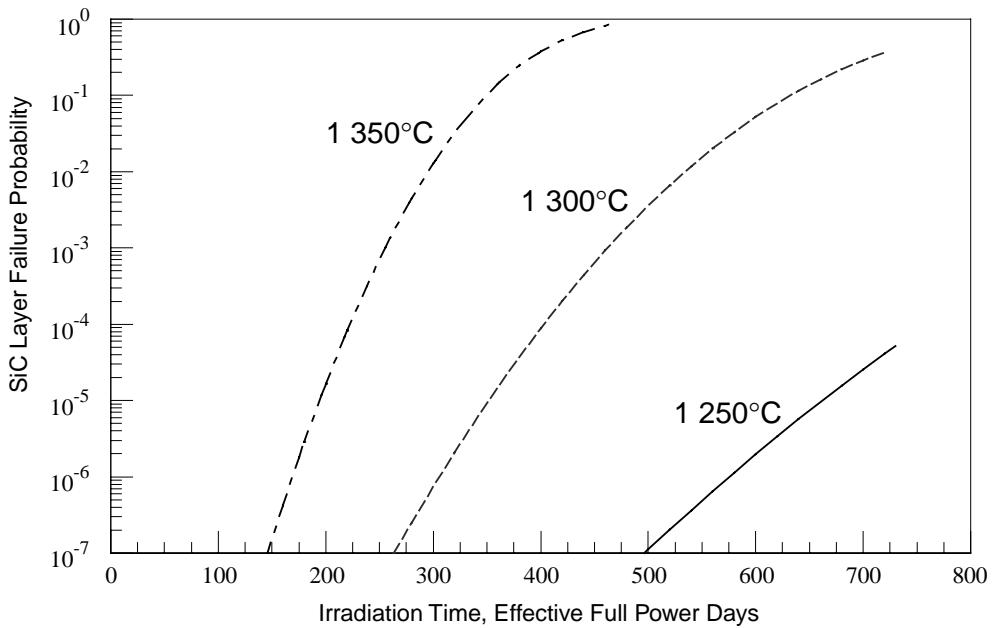
modifications to optimize the core thermal hydraulic and physics designs. These modifications include using lateral restraint mechanisms and sealing keys to reduce the fraction of flow that bypasses the coolant holes (e.g. through gaps between the graphite blocks), improved zoning of fissile/fertile fuel and fixed burnable poison, and improved refueling schemes. As shown in Figure 3, failure of the silicon carbide coating layer by fission-product attack is predicted to be very low for fuel temperatures below 1 250°C.

A potential issue associated with operating at a higher coolant inlet temperature is the impact on the vessel temperature during normal operation and accident conditions. For the GT-MHR, the inlet flow is routed through channel boxes located between the core barrel and the reactor vessel. With this configuration, the vessel temperature during normal operation is approximately 50°C below the core inlet temperature. For the H2-MHR, the inlet flow is routed through holes in the permanent side reflector, which is similar to the configuration used by the Japan Atomic Energy Research Institute (JAERI) for their GTHTTR300 design [5]. As discussed in Reference 2, this configuration should provide enough additional thermal resistance between the inlet flow and reactor vessel to maintain vessel temperatures at acceptable levels. Additional design modifications are being investigated to further lower the vessel temperatures, such that proven light water reactor vessel materials (e.g., SA533 steel) could be used for the MHR vessel.

Table 1. H2-MHR Core Design Parameter

Core thermal power (MW)	600
Number of fuel columns	102
Number of fuel blocks per column	10
Thermal power density (MW/m³)	6.6
Effective inner diameter of active core (m)	2.96
Effective outer diameter of active core (m)	4.83
Active core height (m)	7.93
Fissile fuel (19.8% enriched in U-235)	UC _{0.5} O _{1.5}
Fertile Fuel (natural U)	UC _{0.5} O _{1.5}
Equilibrium fuel cycle length (full-power days)	425
Number of columns per refueling segment	51
Mass of heavy metal per refueling segment (kg)	1748 (fissile fuel)
	514 (fertile fuel)
Core inlet temperature (°C)	590
Core outlet temperature (°C)	950
Core upper plenum inlet pressure (MPa)	7.1
Core pressure drop (MPa)	0.058
Coolant flow rate (kg/s)	320

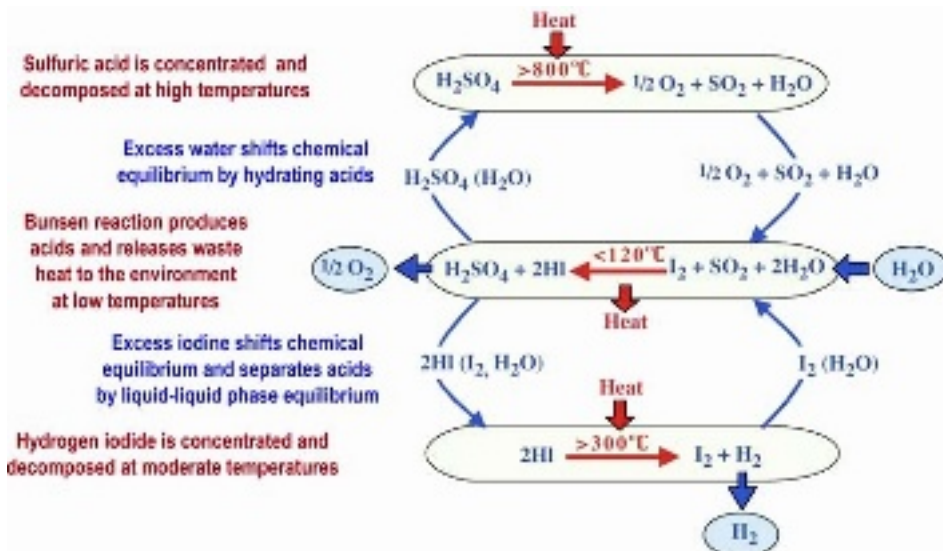
Figure 3. Predicted Failure of the SiC Layer by Fission Product Attack



SI-BASED H2-MHR

As shown in Figure 4, the SI process involves decomposition of sulfuric acid and hydrogen iodide, and regeneration of these reagents using the Bunsen reaction. Process heat is supplied at temperatures greater than 800°C to concentrate and decompose sulfuric acid. The exothermic Bunsen reaction is performed at temperatures below 120°C and releases waste heat to the environment. Hydrogen is generated during the decomposition of hydrogen iodide, using process heat at temperatures greater than 300°C. Figure 5 shows a simplified process flow diagram of the SI cycle.

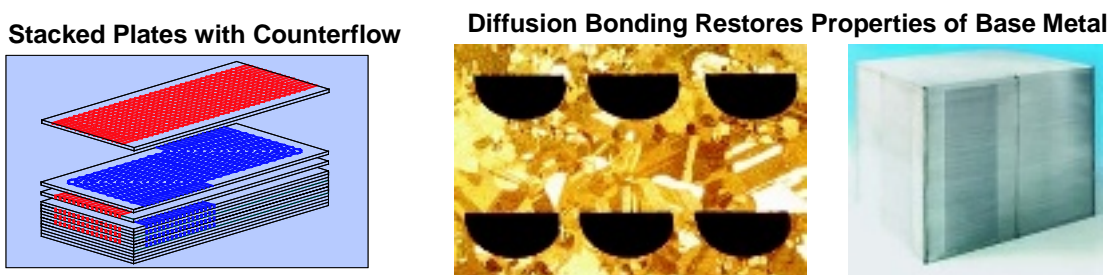
Figure 4. The Sulfur-Iodine Thermochemical Process



volume. The IHX design has been revised to incorporate an improved PCHE module design developed by Heatric. The IHX would consist of 40 modules and associated manifolds within an insulated steel vessel, with each module transferring about 15 MW of heat. The modules would be manufactured from Inconel 617. Each module weighs approximately 5 tonnes and has dimensions of 0.6 m x 0.65 m x 1.5 m. In order to minimize the size and weight of the IHX vessel, it is desirable to use a compact arrangement to house the PCHE modules within the vessel. However, sufficient room must be provided to accommodate differential thermal expansion. Preliminary results indicate that it should be possible to design a 600-MW(t) IHX with a vessel that is of similar size as the MHR vessel.

Two different processes are being investigated for HI decomposition [6]. One process, referred to as extractive distillation, uses phosphoric acid to strip HI from the HI-water-iodine mixture and to break the HI-water azeotrope. The other process is referred to as reactive distillation and involves reacting the HI-water-iodine mixture in a reactive bed to effect the separation process and produce hydrogen. Extractive distillation is a proven process, but requires significant amounts of energy and many components to perform the extraction, distillation, concentration, reaction, and separation steps of the process. The kinetics for reactive distillation are still relatively unknown, but the process can be performed in a single component without requiring concentration of the acid. For the n^{th} -of-a-kind SI-Based H₂-MHR conceptual design, it is assumed that HI decomposition will be performed using reactive distillation. Assuming the electricity needed for the shaft work required by the SI process is supplied by GT-MHRs operating with 48% to 52% thermal efficiency, the overall efficiency for hydrogen production is about 45%, based on the higher heating value (HHV) for hydrogen.

Figure 7. HEATRIC PCHE Design



HTE-BASED H₂-MHR

The HTE-based H₂-MHR couples the GT-MHR to high-temperature, solid-oxide electrolyzer (SOE) modules. Approximately 68 MW(t) of heat from the MHR is used to generate superheated steam for the electrolysis process, and the remaining heat is supplied to the PCS to generate the electricity required by the SOE modules. The SOE modules are based on the planar cell technology (see Figure 8) that has recently been successfully tested as part of a collaborative project between Idaho National Laboratory (INL) and Ceramtec, Inc [7]. Design parameters for a 12.5 kW(e), 500-cell stack are given in Table 2. For the HTE-based H₂-MHR, it is anticipated that a module would contain 40 stacks and consume 500 kW(e). A module would occupy approximately 4.2 m² of floor space, which includes space allocated for internal manifolding, piping, etc. Eight modules could be installed within a structure that is similar in size to the trailer portion of a typical tractor-trailer. Approximately 300 of these 8-module units would be required for a full-scale plant with four 600-MW(t) MHR modules. Figure 9 illustrates this SOE module concept.

Figure 8. Interconnect Plate and Single SOE Cell

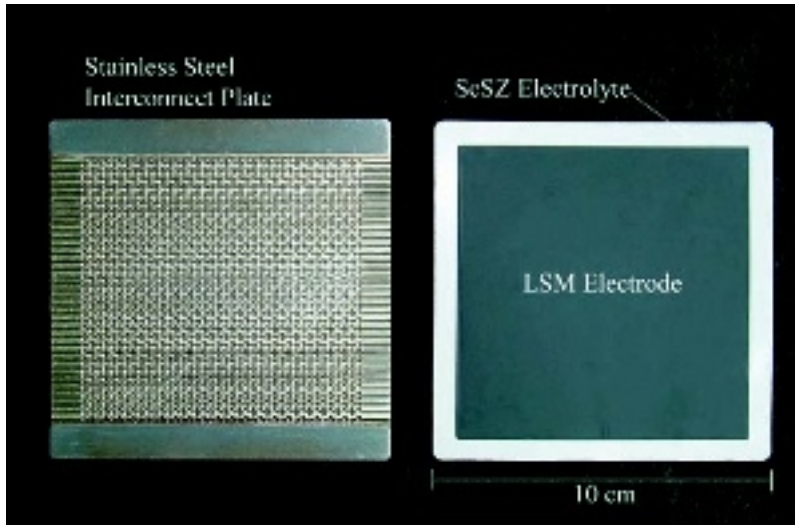


Table 2. Design Parameters for a 500-Cell Stack

Cell Area	
Individual Cell Width	10 cm
Individual Cell Active Area	100 cm ²
Total Number of Cells	12 x 10 ⁶
Total Active Cell Area	120,000 m ²
Cell Thickness	
Electrolyte	10 μm (ScSZ - Scandia Stabilized Zirconia)
Anode	1500 μm (LSM - Strontium Doped Lathanum Manganite)
Cathode	50 μm (Nickel Zirconia Cermet)
Bipolar Plate	2.5 mm (Stainless Steel)
Total Cell Thickness	4.06 mm
Stack Dimensions	
Cells per Stack	500
Stack Height	2.03 m
Stack Volume	0.0203 m ³
Stack Volume with Manifold	0.0812 m ³

Figure 9. SOE Module Concept

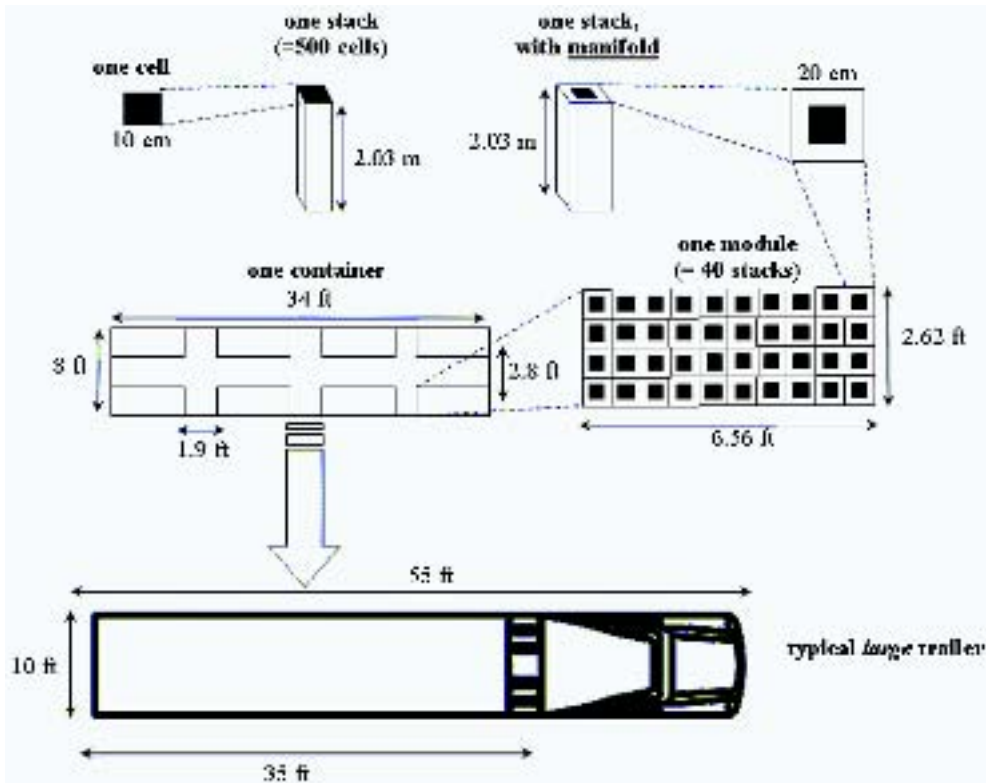
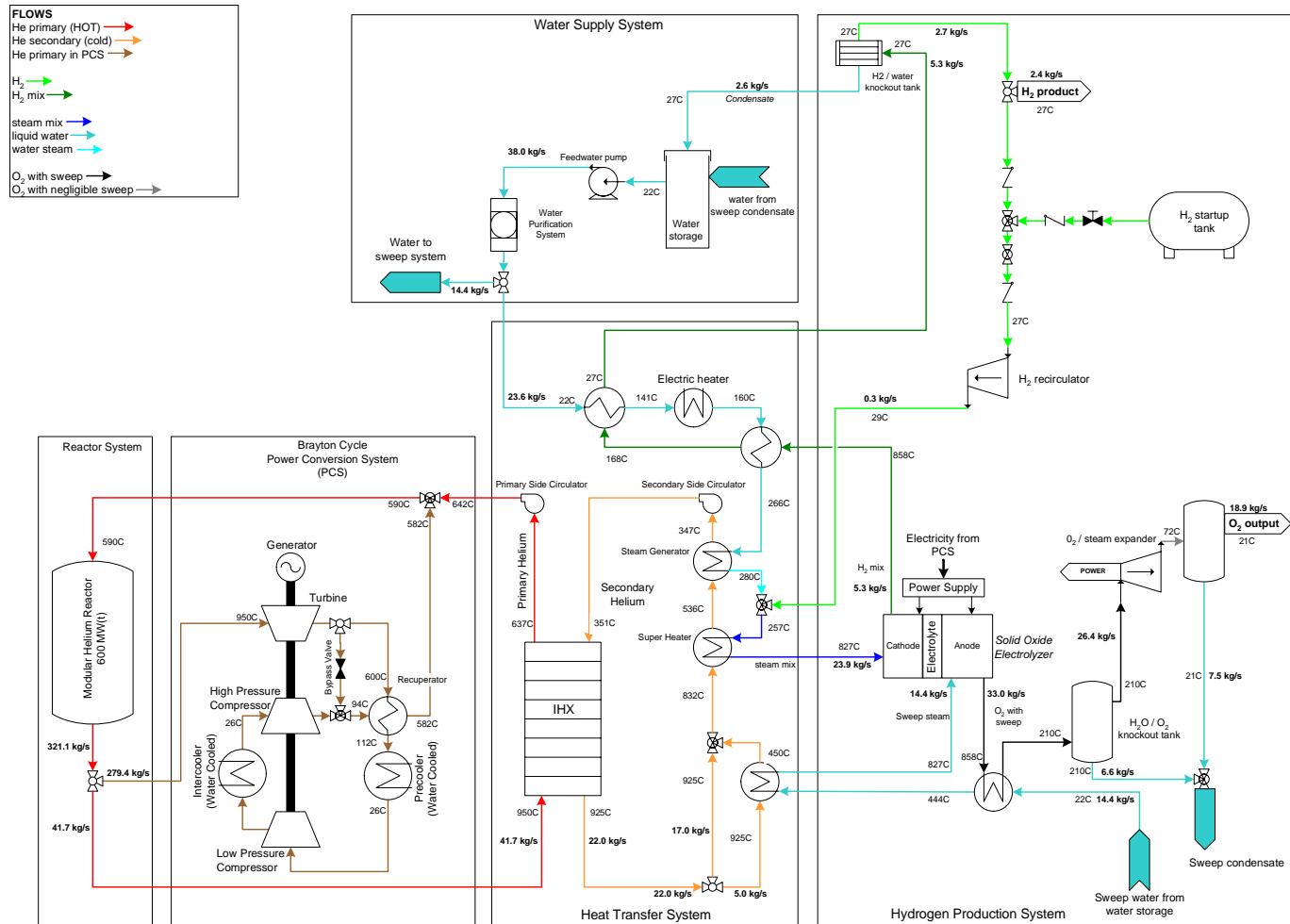


Figure 10 shows a preliminary flow sheet for the HTE-based H₂-MHR (this flowsheet is based on a single 600 MW(t) MHR module). The secondary helium loop is included to preclude the potential for tritium migration from the reactor system to the product hydrogen gas. Steam is supplied to the SOE modules for both electrolysis and sweeping of the oxygen from the anode sides of the SOE modules. Steam (at 827°C) supplied to the cathode sides of the modules is first mixed with a portion of the hydrogen product stream in order to maintain reducing conditions and prevent oxidation of the nickel-zirconia-cermet electrode. To maintain high efficiency, heat is recuperated from the product streams and auxiliary power for pumps, compressors, etc., is generated by expanding the oxygen/steam sweep mixture exiting the electrolyser modules through a turbine.

Figure 10. HTE-Based H2-MHR Process Flow Schematic



The HTE-based H₂-MHR flow sheet was modeled by INL using the HYSYS process modeling software package. For this particular application, INL developed an SOE electrochemical process model that was incorporated into HYSYS. Table 3 provides a summary of results obtained using the HYSYS model.

Table 3. HTE-based H₂-MHR Process Parameters

MHR Module Thermal Power	600 MW(t)
MHR Coolant Outlet Temperature	950°C
PCS Power Generation	312 MW(e)
PCS Thermal Efficiency	52%
Thermal Power Supplied for Hydrogen Production	68 MW(t)
SOE Process Temperature	827°C
Power Supplied to SOE Modules	292 MW(e)
Hydrogen Production Rate	2.36 kg/s
Hydrogen Production Efficiency (based on HHV of H ₂)	55.5%
Auxiliary Power Generation	9.3 MW(e)
Overall Process Efficiency	59.9%

SAFETY AND LICENSING CONSIDERATIONS

Passive safety features for the MHR include ceramic, coated-particle fuel and an annular graphite core with high heat capacity and low power density. Recently, INL has used the ATHENA thermal hydraulic code to model the response of the MHR during loss-of-flow and loss-of-coolant accidents and has confirmed these passivity safety features work to maintain fuel temperatures well below failure thresholds [8].

Another key consideration for safety and licensing is co-location of the MHR modules with a hydrogen production plant. The nth-of-a-kind plants consist of 4 MHR modules coupled to hydrogen production plants. As illustrated in Figure 11, it is proposed to locate the two facilities as close as possible (e.g., within about 100 m) in order to minimise the distance over which high-temperature heat is transferred. INL has recently performed an engineering evaluation for these separation requirements and has concluded separation distances in the range of 60 m to 120 m should be adequate in terms of safety [9]. Other recommendations from the INL study include a 100 kg on-site limit for hydrogen storage, use of double-walled pipes for hydrogen transport, and location of the nuclear plant control room outside of the dispersion zone for chemical release. The below-grade installation of the MHR modules, combined with an earthen berm between the MHR modules and the hydrogen production plant for defense in depth, provide additional safety margin for co-location of the two facilities.

ECONOMIC EVALUATIONS

As shown in Figure 12, economic evaluations for an nth-of-a-kind SI-Based H₂-MHR show the hydrogen-production costs are competitive with those for steam-methane reforming [10]. Economic evaluations for the HTE-based H₂-MHR are currently being evaluated and will depend significantly on the unit costs for the SOE modules. Preliminary evaluations show the hydrogen-production costs for both plants to be comparable if the SOE module unit costs are approximately \$500 per kW(e).

Figure 11. Concept for Interfacing the MHR with a Hydrogen Production Plant

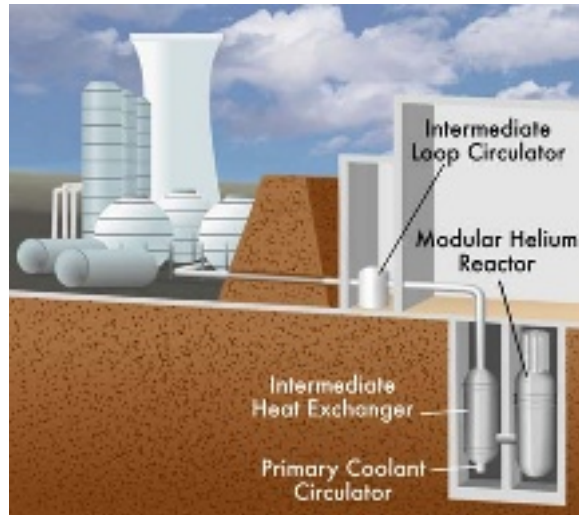
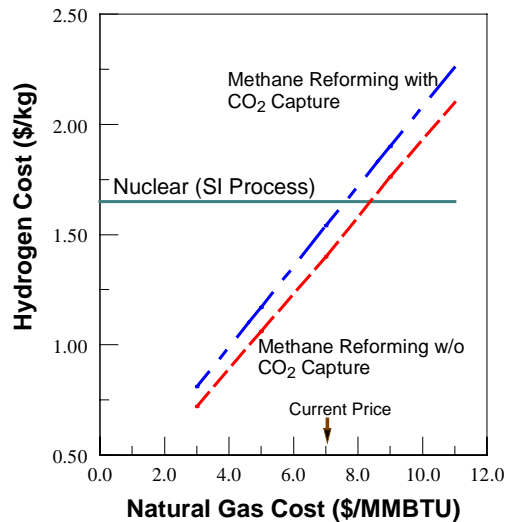


Figure 12. Comparison of Hydrogen Production Costs



CONCLUSIONS

The MHR is well suited for coupling to hydrogen production processes based on thermochemical water splitting and HTE. Both the SI-based and HTE-based H₂-MHR concepts have the potential to produce hydrogen safely, efficiently, and economically. Work on both concepts should continue beyond the conceptual design phase, which will provide a sound basis for a focused technology-development program that could eventually lead to commercial deployment of one or both concepts.

ACKNOWLEDGMENTS

This work was funded in part by the U.S. Department of Energy Nuclear Energy Research Initiative, under grant DE-FG03-02SF22609/A000.

REFERENCES

- [1] “High Temperature Gas-Cooled Reactors for Production of Hydrogen: An Assessment in Support of the Hydrogen Economy,” EPRI Report 1007802, Electric Power Research Institute, Palo Alto, CA (2003).
- [2] M. Richards *et al.*, “The H₂-MHR: Nuclear Hydrogen Production Using the Modular Helium Reactor,” Proceedings of ICAPP ’05, Seoul, Korea, May 15-19, 2005, Paper 5355.
- [3] M.P. LaBar *et al.*, “The Gas Turbine Modular Helium Reactor,” Nuclear News, Vol. 46, No. 11, p. 28 (2003).
- [4] M. Richards, A. Shenoy, Y. Kiso, N. Tsuji, N. Kodochigov, and S. Shepelev “Thermal Hydraulic Design of a Modular Helium Reactor Core Operating at 1 000°C Coolant Outlet Temperature,” Proceedings of the 6th International Conference on Nuclear Thermal Hydraulics, Operations and Safety (NUTHOS-6), October 4-8, 2004, Nara, Japan, Atomic Energy Society of Japan, Tokyo, Japan (2004).
- [5] K. Kunitomi, S. Katanishi, S. Takada, X. Yan, N. Tsuji, “Reactor Core Design of Gas Turbine High Temperature Reactor 300” Nuclear Engineering and Design, Vol. 230, p. 349 (2004).
- [6] B. Russ *et al.*, “HI Decomposition – A Comparison of Reactive and Extractive Distillation Techniques for the Sulfur-Iodine Process,” Proceedings of the 2005 AIChE Spring National Meeting, Atlanta, GA, April 10-14, 2005, Paper 75e.
- [7] J.S. Herring *et al.*, ”Progress in High-Temperature Electrolysis for Hydrogen Production Using Planar SOFC Technology,” Proceedings of the 2005 AIChE Spring National Meeting, Atlanta, GA, April 10-14, 2005, Paper 74f.
- [8] E. Harvego *et al.*, “Hydrogen Production Using the Modular Helium Reactor,” Proceedings of ICONE13: 13th International Conference on Nuclear Engineering, May 16-20, 2005, Beijing, China, Paper 50281.
- [9] C. Smith, S. Beck, and B. Galyean, “An Engineering Analysis for Separation Requirements of a Hydrogen Production Plant and High-Temperature Nuclear Reactor,” INL/EXT-05-00317, Rev. 0, Idaho National Laboratory, Idaho Falls, ID, USA, March 2005.
- [10] W. Summers, *et al.*, “Centralized Hydrogen Production from Nuclear Power: Infrastructure Analysis and Test-Case Design Study,” Interim Project Report, Phase A infrastructure Analysis, WSRC-TR-2004-00318, Rev. 0, Savannah River National Laboratory, Aiken, SC, USA, July 2004.

This page intentionally left blank

COUPLING A HYDROGEN PRODUCTION PROCESS TO A NUCLEAR REACTOR

**Pascal Anzieu, Patrick Aujollet, Dominique Barbier, Anne Bassi, Frédéric Bertrand,
Alain Le Duigou, Jean Leybros, Gilles Rodriguez**
Commissariat à l'énergie atomique, France

Abstract

Work is currently underway to define a pre-conceptual design of a Hydrogen Production Plant. As a reference case, a VHTR is dedicated to Hydrogen production using the Sulphur-Iodine process. The chemical part of the plant is based on a reference very detailed flow-sheet where all components are listed. Considering the volume and flow-rates of the circulating products, a detailed image of the chemical plant is drawn with several shops in parallel. A coupling circuit in gas was also studied with two intermediate heat exchangers at very high temperature. A specific heat transfer circuit is added inside the chemical part to distribute heat at the good temperature level. Optimisation of this circuit should lead to raise the overall efficiency of the process. Finally a methodology is proposed for the safety of the HYPP.

Introduction

To evaluate the viability and the cost of a future process that produces hydrogen, it is necessary to design an industrial plant. Such a design will help looking at the key points and will overcome the efficiency calculation as the best criteria to choose a future technology. We describe here some studies that are relevant to the design of a hydrogen production plant coupled to a high temperature nuclear reactor.

Basic options

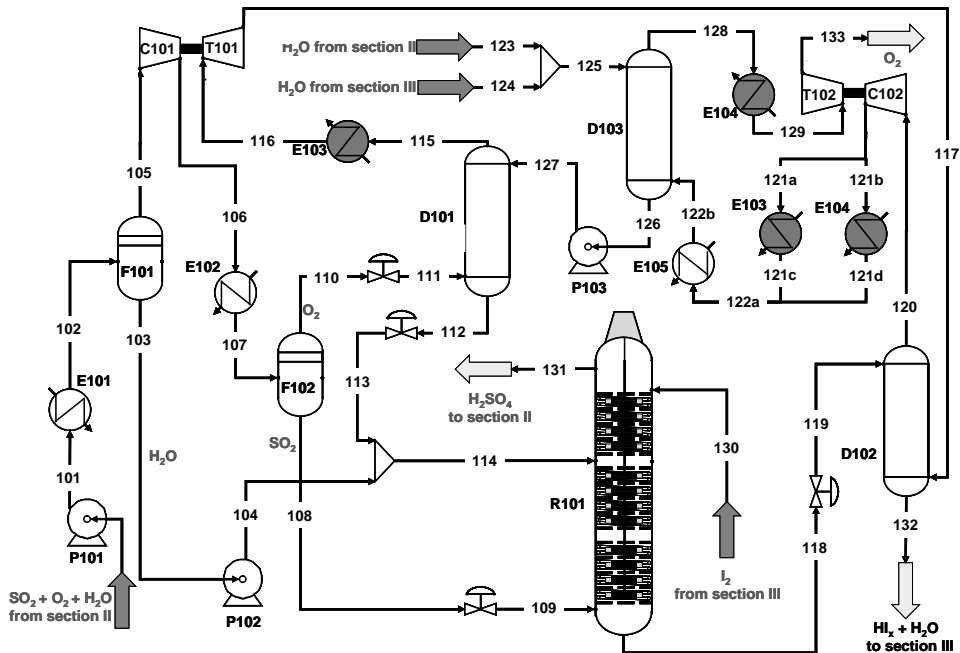
They are numerous possible arrangements to produce hydrogen using a very high temperature nuclear reactor (VHTR). In most of the cases related in the literature, people are dealing with co-generation when electricity and Hydrogen are both produced. In order to reduce the number of open parameters and to find a first set of operating conditions we will here study a dedicated plant. A 600 MWth VHTR will deliver heat to a hydrogen production plant (HYPP) based on a Sulphur-Iodine process. When electricity is needed to operate the process, it comes from the grid. The VHTR produces heat at the temperature needed by the process. The S-I process needs at least a temperature in the range of 840 to 870°C to operate with a sufficient efficiency.

The temperature level of the VHTR has to be established considering the heat delivering system. If one considers three intermediate heat exchangers (IHX), using a dedicated intermediate close loop, and takes a usual temperature pinch of 50°C for a gas-gas heat exchanger, the relevant VHTR temperature is above 990°C. But if optimisation only leads for instance to two IHXs and 30°C for the temperature pinch, the needed VHTR temperature decreases to 900°C. So it is important to optimise the coupling scheme and to validate the results with calculations. This is depending on the one hand of the knowledge we have on the HYPP and the other hand on the design we choose for the coupling. Both of them are presented in the following chapters.

Towards a Hydrogen Production Plant

From the basic studies for the S-I cycle we have derived a very detailed operating flow-sheet. It is based on a reactive distillation scheme. This flow-sheet has been designed taking into account present thermodynamics data and chemical engineering techniques. Expert judgements from people working in various areas related to the system were also used to assess each part of the flow-sheet and to validate its efficiency. Figure 1 shows the flow-sheet obtained for the Bunsen section.

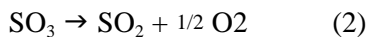
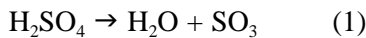
Figure 1. Detailed reference flow-sheet of the Bunsen section.



The complete flow-sheet gives a global efficiency of the process equal to 35% with an estimated range of variation of $\pm 5\%$. For each section, the efficiency of each basic reaction has been studied and discussed and a set of components were designed that are able to operate.

For the Bunsen section I, an excess of Iodine and of water is introduced to make the reaction not reversible. The dissolved Sulphur dioxide must be eliminated from the hydriodic acid at the outlet.

For the sulphuric acid decomposition section II, conversion factors and kinetic were studied for the two main reactions:



For (1), the dissociation factor is high above 530°C . There is no kinetic data. One or more simple heat exchanger is convenient with an outlet temperature that reaches the one needed for (2). (2) needs a catalyst. A vanadium oxide catalyst was assumed, made of granulate. The temperature must be at least 827°C and a value between 840 and 870°C is considered that gives a conversion factor from $0,7$ to $0,8$.

For the hydriodic acid decomposition section III, a first step is the iodine separation, due to contact with phosphoric acid in a counter current contactor. Then a reaction with catalyst in a reactive distillation column separates the Hydrogen from Iodine. This reaction is very slow and a residence time of some 3s is estimated in the column. The mixture that contains Iodine is adjusted and recycled to the main reactor of the Bunsen section, while the unreacted hydriodic acid is re-circulated.

In a first step, the energy is assumed to be mainly recovered. This is not the case for section I where the temperature is too low, less than 120°C . Section II is most well known and it is possible to perfectly adjust the heat demand to the use. Section II is the one that really needs to be optimised. Also the reaction is almost athermic, the great quantity of re-circulated products, especially water that has to be

vaporised, is energy consumer.

The detailed flow-sheet is derived from the expertise of each section. The needs for re-circulating compounds and for compounds separation gives a set of subsections that are composed of several apparatus. Pumps, pressure reducing valves and heat exchangers are part of these sub-sections.

For section I, one unique counter-current flow reactor is set up. At the inlet, Oxygen must be separated from SO₂ and hydriodic acid must be concentrated.

For section II, optimisation leads to concentrate the sulphuric acid up to 80% before it is converted. Finally a temperature of 850°C at the outlet of the converter is required. For section III, a specific column is required. It is composed of 25 theoretical plates, including re-boiler and condenser. Inlet is done at plate n° 22 at a temperature of 316°C. An intermediate partial draught at plate n° 15 is a good compromise from an energetic point of view. The total length of the catalyst bed is adjustable.

In a second step each component is designed separately for a 1 mol/s unit, representative of a laboratory scale experiment. For instance, a heat exchanger is described in detail and mass flow rates, temperatures and compounds composition are calculated. This gives a first idea of the component that should be built.

In a third step, an extrapolation to a HYPP is made, assuming a 1 kmol/s plant, that is more or less a plant that needs some 600 MWth of energy. Hypothesis is the following:

- No heat losses from the heat exchangers.
- Isentropic efficiency of the rotating machines (turbines and compressors) set to 0,75.
- Mechanical efficiency of pumps set to 1.
- Average logarithmic pinch of exchangers are above 10°C.
- Heat to electricity conversion efficiency is set to 0,5.

Energy balance for each section gives values from Table 1.

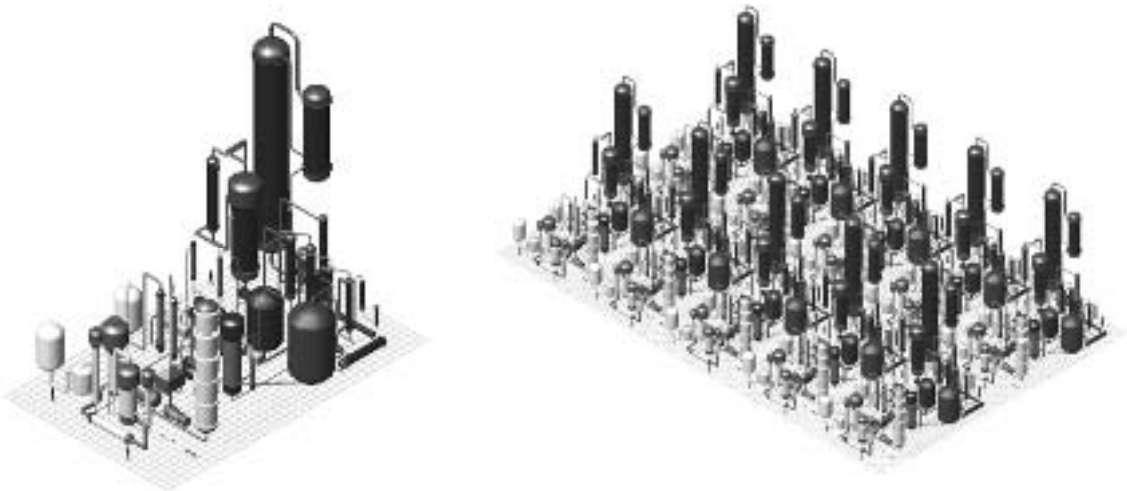
Table 1. Energy balance in each section of 1kmol/s HYPP

	Total Energy need	Heat fraction	Electricity fraction
Section I	34 MW	0	17 MWe
Section II	389 MW	385 MWth	2 MWe
Section III	376 MW	214 MWth	81 MWe
TOTAL	799 MW	599 MWth	100 MWe

This gives a global efficiency of 36%. The VHTR is totally dedicated to the heating of the HYPP. Additional 100 MWe are coming from the grid.

When dimensioning the components for the HYPP, measurements of the Bunsen reactor and the HI distiller are far from today technology. So it is proposed to split the factory into 10 shops. On this basis each component can be designed using available codes and standard. The pre-conceptual design of a shop and the factory are shown on Figure 2.

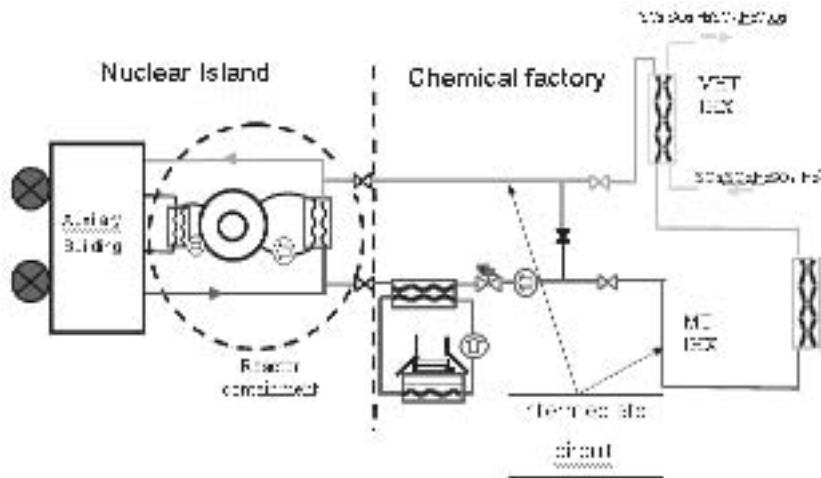
Figure 2. Pre-conceptual design of a shop delivering 100 mol/s H₂ (left) and of the factory of 10 shops (right).



Coupling the HYPP with the VHTR

Coupling the VHTR to the HYPP consists in a first step in designing the system that is used to transfer the energy from the primary circuit of the nuclear reactor to the inlet of the chemical factory. It is necessary to take into account the minimum heat losses in this circuit by reducing the number of IHX and the length of the system. Figure 3 gives a sketch of this coupling circuit.

Figure 3. Sketch of the coupling circuit between the VHTR and the HYPP



The design of the circuit must answer to several problems:

1. Transfer the high temperature heat to section II with the best greatest efficiency.
2. Supply to and recuperate heat from medium and low temperature sections.
3. Respect operating and safety rules in each plant.
4. Maintain a barrel between the two plants.

Present studies are based on a circuit fill with helium. Pressure is set at the mid value between the one of the VHTR (around 5.0 MPa) and the one of the sulphuric acid decomposer (0.5 to 1.0 MPa) to minimise the pressure difference on both sides. So the pressure of the intermediate circuit is around 2.9 MPa. A reference is set to 2.7 MPa. To transport the 600 MW a flow-rate of 220 kg/s is necessary.

For point 1, a specific design of the pipes is necessary to reduce the heat losses and also the pressure drop to minimise the blowing energy. A minimum temperature of 850°C is needed at the inlet of the chemical reactor. When studying the different geometrical arrangement of the pipes, one can easily show that co-axial pipes are not convenient because they generate too high friction losses. So a special design of the thermal isolation of standard pipes has been studied. An optimisation of the isolating material, using an internal coat and an external one plus an outside thermal screen, gives as a result a heat loss of less than 0.001°C/m (1kW/m) and a pressure drop of 400 Pa/m. The temperature of the metallic pipe that withstands the pressure is no more 400°C. This allows to use several 100 m length of pipes.

For point 2, a specific tool was developed to calculate heat exchange coupled to a reactive flow. This tool, called SRDE, is based on the PROSIM chemical tool. It has been used to firstly design a SiC heat exchanger for the sulphuric acid decomposer. The heat exchanger is optimised with 5 heat exchangers of 441 pipes each, 13 m length. Helium circulates inside the 0.03 m diameter pipes. The chemical compounds circulate in an outside counter current flow with a 0.057 m equivalent diameter. The total energy exchange is 70 MW per exchanger. An iteration must be made with the description of the HYPP (see above) concerning the optimum number of shops. The same type of calculation was made for the medium temperature part of the circuit and for the IHX. It has been concluded, among

others, that the minimum pinch temperature for the heat exchanger was around 30°C. This allows to calculate the minimum temperature required from the VHTR: 900°C, if everything works well!

For point 3, a boiler that stabilises the temperature of the helium coming back to the main IHX, has been added on the basis of the work done by JAERI for its Steam Methane Reforming project coupled to the HTTR. The design and the characteristics of this boiler are currently being studied.

Point 4 is achieved through the integration of the main IHX in the main confinement of the VHTR and the intermediate circuit that should prevent rapid interaction of one plant with the other.

Safety issue

The safety approach, guided by the regulation and based on safety analysis methodology, is a synthesis of the nuclear power plant and the conventional plants regulations. It gives a methodology for the safety approach of the VHTR coupled with the HYPP, consistent with both regulations. As a nuclear facility, the VHTR is submitted to safety rules. The strategy and the foreseen provisions are described in a safety report showing the compliance with these safety objectives. Physical barriers are interposed between the radioactive materials (fission product) and the environment, in order to prevent their release. Safety functions are defined to preserve the integrity of these barriers, for instance the control of the nuclear reactivity or the cooling of the fuel. Moreover, conception rules are adopted with respect to the principle of defense in depth (DID) including generally five levels.

For a conventional facility, the regulation consists in laws applicable to the facility “classified for environment” and eventually in the SEVESO II European directive, depending on the quantities of dangerous substances included in the facility. Of course, the conception rules of the art have to be applied. The deterministic approach is declined in a less rigorous way in the conventional industry, but it is more or less based on the DID principle and on studies of postulated major accidents.

According to the previous statements, three overall safety functions can be defined for the whole facility (VHTR/HYPP) in order to prevent and to limit the consequences of dangerous releases in case of accidents [1]:

- the control of the nuclear reactivity and of the chemical reactivity;
- the extraction of the nuclear power, of the thermal power (heat release by chemical reactions, phase changes) and of the mechanical power (compressors, pumps, pressure wave associated to phase changes or very rapid gas expansion due to heat release);
- the confinement of hazardous substances : fission product and chemical substances.

Obviously, the two first safety functions are required to avoid excessive solicitations of components constituting a barrier. The last safety function states the protection of the barriers in itself.

Level 1

The prevention of abnormal operation and failures can be divided into two folds: selection of design rules related to chemical substances specificity and to different operating conditions; provisions regarding parameter variations transmitted from one facility to the other through the coupling system. Items related with this level 1 of the DID are for example:

- Material resistant to the corrosion of acids.
- Hydrogen embrittlement of the walls of cryogenic storages.
- Hydrogen diffusion through metal.
- Control of the heat exchange between the two facilities.

Level 2

The control of abnormal operation forms the level 2 of the DID. This level deals mainly with surveillance, control and regulation systems. The security and limiting systems acting automatically in case of abnormal operation are designed to operate before the triggering of systems of third level of DID, especially, the automatic emergency shutdown of the facilities (for the VHTR and the HYPP) mainly the uncoupling and shutdown of the H2 units that are out of normal operation domain, but also the uncoupling needed when the temperature of the VHTR varies outside the operating range (see for instance the case of a slow starting-up).

Level 3

In the level 3 of the DID, one needs to control the progression of accidents and to limit their consequences. The accidents considered here should be controlled within the design basis conditions and, therefore, should not induce large leakages through the last physical barriers nor explosions/fires being likely to aggress significantly the HYPP or the VHTR. By the way, the safe states of the facilities correspond to an uncoupled state that allows to insure independently the safety functions of each facility. In this level we need provisions and systems devoted to the fulfillment of safety functions.

The control of the nuclear and chemical reactivity in case of accidents is insured by the emergency shutdown systems. The safety function devoted to the thermal power extraction from the HYPP is directly linked to the control of the chemical reactivity because the kinetics of chemical reactions increases with the temperature. The HYPP must be cooled by emergency systems, water streaming on equipments, spraying systems, and so on.

The extraction of the mechanical power has an influence on the chemical reactivity as well, by controlling the pressure in the HYPP components. Provisions like safety valves, expansion tanks, flarestacks, can be foreseen in order to release the pressure, thus avoiding the failure of equipments

The main accidents considered at this level are listed below:

- the loss of electric supply or other support systems (secondary products evacuation, pneumatic systems);
- coupling system failure or rupture as an accident initiator;
- design basis accident in the VHTR;
- equipment failure in the HYPP without external leakage;
- limited leakages without ignition in the HYPP;

- simultaneous rupture of IHX1 and IHX2, eventually initiated by a breach.

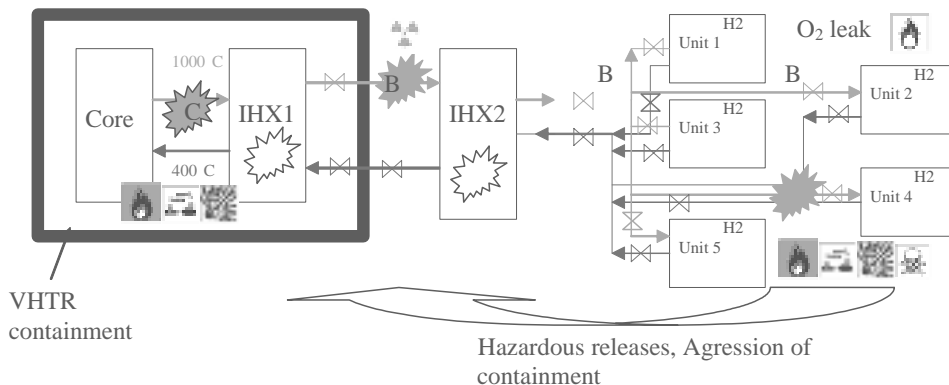
The prevention measures to control the accident consists in the triggering of emergency shutdown systems in VHTR and in HYPP associated to the overall decoupling of the facilities.

Level 4

Here are the control severe plant conditions and mitigation of severe accidents consequences. They results from low probability sequences including multiple failures. Complementary provisions aiming to limit the consequences of such accidents are provided, especially regarding the integrity of the last confinement barrier (containment for VHTR, last wall and safety distances for HYPP). At this level, provisions are also proposed in order to prevent and to mitigate possible “dominoes effects” due to the proximity of the two facilities and of the different units of HYPP.

The consequences of major accident scenarios postulated in the HYPP have to be assessed. The relevance of these scenarios regarding VHTR aggression has to be checked, because the “envelope” accidents are not necessarily the same for out-site consequences as for VHTR aggressions. As an illustration, the toxic consequences of a sulfur dioxide release could impose the larger safety distance regarding the environment, whereas a conservative scenario could be a hydrogen deflagration regarding the VHTR aggressions (Figure 4).

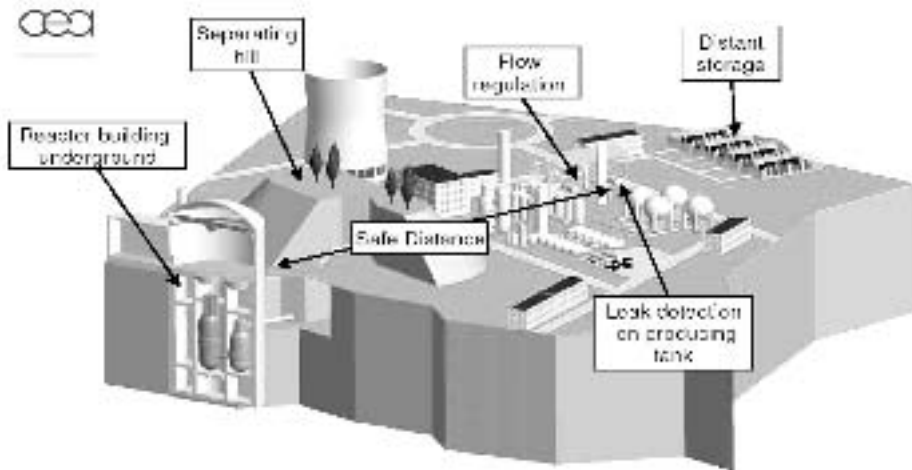
Figure 4. schematic of hypothetical severe accidents consequences



Especially, the containment resistance to an explosion wave must be evaluated in order to size it appropriately. One must limit its consequences by relevant provisions like (Figure 5) :

- reduction of energetic ignition sources (risk of fast combustion regime);
- absence of confinement and of obstacles (pipe agglomerate) to avoid flame acceleration and DDT;
- inerting or igniting systems in confinement;
- events systems, physical barriers between the VHTR and the HYPP, deflectors, reasonable safety distance;
- possible grounding of the coupling system and/or the VHTR;
- training of rescue teams and emergency means optimisation;

Figure 5. Possible provisions to mitigate pressure wave aggression on VHTR



Compounds issues

For the Sulphur-Iodine cycle, an obviously important challenge is related to Iodine itself, which is a not so abundant and rather expensive material. As said previously, a main characteristic of the process is the very important amount of chemicals involved in the process in relation with the quantity of hydrogen produced. This is due on the one hand to the balance of the molecular weight of hydrogen versus iodine (1 versus 127) and on the other hand to the fact that the Bunsen reaction is not stoichiometric and requires, for phase separation, 9 moles of I_2 to produce one mole of H_2 .

As a matter of fact, it is easily shown that, using an average cost of \$ 15 per kg of Iodine [11], the production of 1 kg of H_2 requires the handling of \$ 20 000 of iodine. As a direct consequence, Iodine molar losses of, for instance, 10^{-5} , would increase the hydrogen production cost of \$ 0.2 per kg H_2 : clearly, the control of Iodine losses would be an important question in the operation of a Sulphur-Iodine plant.

Another question relates to the availability of large enough quantities of iodine in the world. First estimates of the Iodine hold-up in a 600 MW VHTR coupled hydrogen production plant, designed using a detailed flow-sheet of the cycle, are on the order of 3 000 t (corresponding to a \$ 45M capital cost, and consequently \$ 0.045 per kg H_2). This amount seems realistic when compared to the world yearly production of 20,000 t and the estimated world reserves of $15 \cdot 10^6$ t [2].

REFERENCES

- [1] A. Bassi *et al.*, Massive H₂ production with nuclear heating, safety approach for coupling A VHTR with an Iodine Sulfur process cycle, ICHS, Pisa, September 8-10, 2005.
- [2] <http://minerals.usgs.gov/minerals/pubs/commodity/iodine/>

This page intentionally left blank

HTTR TEST PROGRAMME TOWARDS COUPLING WITH THE IS PROCESS

**Tatsuo Iyoku, Nariaki Sakaba, Shigeaki Nakagawa, Yukio Tachibana, Seiji Kasahara,
and Kozo Kawasaki**

Japan Atomic Energy Agency (JAEA), Japan

Abstract

High-temperature gas-cooled reactors (HTGRs) are particularly attractive due to its inherent safety, economic viability, high efficiency, very high burnup, and wide industrial application (from electricity generation to hydrogen production). They are expected to play a dominant role in the future hydrogen society. The JAEA's HTTR, which is the first HTGR in Japan, attained its maximum reactor-outlet coolant temperature and successfully delivered 950°C coolant helium outside its reactor vessel. The reactor-outlet coolant temperature of 950°C makes it possible to extend HTGR use beyond the field of electric power. Also, highly effective power generation with a high-temperature gas turbine becomes possible, as does hydrogen production from water. This paper describes the main results of 950°C operation and future test program in order to connect with a hydrogen production system by using a thermochemical IS process, as well as a preliminary project plan of the HTTR-IS system.

Introduction

High-temperature gas-cooled reactors (HTGRs) are particularly attractive due to its inherent safety, economic viability, high efficiency, very high burnup, and wide industrial application (from electricity generation to hydrogen production). They are expected to play a dominant role in the future hydrogen world. The Japan Atomic Energy Agency's (JAEA's) HTTR, which is the first HTGR in Japan, attained its maximum reactor-outlet coolant temperature and successfully delivered 950°C coolant helium outside its reactor vessel [1]. The reactor-outlet coolant temperature of 950°C makes it possible to extend HTGR use beyond the field of electric power. Also, highly effective power generation with a high-temperature gas turbine becomes possible, as does hydrogen production from water.

This paper describes the major results of 950°C operation of the HTTR performed till 2004 and the future test programme in order to connect with the hydrogen production system by using a thermochemical water-splitting IS process as well as a preliminary project plan of HTTR-IS system.

Outline of the HTTR

As the HTTR is the first HTGR in Japan and a test reactor, it has following purposes:

- Establishment of basic HTGR technologies.
- Demonstration of HTGR safety operations and inherent safety characteristics.
- Demonstration of nuclear process heat utilisation.
- Irradiation of HTGR fuels and materials in an HTGR core condition.
- Provision of testing equipment for basic advanced studies.

The reactor core, composed of graphite blocks, is so designed as to keep all specific safety features. In the cooling system, the intermediate heat exchanger (IHX) is equipped to supply high-temperature helium gas to some process heat application system being coupled to the HTTR in the future.

The detailed HTTR design was already reported [2] and the equipment concerning the 950°C operation and HTTR-IS system are described in this chapter.

(1) Core components and reactor internals

The HTTR has a thermal power of 30MW and 950°C maximum reactor-outlet coolant temperature. The main specifications of the HTTR are shown in Table 1. The reactor consists of a reactor pressure vessel (RPV), fuel elements, replaceable and permanent reflector blocks, core restraint mechanism, control-rods, etc. Thirty columns of fuel blocks and seven columns of control-rod guide blocks form the reactor core, called the fuel region, which is surrounded by replaceable reflector blocks and large-scale permanent reflector blocks. The fuel element of the HTTR is pin-in-block type. Enrichment of U-235 is 3 to 10 (average 6) wt%. Sixteen pairs of control-rods in the fuel and replaceable reflector regions of the core control reactivity of the HTTR. A control-rod drive mechanism drives each pair of control-rods using an AC motor. At a reactor scram, electromagnetic clutches of the

control-rod drive mechanisms are separated, and the control-rods fall into holes in the control-rod guide blocks by the force of gravity at a constant speed, shutting down the reactor safely. The vertical cross section of the HTTR reactor is shown in Figure 1.

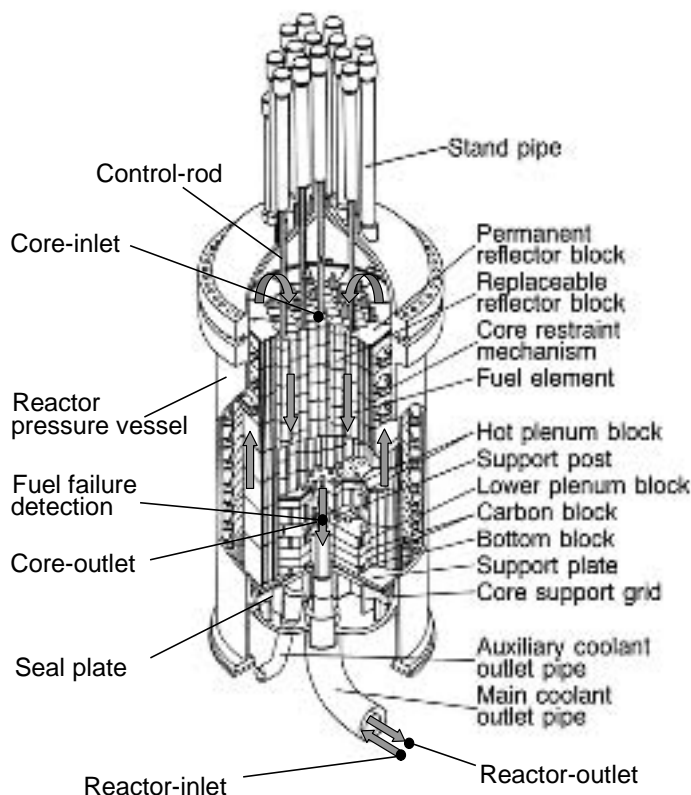
Table 1 Major Specification of the HTTR

Item	Specification
Thermal power	30 MW
Coolant	Helium gas
Reactor-outlet coolant temperature	850 °C *, 950 °C **
Reactor-inlet coolant temperature	395 °C
Primary coolant pressure	4.0 MPa
Primary coolant flow rate	12.4 kg/s *, 10.2 kg/s **
Core structures	Graphite
Core height	2.9 m
Core diameter	2.3 m
Power density	2.5 MW/m ³
Fuel	Low enriched UO ₂
Enrichment	3~10wt % Avg. 6wt%
Fuel element type	Prismatic block
Pressure vessel	Steel (2¼Cr – 1Mo)
Number of main cooling loop	1

* Rated operation mode: operation at reactor-outlet coolant temperature of 850°C.

** High-temperature test operation mode: operation at reactor-outlet coolant temperature of 950°C.

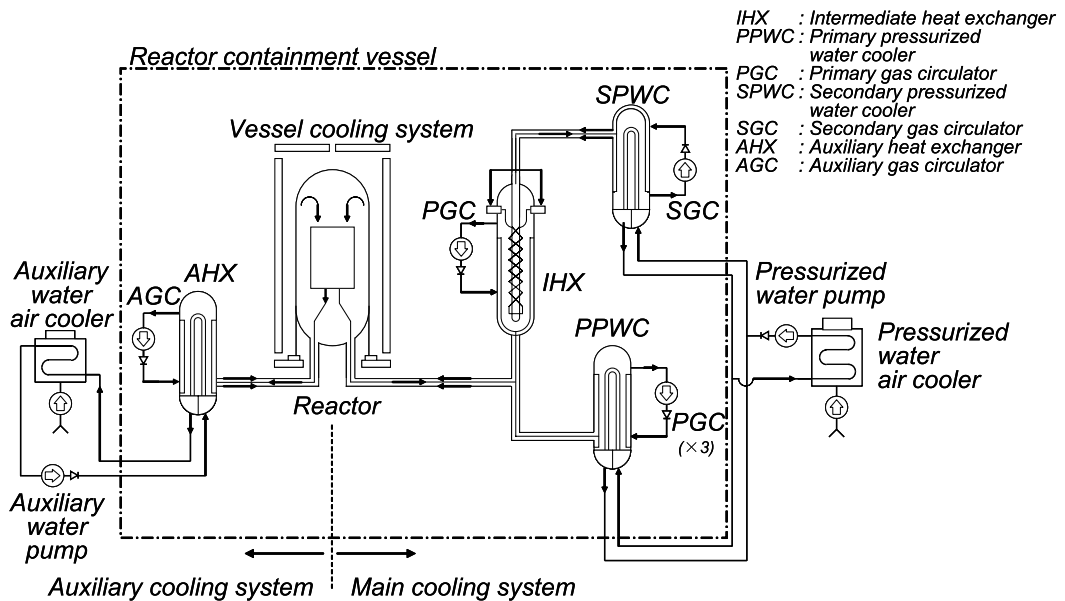
Figure 1. Vertical cross section of the HTTR reactor



(2) Main cooling system

As shown in Figure 2, the cooling system of the HTTR consists of a main cooling system operating at normal operations; and an auxiliary cooling system and a vessel cooling system, the engineered safety features, operating after a reactor scram to remove residual heat from the core. The main cooling system, which consists of a primary cooling system, a secondary helium cooling system, and a pressurized water cooling system, removes heat generated in the core and dissipates it to the atmosphere by a pressurized water air cooler. The primary cooling system consists of an IHX, a primary pressurized water cooler (PPWC), a primary concentric hot gas duct, etc. Primary coolant of helium gas from the reactor at 950°C maximum flows inside the inner pipe of the primary concentric hot gas duct to the IHX and PPWC. The primary helium is cooled to about 400°C by the IHX and PPWC and returns to the reactor flowing through the annulus between the inner and outer pipes of the primary concentric hot gas duct. The HTTR has two operation modes. One is the single-loaded operation mode using only the PPWC for the primary heat exchange. Almost all the basic performance of the HTTR system is confirmed by the single-loaded operation mode. The other is the parallel-loaded operation mode using the PPWC and IHX. In a single-loaded operation mode the PPWC removes 30 MW of heat and in a parallel-loaded operation mode the PPWC and IHX remove 20 MW and 10 MW, respectively. It is planned to use the secondary helium gas of the IHX for nuclear process heat utilisation. The auxiliary cooling system, consisting of an auxiliary helium cooling system, an auxiliary water cooling system, a concentric hot gas duct, etc. is on stand-by during normal operations and starts up to remove residual heat after a reactor scram. The vessel cooling system cools the biological concrete shield surrounding the reactor pressure vessel at normal operations, and removes heat from the core by natural convection and radiation outside the reactor pressure vessel under “accident without forced cooling” conditions such as a rupture of the primary concentric hot gas duct, when neither the main cooling system nor the auxiliary cooling system can cool the core effectively.

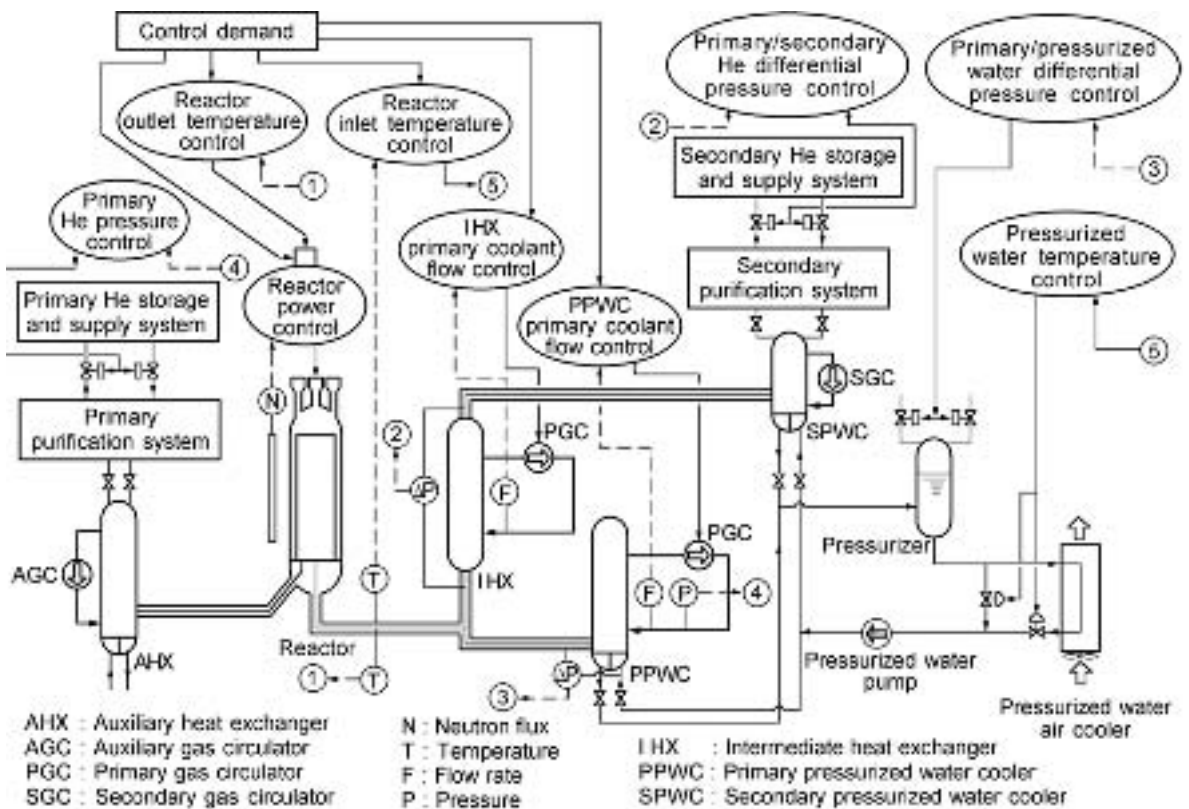
Figure 2. Schematic diagram of the reactor cooling systems consisting the main cooling system, auxiliary cooling system and vessel cooling system of the HTTR



(3) Instrumentation and control system

The reactor power control device consists of control systems for the reactor power and reactor-outlet coolant temperature. These control systems are cascade-connected: the latter control system first gives demands to the reactor power control system. The signals from each channel of the power-range monitoring system are transferred to three controllers using microprocessors. In the event of a deviation between the process-value and set-value, a pair of control-rods is inserted or withdrawn at the speed from 1 mm/s to 10 mm/s according to the deviation. The relative position of 13 pairs of control-rods, except for 3 pairs of control-rods used only for a scram, are controlled within 20 mm of one another by the control-rod pattern interlock to prevent any abnormal power distribution. The plant control device controls plant parameters such as the coolant temperature of the reactor-inlet, flow-rate of the primary coolant, pressure of the primary coolant, and differential pressure between the primary cooling system and pressurised water cooling system. The schematic diagram of the plant control device is shown in Figure 3. The reactor power, the reactor-inlet coolant temperature, and the primary coolant flow-rate are controlled to constant values by each control system. The reactor-outlet coolant temperature is adjustable by the control system of the primary coolant flow-rate.

Figure 3. Plant control device of the HTTR



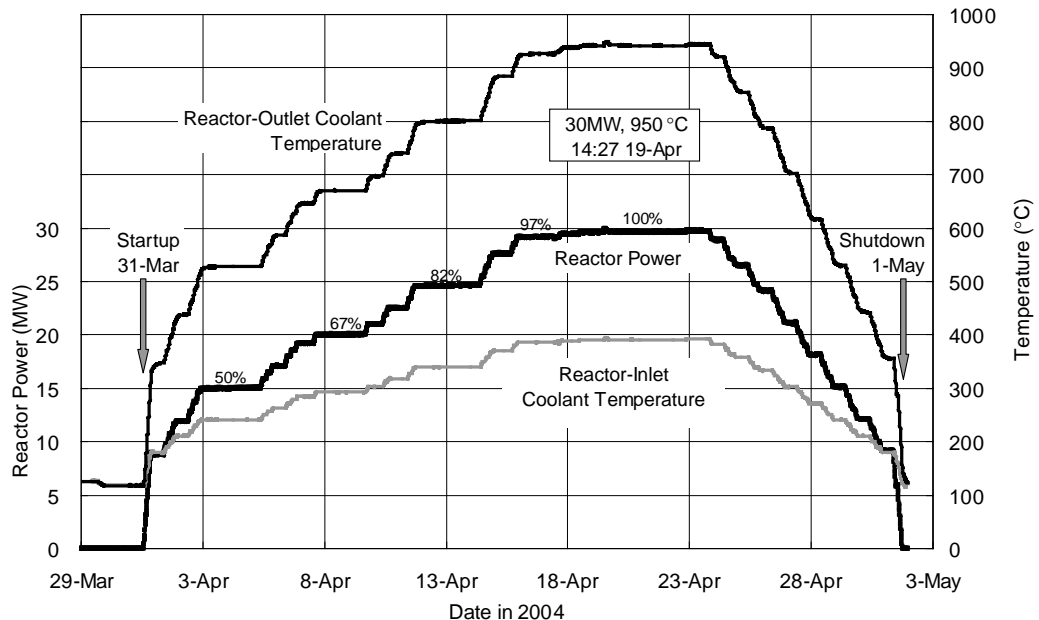
Major results of 950°C high-temperature operation

The high-temperature test operation was conducted in order to achieve the rated thermal power of 30 MW and reactor-outlet coolant temperature of 950°C. The reactor power was increased step-by-step with monitoring all of the parameters, such as thermal parameters, concentrations of coolant impurities. The temperature was raised within the rate of 15°C/h (reactor-outlet coolant temperature above 650°C) and 35°C/h (below 650°C) for the safety of operations. The reactor power was kept at 50% (15 MW),

67% (20 MW), and 100% (30 MW) more than two days in a steady temperature condition in order to measure the power coefficients of the reactivity. The reactor power was also kept at 82%, at which the reactor-outlet coolant temperature is a little below 800°C, in order to remove the chemical impurities by a helium purification system. The calibration of the neutron instrumentation system with the thermal reactor power was performed at 97% power. Figure 4 shows the operation history of the reactor-inlet and -outlet coolant temperature and the reactor power. The reactor-outlet coolant temperature of 950°C was achieved on 19 April 2004 during the single-loaded operation mode. During the parallel-loaded operation mode the reactor-outlet coolant temperature reached 941°C and the secondary helium temperature at the IHX-outlet reached 859°C on 24 June 2004. The differences of the reactor-outlet coolant temperature from the design value of 950°C were caused by a permitted margin for error of the flow-rate indicators of the primary cooling system. The attained temperatures implied that the flow-rate of the parallel-loaded operation mode was about 1% higher than that of the single-loaded. As the flow-rate was designed to keep its control demand constantly, some correction will be added to the target value of the primary coolant flow-rate in next parallel-loaded operations.

The following are the major test results obtained during the 950°C operation.

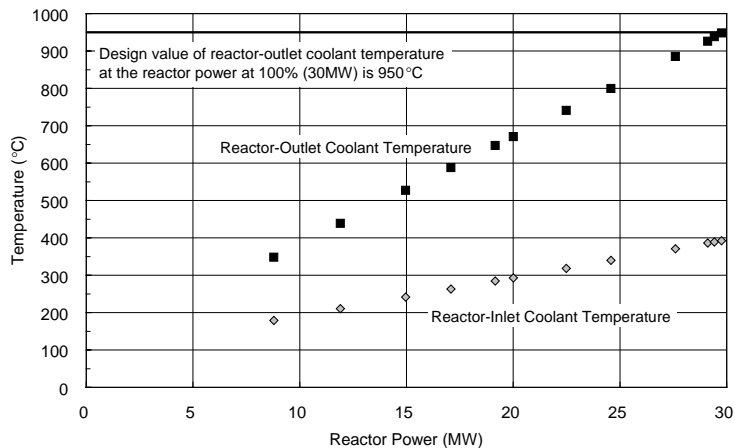
Figure 4. Operation history during the high-temperature test operation by the single-loaded mode. Maximum reactor-outlet coolant temperature of 950°C had attained on 19 April 2004.



Reactor-outlet coolant temperature and heat balance

The maximum values of temperature and pressure of the primary coolant were measured during steady state conditions at the full power of 30MW and they were confirmed to be less than the criteria of 957°C and 4.0 MPa. Figure 5 shows the relation between the reactor thermal power and the reactor-inlet and -outlet coolant temperature. The heat transfer performance was estimated in order to confirm the performance of the PPWC and air fin cooler (ACL). The PPWC is the only primary heat exchanger used at the primary circuit during the single-loaded operations and the ACL is the final heat sink during any operations excluding after a reactor shutdown.

Figure 5. Relation between the reactor power and reactor-inlet and -outlet coolant temperature



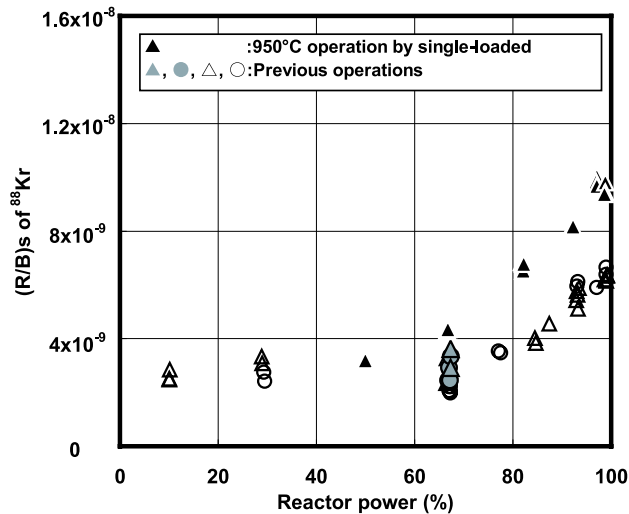
Thermal hydraulics

The core-internal thermal-hydraulic performance of fuel temperature, core-internal structure, and core-internal coolant distribution were confirmed to be appropriate to their design during the full power operation. The maximum temperature of the core support-plate measured at the upper surface of the centre core support-plate was 450°C that was sufficiently below its limited value of 530°C. Also, it was confirmed that other core-internal structure temperatures were well below their design criteria. From the result that no core-internal structure temperature measurement showed an abnormal value, it was confirmed that there was no abnormal leak flow of coolant such as cross and bypass flows between fuel blocks, replaceable reflector blocks, permanent reflector blocks, etc. The maximum fuel temperature was evaluated to be 1 463°C prior to the high-temperature test operation. It was re-evaluated using the measured temperature data i.e. core-inlet and -outlet coolant temperatures and the calculated value of 1478°C does not exceed the normal operation limit of 1 495°C.

Fuel and fission product gases behaviours

Fuel and fission product gases behaviour was monitored in order to evaluate the release behaviours of the fission product gases and to confirm that the levels of the released fission product gases were within their limits during the operation. The primary coolant radioactivity instrumentation of the safety protection system, the fuel failure detection (FFD) system, and the primary coolant sampling system have been installed in the primary circuit for the measurement of the primary coolant radioactivity [3]. The primary coolant radioactivity was measured continuously during this operation. Results were that, not only all signals were less than the alarm level of 10 GBq/m³ which corresponds to 0.2% of fuel failure, but also all signals were less than the detection limits (1 GBq/m³). The measured release-to-birth ratios, (R/B), of 88 Kr as a function of the reactor power are plotted in Figure 6. In this operation, the measured fractional release at 50% of the reactor power shows the same levels as in rated operation mode, and then increase exponentially to 1.0x10⁻⁸ at the full power operation, which was slightly larger than in the rated operation mode, 7x10⁻⁹. The measured (R/B) at the full power was three orders lower than the limitation of 5.35x10⁻⁴, which corresponds to 1% fuel failure. It suggests that the measured values were within the release level by diffusion of the generated fission gas from the contaminated uranium in the fuel compact matrix, and no significant failure occurred during the 950°C operation.

Figure 6. Fractional release fractions of ^{88}Kr during the rise-to-power tests



Future test programme

(1) Simulation tests of abnormal transients caused by the nuclear heat utilization system

After obtaining new licences from Japanese government, some simulation tests of abnormal transients caused by the nuclear heat utilization system which will be connected to the HTTR are planned in order to contribute the design of the nuclear heat utilisation system. The test results will be utilized for the validation of analytical codes as well as both of the HTTR-IS system design and the future VHTR design. Two kinds of simulation tests are planned.

One is the secondary coolant reduction test by partial secondary loss of coolant flow in order to simulate the load change of the nuclear heat utilization system. This test will demonstrate that the both of negative reactivity feedback effect and the reactor power control system brings the reactor power safely to a stable level without a reactor scram, and that the temperature transient of the reactor core is slow in a decrease of the secondary coolant flow rate. The test will be performed at a rated operation and parallel-loaded operation mode. The maximum reactor power during the test will limit within 30 MW (100%). In this test, the rotation rate of the secondary helium circulator will be changed to simulate a temperature transient of the heat utilisation system in addition to cutting off the reactor-inlet temperature control system. This test will be performed under anticipated transients without reactor scram (ATWS).

The other is the loss of final heat sink test by stopping the pressurised water air cooler. The final heat sink of the HTTR will be lost in order to simulate the abnormal stop of the nuclear heat utilization system. This test will demonstrates that the negative reactivity feedback effect of the reactor core brings the reactor power safely to a stable level without a reactor scram, and that the temperature transient of the reactor core is sufficiently slow in a rapid loss of the final heat sink. The test will be performed at a rated operation and single-loaded operation mode. The maximum reactor power during the test will be decided by evaluating the temperatures of the heat transfer tubes, pressurised water (secondary coolant), etc. This test will also be performed under ATWS.

(2) Plan of the HTTR-IS system

A hydrogen production system based on the thermochemical water-splitting iodine sulphur (IS) process is planned to be connected to the HTTR in the near future. This will establish the hydrogen production technology with an HTGR including the system integration technology for connection of hydrogen production system to HTGRs. The image of HTTR-IS system is shown in Figure 7. It will probably be the world's first demonstration of hydrogen production directly using heat supplied from a nuclear system. The HTTR-IS system aims to:

- Establish procedures on safety design and evaluation.
- Add to experience of construction, operation, and maintenance.
- Establish the control technology for both of IS process and reactor.
- Establish the technology on key high-temperature components, such as high-temperature valves, high-temperature bellows.
- Verify analysis codes.

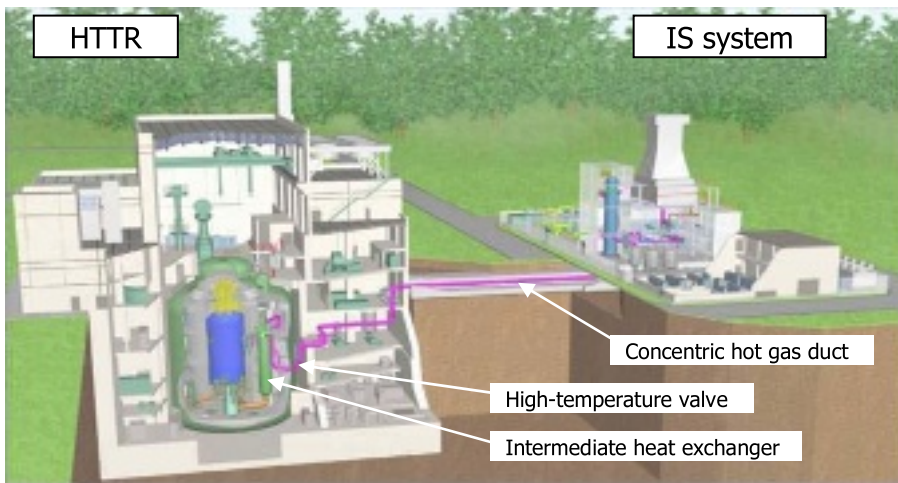
The requirements of users, such as efficiency, amount and cost of produced hydrogen, safety scenario of the connection between a nuclear reactor and chemical plant, should be satisfied or should be shown its way to commercial reactors by the HTTR-IS system development. Since the secondary helium of the HTTR will be utilised in this system, the possibility of utilization of a non-nuclear class IS system as a chemical plant is investigated. Hydrogen explosion, tritium transfer, etc. will be evaluated in order to separate IS process from nuclear facilities by high-temperature valves.

Development of the HTTR-IS system started from a conceptual design in the fiscal year 2005. Available structure of the system and its heat mass balance is evaluated initially. Basic design will be performed from design of apparatuses, kinetic analysis, and design of instrumentation and control systems in 2007. Safety case studies, detailed design, cost evaluation, and risk evaluation will be carried out in 2008. The safety analysis codes will be validated by using the component tests data and IS pilot plant operation data. The know-how of the pilot plant tests will be applied to the HTTR-IS system design. In 2009, safety assessment will be started. The assessment will may need about two years, while some studies for the higher efficiency of the HTTR-IS system continues. The design of the HTTR-IS system will be completed until 2010. Separation technology of hydrogen will also be expected to be applied.

Prior to the abnormal event study, the number of main apparatuses in the IS system should be decided. The most severe event will be selected as a representative event in the HTTR-IS system. Then the event will be compared with the abnormal transient of the HTTR secondary system which was already evaluated during the HTTR design stage. The IS process is designed conceptually using results of the component tests performed from 2005 and the concept of the GTHTR-300C which is a Japanese future HTGR designed by JAEA. In order to achieve higher efficiency in the HTTR-IS system, for instance, concentration of hydrogen iodide, intermediate chemical of hydrogen production, membrane developed by JAEA, will be studied.

The verification of the hydrogen production by the HTTR-IS system by using heat from a nuclear reactor is greatly expected to contribute to the commercialization of nuclear hydrogen in coming hydrogen society.

Figure 7. Image of the HTTR-IS system



Summary

The HTTR attained its maximum reactor-outlet coolant temperature of 950°C in 2004. The main results of 950°C operation were described. Simulation tests of abnormal transients caused by the nuclear heat utilisation system planned to be connected to the HTTR were proposed in order to contribute to the code validation for both of the HTTR-IS system design and future VHTR design, in addition to summarising the preliminary project plan of the HTTR-IS system.

REFERENCES

- [1] S. Fujikawa, H. Hayashi, T. Nakazawa, K. Kawasaki, T. Iyoku, S. Nakagawa, N. Sakaba, "Achievement of Reactor-Outlet Coolant Temperature of 950°C in HTTR", *J. Nucl. Sci. Technol.*, 41[12], 1245, (2004).
- [2] "Topical issue on Japan's HTTR", *Nucl. Eng. Des.*, 233, (2004).
- [3] S. Ueta, J. Sumita, K. Emori, M. Takahashi, K. Sawa, "Fuel and fission gas behavior during rise-to-power test of the High Temperature Engineering Test Reactor (HTTR)", *J. Nucl. Sci. Technol.*, 40[9], 679, (2003).

CURRENT STATUS OF RESEARCH AND DEVELOPMENT ON SYSTEM INTEGRATION TECHNOLOGY FOR CONNECTION BETWEEN HTGR AND HYDROGEN PRODUCTION SYSTEM AT JAEA

**Hirofumi Ohashi, Yoshitomo Inaba, Tetsuo Nishihara,
Tetsuaki Takeda, Koji Hayashi and Yoshiyuki Inagaki**

Japan Atomic Energy Agency, Japan

Abstract

Japan Atomic Energy Agency (JAEA) has been promoting R&D on the hydrogen production technology with a high temperature gas-cooled reactor (HTGR) with a view to contributing to the global warming issue and hydrogen energy society in the near future. The system integration technology for connection of the hydrogen production system to HTGR is one of the key technologies to put hydrogen production with nuclear energy to commercial use. Research on the system integration technology has been carried out about four items, that is, a) control technology to keep reactor operation against thermal disturbance caused by the hydrogen production system, b) estimation of tritium permeation from reactor to hydrogen, c) countermeasure against explosion and d) development of high temperature valve to isolate reactor and hydrogen production systems in accidents. This report describes current status of research activities on the system integration technology at JAEA.

Introduction

Research and development (R&D) for clean, economical, stable, safe and abundant energy should be promoted from the viewpoint of technology as a potential measure to mitigate the global warming issue as well as for massive and stable energy supply and utilisation. There are various options as alternative energy for fossil fuels: solar, geothermal, hydropower and nuclear energy and so on. While available natural energy is limited due to its stability, quality, quantity and density, it is sure that nuclear energy by a high-temperature gas-cooled reactor (HTGR) has the potential to come up with a share as regards a satiable energy supply and utilisation. Nuclear energy has been exclusively utilised for electric power generation, but the direct utilisation of nuclear thermal energy is necessary and indispensable so that the energy efficiency can be increased and energy savings can be promoted in the near future. The hydrogen production is one of the key technologies for direct utilisation of nuclear thermal energy. Japan Atomic Energy Agency (JAEA) has carried out the R&D on hydrogen production with HTGR, that is the HTGR technology [1], the hydrogen production technology on the thermochemical water splitting by IS process [2] without CO₂ emission and the system integration technology to connect the hydrogen production system to HTGR.

R&D Items on System Integration Technology

Figure 1 shows the concept of the HTGR hydrogen production system. The high-temperature heat generated in the reactor core is exchanged from the primary helium gas to the secondary helium gas with the intermediate heat exchanger (IHX), and the secondary helium gas is transported to the hydrogen production system through the hot gas duct. The transported heat is used in the hydrogen production system for the endothermic reaction of hydrogen production.

Figure 1. Concept of the HTGR hydrogen production system

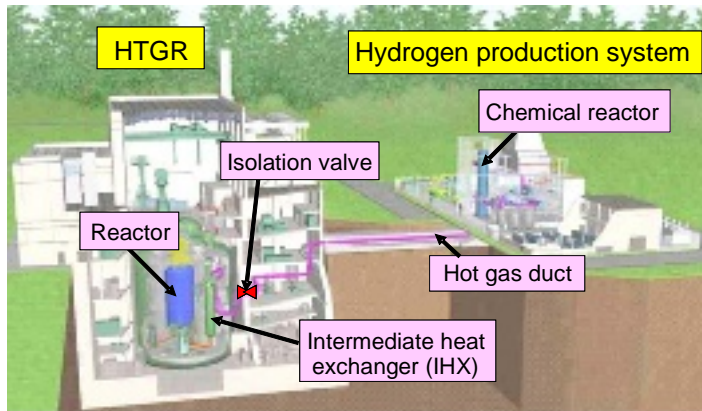
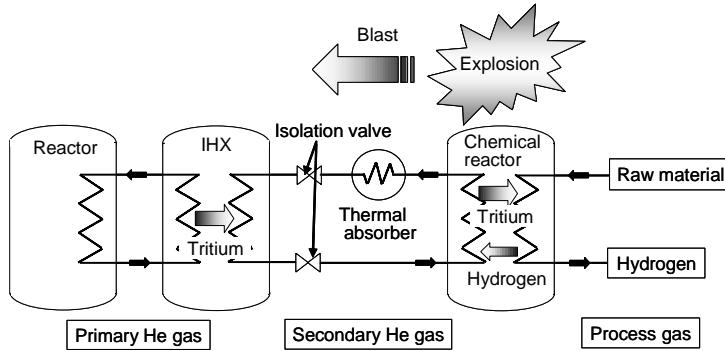


Figure 2 shows the flow diagram of the HTGR hydrogen production system and research items on the system integration technology, that is, a) control technology to keep reactor operation against thermal disturbance caused by the hydrogen production system, b) estimation of tritium permeation from reactor to hydrogen, c) countermeasure against explosion of combustible gas and d) development of high temperature isolation valve to separate reactor and hydrogen production systems in accidents.

Figure 2. Flow diagram of HTGR hydrogen production system and research items on system integration technology



Control technology

The reactor and the hydrogen production system are connected by the helium gas loop. A chemical reactor causes the temperature fluctuation of the secondary helium gas by the fluctuation of the chemical reaction that occurs at the normal start-up and the shutdown operation as well as malfunction or accident of the hydrogen production system. If the temperature fluctuation is transferred to the reactor, the reactor will be stopped. Therefore, the control technology should be developed to mitigate the temperature fluctuation within an allowable range to keep reactor operation, using a thermal absorber. JAEA proposed to use a steam generator (SG) as the thermal absorber that is installed downstream the chemical reactor in the secondary helium gas loop.

Tritium permeation

It is well known that hydrogen isotopes, hydrogen, deuterium, and tritium, permeate through solid metals. Tritium produced in the reactor core tends to permeate through heat transfer tubes of IHX and the reaction tubes of the chemical reactor. Further, it is probable that the tritium will mix with the product hydrogen. Therefore, estimation of tritium permeation should be done, and a countermeasure to reduce tritium permeation, if necessary.

Countermeasure against explosion

The explosion of combustible gas is a very severe problem to keep the reactor safety. The problem can be considered as overpressure caused by blast to the safety-related components. There are three principal countermeasures against explosion, that is, i) place a distance between the reactor and the hydrogen production system enough to mitigate the overpressure within an allowable range, ii) limit the leak amount of combustible gas, and iii) protect blast with barriers such as wall, bank and so on. As for the hydrogen production system connected to HTTR, the countermeasure-ii) was mainly considered.

High temperature isolation valve

The isolation valve is a key component to assure the safety, that is, protection of radioactive material release from the reactor to the hydrogen production system and combustible gas ingress to the reactor at the accident of fracture of IHX and the chemical reactor. The high temperature isolation valve

(HTIV) used in the helium condition over 900°C, however, it has not yet been fabricated for actual use. JAEA has been conducting design and a component test on HTIV.

Current Status of R&D at JAEA

Control Technology

In the design of the HTTR hydrogen production system (HTTR-H2), SG is installed as the thermal absorber downstream the chemical reactor in the secondary helium gas loop to mitigate the temperature fluctuation within 10°C at the SG outlet, because the temperature rise above 15°C compared with the normal temperature at the reactor inlet causes the HTTR reactor scram [3].

Figure 3. Flow diagram of mock-up test facility for development of control technology

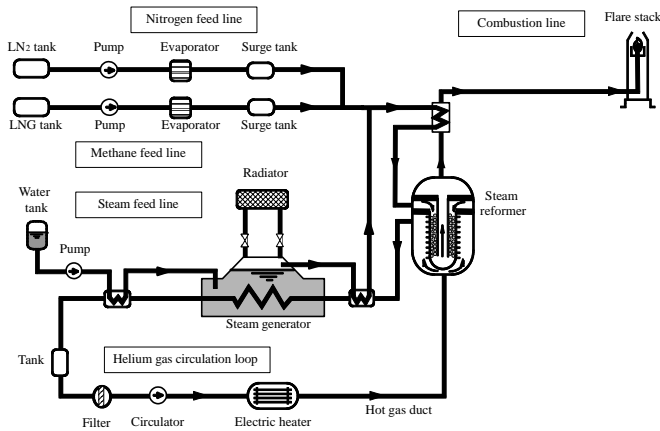
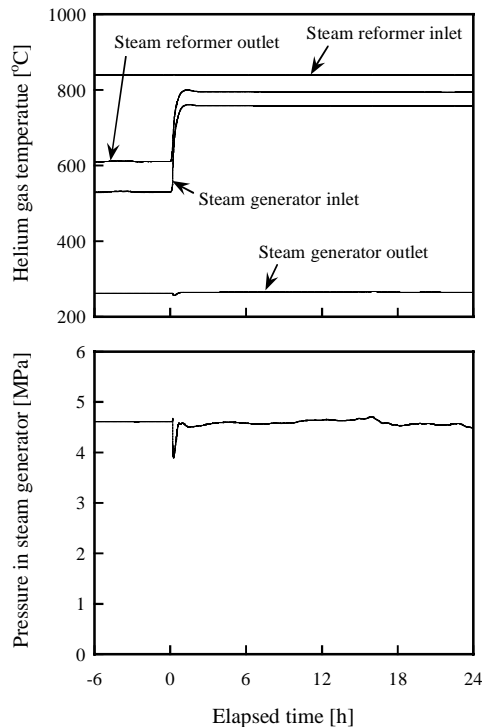


Figure 4. Experimental result of simulation test on the loss of chemical reaction



A simulation test with a mock-up test facility was carried out to investigate performance of SG for the mitigation of the temperature fluctuation and transient behavior of the hydrogen production system and to obtain experimental data for verification of a dynamic analysis code [4-7]. Figure 3 shows the schematic flow diagram of the test facility. The test facility has an approximate production capacity of 120 m³/h and simulates key components downstream from IHX. An electric heater is used as a heat source instead of the reactor in order to heat helium gas up to 880°C (4 MPa) at the chemical reactor inlet which is the same temperature as HTTR-H2. The steam reforming process of methane; $\text{CH}_4 + \text{H}_2\text{O} = 3\text{H}_2 + \text{CO}$, instead of the IS process is used for hydrogen production of the test facility.

Figure 4 shows the experimental results of the simulation test on the loss of chemical reaction accident that is the severest accident for the temperature fluctuation of the secondary helium gas. The supply of the raw gas for the hydrogen production, methane, was suspended during the normal operation to simulate an accident at the hydrogen production system. The SG inlet helium gas temperature increased 228°C due to the loss of chemical reaction, however, helium gas temperature at SG outlet showed almost stable value. The fluctuation range of the helium gas temperature was from -5.5°C to +5.0°C at SG outlet, which is within the target range of HTTR-H2.

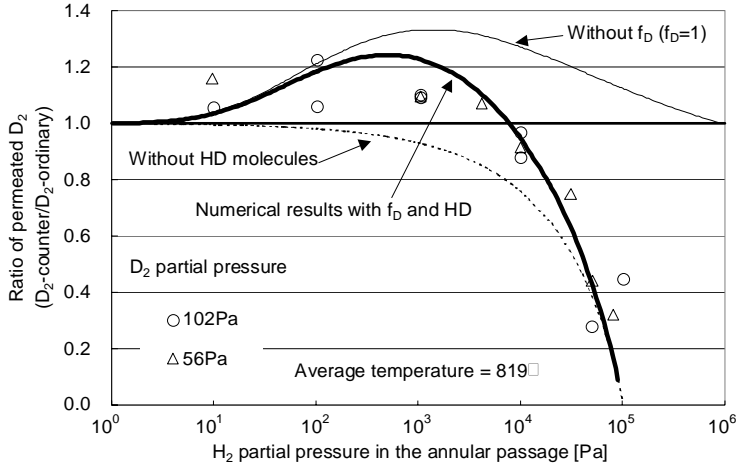
As a result, it was confirmed that SG can be used as a thermal absorber to mitigate the temperature fluctuation of the secondary helium gas caused by the chemical reactor. This technology can keep reactor operation at normal start-up and shutdown operation as well as malfunction or accident of the hydrogen production system.

Tritium Permeation

A component test was carried out to investigate the permeability of the material of the IHX tubes, Hastelloy XR, and the permeation phenomenon of the reaction tubes where hydrogen and tritium permeate in the counter direction as shown in Figure 2 [8, 9]. A test section of an experimental apparatus was made a coaxial double pipe structure, which inserted the permeation test pipe, Hastelloy XR or Inconel 600, into the measurement pipe, Hastelloy X of which hydrogen permeability is already known. Hydrogen (H₂) and deuterium (D₂) instead of tritium were flowed with helium and argon gases into the inside and outside of the permeation test pipe and the partial pressure of hydrogen isotope was measured by a quadrupole mass spectrometer.

Experiment and analysis on counter-permeation of D₂ and H₂ were performed to investigate the effect of the existence of high pressure H₂ on the amount of permeated D₂, instead of tritium, when the rate-limiting step of the permeation becomes the diffusion process in metals [9]. Figure 5 shows the experimental (symbols) and numerical (lines) results on the counter- permeation. When D permeates from the inside of the test pipe and H permeates from the outside, the amount of permeated D₂ through the test pipe depends not only on the partial pressure of D₂ but also on that of H₂ existing outside the test pipe. When the partial pressure of D₂ in the test pipe is lower than 102 Pa and the one of H₂ outside the test pipe is higher than 10 kPa, the amount of permeated D₂ in counter-permeation decreases compared with the one in ordinary permeation. This is because the interstitial sites where D atoms can be dissolved on the metal surface decrease by occupation by a large amount of dissolved H atoms on the surface. On the other hand, when the partial pressure of D₂ and H₂ are lower than 1 kPa, the interstitial sites do not decrease so much because the amount of dissolved H atoms decrease. In this case, the partial pressure of D₂ and HD molecules becomes almost equal as taking account of the equilibrium state of D₂, H₂ and HD molecules on the surface. Consequently, the amount of permeated D₂ on counter-permeation increases relative to the one for ordinary permeation because the amount of dissolved D atoms increases.

Figure 5. Experimental and numerical results of permeated deuterium on counter-permeation of deuterium and hydrogen



The amount of permeated D_2 on counter-permeation, Q_D [$m^3(STP) s^{-1}$], can be predicted by the following in consideration of occupation ratio of the interstitial sites, at which D atoms can be dissolved on the metal:

$$Q_D = \frac{2\pi \cdot L \cdot f_D \cdot D_D}{\ln(r_o / r_i)} (C_{D,i} - C_{D,o}), \quad (1)$$

$$f_D = 1 - C_{H,o} / C_{H,po} . \quad (2)$$

where D_D , $C_{D,i}$, $C_{D,o}$, $C_{H,o}$ and $C_{H,po}$ are diffusivity of D_2 [$m^2 s^{-1}$], atomic mole concentration of D on the inside and outside surfaces of the test pipe, atomic mole concentration of H on the outside surfaces of the test pipe, and saturated atomic mole concentration of H, respectively.

Explosion of Combustible Gas

The simplest countermeasure against explosion of combustible gas is to place a long distance between the reactor and the hydrogen production system. However, this countermeasure brings about the rise of the construction cost and the decline of the helium gas temperature, i.e. the decline of the hydrogen production efficiency. Therefore, the hydrogen production system should be arranged closed by the reactor to achieve economical hydrogen production.

The probabilistic safety assessment (PSA) for the steam reforming process was carried out to investigate the cause of an accident on combustible gas leak and a conceptual design on a countermeasure against explosion was carried out aiming at reducing the probability of the combustible gas leak less than 10^{-6} /year. The rupture of combustible gas pipes is considered as the cause of the leakage.

A coaxial pipe of combustible gas was designed from the viewpoint of protection of the leakage. The coaxial pipe is composed of an inner pipe in which combustible gas flows and an outer pipe in which nitrogen gas is filled. If the inner pipe is fractured, the outer pipe can protect leak of combustible gas to atmosphere and the leak from the inner pipe can be easily detected. In case of fracture of the outer pipe by detection of pressure down of nitrogen gas, hydrogen production is stopped and combustible gas in the inner pipe is purged with nitrogen gas.

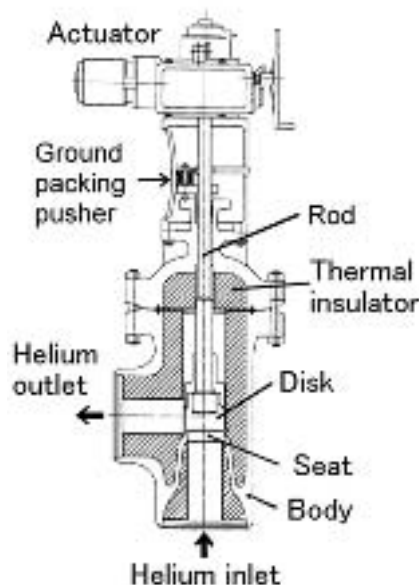
At present, a conceptual design using a wall and/or a bank is under way from the viewpoint of mitigation of blast.

High Temperature Isolation Valve (HTIV)

The HTIV has functions to protect radioactive materials release to the hydrogen production system in case of fracture of IHX and to prevent combustible gas ingress to the reactor in case of fracture of the chemical reactor. JAEA has been conducting the design focusing on prevention of a valve seat from thermal deformation and a new material for the valve seat surface was developed to keep face roughness of the seat within allowable level against open and close. An angle valve was selected from the viewpoint of workability of inner thermal insulator as shown in Figure 6, and the detailed structure was decided by the thermal stress analysis to prevent the deformation of the valve seat. The building material of the valve seat, which can keep hardness and wear resistance at high temperature over 900°C, is necessary to assure the seal performance. A new building material was developed [10].

A component test was carried out with a 1/2 scale model of HTIV for HTTR-H2 to confirm the structural integrity and the seal performance of the valve seat. An experimental apparatus is composed of the 1/2 scale mode of HTIV, electric heaters, gas supply systems, an actuator, a concentration measurement system and so on. Helium gas at 4.0 MPa was supplied to the 1/2 scale model of HTIV, and the pressure difference across the valve seat was set to 4.0 MPa. The leaked helium gas from the closed valve seat was mixed with argon gas and the leak amount was measured by a helium gas detector. Before closing at 900°C, the helium gas leak rate from the valve seat at a room temperature was less than 1 cc/s, which satisfied the design target, 4.4 cc/s. The leak rate decreased less than 0.1 cc/s after closing at 900°C, and then it increased up to around the design target at a room temperature after opening at a room temperature. By lapping the valve seat, the leak rate at a room temperature became less than 1 cc/s again. The current technology can be applied to HTTR-H2, however, the work to lap the valve seat is necessary after closing at a high temperature. Therefore, the next research item is improvement of durability of the valve seat by refinement of the building metal and so on.

Figure 6. Schematic view of high temperature isolation valve



Conclusion

The system integration technology has been developed for connection of the hydrogen production system to HTGR. The following conclusions were obtained on the research items, a) control technology to keep reactor operation against thermal disturbance caused by the hydrogen production system, b) tritium permeation from reactor to hydrogen, c) countermeasure against explosion of combustible gas and d) HTIV to isolate reactor and hydrogen production systems in accidents.

As for the control technology, JAEA proposed to use SG as the thermal absorber, which is installed downstream the chemical reactor in the secondary helium gas loop, to mitigate the temperature fluctuation of the secondary helium gas. By the simulation test with the mock-up test facility, it was confirmed that the SG could be used as the thermal absorber.

As for the tritium permeation, the permeability on Hastelloy XR was obtained and the numerical equation was introduced to predict the behavior on the counter-permeation of hydrogen and tritium at the chemical reactor.

As for the countermeasure against explosion, it was found that the rupture of combustible gas pipes was the main cause of the leak having a large impact on the reactor safety by PSA, and the coaxial pipe of combustible gas was designed from the viewpoint of protection of the leakage aiming at arrangement of the hydrogen production system closed by the reactor.

As for HTIV, the new building material of the valve seat used over 900°C was developed and the seal performance of the angle valve was confirmed to satisfy the design target with the 1/2 scale model of HTTR-H2. The improvement of durability of the valve seat is the next target for development.

Acknowledgments

The present study is the results of “Development of Nuclear Heat Utilisation Technology“ in fiscal year from 1997 to 2001, 2003 and 2004 entrusted by Ministry of Education, Culture, Sports, Science and Technology (MEXT) to Japan Atomic Energy Research Institute (JAERI) succeeded by into Japan Atomic Energy Agency (JAEA). The authors are indebted to Dr. S. Shiozawa and Dr. M. Ogawa for their useful advice and discussion in this research.

REFERENCES

- [1] S. Saito, *et al.*, “Design of High Temperature Engineering Test Reactor,” JAERI-1332, Japan Atomic Energy Research Institute (JAERI), (1994).
- [2] S. Kubo, *et al.*, “A demonstration study on a closed-cycle hydrogen production by the thermochemical water-splitting iodine-sulfur process” Nucl. Engng. Des ., 233, 347 (2004).
- [3] S. Uchida, *et al.*, “A Conceptional Design Study on the Hydrogen Production Plant Coupled With the HTTR,” Proc. 11th Int. Conf. on Nucl. Eng., Tokyo, Japan, April 20-23, 2003, ICONE11-36319 (2003).
- [4] Y. Inagaki, *et al.*, “Out-of-Pile Demonstration Test of Hydrogen Production System Coupling with HTTR,” Proc. 7th Int. Conf. on Nucl. Eng., Tokyo, Japan, April 19-23, 1999, ICONE-7101 (1999).
- [5] H. Ohashi, *et al.*, “Performance Test Results of Mock-up Test Facility of HTTR Hydrogen Production System,” J.Nucl. Sci. Tech ., 41, 3, 385 (2004).
- [6] Y. Inaba *et al.*, “Study on Control Characteristics for HTTR Hydrogen Production System with Mock-up Test Facility System Controllability Test for Fluctuation of Chemical Reaction,” Nucl. Engng. Des ., 235, 111 (2004).
- [7] H. Ohashi, *et al.*, “Experimental and Analytical Study on Chemical Reaction Loss Accident with a Mock-up Model of HTTR Hydrogen Production System,” Proc. 12th Int. Conf. on Nucl. Eng., Arlington, Virginia USA, April 25-29, 2004, ICONE12-49419 (2004).
- [8] T. Takeda, *et al.*, “Permeability of Hydrogen and Deuterium of Hastelloy XR,” J. Nucl. Mater., 326, 47 (2004).
- [9] T. Takeda, *et al.*, “Counter-Permeation of Deuterium and Hydrogen through Inconel 600,” Nucl. Tech., 146, 83 (2004).
- [10] N. Nishihara, *et al.*, “Development of High Temperature Isolation Valve for the HTTR Hydrogen Production System,” JANS, 3, 4, 69 (2004) (in Japanese).

This page intentionally left blank

SESSION IV

NUCLEAR HYDROGEN TECHNOLOGIES AND DESIGN CONCEPTS

Chairs: K. Kunitomi, J.S. Herring, Y.S. Shin, T. Takeda

This page intentionally left blank

STUDY ON THERMOCHEMICAL IODINE-SULFUR PROCESS AT JAEA

Kaoru Onuki, Shinji Kubo, Atsuhiko Terada, Nariaki Sakaba, and Ryutaro Hino
Japan Atomic Energy Agency, Japan

Abstract

Thermochemical water-splitting process of Iodine-Sulfur family (IS process) has been studied in various research institutions. Previous studies cover the chemistry of each reaction section, heat/mass balance analysis of the process flowsheet, screening of corrosion-resistant materials of construction, development of advanced chemical reactor made of ceramics, and small-scale demonstration of the closed-cycle hydrogen production. Based on these studies, a pilot test of IS process is planned at Japan Atomic Energy Agency (JAEA), which consists of (1) hydrogen production test using test apparatus made of industrial materials and electrically-heated helium gas as the process driver, (2) development of analytical code system, (3) R&D on efficient unit operations and on advanced materials, (4) design study on a next-stage test plant to be connected to the HTTR.

Introduction

“Thermochemical method” for hydrogen production offers a technology with which nuclear energy is transformed into hydrogen, the energy carrier. This paper briefly describes the present status of study on Iodine-Sulfur cycle, a promising thermochemical cycle, at JAEA.

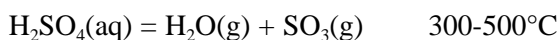
Hydrogen production by direct thermal decomposition of water requires high temperature heat of a few thousand Kelvin. However, by combining high-temperature endothermic chemical reactions and low-temperature exothermic chemical reactions, in which the net chemical change resulting from the sequence of component chemical reactions is the water decomposition, it is possible, in principle, to decompose water only with the heat of lower temperature. The cycle of chemical reactions produces the free energy required for water splitting. It is called thermochemical method and has a possibility of large-scale carbon-free hydrogen production.

Thermochemical water splitting cycle was first studied by Funk [1], and an actual example was proposed by researchers of CEC, JRC Ispra establishment, in early 70s [2]. Since then, a number of thermochemical cycles have been proposed assuming high temperature gas-cooled reactor (HTGR) as the heat source, which can supply heat with its maximum temperature of close to 1 000°C. After mid-80s, activities in Europe and in North America slowed down in accordance with the slowing down of their HTGR projects. Recently, however, with the emerging interest in the “hydrogen energy system” in accordance with the progress of fuel cell technology, the thermochemical method attracts growing interest again.

Previous studies on Iodine-Sulfur cycle focusing on the activities of JAERI

Hundreds of cycles have been studied from the viewpoints of the feasibility of component chemical reactions in terms of conversion ratio and/or products separation, theoretical thermal efficiency of hydrogen production etc [3]. Among them, those that utilise thermal decomposition of sulfuric acid, which are categorised as “sulfur cycles”, have been considered one of the most promising cycles.

Thermal decomposition of sulfuric acid, reaction (1), proceeds in the following two steps.



Both steps are highly endothermic and proceed smoothly without side reactions and with high conversion ratio at the temperature range indicated. The endothermic characteristics match well with the temperature distribution of the heat source, HTGR. The heat of HTGR is transferred to the chemical process through the sensible heat of helium gas, the temperature of which varies, e.g. 900-400°C. Therefore, the reaction is quite suited as the high temperature endothermic reaction for thermochemical water splitting cycle [4].

Iodine-Sulfur cycle (or Sulfur-Iodine cycle, or ISPR Mark 16 cycle) combines following chemical reactions with the sulfuric acid decomposition reaction.



Here, reaction (2), known as “Bunsen reaction”, is the low-temperature exothermic reaction, where raw material, water, reacts with iodine and gaseous sulfur dioxide producing an aqueous solution of hydriodic acid and sulfuric acid. The acids are then separated and thermally decomposed to produce hydrogen and oxygen.

The cycle has been studied in US, Europe and Japan since 1970s, and some important breakthroughs were attained by General Atomics (GA). So far, the research has been carried out in the following fields:

- (a) study on the chemistry of each reaction section;
- (b) demonstration of the closed-cycle hydrogen production;
- (c) heat/mass balance analysis of the process flowsheet;
- (d) screening of corrosion-resistant materials and development of advanced chemical reactors.

There are two main issues concerning the chemistry of the reaction and the separation. One is how to separate the hydriodic acid and sulfuric acid produced by the Bunsen reaction. The other is how to carry out the hydrogen iodide decomposition section, where the presence of azeotrope in the vapor-liquid equilibrium of hydriodic acid makes the energy-efficient separation of HI from its aqueous solution difficult and also unfavorable reaction equilibrium limits the attainable conversion ratio of HI to a low level, ca. 20%.

As for the former problem, the researchers of GA found that the mixed acid solution produced by the Bunsen reaction separates spontaneously into two liquid phases in the presence of excess amount of iodine [4]. The heavier phase is mainly composed of HI, I₂, and H₂O, and is called “HIx” solution. The main components of the lighter phase are H₂SO₄ and H₂O. The phenomenon (LL phase separation) offered an easy way of separating the hydriodic acid and the sulfuric acid. As for the hydrogen iodide processing, some ideas have been proposed by GA [4], RWTH Aachen [5] and JAERI. JAERI studied a utilization of membrane technologies for concentrating the HIx solution to facilitate the HI separation and also for enhancing the one-pass conversion of HI decomposition [6,7].

One of the specific and important characteristics of thermochemical water splitting cycles is that the reactants except water are cyclically used in the process. The closed-cycle continuous hydrogen production by Iodine-Sulfur process featuring the LL phase separation has been examined at JAERI. Although the chemistry of sulfuric acid decomposition section and that of hydrogen iodide decomposition section are rather straightforward in terms of reaction and separation, in the Bunsen reaction section, occurrence of side reactions forming sulfur and/or hydrogen sulfide should be suppressed while maintaining the liquid-liquid phase separation. JAERI has devised a basic methodology for the closed-cycle continuous hydrogen production and also for the reaction control in the Bunsen reaction step. Feasibility of the methodology has been demonstrated in small-scale continuous hydrogen production experiments of 1NL-H₂/h and of 30NL-H₂/h, as well [8,9].

Preliminary flowsheeting studies carried out at GA [10,11], RWTH Aachen [5,12], Ecole Polytechnique Montreal [13], CEA [14] and JAERI [15] suggested that the “process thermal efficiency” in the range of 35-50% could be possible assuming intensive heat recovery. Here, the thermal efficiency is defined as the ratio of the Higher Heating Value (HHV) of hydrogen to the net energy input for the process. Precise thermodynamic data concerning the concentrated process solutions is desired for the accurate evaluation of the heat/mass balance.

Since sulfuric acid and halogen are very corrosive, selection of the structural materials is an important issue. Screening tests have been carried out using test pieces of commercially available materials at GA [16], JAERI [17] etc. As for the gas phase environment of H_2SO_4 decomposition step, some refractory alloys that have been used in conventional chemical plants showed good corrosion resistance. Also, in the gas phase environment of HI decomposition step, a Ni-Cr-Mo-Ta alloy was found to show good corrosion resistance. As for the Bunsen reaction step, glass-lining materials, Ta etc showed corrosion resistance. In the environment of HIX distillation, Ta showed excellent corrosion resistance. The severest environment is the boiling condition of concentrated sulfuric acid under high pressure (e.g. 20bar), where ceramic materials containing Si such as SiSiC, SiC, and Si₃N₄ were the only materials that showed excellent corrosion resistance [18]. In summary, for gas phase service, there exists little concern on the structural materials. As for the equipments used in the Bunsen reaction step, lining materials should be used. Special design consideration is required for the equipments to be used in the boiling and condensing conditions of the acids.

One of the key components to be used in the boiling sulfuric acid environments is the sulfuric acid decomposer, in which sulfuric acid solution with concentration of more than 90 wt% is evaporated and, simultaneously, H_2SO_4 is decomposed into gaseous SO_3 and H_2O under high temperature conditions of up to 500°C. Recently, JAERI proposed a concept of the sulfuric acid decomposer, in which multi-hole-blocks made of SiC is used as the heat exchanging units. Feasibility of the concept has been confirmed by preliminary analysis of the mechanical strength and thermal-hydraulic performance, and also by a test-fabrication of prototype ceramic block [19].

JAEA's Pilot Test Plan

At present, JAEA is conducting R&D programmes to develop technologies for the thermochemical hydrogen production using HTGR. The programme covers R&D on HTGR technology, R&D on the system integration technology to connect HTGR and hydrogen production plant, and R&D on Iodine-Sulfur cycle.

As for Iodine-Sulfur cycle, a pilot test is planned as a logical evolution of the above-mentioned studies. In the pilot test, following studies will be carried out [20].

- (1) Development of IS process test plant made of engineering materials. Capacity of the plant may be in the range of 10-30m³-H₂/h, with which smallest components used in industrial chemical plants can be tested such as valves, pumps, etc.
- (2) Hydrogen production test using the test apparatus driven by electrically-heated helium gas. Operation of the test plant will demonstrate the technical feasibility of Iodine-Sulfur cycle, and, also, the test data will be used to verify the analytical codes to be developed.
- (3) Development of computer code system for analysing the heat/mass balance, for dynamic process simulation, for supporting the component design works, etc.

- (4) R&D on advanced low-cost materials that exhibit corrosion resistance in the severe process environments.
- (5) R&D on advanced unit operations that enable to improve the heat/mass balance.
- (6) Design study on a next-stage test plant to be connected to the HTTR.

After completion of the pilot test of Iodine-Sulfur cycle, it is planned to proceed to the demonstration test of nuclear hydrogen production using HTTR.

REFERENCES

- [1] J.E. Funk and R.M. Reinstrom, "Energy requirements in the production of hydrogen from water," *I&EC Process Design and Development*, 5 (1966) 336-342.
- [2] G.E. Beghi, "A decade of research on thermochemical hydrogen at the Joint Research Centre, ISPRA," *Int. J. Hydrogen Energy*, 11 (1986) 761-771.
- [3] J.E. Funk, "Thermochemical hydrogen production: past and present," *Int. J. Hydrogen Energy*, 26 (2001) 185-190.
- [4] J.H. Norman, G.E. Besenbruch, D.R. O'Keefe, "Thermochemical water-splitting for hydrogen production," GRI-80/0105, 1981.
- [5] H. Engels, K.F. Knoche, M. Roth, "Direct dissociation of hydrogen iodide - an alternative to the General Atomic proposal," *Proc. 6th World hydrogen Energy Conf.*, Vienna, Austria, July 1986, vol.2, pp.657-662.
- [6] K. Onuki, G.-J. Hwang, Arifal, S. Shimizu, "Electro-electrodialysis of hydriodic acid in the presence of iodine at elevated temperature," *J. Membr. Sci.*, 192 (2001) 193-199.
- [7] G.-J. Hwang, K. Onuki, S. Shimizu, "Separation of hydrogen from a H₂-H₂O-HI gaseous mixture using a silica membrane," *AIChE J.*, 46 (2000) 92-98.
- [8] H. Nakajima, M. Sakurai, K. Ikenoya, G.-J. Hwang, K. Onuki, S. Shimizu, "A study on a closed-cycle hydrogen production by thermochemical water-splitting IS process," *Proc. 7th Int. Conf. Nucl. Eng. (ICONE-7)*, Tokyo, Japan, April 1999, ICONE-7104.
- [9] S. Kubo, H. Nakajima, S. Kasahara, S. Higashi, T. Masaki, H. Abe, K. Onuki, "A demonstration study on a closed-cycle hydrogen production by thermochemical water-splitting Iodine-Sulfur process," *Nucl. Eng. Des.*, 233 (2004) 347-354.
- [10] J.H. Norman, G.E. Besenbruch, L.C. Brown, D.R. O'Keefe, C.L. Allen, "Thermochemical water-splitting cycle, bench-scale investigations and process engineering," GA-A 16713, 1982.
- [11] L.C. Brown, G.E. Besenbruch, R.D. Lentsch, K.R. Schultz, J.E. Funk, P.S. Pickard, A.C. Marshall, S.K. Showalter, "High efficiency generation of hydrogen fuels using nuclear power," GA-A24285, June 2003.
- [12] K.F. Knoche, H. Schepers, K. Hesselmann, "Second law and cost analysis of the oxygen generation step of the General Atomic Sulfur-Iodine cycle," *Proc. 5th World hydrogen Energy Conf.*, Toronto, Canada, July 1984, vol.2, pp.487-502.
- [13] I.T. Oeztuerk, A. Hammache, E. Bilgen, "An improved process for H₂SO₄ decomposition of the sulfur-iodine cycle," *Energy Convers. Mgmt.*, 36 (1995) 11-21.

- [14] S. Goldstein, J. Borgard, X. Vitart, "Upper bound and best estimate of the efficiency of the iodine sulphur cycle," *Int. J. Hydrogen Energy*, 30 (2005) 619-626.
- [15] S. Kasahara, G.-J. Hwang, H. Nakajima, H.-S. Choi, K. Onuki, M. Nomura, "Effects of process parameters of the IS process on total thermal efficiency to produce hydrogen from water," *J. Chem. Eng. Jpn.*, 36 (2003) 887-899.
- [16] P.W. Trester and H.G. Staley, "Assessment and investigation of containment materials for the Sulfur-Iodine thermochemical water-splitting process for hydrogen production," GRI-80/0081, 1981.
- [17] K. Onuki, H. Nakajima, I. Ioka, M. Futakawa, S. Shimizu, "IS process for thermochemical hydrogen production," *JAERI-Review* 94-006, 1994.
- [18] S. Kubo, M. Futakawa, I. Ioka, K. Onuki, S. Shimizu, K. Ohsaka, A. Yamaguchi, R. Tsukada, T. Goto, "Corrosion test on structural materials for Iodine-Sulfur thermochemical water splitting cycle," *Proc. 2nd Topical Conf. on Fuel Cell Technology, AIChE 2003 Spring National Meeting*, New Orleans, La, USA.
- [19] H. Ota, A. Terada, S. Kubo, S. Kasahara, M. Hodotsuka, R. Hino, T. Inatomi, K. Ogura, M. Kobayashi, S. Maruyama, "Conceptual design study on sulfuric-acid decomposer for thermochemical Iodine-Sulfur process," *Proc. 13th Int. Conf. Nucl. Eng. (ICONE-13)*, Beijing, China, May 2005, ICONE-13-50494.
- [20] A. Terada, S. Kubo, H. Okuda, S. Kasahara, N. Tanaka, H. Ota, A. Kanagawa, K. Onuki, R. Hino, "Development program of hydrogen production by thermochemical water splitting IS process," *Proc. 13th Int. Conf. Nucl. Eng. (ICONE-13)*, Beijing, China, May 2005, ICONE-13-50183.

This page intentionally left blank

STUDIES ON CONTINUOUS AND CLOSED-CYCLE HYDROGEN PRODUCTION BY A THERMOCHEMICAL WATER-SPLITTING IODINE-SULFUR PROCESS

Shinji Kubo, Sabro Shimizu, Hayato Nakajima and Kaoru Onuki
Japan Atomic Energy Agency, Japan

Abstract

The use of the iodine-sulfur process for hydrogen production, which utilizes nuclear energy, has attracted considerable interest for applications in areas including the economy, environmental conservation and mass production. One of the primary merits of the process is the fact that it is operable on continuous and closed-cycle operations. Studies on the process operation have been implemented on lab-scale R&D and bench-scale stages to develop key technologies to achieve such operations. Techniques for recycling chemicals to complete the closed-cycle and the fundamental concepts of the control method used to stably maintain the process were developed and demonstrated through hydrogen production tests using glass facilities.

Introduction

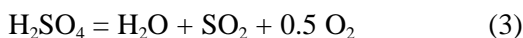
Thermochemical water-splitting processes offer the potential for the mass production of hydrogen without using carbon dioxide, supplied with heat from high-temperature gas-cooled reactors (HTGRs).

The IS process that uses iodine and sulfur is a variation of those proposed by the General Atomic Co [1]. Since it features such attractive characteristics, we have implemented studies to develop a hydrogen production system using the IS process with HTGR. The IS process should include features whereby all process fluids act in the liquid or gaseous phase, and all chemicals except hydrogen and oxygen circulate through the process. This enables continuous and closed-cycle operations, which cannot be performed in other chemical plants, leading to various difficulties in actually implementing such operations. To ensure the IS process can become a reality in an operational chemical plant, studies on the process operation were implemented at lab-scale R&D and bench-scale stages respectively. This paper describes the essential technologies used to achieve continuous and closed cycle operation, which were developed through both R&D stages.

Continuous and closed-cycle Operation

The IS process features a unique characteristic, namely, its operability under continuous and closed-cycle conditions. This feature is important for running the IS process using continuous heat from HTGRs with no external waste generated.

Figure 1. shows a brief scheme of the process, which comprises the following chemical reactions



These three reactions establish a chemical cycle, which converts water, as the raw material, into products of hydrogen and oxygen by absorbing heat. The first reaction is called the Bunsen reaction (eq. 1). This reaction in the aqueous solutions produces two acids, namely hydriodic acid and sulfuric acid, from water, sulfur dioxide and iodine. After separation of the acids by the liquid-liquid phase separation process, each acid is purified and concentrated to remove excess water, before decomposing in the other two reactions during the gaseous phases. The hydriodic acid decomposes into iodine and hydrogen with a small endothermic reaction (eq. 2). The sulfuric acid decomposes into water, sulfur dioxide and oxygen with an endothermic reaction (eq. 3). For all chemicals acting in the fluid phase, the process, including the three aforementioned reactions, can be operated continuously. For completion of the closed-cycle, the impurities, excess water and decomposition products have to be completely recycled into the Bunsen reaction section.

Development of the continuous and closed-cycle process

(1) Studies on the process operation

To establish the IS process in an operational chemical plant, studies on the process operation were carried out in various stages. Figure 2 shows the R&D stages for the IS process at the Japan Atomic

Energy Agency (JAEA), while photographs of the lab- and bench-scale test facilities are respectively shown in Figure 3. The first stage, techniques for recycling chemicals, was investigated through a laboratory scale test to complete the closed-cycle. The test facility was mainly made of glass, with the required heat supplied by electricity. By developing chemical recycling techniques, we succeeded in producing 1 L/h of hydrogen over 48 hours [2]. For the second stage, involving stable and durable hydrogen production, control methods for the closed-cycle operation were essential, hence we constructed a larger test facility [3] to develop such methods. The facility was of sufficient size to allow instruments for the measurements and controls to be integrated. By further developing the process control method, stable hydrogen production of 31 L/h was successfully accomplished for 175 hours [4]. In the next stage, namely a preliminary step toward the HTTR-IS test [5, 6], we hope to proceed to the pilot test [7]. The plant for this test will be made of industrial materials, like refractory alloys, glass linings, and ceramics, and high temperature helium gas will be supplied for its operation.

Figure 1. Reaction scheme of the IS process

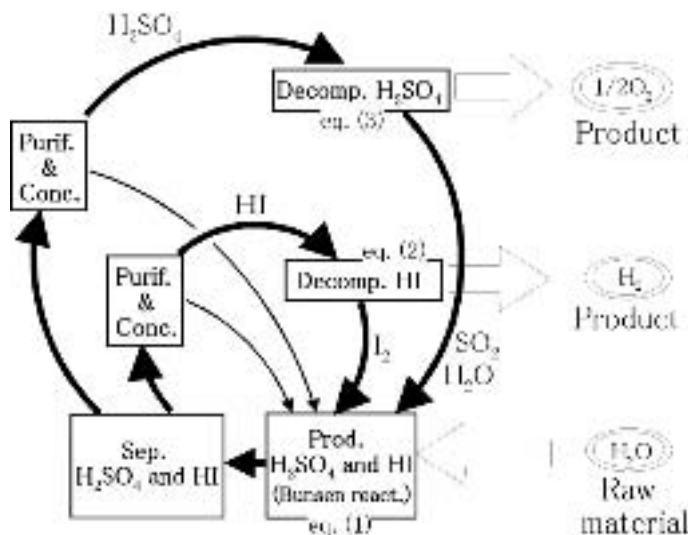
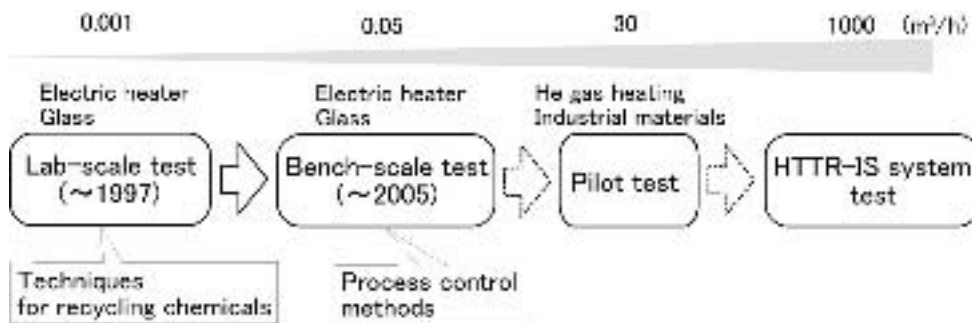


Figure 2. R&D stages for the IS process at the JAEA



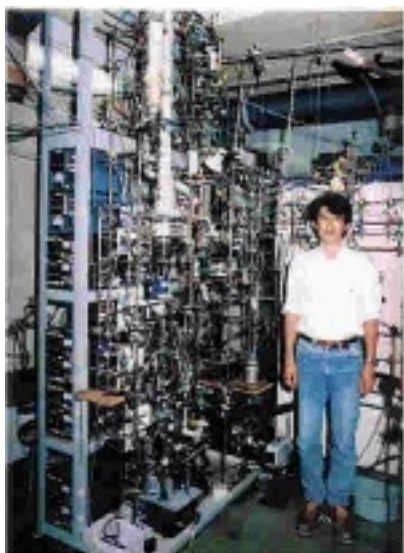
(2) Techniques for recycling chemicals during the lab-scale stage

All chemicals circulate throughout the process, changing their chemical forms under the closed-cycle condition, and are thus completely recycled. However, conducting such an operation involves various practical difficulties. During the lab-scale stage, key techniques for recycling chemicals were investigated.

Purification, to remove and recycle impurities, was a key technique making up part of the closed-cycle, which targeted the complete separation of the residual acid to prevent any side reactions forming sulfur or hydrogen sulfide. Although the solution produced from the Bunsen reaction can be separated into upper and lower phases in the presence of an excess amount of iodine, they are contaminated by each other's components. The upper phase (sulfuric acid phase) is rich in sulfuric acid, which contains impurities of HI and iodine as minor components. The lower phase (HIx phase) is rich in HI, which contains an impurity in the form of sulfuric acid as its minor component. To purify the phase separated acids, wetted-wall columns were adopted for the purifiers using nitrogen as a stripping gas for the evolved SO_2 ; and their process was implemented utilizing the reverse reaction of the Bunsen reaction. Based on examinations of the purifier [8], complete separation of the sulfuric acid involved in the HIx phase was attained above a wall temperature of 170°C . By adapting the purifier, the sulfur, separated from the HIx phase in the form of sulfur dioxide, could be recycled during the Bunsen reaction step. In addition, the purification of the sulfuric acid phase was possible in the same manner.

Compositions of the Bunsen reaction and liquid-liquid phase separation solutions represent basic design data, used to determine the precise material balances for close-cycle operation. The compositions, which were dependant upon the Bunsen reaction, were investigated experimentally [8,9] for the $\text{HI-H}_2\text{SO}_4\text{-I}_2\text{-H}_2\text{O}$ mixture produced by absorbing SO_2 until saturation. In addition, the compositions of both phases in the liquid-liquid phase separation were investigated. The compositions of solutions were quantified by a chemical titration method, devised for the multicomponent mixed solutions [10]. For the Bunsen reaction, the acid concentration in the final solution under iodine saturation increased with rising temperature, due to an increase in the iodine solubility. For the phase-separated solutions, high concentrations of acids and iodine were vital to attain the high separation factor. In contrast, the high acid concentration caused side reactions, forming sulfur and/or hydrogen sulfide, while high iodine concentration resulted in the precipitation of solid iodine. Based on the investigations, the acquired compositions of the phase-separated solutions were adopted to evaluate the flow rates from the separation section into the decomposition section. Besides, the conditions of the solutions for the lab-scale hydrogen production test were determined as required, to prevent side reactions and solid iodine precipitation and thus facilitate handling.

Figure 3. Lab- and bench-scale test facilities



Lab-scale



Bench-scale

Transportation of the melting iodine involved technical difficulties, linked to the need to recycle them from the decomposition section into the Bunsen section. The iodine during transportation had to be maintained in a liquid phase, namely between melting and boiling points; which in case of pure iodine represented temperatures of 113.6°C and 184.4°C respectively. The materials used for pumps to transport this material also had to be capable of resisting such a corrosive environment, hence non-seal structures were desirable for the pumps. In order to boost the low volume flow rate for the lab-scale hydrogen production test, a new pump system was devised [11], employing a glass capillary tube with an injection nozzle for the carrier gas. The melting iodine was forced by the gas pressure to rise in the tube until it gained a level sufficient to facilitate flow down into the destination vessels.

(3) Process control methods during the bench-scale stage

The IS process had to include the desirable and unique feature of being operable on a closed cycle condition. This involved all chemicals circulating through the process as the chemical forms change by plural reactions, meaning they had to be recycled. Because of influences on the recycling chemicals in the closed-loop, establishing stable hydrogen production was quite difficult during practical operations. Therefore, the ability to develop process control methods for stable hydrogen production, which maintain the process in a stable state, was vital. To achieve this, the process had to be controlled artificially, to produce hydrogen and oxygen at a rate of 1:0.5. To realise this object, a fundamental concept of a process control method [4] was developed to maintain a balance between the reacting constituents of chemical reactions and the raw material supply, which involved both the manipulated and controlled variables, with the latter controlled by the former, being created during the process.

To construct the bench-scale test facility, techniques for recycling chemicals and technical knowledge collected at the lab-stage, such as the means of preventing side reactions, were incorporated into the facility. Moreover, the experimental examinations of the process fluid at atmospheric pressure, and the temperature and compositions of the solutions for the Bunsen reaction were investigated [3] using a small glass apparatus. Throughout the examinations, the molar flow rate for the detailed design of the facility was fixed. Equipment and operational designs were established, based on the molar flow rate and from which the throughput of process fluids was estimated.

The operating temperature of the Bunsen reaction was investigated during the examination. It is advantageous when processing concentrations to obtain rich acids, HI and H₂SO₄ with H₂O, as the products of the Bunsen reaction. Reducing impurities, namely HI and I₂ in the upper phase and H₂SO₄ in the lower phase, facilitates the processing of purifications. Examinations show the I₂ fraction of the lower phase increases in correlation to the reaction temperature, while the concentrations of acids also increase with the I₂ fraction. However, the concentrations of impurities decrease further as the I₂ fractions gain, and bottom out at about 70°C. With these results and optimized handling of the solutions in mind, a temperature of 70°C was chosen to operate the Bunsen reaction for the bench-scale hydrogen production test.

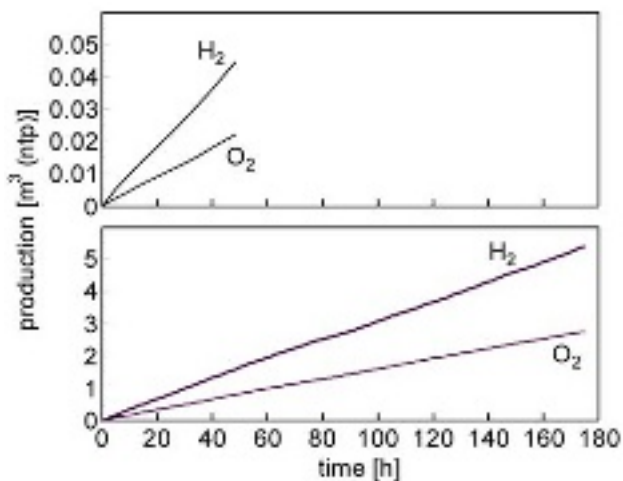
Maintaining the compositions of the Bunsen reaction solutions was investigated throughout the examinations. With the Bunsen reaction in mind, the following were essential for it to work. First, the SO₂ had to be entirely reacted, to ensure the sulfur compounds involved in the process operated at atmospheric pressure. Next, I₂ had to be completely dissolved in the solution to prevent any clogging of pipes due to I₂ forming a solid cake. Additionally, the solution had to be separated into two phases, to obtain two rich acids for either HI or H₂SO₄. Based on examinations, the target compositions of the Bunsen reaction to be maintained during the bench-scale hydrogen production test were resolved, hence allowing demands for the Bunsen reaction to be satisfied.

Continuous and closed-cycle hydrogen production tests

Both the lab- and bench-scale facilities were made of fluorine resin, glass and quartz; comprising fundamental reactors and separators and operated at atmospheric pressure. The heat required for the operations was supplied by electricity. The lab-scale facility adopted techniques for recycling chemicals, while the bench-scale facility employed automated control methods for longer term hydrogen production.

Continuous and closed-cycle hydrogen production tests were carried out to demonstrate the techniques and control methods respectively and this was successfully accomplished for 48 and 175 hours respectively. The respective levels of hydrogen productions were maintained at virtually constant rates of 1 L/h and 31 L/h, while the production ratio of oxygen to hydrogen correlated almost exactly to the ratio 0.5:1; evidence of stoichiometric water-splitting.

Figure 4. Hydrogen and oxygen production over time in lab- and bench-scale test



Regarding the evaluation of operating stability, the consumption volume of circulatory chemicals was determined; and the number, N , was given by,

$$N_i = \frac{r_i}{n_i} \quad (4)$$

where r_i is the total amount of the reacted chemical, n_i is the total contents of the chemical in the test facility and i represents the components of HI, H₂SO₄, I₂ and H₂O. Since r_i was estimated based on the volumes of hydrogen and oxygen production, N_i was counted in Table 1 for both the hydrogen production tests. During the lab-scale test, N_{HI} and $N_{NH_2SO_4}$ were recorded as 1. In particular, the bench-scale test achieved a level 1 of NH₂O, representing the largest amount of constituents in the facility. Therefore, the test span was longer than that required for the single replacement of all the water contained in the facility by chemical reactions. Based on this evaluation, the stability of this control method was confirmed.

Table 1. Number of times for the consumptions of circulatory chemicals

N_2	Lab	Bench
HI	1	15
H ₂ SO ₄	1	15
I ₂	0.2	2
H ₂ O	0.1	1

Conclusions

The IS process should have a desirable and unique feature, namely operability on a closed cycle condition. To establish the IS process at an operational chemical plant, studies on the process operation required to complete the closed-cycle have been conducted involving various R&D stages. The key techniques for recycling chemicals and the fundamental concept of the control methods used to maintain the process in a stable state were developed through the lab- and the bench-scale stages. Their usefulness was demonstrated by the accomplishments during the hydrogen production tests.

REFERENCES

- [1] J.H. Norman, G.E. Besenbruch and D.R. O'Keefe, Thermochemical Water-splitting for Hydrogen Production, Final Report (January 1975-December 1980), GRI-80/0105, March 1981.
- [2] H. Nakajima, M. Sakurai, K. Ikenoya, G. Hwang, K. Onuki, S. Shimizu, A study on a closed-cycle hydrogen production by thermochemical water-splitting IS process, Proc. 7th Int. Conf. on Nuclear Engineering, (1999).
- [3] S. Kubo, H. Nakajima, S. Kasahara, S. Higashi, T. Masaki, H. Abe and K. Onuki, A demonstration study on a closed-cycle hydrogen production by the thermochemical water-splitting iodine-sulfur process, Nuclear Engineering and Design 233 (2004).
- [4] S. Kubo, H. Nakajima, S. Shimizu, K. Onuki, R. Hino, A bench scale hydrogen production test by the thermochemical water-splitting Iodine-Sulfur process, Proc. GLOBAL 2005, No. 474, Oct 9-13, Tsukuba, JAPAN (2005).
- [5] T. Iyoku, N. Sakaba, S. Nakagawa, Y. Tachibana, S. Kasahara, K. Kawasaki, HTTR test program towards coupling with the IS process, Proceedings of the third information exchange meeting on the nuclear production of hydrogen, including the second HTTR workshop on hydrogen production technologies, 5-7 October 2005, Oarai, Japan, (2005).
- [6] N. Sakaba, Y. Tachibana, K. Onuki, Y. Komori, M. Ogawa Japan's HTTR and its hydrogen production Nuclear Engineering International, Vol. 50, No. 612, pp. 20-22, (2005).
- [7] A. Terada, S. Kubo, H. Okuda, S. Kasahara, N. Tanaka, H. Oota, A. Kanagawa, K. Onuki and R. Hino, Development program of hydrogen production by thermochemical water splitting IS process, Proc. 13th Int. Conf. Nucl. Eng., May 16-20, Beijing, China, (2005) ICONE13-50183.
- [8] K. Onuki, H. Nakajima, M. Futakawa, I. Ioku and S. Shimizu, A study on the Iodine-Sulfur thermochemical hydrogen production process, Principle of Exergy Reproduction (No. 256) supported by the Grant-Aid on Priority Areas, Ministry of Education, JAPAN (1998).
- [9] K. Onuki, H. Nakajima, I. Ioku, M. Futakawa and S. Shimizu, IS Process for thermochemical hydrogen production, JAERI-Review 94-006 (1994).
- [10] M. Sakurai, H. Nakajima, K. Onuki and S. Shimizu, Investigation of 2 liquid phase separation characteristic on the iodine-sulfur thermochemical hydrogen production. Int. J. Hydrogen Energy 25, 605-611 (2000).
- [11] H. Nakajima, S. Shimizu, K. Onuki, Jap. P. Appl. 9-60885 (1997).

EXPERIMENTAL AND ANALYTICAL RESULTS ON H₂SO₄ AND SO₃ DECOMPOSERS FOR IS PROCESS PILOT PLANT

**Atsuhiko Terada, Yoshiyuki Imai, Hiroki Noguchi, Hiroyuki Ota, Akihiro Kanagawa, Syuichi
Ishikura, Shinji Kubo, Jin Iwatsuki, Kaoru Onuki and Ryutaro Hino**

Japan Atomic Energy Agency
Nuclear Science and Energy Directorate
4002 ,Narita-cho, Oarai-machi, Ibaraki-ken, 311-1393 JAPAN
Tel: +81-29-266-7572, Fax: +81-29-266-7741,

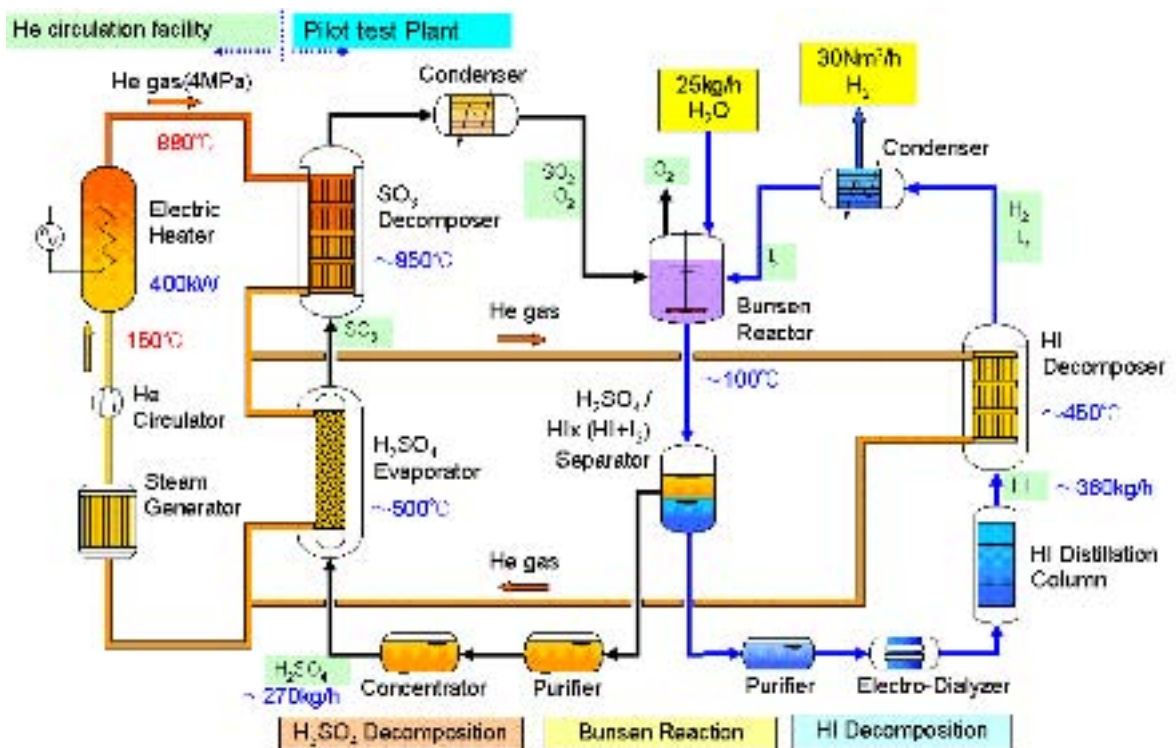
Abstract

The Japan Atomic Energy Agency (JAEA), whose former organisation name is the Japan Atomic Energy Research Institute (JAERI), is conducting R&D on high temperature gas-cooled reactor (HTGR) and also on thermochemical hydrogen production iodine-sulfur cycle (IS process). The continuous hydrogen production was demonstrated with the hydrogen production rate was about 30 NL/hr for one week using a bench-scale test apparatus made of glass. Based on the test results and know-how obtained through the bench-scale tests, a pilot plant that can produce hydrogen of about 30 Nm³/hr is being designed as the next step of the IS process development. In parallel to the pilot plant design, key components of the IS process such as the sulfuric acid (H₂SO₄) and the sulfur trioxide (SO₃) decomposers working under high-temperature corrosive environments were designed to confirm their fabricability. In this paper, we will introduce latest experimental and analytical results on the H₂SO₄ and the SO₃ decomposers.

1. Introduction

The Japan Atomic Energy Agency (JAEA), whose former organization name is the Japan Atomic Energy Research Institute (JAERI), is conducting R&D on high temperature gas-cooled reactor (HTGR) and also on thermochemical hydrogen production by an iodine-sulfur cycle (IS process). In the IS process, raw material, water, is to be reacted with iodine (I_2) and sulfur dioxide (SO_2) to produce hydrogen iodide (HI) and sulfuric acid (H_2SO_4), the so-called Bunsen reaction, which are then decomposed endothermically to produce hydrogen (H_2) and oxygen (O_2), respectively. Iodine and sulfur dioxide produced in the decomposition reactions can be used again as the reactants in the Bunsen reaction. In JAERI, continuous hydrogen production was demonstrated with the hydrogen production rate was about 30 NL/hr for one week using a bench-scale test apparatus made of glass. Based on the test results and know-how obtained through the bench-scale tests, a pilot plant that can produce hydrogen of about 30 Nm³/hr is being designed as the next step of the IS process development. The pilot plant will be fabricated with industrial materials such as glass coated steel, SiC ceramics etc, and operated under high pressure condition up to 2 MPa. Figure 1 shows a tentative scheme of the test facility, which consists of the IS process pilot plant and a helium gas (He) circulation facility (He loop). The He loop can simulate HTTR operation conditions, which consists of a 400 kW-electric heater for He heating, a He circulator and a steam generator working as a He cooler.

Figure 1. Schematic flow diagram of the IS process pilot test plant



In parallel to the pilot plant design, key components of the IS process such as the sulfuric acid (H_2SO_4) and the sulfur trioxide (SO_3) decomposers working under high-temperature corrosive environments were designed to confirm their fabricability. The H_2SO_4 decomposer is a multi-hole-block type heat exchanger composed of SiC ceramics. The thermal stress analyses were carried out under the operating condition of axial temperature distribution along the flow channels, in order to clarify its structural strength. Also, leak tests were carried out with a mock-up model of the H_2SO_4 decomposer. As for the SO_3 decomposer, catalyst performance was examined with Pt/SiO₂ catalyst

under the pressure up to 1 MPa and the space velocity of around 1 000.

In this paper, we will recently introduce R&D on the H₂SO₄ and the SO₃ decomposers.

2. H₂SO₄ Decomposer

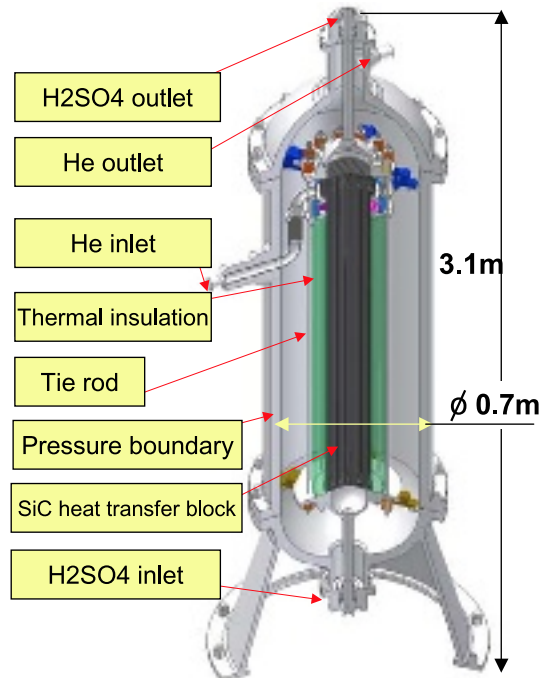
2.1 Concept of H₂SO₄ decomposer

The sulfuric acid decomposer is the equipment by which concentrated sulfuric acid is made evaporate with the heat of He and decomposed into SO₃ and H₂O. The design conditions for the sulfuric acid decomposer for the pilot test plant are shown in Table 1, which are defined based on the heat-mass balance of the sulfuric acid decomposition section performed by Knoche *et al.* [1]. The evaporation temperature of H₂SO₄ is assumed to be 455°C.

Table 1. Design condition of sulfuric acid decomposer

	Conditions
Thermal Rating	82.7 kW
He Inlet / Outlet Temp.	710 / 535°C
Process Inlet / Outlet Temp.	435 / 460°C
He Pressure	4 MPaG
Process Pressure	2 MPaG
He Flow Rate	0.091 kg/s
Process Flow Rate	0.066 kg/s

Figure 2. Concept of H₂SO₄ decomposer



Corrosiveness of the boiling sulfuric acid environment is very severe, and it has been clarified that only silicon containing ceramics show good corrosion resistance [2]. In the present study, ceramic heat-exchanger type reactor made of atmospheric pressure sintered SiC was adopted. Figure 2 shows a concept of the H₂SO₄ decomposer featuring the SiC ceramic block as the heat exchanger.

2.2 Mechanical strength analyses of SiC blocks

Considering the fabricability and manufacture- ability, the shape of heat exchanging component made of atmospheric pressure sintered SiC was selected to provide the flow channels of He and sulfuric acid alternately in the cylindrical block. Sizing of the ceramic block was decided under the design conditions listed in Table 1. The block was 0.25 m in outer diameters, and 1.5 m in height. The flow channels of He and sulfuric acid were arranged in the block. The number of the flow channels for sulfuric acid and He were 32 and 38, respectively; diameter of these flow channels was 14.8 mm. From the viewpoint of keeping high yield rate of a 0.25 m-diameter SiC ceramic block, the ceramic block was divided into 2 parts in the axial direction; block height was 0.75 m. These block parts were connected with a seal part. This type of seal technology between the ceramic blocks is useful for decreasing fabrication cost of large scale ceramic structures.

Figure 3 shows the axial temperature distributions of fluids under the normal operating condition. Temperature distribution in the ceramic block was analysed with ABAQUS Ver.6.4. Figure 4 shows a computational grid of a 1/4 sector of the upper half part of the block.

In the case of heat transfer analysis, axial temperature distribution, shown in Figure 3 are specified for the surfaces of both He and sulfuric flow cannels, considering heat transfer coefficients. And outer surface of block is modeled as adiabatic condition. Figures 5 and 6 show the temperature and the stress distributions in the block, respectively. The stress shown in Figure 6 is a coupled stress with thermal stress and static stress caused by the operating pressure difference between He and sulfuric acid. Analytical conditions are as follows :

- Density of block : 3.1 X 10³ kg/m³
- Young's modulus : 3.98 X 10⁵ N/mm²
- Thermal conductivity : 0.12 W/mm • K (R.T.)
0.08 W/mm • K (800°C)

Figure 3. Axial temperature distribution

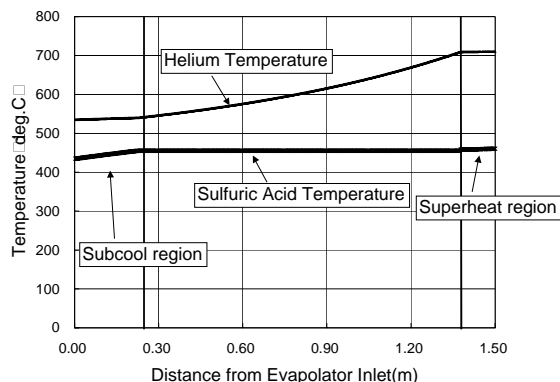


Figure 4. Computational grid

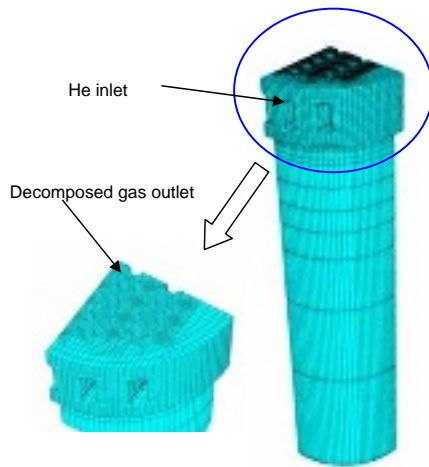


Figure 5. Temperature distribution in block

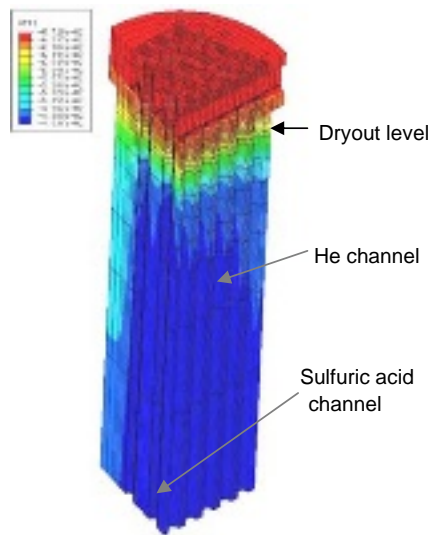
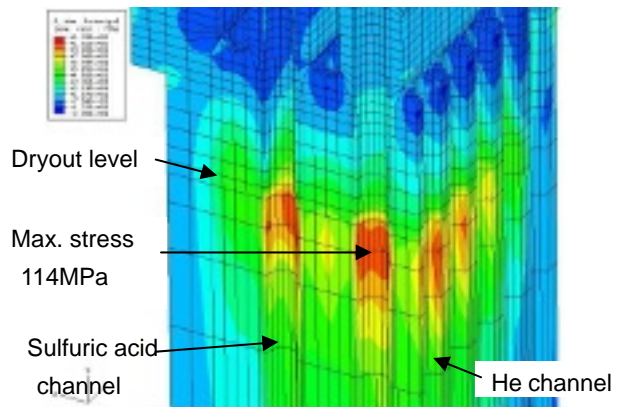


Figure 6. Computational grid (thermal stress + static stress)



- Thermal expansion coef. : $3.47 \times 10^{-6} /\text{K}(\text{R.T.})$
 $3.90 \times 10^{-6} /\text{K}(800^{\circ}\text{C})$

As seen in Figure 5, high temperature region is located after the dryout region. Then the temperature difference between He and sulfuric acid flow channels are about 250°C at maximum. Then the maximum stress, about 114 MPa as seen in Figure 8, was occurred around the dryout region on the sulfuric acid flow channels. This value is much lower than the average bending strength of high strength atmospheric pressure sintered SiC, 450 MPa [3].

To verify fabricability of the SiC ceramic block, a real-scale model was manufactured experimentally. Through the manufacturing of the block, the production technology of large blocks was established.

2.3 Seal performance test with mock-up model of H_2SO_4 decomposer

Seal performances at the connections of metal/metal, metal/SiC, and SiC/SiC, which are the boundary of He-He and He- H_2SO_4 , were investigated with scaled models under hydrostatic and He conditions. Figure 7 and 8 show the schematic and an outer view of the test apparatus, respectively. A SiC block model (120 mm in diameter and 50 mm in thickness) shown in Figure 9 was installed in the test apparatus.

Figure 7. Schematic of leak test apparatus

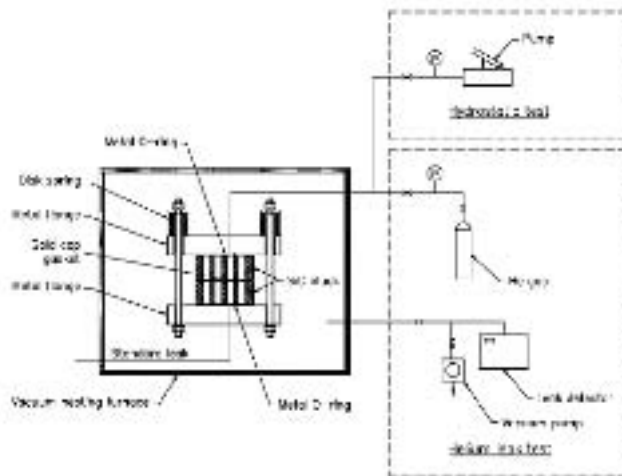


Figure 8. Leak test apparatus



Figure 9. SIC block for seal performance test



Figure 10. Attachment of gold wire gasket



Figure 11. Attachment of gold cap gasket



Table 2. He leak rate at 500°C

Connection	He leak rate at 3 heat cycle Pa•m ³ /s	Maximum pressure	Line load or seating stress
Metal/Metal	3.6x10 ⁻⁴	3.6 MPa	1.0x10 ⁵ N/m (3.2x10 ⁴ N)
Metal/SiC	2.2x10 ⁻⁶	2.6 MPa	1.2x10 ⁵ N/m (4.0x10 ⁴ N)
SiC/SiC	7.5x10 ⁻⁸	4.0 MPa	24 MPa (5.9x10 ³ N)

Table 3. He leak rate at 20°C

Connection	He leak rate after 3 heat cycle Pa•m ³ /s	Maximum pressure	Line load or seating stress
Metal/Metal	6.4x10 ⁻⁸	4.0 MPa	2.8x10 ⁵ N/m (8.9x10 ⁴ N)
Metal/SiC	2.7x10 ⁻⁴	3.4 MPa	3.0x10 ⁵ N/m (9.3x10 ⁴ N)
SiC/SiC	2.8x10 ⁻⁷	4.0 MPa	58 MPa (1.4x10 ⁴ N)

Wire gaskets and the cap gaskets made of the pure gold are to be used in the H₂SO₄ decomposer for the pilot tests. The wire gasket is to be used at the connections of metal/metal and metal/SiC, and the cap gasket will be used to the SiC block parts connection. Figure 10 shows the state after the seal performance test. Figure 11 shows the cap gasket mounted in a SiC block model.

Helium leak tests were carried out under load pressure up to 4 MPa and surface temperature of the models up to 500°C. All connections were installed in a vacuum electric furnace, and leak rates were measured with a helium leak detector. Table 2 shows the leak rates obtained at 500°C in the third times at the heat cycle up to 500°C, and Table 3 obtained under 20°C after the leak measurement at 500°C shown in Table 2. In these tables, line loads and seating stresses (tightening forces) are also indicated. As seen these tables, although the tightening forces under 500°C decreased down to less than

half of the forces shown in Table 2, the leak rates under 500°C were decreased in metal/SiC and SiC/SiC connections. This would be due to softening and adhesion effect of gold.

2.4 H₂SO₄ thermal-hydraulic test loop

Figure 12. Schematic diagram of the H₂SO₄ flow test loops

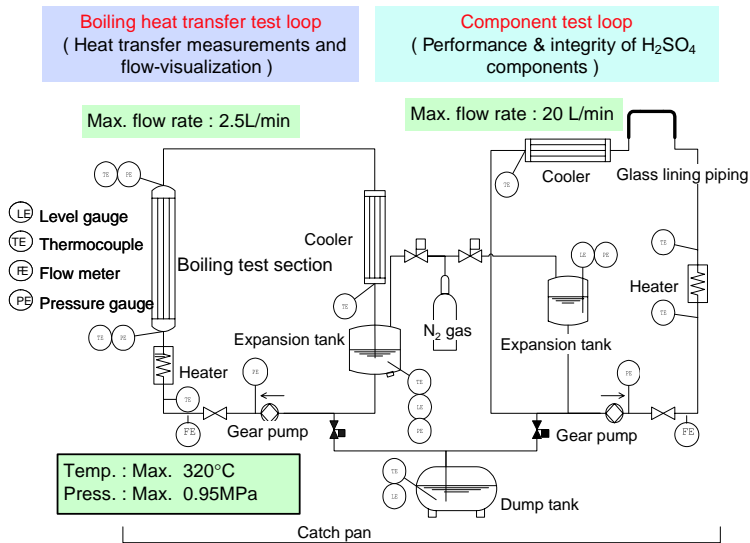
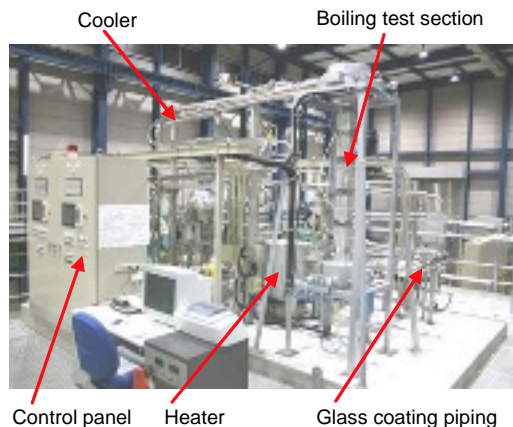


Figure 12 shows the schematic diagram of the sulfuric acid flow test loops, which consists of a boiling heat transfer test loop and a component test loop. Figure 13 shows outer view of sulfuric acid flow test loops under construction. In the boiling heat transfer test loop, the concentric annulus test section composed of an electric heater with SiC heat transfer surface and an outer tube made of quartz glass were installed. We will measure heat transfer coefficients under flow boiling and visualize boiling situation. In the component test loop, the integrity of components such as gear pump, electro-magnet flow meter and glass lining pipeline will be examined. Maximum flow rates of these loops are 2.5 L/min and 20 L/min. As the result of preliminary test, we had confirmed the boiling of H₂SO₄ visually.

Figure 13. Outer view of H₂SO₄ thermal-hydraulic test loop



3. SO₃ Decomposer

3.1 Concept of SO₃ decomposer

JAERI is developing the SiC plate-type SO₃ decomposer, which can make a large heat transfer surface relatively and consequently can make the decomposer more compact. And in a future it also has a possibility to add gas-separation function as a membrane reactor to enhance equilibrium conversion rates of SO₃ decomposition under high operation pressure of 2 MPa (equilibrium conversion rates is less than 50% at 850°C).

Tables 4 and 5 show the design conditions for the SO₃ decomposer in the pilot test plant based on the conditions in literature [1]. SiC ceramics, which is a high thermal resistant material, is presently the most promising material for the SO₃ decomposer to meet following requests:

- High thermal conductivity necessary to transfer heat effectively by high temperature He gas (max 880°C)
- Anti-corrosiveness against the process gases such as the SO₃, SO₂, H₂O and O₂ gases
- High mechanical strength to withstand static the pressure difference between He gas and process gas

Table 4. Design conditions of SO₃ decomposer in pilot test plant

Item	Conditions for hydrogen production 30 N m ³ /h
Process gas pressure	2.0 (MPaG)
Process gas temperature (inlet/outlet)	527/850 (°C)
He pressure (inlet)	4.0 (MPaG)
He flow rate	100 (g/s)
He temperature (inlet)	880 (°C)
Heat exchange	100(kW)

Table 5. Flow conditions of process gas

Process gas	Mol flow (mol/s)	
	Inlet (527°C)	Outlet (850°C)
H ₂ O	0.931	1.210
H ₂ SO ₄	0.286	0.005
SO ₃	0.441	0.307
SO ₂	0.032	0.446
O ₂	0.016	0.223
Total	1.71	2.19

Figure 14. Concept of the SiC plate type SO₃ decomposer for pilot test plant

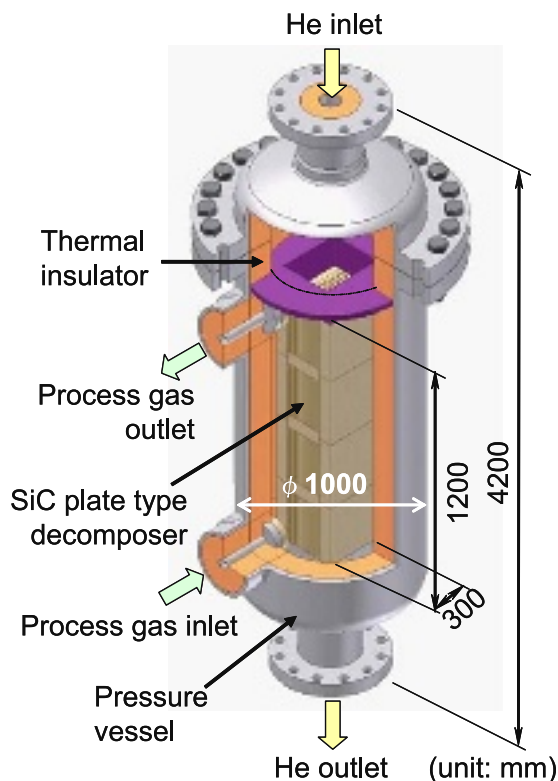


Figure 14 shows the concept of a SO₃ decomposer for the pilot test plant. The SO₃ decomposer is installed in a pressure vessel lined internally with thermal insulator. One unit of SO₃ decomposer is a stack of SiC plate-type heat exchanger segment. He gas (heating source) comes from the top of pressure vessel, and is introduced to the upper unit of the SO₃ decomposer by way of partition plate. Process gases flowing up in the unit are heated by He gas flowing down to the unit bottom, so that the SO₃ decomposer works as a counter-flow type heat exchanger. The space between the heat insulator and the heat exchanger unit is also filled with He.

Then, necessary heat transfer area of the SO₃ decomposer was more than 3.6 m², which was decided on the basis of conservative heat transfer evaluation. This value was verified with the numerical analytical works.

The dimension of a SO₃ decomposer unit is shown in Figure 15. 4-stage stack of the heat exchangers makes one unit, which ensures about 1.2 m² of the heat transfer area. One stage of the stack is around 250 mm wide, 300 mm long and 200 mm high. In the pilot test plant, it is necessary to integrate 3 units of the stack. Figure 16 shows the structure of the decomposer unit. He gas flow channels have many arranged cylindrical ribs to keep mechanical strength of the channel, which work as heat transfer promoters.

The rated space velocity (SV) in a SO₃ catalyst layer is necessary to be kept less than 10 000 hr⁻¹ in order to keep high reactivity of SO₃ decomposition. In this unit, the internal volume charged with catalyst is around 17.64 liters. Then, the space velocity (SV) becomes $1.71 \text{ (mol/s)} \times 22.4 \text{ (NL/mol)} \times 3600 / 17.64 \text{ (L)} = 7817 \text{ h}^{-1}$.

3.2 Mock-up model of plate-type SO₃ decomposer

The thermal-hydraulic analysis and thermal stress analysis of plate-type SO₃ decomposer had been carried out with analytical codes. So, structural feasibility of plate-type SO₃ decomposer was analytically verified by them.

Figure 15. Dimension of one SO₃ decomposer unit

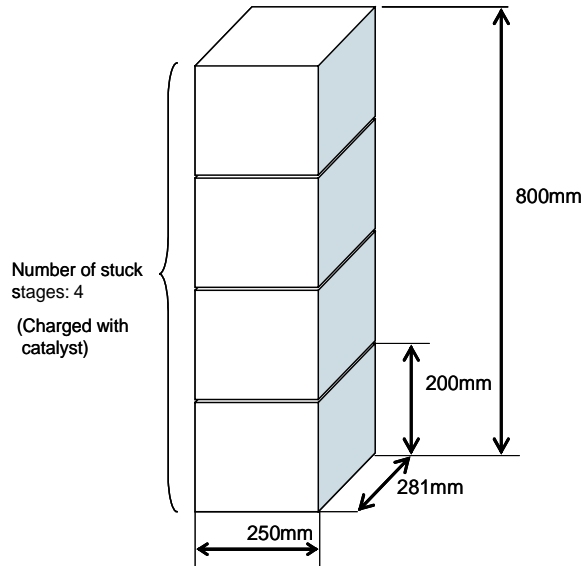
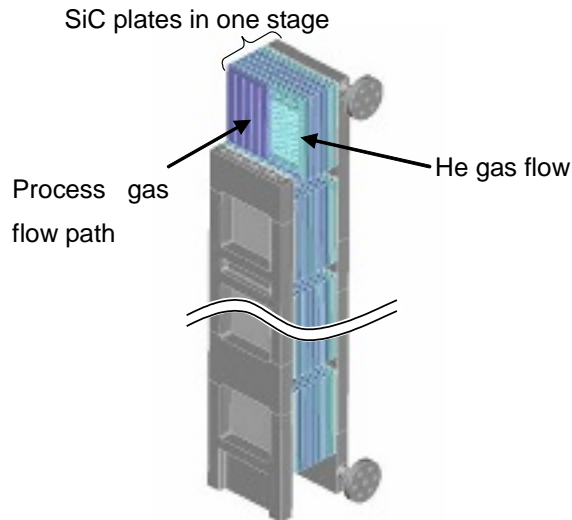
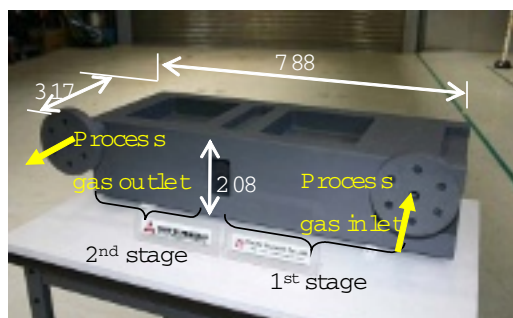


Figure 16. Structure of the SO₃ decomposer unit



A mock-up model of plate-type SO₃ decomposer was test fabricated to verify manufacturing feasibility such as a stacked structure and pipe connections with flanges. Figure 17 shows an outer view of one stage of the prototype. It has been confirmed that the prototype of the heat exchanger can be produced as designed by the inspection through .an appearance inspection (crack, omission) and a dimensional inspection.

Figure 17. Outer view of prototype model of plate-type SO₄ decomposer

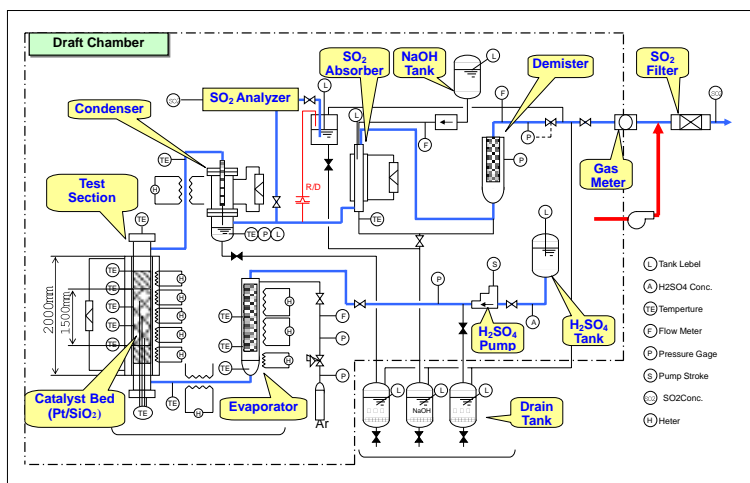


3.3 Catalyst test for SO₃ decomposition

Figure 18 shows the schematic diagram of catalytic test apparatus for SO₃ decomposer. 98wt% H₂SO₄ is vaporized by a electric heater, and sent to the catalytic reactor with Argon (Ar) gas as carrier, then sulfuric-acid vapor is decomposed. At the normal operation, sulfuric-acid is supplied from the H₂SO₄ tank by the H₂SO₄ pump, and vaporised to the SO₃ gas at the evaporator, and decomposed to SO₂ and O₂ gases. The decomposed gases are cooled to around the room temperature (40°C) and condensed at a condenser. SO₂, O₂, unreacted H₂SO₄ and carrier Ar-gas are separated to gas and liquid at the condenser, and the separated gases are sent to the SO₂ absorber. The trapped SO₂ gas is neutralized with NaOH, and removed.

The catalytic reactor is composed of double-pipe structure. The inner pipe (I.D. : 30mm) is a catalytic reactor made of SiC filled with SiO₂ loading Pt catalyst (size is about Ø 1mm). The outer pipe (I.D. 48mm) is a pressure retaining pipe made of Alloy 800H. In the gap between inner pipe and outer pipe (width 5.5mm), Ar gas is vented in order to prevent process gases from mixing to the gap. The performance of the catalyst is evaluated by SO₃ gas decomposing rate to the space velocity in a catalyst bed, and the SO₃ gas decomposing rate is evaluated by SO₂ concentration and O₂ flow rate. The SO₂ concentration is measured by non-dispersive SO₂ concentration meter, and O₂ flow rate is measured by wet gas meter.

Figure 18. Schematic diagram of catalytic test apparatus for SO₄ decomposer



The main testing condition is as follows. The SO₃ decomposing test which parameter of space velocity, pressure, and temperature, will be performed and evaluate the performance of the catalyst.

- maximum test temperature: 850°C
- maximum test pressure: 0.75 MPa
- space velocity in a catalyst layer: 1 000 ~ 1 000h⁻¹

4. Conclusion

Concepts of the H₂SO₄ and SO₃ decomposers for the pilot test plant were proposed featuring corrosion resistant performance under high-temperature H₂SO₄ and SO₃ operations, which were mainly composed of SiC ceramics. The feasibility of the proposed concepts were confirmed by mechanical strength analyses and test fabricated mock-up models. As for the H₂SO₄ decomposer, the seal performance with gold gaskets showed very good seal performance. We will confirm the thermal-hydraulic performance of the H₂SO₄ decomposer and the SO₃ decomposition rate in the packed catalyst layer by using the sulfuric acid flow test loops and the catalyst test apparatus.

Acknowledgements

A part of study was carried out in the “Development of Nuclear Heat Utilization Technology” in fiscal year of 2004 entrusted by Ministry of Education, Culture, Sports, Science and Technology (MEXT) to Japan Atomic Energy Research Institute (JAERI).

REFERENCES

- [1] K.F. Knoche *et al.*, 1984, Proc. 5th World Hydrogen Energy Conf., Toronto, Canada, July vol.2, pp.487-502.
- [2] A.Terada *et al.*, 2005, 13th Int. Conf. Nucl. Eng., Beijing, China, May 16-20, ICONE13-50183.
- [3] S. Suyama *et al.*, 2004, proceeding of 15th World Hydrogen Energy Conf., Yokohama, Japan, June 27 – July 2, pp.05-07

A SCOPING FLOWSHEET METHODOLOGY FOR EVALUATING ALTERNATIVE THERMOCHEMICAL CYCLES

Michele A. Lewis, Mark C. Petri, and Joseph G. Masin
Argonne National Laboratory, Argonne, IL 60439

Abstract

Four thermochemical cycles were identified as potentially promising alternative cycles. Two were metal sulfate cycles and two were metal chloride cycles. All are hybrid cycles, i.e., they have an electrochemical step. These cycles were evaluated with a recently developed scoping flowsheet methodology to determine their maximum theoretical efficiency and their ability to function as a cycle. Thus, their efficiencies were calculated for two levels of knowledge. The first uses heat and work inputs only whereas the second also includes free energy changes to obtain an estimate of possible equilibrium yields. Reaction conditions are modified when competing products form or when experimental data on yields and/or rates indicate changes are necessary. The results indicate that the copper sulfate and the copper chloride cycles merit further investigation because efficiencies are reasonably high, their heat needs are consistent with process heat from a high temperature gas reactor (VTGR), and because experimental work has proven cycle feasibility.

Introduction

Thermochemical cycles take in water and heat and produce hydrogen and oxygen without greenhouse gas emissions when the heat source is nuclear or solar. The U.S. R&D effort in thermochemical cycles started in the 1970s and nearly all work stopped after the mid 1980s. From this period, several cycles were identified as promising. These included the sulfur cycles and the UT-3 (a calcium bromide cycle). Interest in thermochemical cycles has recently been revived. Currently, a large international effort is ongoing to develop a pilot plant demonstration for the sulfur-iodine (S-I) cycle, which will be coupled with a very high temperature gas reactor (VHTGR). Smaller R&D efforts for the hybrid sulfur cycle and the calcium bromide (Ca-Br) cycle are also ongoing. These cycles are referred to as baseline cycles within the U.S. DOE thermochemical cycle program. The objective of our research is to identify alternative cycles. Such cycles may have been identified as promising late in the active research phase and were not subject to in-depth scrutiny. In addition, new technologies may remove barriers previously seen to further development of the alternative cycles. A method to evaluate these alternative cycles early in their development stage is important to focus time and money on the most promising ones. Consequently the goals of our research program are threefold: (1) identify potential cycles from a variety of sources, (2) characterise potential advantages and issues, and (3) perform scoping flowsheet analyses and identify R&D needs for the highest priority cycles.

We surveyed the literature and identified over 200 thermochemical cycles most of which are included in two summary reports [1, 2]. Based on the reported values for the maximum theoretical efficiency and chemical workability for these cycles, we eliminated all but 20. Further screening was based on other considerations. For example, cycles containing cadmium, mercury, or selenium were eliminated on the basis of the very low allowable EPA release rates. Other cycles were eliminated because of low conversions at the process temperatures expected to be available from the very high temperature gas reactor (VTGR), expected to be $900 \pm 50^\circ\text{C}$. A few cycles were eliminated on the basis of low elemental abundance from a survey of worldwide resources.

After applying these selection criteria, we identified three promising alternative cycles, the copper sulfate, the zinc sulfate, and the copper chloride cycles. High maximum theoretical efficiencies were reported for the metal sulfate cycles [1]. In addition, the metal sulfate cycles present a less corrosive system than the sulfur cycles. In the metal sulfate cycles, water is removed from the metal sulfate solution rather than from sulfuric acid as in the sulfur cycles. Anhydrous SO_3 is decomposed to SO_2 and oxygen. The high temperature reactions are less corrosive in the absence of water vapor. In addition, the metal sulfate cycles have some common features to the baseline sulfur cycles and R&D for these cycles may be leveraged for use with the metal sulfate cycles. For example, membranes currently under development for the baseline sulfur cycles could also be used to advantage in this cycle. Such a membrane, if successfully developed, would lower the maximum temperature and facilitate SO_3 decomposition and separations. For these reasons, we decided to take a second look at the metal sulfate cycles. The copper chloride cycle was identified as promising in 1980 but little experimental work was reported. The primary advantage of this cycle is its relatively low maximum temperature requirement.

The most often used metric for assessing the potential of a thermochemical cycle is its efficiency.

Efficiency is defined by the following equation
$$E = \frac{-\Delta H_{25^\circ\text{C}}^\circ (\text{H}_2\text{O})}{Q_{\text{hot}} + \frac{W}{0.5}} \quad [3].$$

The numerator is the standard enthalpy of the formation of water at 25°C or 68.3 kcal/mol for the higher heating value (HHV) or 57.8 kcal/mol for the lower heating value (LHV). The denominator includes thermal heat or enthalpy, Q , supplied externally, and different types of work (chemical,

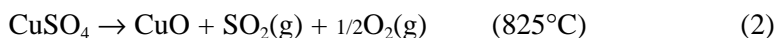
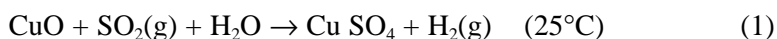
electrochemical, mechanical, electrical, separations, etc.) converted to the thermal equivalent (assuming a 50% heat-to-electricity conversion factor). Electrochemical work is defined by the Nernst equation, or $\Delta G = nFE$ where E is the cell potential in volts, F is Faraday's Constant, 96,493 coulombs/mol [ΔG is in J.]. Work of separation is defined by the equation, $\Delta G_{\text{sep}} = -RT \sum_i n_i \ln y_i$, where R is the gas constant, T is the absolute temperature, n is the flow rate of each component and y is the mole fraction. Chemical work is given by positive free energy for the reaction. Methods for accomplishing the separations or the chemical work are undefined in these early evaluations. Efficiency calculations are not static and will change as more knowledge of the cycle's chemistry is learnt and as processes within the cycle are optimised. In the scoping flowsheet methodology we define two levels for efficiency calculations.

For a Level 1 evaluation, we calculate an idealised efficiency where the reactions are assumed to go to 100% completion. We use the reaction temperatures given in the cycle's definition and pinch analysis for optimising energy usage. In pinch analysis, the exothermic heat is recovered and used for endothermic processes only when temperatures can be matched. These calculations are normalized to one mole of water. For cycles that appear promising after the Level 1 analysis, we calculate a more detailed Level 2 efficiency that is based on equilibrium data. The effect of less than 100% yield is explicitly considered. Reaction temperatures may be adjusted to increase yields. For promising cycles, a process flow diagram (PFD) is designed and energy usage is usually optimised with a heat exchange network, but we are currently using only pinch analysis. Level 2 evaluations allow consideration of more realistic separations and recycle streams. Mechanical work may be estimated from the unit operations in the PFD. Shaft work is usually a relatively small component of the total work load and can be ignored unless gas compressors are used in the PFD. In Level 2 evaluations, reaction temperatures may be adjusted again when kinetic data are taken into account.

Results

We have used the scoping flowsheet methodology to calculate Level 1 and Level 2 efficiencies for the Cu-SO₄, Zn-SO₄, and CuCl cycles, as well as for a new cycle, Mg-Cl [1, 4]. All are hybrid cycles; i.e., they contain an electrochemical reaction. The methodology is illustrated in detail for the Cu-SO₄ cycle. Only the results are presented for the other cycles evaluated.

The two major reactions in Cu-SO₄ cycle and their temperatures are the following:



The above temperatures are from the Carty *et al.* report [1]. At these temperatures the free energy of the reactions are slightly positive, 1.08 and 1.73 kcal for reactions 1 and 2, respectively. These values are used to estimate the chemical potential work because they are positive. Negative free energy changes are ignored because this work is not usable. We ignored the insolubility of CuO in water.

Level 1 Efficiency Calculations

We used HSC as the thermodynamic database [5]. Table 1 lists the enthalpy balance (heats of reaction, sensible heat, and latent heat for phase changes) for both the endothermic and the exothermic reactions defined above.

Table 1. Energy balance for the Level 1 analysis for the Cu-SO₄ cycle

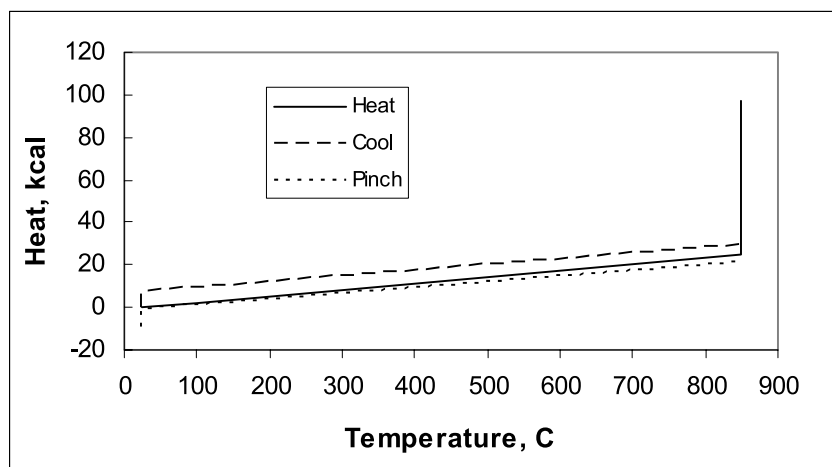
	Reaction #	Type	Mole	T _{in} ^a (°C)	T _{out} ^b (°C)	ΔH, kcal	ΔG, kcal
CuO	1	Reaction		25	25	-7.54	1.08
CuSO ₄	2	Reaction		850	850	71.95	1.73
CuSO ₄		Sensible	1	25	850	27.26	
CuO		Sensible	1	850	25	-10.15	
SO ₂ (g)		Sensible	1	850	25	-9.98	
O ₂ (g)		Sensible	0.5	850	25	-3.23	
Total						68.31	

^aT_{in} = Initial temperature

^bT_{out} = Final temperature

Figure 1 shows the heating, cooling, and pinch curves. In pinch analysis, cumulative heating and cooling loads are plotted vs. temperature level, and the pinch curve is obtained by offsetting the cooling curve (exothermic heat) so that the pinch curve lies below the heating curve (endothermic heat) at all points. The offset, 8.7 kcal, is determined by the desired driving force, in this case 10°C.

Figure 1. Pinch analysis for optimising energy usage in the Cu-SO₄ Cycle – Level 1 (Cumulative heating and cooling requirements shown. The pinch temperature is 849.9°C.)



The total enthalpy or heat demand, Q, requirement is the sum of the offset (determined from the pinch analysis) and the endothermic external heat load. Work terms for chemical potential and separations are converted to their heat equivalent. Table 2 shows the details of the efficiency calculation. The resulting efficiency is 66.9% (LHV).

Table 2. Level 1 efficiency calculation for the Cu-SO₄ cycle

	Energy, kcal/mol H ₂	Heat Equivalent ^a , kcal/mol H ₂	Energy, kcal/mol H ₂	Heat Equivalent ^a , kcal/mol H ₂
Total heat-in	68.3		68.3	
Pinch heat	8.2		8.2	
Chemical potential work	2.81 ^b	5.62	1.73	3.46
Separation work	2.15	4.3	2.15	4.3
Electrochemical work	0	0	20.75	41.5
Enthalpy of formation, H ₂ (LHV)	57.8		57.8	
Efficiency	66.9%		46.0%	

^a Assumes 50% conversion factor for heat to electricity

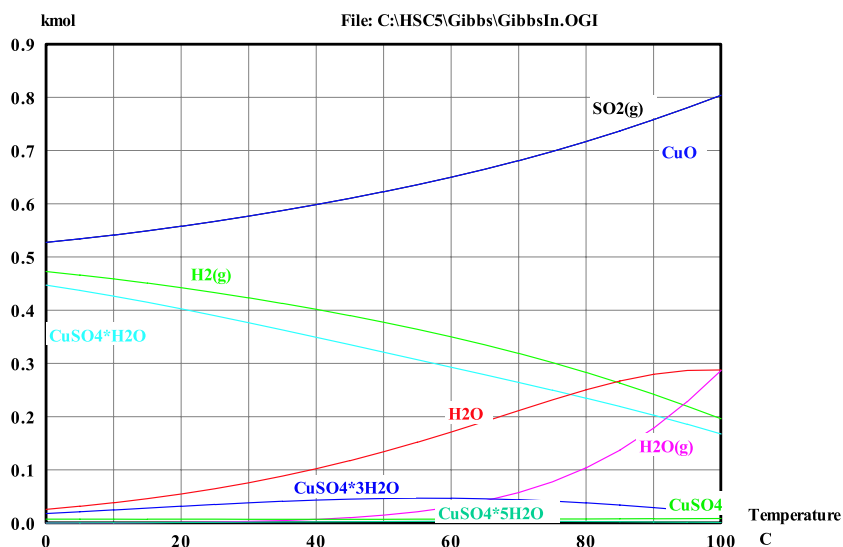
^b Includes the contribution of the free energy change for reaction 1

The Carty *et al.* report specifies that reaction 1 cannot be thermally driven. Their experimental work indicates a minimum cell potential of 0.45V that might be achieved with an optimized cell design and electrocatalysts [1,6]. This value was used to calculate the electrochemical work. The corresponding efficiency with the electrochemical work is 46.0% (LHV) as shown in Table 2. The drop in efficiency illustrates the high cost of the work terms in the energy balance.

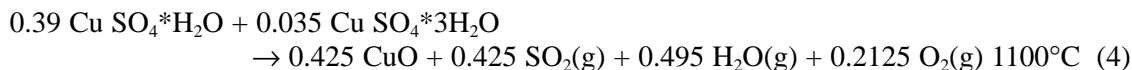
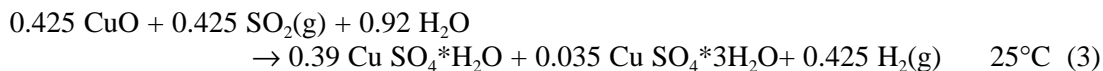
Level 2 Efficiency Calculations

For the Level 2 analysis, we used the equilibrium module of HSC to obtain equilibrium data [HSC]. Figure 2 shows the equilibrium compositions for reaction 1, the hydrogen generation reaction, versus temperature.

Figure 2. Equilibrium composition for a system with equimolar amounts of CuO, SO₂(g) and H₂O

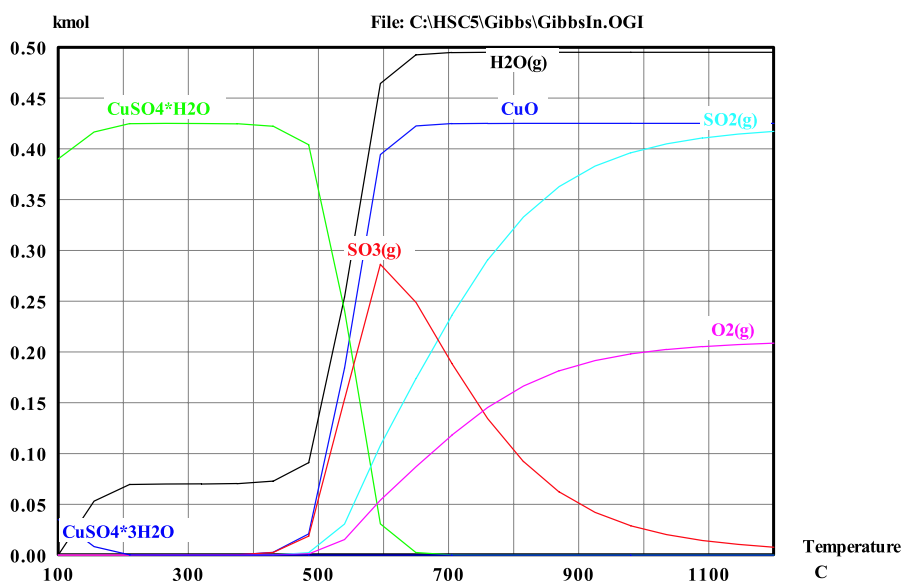


One mole of water is converted to 0.43 moles of hydrogen at 25°C and the amount decreases at higher temperatures. We have rewritten reactions 1 and 2 as reactions 3 and 4 to show the new material balance. Note that in Level 2, less than 1 mole of H₂ may be produced from 1 mole of water feed, resulting in unreacted or excess water, resulting in additional separation work.



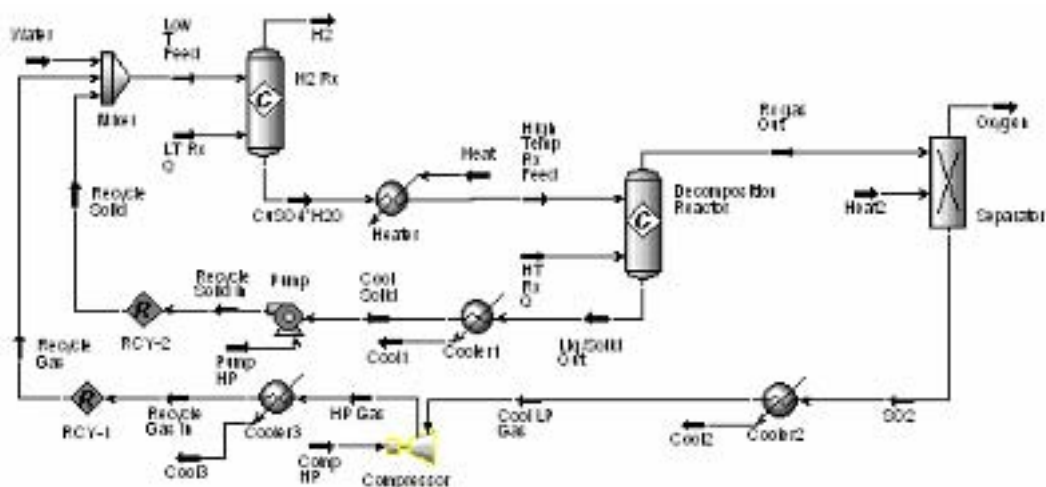
The equilibrium compositions versus temperature for reaction 4 in Figure 3 indicates that the reaction goes nearly to completion at 1 100 °C (1373K) and we chose to use 1 100°C to eliminate recycle of the high temperature streams for this Level 2 analysis.

Figure 3. Equilibrium composition for the high temperature decomposition of reaction 4



The corresponding stream energy balance was prepared, the pinch analysis completed, and the energy efficiency calculated as 38.1% (LHV) after normalisation to one mol of hydrogen. The corresponding process flow diagram is shown in Figure 4. This Level 2 process now has a difficult SO₂/O₂ separation, a very high temperature reaction step, and substantial recycle quantities in the electrochemical cell.

Figure 4. Process flow diagram for the Level 2 Cu-SO₄ process



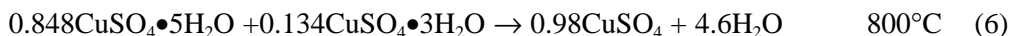
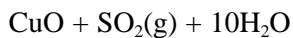
Effect of Competing Product Formation

In the Level 2 analysis above we have not explicitly considered any species other than the cupric sulfates and their hydrates as reaction products. We did check equilibrium compositions in the HSC equilibrium composition module when different species were allowed to form. If one allows the formation of various other salts, the hydrogen and CuSO₄ yields can be significantly reduced. For example, if the cuprous species, Cu₂O and/or Cu₂SO₄ form, hydrogen does not form to any measurable extent. The inclusion of another compound, CuSO₄•3Cu(OH)₂, into the allowable products list primarily affects the yield of CuSO₄. When this compound forms, most of the copper is tied up as the hydroxide, which results in less CuSO₄ and ultimately lower oxygen yields. We expect that the formation of this compound can be controlled by adjusting the pH of the aqueous solution in the electrochemical cell. Likewise, the sulfides impact hydrogen yields. If CuS is allowed to form, no hydrogen is produced. These data indicate that operating conditions have to be controlled such that these competing products, which can be thermodynamically favored, do not interfere with the desired reaction. Typical methods to increase conversion of a desired product are adjusting the temperature, increasing the relative concentration of one of the reactants, or adjusting the pH.

Effect of Excess Water

According to the literature, CuSO₄•5H₂O rather than CuSO₄ is formed experimentally in the electrochemical cell [1, 6]. No other products were specifically mentioned. Thermodynamics predicts the pentahydrate is the major product when reaction 1 is run in an excess of water at 25°C [5]. We have therefore reran the equilibrium module with increasing amounts of water. The amounts of CuO and SO₂(g) remain fixed at one mole each and we have assumed that all competing products (cuprous species, the sulfide species, and the hydroxides) are prevented from forming by the choice of operating conditions. Figure 5 shows that the hydrogen yield is 99% when the molar ratio of water to CuO is increased to 10. The pentahydrate also becomes the predominant species.

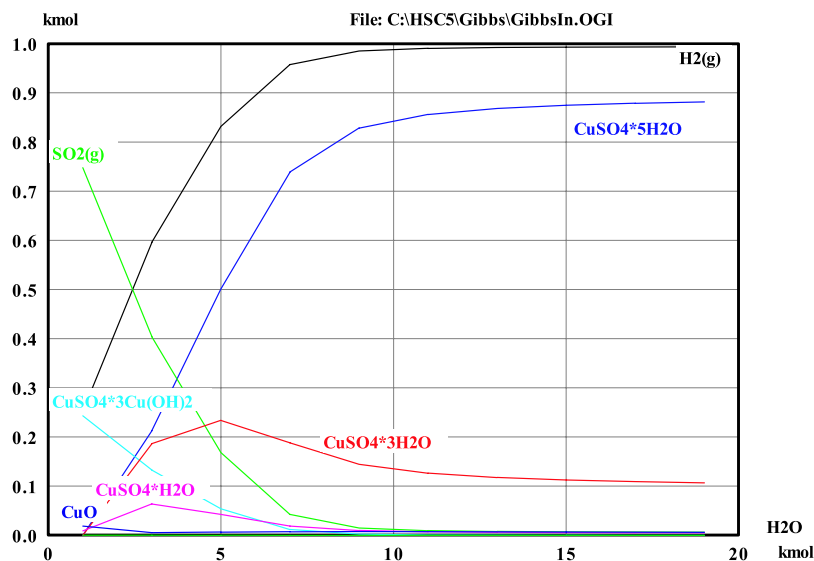
For the final Level 2 analysis, we used new reactions, 5-7, shown below. New temperatures were chosen to increase the yields of hydrogen and oxygen to 100% with excess water (10 times stoichiometric) in the feed. Though this increases the yields of hydrogen and oxygen, it also requires increased energy costs for removing free water and hydrated water.



In this evaluation the energy balance considers the requirements for removing water from the hydrated species shown in reaction 6. The pinch analysis (not shown) shows that 135 kcal of extra heat is needed to maintain a 10°C driving force because the heat from the CuO reaction (reaction 5) is not recoverable. In addition, the complete removal of water from the product of reaction 6 causes the maximum temperature for complete conversion of the anhydrous CuSO₄ (reaction 7) to shift from 1 100°C to 1 200°C. The energy efficiency in this case is 30.7% (LHV). This calculation is not shown in detail. Our value agrees reasonably well with a value of 30.9% (LHV) from a preliminary and unoptimised flowsheet analysis by Carty *et al.* [1, 6].

One of the biggest advantages of this cycle is that it has been demonstrated [6]. While most of the details of the experimental programme have been lost, published results indicate that all of the reactions occur with recycled materials and that the electrochemical reaction produces hydrogen and CuO with a potential of 0.45V albeit with low current densities and reaction rates. The primary effort required for going forward is the optimisation of the electrochemical cell such that the components are highly mixed. Foh *et al.* suggest the use of a fluidised electrolyte system to allow large current densities at low polarizations [6, 7, 8].

Figure 5. Equilibrium yields when the molar ratio of water to CuO (or SO₂(g)) is varied in the CuO reaction



Other Promising Alternative Cycles

Efficiency Calculations.

The results of our evaluations for the other hybrid cycles are summarized in Table 3. The advantages of the Cu-Cl cycle are its low maximum temperature requirement and its relatively high efficiencies. The Level 1 and 2 efficiencies exceed 40% (LHV). All reactions in this cycle have been proven [1, 9, 10]. The Mg-Cl cycle has a low maximum temperature requirement but comparatively low Level 1 and 2 efficiencies. The chemistry for the thermal reactions has not been demonstrated. The low maximum temperatures, 550 and 600°C, respectively, for the two chloride cycles provide more flexibility in coupling them with heat sources other than the VHTGR. The advantages of the metal sulfate cycles are their lower corrosivity and the common high temperature decomposition reaction with the sulfur cycles. Of the two metal sulfate cycles, the copper sulfate cycle appears more promising because the copper sulfate cycle requires somewhat lower temperatures than the zinc sulfate cycle. The copper sulfate cycle has also been demonstrated with recycled materials, but no experimental work has been reported for the zinc sulfate cycle [1].

Table 3. Summary of the efficiency calculations for the candidate cycles evaluated with the scoping flowsheet methodology

Cycle	Level	Efficiency % (LHV)	Maximum Temperature, °C	Other Conditions
Cu-SO ₄	1	46.0	850	1 mol water
	2	38.1	1100	1 mol water
	2	30.7	1200	10 mols water
Zn-SO ₄	1	40.5	850	1 mol water
	2	40.8	1400	2.7 mols water
Cu-Cl	1	48.0	550	1 mol water
	2	42.4 From Aspen-Plus	550	Excess water and HCl
Mg-Cl	1	35.2	600	1 mol water
	2	30.0 to 33.1	600	2 mols water

Recommendations for needed R&D

The most significant R&D issue for further development of all of these cycles is the development of the electrochemical cell. For the two sulfate cycles and the Cu-Cl cycle, the electrochemical step involves a nearly insoluble reagent (CuO, ZnO, or CuCl) in aqueous solution. The solubility of CuCl can be increased by using an aqueous solution of HCl. For the Cu-SO₄ cycle, Foh suggests the use of fluidized electrolyte system and electrocatalysts. Research in these areas may also be leveraged for use in the ZnSO₄ and the Cu-Cl cycles. Another area for future R&D effort regards materials development. For example, materials for the Cu-Cl cycle must withstand HCl with various quantities of moisture and be inert with respect to the oxidizing properties of CuCl₂. Materials for the metal sulfate cycles must withstand SO₂ and O₂ at 900°C.

Summary

We developed a scoping flowsheet methodology to evaluate the potential of alternative cycles. The methodology was designed to rapidly screen processes at Level 1 with reasonable realism. More accurate simulations are done in Level 2 analyses to find problem areas (unexpected by-products,

unrealistic process conditions, problematic separations, etc.) so that process development efforts can be focused. Where possible, we incorporate published experimental information regarding the cycle's chemistry. We used this methodology to evaluate four cycles that were identified as promising. In this paper, we report detailed results of our analysis for the Cu-SO₄ cycle and a summary of results for the other cycles.

We calculated the Level 1 efficiency for the Cu-SO₄ cycle from the heat and work inputs for two cases. One case used chemical potential work and the other used electrochemical work for the hydrogen generation reaction. Experimentally it was determined that electrochemical work was required and the Level 1 efficiency was calculated as 46.0% (LHV), a large drop from the 66.9% (LHV) calculated without electrochemical work. The Level 2 efficiency was calculated for two cases, one with a 1 to 1 molar ratio of water to CuO and one with a 10 to 1 molar ratio of water to CuO. The larger amount of water was used to increase hydrogen yields and to obtain experimentally reported products. Handling the excess water exacted an energy penalty and dropped the efficiency to 30.7% (LHV). Even though this value is relatively low, we still consider this cycle as a promising alternative cycle for the following three reasons: (1) its chemistry has been demonstrated; (2) its highest temperature reaction is less corrosive than that for the other sulfur cycles; and (3) improvements in efficiency are expected with process design optimization. An evaluation at higher levels would include process design optimization as well as a consideration of non-idealities, such as the insolubility of CuO, enthalpies of solvation and mixing, azeotrope formation, etc.

We used the same methodology to evaluate the three other cycles identified as promising. Of the four examined, the Cu-Cl had higher Level 1 and Level 2 efficiencies, 48 and 42.4%, respectively, than the others. In addition, proof-of-concept experiments have been completed for all reactions. It is therefore one of the more promising candidates for further development. Both cycles can be coupled with the very high temperature gas reactor.

REFERENCES

- [1] R.H. Carty, M.M. Mazumder, J.D. Schreider, and J.B. Panborn, "Thermochemical Hydrogen Production," Vols. 1-4, Gas Research Institute for the Institute of Gas Technology, GRI-80/0023, Chicago, IL 60616 (1981).
- [2] B.W. McQuillan *et al.*, "High Efficiency Generation of Hydrogen Fuels Using Solar Thermochemical Splitting of Water: Annual Report, October 1, 2003 through September 30, 2004," to be published as GA-A24972, San Diego, CA.
- [3] G.E. Beghi, *Int. J. Hydrogen Energy*, **11**, pp. 761-771 (1986).
- [4] M.F. Simpson, Personal communication, Idaho National Laboratory, May, 2005
- [5] HSC Software "Outokumpu HSC Chemistry for Windows," Version 5.1, Antti Roin, 02103-ORC-T, Pori, Finland, 2002.
- [6] S.E. Foh, J.D. Schreiber, and J.R. Dafler, Report # Conf-780801-12 (1978).
- [7] R.E. Soida, "Flow-through Electrodes Composed of Parallel Screens," *Electrochimica Acta*, **22**, pp. 439-43 (1977).
- [8] F. Goodridge, C.J.H. King, and A.R. Wright, "The Behavior of Bipolar Packed-Bed Electrodes," *Electrochimica Acta*, **22** pp. 347-52 (1977).
- [9] M.A. Lewis, J.G. Masin, and R.B. Vilim, "Development of the Low Temperature Cu-Cl Thermochemical Cycle," International Congress on Advances in Nuclear Power Plants, Seoul, Korea presented May 15-19, 2005, to be published.
- [10] M. Serban, M.A. Lewis, J.K. Basco, "Kinetic Study of the Hydrogen and Oxygen Production Reactions in the Copper-Chloride Thermochemical Cycle," 2004 AIChE Spring National Meeting, Conference Proceedings, 2004 AIChE Spring National Meeting, Conference Proceedings, pp. 2690-2698 (2004).

This page intentionally left blank

STUDY OF THE HYBRID CU-CL CYCLE FOR NUCLEAR HYDROGEN PRODUCTION

Sam Suppiah, J. Li, R. Sadhankar and K.J. Kutchcoskie

Atomic Energy of Canada Limited, Canada

and

Michele Lewis

Argonne National Laboratory, U.S.A.

Abstract

AECL is collaborating with Argonne National Laboratory in the development of the Hybrid Cu-Cl Cycle for hydrogen production using nuclear energy. This cycle is well suited for integration with the Supercritical Heavy Water Cooled Reactor (SCWR) under development by AECL as part of the fourth generation Advanced CANDU[®] Technology. AECL's electrolysis expertise has been identified as a potential contributor to the development of the electrochemical step involved in the Cu-Cl cycle. Work has been initiated at AECL to focus on the development of an electrolytic cell for the disproportionation of CuCl in an aqueous system to provide the Cu required for this closed cycle requiring only water and energy inputs. As part of this effort, AECL would also explore a variant of the Hybrid Cu-Cl Cycle involving direct electrochemical production of hydrogen from CuCl/HCl. In addition, AECL would explore the Reverse Deacon Reaction-based cycle involving electrolysis of anhydrous HCl.

Introduction

Availability of economical hydrogen from non-greenhouse gas emitting processes is a prerequisite for the success of the evolving hydrogen economy. Countries around the world are making significant contributions to the development of economical hydrogen production processes based on their own governmental energy policies. High and moderate temperature thermochemical processes are touted as potential routes for the supply of economical hydrogen using very high temperature nuclear reactors (VHTR) and supercritical water cooled reactors (SCWR), respectively. Argonne National Laboratories (ANL) has identified the Hybrid Cu-Cl Cycle as one of the most promising cycles to split water to produce hydrogen at a moderate temperature of around 550°C [1].

AECL is developing a supercritical heavy water moderated nuclear reactor (SCWR) [2] based on its successful CANDU[®] reactor system currently deployed around the world. Since the Mark 2 [2] version of the heavy water moderated SCWR can satisfy the temperature requirements of the hybrid Cu-Cl cycle, AECL is collaborating with ANL in the development of this cycle. Also, AECL is particularly interested in this process since some of its hydrogen-economy related technologies are a good match for the developmental needs of this process, in particular for the development of the electrochemical step involved.

Apart from the ANL's current effort on Hybrid Cu-Cl Cycle, there have been only a limited number of other processes proposed for moderate temperature thermochemical hydrogen production. Dokiya and Kotera [3] proposed a cycle with a significant variant of the Hybrid Cu-Cl Cycle involving a direct electrochemical hydrogen generation reaction. More recently, Simpson et al. [4] have proposed a hybrid thermochemical electrolytic process for hydrogen production based on modified Reverse Deacon Reaction (generation of HCl gas) and gas phase electrolysis of HCl.

As a way of maximising the overall efficiency of the developmental effort on the Hybrid Cu-Cl Cycle, AECL is providing input from its in-house expertise to the development of the electrochemical step. This paper presents AECL's initial effort in the development of the electrochemical step involved in the hybrid Cu-Cl cycle and in the cycles proposed by Dokiya and Kotera [3] and Simpson *et al.* [4].

The Cu-Cl Hybrid Cycle

The five main steps identified by ANL in the hybrid Cu-Cl Cycle are shown in Table 1 with details pertaining to the operating conditions. Basically, the cycle is mainly a closed one, as shown pictorially in Figure 1, except for feed water, heat and electricity requirements. In Step 1, solid Cu is reacted with HCl gas to produce H₂ gas and Cu-Cl in a molten state. Step 2 uses the Cu-Cl from Steps 1 and 5 to produce the Cu required for Step 1 through an electrochemical process. The reaction between solid CuCl₂ and steam (Step 4) produces the HCl gas required in Step 1. In Step 5, the CuO*CuCl₂ complex formed in Step 4 is decomposed to produce O₂ gas as output and CuCl for Step 1. Hence, all chemicals are recycled with only H₂ and O₂ as products from the process.

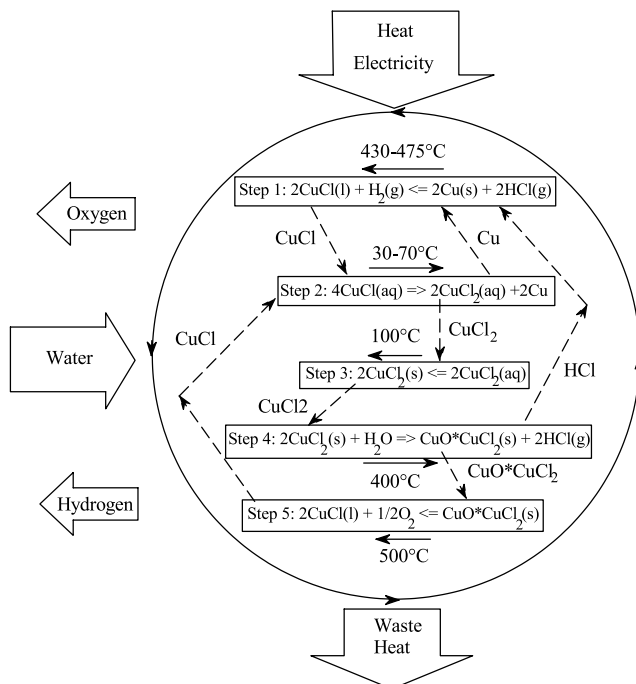
Table 1. The reaction steps involved in the hybrid Cu-Cl cycle

Step #	Reaction	T range (°C)	Feed/Output	
1	$2\text{Cu(s)} + 2\text{HCl(g)} = 2\text{CuCl(l)} + \text{H}_2\text{(g)}$	430-475	Feed:	Electrolytic Cu + dry HCl + Q
			Output:	H ₂ gas + CuCl(l) salt
2	$4\text{CuCl(s)} \rightarrow 4\text{CuCl(aq)} = 2\text{CuCl}_2\text{(aq)} + 2\text{Cu(s)}$	30-70	Feed:	Powder/granular CuCl and HCl + V
			Output:	Aqueous slurry containing Cu, HCl & CuCl ₂
3	$2\text{CuCl}_2\text{(aq)} = 2\text{CuCl}_2\text{(s)}$	>100	Feed:	Aqueous CuCl ₂ with HCl + Q
			Output:	Powder/granular CuCl ₂ + H ₂ O/HCl vapours
4	$2\text{CuCl}_2\text{(s)} + \text{H}_2\text{O(g)} = \text{CuO*CuCl}_2\text{(s)} + 2\text{HCl(g)}$	400	Feed:	Powder/granular CuCl ₂ + H ₂ O(steam) + Q
			Output:	Powder/granular CuO*CuCl ₂ + 2HCl (g)
5	$\text{CuO*CuCl}_2\text{(s)} = 2\text{CuCl(l)} + 0.5\text{O}_2\text{(g)}$	500	Feed:	Powder/granular CuO*CuCl ₂ (s) + Q
			Output:	Molten CuCl salt + oxygen

Q – Thermal energy
V – Electrical energy

Lewis *et al.* [1] at ANL have confirmed that all the reactions shown in Table 1 are thermodynamically viable. They have also conducted proof of principle experiments for the generation of H₂ (Step 1), Cu (Step 2), HCl (Step 4) and O₂ (Step 5). However, there are numerous challenges associated with each step involved in this cycle, in addition to the challenges related to the integration of this cycle to SCWR. The challenges involved in the development of the electrochemical step (Step 2) of disproportionating CuCl in an aqueous system are considered to be quite significant from technological and economical points-of-view.

Figure 1. A schematic of the closed loop nature of the hybrid Cu-Cl cycle



Electrochemical Disproportionation of Cu-Cl in Aqueous System

The anode and cathode reactions involved in the disproportionation of Cu-Cl are presented in Equations (1) and (2) and shown pictorially in Figure 2.

Anode reaction:



Product: $CuCl_2$

Cathode reaction:

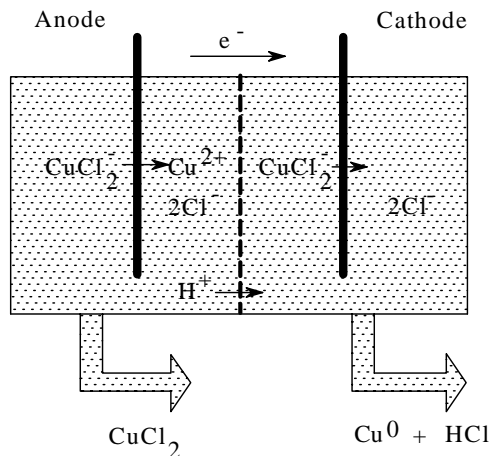


Product: Cu^0 and HCl

One of the main initial concerns with respect to this electrochemical process was that the theoretical voltage requirement would be too high at 1.4V as given in the U.S. Patent [5]. However, calculations at ANL revealed a significantly lower value, and therefore confirmation of the lower value was sought through bench-top experiments conducted at ANL using single compartment cells. These results are given in Table 2 with those from Gas Technology Institute (GTI) and AECL. As can be seen from these results, good levels of current densities have been achieved at considerably lower than 1.4V from the work carried out at all three organisations. Since lower voltage would produce higher efficiency, these preliminary results are very encouraging.

As the summary of the experimental work presented in Table 2 show, the cell used at GTI separated the anode and cathode compartments using an anion exchange membrane while the cells used at ANL and AECL did not have such a separator. Since in a real operational cell separation of the electrodes will be necessary, identification or development of useful membranes for this process is one of the main objectives.

Figure 2. The electrolytic step involved in the hybrid Cu-Cl cycle



Lewis *et al.* [1] have summarised the various challenges facing the development of the electrochemical step. The design of the electrochemical cell, selection of appropriate membranes and electrode materials, determination of operating parameters that will produce removable Cu particles at the cathode and a concentrated $CuCl_2$ solution at the anode. Because of the low solubility of $CuCl$, a dilute solution at the anode would lead to an excessive heat requirement for drying of $CuCl_2$ (Step 3 in Table 1), which can render the overall cycle uneconomical. Using an HCl solution can increase the solubility of $CuCl$, but it leads to the requirement for separating $CuCl_2$ from an acid solution. Apart

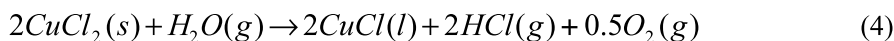
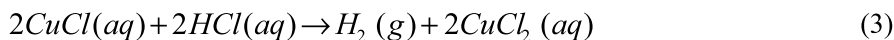
from these challenges, selection of materials, minimising concentration polarisation and maximising ionic conductivity of electrolyte are expected to provide a significant challenge in the development of the e-cell.

Table 2. A summary of experimental work conducted in different organisations on the electrochemical step of the hybrid Cu-Cl cycle.

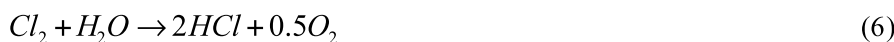
Organisation	Details of work
ANL	Temperature: 20-80°C 0-4M HCl, 0.01-0.3M CuCl, 0-0.1M CuCl ₂ Anode current density: 21 mA·cm ⁻² @ 0.4V 135 mA·cm ⁻² @ 0.6V
GTI	Voltage as low as 0.4V Current density: unknown CuCl ₂ concentration as high as 5N Proprietary anion exchange membrane Graphite plates with channel as electrodes
AECL	<u>With Graphite electrodes:</u> 0.3 M CuCl in 4M HCl Voltage: 0.4 to 0.8 V Current density: 29 to 37 mA·cm ⁻² <u>With copper cathode and platinum anode:</u> 0.3 M CuCl in 4M HCl Voltage: 0.5 to 0.8V Current density: 14 to 86 mA·cm ⁻²

Cu-Cl Cycle with Direct Electrochemical Hydrogen Generation Reaction

The cycle proposed by Dokiya and Kotera [3] can be expressed by Equations (3) and (4).



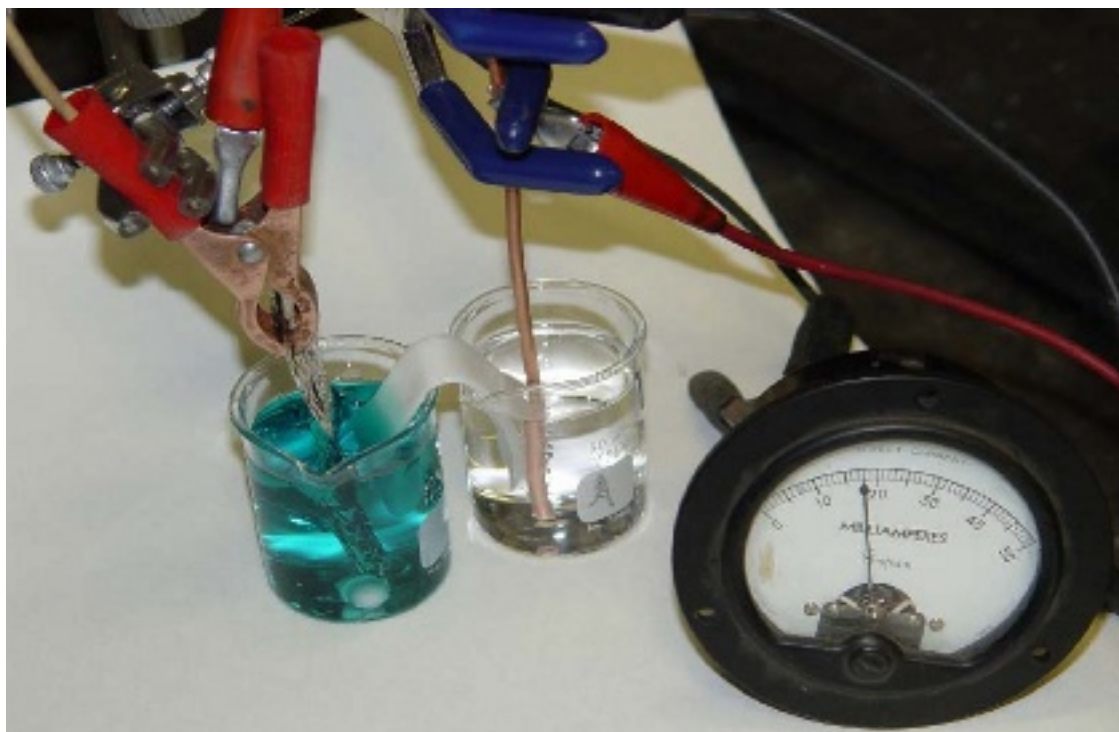
The first reaction is the electrolysis step conducted at room temperature and the second step, which involves reaction of solid CuCl₂ with steam at around 600°C, closes the cycle. As can be seen, a single step of Equation (4) combines Steps 4 and 5 of the ANL's cycle presented in Table 1. The reaction given in Equation (4) may be expressed more precisely in two steps as shown in Equations (5) and (6). Equation (6) is known as the Reverse Deacon Reaction.



Dokiya and Kotera [3] reported current densities of >250 mA·cm⁻² at 0.6 to 1.0 V using a cell with two chambers separated by an anion exchange membrane, Celemion (Asahi Glass Co, Japan). The cathode was a copper plate immersed in HCl (35%) and the anode was platinum plate in 2.5M CuCl in HCl.

At ANL a similar cell was used to obtain $\sim 50 \text{ mA}\cdot\text{cm}^{-2}$ at 1.0 V. The scoping experiment at AECL involved the set-up shown in Figure 3. The anode part of the cell consisted of platinum foil submerged in a 40 mL of solution containing 1M CuCl and 2M HCl. The cathode was a 1/8 inch diameter copper tube inserted 3 cm deep into 40 mL of 2M HCl. An ion bridge was provided with several layers of Whatman #1 filter paper soaked in 2M HCl. A variable voltage DC power supply was used to control the cell voltage and an inline 50mA ammeter was used to measure the current. The negative power lead was connected to the copper tube (cathode) and the positive lead was connected to the Pt foil (anode). A multimeter was connected directly to the cathode and anode to read cell voltage. Hydrogen production was observed at as low as 0.6 V with significant bubble formation at 1 V.

Figure 3. Demonstration of the electrochemical step involved in the variant of the hybrid Cu-Cl cycle proposed by Dokiya and Kotera [3].



Dokiya and Kotera [3] proposed to carry out the reactions shown in Equations (5) and (6) in one step as shown in Equation (4) to produce the HCL to close the loop and provide O_2 as a by-product. The electrolysis step given by Equation (3) may be incorporated in the ANL cycle (Table 1) to replace Steps 1, 2 and 3, but maintain Steps 4 and 5.

Hybrid Thermochemical Electrolytic Process for Hydrogen Production Based on Modified Reverse Deacon Reaction

From preliminary efficiency estimates and proof of principle experiments, Simpson *et al.* [4] have recently proposed a hybrid process based on the reverse Deacon cycle as a promising moderate temperature thermochemical process to produce hydrogen. The basic reactions involved are shown in the three steps in Table 3. As can be seen from the equations given in Table 3, the two-step sequence involving magnesium chloride hydrolysis (Step 1) followed by magnesium oxide chlorination (Step 3) reduces to the Reverse Deacon Reaction. The moderate temperatures involved in these reactions would

prevent recombination of oxygen and hydrochloric acid [4]. Separation of gas and solids is expected to be somewhat easier (compared liquid/solid separations) and help the hydrolysis step. The electrolysis of anhydrous HCl requires less energy (reversible voltage of 1.0 V) than water electrolysis (reversible voltage of 1.25 V). Also, electrolysis of anhydrous HCl is well established from DuPont's early development efforts [6].

Table 3. The steps involved in the modified Reverse Deacon Cycle

Step #	Reaction	Temperature Range (°C)	Remarks
1	$MgCl_2(s) + H_2O(g) \rightarrow MgO(s) + 2HCl(g)$	500-550	gas-solid reaction $\Delta H = 23 \text{ kcal}\cdot\text{mol}^{-1}$ @ 500°C
2	$2HCl(g) \rightarrow H_2(g) + Cl_2(g)$	25-100	anhydrous HCl electrolysis 8 kA·m ⁻² @ 1.6V
3	$MgO(s) + Cl_2(g) \rightarrow MgCl_2(s) + 0.5O_2(g)$	400-500	gas-solid reaction $\Delta H = -9 \text{ kcal}\cdot\text{mol}^{-1}$ @ 500°C

Simpson *et al.* [4] propose to carryout the two-step Deacon reaction through supported magnesium compounds on a zeolite such as Silicalite. Though they have addressed many of the development requirements of this process, some still need considerable effort for assessment of the commercial viability of the overall process. Due to the lower temperature requirements of this process (compared to high temperature thermochemical processes), the less stringent demand on materials, and the well-established status of the electrolysis step, this process deserves further evaluation.

Conclusions

The hybrid Cu-Cl cycle is a potentially suitable hydrogen production process for integration with the SCWR being developed by AECL. A number of challenges face the development of the Hybrid Cu-Cl cycle into a commercially viable one. ANL is addressing some of these challenges with AECL collaborating with them on the electrolytic step. The variant of the hybrid Cu-Cl cycle, proposed by Dokiya and Kotera [3], also appears to be a suitable process for further consideration. AECL is planning to explore the development opportunities in the electrolytic step involved in this variant hybrid Cu-Cl cycle.

Since the Reverse Deacon Cycle-based process proposed by Simpson *et al.* [4] appears to be more efficient than water electrolysis and involves a well-developed electrolysis cell, AECL is planning to spend some effort into the evaluation of this process for further development.

REFERENCES

- [1] M. Lewis, M. Serban, J. Basco and J. Figueroa, “Low Temperature Thermochemical Cycle Development”, Presented at the NEA/OECD meeting, October 2-3, 2003.
- [2] N.J. Spinks, N. Pontikakis and R.B. Duffey, “Thermo-Economic Assessment of Advanced, High-Temperature CANDU Reactors”, Proceedings of ICONS 10, 10th International Conference on Nuclear Engineering, Arlington, VA, April 14-18, 2002.
- [3] M. Dokiya and Y. Kotera, “Hybrid Cycle with Electrolysis Using Cu-Cl System”, Presented at the U.S.-Japan Seminar on Key Technologies for the Hydrogen System, Tokyo, Japan, July 1975.
- [4] M.F. Simpson, S.D. Herrmann and B.D. Boyle, “A hybrid thermochemical electrolytic process for hydrogen production based on the reverse Deacon reaction, International Journal of Hydrogen Energy, in press December 2005.
- [5] U.S. Patent 3,692,647, “Electrolytic Copper Producing Process”.
- [6] S. Motupally, D.T. Mah, F.J. Freire and J.W. Weidner, “Recycling Chlorine from Hydrogen Chloride – A New and Economical Electrolytic Process”, The Electrochemical Society Interface, Fall 1998.

PRELIMINARY PROCESS ANALYSIS AND SIMULATION OF THE COPPER-CHLORINE THERMOCHEMICAL CYCLE FOR HYDROGEN GENERATION

Mohammad Arif Khan and Yitung Chen

Department of Mechanical Engineering
University of Nevada, Las Vegas

Abstract

Hydrogen is an attractive fuel for the future because it is renewable as an energy resource and it is also flexible as an energy carrier. Process analysis and simulation flowsheets for thermochemical cycles have been developed in the framework of ASPEN PLUS (chemical analysis simulator) in order to study hydrogen generation. Chemical mass balance, conversion rate, operating temperature and pressure are comparatively assessed for a wide range of hydrogen production processes, including processes which are hydrocarbon based (methane reforming), non hydrocarbon based (copper-chlorine cycle) and water splitting thermochemical cycles. Then process analysis and simulation models have been built up with the help of detailed reaction models, chemical components data, reactor dimensions, specification, and operating parameters. Copper-chlorine (Cu-Cl) cycle has been studied and analyzed in this study as a promising cycle which can produce hydrogen at a lower temperature (550°C). Argonne National Laboratory (ANL) has recently initiated an exploratory research to develop Cu-Cl cycle that operates at 550°C. In the Cu-Cl cycle chemicals are combined with water and heated to cause chemical reactions that produce hydrogen at 550°C – a temperature compatible with current power plant technologies. A process analysis and simulation model has been developed for this cycle. Preliminary assessment of cycle efficiency is also completed. Details of the simulation flowsheet and efficiency are discussed.

Introduction

Hydrogen production using thermochemical cycles has been studied in the last three decades. Various thermochemical cycles have been successfully developed including their chemistry, bench scale studies and process flowsheet analysis. Of the identified thermochemical processes, the sulfur family of processes, including sulfur-iodine (S-I) and hybrid-sulfur, appear to have the highest efficiencies and hence to be the most promising. The S-I cycle (850°C) proposed by the General Atomics (GA) Company is one such cycle developed for large-scale hydrogen production. The calcium-bromine cycle, also known as the UT-3 cycle (760°C), invented by the University of Tokyo, gained considerable attention in addition to the GA proposed the S-I cycle. The chemistry of these cycles has been studied extensively. The efficiency of hydrogen generation, for a stand alone plant, is predicted to be 36-40%, depending upon the efficiency of the membrane separation processes. Higher overall efficiencies, 45-49%, are predicted for a plant that co-generates both hydrogen and electricity [1-2]. On the other hand, Copper-Chlorine thermochemical cycle has the option of producing much needed hydrogen gas at a very low temperature (550°C) which is very encouraging. At the same time it may be very economical process as this cycle uses inexpensive raw materials. The process involves six separate reactions: four thermal steps driven by heat and two electrolytic steps driven by electric energy.

In this paper, we present a detailed process analysis of the Cu-Cl cycle as a potential alternative of the S-I cycle. Thermodynamic feasibility of the reactions involved in this cycle has been evaluated by HSC Chemistry 5.11 (commercially available thermodynamic database software). Simulation flowsheet has been developed by using chemical analysis simulator ASPEN PLUS 12.1.

Basics of thermochemical cycles

Thermochemical production of hydrogen involves the separation of water into hydrogen and oxygen through chemical reactions at high temperatures. Ideally, water can be separated directly (thermolysis); however this process requires temperatures in excess of 2 500°C.



Because these temperatures are impractical, the thermochemical water-splitting cycles achieve the same result (i.e., separation of water into hydrogen and oxygen) at lower temperatures. A thermochemical water-splitting cycle is a series of chemical reactions that sum to the decomposition of water. To be useful, each reaction must be spontaneous and clean. Chemicals are chosen to create a closed loop where water can be fed to the process, oxygen and hydrogen gas are collected, and all other reactants are regenerated and recycled [2].

Recent studies conducted through the Nuclear Energy Research Initiative (NERI) have identified more than 100 thermochemical water-splitting cycles. A few of the most promising cycles have been selected for further research and development, based on the simplicity of the cycle, the efficiency of the process, and the ability to separate a pure hydrogen product. The Cu-Cl cycle is one of the promising cycles which can produce hydrogen at a lower temperature (550°C) compare to that of direct thermolysis.

Copper-chlorine (Cu-Cl) thermochemical cycle

Copper-chlorine (Cu-Cl) cycle is a good alternative for hydrogen gas generation at low temperature in which chemicals are combined with water and heated to cause chemical reactions that produce hydrogen (and oxygen) at 550°C – a temperature compatible with current power plant technologies.

The chemicals are not consumed, and are recycled. Chemical Engineering Division of ANL is currently working on this cycle. The cycle is referred as Argonne Low Temperature Cycle-1 (ALTC-1). This cycle is considered promising over other cycles for the following reasons [3-4]:

1. The maximum cycle temperature (<550°C) allows the use of multiple and proven heat sources.
2. The intermediate chemicals are relatively safe, inexpensive and abundant
3. Minimal solids handling is needed.

All reactions have been proven in the laboratory and no significant side reactions have been observed.

One potential disadvantage with ALTC-1 cycle is that one of the reactions is electrochemical, which imposes a significant energy cost. However, the experimental data suggest that the electrolytic step can be performed at voltages significantly lower than in direct water electrolysis. The reactions involved in ALTC-1 cycle are given in the following Table:

Table 1. Reactions involved in the Cu-Cl cycle

Reaction No.	Reaction	Temp. °C	ΔG kcal/mol	ΔH kcal/mol
1.	$2\text{Cu(s)}+2\text{HCl(g)}=2\text{CuCl(l)}+\text{H}_2\text{(g)}$	450	3.85	-13.50
2.	$4\text{CuCl(s)} + 4\text{Cl}^-\text{(aq)} = 4\text{CuCl}_2^-\text{(aq)}$ Electrochemical step	30	8.27	0.06
3.	$4\text{CuCl}_2^-\text{(aq)}=2\text{CuCl}_2\text{(aq)}+2\text{Cu(s)}+4\text{Cl}^-\text{(aq)}$ Electrochemical step	30	14.50	2.93
4.	$2\text{CuCl}_2\text{(aq)} = 2\text{CuCl}_2\text{(s)}$	100	6.0	19.90
5.	$2\text{CuCl}_2\text{(s)}+\text{H}_2\text{O(g)}=\text{CuO(s)}+\text{CuCl}_2\text{(s)}+$ 2HCl(g)	400	9.50	28.00
6.	$\text{CuO(s)} + \text{CuCl}_2\text{(s)}=2\text{CuCl(l)}+1/2\text{O}_2\text{(g)}$	550	-1.93	31.00

The Cu-Cl thermochemical cycle was first proposed by Carty *et al.* and was designated H-6 in a Gas Research Institute (GRI) report [5]. In that study, H-6 consisted of four reactions, three thermal and one electrochemical. ANL's preliminary study indicated that two additional reactions should be added to the original H-6 cycle. So the proposed ALTC-1 cycle consists of six reactions. Reaction-1 is the hydrogen generation reaction and Reaction-6 is oxygen generation reaction [5]. The other reactions close the cycle.

The first step in cycle development is to determine its thermodynamic feasibility. The free energies and the enthalpies for the reactions shown in the above Table were obtained by using HSC Chemistry 5.11 which contain a thermodynamic database. At the temperature indicated in the table, based on cycle stoichiometry to produce 1 mol of hydrogen, the free energy change of each reaction step is ± 10 kcal, except for the electrochemical step, which has ΔG of 14.50 kcal/mol at 30°C. The current research of

this cycle at ANL concludes that all of these reactions are viable on thermodynamic basis using the values of the free energies.

According to Carty [5], who proposed this cycle in a Gas Research Institute (GRI) report in 1981, reactions whose free energy change lies within ± 10 kcal for a given temperature are considered likely candidates for a cyclic process. Small positive free energy changes are acceptable if nonequilibrium reactor configurations can be utilized, such as continuous product removal, reactants in excess, and where there are a smaller number of product gases than reactant gases. Reactions with a positive free energy change of 10 to 25 kcal/mol can generally be accomplished electrochemically.

Study of the reaction kinetics of Cu-Cl cycle

H₂ Production

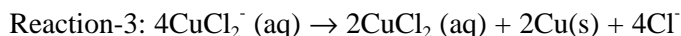
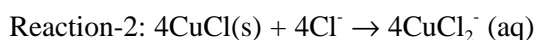


The reaction between HCl and Cu is a heterogeneous exothermic reaction. It has been suggested that the reaction proceeds rapidly at 230°C, the temperature at which 93% of HCl is decomposed and the Gibbs free energy change is -3.95 kcal/mol. However no hydrogen is detected at this temperature. Hydrogen starts to be produced in significant amounts at temperature above 350°C. The kinetics of the reaction are accelerated at temperatures higher than 430°C, the temperature at which CuCl melts, facilitating the interaction between HCl and Cu [4].

For a batch process, a reaction tank in which Cu powder/granules are fed with a

continuous bleed of HCl gas could be utilized. However, a continuous process reactor can be used in this step. Process heat from an external heat source is used to heat the mixture to the reaction temperature. The copper could be introduced at room temperature and heated to the desired reaction temperature, or it could be preheated before placing it in the reactor. Obviously, preheating will reduce the overall length of this reactor [6].

Copper Production by Electrolysis



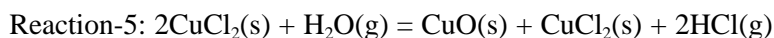
CuCl is very sparingly soluble in water but soluble in HCl. The electrochemical disproportionation of CuCl is therefore being conducted at room temperature in an HCl aqueous solution [4].

Recovery of CuCl₂(s) from the Aqueous Solution Containing CuCl₂ and HCl



The output from the electrolyzer will be an aqueous solution containing CuCl₂ and HCl. This step involves recovery of the CuCl₂(s) from the solution for the subsequent oxygen production step. This step also involves addition of sufficient thermal energy to remove (by vaporisation) the water and HCl in order to recover the solid CuCl₂. Process heat from external heat source should be used to preheat the solution to 110°C before the mixture is forced through settling chamber [6].

Oxygen Production Step



The first step of this two-step process involves steam oxidation of CuCl_2 at 400°C . The second step involves additional heating of the reaction byproduct to 550°C where the $\text{CuO}(\text{s}) + \text{CuCl}_2(\text{s})$ react to form $\text{CuCl}(\text{l})$ and $\text{O}_2(\text{g})$. Process heat from external heat source is used to provide the thermal energy needed to carry out these reactions [6].

Potential Heat Source for Cu-Cl Cycle

The net heat input to the Cu-Cl thermochemical cycle is to be provided by potential external heat source. Of the chemical reactions, the oxygen production step has the highest temperature requirement, 550°C . Several factors require raising the design value to achieve the necessary oxygen production temperature. First, the process heat will be delivered through a heat exchanger and there will be an associated temperature drop along the length of the heat exchanger as heat is transferred. If this temperature drop is taken as 40°C , then to achieve an average temperature on the primary side of the heat exchanger of 550°C , the coolant must enter at 570°C . Second, there is a temperature drop of roughly 20°C when passing across sodium heat exchanger tubes. Thus, an external heat source (nuclear or solar) capable of delivering temperature of about 580°C is needed to satisfy the oxygen production process step [6].

Process Analysis and Simulation of Cu-Cl Cycle

The Cu-Cl cycle is considered as a closed cycle since all materials are recycled with the exception of water which is split into hydrogen and oxygen. The process involves six separate reactions: four thermal steps driven by heat and two electrolytic steps driven by electric energy. The reactor provides the heat while a Rankine cycle driving a generator provides the electrical energy. A schematic diagram (Figure 1) of Cu-Cl cycle is shown above for better understanding.

In the given diagram solar panels are used to produce the heat to complete the last three steps of this cycle. Heated steam coming from the external heat source will enter into the reactor to generate HCl at 400°C . CuCl_2 from the aqueous CuCl_2 dryer reacts with steam to produce HCl. The other products of this reaction, CuO and CuCl_2 are then sent to another reactor to form O_2 at 500°C . The other product of this reaction, CuCl, recycles back to the electrolysis step. HCl produced by the HCl generation reactor then passes through the HCl-dryer where dry and pure HCl is stored in a tank and some portion of it along with H_2O is stored in another tank. HCl from the dry HCl tank is sent to the hydrogen generation reactor where it reacts with Cu recovered from the electro-refiner at 450°C . The copper could be introduced at room temperature and heated to the desired reaction temperature, or it could be preheated before placing it in the reactor. The produced gas is not pure and a small amount of HCl is mixed with H_2 . To extract pure H_2 gas, this mixture passes through a separator where pure H_2 gas recovery takes place and the unwanted HCl is sent back to the dry HCl tank.

The reactions have been defined in the individual reactor blocks instead of globally. Block ELCTRLYZ does the electrolysis reactions, Block CU-HYDRO does the CuCl₂ hydrolysis which produces HCl, Block O2-REACT does the oxygen production reaction, and Block H2-REACT contains the hydrogen production reaction. The reaction mechanisms specified for these blocks can be found in the reaction tab of these blocks. Sometimes it took two reaction definitions to get the desired reaction to take place: one reaction for the solid species and another for the dissolved species [7].

Efficiency analysis of the Cu-Cl cycle

Efficiency of the Cu-Cl cycle can be calculated following the efficiency calculation procedure of the sulfur-iodine cycle. All the energy values are based on the generation of one mole of hydrogen by the process. Efficiency is defined as the ratio of hydrogen heating value to the sum of the heat and electrical inputs required. For the electrical energy, an efficiency of 50% is assumed for any electrical generation not supplied by the process. In equation form:

$$\varepsilon = \frac{\Delta H}{Q + \frac{E}{\eta}}$$

ε = Thermal efficiency

ΔH = Hydrogen heating value

Q = External heat demand for cycle

E = External power demand for cycle

η = Efficiency of external electrical power

Here Q is the sum of the endothermic enthalpies (heat inputs) and E is the sum of the work inputs, which are converted to heat inputs by dividing the work inputs by the efficiency for converting heat to electricity, η . This calculation is referred to as the lower heating value (LHV) basis.

Based on thermodynamic analysis, the efficiency of the Cu-Cl cycle for the simulation is found to be 29.15%. The efficiency (based on thermodynamics) calculated by ANL is 41%. More reliable efficiency values can be obtained after the chemistry of the cycle is well defined.

Result summary of the simulation of Cu-Cl cycle:

1. The thermodynamic feasibility of the reactions involved in the Cu-Cl cycle has been checked out. It can be concluded that all reactions are thermodynamically viable based on the values of the free energy.
2. A process flowsheet for the Cu-Cl cycle has been developed for hydrogen generation with a solar heat source.
3. Though the simulation results converged, operating conditions for the heat exchanger and reactors should be modified for better efficiency.
4. Based on thermodynamic analysis, the efficiency of the Cu-Cl cycle is 29% which is less than the efficiency calculated by the Chemical Engineering Division of ANL (41%).
5. More reliable efficiency values can be obtained after the chemistry model of the cycle is well defined.

A process analysis flowsheet has been developed by following the current experimental and simulation work done by ANL. Thermodynamic feasibility of the reactions involved in the Cu-Cl cycle has been determined using HSC Chemistry 5.11 Simulation models have been developed based on the experimental setup and data. Though one of the reactions is electrochemical, this cycle poses advantages over the S-I cycle because of its lower operating temperature (550°C). Efficiency has been found to be 29% for this cycle. The efficiency of this cycle calculated by ANL based on the thermodynamics is 41%. More reliable efficiency values can be obtained after the chemistry of the cycle is well defined. It is important to note that the energy required for compression and separation, and for any inefficiencies and irreversibilities, has not been included in the efficiency calculation. Nevertheless, the efficiency estimates indicate that further development is justified. Though the simulation model presented for this cycle is preliminary, it will be very helpful for producing insights for future improvement of this cycle. The cost analysis of Cu-Cl cycle has not been done. But it is very necessary to conduct cost analysis and estimation for the economic feasibility of the cycle. The external heat input must be matched to the chemical process such that high thermal efficiency is obtained, but not at the expense of sacrificing the operability of the combined plant. The matching must be done in a way that promotes operational stability of the chemical process. Significant research should continue to fully characterize cycles to realistically estimate cost and efficiency, demonstrate the feasibility of the processes to produce significant amounts of hydrogen, and understand tradeoffs between different thermochemical cycles.

REFERENCES

- [1] Ozturk, I.T.; Hammache, A.; Bilgen, E., An improved process for H₂SO₄ decomposition step of the sulfur-iodine cycle, *Energy Conversion Management*, 36 (1995), 11-21.
- [2] Brown, L.C.; Besenbruch, G. E.; Lentsch, R.D.; Schultz, K.R.; Funk, J. F.; Pickard, P.S.; Marshall, A.C.; Showalter, S.K., High efficiency generation of hydrogen fuels using nuclear power, Final Technical Report, August 1, 1999 through September 30, 2002, General Atomics Report GA – A24285 (2003).
- [3] Lewis, M. A.; Serban, M.; Basco, J., Kinetic study of the hydrogen and oxygen production reactions in the Copper-Chlorine Thermochemical Cycle, AIChE 2004 Spring National Meeting, New Orleans, LA, April 25-29, 2004.
- [4] Lewis, M. A.; Serban, M.; Basco, J., Hydrogen production at 550°C using a low temperature thermochemical cycle, Proceedings of the OECD/NEA Meeting, Argonne National Laboratory, 2003.
- [5] Carty, R. H.; Mazumder, M. M.; Schreiber, J. D.; Pangborn, J. B., Thermochemical Hydrogen Production, GRI-80-0023, Institute of Gas Technology, Chicago, IL 60616 (June, 1981).
- [6] Vilim, R.B. (Argonne National Laboratory); Miron, A.; Feldman, E.; Bauer, T.; Farmer, M., Nuclear-chemical plant for low temperature hydrogen co-production, Global 2003: Atoms for Prosperity: Updating Eisenhower's Global Vision for Nuclear Energy, Global 2003: Atoms for Prosperity: Updating Eisenhower's Global Vision for Nuclear Energy, 2003, p 676-680.
- [7] ASPEN PLUS 12.1 Help Documentation from ASPEN Tech.

This page intentionally left blank

DEVELOPMENT OF THE HYBRID SULFUR THERMOCHEMICAL CYCLE

William A. Summers and John L. Steimke
Savannah River National Laboratory, USA

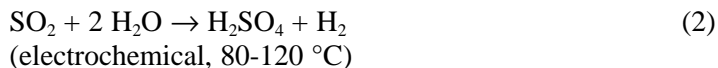
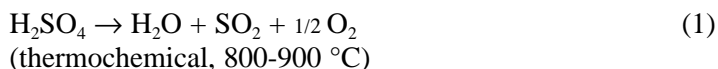
Abstract

The production of hydrogen via the thermochemical splitting of water is being considered as a primary means for utilising the heat from advanced nuclear reactors to provide fuel for a hydrogen economy. The Hybrid Sulfur (HyS) Process is one of the baseline candidates identified by the U.S. Department of Energy [1] for this purpose. The HyS Process is a two-step hybrid thermochemical cycle that only involves sulfur, oxygen and hydrogen compounds. Recent work has resulted in an improved process design with a calculated overall thermal efficiency (nuclear heat to hydrogen, higher heating value basis) approaching 50%. Economic analyses indicate that a nuclear hydrogen plant employing the HyS Process in conjunction with an advanced gas-cooled nuclear reactor system can produce hydrogen at competitive prices. Experimental work has begun on the sulfur dioxide depolarized electrolyzer, the major developmental component in the cycle. Proof-of-concept tests have established proton-exchange-membrane cells (a state-of-the-art technology) as a viable approach for conducting this reaction. This is expected to lead to more efficient and economical cell designs than were previously available. Considerable development and scale-up issues remain to be resolved, but the development of a viable commercial-scale HyS Process should be feasible in time to meet the commercialisation schedule for Generation IV gas-cooled nuclear reactors.

Introduction

U.S. President George W. Bush has established the Hydrogen Fuel Initiative to ensure the nation's long-term energy security and a clean environment. To this end, the U.S. Department of Energy (DOE) is exploring clean hydrogen production technologies using fossil, nuclear and renewable resources to revolutionize the way we power cars, homes and businesses. The DOE Office of Nuclear Energy, Science and Technology has established the Nuclear Hydrogen Initiative (NHI) to develop the technologies that can most effectively be coupled to next generation nuclear reactors for hydrogen production. The NHI R&D plan [2] identifies sulfur-based thermochemical cycles and high temperature steam electrolysis as the leading approaches. Thermochemical cycles produce hydrogen through a series of chemical reactions that result in the splitting of water, with all other chemical species regenerated and recycled within the process. Overall thermal efficiencies approaching 50% are possible for converting the heat from the nuclear reactor to hydrogen chemical energy (higher heating value basis) using thermochemical cycles.

The Hybrid Sulfur (HyS) Process is one of the two baseline thermochemical cycles identified for development in the NHI program. (The sulfur-iodine cycle is the other). HyS is an all-fluids, two-step hybrid thermochemical cycle, involving a single thermochemical reaction and a single electrochemical reaction. The chemical reactions are shown below:



The net result of the two reactions is the decomposition of water into hydrogen and oxygen. Since the chemistry involves only sulfur, oxygen and hydrogen compounds, many of the development issues associated with more complex thermochemical processes, such as cross-contamination and halide-induced stress corrosion cracking, are eliminated.

In recent years the sulfur-iodine thermochemical cycle has received considerable attention in development programmes in the United States, Japan, France and elsewhere [3,4]. The HyS Process, however, has seen little research since the early 1980s. The goals of the research programme at SRNL were to perform a conceptual design analysis of the process, identify major technical issues and challenges, and initiate development of the electrolyzer.

Background

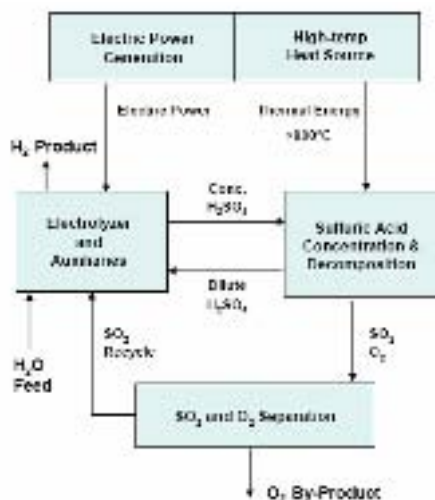
The Hybrid Sulfur Cycle, also known as the Westinghouse Sulfur Cycle or the Ispra Mark 11 Cycle, was originally proposed and investigated by Westinghouse Electric Corporation in the 1970s [5,6]. All basic chemistry steps were successfully demonstrated. By 1978, a closed-loop, integrated laboratory bench-scale model was successfully operated producing 120 liters (STP) of hydrogen per hour. Work continued on equipment design and optimisation, materials of construction, integration with a nuclear/solar heat source, process optimisation, and economics until 1983. However, the general decline of support for alternative energy programs, combined with reduced interest in developing either advanced nuclear reactors or high-temperature solar receivers, led to the termination of the work on this promising process.

All sulfur-based thermochemical cycles have a common oxygen-generating, high temperature step (Reaction 1). This is an equilibrium reaction, which is carried out over a catalyst at 800 to 900 °C. It is highly endothermic, and accounts for the primary input of high temperature heat. In the case of a nuclear hydrogen plant, this heat is supplied by a hot secondary helium stream that is heated in an intermediate heat exchanger by primary helium used to cool the nuclear reactor. In reality the acid decomposition process involves multiple processing steps, including preheating, acid concentration, acid vaporisation, acid dissociation, and sulfur trioxide decomposition. The processing environment is highly corrosive, requiring super alloys or non-metallic components. Considerable work is being done on the acid decomposition process in relationship to the sulfur-iodine process development, and this can be directly applied to the HyS cycle.

The unique aspect of the HyS Process is the use of an electrochemical step (Reaction 2) to convert sulfur dioxide back to sulfuric acid and to generate hydrogen. Sulfur dioxide is oxidized at the anode of an electrochemical cell, while protons are reduced at the cathode to produce hydrogen. The presence of sulfur dioxide depolarises the anode and reduces the reversible (theoretical minimum) voltage relative to that required for the direct dissociation of water into hydrogen and oxygen. Whereas at 25°C direct water dissociation by electrolysis requires a reversible cell voltage of 1.23 volts, the sulfur dioxide depolarised electrolyzer (SDE) requires a reversible voltage of only 0.17 volts per cell. Dissolving the SO₂ feed in 50 wt% sulfuric acid increases the reversible cell voltage to 0.29 volts [7]. Actual performance, including ohmic losses and reaction irreversibilities, is expected to be approximately 0.60 volts per cell. This is significantly less than the performance of commercial direct water electrolyzers that operate with 1.8 to 2.6 volts per cell [8]. Therefore, an SDE requires substantially less electricity than a conventional electrolyzer for the same hydrogen output. When combined with the endothermic decomposition of H₂SO₄, the net thermal efficiency for water-splitting by the HyS process is 30-50% higher than that for a process consisting of all electric production followed by direct water electrolysis, even when highly efficient gas-cooled nuclear reactors using a Brayton Cycle are used for electrical energy generation.

The current work by SRNL included the creation of high-efficiency process design for the HyS Process. A block flow schematic for the process is shown in Figure 1. Since HyS is a hybrid thermochemical cycle, energy input in the form of both electricity and thermal energy is required. For a commercial nuclear hydrogen plant, approximately 38% of the nuclear reactor thermal output would be directed to electricity production and 62% to provide process heat.

Figure 1. Hybrid Sulfur Process Block Schematic



Significant improvements were realized in several processing sections compared to previous work performed by Westinghouse Electric. A baseline plant thermal efficiency for a commercial nuclear hydrogen plant of 48.8% was calculated. The efficiency was based on the higher heating value (HHV) of the hydrogen product divided by the total thermal energy output of the nuclear reactor, including the thermal energy used to generate electricity and allowances for auxiliaries such as pumps, compressors and cooling towers. Higher thermal efficiencies, exceeding 50% HHV-basis, are deemed feasible for plants based on further optimised process flowsheets.

An economic analysis was performed to determine the projected cost of hydrogen from an integrated Nth-of-a-kind plant consisting of an advanced helium-cooled nuclear reactor and the HyS thermochemical process. The hydrogen production cost for the base case was \$1.60 per kilogram at the plant gate. The hydrogen production cost ranged from \$1.49 to \$1.77 per kilogram for low and high estimates for the capital cost of the electrolyser system, the major component with the greatest cost uncertainty. The inclusion of by-product credits for oxygen production lowered the baseline cost to \$1.31 per kilogram. Hydrogen costs at this level are very competitive with costs projected for other means of hydrogen production, including steam reforming of methane, coal gasification with CO₂ sequestration, and renewable energy processes. It is cautioned, however, that estimates for production costs can vary widely dependent on the underlying assumptions. A revised cost analysis using a recent standardized DOE approach to determining hydrogen costs is warranted. More discussion of the systems design and economic analysis performed for the HyS Process can be found in a recent technical paper on this subject [9]. The balance of the current paper will describe the development of the sulfur dioxide depolarised electrolyser and the experimental results.

Concept Definition

The key component in the HyS Process is the sulfur dioxide depolarized electrolyzer (SDE). In order for HyS to be a viable thermochemical cycle, the SDE must be efficient and cost effective. The process design and economic analyses discussed above indicate that an SDE should perform with a voltage of <600 mV per cell. The current density should be high in order to minimise the size and capital cost of the electrolyzer system. The final selection of operating current density will be a tradeoff between performance and capital cost and will be influenced by the cell's polarization characteristics (V vs. I) and the unit capital costs (\$ per square meter of active cell area). Initial estimates indicate that a current density of 500 mA/cm² with electrolyser operating conditions of 100°C and 20 bar will be required for commercial systems. The goal of the SRNL electrolyzer programme is to develop an SDE using PEM cell technology that satisfies these design requirements. PEM cell technology is being developed for automotive fuel cells and onsite hydrogen generators, and cost reductions and performance improvements developed for these applications are expected to lead to similar improvements for the HyS application.

Previous SDE development by Westinghouse Electric [10] utilised a two-compartment, flow-through parallel plate cell with a porous rubber diaphragm separating the reaction compartments. The half-cell reactions are as follows:



The anode reaction results in the greatest irreversibility, and Westinghouse tested various electrocatalysts, including palladium and platinum. The majority of research has employed platinum electrocatalyst, but this is an area of research that requires further investigation. The Westinghouse

cell utilised separate liquid streams fed to the anode and cathode compartments of the cell. The anolyte consisted of a solution of sulfuric acid, water and dissolved sulfur dioxide. The catholyte consisted of sulfuric acid and water. Sulfuric acid concentrations were similar in both streams and were varied between 30 and 70 wt%. The rubber diaphragm served to allow hydraulic communication between the two parallel flow channels. A slight positive pressure differential between the catholyte to the anolyte channels was imposed to minimise SO₂ crossover to the cathode, while still allowing the diffusion of hydrogen ions (protons) from the anode to the cathode.

The PEM cell design chosen for the current work employs a significantly different geometry than the Westinghouse cell. The PEM electrolyzer consists of a membrane electrode assembly (MEA) inserted between two flow fields. Behind each flow field is a back plate, copper current collector and stainless steel end plates. The MEA consists of a Nafion proton-exchange-membrane with catalyst-coated gas diffusion electrodes bonded on either side.

Experimental Procedure

Test Facility

A test facility for testing SO₂-depolarized electrolyzers was designed and constructed. The facility was located in a large chemical hood as shown in Figure 2. A 100 lb. cylinder of sulfur dioxide is shown on the left. To the right of it is the SO₂ Absorber. In the upper middle of the picture is the electrolyser cell. Below it is the anolyte flowmeter, and below that is the anolyte pump. Further to the right is the hydrogen collector. Air flow was maintained whenever hydrogen or sulfur dioxide was present in the hood. The hood was effective, no sulfur dioxide odor leaked out.

Figure 2. Electrolyzer Test Facility.



The cathode side of the electrolyser being tested was connected to the hydrogen handling side of the facility. For safety purposes, a pressure relief valve was connected to the hydrogen outlet of the electrolyser. There are two backpressure regulators. The first one controls the pressure in the sulfur dioxide absorber on the anode side of the cell. The absorber is used to dissolve sulfur dioxide gas in

either water or solutions of sulfuric acid and water to form anolyte. The absorber column is packed with Raschig Rings and operates in countercurrent operation; anolyte flows into the top and sulfur dioxide gas flows upward. Below the packed bed is a reservoir for approximately one liter of anolyte. An excess of sulfur dioxide gas was fed to the absorber, and the excess gas was vented. Anolyte is pumped out the bottom of the absorber, through a flowmeter, through the anolyte side of the electrolyser and back into the top of the absorber. All tubing, valves and connectors in the anolyte flow loop were made from fluorocarbon polymer (PTFE or PFA). The translucent tubing was useful in determining if lines were full of liquid or were passing a two-phase mixture. The second backpressure regulator controls the hydrogen pressure at the cathode side of the electrolyser. It is important to demonstrate the ability of the electrolyser to generate hydrogen at elevated pressures, since this will be required in commercial operation in order to reduce compressor requirements for hydrogen delivery. Downstream of the backpressure regulator is a three-way valve that can direct product hydrogen either directly to a vent or to the hydrogen collector for flow measurement. The inner cylinder of the hydrogen collection cylinder was made from glass; an outer cylinder made from acrylic protected the glass cylinder. Upstream of the hydrogen collector is a water collection chamber with a purge valve to allow capture and sampling of any condensate that might appear.

Electrolyzer Test Units

Two different SDE's were designed, procured and tested. The first electrolyser was based on a commercially available PEM water electrolyser manufactured by Proton Energy Systems, Inc. (PES) of Wallingford, CT. The commercial-type electrolyser was built with Hastelloy B and Teflon wetted parts, a PEM electrolyte, and porous titanium electrodes. It had an active cell area of 86 cm², and a Pt catalyst loading of 4 mg/cm². SRNL requested that the titanium electrodes be changed to carbon or other more corrosive-resistant material, but they were an integral part of the commercial design and could not be modified. During testing there was evidence of severe corrosion of the metal wetted parts of the electrolyzer due to the sulfuric acid environment of the SDE.

The second electrolyser was a research unit assembled for SRNL by the University of South Carolina (USC). It was constructed with platinised carbon cloth electrodes, a Nafion 115 PEM electrolyte, carbon paper flow fields, solid graphite back plates, copper current collectors and stainless steel end plates. The USC electrolyser had an active cell area of 40 cm² and a Pt catalyst loading of 0.5 mg/cm² (only one-eighth that of the commercial cell). The carbon-based configuration proved to be much more corrosive resistant than the commercial-type electrolyzer. A photograph of the two electrolyzer units is shown in Figure 3.

Figure 3. Photograph of the commercial-type PEM electrolyser on the left and the USC research electrolyser installed in the test facility on the right



Test Procedures

The following procedure was followed preceding each test. Any previous contents of the facility were drained. A liter of the desired acid solution was mixed in a bottle. A tube was attached to the acid feed valve and inserted into the bottle of acid solution. The pump was used to draw the acid into the absorber. The acid solution was circulated through the cell and absorber at flowrates ranging from 0.3 to 1.5 liters per minute and sulfur dioxide gas was passed through the absorber at 1 liter per minute. After about 20 minutes the sulfur dioxide flow was reduced to 0.5 liters per minute and current was passed through the cell. At the end of the day of testing, the cell was drained and both sides of the cell were flushed with deionised water. The cell was filled with deionised water for overnight and weekends.

The method for measuring hydrogen generation with the hydrogen collector was to displace water from an inverted cylinder positioned with its base in a shallow pool of water. This method is simple yet allows accurate measurement of low flow rates. The water temperature, hydrogen gage pressure in the inverted cylinder, and atmospheric pressure were measured to allow for volume correction. The inner cylinder of the hydrogen collection cylinder was made from glass, and an outer cylinder made from acrylic protected the glass cylinder and facilitated filling the inner cylinder with water between runs.

The power supply to the electrolyser was a Model 710 from The Electrosynthesis Company, Inc. of Lancaster NY. It was operated in constant current mode rather than in constant voltage mode. The maximum current and maximum voltage available was 50 amperes and 20 volts, respectively. In addition to current measurement provided by the power supply, a calibrated shunt was connected to the output to allow for independent measurement of current. Voltage taps independently connected to the cell electrodes were connected to the data acquisition system (DAS). The instrument signals from thermocouples, pressure gages, and flowmeters were connected to the DAS, which was comprised of a Dell computer with special acquisition boards and Labview software. Observations and some data were manually recorded in a laboratory notebook.

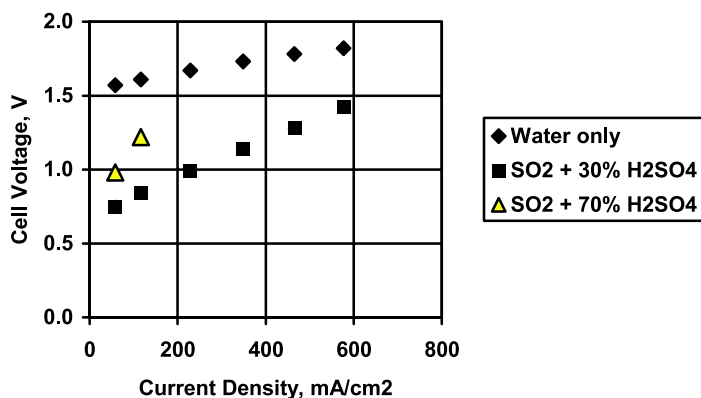
Results and Discussion

Plots of cell potential vs. current density, called polarization curves or Tafel plots, for the commercial-type electrolyzer are shown in Figure 4 for various anode feed conditions. Anolyte flowrate was 0.35 liters per minute; temperature was 20°C and pressure was 1.0 bar. For direct water electrolysis, the cell potential increased linearly from 1.57 volts at very low current density to 1.82 volts at nearly 600 mA/cm². Hydrogen production at the maximum current density was approximately 20 liters per hour. The minimum possible cell voltage is the reversible cell voltage for direct water electrolysis, which is 1.23 volts at 25°C. The excess voltage, which ranged from 0.3 to 0.6 volts, is the result of ohmic losses and various polarisations. When the cell was operated in the direct electrolysis mode (water feed only), the anolyte effluent contained a two-phase mixture of water and oxygen. When sulfur dioxide dissolved in sulfuric acid was used as the anolyte, a substantial drop in cell voltage was measured. This is the result of SO₂ depolarisation caused by the oxidation of SO₂ to H₂SO₄ at the anode in place of oxygen generation, which could be observed visibly by the absence of oxygen bubbles in the anolyte effluent.

At low current density of approximately 50 mA/cm², the cell voltage was 0.75 volts using 30 wt% acid. This increased to approximately 1.4 volts at near 600 mA/cm². These performance results were very encouraging, particularly for operation at room temperature and atmospheric pressure. However, during testing of the commercial-type electrolyser with sulfuric acid, a black liquor containing a very fine metal powder was observed. This was a result of corrosion of some of the metal components in the cell, including the titanium electrodes. Testing was then performed with 70 wt% sulfuric acid, which is

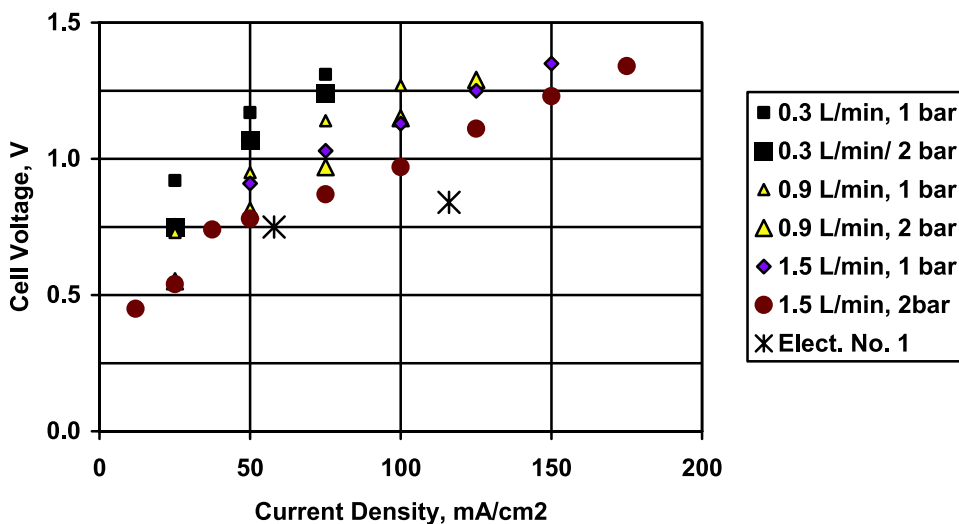
considerably more corrosive than 30 wt%. Cell potential at 50 mA/cm² was 0.98 volts and increased to 1.22 V at 116 mA/cm². Testing had to be discontinued after a short period due to excessive corrosion, including suspected loss of electrocatalyst and surface area. Unfortunately, the purchase agreement with the electrolyser supplier did not permit cell disassembly and post-test examination.

Figure 4. Polarisation Curve for Commercial-type PEM Electrolyser.



Test data for the research electrolyser provided by USC is shown in Figure 5. Tests were conducted with an anolyte feed consisting of 30 wt% sulfuric acid saturated with SO₂ at a pressure of 1 and 2 bar. The calculated concentration of SO₂ in the feed at the two pressures was 5 wt% and 10 wt%, respectively. The anolyte feedrate was varied from 0.3 to 1.5 liters per minute.

Figure 5. Polarisation data for USC Research Electrolyser



The second electrolyser achieved very good performance at low currents, with hydrogen generation occurring at a cell voltage of less than 0.5 volts at the lowest point. However, the performance indicated that the design suffered from high mass transfer resistance as evidenced by the improvement of performance with increases in anolyte flowrate. Furthermore, increasing the pressure, which increased the concentration of sulfur dioxide, had a measurable effect on reducing the voltage.

Under the highest anolyte flow and pressure conditions, the performance of the second electrolyzer was similar to that of the commercial-scale electrolyser at a modest current density

(approximately 0.75 V at 50 mA/cm²). However, the voltage of the second electrolyser increased more rapidly with increasing current. This could partially be a result of the much lower catalyst loading in the second electrolyser. A further explanation for this behavior is likely the hydraulic design of the cells. The commercial-type cell was designed for liquid water feed, and it had relatively low fluid flow resistance and good mass transfer characteristics. The second cell was a modified design originally based on gaseous reactants, and it had poor mass transfer characteristics when using liquid sulfuric acid feed with dissolved SO₂. Future work will focus on improved cell designs and operation at higher temperature and pressure. The membranes in both cells permitted the passage of some sulfur dioxide from the anode to the cathode, where it reacted with hydrogen gas to form elemental sulfur. However, the sulfur did not appear to poison the cathode electrocatalyst, and it was easily washed out of the cells. Future designs should eliminate or minimise SO₂ crossover, or should be designed to mitigate its effects on long-term cell performance.

Conclusions

Process design analysis and preliminary economic assessments indicate that the Hybrid Sulfur Process is a viable and attractive method for utilising high-temperature heat from an advanced nuclear reactor to produce hydrogen. The key processing step that determines both the efficiency and economics of the process is the production of hydrogen using sulfur dioxide depolarised electrolysis. Proof-of-concept testing has shown that modern proton-exchange-membrane electrochemical cell designs can be utilised to conduct this reaction. Further research and cell development are necessary to establish the cell performance at commercial operating conditions and to minimize the formation of sulfur caused by diffusion through the membrane. In order to demonstrate the complete Hybrid Sulfur cycle, an integrated, closed-loop laboratory model should be constructed consisting of both the electrolyser subsystem and the sulfuric acid decomposition section.

Acknowledgements

This work was performed by the Savannah River National Laboratory under U.S. Department of Energy Contract No. DE-AC09-96SR18500. Funding was provided by the DOE Office of Nuclear Energy, Science and Technology under the Nuclear Hydrogen Initiative, Work Package SR15TC21. Mr. David Henderson was the technical programme monitor. His support and guidance are acknowledged and greatly appreciated.

REFERENCES

- [1] U.S. Department of Energy Office of Nuclear Energy, Science and Technology, "Nuclear Hydrogen R&D Plan", March, 2004. <http://nuclear.gov/hydrogen/RandDPlan.pdf>
- [2] Ibid.
- [3] Denis Doizi *et al.*, "Hydrogen Production by the Iodine-Sulphur Thermochemical Cycles: Partial Pressure Measurements", Transactions of American Nuclear Society 2005 Annual Meeting, Volume 92, San Diego, California, June 5-9, 2005.
- [4] Shinji K. *et al.*, R&D on Water Splitting IS Process for Hydrogen Production Using HTGR at JAERI, AIChE Spring National Meeting, April 25-29, 2004, New Orleans.
- [5] G.H. Farbman, "The conceptual design of an integrated nuclear-hydrogen production plant using the sulfur cycle water decomposition system", NASA Contractor Report, NASA-CR-134976, Washington, D.C., April, 1976.
- [6] Gerald H. Parker, "Solar thermal hydrogen production process", Final Report, December, 1982, to US DOE, DOE/ET/20608-1, Westinghouse Electric Corp., Pittsburgh, Pennsylvania, January 21, 1983.
- [7] Lu, P.W.T., and; R.L. Ammon, "An Investigation of Electrode Materials for the Anodic Oxidation of Sulfur Dioxide in Concentrated Sulfuric Acid," J. Electrochem. Soc.: Electrochemical Science and Technology, Vol. 127, No. 12, pp. 2610-2616, December, 1980.
- [8] Jacqueline I.Kroschwitz (executive editor), Kirk-Othmer, Encyclopedia of Chemical Technology, Fourth Edition, John Wiley and Sons, New York, NY, c1991-c1998.
- [9] William A. Summers *et al.*, "The Hybrid Sulfur Cycle for Nuclear Hydrogen Production," Proceedings of GLOBAL 2005 , Paper 097, Tsukuba, Japan, October 9013, 2005 (in progress).
- [10] Peter W.T. Lu, "Technological Aspects of Sulfur Dioxide Depolarized Electrolysis for Hydrogen Production", *Int. J. Hydrogen Energy* **1983**, 8, 773-781.

THE SULFUR-IODINE AND OTHERS THERMOCHEMICAL PROCESSES STUDIES AT CEA

Pascal Anzieu, Philippe Carles, Alain Le Duigou, Xavier Vitart, Florent Lemort
Commissariat à l'énergie atomique, France

Abstract

The thermochemical Sulphur-Iodine process is studied by CEA with the objective of massive Hydrogen production using the heat at high temperature coming from a very high temperature reactor. A two folds programme was set up in 2000. The main part is devoted to the study of the basic process, including optimisation of a detailed flow-sheet using existing knowledge from literature, thermodynamics measurements of each section of the process and studies for a hydrogen production plant. Several devices are currently under test phase to get precise measurements of the Bunsen section and the HI distillation liquid vapour equilibrium. Measurements techniques have been prepared to obtain data under pressure and temperature values outside the existing domain. In parallel, an operating flow-sheet was studied that gives the best efficiency one could obtain today when building a loop using either a reactive or a direct distillation, i.e. 35%. From the analysis of those flow-sheets, an innovative programme was derived that could lead to raising the efficiency up to 50%. This program includes membranes studies, process operating point optimisation (by reducing water and iodine quantity, and by optimising temperature and pressure in each device of the flow-sheet).

In parallel, international collaborations are used to develop laboratory loops to get experience from materials and components, and to verify the existence of limited side reactions and of limited re-circulating products. A Bunsen section is under construction in CEA/Marcoule to be coupled later on to two other sections, sulphuric decomposer and HI distillation, built in the US by SNL and GA respectively, thanks to an International NERI contract.

On the other hand, several cycles are presented with a first set of analysis: the hybrid Sulphur cycle, the UT_3 cycle and Cerium-Chloride cycle.

Introduction

The thermochemical Sulphur-Iodine process is being studied by the CEA, the French Atomic Energy Authority, with the objective of massive hydrogen production using high-temperature heat from a very high temperature reactor. A two-fold programme was set up in 2000. The main part is devoted to the study of the basic process, including optimisation of a detailed flow-sheet using existing knowledge from literature, thermodynamics measurements of each section of the process and studies for a hydrogen production plant. In parallel, operating flow-sheets was studied that gives the best efficiency one could obtain today when building a loop. From the analysis of those flow-sheets, an innovative programme was derived that could lead to raising the future efficiency. This programme includes membranes studies and process optimisation.

Besides the two main streams of the CEA programme, S/I cycle and HTE studies and development, a limited programme considers alternative cycle that could backup these two if optimization fails. In a first part, a methodology is being studied, that can be applied to each process and could lead to a more standardise comparison of advantages and disadvantages. Another point concerns economic evaluation of the cycles that is not reported here. Finally, several cycles are presented with a first set of analysis.

Technical issues

The Bunsen section (section I)

The Bunsen reaction involves an excess of both water, to make the reaction spontaneous, and iodine, to induce the phase separation which is a key point of the process. However, such excesses are quite unfavourable for the following HIX section (as will be described below). Hence, research and development efforts are devoted to find new operation points for the Bunsen reaction with lower amounts of I_2 and H_2O , in order to find the best compromise between completion of reaction, phase separation, limitation of side reactions and energy loss in this low temperature exothermic step [1].

The experimental study of the Bunsen reaction which is currently underway at the CEA has required the development of analytical methods to allow a quantitative determination of the total amount of H^+ ions by potentiometry, Sulphur by ICP-AES, iodine by UV-visible spectro-photometry after iodine reduction, and total water by density, in each phase. Specific devices have also been designed (Figure 1), ranging from simple glass devices to develop the analytical methods to a tantalum pressure vessel allowing studying the Bunsen reaction in actual process conditions, including the possibility of varying the SO_2 pressure.

Figure 1. Glass device for the study of the Bunsen reaction

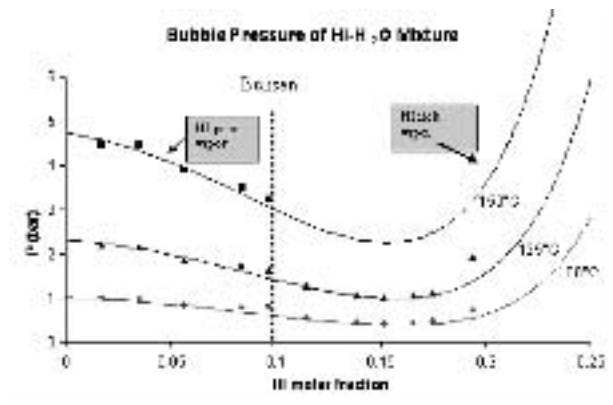


The HIx section (section III)

In the S-I cycle, HI decomposition must be achieved from the HIx mixture produced during the Bunsen reaction described above. Four main difficulties have to be overcome:

- the extraction of HI from the HIx mixture is difficult because of the presence of an azeotrope (Figure 2) in the mixture, which prevents simple distillation;
- the extraction of HI from the HIx mixture requires very large heat exchanges, due to the large heat capacity induced by the high water content of the mixture;
- the decomposition reaction is slow and incomplete.

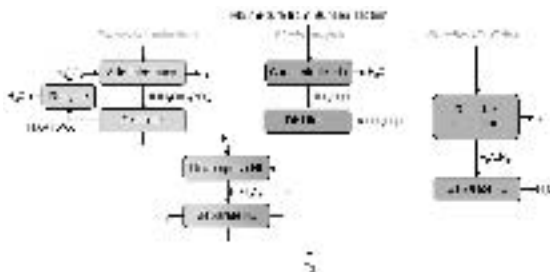
Figure 2. Azeotropic lines of HIx mixture



Three main options are currently being considered for the HI section (Figure 3):

- Extractive distillation was proposed by General Atomics [2]: the introduction of phosphoric acid induces first the separation of iodine, and then allows simple distillation of HI. HI is then decomposed in gaseous (or possibly liquid) phase around 450°C to yield H₂, which has to be separated from the gaseous mixture using membranes.
- The present Japanese scheme favours electro dialysis [3], which removes some water of the HIx mixture to concentrate it beyond the azeotropic limit. Excess HI is then removed by simple distillation. The final decomposition and extraction steps are the same as in the extractive distillation process.
- Reactive distillation was proposed in the 1980s by RWTH Aachen [4]. HIx distillation and HI decomposition are performed in the same reactor at 350°C. A liquid-gas equilibrium is obtained in the middle of the column, I₂ is solubilised in the lower liquid phase and a mixture of gaseous H₂ and water is recovered at the top of the column.

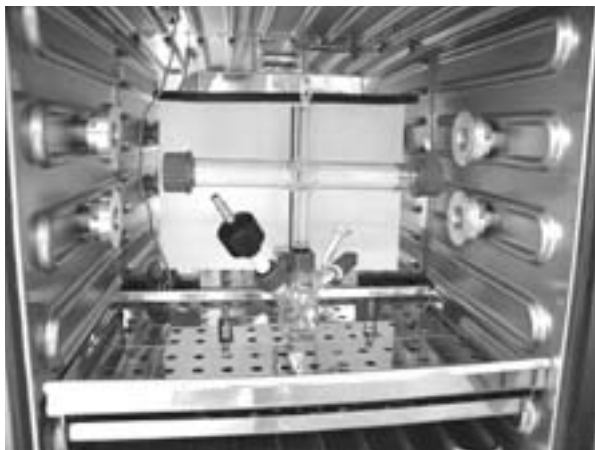
Figure 3. Schematic representation of the main options for the HI section



Apart from the membranes required for H_2 separation in the extractive distillation and electro dialysis schemes, membranes could be used at other places in the cycle. In particular, pervaporation membranes [5] could allow removing water from the HIx mixture, thus providing a low energetic cost alternative to bypass the azeotrope.

Reactive distillation is the reference scheme chosen by the CEA [6]. However, the amount of hydrogen produced during the process depends closely on the I_2 and HI concentrations in the vapour, which means that the correct evaluation of the actual efficiency of reactive distillation requires the knowledge of liquid-vapour equilibrium data for the HIx mixture. The model currently used to represent this equilibrium is based on total pressure measurements performed at RWTH Aachen, and CEA has launched a program to measure the relevant partial pressures under process conditions (up to $300^\circ C$ and 5 MPa). Like for the Bunsen section, this programme involves specifically designed experimental devices (Figure 4) as well as the development of suitable analytical methods. In particular, we have developed optical diagnostics (FTIR spectrometry, UV-visible spectrophotometry, Spontaneous Raman Scattering) to measure the composition of the vapour phase in the very concentrated conditions encountered in the process.

Figure 4. Device for the study of partial pressures around $120^\circ C$



The Sulphuric acid section (section II)

This section appears to be the best known one of the cycle, because of the experience gained in the sulphuric acid industry. In the proposed flow-sheet [6], sulphuric acid is concentrated through a series of flashes starting from low pressure. It is then dehydrated, before SO_3 is decomposed into SO_2 . This decomposition being only partial, non decomposed SO_3 is recombined with water, which allows to recovering its heat content.

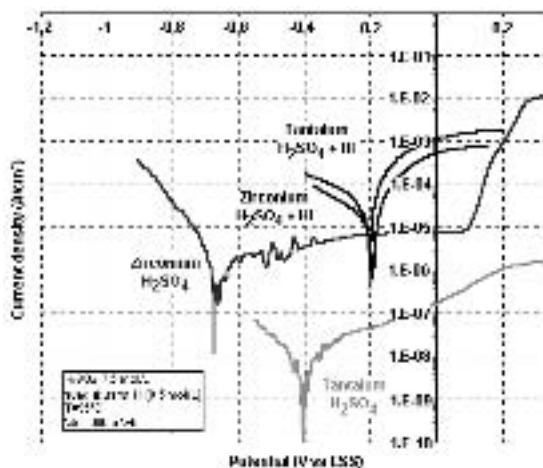
The main remaining questions concern the high temperature step of the process, namely SO_3 into SO_2 decomposition. The reaction, which requires a temperature in the 870°C range, will take place in a reactor and use the heat from a VHTR. This reactor will therefore also be a very high temperature heat exchanger, which will raise technological issues. Furthermore, a low pressure will be sought on the reaction side, whereas the heat transfer fluid will more likely be at high pressure. Finally, the temperature provided by a VHTR is not high enough to avoid the use of a catalyst for the reaction, and the long term resistance of this catalyst under the severe conditions that prevail will have to be ensured.

Corrosion of materials

The Sulphur-Iodine cycle is very demanding on materials, which are exposed to very corrosive species at elevated temperatures and pressures.

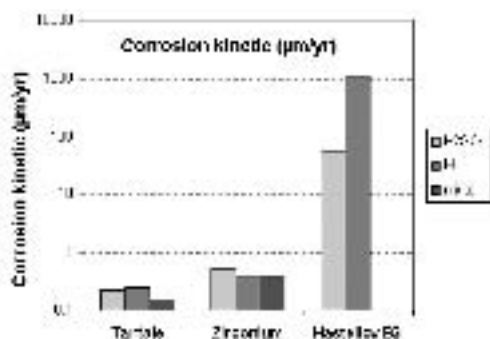
A literature review was conducted, which provided some materials as candidates for the section I (Bunsen) of the process: ceramics (SiC , Si_3N_4 , Al_2O_3), glass, fluorocarbons, Tantalum and Zirconium or Ni alloys. However, corrosion tests are necessary to assess the maximum temperature and acidity acceptable conditions, the long term behaviour and the corrosion mechanisms.

Figure 5. Electrochemical tests on metallic materials



As a first step, electrochemical and dipping tests have been conducted in each acid produced by the Bunsen-reaction (aqueous sulphuric acid and a mixture of hydriodic acid, iodine and water named HIx), up to 95°C , so that first operating ranges are given for the candidate materials. Immersion tests performed in separate acids up to 140°C showed that Tantalum and Zirconium seem to be the most metallic relevant materials; nevertheless localized corrosion has been observed on Zirconium in liquid Bunsen condition ($\text{H}_2\text{SO}_4\text{-HI-I}_2$ 10wt%-10wt%-70wt%), (Figures 5 and 6).

Figure 6. Corrosion rates of metallic materials



The next step will be the study the long term behaviour of selected materials in separate and both acids, under the standard temperature and pressure conditions given by the flow-sheet of the process, in a pressurised reactor.

Flow-sheet evaluation

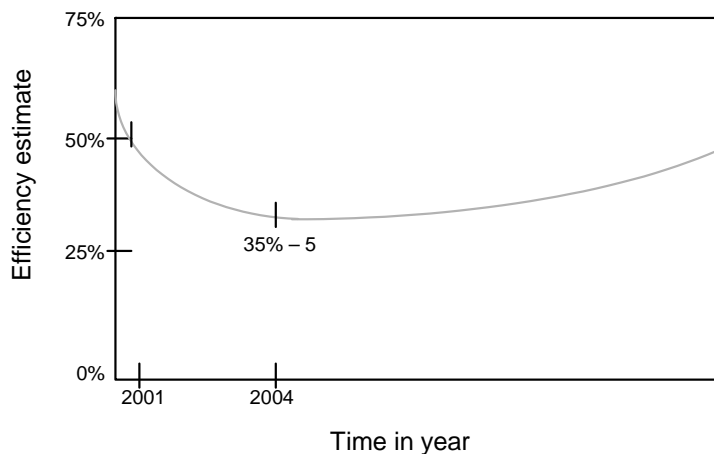
Another important fact is to describe the flow-sheet of the process to derive with sufficient accuracy the efficiency that remains the main criteria for the process evaluation. Obviously, we need to describe in detail each part of the process, including the various types of losses that can reduce the efficiency.

Several sub-sections are needed by the decomposition of a global reaction into several steps. For instance the sulphuric acid decomposition needs at least two or three steps, the first one to eliminate most of the water, the last one to crack the SO₃. So you have to look precisely at the way you want to operate, and for instance to introduce a re-circulation circuit and separate chemical reactors. Technology means are essential as they represent an actual part of the losses. Sometimes a component should not be feasible, for instance a compressor at high temperature or a heat exchanger with no temperature pinch. The way by which heat transfers and conveyance can be organized is dependent of the technology and also of the spatial organisation of the process.

One can illustrate the scientific approach generally used in process evaluation by drawing a curve giving the estimated efficiency versus time spent for research. In a first step, expert and manager judgments are used to enhance the ability of the process on a rough thermodynamic basis. The estimated efficiency is high. As a second step, a provisional flow-sheet is drawn and first thermodynamic calculations give a more realistic view based on existing or extrapolated data from literature. Some difficulties are arising, but there is no way to quantify them. Efficiency is decreasing. The third step needs more effort. It includes a first set of research. Detailed operational flow-sheets are presented based on the one hand on known technology and on the other hand on detailed calculation including some kinetics features. New experimental data become available. Process losses are accounted for. Laboratory scale experiments for the global process are scheduled and designed. Efficiency is low but realistic. Next step is carrying out a R&D programme in order to increase the efficiency and overcoming the difficulties encountered before. This is the longer step.

The example of the Sulphur-Iodine process studies is illustrated on Figure 7 based mainly on the work done at CEA and together with SNL and GA in the US, in the framework of an International NERI contract. For the last step, not yet achieved, several tracks are yet identified as described above in this paper.

Figure 7. Estimated efficiency of a Hydrogen production process as a function of time spent in research. The case of the S/I process



This curve shows that efficiency evaluation involves several steps so that to compare various processes among them, one needs to know the step he reached, that is depending on the level of knowledge he has got on the process. For that purpose, we try to identify clearly the various steps and to fix some data that could be used in each of them. For instance step 1 is based only on thermodynamics evaluation. Step 2 deals with reversible heat and work requirement calculations of the reactions, giving an upper bound of the efficiency. Step 3 needs detailed flow-sheet calculations including components efficiencies such as pumps, compressors and heat exchangers pinch. In this later step, we propose to set up a list of standard parameters to be used in the calculation. For instance the pinch for a gas-gas heat exchanger could be set to 50°C as a reference; the heat coming from the reactor is at 950°C, and so on. This work is underway in collaboration with ANL in the US.

Alternative cycles evaluation

Other cycles working at a temperature compatible with the use of a nuclear reactor, that is to say less than 1 000°C, are currently under evaluation at CEA.

The UT_3 cycle from Tokyo University with Calcium Bromide has been studied including some experiments on basic reactions. It was shown that the transformation of CaBr_2 in CaO was largely unfinished around 750°C with a bulk solidification. The transformation of FeBr_2 in Fe_3O_4 was not effective with preferably the formation of Fe_2O_3 (in a range of 600 to 700°C) which modifies considerably the cycle. Also was noticed the azeotropic mixture H_2O - HBr at 47% HBr and the eutectic CaBr - CaO above 700°C. Finally, the MASCOT pilot experiment conducted in 1980 was considered too complex, far from an easy to ride process, especially due to the rapid ageing of the compounds and the formation of clusters. Knowing that Bromide is a toxic compound, this cycle has been given up.

The Sulphate cycle using a metal M (M = Fe, Ni, Co or Mn) has been evaluated on a theoretical basis. Tests are underway to verify the efficiency of the elementary reactions and the presence of side reactions. The process needs to transfer solids from one reaction to another, which is not easy generally speaking.

Concerning the Cerium Chloride cycle, a first flow-sheet has been issued and separate reactions were experimentally tested. Two of them indicated a correct behaviour with a good kinetics. Work is ongoing to achieve the experiment and to derive data for flow-sheet calculations.

The hybrid Sulphur cycle is the one that benefits from the most important program of evaluation, due to its synergy with the Sulphur-Iodine cycle on the sulphuric acid decomposition and the potential simplification that it introduces in the full process suppressing the Iodine utilisation. A first flow-sheet has been issued and calculations associated to this flow-sheet gives 35% efficiency at least but with some hypothesis on the electrolysis part. Work is underway to achieve a detailed flow-sheet at the same level of knowledge than the one used on the S/I process. Specific tests on the $\text{SO}_2+\text{H}_2\text{O}$ electrolysis are scheduled to determine the operating voltage and to test various combinations of anodic, cathodic and electrolytic materials in order to enhance the efficiency.

Conclusion

Thermochemical cycles, and in particular the Sulphur-Iodine cycle, have been the subject of renewed intense interest in the last years. The accurate evaluation of their industrial potential is difficult, as it involves many aspects, from scientific questions such as the knowledge of thermodynamic data to safety, acceptability and economic assessments.

In particular, as the Sulphur-Iodine cycle is investigated worldwide, the problems that have to be solved appear more and more clearly. However, the basic advantages of this cycle remain valid:

- it only involves the handling of fluids;
- it is purely thermochemical, which is associated with low electricity need and therefore high potential efficiency;
- its coupling to a VHTR seems promising.

The CEA has launched an integrated program to choose by 2008 the most promising way to produce hydrogen using the high temperature heat available from a VHTR. In order to develop its own expertise on thermochemical cycles assessment, the CEA has chosen to develop a scientific approach based on data acquisition (development of devoted devices and specific analytical methods) and modelling (physical models, flow-sheet analysis, systemic approach). This approach comprises:

- Development of a methodology for process comparison.
- Acquisition of basic thermodynamic data.
- Flow-sheet analysis and development.
- Pre-conceptual design of a hydrogen production plant coupled to a VHTR, including energy distribution and safety issues.
- Efficiency and cost analysis based on the previous items.

The CEA has chosen to concentrate on a limited number of processes, namely the Sulphur-Iodine cycle and high temperature electrolysis, with the hybrid Sulphur cycle as a back-up, cycles that have been selected as being the most promising. Experience gained on the evaluation of these options is built on to perform a more theoretical assessment of other potentially interesting cycles.

REFERENCES

- [1] X. Vitart *et al.*, “Investigation of the IS cycle for massive hydrogen production”, ANL Symposium, Argonne (2004).
- [2] G.E. Besenbruch *et al.*, GA-A18257 report (1982).
- [3] Y. Miyamoto *et al.*, “R&D Program on Hydrogen Production System with High Temperature Cooled Reactor”, in: Proc. Int. Hydrogen Energy Forum 2000, Munich, Germany; 2:271-8 (2000).
- [4] M. Roth and K.F. Knoche, “Thermochemical water splitting through direct HI decomposition from H₂O–HI I₂ solutions”, Int. J. Hydrogen Energy 14:545-9 (1989).
- [5] R.H. Elder, J.M. Borgard, G.H. Priestman, B.C.R. Ewan, R.W.K. Allen, “Use of Membranes and Reactive Distillation for the Separation of HIx in the Sulphur-Iodine Cycle”, Proc. AIChE 2005 Annual Meeting (to be published).
- [6] S. Goldstein, J.M. Borgard and X. Vitart, “Upper bound and best estimate of the efficiency of the iodine sulfur cycle”, Int. J. Hydrogen Energy, 30:619-626 (2005).

This page intentionally left blank

A STUDY ON HYDROGEN PRODUCTION BY THERMOCHEMICAL WATER-SPLITTING IS (IODINE-SULFUR) PROCESS

**Ki-Kwang-BAE, Kyung-Soo KANG, Sung-Dae HONG, Chu-Sik PARK, Chang-Hee KIM,
Sang-Ho LEE and Gab-Jin HWANG**

Hydrogen Production Research Center, Korea Institute of Energy Research, Korea

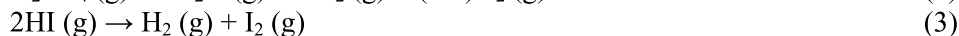
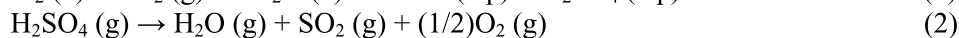
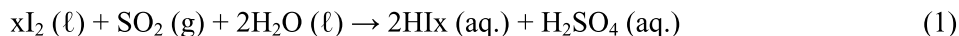
Abstract

Thermochemical water-splitting IS(iodine-sulfur) process produces the hydrogen from water using high temperature nuclear heat supplied by VHTR (very high temperature gas-cooled reactor). In KIER, a study on IS process was started at last year in association with KAERI (Korea Atomic Energy Research Institute) and KIST (Korea Institute of Science and Technology). Bunsen reaction, HI decomposition reaction and closed-loop cycle operation is carrying out in KIER. This paper presents a concept of the experiments conducting in KIER.

Introduction

Hydrogen is an attractive fuel for the future because it is renewable as an energy resource and also flexible as an energy carrier. One of the promising methods for large-scale hydrogen production is thermochemical water-splitting using heat energy from nuclear, solar sources and so on. IS (Iodine-Sulfur) process [1] have been investigating for the thermochemical hydrogen production processes using heat energy from nuclear.

In KIER (Korea Institute of Energy Research), IS process which was first proposed by General Atomic Co. [2] and laboratory scale closed-loop operated in JAERI (Japan Atomic Energy Research Institute) [1,3], is under investigation with KAERI (Korea Atomic Energy Research Institute) and KIST (Korea Institute of Science and Technology). IS cycle is composed of the following reactions:



The so-called Bunsen reaction (1) is an exothermic SO_2 gas absorbing reaction, which proceeds spontaneously in the temperature range of 20-100°C. Sulfuric acid (H_2SO_4) decomposition reaction (2) is an endothermic reaction, which proceeds in two stages, i.e. gaseous H_2SO_4 decomposes spontaneously into H_2O and SO_3 at 400-500°C, and then SO_3 decomposes into SO_2 and O_2 at about 800°C in the presence of a solid catalyst. Hydrogen iodide (HI) decomposition reaction (3) can be carried out in the gas phase or in the liquid phase. The process has such attractive characteristics that all chemicals circulate in the process as fluid, H_2SO_4 decomposition proceeds stoichiometrically with high conversion ratio and large entropy change, temperature range of which is suitable for utilising the nuclear heat supplied by VHTR (very high temperature gas-cooled reactor). In HI decomposition reaction, hydrogen was produced by thermal decomposition of gaseous HI.

Bunsen reaction, HI decomposition reaction and closed-loop cycle operation are carrying out in KIER. H_2SO_4 decomposition reaction is carrying out in KIST

In KIER, the process was studied from 2004. Our first target is to demonstrate continuous hydrogen production using a small-scale apparatus (~ 20 ℓ/h) at atmosphere condition in 2006. Figures 1 and 2 show the schematic flowsheet of the small-scale apparatus and mass balance, respectively. After a successful demonstration using a small-scale apparatus, we will carry out the continuous hydrogen production using a laboratory scale apparatus (~ 1,000 ℓ/h) at pressure condition in 2007-2009.

This paper presents the outline of our state of the art. The R&D plan is also described.

State of the art

Bunsen reaction

In the Bunsen reaction, the product can be separated into a H_2SO_4 phase, the lighter phase, and a poly-hydriodic acid (HIx) phase, the heavier phase, in the form of a liquid phase in the liquid phase separator. Each of the phases, H_2SO_4 and HIx, are introduced into the H_2SO_4 decomposition and HI decomposition reaction, respectively. The decomposition reaction proceeds after a purification step at each decomposition section

To establish the closed-loop operation technology, the composition and the flow rate of the process solution maintain to be constant for the steady state operation. The separation properties of solution in the liquid phase separator to keep the constant composition and flow rate of the process solution. Sakurai *et al.* [4] was reported the effects of solution temperature and composition of initial solution in the liquid phase using HI-H₂SO₄-I₂ solution. They found that the separation properties were improved with the increase in iodine concentration. The control of the side reaction in the liquid phase separation of Bunsen reaction is also important to establish the closed-cycle operation technology.

It was measured the side reaction and effect of the I₂ concentration with an increase in temperature in the 2-liquid phase separation for a preliminary study [5].

Figure 3 shows the 2-liquid phase separation point and I₂ solidification point at each temperature using an initial molar ratio of H₂SO₄/HI/H₂O=1/2/14.

At each temperature, the 2-phase separation did not show in about 0.1 of I₂ molar fraction. I₂ solidification point was about 0.25, 0.25 and 0.35 of I₂ molar fraction at 298K, 313K and 333K, respectively. At 298K and 313K, I₂ saturation point was same, and that at 333K was increased. This means that I₂ solidification point did not dependent to temperature until 313K. The excess iodine exists in the solution as the state of solid phase, therefore, this solid iodine is supposed not to affect the separation properties. At 353K, I₂ solidification point was not shown. In the case of this solution mixture system, the mutual solubility of the H₂SO₄ and HIx phase solution is supposed to increase with an increase in the solution temperature. This result means that an increase in the I₂ saturation concentration combined with an increase in temperature can improve separation properties.

HI decomposition reaction

In HI decomposition reaction, hydrogen was produced by thermal decomposition of gaseous HI. HI is separated from HIx solution and then decomposed to produce hydrogen. The HIx solution (H₂O-HI-I₂ mixture) was produced in Bunsen reactor. Simple option to realise the chemical change was the distillation of HIx solution and the gas phase thermal decomposition of HI. However, the conventional distillation requires a lot of excess thermal burden because of the presence of an azeotropic composition in HI-H₂O system (the molal ratio of H₂O/HI is about 5). Also, the low equilibrium conversion of HI decomposition (ca 20% at 400°C) imposed a large amount of HI circulation within the process, which results in the increase of thermal burden [6].

To improve the HI processing scheme, there are two kinds application of membrane technology [7]. One is membrane reactor to enhance one pass conversion of equilibrium limited HI decomposition reaction in the gas phase using the hydrogen permselective membrane. The other is concern with the membrane application to enhance the HI molality of HI-I₂-H₂O mixture in order to facilitate the separation of pure HI. These second application is caused by the lack of capability to distill the HIx solution for the concentration HI more than 56%. To reach the HI concentration of 56% by conventional distillation, even consume a significant huge of heat, the distillation process would be decreased the over all thermal efficiency of the process.

In KIER, the system of electro-electrodialysis(EED)-distillation-membrane reactor employ in HI decomposition reaction. HI concentrates over 56% by EED from HIx solution, and more concentrate by distillation. Pure HI (include a little H₂O) gas come out from the bottom of distillation tower. Pure HI gas decomposes in membrane reactor and produce H₂. I₂ and non-decomposed HI gas go to the HI-I₂ recovery tower, and separated HI gas and I₂ gas. I₂ gas recycles to Bunsen reactor and HI gas recycles to vapor tank set the front to membrane reactor.

Figure 4 shows the H₂ and N₂ gas permeability in the membrane prepared by CVD (chemical vapour decomposition) using multi-membrane preparation apparatus.

In operation temperature of membrane reactor (450°C), the separation factor of H₂ to N₂ was 27 and hydrogen permeability was about 5x10⁻⁸ mol/Pa·m²·s. This membrane having the separation factor of H₂/N₂ of 27 will be had over the separation factor of H₂ to N₂ of 500 [8].

In the small-scale apparatus, the area of EED cell is about 600cm², and 13 numbers of membranes (membrane length, 15cm) pack in membrane reactor. Two membrane reactors will be connecting to a series.

Closed-loop operation for continuous hydrogen production

The small-scale apparatus will be built up in Oct. 2005. The apparatus was designed to produce hydrogen at the maximum rate of 20Nℓ/h, and is made of glass and Teflon. The operation will be carried out at atmosphere condition. A higher iodine concentration of HIx solution will be handled with an apparatus. The closed-loop operation technique for continuous hydrogen production will be developed using this apparatus. The experiments will start in November 2005.

R&D Plan

Figure 5 shows KIER's R&D plan for the IS process. Studies on the closed-loop operation technologies at atmosphere condition using the small-scale apparatus will be carried out until 2006. Studies on process improvement and collection of data in each reaction will be carried out until 2010 for the laboratory and pilot scale equipment that will demonstrate hydrogen production at the rate of 1,000Nℓ/h and 30~100Nm³/h, respectively.

Studies on the closed-loop operation technologies at pressure condition will be carried out until 2009 to acquire knowledge on process control and to establish the detailed process scheme required for the scale-up experiment.

The pilot-scale demonstration will represent the important part of engineering where the expected thermal efficiency of hydrogen production is higher than 45%, and will connect with He heating loop to acquire knowledge on connecting with VHTR.

The laboratory scale apparatus (reactors, separators, heat exchanger, line, pump etc.) will be fabricated using the materials selected.

ACKNOWLEDGEMENT

This work has been done under "Nuclear Hydrogen Production Technology Development and Demonstration(NHDD) Project" and we are grateful to MOST for financial help.

REFERENCES

- [1] Nakajima, H., Ikenoya, K., Onuki, K., and Shimizu, S., "Closed-cycle continuous hydrogen production test by thermochemical IS process", *Kagaku Kogaku Ronbunshu*, 24(2), 352-355, 1998.
- [2] Norman, J.H., Besenbruch, G.E., and O'keefe, D.R., "Thermochemical water-splitting for hydrogen production", GRI-80/0105, March, 1981.
- [3] Onuki, K., Nakajima, H., Kubo, S., Futakawa, M., Higashi, S., Hwang, Gab-Jin, Masaki, T., Ikenoya, K., Ishiyama, S., Akino, N., and Shimizu, S., "Thermochemical hydrogen production by iodine-sulfur cycle", *Proceedings, 14th World Hydrogen Energy Conference*, Montreal, Canada, 2002.
- [4] Sakurai, M., Nakajima, H., Onuki, K., and Shimizu, S., "Investigation of 2 liquid phase separation characteristics on the iodine-sulfur thermochemical hydrogen production process", *International Journal of Hydrogen Energy*, 25, 605-611, 2000.
- [5] Hwang, G.-J., Kim Y.-H., Park, C.S., LEE, S.-H., Kim, C.-H., and Bae, K.-K., "Bunsen reaction in IS (Iodine-sulfur) process for the thermochemical hydrogen production", *Proceedings, 18th International Hydrogen Energy Congress & Exhibition (IHEC2005)*, July 13-15, Istanbul, Turkey, 2005.
- [6] Hwang, G.-J., Onuki, K., Shimizu, S., and Ohya, H., "Hydrogen separation in H₂-H₂O-HI gaseous mixture using the silica membrane prepared by chemical vapor deposition", *Journal of Membrane Science*, 162, 83-90, 1999.
- [7] Hwang, G.-J., Onuki, K., Nomura, M., Kasahara, S., and Kim, J.-W., "Improvement of the thermochemical water-splitting IS(iodine-sulfur) process by electro-electrodialysis", *Journal of Membrane Science*, 220, 129-136, 2003.
- [8] Hwang, G.-J., Onuki, K., and Shimizu, S., "Separation of hydrogen from a H₂-H₂O-HI gaseous mixture using a silica membrane", *AIChE J.*, 14, 92-98, 2000.

Figure 1. Schematic flowsheet of the small-scale apparatus

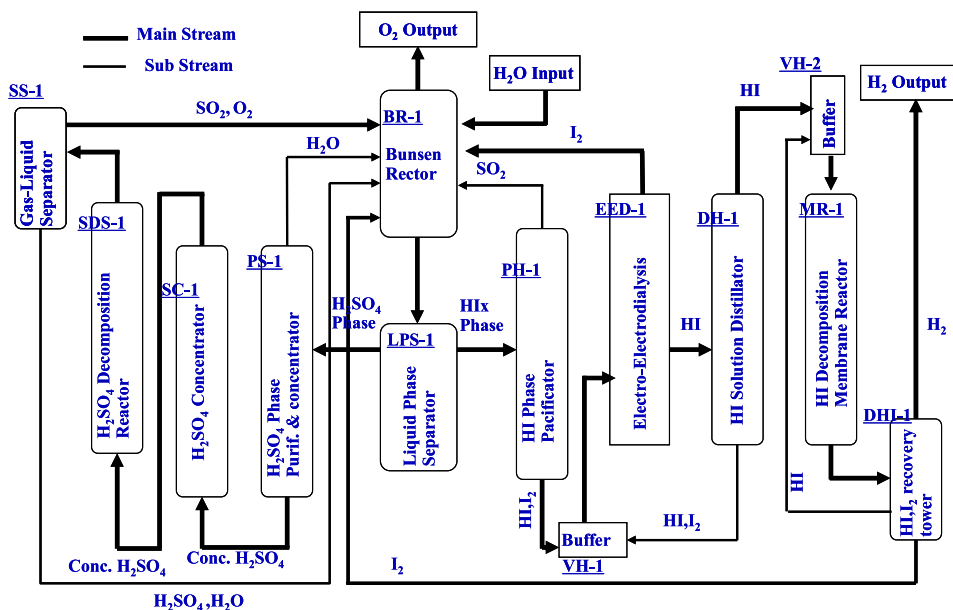


Figure 2. Mass balance of the small-scale apparatus

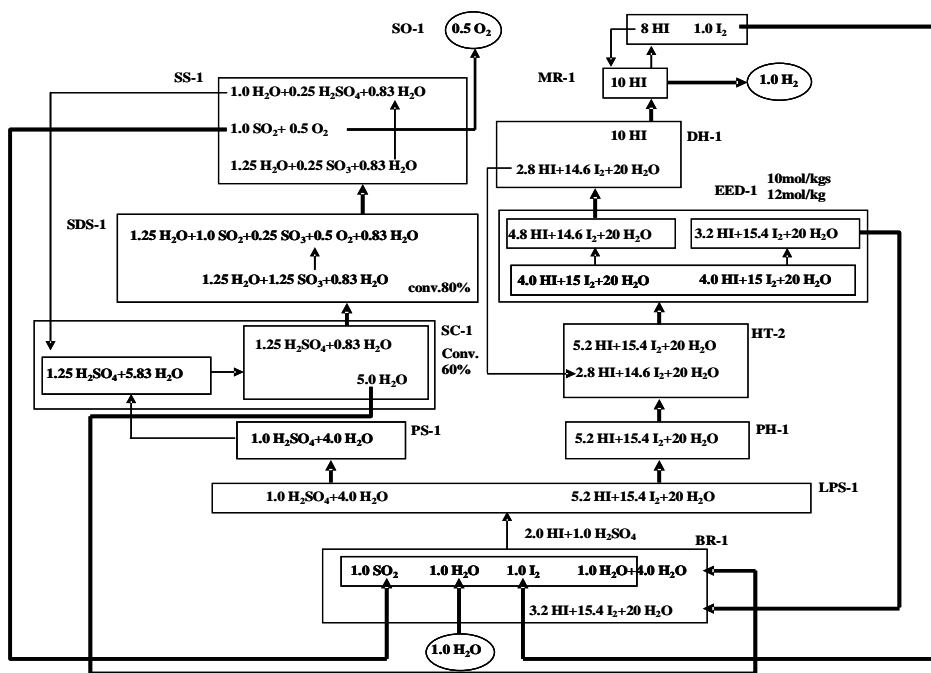


Figure 3. 2-liquid phase separation point and I₂ solidification point at each temperature using an initial molar ratio of H₂SO₄/HI/H₂O=1/2/14

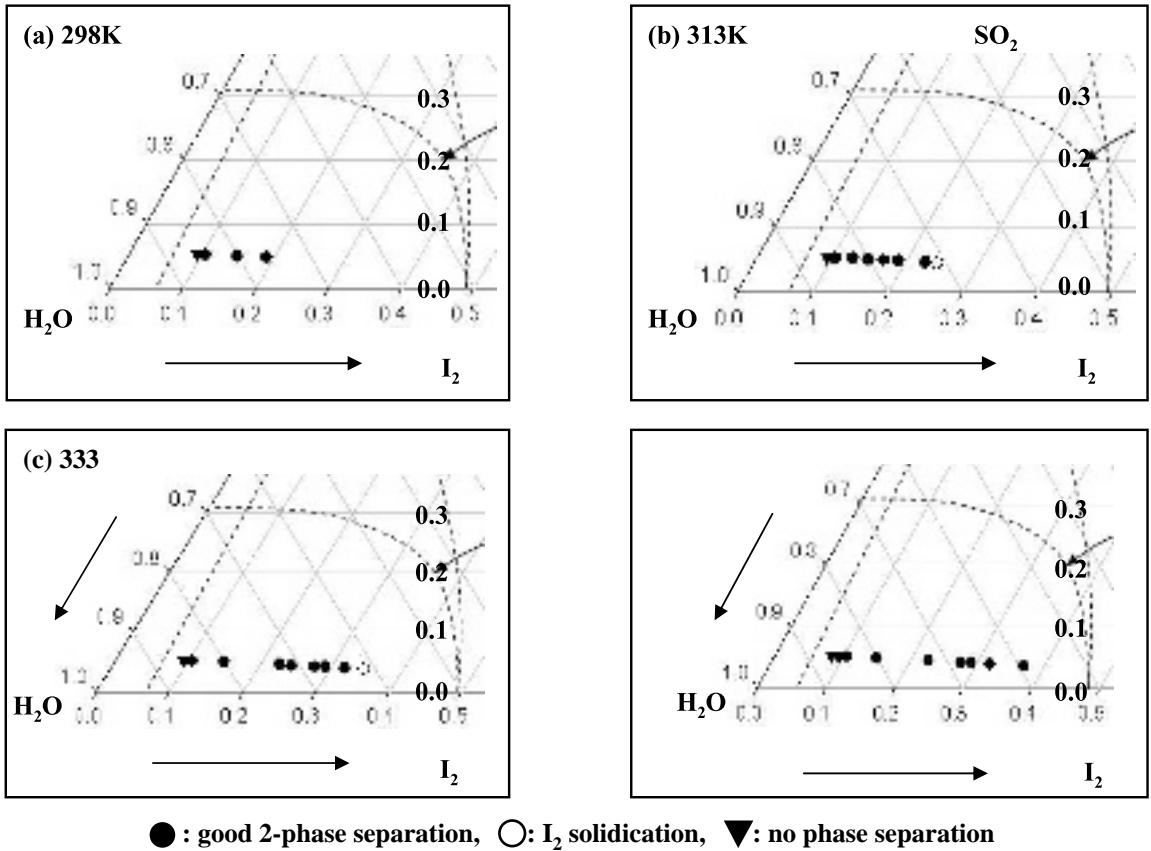


Figure 4. H₂ and N₂ gas permeability in the membrane prepared by CVD using multi-membrane preparation apparatus

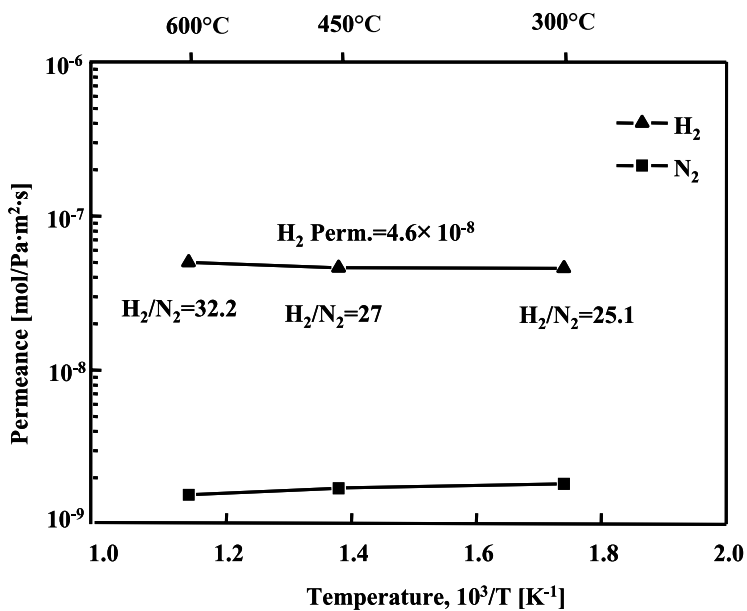
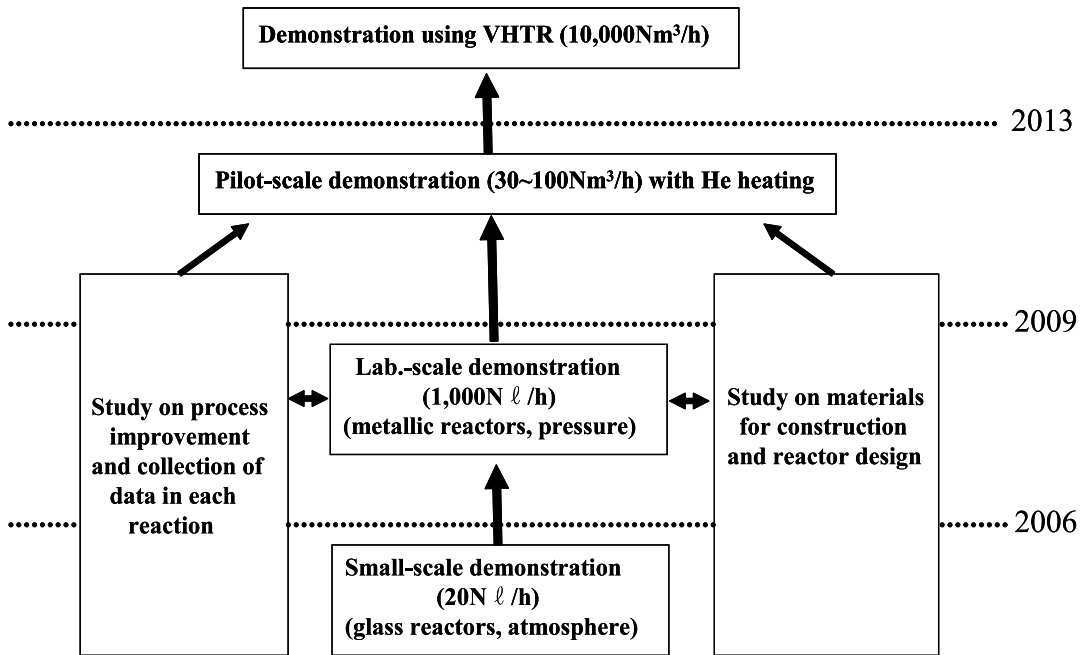


Figure 5. R&D plan of IS process at KIER



PRESENT RESEARCH STATUS AND DEVELOPMENT PLAN OF NUCLEAR HYDROGEN PRODUCTION PROGRAMME IN INET

Ping Zhang, Bo Yu, Lei Zhang, Jing Chen, Jingming Xu

Institute of Nuclear and New Energy Technology, Tsinghua University
Beijing, 10084, P.R.China

Abstract

At the institute of nuclear and new energy technology (INET) of Tsinghua University, P.R. China, a high temperature gas-cooled reactor, HTR-10, has been constructed and reached criticality, the relative research activities on nuclear hydrogen production were initiated since 2004. Thermochemical water splitting cycles based on metal oxides were developed, several metal oxides (such as copper ferrite, CuFe_2O_4 , and manganese ferrite, MnFe_2O_4) were prepared and the thermo-decomposition conditions to form the oxygen deficient oxides were investigated. The oxygen-deficient metal oxide was employed to split water at about 800°C and the feasibility of the thermochemical cycle was demonstrated. In addition, research works on the other two promising techniques of hydrogen production using nuclear heat, i.e., iodine-sulfur process and high temperature steam electrolysis, were also started at INET, and the R&D plan of the of the nuclear hydrogen production programme was presented.

Introduction

The utilisation of fossil fuel for energy generates enormous amounts of CO₂ emission, which was considered to be responsible for global warming. While trying to take effective measures to decrease the threaten to environment caused by consumption of fossil fuel, people are making efforts to seek new energy resources having potentiality to replace fossil fuel.

Hydrogen could become an important and potential option for a sustainable energy system as it can be use to meet most energy needs without harming the environment. In fact, hydrogen has the potential for contributing to the reduction of CO₂ emission and other air pollutants as it exhibits clean combustion with no sulphur oxide emissions. However, widespread use of hydrogen is not feasible currently because of economic and technological difficulties. One of them is to produce hydrogen massively with clean, economic and sustainable way.

Hydrogen can be produced by splitting water into hydrogen and oxygen by way of electrolysis or by stripping the carbon atom from fossil fuel or biomass sources (such as steam methane reforming (SMR), partial oxidation of oil, pyrolysis of coal or biomass, or gasification of coal and biomass, etc.). Presently, global hydrogen production is dominated by SMR followed by electrolysis [1]. The former is a CO₂ emission process in which both the feedstock and process heat source are CO₂ emitters. The latter is a expensive way of hydrogen production; besides, most of the electricity generating process are associated with CO₂ emission. Therefore, the current hydrogen production ways can not meet the demands of hydrogen economy.

Hydrogen production by thermochemical water-splitting can achieve the decomposition of water into hydrogen and oxygen using only heat with the temperature much lower than that of direct water splitting [2]. If the heat is supplied by a nuclear reactor, the whole hydrogen production process could meet the goal of low or no CO₂ emission.

In the institute of nuclear and new energy technology (INET) of Tsinghua University, CHINA, a high temperature gas cooled reactor, HTR-10, has been constructed and reached criticality in 2000. In 2003, the full power operation test was successfully made. Besides electricity generating, HTR-10 can provide process heat with various temperatures up to 900°C, which is promising to couple with some thermochemical water-splitting processes as well as high temperature steam electrolysis technique. As an important application of high temperature heat,, the nuclear hydrogen programme was initiated since 2004. In this paper, the present status of the programme, mainly on development of 2-step metal oxide water-splitting cycle, was presented. In addition, the R&D plan of nuclear hydrogen program of the next five years was briefly introduced.

I. Hydrogen production with two-step water splitting of CuFe₂O₄

The two-step water splitting cycle using metal oxide for hydrogen production has been extensively studied [3,4]. The process consists of two steps: in the decomposition step, oxidised metal oxide (MO_{ox}) is thermally reduced with oxygen releasing, forming the reduced metal oxide (MO_{red}); in the hydrogen production step, MO_{red} reacts with H₂O to generate hydrogen and restore the original MO_{red}. By repeating the two steps, oxygen and hydrogen were produced alternatively. The cycle could be represented with following formulas:



The two-step water splitting cycle using $\text{Fe}_3\text{O}_4/\text{FeO}$, ZnO/Zn redox systems have been reported [5,6]. The decomposition temperatures are above 2300K when the process was operated in air or at $p\text{O}_2 = 0.1$ MPa. The $\text{Mn}_3\text{O}_4/\text{MnO}$ and $\text{Co}_3\text{O}_4/\text{CoO}$ systems were studied [7] and they can be reduced in air at 1810K and 1175K respectively. However, the hydrogen production yield was too low for economical production. Recently, the metal ferrite systems were paid much attention, as the O_2 releasing step can be implemented at around 1273K. Tamaura et al [8] demonstrated the two-step water splitting with (Ni, Mn)-ferrite using a solar furnace. The oxygen-deficient (Ni, Mn)-ferrite was formed in the oxygen releasing step at $> 1173\text{K}$ in Ar and the water-splitting step was implemented at $< 1173\text{K}$. In that case, the water splitting was caused by stripping of O from water molecule by active oxygen deficient ferrite, therefore, the reactivity and H_2 production rate depend on the oxygen deficient degree.

In this work, we prepared various ferrite and cation-excess ferrite, to investigate their decomposition temperature and the influence of factors in the preparation process on the oxygen deficient values, δ . In addition, the two-step cycle using CuFe_2O_4 was demonstrated

Experimental

Preparation of MFe_2O_4

The MFe_2O_4 was prepared by co-precipitation method. The mixture of $\text{Cu}(\text{NO}_3)_2$ and $\text{Fe}(\text{NO}_3)_3$ was added into the KOH solution by peristalsis pump under the mixing condition, during the process, the pH values of the solutions were measured continuously using pH meter. Then the temperature was raised to desired ones and the solution was stirred for 8 hours. The precipitation was filtrated, washed with de-ionized water and acetone respectively, dried at 120°C for 24 hours. Then the samples were calcined at various temperature for different time in air or nitrogen atmosphere. Thus obtained products were grinded and the portion of 200-300 mesh was chosen for use. All the reagents are of analytical purity.

Identification of copper ferrite and its decomposition characteristics

The ferrite samples were analysed by X-ray diffractometer (XRD) with $\text{CuK}\alpha$ radiation (Rigaku D/max-RB), $\lambda = 0.154\text{nm}$, the scan range (2θ) is $20\sim 80^\circ$. The lattice constant was calculated by extrapolating the values of a_0 vs the Nelson-Riley function, $\cos^2\theta/\sin\theta + \cos^2\theta/\theta$, to zero using the least squares method.

TGA-DTA analysis was made by SDT 2960 TG-DTA thermo-analyser (Thermal Analysis, US)

Preparation of oxygen-deficient metal oxide ($\text{MFe}_2\text{O}_{4-\delta}$) and the determination of δ

The oxygen-deficient ferrite was prepared by calcinations of the stoichiometric ferrite in nitrogen atmosphere at different temperatures for desired time. The obtained oxygen-deficient products were covered with liquid paraffin for XRD analysis and chemical determination.

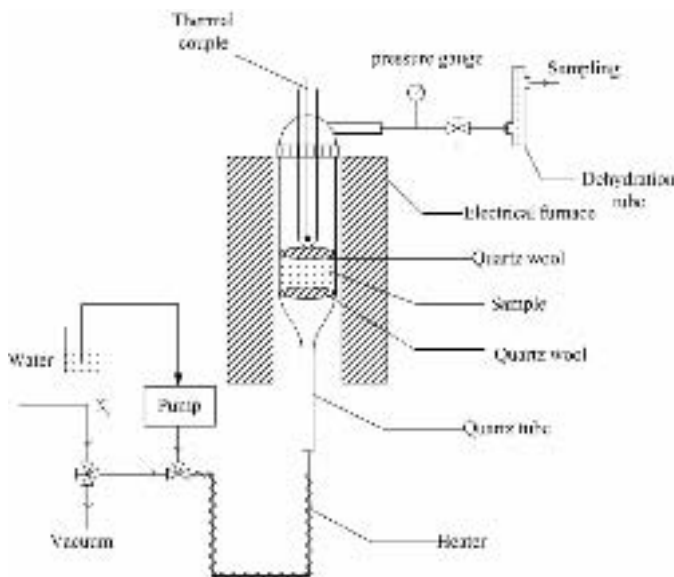
The δ value was determined as follows: samples were resolved in concentrated HCl solution, Fe^{2+}

was determined by colorimetry using 2,2'-bipyridyl (Perkin Elmer L800) Fe_{Total} and Cu were measured by AAS (Hitachi 180-80). The chemical composition and δ value was calculated by the ratio of $n(\text{Cu}^{2+}):n(\text{Fe}^{2+}):n(\text{Fe}^{3+})$.

Oxygen releasing and water-splitting experiment

Oxygen releasing and water-splitting was studied using an experimental setup shown in Figure 1. Ferrite sample was placed in quartz reactor and nitrogen was passed through. The sample was heated to around 1273K for different time, then water was bunched quantitatively into the pre-heater, generated steam reacts with the sample. Excess water was removed by a water trap or by a dehydration tube. The evolved O_2 and H_2 gases were detected by gas chromatography (GC). The sample was analysed by XRD before and after reacting with water.

Figure 1. Experimental setup for water splitting with copper ferrite



Results and Discussion

XRD of the copper ferrite sample

Figure 2 shows the XRD pattern of the copper ferrite prepared by co-precipitation. The diffraction peaks in the scanning range include 112, 103, 211, 220, 224 and 321; and the strongest peak appears at around 35° , these correspond to the structure characteristics of the spinel compounds. the strongest peak corresponds the 211 crystal surface. There is no other peak in the spectrum, indicating that the product is pure compound. The crystalline data were shown in Table 1.

Figure 2. The XRD pattern of copper ferrites calcined for 6h at 1 000°C

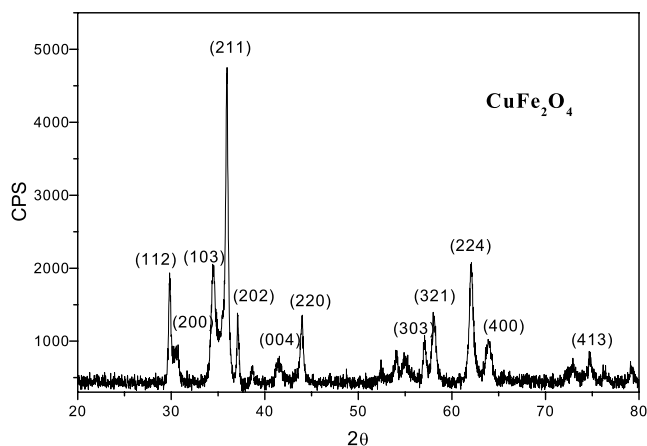


Table 1. Experimental conditions and crystalline data

Formula	CuFe ₂ O ₄
2θ	0°~80°
λ	0.154nm
a=b	5.8440Å
c	8.6302Å
α=β=γ	90°
Z	4

The influence of pH value and co-precipitation temperature on ?

The oxygen-deficient value (δ), which predominantly decides the reactivity of the ferrite after O₂ releasing, would be affected by the pH value and co-precipitation temperature. Tables 2 and 3 show the δ values of the samples prepared under different pH values and various co-precipitation temperatures.

Table 2. Effect of pH value on δ

pH	Initial composition	After calcination	δ
8	CuFe _{1.98} O _{3.97}	CuFe _{1.98} O _{3.86}	0.11
9	CuFe ₂ O ₄	CuFe ₂ O _{3.87}	0.13
10	CuFe _{1.99} O _{3.98}	CuFe _{1.99} O _{3.88}	0.10
11	CuFe _{1.99} O _{3.98}	CuFe _{1.99} O _{3.85}	0.13
12	CuFe _{1.97} O _{3.955}	CuFe _{1.97} O _{3.845}	0.11

Table 3. Effect of co-precipitation reaction temperature on δ

Co-precipitation (°C)	Initial composition	After calcination	δ
30	CuFe _{1.99} O _{3.98}	CuFe _{1.99} O _{3.78}	0.20
50	CuFe _{1.98} O _{3.97}	CuFe _{1.98} O _{3.79}	0.18
70	CuFe _{1.96} O _{3.94}	CuFe _{1.96} O _{3.69}	0.25
90	CuFe ₂ O ₄	CuFe ₂ O _{3.86}	0.24

The sintering condition: 0.6g sample was sintered at 950°C in 100ml/L N₂ for 2 hours.

From the data shown in Table 2, it could be observed that pH values of the solution has little effect on δ values of ferrite. This may attribute to the facts that the pH value needed of complete precipitation for Cu²⁺ and Fe³⁺ is 6.5 and 4, respectively. When the pH value exceeds 8, all Cu²⁺ and Fe³⁺ are precipitated totally. After calcinations, the size of the crystal increased gradually and the crystal process trends to be complete, the effect of calcinations temperature becomes predominant and other factors were weakened. By the way, the δ values obtained from chemical analysis are well matched with those calculated based on thermal analysis. Table 3 presents the effect of co-precipitation reaction temperature on δ , results show that the temperature of the co-precipitation has neglectable influence on the oxygen deficient value, the reason is assumed to be similar with those mentioned above, i.e., the calcination process eliminate the effects of the temperature in the co-precipitation step.

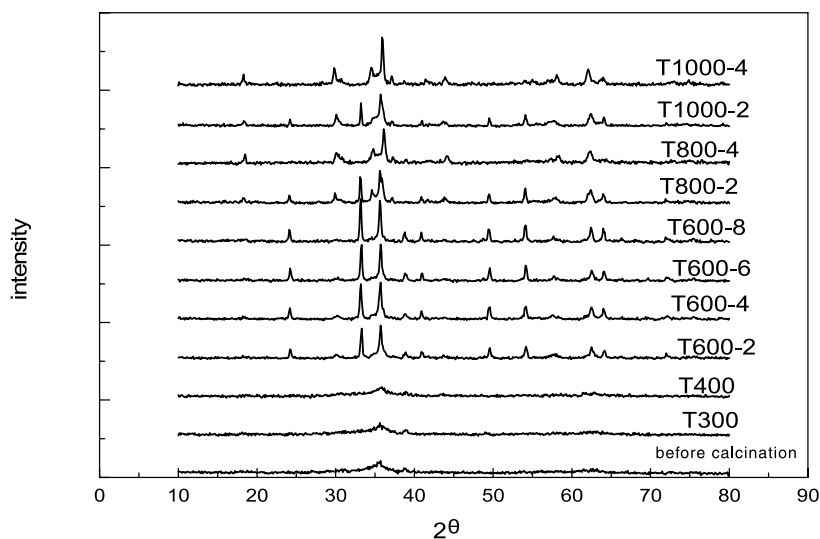
The influence of sintering temperature on the formation of ferrite

Figure 3 gives the XRD patterns of the ferrites obtained at various calcination temperatures. From the figure, following facts can be observed: when the calcination temperature is lower than 400°C, the obtained products is amorphous and no crystal formed. As the temperature raised to 600°C, the characteristic diffractive peaks of Fe₂O₃ appear and the structure does not varied with the prolonged calcinations time. As the calcinations increased to 800°C, the diffractive pattern presents the spinel structure of CuFe₂O₄; furthermore, the content of CuFe₂O₄ increased with the increasing of calcinations time. Two hours later the contents of Fe₂O₃ and CuFe₂O₄ are 31.7% and 68.3% respectively. After 4 hours calcinations and above, the product transform to complete spinel phase. In addition, the content of CuFe₂O₄ increases at elevated temperature. Compare to those of the products calcined at 800°C for 2 hours, the content of CuFe₂O₄ increased to 72.5% at 1000°C. Similarly, when the sample was calcined for 4 hours above, the crystal structure becomes complete spinel type.

The formation of the spinel consists of two steps. Firstly, the hydroxide formed in co-precipitation occurs dehydration reaction to form oxides, then the oxides was calcined to form copper ferrite with spinel structure. If the calcinations temperature is not high enough or the time is not long enough, the phase transformation could not be finished. Therefore, only the temperature exceeds 800°C, it is possible to form homogenous spinel type CuFe₂O₄; furthermore, the longer calcinations process is beneficial to the formation of pure spinel type ferrites.

With the elevation of the calcinations temperature, the oxygen in the crystal lattice releases and forms oxygen-deficient structure, which breaks the electrical neutrality of the compound, and cause the excess Fe³⁺ to be reduced to Fe²⁺ and congregate interiorly. This leads to distorted crystal lattice and make the oxygen-deficient compound unstable. When reacting with water, it strips oxygen from water molecule to restore the original stable state. In this process, water was split and hydrogen was generated.

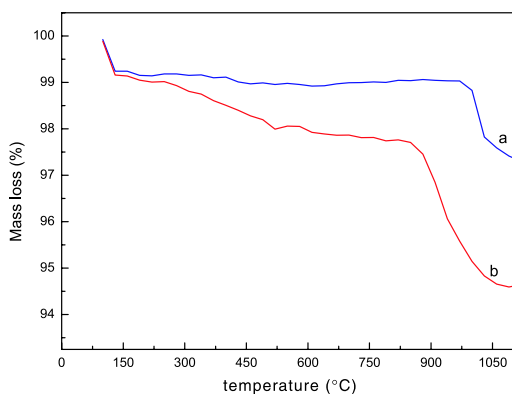
Figure 3. The comparison of XRD patterns under different calcined conditions



The effects of thermo-decomposition atmosphere on δ

The decomposition characteristics in air and nitrogen of copper ferrite were studied respectively with TG-DTA. The weight loss process is composed of two stages: the water in copper ferrite and oxygen absorbed on the surface lost at first, and then oxygen in lattice lost and form oxygen deficient ferrite. XRD patterns of the samples in the different decompose stages shows that the spinel structure of the copper ferrite remains during the whole process. In nitrogen atmosphere, oxygen in lattice of CuFe_2O_4 began to lose as the temperature was raised to 1373K, the weigh loss reaches to 2.87% and δ value is 0.43. Comparatively, decomposition of CuFe_2O_4 in air occurs at 1000°C and the δ value is 0.28 when temperature reaches to 1 100°C. These factors indicate that the preparation of oxygen deficient CuFe_2O_4 should be implemented in lower O_2 partial pressure or non oxygen atmosphere.

Figure 4. Thermogravimetric measurements of copper ferrite at different atmosphere (a: in air; b: in N_2 ; crucible: Al_2O_3 ; temperature: 100 to 1 100°C at 30°C/min)

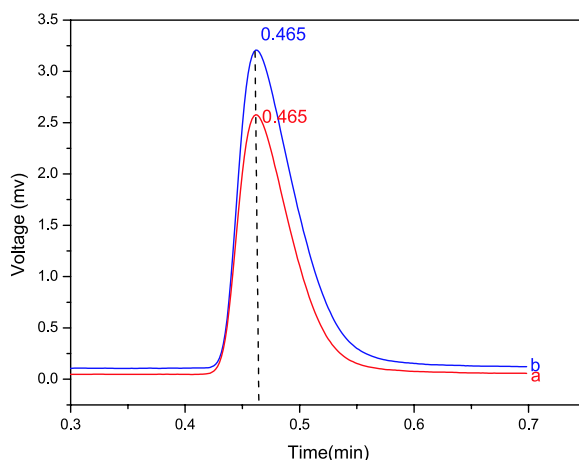


Oxygen releasing and water splitting

A charge of 5 g of CuFe_2O_4 power (100-200 mesh) was loaded in the quartz reactor. During the activation step (O_2 releasing), the reactor was heated to about 1 273K and a flow of 100 mL/min of

N₂ was passed through the sample at slightly above ambient pressure. O₂ was detected with GC. When O₂ can not be detected any more, the reactor was cooled to 673K, and quantitative amount of water was pumped and vaporised into the reactor, until the pressure reached to 1 atm. Afterwards, the reactor temperature was raised to 973K and 1073K. Gas samples was collected at 2 minutes interval. Figure 75 shows the GC spectrum of gas sample taken from the reactor after 8 minutes reaction with steam. The results showed that H₂O was split and H₂ evolved in the process. By repeating both activation and water splitting steps following the same procedures, the cycling capability of the copper ferrite was confirmed. Thus the proposed two step water-splitting cycle with copper ferrite was demonstrated.

Figure 5. The result of GC (a: standard H₂; b: gas samples from reactor)



Summary

Two steps thermochemical water splitting cycle based on CuFe₂O₄ was developed. The preparation conditions of CuFe₂O₄ and CuFe₂O_{4-δ}, were studied. Results show that the spinel type copper ferrite could be easily prepared by co-precipitation method; pH value and temperature of the co-precipitation process has little effect on the oxygen deficient value, δ, while, the calcination temperature apparently affects the formation of CuFe₂O₄. Pure spinel type copper ferrite could be formed only when temperature is above 800°C and calcinations time is longer than 4 hours. The thermo decomposition research of the CuFe₂O₄ indicates that the ferrite began to lose lattice oxygen at ~850°C in nitrogen and ~1 000°C in air, respectively. In addition, the water splitting cycle with CuFe₂O₄ was demonstrated; and oxygen and hydrogen generated in the process were detected by GC. The cycling capability of the copper ferrite was proved.

II. R&D plan of Chinese nuclear hydrogen production plan in the following five years

In INET, a high temperature gas-cooled reactor, HTR-10, was constructed and reached first criticality in 2003. Besides power generation, one of the most important application of the high temperature heat is hydrogen production. Among the technologies for nuclear hydrogen production, the iodine-sulfur thermochemical water splitting cycle and high temperature steam electrolysis were considered as the most promising ones. the nuclear hydrogen production programme was initiated in INET since 2004, and IS process and HTSE were the two candidates for further development.

The aims of the nuclear hydrogen production programme in INET are developing and optimizing the iodine-sulfur thermochemical water splitting process and high temperature steam electrolysis technology.

IS cycle: the main research works in the following five years consists of:

- Acquisition of thermodynamic and kinetic data of the reactions of IS process (Bunsen reaction, HI concentration and decomposition with reactive distillation and SO₃ catalytic decomposition).
- Advanced technological solutions to improve the process efficiency (membrane separation, new reactor, catalysts,).
- Screening and development of Corrosion resistant materials.
- Simulation code and control technology of the process.
- Design and construction of chemical reactors
- Development of catalyst for decomposition reaction of SO₃ HI.
- Construction of a close-loop facility with the hydrogen production rate of 100NL/h.

HTSE: the main research works consists of:

- Development of SOEC materials, including anode, cathode, and electrolyte; and development of single cell testing system.
- Development and fabrication of cell stack system and materials (connection and sealing system).
- Construction of HTSE and experimental test loop.
- HTE cell/module optimisation.
- Construction of a HTSE facility with the hydrogen production rate of 100NL/h.

REFERENCE

- [1] IAEA-TECDOC-1085. Hydrogen as an energy carrier and its production by nuclear power. IAEA, May 1999,101-130.
- [2] Kogan A., Spiegl E., Wolfshtein M., Direct solar thermal splitting of water and on-site separation of the products. *Inter. J. Hydrogen Energy*, 2000, 25: 739-745
- [3] Nakamura T., Hydrogen production from water utilizing solar heat at high temperatures. *Solar Energy* 1977; 19:467-475.
- [4] Lundberg M., Model calculations on some feasible two-step water splitting process. *Inter. J. Hydrogen Energy*, 1993; 18:369-376.
- [5] Sibieude F., Ducarroir M., Tofighi A., Ambriz J., High temperature experiments with a solar furnace : the Decomposition of Fe_3O_4 , Mn_3O_4 , CdO . *Inter. J. Hydrogen Energy*, 1982; 7:79-88.
- [6] Weidenkaff A., Reller A.W., Wokaun A., Steinfeld A. Thermogravimetric analysis of the ZnO/Zn water splitting cycle. *Thermochimica Acta* 2000; 359:69-75.
- [7] Ehrensberger K., Kuhn P., Shklover. V., Temporary phase segregation processes during the oxidation of $(\text{Fe}_{0.7}\text{Mn}_{0.3})_{0.99}\text{O}$ in $\text{N}_2\text{-H}_2\text{O}$ atmosphere. *Solid state ionics*, 1996 90:75-81.
- [8] Tamaura Y., Steinfeld A., Kuhn P., Ehrensberger K., Production of solar hydrogen by a novel, 2-step, water-splitting thermochemical cycle. *Energy*, 1995 20:325-330.

DEVELOPMENT OF THE THERMOCHEMICAL AND ELECTROLYTIC HYBRID HYDROGEN PRODUCTION PROCESS FOR SODIUM COOLED FBR

Toshio Nakagiri* , Takeshi Kase, Shoichi Kato and Kazumi Aoto

Advanced Material Technology Group, Advanced Nuclear System Research and
Development Directorate,
Japan Atomic Energy Agency, O-Arai-machi, Higashi Ibaraki-gun, Ibaraki 311-1393.

Abstract

The thermochemical and electrolytic hybrid hydrogen production process has been developed by Japan Nuclear Cycle Development Institute (JNC). The process is based on sulfuric acid (H_2SO_4) synthesis and decomposition process developed earlier (Westinghouse process) and sulfur trioxide (SO_3) decomposition process is facilitated by electrolysis with ionic oxygen conductive solid electrolyte at 500°C - 550°C . Stable hydrogen and oxygen production for several hours by the process was already confirmed in the experiments performed by JNC.

The experiment for about 60 hours was performed to investigate the durability of the experimental apparatus by the hybrid process. In the experiment, 50wt% sulfuric acid was circulated in the experimental apparatus at the flow rate of 0.6ml/min, and SO_3 electrolysis cell was operated at 550°C . The cell voltage of SO_3 electrolysis cell and SO_2 solution electrolysis cell were kept to 0.13V and 0.9V, respectively. Stable oxygen generation from SO_3 electrolysis cell was observed during the experiment and no degradation was observed in the Pt plated YSZ electrolyte. Nevertheless, outlet pipe of SO_3 electrolysis cell was corroded by high temperature sulfuric acid and hydrogen generation rate in SO_2 solution electrolysis cell decreased in several hours. The cause of the corrosion of outlet pipe of SO_3 electrolysis cell and the decrease of hydrogen generation rate was investigated and the technical problems for manufacturing a higher performance (1NL/h) experimental apparatus were extracted.

* e-mail: nakagiri.toshio@jaea.go.jp

I. INTRODUCTION

The thermochemical and electrolytic hybrid hydrogen production process (thermochemical and electrolytic hybrid hydrogen process in lower temperature range: HHLT) for sodium cooled FBR is proposed by Japan Nuclear Cycle Development Institute (JNC) [1]. HHLT is based on the sulfuric acid (H₂SO₄) synthesis and decomposition processes (named “Westinghouse process”) developed earlier [2, 3], and SO₃ decomposition process is facilitated by electrolysis with ionic oxygen conductive solid electrolyte which is extensively utilised for high-temperature electrolysis of water. The hydrogen production experiments to substantiate the whole process of HHLT were already performed and stable production of hydrogen and oxygen for several hours was confirmed. Furthermore, conceptual design of hydrogen production plant with HHLT using a small sized sodium cooled reactor was performed.

In the present study, experiment for about 60 hours was performed to investigate the durability of the experimental apparatus in long time operation and technical problems were extracted to manufacture 1NL/h hydrogen production experimental apparatus.

II. LONG TIME HYDROGEN PRODUCTION EXPERIMENT

1. Principle of HHLT

Westinghouse process requires high temperature over 800°C only for SO₃ decomposition reaction, and other reactions can be performed below 500°C. If SO₃ decomposition can be performed in lower temperature than 800°C, hydrogen production using lower temperature heat source such as FBR can be realized, and corrosion problems can be reduced.

Only 7.8% SO₃ thermally decomposes in equilibrium condition at 500°C as shown in Figure 1, and also only about 20% in the case membrane reactor technique is used to increase decomposition fraction of SO₃ at 500°C. Therefore, some other energy is required to obtain higher decomposition fraction of SO₃. Electrolysis by ionic oxygen conductive solid electrolyte is applied to increase decomposition fraction of SO₃ in HHLT. HHLT is composed of the reactions shown below.

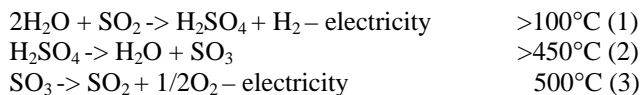


Figure.1 Thermal decomposition fraction of SO₃

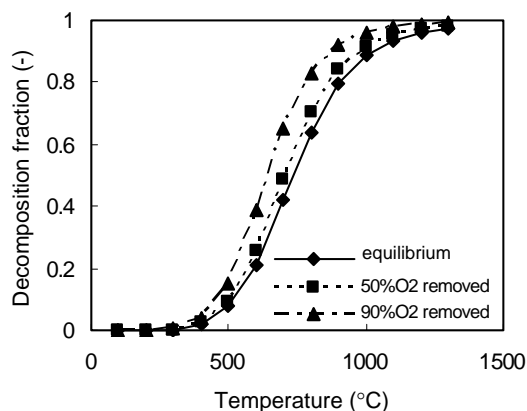
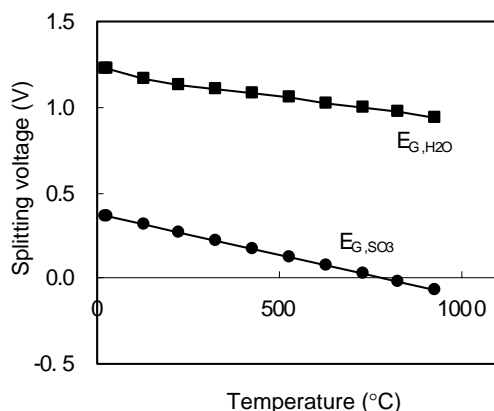


Figure 2. Splitting voltages of H₂O and SO₃



Characteristics of HHLT are summarised below.

(1) Low electrical energy required

Required energies and entropy changes of reaction for HHLT are shown in Table 1. In HHLT, total required electrical energy is 113.4 kJ/mol for 1 mol H₂ production and it is about half of direct water splitting (204.9 kJ/mol at 500°C, [5]).

Furthermore, required splitting voltage for reaction (3) (E_{G,SO_3}) is expected to be lower than 0.2V at 500°C as shown in Figure 2. EG is calculated by equation (4)

$$EG = -\Delta G/(nF) \quad (4)$$

In equation (4), n is number of electron (= 2 for 1 oxygen atom) and F is Faraday constant. Theoretical voltage of sulfuric acid synthesis reaction (equation (1)) is 0.17V-0.29V, therefore, total theoretical voltage in HHLT is expected to be lower than 0.5V which is about half of the theoretical voltage of direct water splitting (E_{G,H_2O}), about 1V.

(2) Simple process flow

HHLT does not require decomposition and separation processes of HI, HBr and separation of O₂ which are required in Iodine-Sulfur (IS) process or sulfur-bromide process [2, 3], therefore, numbers of reactors are much less than those of IS process or sulfur-bromide process, and simple process flow can be achieved.

(3) Decrease in corrosion of structural materials

Corrosion of structural materials is expected to be suppressed in HHLT than in IS process etc., because high corrosive iodine or bromine is not used.

(4) Higher safety

In the case hydrogen and oxygen can be mixed at the temperature higher than spontaneous ignition temperature of hydrogen (500°C in air [6]), hydrogen explosion can take place.

In HHLT, hydrogen is produced in reaction (1), at the temperature lower than 100°C, therefore, possibility of hydrogen explosion is considered to be quite a low.

2. Experimental apparatus and experimental conditions

The flow sheet of experimental apparatus and experimental conditions are shown in Figure 3 and Table 1, respectively. The sulfuric acid thermal decomposition reaction was performed in “H₂SO₄ vaporiser” at 400°C. Electrolytic SO₃ decomposition reaction was performed in “SO₃ electrolysis cell” at 550°C and cell voltage was controlled to be 0.13V by potentiostat. Stainless steel pipes of the SO₃ electrolysis cell exposed to high temperature sulfuric acid were all plated by gold. O₂ generated in the SO₃ electrolysis cell is purged by N₂ and O₂ concentration in N₂ purge gas was measured by O₂ meter. A tubular 8mol% yttria stabilised zirconia (YSZ) with a dimension of 2 mm in thickness was used as electrolyte in the SO₃ electrolysis cell, and Pt electrodes were manufactured on both (inner and outer) surface of the YSZ tube. In this experiment, Pt electrodes were manufacture by Pt plating for higher durability and higher cell current. Furthermore, the diameter of outlet piping of the SO₃ electrolysis cell was increased from 1/2 inch to 3/4 inch to increase gas flow rate in SO₃ electrolysis cell. The cell current of SO₃ electrolysis cell was increased about one order as compared to previous cell.

H₂ was produced in “H₂SO₃ solution electrolysis cell” at room temperature. The cell voltage of H₂SO₃ electrolysis cell was controlled by potentiostat and cell current was also measured by the potentiostat. Liquids (H₂SO₄ and H₂O) were carried by roller pumps and flow rate was 0.6ml/min, and gases (SO₃, H₂O, SO₂, O₂) were carried by N₂ purge gas and flow rate of N₂ purge gas was 100ml/min. Solid polymer electrolyte Nafion 117 was used as membrane between anode and cathode, and anolyte and catholyte of the electrolysis cell were 50wt% H₂SO₄ solution.

Table 1. Experimental conditions

Reactor	Temperature (deg-C)	Cell voltage (V)
H ₂ SO ₄ vaporizer	400	-
SO ₃ electrolysis cell	550	0.13
SO ₂ absorber	Approx. 10	-
H ₂ SO ₃ solution electrolysis cell	Room Temp.	0.85~0.9

3. Experimental results

Total duration of present experiment was about 56 hours. H₂ and O₂ generation rate calculated from measured cell current are shown in Figure 4. O₂ generation rate was about 5ml/h and almost stable generation of O₂ was continued in SO₃ electrolysis cell. O₂ amount measured with O₂ meter agreed well with the amount calculated from cell current. H₂ generation rate in H₂SO₃ electrolysis cell decreased in several hours and H₂ generation rate was lower than 5ml/h during the experiment. H₂SO₃ solution was added in the anolyte and the anode surface was polished by emery paper at about 20 hours after the experiments started, and stirring by N₂ gas bubbling around the anode was started at about 40 hours after the experiment started, to increase H₂SO₃ amount supplied for the anode surface. Cell current of H₂SO₃ solution electrolysis cell increased for a time by the operations mentioned above, but decreased in several hours again.

III. DISCUSSION

1. *Durability of SO₃ electrolysis cell for high temperature sulfuric acid*

The performance of Pt plated YSZ electrolyte for SO₃ electrolysis was stable for about 60 hours, and no degradation was observed in post experiment examination.

Nevertheless, corrosion of the outlet piping of SO₃ electrolysis cell was observed in post experiment observation as shown in Figure 6. SEM-EDS analysis of white powder remained in SO₂ absorber was performed, and constituents of stainless steel (Fe and Cr) and sealing metal (Cu), and sulfur were detected as shown in Table 2. Therefore, white powder is considered to be sulfate of stainless steel and sealing metal constituent. The cause of the corrosion was estimated to be the peeling of plated gold by condensed sulfuric acid. To improve the durability of the outlet piping of SO₃ electrolysis cell, sulfuric acid resistant material, such as high Si cast steel, should be used.

2. *Technical problems to manufacture 1NL/h hydrogen production test apparatus*

(1) *Development of higher performance of SO₃ electrolysis cell*

In the present experiment, Pt plated YSZ electrolyte was used, and its performance was one order higher than YSZ with Pt paste electrode. The thickness of the Pt plated electrode is much thinner than Pt paste electrode as shown in Figure 7, therefore, SO₃ or O₂ molecule diffusion on the Pt plated electrode surface to the reaction area called three phase (gas/electrode/electrolyte) boundary is assumed to be much faster than on Pt paste electrode.

Nevertheless, further improvement of the SO₃ electrolysis performance of Pt/YSZ electrolyte is required. Therefore, the total area of three phase boundary must be increased by improving the microstructure of Pt electrode.

(2) *Development of higher performance H₂SO₃ solution electrolysis cell*

In this experiment, the hydrogen production rate in H₂SO₃ solution electrolysis cell was almost lower than 5ml/h, and the cause of low production rate is considered to be the lack of H₂SO₃ supply to anode surface. Therefore, improvement to increase the amount of H₂SO₃ solution supplied to the anode surface, for instance, use of flow type electrolysis cell and gas diffusion type electrode, should be required.

Figure 5. Blockage of inlet pipe of SO₂ absorber

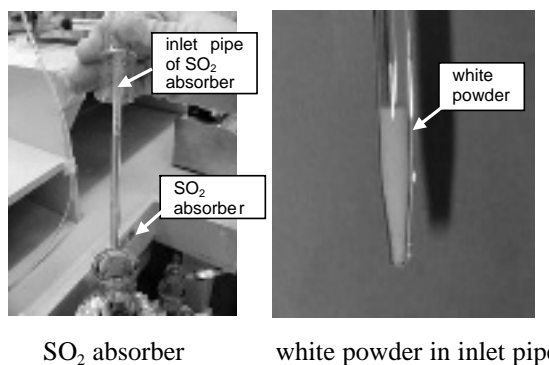


Figure 6. Cut image of outlet piping of SO₃ electrolysis cell

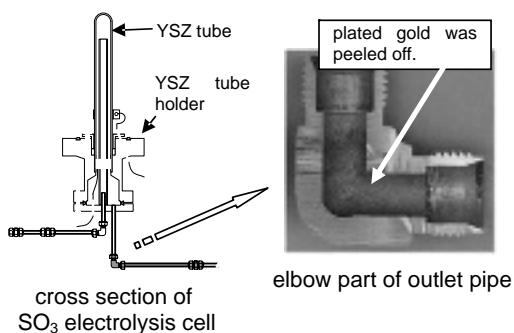
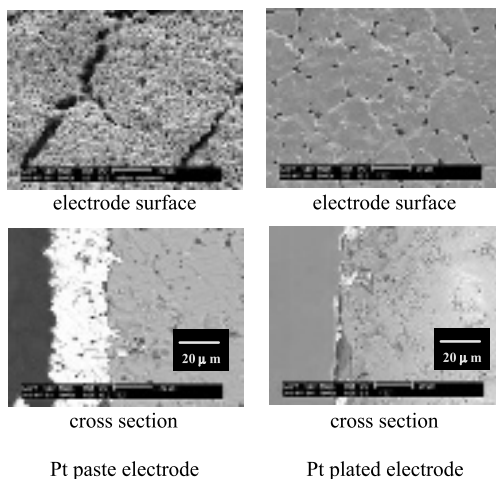


Table 2. Composition of white powder in the SO₂ absorber by SEM-EDS analysis

element	weight fraction (wt%)
S	56.07
Cr	6.35
Fe	33.97
Cu	3.61

Figure 7. SEM images of Pt paste and Pt plated electrodes



IV. CONCLUSIONS

The experiment for about 60 hours was performed to investigate the durability of the experimental apparatus by HHLT, and technical problems to manufacture 1NL/h hydrogen production experimental apparatus were extracted. Conclusions are summarized as follows.

(1) The performance of Pt plated YSZ electrolyte for SO_3 electrolysis did not degrade during about 60 hour operation in 550°C gaseous sulfuric acid. Nevertheless, outlet piping of the SO_3 electrolysis cell was corroded by condensed sulfuric acid. Sulfuric acid resistant material should be used in the new experimental apparatus.

(2) It is considered to be necessary to increase the total area of three phase boundary on Pt plated YSZ electrolyte to obtain higher performance of SO_3 electrolysis cell.

(3) The hydrogen production rate in H_2SO_3 solution electrolysis cell for decreased in several hours, and the amount of H_2SO_3 solution supplied to the anode surface is considered to be not enough. It is considered to be necessary to increase the amount of H_2SO_3 solution for higher cell hydrogen production rate.

Experiments apparatus for 1NL/h hydrogen production will be manufactured in this year and hydrogen production efficiency of the apparatus will be evaluated. Furthermore, designing study of a 5Nm³/h hydrogen production plant will be started.

NOMENCLATURE

EG: splitting voltage (V)

DG: Gibbs energy change (kJ/mol)

n: number of electron (=2 for 1 oxygen atom)

F: Faraday constant.

REFERENCES

- [1] Y. Kani, "Investigation on hydrogen production by Fast Breeder Reactor (FBR)", Nuclear Viewpoints, Vol.49 No.1, 26, pp.26-29 (2003), [in Japanese].
- [2] IAEA, "Hydrogen as an energy carrier and its production by nuclear power", IAEA-TECDOC-1085 (1999).
- [3] W. Weirich, K.F. Knoche, F. Behr *et al.*, "Thermochemical processes for water splitting – Status and outlook", Nuclear Engineering and Design 78, pp.285-291 (1984).
- [4] T. Nakagiri *et al.*, "Development of a new thermochemical and electrolytic hybrid hydrogen production system for sodium cooled FBR", ICONE13-50147, Beijing, 2005.
- [5] M.W. Chase, Jr *et al.*, " JANAF Thermochemical tables third edition", American Chemical Society and American Institute of Physics, (1985).
- [6] National Astronomical Observatory, "Rika nenpyo (Chronological Scientific Tables)", Maruzen Co., Ltd, pp.491 (1996), [in Japanese]

This page intentionally left blank

PROGRESS IN HIGH-TEMPERATURE ELECTROLYSIS FOR HYDROGEN PRODUCTION

**J. Stephen Herring, James E. O'Brien, Carl M. Stoots, G.L. Hawkes, Paul Lessing,
William Windes, Daniel Wendt, Michael Mc Kellar and Manohar Sohal**

Idaho National Laboratory
P.O. Box 1625 MS 3860
Idaho Falls, ID, 83415-3860, USA

Joseph J. Hartvigsen
Ceramatec, Inc.
2425 South 900 West
Salt Lake City, UT 84119, USA

Abstract

A research program is under way at the Idaho National Laboratory to assess the performance of solid-oxide cells operating in the steam electrolysis mode for hydrogen production over a temperature range of 800 to 900°C. The research program includes both experimental and modeling activities. Selected results from both activities are presented in this paper. Experimental results were obtained from a ten-cell planar electrolysis stack, fabricated by Ceramatec, Inc. The electrolysis cells are electrolyte-supported, with scandia-stabilised zirconia electrolytes (~140 μm thick), nickel-cermet steam/hydrogen electrodes, and manganite air-side electrodes. The metallic interconnect plates are fabricated from ferritic stainless steel. The experiments were performed over a range of steam inlet mole fractions (0.1 – 0.6), gas flow rates (1 000-4 000 sccm), and current densities (0 to 0.38 A/cm²). Hydrogen production rates up to 115 Normal liters per hour were demonstrated. Stack performance is shown to be dependent on inlet steam flow rate. A three-dimensional computational fluid dynamics (CFD) model was also created to model high-temperature steam electrolysis in a planar solid oxide electrolysis cell (SOEC). The model represents a single cell as it would exist in the experimental electrolysis stack. Mass, momentum, energy, and species conservation and transport are provided via the core features of the commercial CFD code FLUENT. A solid-oxide fuel cell (SOFC) model adds the electrochemical reactions and loss mechanisms and computation of the electric field throughout the cell. The FLUENT SOFC user-defined subroutine was modified for this work to allow for operation in the SOEC mode. Model results provide detailed profiles of temperature, Nernst potential, operating potential, anode-side gas composition, cathode-side gas composition, current density and hydrogen production over a range of stack operating conditions. Integrated model results are shown to compare favorably with the experimental results obtained from the ten-cell stack tested at INL.

Introduction

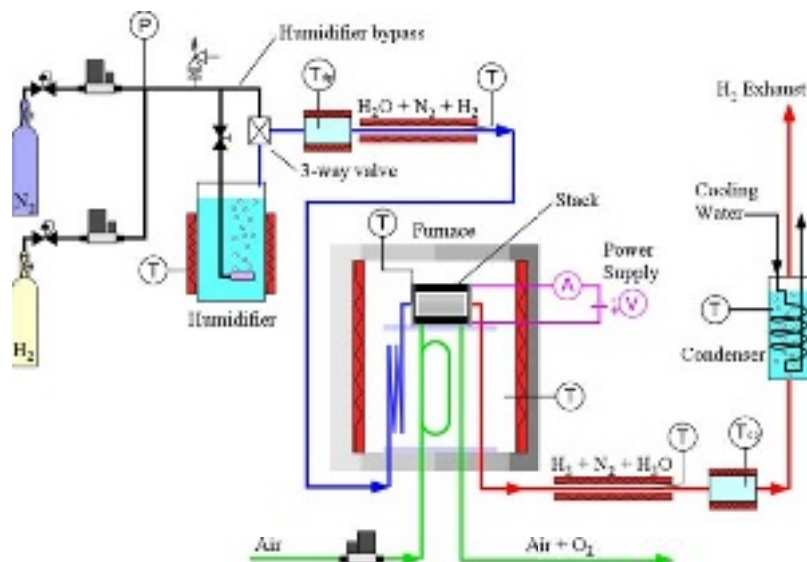
As part of the US Department of Energy Nuclear Hydrogen Initiative a research programme is being conducted at the Idaho National Laboratory (INL) to simultaneously address the research and scale-up issues associated with the implementation of planar solid-oxide electrolysis cell technology for hydrogen production from steam. We are conducting a progression of electrolysis stack testing activities, at increasing scales, along with a continuation of supporting research activities in the areas of materials development, single-cell testing, detailed computational fluid dynamics (CFD) and systems modeling. This paper describes a series of high-temperature electrolysis stack tests performed at the INL in October, 2004 and in July and August, 2005, with a 10-cell and a 22-cell stack fabricated at Ceramtec, Inc. These tests culminated in the demonstration of hydrogen production rates of 50 normal (ref. 0° C, 101.33 kPa) liters per hour (NL/hr) for the October, 2004 test and greater than 100 NL/hr for the July-August 2005 test.

In addition to the work at the INL, the Argonne National Laboratory is performing CFD and systems-level modeling of high temperature electrolysis using Star-CD and ASPEN, in order to compare with both the results of the INL experiments and modeling. ANL is also developing electrode materials that show promise of better conductivity than those presently used. The Oak Ridge National Laboratory is investigating the application of high temperature inorganic membranes for the separation of hydrogen from the residual steam exiting the electrolytic cells.

Test Configuration

A schematic of the stack-testing apparatus is presented in Figure 1. Primary components include gas supply cylinders, gas mass-flow controllers, a humidifier, dewpoint measurement stations, temperature and pressure measurement, high temperature furnace, and a solid oxide electrolysis stack. Nitrogen was used as an inert carrier gas. The use of a carrier gas allows us to independently vary both the partial pressures and the flow rates of the steam and hydrogen gases while continuing to operate at atmospheric pressure. The flow rates of nitrogen, hydrogen and air are established by means of precision mass-flow controllers. Air flow to the stack is supplied by the laboratory shop air system, after passing through a two-stage extractor/dryer unit.

Figure 1. Schematic of experimental apparatus for electrolysis stack testing



Downstream of the mass-flow controller, nitrogen is mixed with a smaller flow of hydrogen gas. Hydrogen is included in the inlet flow as a reducing gas in order to help prevent oxidation of the nickel-zirconia cermet electrode material. The nitrogen/hydrogen gas mixture is mixed with steam by means of a heated humidifier. The humidifier consists of a heated stainless-steel vessel containing demineralized/deionized water through which the nitrogen/hydrogen flow is bubbled. An aquarium-style bubbler was used for this purpose. The dewpoint temperature of the nitrogen/hydrogen/steam gas mixture exiting the humidifier is monitored continuously using a precision dewpoint sensor. All gas lines located downstream of the humidifier are heat-traced in order to prevent steam condensation. Gas line temperatures are monitored by thermocouples and controlled by means of variable transformers.

Close-up photographs of the 22-cell solid-oxide electrolysis stack used for these tests are shown in Figure 2. The stacks were fabricated by Ceramtec, Inc. of Salt Lake City, Utah. The stacks have a per-cell active area of 64 cm². They are designed to operate in cross flow, with the steam/hydrogen gas mixture entering the inlet manifold on the right in the photographs, and exiting through the outlet manifold, visible on the left in the photographs. Air flow enters at the rear though an air inlet manifold (not visible in the figures) and exits at the front directly into the furnace. The power lead attachment tabs, integral with the upper and lower interconnect plates are also visible in the photograph. The 22-cell stack incorporated new steam/hydrogen manifolds fabricated from alloy 440C.

The interconnect plate is fabricated primarily from ferritic stainless steel (alloy 441). It includes an impermeable separator plate (~0.46 mm thick) with edge rails and two corrugated “flow fields,” one on the air side and one on the steam/hydrogen side. The height of the flow channel formed by the edge rails and flow fields is 1.02 mm. Each flow field includes 32 perforated flow channels across its width to provide uniform gas-flow distribution. The steam/hydrogen flow field is fabricated from nickel. The air-side flow field material is ferritic stainless steel. The interconnect plates and flow fields also serve as electrical conductors and current distributors. To improve performance, the air-side separator plates and flow fields are surface-treated to form a rare-earth conductive oxide scale. A perovskite rare-earth bond layer is also applied to the separator-plate on the air side by either screen printing or plasma spraying. On the steam/hydrogen side of the separator plate, a thin (~10 μm) nickel metal coating is applied. The steam/hydrogen side flow field is fabricated from nickel foil. The alloy-441 separator plates of the 22-cell stack were treated with the usual Ceramtec environmental barrier coating (EBC) and were thermal-sprayed on one side with a nickel coating. The other side was treated with a rolled-on perovskite coating of Lanthanum Strontium Cobaltite (LSC), with an extra green layer. The edge rails were brazed to the separator plates and also treated with the Ceramtec EBC. “Q glass” paste was used on the outside of the edge rails to bond the edge rails to the electrolytes. This paste was chosen based on the results of recent separate-effects corrosion tests performed at Ceramtec.

Figure 2. 22-cell planar stack

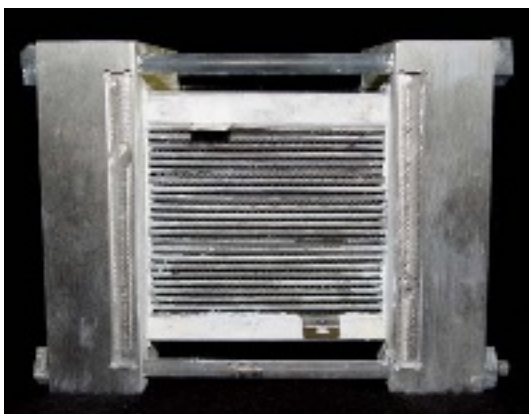
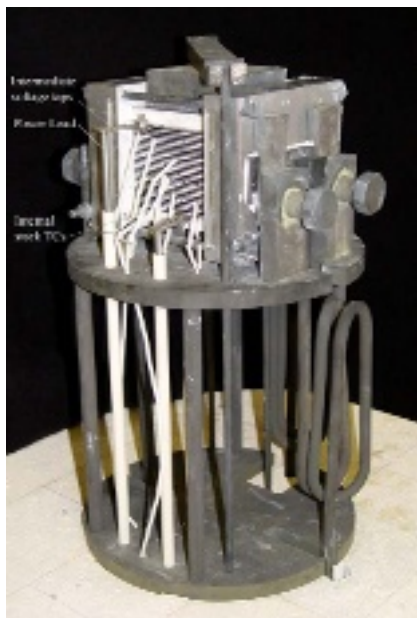


Figure 3. 22-cell stack mounted on test fixture in furnace. Power leads, internal stack thermocouples and intermediate voltage taps are visible



The electrolyte is scandia-stabilised zirconia, about 160 μm thick. The air-side electrode (anode in the electrolysis mode), visible in the figure, is a strontium-doped manganite. The electrode is graded, with an inner layer of manganite/ zirconia ($\sim 13 \mu\text{m}$) immediately adjacent to the electrolyte, a middle layer of pure manganite ($\sim 18 \mu\text{m}$), and an outer bond layer of cobaltite. The steam/ hydrogen electrode (cathode in the electrolysis mode) is also graded, with a nickel-zirconia cermet layer ($\sim 13 \mu\text{m}$) immediately adjacent to the electrolyte and a pure nickel outer layer ($\sim 10 \mu\text{m}$).

A photograph of the 22-cell stack, mounted on the inconel test fixture at the May St. North Laboratory, and resting on the furnace base, is shown in Figure 3. New power leads fabricated from 3/16-inch diameter stainless-steel (304) rods were used for this test. The power lead rods are insulated with alumina tubing. Additional instrumentation is also visible in the photograph. These include 4 intermediate voltage taps and 5 miniature thermocouples inserted into the air-side flow channels to monitor internal stack temperatures. These were inconel-sheathed 0.020-inch OD, mineral-insulated, type-K, ungrounded thermocouples. The thermocouples were all inserted into the middle cell, about one inch apart, with one in the middle of the cell, two to either side of it, one near the steam/hydrogen inlet, and one near the steam/hydrogen outlet.

For these tests, with the 22-cell stack, initial sweep data were obtained at 800°C, and long-term testing was performed at 830°C.

Measurement of the outlet dewpoint temperature, downstream of the electrolysis stack, allows for direct determination of the change in dewpoint, the rate of steam reduction and the corresponding rate of hydrogen production during electrolysis testing. During stack tests, pressure at the humidifier is higher than the laboratory ambient pressure by an amount that is dependent on the flow rates of nitrogen, hydrogen and steam. Higher flow rates yield higher back pressure due to flow losses in the line. The actual pressure at the humidifier has to be taken into account when calculating the dewpoint-based hydrogen production rates.

Test Procedure

Prior to testing, a slow automated heat-up of the electrolysis stack was performed with the stack in the open-cell condition until the desired test temperature was achieved. A heating time of 8 hours was used to take the cell from room temperature to 800°C. During this time, the humidifier, humidity sensing station, and heat tracing temperatures were also established. Nitrogen, hydrogen, and air gas flow rates were established by adjusting the set points on the mass-flow controller electronics unit. .

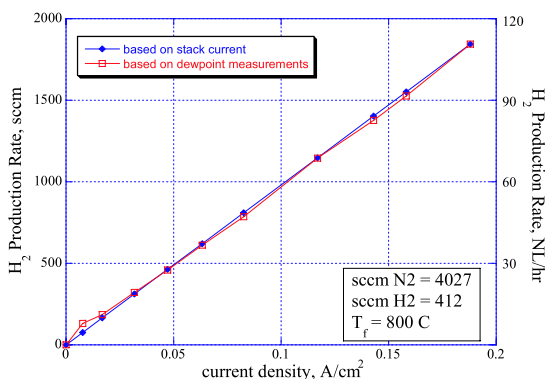
Two types of stack characterisation tests were performed: DC potential sweeps and a long-term test for the 22-cell stack. The initial DC potential sweep for this stack was performed in a stepwise fashion in order to allow the internal stack temperatures to achieve steady-state values before proceeding to the next voltage setting. Results of the DC potential sweep allowed for determination of the stack area-specific resistance and hydrogen production rates. The long-term test was performed in the constant-current mode by selecting a stack current that corresponded to a hydrogen production rate just above the 100 NL/hr threshold desired for this test. Under constant-current operation, any long-term performance degradation is reflected in a slow increase in the stack operating voltage.

Experimental Results

Hydrogen production rates for the stepwise sweep performed with the 22-cell stack are presented in Figure 4. The rate of hydrogen production based on dewpoint measurements is also shown in Figure 4. These values agree very closely with the current-based values. Note that hydrogen production rates in excess of 100 NL/hr were achieved during this sweep.

Internal stack temperatures were monitored during the initial DC potential sweep performed with the 22-cell stack. Each operating voltage during the sweep was maintained for about ten minutes in order to allow the internal stack temperatures to achieve steady-state values before proceeding to the next operating condition. Results of the internal stack temperature measurements are presented in Figure 5 as a function of stack operating voltage. As expected, stack internal temperatures are lower than the external furnace temperature when the operating voltage is between open-cell and thermal neutral. The thermal neutral voltage is 28.4 V for the 22-cell stack. Note that the internal stack temperatures cross from below to above the 800°C furnace setpoint temperature at a voltage very close to the thermal neutral value. The stack centerline temperature is indicated by temperature T_{internal3} in the Figure. Note that in the range of operating voltages between open-cell and thermal neutral, this thermocouple has the lowest value of the 5 internal temperatures, indicating that the center of the electrolyte is coolest in this voltage range.

Figure 4. Hydrogen production rates for the 22-cell stack measured during stepwise sweep

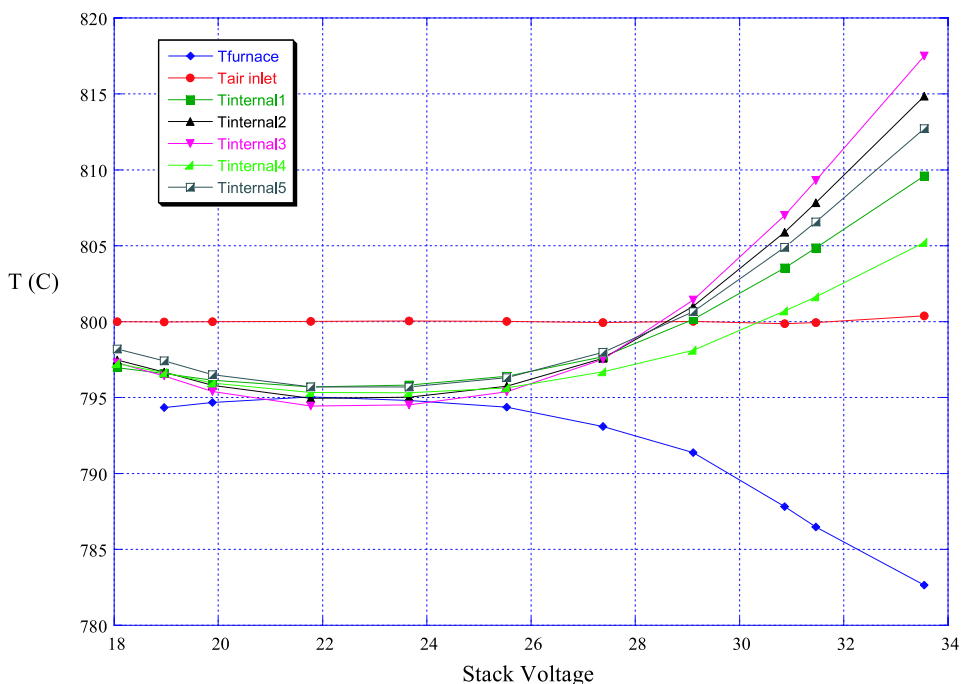


The center temperature reaches a minimum value of about 794 C for these operating conditions. At operating voltages above thermal neutral, this center thermocouple reading is the highest of the five internal temperatures, indicating that at voltages above thermal neutral, the center portion of the electrolyte is hottest. These results are consistent with our computational fluid dynamic calculations. During our tests, the furnace temperature is feedback-controlled using the air inlet manifold temperature as the process variable. This temperature is also shown in Figure 5. Note that its value remains fixed during the sweep. The “furnace” temperature shown in Figure 5 is the reading from a thermocouple that is positioned in the furnace outside of the test fixture. Its value responds relatively quickly to any change in the heater power level. Since the stack tends to cool off at operating voltages between open-cell and thermal neutral, the feedback control increases the furnace power, as indicated by the increase in the “furnace” temperature. Beyond thermal neutral, the stack is somewhat self-heating, and the furnace temperature decreases as the stack internal temperatures increase.

Long-term Test Results

The 22-cell stack was operated for long-term testing with the power supply in constant-current mode at a current of 11.0 A (0.172 A/cm²), yielding a hydrogen production rate in excess of 100 NL/hr. The stack was allowed to operate in this mode until approximately 6:00 PM, August 3, 2005, when an uninterruptible power supply failure forced termination of the test. A plot of the stack operating voltage, current, and hydrogen production rate as a function of time is presented in Figure 13. The large negative spikes in voltage and current correspond to the times when the stack was placed briefly in the open-cell condition in order to check the open-cell voltage and to refill the liquid water reservoir. This was done on roughly 12-hour increments. The stack operating voltage increased over the 196 hours from 30.3 to 32.4 V, representing about a 7% degradation in electrolysis efficiency over that time period. Stack per-cell ASR during the long-term testing corresponding to these operating voltages and the fixed current increased slightly from 3.3 to 3.8 Ohm cm². These ASR values are lower than what we observed during the initial sweep.

Figure 5. Stack and furnace temperature during sweep

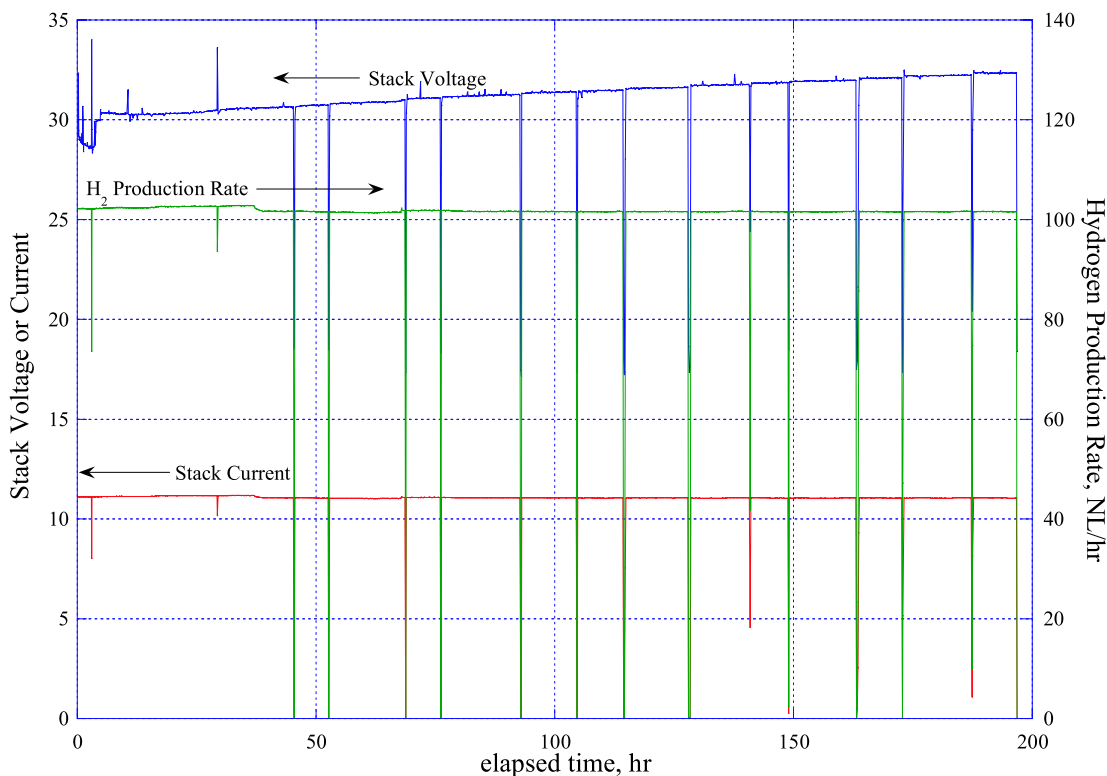


Numerical Modelling

The numerical model developed for this paper was based on the geometry of a single SOEC cell taken from the stack described previously. The numerical domain extends from the center plane of one separator plate to the center plane of the next separator plate. Symmetry boundaries are applied at the top and bottom of the model. Representations of the numerical model are presented in Figure 7. In the top left portion of Figure 7, the full model is shown to scale. Since the model includes only one cell, the model geometry is quite thin in the vertical (z) direction. To show more detail, the model is shown in the bottom left portion of Figure 7 with a vertical exaggeration of 10x in the z -direction. An exploded view with the 10x vertical exaggeration is shown in the right half of the figure.

In the exploded view, the bottom element is the bottom separator plate. Since we are trying to represent a unit cell extracted from a larger stack, the bottom and top separator plates in the numerical model are only half as thick (i.e., 0.19 mm) as the hardware separator plates. Therefore, the top and bottom boundaries of the numerical model represent symmetry planes and the boundary conditions on those faces are set accordingly. The edge rails are shown attached to the bottom separator plate. In the stack hardware, the edge rails are fabricated from the same material as the separator plates, but they are separate pieces.

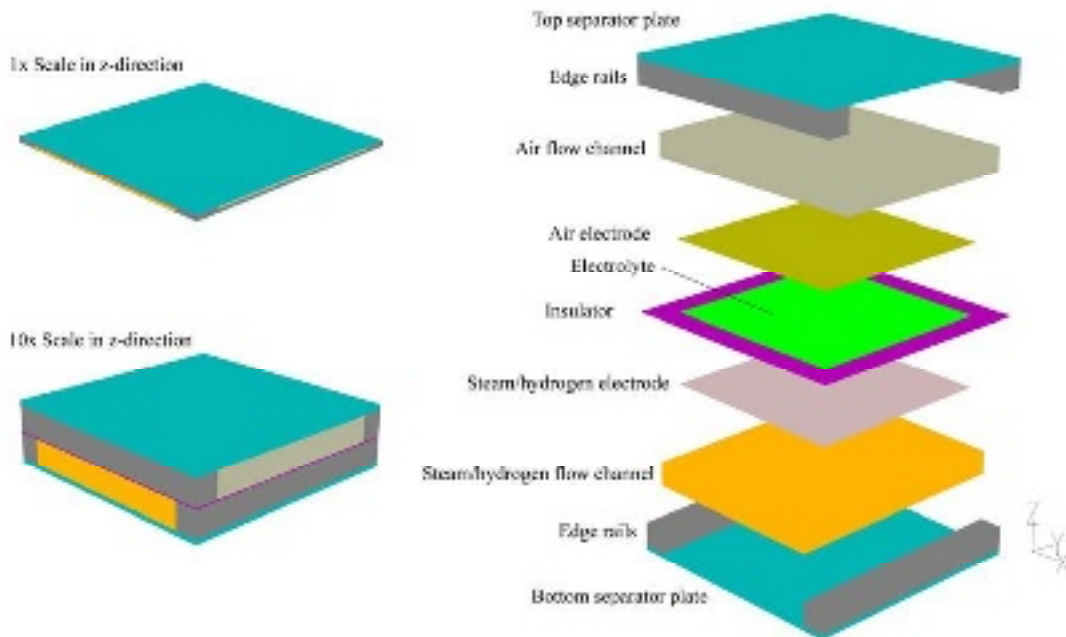
Figure 6. Stack voltage, current, and hydrogen production rate during long-term test



The next element in the numerical model is the steam/hydrogen flow channel. The flow channels are the regions in the stack between the separator plate, the edge rails and the electrodes in which the corrugated/perforated “flow fields” are located. The steam/hydrogen flow channel has been specified as a high-porosity porous-media region with metallic nickel as the solid material and with anisotropic permeability, much higher in the primary flow direction than in the cross flow directions. The height of the flow channel is the set by the thickness of the edge rails, 1.019 mm.

The next three layers in the numerical model are associated with the electrolyte/electrode assembly, as shown in the right half of Figure 7. The FLUENT SOFC module treats the electrolyte as a 2-D planar element. Therefore the electrolyte in the model has geometrical thickness of zero. On either side of the electrolyte are the electrodes which are created with 3-D elements. Therefore, the electrolyte/electrode assembly in the model is only as thick as the two electrodes. Around the outer periphery of the electrolyte/electrode assembly, we have include an “insulator” with the properties of YSZ. The insulator prevents an electrical short circuit between the top and bottom edge rails. No ionic transport occurs through this insulator.

Figure 7. Fluent single-cell SOEC model



The next element in the numerical model is the air/oxygen flow channel. It has also been specified as a high-porosity porous media region with ferritic stainless steel as the solid material and with the same anisotropic permeabilities and flow channel height used in the steam/hydrogen flow channel. The top separator plate and edge rails are identical to those on the bottom, but the edge rails are oriented perpendicular to the bottom edge rails to allow for the cross flow arrangement. The bottom separator plate in the FLUENT model serves as the electrical ground and the top separator plate serves as the current source.

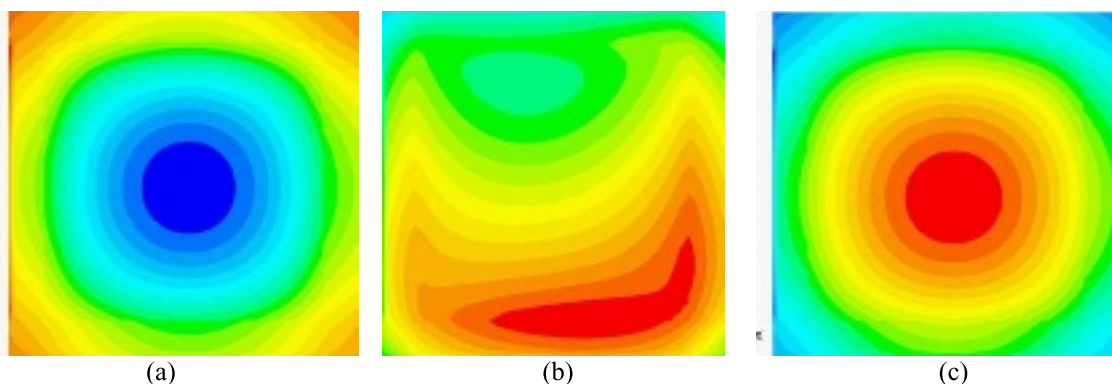
Additional parameters specified in the numerical model include the electrode exchange current densities and several gap electrical contact resistances. These quantities were determined empirically by comparing FLUENT predictions with stack performance data. The FLUENT model uses the electrode exchange current densities to quantify the magnitude of the activation overpotentials via a Butler-Volmer equation [1]. A radiation heat transfer boundary condition was applied around the periphery of the model to simulate the thermal conditions of our experimental stack, situated in a high-temperature electrically heated radiant furnace. The edges of the numerical model are treated as a small surface in a large enclosure with an effective emissivity of 1.0, subjected to a radiant temperature of 1 103 K, equal to the gas-inlet temperatures.

The gas flow inlets are specified in the FLUENT model as mass-flow inlets, with the gas inlet temperatures are set at 1 103 K and the inlet gas composition determined by specification of the mass

fraction of each component. The gas flow rates used in the model were the same as those used for the experimental base case, on a per-cell basis. For example, the base case for the steam/hydrogen inlet used a total inlet mass flow rate of 8.053×10^{-6} kg/s, with nitrogen, hydrogen and steam mass fractions of 0.51, 0.0074, and 0.483, respectively. The base case air flow rate was 4.33×10^{-6} kg/s.

Details of the core mass, momentum, energy, and species conservation and transport features of FLUENT are documented in detail in the FLUENT user manual [2]. Details of the electrochemical reactions, loss mechanisms, electric field computation, and electrode porous media constitutive relations are documented by Prinkey (ref. 1). This reference also documents the treatment of species and energy sources and sinks arising from the electrochemistry at the electrode-electrolyte interfaces.

Figure 8. 2 Temperature (K) contours on the electrolyte and insulator for currents of 10, 15, and 30 amps. Ranges (a) min (blue): 1 091 K, max (red): 1 100 K; (b) min: 1 102.5 K, max: 1 103.5 K ; (b) min: 1 139 K, max: 1 197 K



Results of Numerical Modelling

The air inlet temperature remains virtually fixed during the DC potential sweep because this temperature is used for feedback control to maintain a constant stack operating temperature. The four internal stack thermocouples respond as expected during the sweep. At voltages between the open-cell potential and the thermal neutral voltage, in the electrolysis mode, the stack internal temperatures are lower than the gas inlet and furnace setpoint temperatures because at this operating condition, the endothermic reaction heat requirement is greater than the ohmic heating^{3,4} and there is a net cooling effect on the stack. A thermal minimum point is reached at a cell operating voltage near 1.12 V and full thermal recovery is observed near the cell thermal neutral voltage of 1.29 V. The magnitude of the stack cooling and heating effects is greatest at the center of the stack, as indicated by the response of internal stack temperature 1. Internal stack temperatures 2 and 3 respond similarly to the center thermocouple, but with smaller amplitude, due to convective and radiative heat transfer effects near the edges of the stack. Stack internal #4 is in the top air flow channel, so its response is also constrained by radiant heat transfer. Note that the “furnace” thermocouple responds in a direction that is opposite of the stack internal thermocouples. This is because the feedback control demands more furnace power when the stack is tending to cool off and less power when the stack is tending to heat up. The mean electrolyte temperature was predicted in a FLUENT simulation obtained at the operating conditions of shown in Figure 5. The trend of the mean electrolyte temperatures with respect to operating voltage is similar to the trend observed with the thermocouple readings. However, the magnitude of the predicted temperature variation is greater than what was measured. This could be due to the fact that the FLUENT model, as it was configured for these calculations, does not include internal radiation heat transfer. We plan to investigate this effect further in our future modeling efforts.

Contour plots representing local FLUENT results for electrolyte temperature and current density are presented in Figure 8. In this figure, the steam/hydrogen flow is from top to bottom and the air flow is from left to right. Figure 8 shows electrolyte temperature contour plots for amperages of 10, 15, and 30 amps. These current values correspond to operating voltage regions near the minimum electrolyte temperature (10 amps), near thermal neutral voltage (15 amps), and in the region dominated by ohmic heating (30 amps). The radiant boundary condition at 1103 K tends to hold the outside of the model at a higher temperature for the 10-amp case (Figure 8 (a)), while the endothermic heat requirement maintains the center of the electrolyte at a lower temperature. Minimum and maximum temperatures for this case are 1 091 K and 1 100 K respectively. The center Figure 8 (b) shows a temperature difference across the electrolyte of only one degree K, with values very near 1 103 K; this current density is very near the thermal neutral voltage. Figure 8 (c) shows that ohmic heating in the electrolyte is dominating and the thermal boundary condition is keeping the edges cooler than the inside. Minimum and maximum temperatures are 1 139 K and 1 197 K, respectively, for this case.

Summary

A research program is under way at the Idaho National Laboratory to assess the performance of solid-oxide cells operating in the steam electrolysis mode for hydrogen production over a temperature range of 800 to 900°C. The research program includes both experimental and modeling activities. Selected results from both activities have been presented in this paper. Experimental results were obtained from a ten-cell planar electrolysis stack, with a per-cell active area of 64 cm², fabricated by Ceramtec, Inc. The electrolysis cells are electrolyte-supported, with scandia-stabilised zirconia electrolytes (~140 μm thick), nickel-cermet steam/hydrogen electrodes, and manganite air-side electrodes. The metallic interconnect plates are fabricated from ferritic stainless steel. The experiments were performed over a range of steam inlet mole fractions (0.1–0.6), gas flow rates (1 000–4 000 sccm), and current densities (0 to 0.38 A/cm²). Steam consumption rates associated with electrolysis were measured directly using inlet and outlet dewpoint instrumentation. Cell operating potentials and cell current were varied using a programmable power supply. DC potential sweeps performed on this stack demonstrated the effects of steam flow rate on stack performance. High ASR values and steam starvation were observed for the low-steam-content sweeps. A per-cell ASR value of 2.2 was demonstrated for a high-steam-content DC potential sweep at 830°C. Hydrogen production rates measured by the change in dewpoint of the gas flows were shown to be in excellent agreement with hydrogen production rates based on stack current. Internal stack temperatures measured with miniature thermocouples A stack cooling effect was directly observed for stack operating voltages between the open-cell potential and the thermal neutral voltage.

Hydrogen production rates in excess of 50 NL/hr were achieved with a 10-cell stack on several occasions during the time period from October 13 to October 20, 2004. At that time, we were not set up to do long-duration stack testing. The objectives of the 10-cell stack tests were to document stack performance characteristics such as ASR and hydrogen production rates over a range of operating conditions. Hydrogen production rates in excess of 100 NL/hr were maintained with a 22-cell stack for over 196 hours over the time period from July 26 to August 3, 2005. The stack endurance test was terminated due to instrumentation failure (an uninterruptible power supply failed), not due to any problem with the stack itself. Stack performance as measured by the per-cell ASR was good, although a lower value of ASR would be desirable.

A three-dimensional computational fluid dynamics (CFD) model was also created to model high-temperature steam electrolysis in a planar solid oxide electrolysis cell (SOEC). The model represents a single cell as it would exist in the experimental electrolysis stack. Mass, momentum, energy, and species conservation and transport are provided via the core features of the commercial

CFD code FLUENT. A solid-oxide fuel cell (SOFC) model adds the electrochemical reactions and loss mechanisms and computation of the electric field throughout the cell. The FLUENT SOFC user-defined subroutine was modified for this work to allow for operation in the SOEC mode. Model results provide detailed profiles of temperature, Nernst potential, operating potential, anode-side gas composition, cathode-side gas composition, current density and hydrogen production over a range of stack operating conditions. Mean model results were shown to compare favorably with the experimental results obtained from the ten-cell stack tested at INL. At operating voltages between the open-cell potential and thermal neutral, electrolyte temperatures are below 1103 K. A thermal minimum temperature occurs near 1.08 V. For operating voltages above thermal neutral, ohmic heating dominates and resultant electrolyte temperatures rapidly increase beyond 1103 K. Contour plots of local electrolyte temperature and current density indicated the effects of heat transfer, reaction cooling/heating, and change in local gas composition.

Acknowledgements

This work was supported by the US Department of Energy, Office of Nuclear Energy, Nuclear Hydrogen Initiative.

REFERENCES

- [1] Prinkey, M., Shahnam, M., and Rogers, W.A., "SOFC FLUENT Model Theory Guide and User Manual," Release Version 1.0, FLUENT, Inc., 2004.
- [2] FLUENT Theory Manual, version 6.1.22, Fluent Inc., Lebanon, New Hampshire, 2004.
- [3] O'Brien, J.E., Stoots, C.M., Herring, J.S., and Lessing, P.A., "Characterization of Solid-Oxide Electrolysis Cells for Hydrogen Production via High-Temperature Steam Electrolysis," Proceedings, 2nd International Conference on Fuel Cell Science, Engineering, and Technology, June 14-16, 2004, Rochester, NY, paper# 2474, pp., 219 – 228.
- [4] O'Brien, J.E., Stoots, C.M., Herring, J.S., and Lessing, P.A., "Performance Measurements of Solid-Oxide Electrolysis Cells for Hydrogen Production from Nuclear Energy," Proceedings, 12th ICONE Meeting, April 25-29, 2004, Arlington, VA, paper # ICONE12-49479.

POSSIBILITY OF A CHEMICAL HYDROGEN CARRIER SYSTEM BASED ON NUCLEAR POWER

Yukitaka Kato

Research Laboratory for Nuclear Reactors, Tokyo Institute of Technology

Abstract

Possibility of a chemical hydrogen carrier system for fuel cell vehicles, which utilised chemical reactions and capable to realise efficient hydrogen transportation with zero carbon dioxide emission and small explosion risk, was discussed in this study. The reactivity of metal oxide to carbon dioxide is used for the carbon dioxide fixation and also for heat source of fuel reforming. The performance of the combination of the chemical hydrogen carrier system and a high temperature gas reactor was estimated using experimental results. It was expected that the system realised low-pressure and safe storage of hydrogen carrier media consisting with the same energy efficiency of conventional water electrolysis system.

Introduction

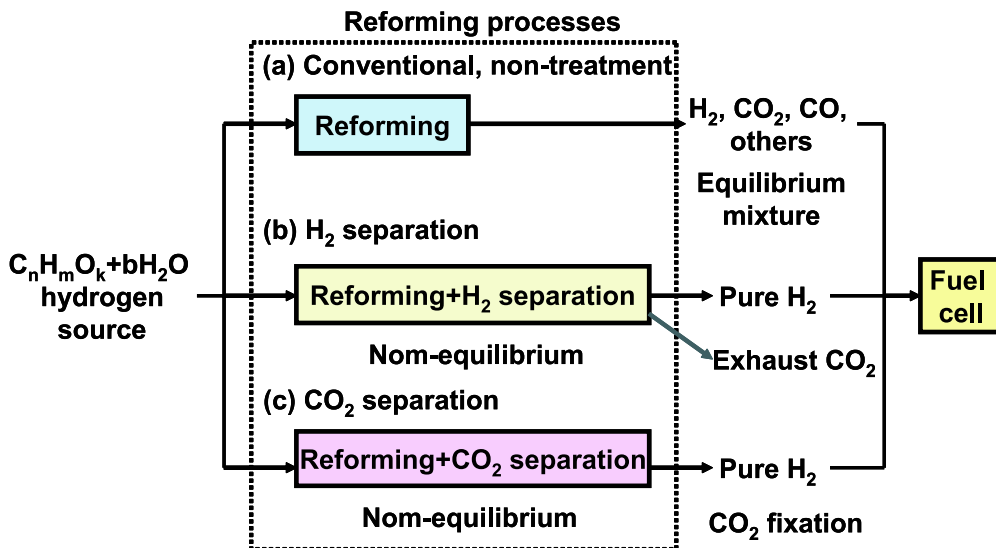
Fuel cell (FC) offers the possibility of expanding the electricity utilization market. Vehicles are seen as particularly good candidates for FC application, because FC is more compact, quieter and emit cleaner exhaust gas than conventional internal combustion engines. One of the key technologies that will make the widespread use of FC possible is a hydrogen (H_2) supply system. The uses of liquefied or compressed H_2 are candidates for this technology. However, the storage and transportation of either of these forms of H_2 require large amounts of energy as well as stringent safety precautions. These drawbacks make steam reforming of common fuels, such as methane, propane, methanol and kerosene, more practical solution for storing and supplying H_2 . Steam reforming can occur at the site of the FC. The use of these chemical reactants as a H_2 storage medium presents the possibility of a safe H_2 carrier and supply system. On the other hand, the reforming requires additional apparatuses for H_2 production, including at least three: a steam reforming reactor, a burner for reforming heat supply and a carbon monoxide converter. It is especially important for a reformer of FC vehicle to be compact and lightweight. A concept of a thermally regenerative steam fuel reformer for a vehicle had been proposed [1]. The reformer can realize compact reforming and achieve zero carbon dioxide (CO_2) emission by using chemical fixation of CO_2 . Finally, zero CO_2 emission H_2 carrier system using the reformer can be established. The system needs energy input for fuel reforming and fuel regeneration processes. Nuclear power plant is good candidate as energy source because it emits zero CO_2 in operation. This paper discussed the possibility of the chemical H_2 carrier system based on the above concept. The energy balance of the carrier system combined with a high temperature gas reactor (HTGR) was estimated using experimental results. The possibility of the carrier system was compared with other hydrogen system.

Concept of Chemical H_2 Carrier System

Separation Process for Fuel Reforming

Separation process would be key technique for high-efficient fuel reforming. Figure 1 shows concept of the separation processes to enhance H_2 yield. Conventional steam reforming in Figure 1 (a) for hydrocarbons attains to equilibrium and produces H_2 , carbon dioxide (CO_2) and carbon monoxide (CO). The yield of H_2 is restricted by equilibrium. Removing H_2 from reforming reaction system induces the system into non-equilibrium state by Le Chaterier's principle, and H_2 production is going on to establish the next equilibrium state in Figure 1(b). The yield of H_2 will be enhanced in the result. Removing CO_2 in Figure 1(c) induces also non-equilibrium state and enhances CO_2 production, then H_2 productivity and purity are also enhanced. These separation processes would realize not only high-yield of H_2 , but also decrease of temperature of the endothermic reforming. This study aims the demonstration of the CO_2 separation process for high-yield production of high-purity H_2 under lower temperature.

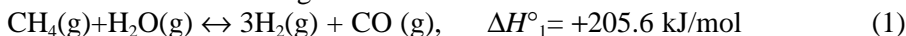
Figure 1. Separation processes for enhancement of H₂ yield in fuel reforming.



Regenerative Reformer

In this study, methane (CH₄) was chosen at first as a candidate reactant for steam reforming, because it is the most popular natural fuel resource and has a simple hydrocarbon fuel structure. The following regenerative reformer methodology is applicable also to kerosene and propane, both of which have reforming temperatures in the range of 700-900°C, similar to that of methane. The CH₄ steam reforming process consists of the following two gas phase reactions with various catalysts.

Methane steam reforming:

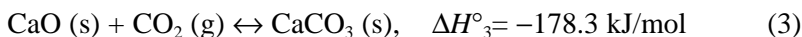


Carbon monoxide (CO) shift reaction:



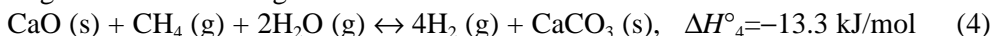
The study attempts to use calcium oxide (CaO) carbonation to remove carbon dioxide (CO₂) from the reformed gas and fix it.

Carbonation of calcium oxide:



This study aims to cause Eqs. (1), (2) and (3) reactions in the same reactor at once. These reactions, taken as a whole, are defined as regenerative reforming.

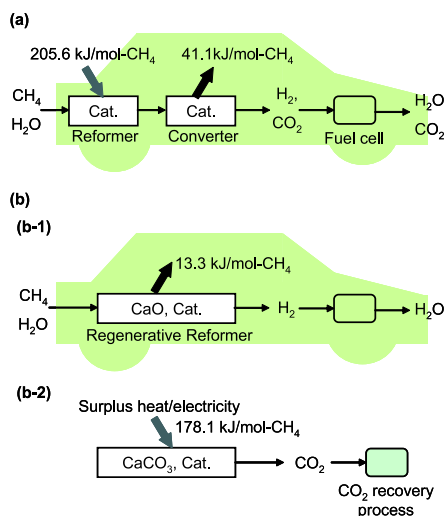
Regenerative reforming:



Conventional steam reforming is depicted in Figure 2 (a). CH₄ and water (H₂O) react by Eq. (1) in a catalytic reformer, and the generated CO is shifted by Eq. (2) into CO₂ and H₂ in a catalytic converter. The endothermic reforming process needs a heat supply of ΔH°_1 . The proposed process is shown in Figure 2 (b). This process consists of a reforming process (Figure 2 (b-1)) while the vehicle

is driving and a regenerating process (Figure 2 (b-2)) for calcium oxide regeneration and CO₂ recovery while the vehicle is turned off. CaO and a reforming catalyst mixture are packed in a regenerative reformer. Reactants are reformed by Eq. (1), and generated CO₂ is removed from the gas phase by the CaO carbonation of Eq. (3). The CO shift reaction of Eq. (2) is enhanced under the non-equilibrium condition realized by the CO₂ removal. Purified H₂ is generated from the reactor finally. The whole reaction of Eq. (4) is exothermic, hence the reaction needs no heat supply and can proceed spontaneously. A zero CO₂ emission drive is possible due to CO₂ fixation resulting from the carbonation. In the regenerating process, CaCO₃ is decomposed endothermically into CaO in the reactor using high-temperature heat, which is assumed to be supplied as heat from high temperature gas reactor, or as joule heat generated from off-peak electric output of other type nuclear power plants. The reformer is regenerated, and used again for the reforming. The proposed regenerative reformer is intended to be contained in a removable package for use in a FC vehicle. The package is loaded into and recovered from a vehicle at a regeneration station that supplies new packages and regenerates used ones. Regenerated CO₂ is managed according to a CO₂ recovery process.

Figure 2. Concept of a zero CO₂ emission FC vehicle using a thermally regenerative reformer; (a) conventional reforming, (b) proposed thermally regenerative reforming, (b-1) reforming mode, (b-2) regenerating and CO₂ recovering mode

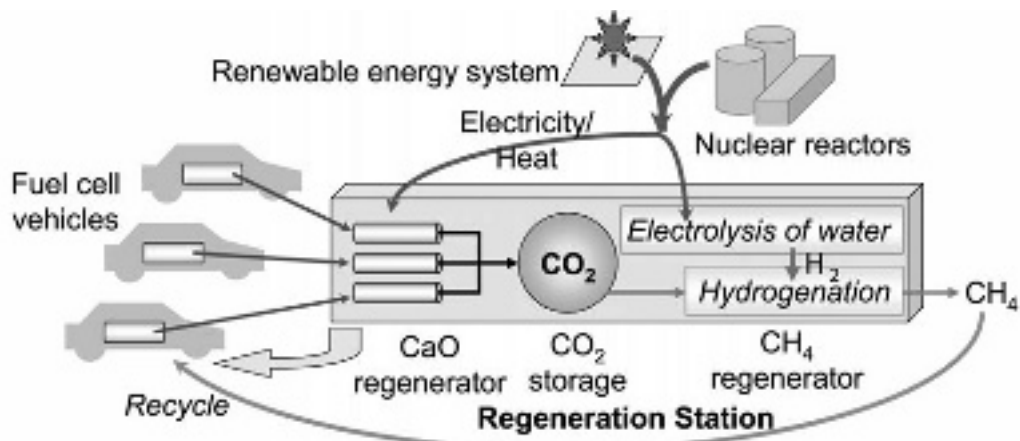


Zero CO₂ Emission chemical H₂ Carrier System

The concept of a zero CO₂ emission chemical H₂ carrier system using the regenerative reforming process depicted in Figure 2(b) is proposed in Figure 3. The zero CO₂ emission system consists of FC vehicles using packages of the regenerative reformer, a decentralised package regeneration station, and power systems for energy supply to the system. The regeneration station plays central role in the system. The packages are loaded in FC vehicles. The vehicles are driven by H₂ fuel produced from the packages. The packages after reforming are collected to the regeneration station. The packages are regenerated, that is, decarbonated thermally using thermal output or joule heat produced from renewable energy or nuclear power plant. Regenerated packages are reused repetitively in the vehicles. Generated CO₂ is recovered in a storage vessel, and is regenerated in hydrocarbons at a hydrocarbon regenerator by hydrogenation process using H₂, which is generated from water electrolysis consuming the power plant output. Regenerated hydrocarbons are reused cyclically in the vehicles. A comprehensive zero CO₂ emission system is formed using the hydrocarbon regeneration process. The system was expected to contribute on load leveling of renewable energy or nuclear power plant

operations by utilizing off-peak electricity or thermal output of the plants as heat source for the CaO and hydrocarbons thermal regeneration processes. Especially a high temperature gas reactor is appropriate for the power plant because thermal output from the reactor can be used in cascade from CaO regeneration process and CH₄ regeneration process.

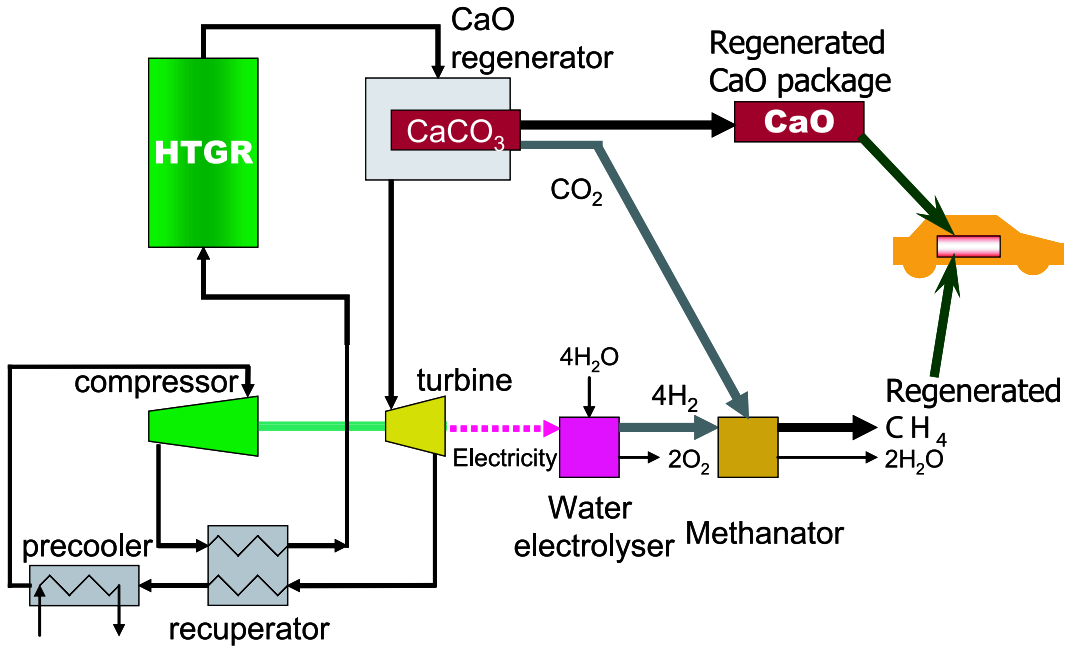
Figure 3. Zero CO₂ emission H₂ carrier system using the thermally regenerative reformer driven by off-peak electricity and heat from renewable energy and nuclear power plants.



The proposed H₂ carrier system for FC vehicles has several merits. Firstly, because the FC system using the proposed process emits no CO₂ during operation, a zero CO₂ emission vehicle system could be established, so long as the treatment of CO₂ is managed well after it is removed from the package, and the system can transport H₂ safely under low-pressure and as low-explosive chemicals. The reforming process is simpler than conventional reforming systems. Because the regenerative reforming is exothermic, the reforming proceeds automatically by self-heating, then, heat conduction control step arisen by heating for conventional reforming can be removed. The power-generation efficiency of a FC after with the reformer will be enhanced by the supply of the reformed high-purified H₂. In a conventional system, H₂ effluent gas from the FC is burned for the next reforming, because the CO₂ concentration in the gas is too high for the cell to use. In the proposed system, on the other hand, the H₂ concentration is higher enough than one of a conventional system, enabling the H₂ to be consumed highly in the cell. Therefore, the proposed system also enhances the H₂ economy of the FC. Because the reformation equilibrium temperature is shifted to a lower temperature than in a conventional system, the exothermic CO shift reaction is enhanced naturally. Furthermore, the CO reduction induced by the enhancement is advantageous for FC durability.

The simultaneous reaction concept for H₂ production from methane steam reforming had been patented by Williams [2]. A fluidised bed concept using a reforming catalyst and carbon dioxide acceptor for H₂ production was patented by Gorin and Retallik [3]. Shift reaction and carbon dioxide removal in a single-reactor packed with a calcium oxide mixture were examined by Chun Han [4]. Calcium oxide as a CO₂ absorber was also applied to regenerative H₂ production by Balasubramanian [5]. Those proposals were based on the use of the regenerative reforming process in fixed plants for H₂ production, such as a fluidised bed or a combined system of a packed-bed reactor and gas turbine. Continuous batch-wise H₂ production system using two regenerative reformers is proposed for a vehicle use by Specht [6]. This study proposed a new concept of zero CO₂ emission H₂ carrier system utilizing the reaction concept.

Figure 4. Combination of the zero CO₂ emission H₂ carrier system using the thermally regenerative reformer driven with a high-temperature gas reactor.



Combination with nuclear reactors

The H₂ carrier system has compatibility with HTGR. Figure 4 shows combination with the H₂ carrier system with an HTGR. The HTGR thermal output is utilised in cascade at the CaO regenerator and gas-turbine. CaO package and hydrocarbon fuels are regenerated in the system. CaO regenerator is placed in the primary coolant loop of the HTGR. Regeneration of CaO from CaCO₃ of the package is proceeded in the reactor. CaO regeneration process is relatively safe process, and then the reactor can be placed in the primary loop directly. The coolant is used secondary at gas turbine for electricity production. Electricity output is used in a water electrolyser for hydrogen production. CO₂ generated from the regenerator and H₂ from the electrolyser are supplied into a methanator, and then, CH₄ is regenerated. Finally this process regenerates CaO and the reforming fuel.

The HTGR is zero CO₂ emission energy source to establish zero CO₂ emission H₂ carrier system. Although the carrier system is applicable to use renewable energy, nuclear reactor has good combination with the H₂ carrier system on the stand point of stable and large-enough energy supply.

Performance Evaluation

Evaluation of the chemical H₂ carrier system

To evaluate the advantage of the chemical H₂ carrier system depicted in Figure 4, the system was compared with conventional H₂ production process using water electrolysis. Enthalpy balances of those systems per 1 mole of H₂ production were shown in Figure 5. Conventional water electrolysis in Figure 5(a) consumes electricity for water electrolysis process of 282 kJ-electric/H₂-mol, and H₂ compression of 29 kJ-e/H₂-mol. The compression is assumed isentropic and 5 stages compression up to 700 bar. Total enthalpy of 311 kJ/H₂-mol is required. The H₂ carrier system in Figure 4(b) needs

thermal input of 44.6 kJ-thermal/H₂-mol for CaO regeneration, electricity input of 282 kJ-e/H₂-mol for water electrolysis, and 4.9 kJ-e/H₄-mol equivalent for CH₄ compression to 175 bar. The compression is assumed also isentropic and 5 stages compression. Enthalpy of 332 kJ/H₂-mol is needed totally. The H₂ carrier system needs enthalpy input slightly larger than the electrolysis. On the other hand, a methanation process of generated CO₂ and H₂ produces exothermically thermal output of 41.1 kJ-t/H₂-mol at around 300-700 °C. When thermal output from the methanation is utilized in some heating process, total enthalpy consumption would be reduced. Enthalpy input for water electrolysis process is dominant in total input at both the conventional and the carrier systems. On-board reforming in Figure 5(c) needs smaller enthalpy input than one of other systems which have water electrolysis process. However, CO₂ is emitted from the former system.

Figure 5. Enthalpy balance of H₂ systems, (a) conventional H₂ system using water electrolysis, (b) the zero CO₂ emission H₂ carrier system, (c) conventional methane steam reforming.

* Isenthalpic & 5 stages compression up to 700 bar. ** Isenthalpic & 5 stages compression up to 175 bar.

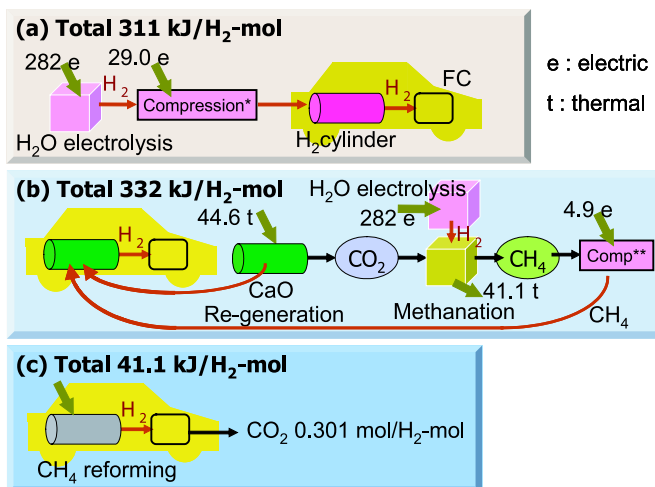


Table 1. Estimated contribution of an HTGR power plant on hydrogen systems

	Proposed H ₂ carrier system	Conventional water electrolysis system
HTGR thermal power ¹		600 MWt
Outlet coolant temperature from HTGR		850°C
HTGR operation duration for hydrogen processes		8 h/day
Inlet/outlet coolant temperature for CaO regenerator	850/835 °C	-
Inlet/outlet coolant temperature for gas-turbine	835/587 °C	850/587 °C
Power input for CaO regeneration	34.8 MWt	-
Plant power input for gas-turbine power generation	565.2 MWt	600.0 MWt
Gas-turbine power efficiency ²	44.3 %	45.0 %
Water electrolysis efficiency (ΔH base) ³		90 %
Compression pressure	175 bar-CH ₄	700 bar-H ₂
Power for H ₂ electrolysis	245.8 MWe	247.1 MWe
Power for compression	3.8 MWe-CH ₄	22.9 MWe-H ₂
H ₂ production/equivalent	2.26E+07 H ₂ -mol equiv.	2.27E+07 H ₂ -mol
Number of FC vehicles for 100 km mileage each ⁴	4.52E+04 -	4.54E+04 -

1. Based on GTHTTR300 [7], 2. Power efficiency for the carrier system is estimated by Carnot's efficiency ratio of turbines between the carrier system and the conventional electrolysis system. 3. Ref. [8], 4. It is assumed that H₂ of 500 mol is required for 100 km mileage.

Estimation of the system combined with HTGR

Thermal feasibility of the H₂ carrier system and conventional water electrolysis systems depicted in Figure 5 was evaluated. Optimized energy balances of both hydrogen systems based on HTGR is shown in Table 1. It was assumed that the gas turbine high temperature reactor named as GTHTTR 300 designed by JAERI [7] circulating helium coolant was used as the HTGR in the estimation. Off-peak output of 600 MWt for 8 h/day from the HTGR was used for the regeneration of the reformer and hydrogen production.

In conventional water electrolysis system, thermal output from the HTGR at 850°C is used at a gas turbine for electricity power generation with efficiency of 45.0% [7]. Hydrogen is produced by water electrolysis consuming the electric power with efficiency of 90% [8]. Produced hydrogen is compressed for on-board use up to 700 bar by a compressor consuming a part of the electric power. In the chemical H₂ carrier system, thermal output from HTGR between 835°C and 850°C is used for CaO regeneration firstly, and rest of heat is consumed for power production at the gas turbine. Power efficiency for the carrier system is estimated by Carnot's efficiency ratio between the carrier system and the electrolysis system, which is calculated from both inlet coolant temperatures for the turbine.

Hydrogen is produced by the same process of the water electrolysis system [8]. Methane is produced exothermically from recovered CO₂ and produced H₂. Produced methane is compressed for on-board use up to 175 bar by a compressor consuming a part of the power. Finally the carrier system is capable to supply hydrogen of 2.26x10⁷ mol to FC vehicles of 4.52 x10⁴, assuming that H₂ of 500 mol is required for 100 km mileage.

The vehicle number is almost same with the value of the conventional electrolysis system of 4.54×10^4 . Required amounts of electric and thermal energy are shown also in the table. Because thermal energy consumption for CaO is only 5.8% of the whole HTGR output, and the compression work is fairly smaller than one of the electrolysis system, then, energy for both hydrogen production processes are closed, and finally both vehicles number are quite similar. It is reduced from the evaluation that the carrier system can deliver hydrogen to FC vehicles on-board under the same efficiency with conventional water electrolysis system. The carrier system stores fuel source, CH₄, under relatively lower pressure at 1/4 of the storage pressure for the conventional electrolysis H₂ system. The result shows that the H₂ carrier system has advantage to conventional H₂ system in the point of the reduction of fuel storage pressure and the compressor work cost. The regenerative reforming is applicable for higher-hydrocarbon fuels, such as propane and kerosene. Especially the carrier system based on liquid fuel would be candidates of attractive hydrogen carrier media because the compression work would be reduced more.

Conclusion

The proposed zero CO₂ emission H₂ carrier system for FC vehicles using a regenerative fuel reformer based on nuclear power has unique performance comparing with conventional H₂ production systems.

The carrier system is capable to reduce hydrogen media storage pressure, and realise more safety H₂ transportation to FC vehicle.

The carrier system has good compatibility with a high temperature gas reactor, because the regeneration process, which is relatively safe, can be applicable at the primary loop of the reactor. Off-peak power of 600 MWt for 8 h from a reactor can supply H₂ for FC vehicles of 45 thousands, which is the similar number for conventional electrolysis system under the same thermal input from the reactor. The carrier system shows a new possibility of chemical energy carrier system.

REFERENCES

- [1] Kato, Y., K. Ando, Y. Yoshizawa, J. Chem. Eng. Japan, 36(7), 860-866 (2003).
- [2] Williams, R.; "Hydrogen production," U. S. Patent 1,938,202 (1933).
- [3] Gorin, E., W.B. Retallik, U. S. Patent 3,108,857 (1963).
- [4] Chun Han, D.P. Harrison, Chem. Eng. Sci., 49, 5875-5883 (1994).
- [5] Balasubramanian, B., B.A. Lopez, S. Kaytakoglu, D.P. Harrion, Chem. Eng. Sci., 54, 3543-3552 (1999).
- [6] Specht, M., A. Bandi, F. Baumgart, T. Weimer, PCT patent WO01/23302 (2001).
- [7] Kunitomi, K., S. Katanishi, S. Takada, T. Takizuka, T. Nakata, X. Yan, M. Takei, S. Kosugiyama, S. Shiozawa; "Design Study on Gas Turbine High Temperature Reactor (GTHTR300)", Journal of Atomic Energy Society of Japan (in Japanese), 1(4), 352-360 (2002).
- [8] Takenaka, H., "R&D on solid polymer electrolyte water electrolysis in Japan", Proceedings of International Hydrogen and Clean Energy Symposium '95, p165.

SESSION V

**BASIC AND APPLIED SCIENCE IN SUPPORT OF NUCLEAR HYDROGEN
PRODUCTION**

Chairs: Y. Kato, P. Anzieu, Y. Sun

This page intentionally left blank

A STUDY ON THE HI CONCENTRATION BY POLYMER ELECTROLYTE MEMBRANE ELECTRODIALYSIS

**Chang-Hee Kim, Byung Kyun Kim, Kyoung-Soo Kang, Chu-Sik Park, Sang-Ho Lee,
Seong-Dae Hong, Gab-Jin Hwang and Ki-Kwang Bae**

Hydrogen Production Research Center
Korea Institute of Energy Research
71-2 Jang-dong, Yuseong-gu, Daejeon 305-343, Republic of Korea

Abstract

Concentration of HI over HIx solution by polymer electrolyte membrane electro dialysis was investigated using galvanodynamic and galvanostatic polarisation method. For this purpose, HIx solution with sub-azeotrope composition ($\text{HI} : \text{I}_2 : \text{H}_2\text{O} = 1.0 : 0.5 : 5.8$) was prepared. It was noticed that the electrical energy demand for electro dialysis of HIx solution decreases with increasing temperature. From the experimental results, it is concluded that the system resistance crucially affects the electro dialysis cell overpotential and hence the optimisation of cell assembly as well as the selection of low resistance materials should be carried out in order to obtain high performance electro dialysis cell.

Introduction

Thermochemical water-splitting iodine sulphur (IS) process is considered as the most promising method for large scale, high efficiency, and environmentally benign hydrogen production [1]. The IS process is comprised of three coupled chemical reactions such as Bunsen reaction, sulphuric acid decomposition reaction, and HI decomposition reaction [2]. The reaction scheme is described as follows:



Many works have been done on the evaluation of the thermal efficiency of the IS process by optimizing their closed-cycle loop [1, 3-5]. They reported that the hydriodic acid concentration part is the most energy consuming process since the HIx solution (HI - I₂ - H₂O mixture) produced from the Bunsen reaction present in an azeotrope composition. And hence the distillation part to concentrate hydriodic acid needs lots of excess thermal energy, giving rise to total thermal efficiency drop in IS process.

To solve these problems, GA researchers [2] adopted an extractive distillation by using phosphoric acid. In this process, the phosphoric acid extracts only I₂ and H₂O and finally HI can be concentrated. However, it contains phosphoric acid concentration process by steam recompression, making the whole process to be complicated and corrosive. In 2003, Hwang *et al.* [6], tried to concentrate HI in HIx solution by electro-electrodialysis method. They reported that the energy demand of electro-electrodialysis to produce 1mole of hydrogen was much lower than that of steam recompression in GA process and the application of electro-electrodialysis in IS process seems to be very useful with proposing the possibility of high thermal efficiency.

In this respect, the present work discusses the polymer electrolyte membrane electro-dialysis method to concentrate the HI over HIx solution. For this purpose, we prepared HIx solution with sub-azeotrope composition (HI : I₂ : H₂O = 1.0 : 0.5 : 5.8) and the polymer electrolyte membrane electro-dialysis was investigated using galvanodynamic and galvanostatic polarisation method.

Experimental

The activated carbon fiber cloth was cut into the size of 5 cm x 5 cm to form the carbon electrode. The carbon electrode was immersed in ethanol solution overnight to remove the residuals and then dried at room temperature.

The Nafion 117 (Du Pont, USA) was used as a polymer electrolyte membrane. The membrane was pretreated by boiling in 3 wt.% H₂O₂ solution for 1 h, followed by boiling in 0.5 M H₂SO₄ for 1h. Thereafter, the membrane was placed in boiling water for 1 h, and the procedure was repeated at least twice to remove completely the sulfuric acid.

The HIx solution was prepared from the mixing of hydriodic acid (55~58 wt.%, Kanto Chemicals Co., Japan) and Iodine (99%, Junsei Chemicals Co., Japan) with mole ratio of HI : I₂ = 1.0 : 0.5. From the titration result of HIx solution, it was confirmed that the mole ratio of as-prepared HIx solution was HI : I₂ : H₂O = 1.0 : 0.5 : 5.8. This indicated that the HI molarity of starting solution was 9.55 mol kg⁻¹-H₂O, which is lower than the azeotrope composition of 11.11 mol kg⁻¹-H₂O.

A single cell assembly was composed of polymer electrolyte membrane sandwiched with two carbon electrodes, gaskets, and carbon blocks with flow channels for the distribution of reactant HIx solution as shown in Figure 1 (a). The single cell was placed in a mantle heater to maintain a desired temperature. Figure 1 (b) shows the schematic illustration of the experimental arrangements for electrochemical measurements. The volumes of HIx solution (HI : I₂ : H₂O = 1.0 : 0.5 : 5.8) were 430 and 190 ml in anolyte and catholyte reservoirs, respectively. The reservoirs and all glass lines were cast in double jacket that were heated with silicon oil at the same temperature.

Results and discussion

Figure 2. displays cell potential measured from the electro dialysis cell as a function of operation temperature. As operation temperature increased from 35 to 90°C, the cell potential decreased from 0.68 to 0.41 V at the applied current of 2 A. This is because high temperatures reduce the amount of electrical energy required to concentrate HI molarity from a thermodynamic standpoint and hence electrical energy demand ΔG for electro dialysis of HIx solution decreases with increasing temperature [7]. Furthermore, high temperature operation quite generally favours reaction kinetics decreasing activation overpotential.

In this respect, it is assured that high temperature operation is advantageous for electro dialysis of HIx solution. In this work, the operation cell temperature was selected as 90°C. If not specifically indicated, all the electrochemical measurements in the present study were carried out at 90°C.

Figure 3 illustrates the current-potential curves measured on the electro dialysis cell. The potential exhibited linear increase with the applied current over all current ranges. It is well known [8] that current-potential curve has a characteristic shape and clearly shows three distinct regions with respect to the applied current. In the low current range, the shape of current-potential curve is convex and transformed to linear in the intermediate current range. Then the shape changed to concave in the high current range.

The overpotential in the low current range is ascribed to the activation overpotential, which is caused by the slowness of the reactions taking place on the surface of the electrode. In the intermediate current range, the overpotential is mainly due to the ohmic losses of the system. The appearance of overpotential in the high current range is primarily ascribed to the mass transfer limitation of the involved species.

Under the circumstances, it is reasonable to say that the reaction kinetics on the surface of carbon electrode is facilitated and hence the activation overpotential is not observed. However, the system resistance such as electrode, electrolyte, polymer electrolyte membrane, and carbon block could be dominant, influencing cell overpotential over all current ranges. Therefore, it is necessary to reduce the system resistance by selecting the cell constituents with low resistance and optimising the cell assembly.

It is noticed that the vapour pressure of HI over HIx solution steeply increases right after the azeotrope composition [9]. Accordingly, the thermal burden imposed on the distillation could be drastically diminished. The azeotrope composition of HIx solution is HI : H₂O = 1.0 : 5.0 (HI molarity: 11.11 mol kg⁻¹-H₂O). However, as mentioned earlier, the HIx solution prepared in this work was of sub-azeotrope composition with HI molarity 9.55 mol kg⁻¹-H₂O. Therefore, we tried to concentrate HI over azeotrope composition from sub-azeotrope composition examining electrochemical behaviour of the cell.

Figure 4 (a) plots the cell potential against elapsed time with applied current of 2 A. The cell potential steadily increased from 0.40 to 0.47 for 2 h. At the same time, the HI molarity increased up to 11.9 mol kg⁻¹-H₂O in catholyte, while that in anolyte decreased up to 8.7 mol kg⁻¹-H₂O. The ratio of HI molarity change between catholyte and anolyte from the starting composition is about 2.6. Taking into account that the volume of HIx solution in anolyte is almost 2.3 times as much as that in catholyte, it can be said that the amount of HI molarity change in two solutions is roughly the same.

From the experimental results, we concluded that electrical energy demand ΔG for electro dialysis of HIx solution decreases with increasing temperature. Moreover, the electro dialysis cell overpotential is primarily influenced by the system resistance and hence the thermal efficiency of the cell could be improved by reducing the constituent resistance and by optimizing the cell assembly.

Acknowledgement

This work has been done under “Nuclear Hydrogen Production Technology Development and Demonstration (NHDD) Project” and we are grateful to MOST for financial help.

REFERENCES

- [1] L.C. Brown, G.E. Besenbruch, R.D. Lentsch, K.R. Schultz, J.F. Funk, P.S. Pickard, A.C. Marshall, S.K. Showalter, "High efficiency generation of hydrogen fuels using nuclear power", Final Technical Report GA-A 24285, General Atomic, Inc., San Diego, CA (2002).
- [2] J.H. Norman, G.E. Besenbruch, and D.R. O'keefe, "Thermochemical water-splitting for hydrogen production", GRI-80/0105, (1981).
- [3] D.R. O'keefe, C. Allen, G. Besenbruch, L. Brown, J. Norman, and R. Sharp, "Preliminary results from bench-scale testing of a sulfur-iodine thermochemical water-splitting cycle", International Journal of Hydrogen Energy, 7, 381-392 (2000).
- [4] S. Kasahara, S. Kubo, K. Onuki, M. Nomura, "Thermal efficiency evaluation of HI synthesis/concentration procedures in thermochemical water splitting IS process", International Journal of Hydrogen Energy, 29, 579-587 (2004).
- [5] S. Goldstein, J.-M. Borgard, X. Vitart, "Upper bound and best estimate of the efficiency of the iodine sulphur cycle", International Journal of Hydrogen Energy, 30, 619-626 (2005).
- [6] G.-J. Hwang, K. Onuki, M. Nomura, S. Kasahara, and J.-W. Kim, "Improvement of the thermochemical water-splitting IS (iodine-sulfur) process by electro-electrodialysis", Journal of Membrane Science, 220, 129-136 (2003).
- [7] H. Wendt, Electrochemical Hydrogen Technologies: Electrochemical Production and Combustion of Hydrogen, p. 213, Elsevier Science Publishers B.V., The Netherlands (1990).
- [8] J. Larminie and A. Dicks, Fuel Cell Systems Explained, p. 37, John Wiley & Sons, England (2000).
- [9] D. Neumann, "Phasengleichgewichte von $H_2/H_2O/H_2$ loesungen", Diplomarbeit, RWTH Aachen (1987).

Figure 1. Schematic diagram of (a) electro dialysis cell and (b) experimental arrangements used for concentrating HI over HIx solution

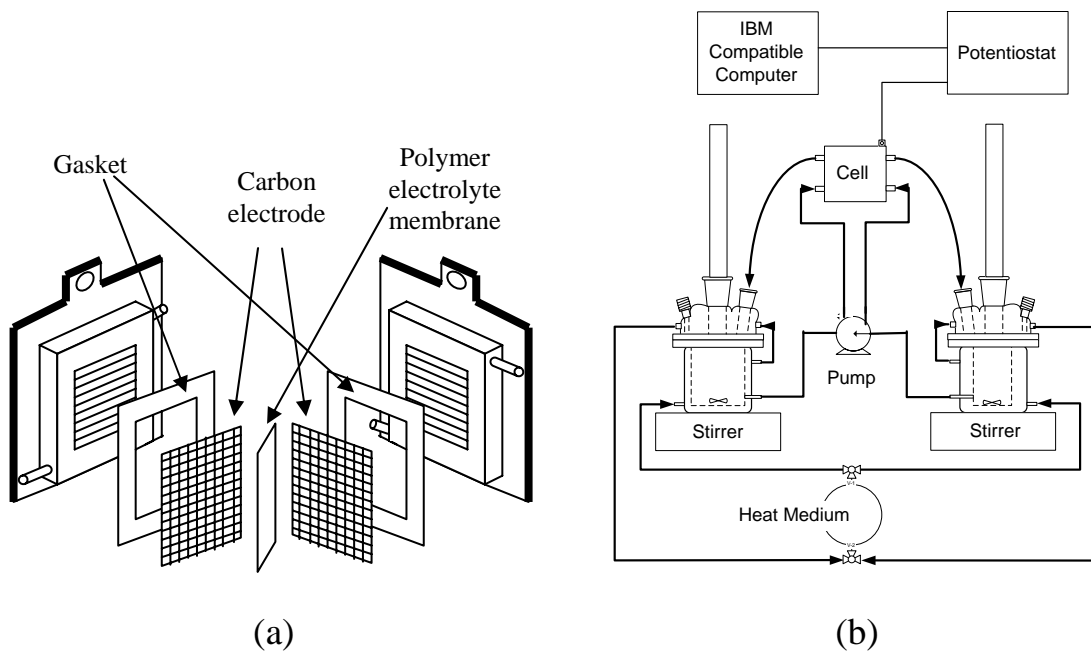


Figure 2. Plots of cell potential against operation temperature measured on the electro dialysis cell at the applied current of 2A. The apparent area of activated carbon electrode was 25 cm².

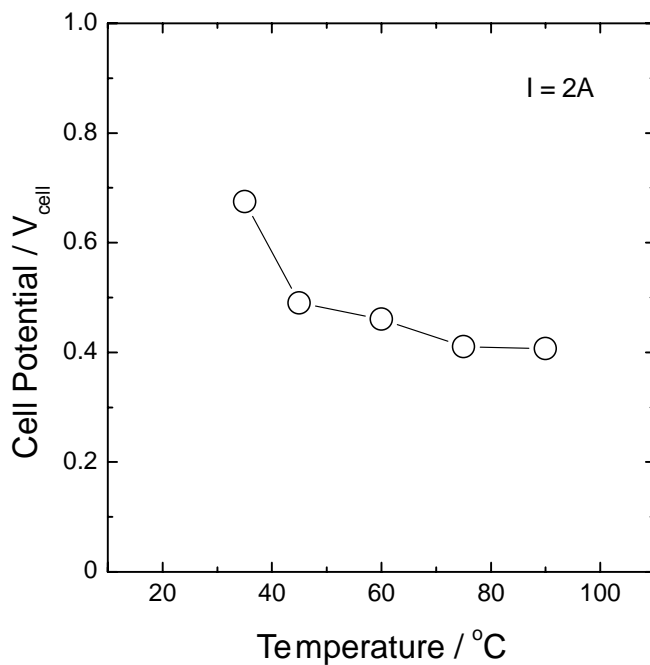


Figure 3. Galvanodynamic polarization curves measured on the electro dialysis cell at the operation temperature of 90°C.

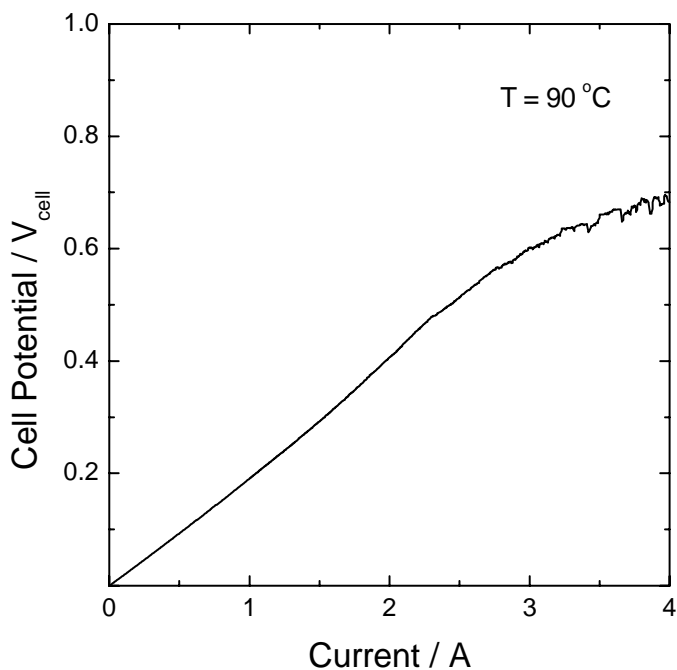
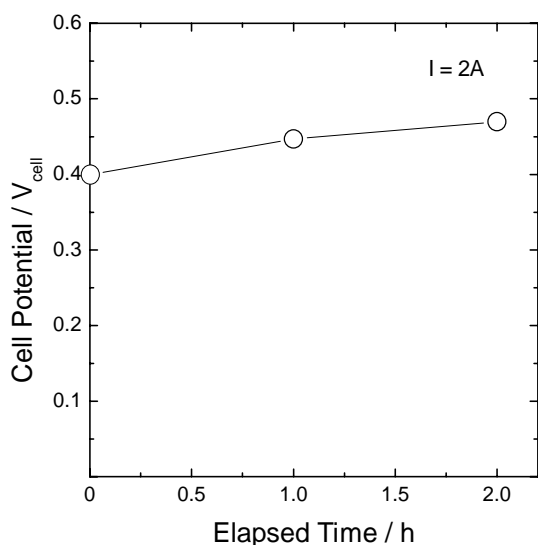
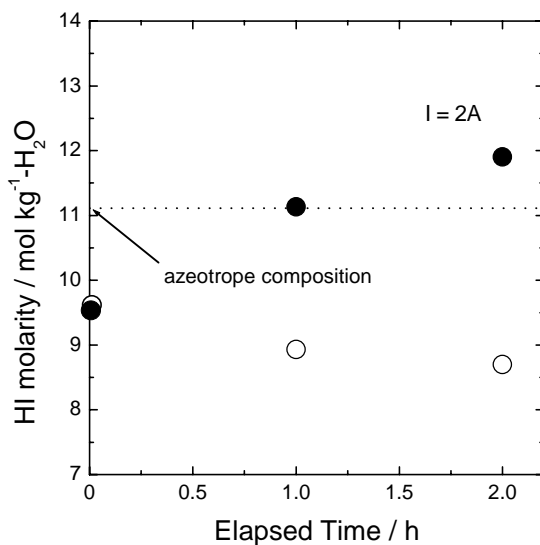


Figure 4. Plots of (a) cell potential and (b) HI molarity against elapsed time measured on the electro dialysis cell at the operation temperature of 90°C. The applied current on the cell remained constant with 2 A throughout the measurement.



(a)



(b)

This page intentionally left blank

THE PREPARATION CHARACTERISTICS OF HYDROGEN PERMSELECTIVE MEMBRANE FOR HIGHER PERFORMANCE IN IS PROCESS OF NUCLEAR HYDROGEN PRODUCTION

Ho-Sang Choi^a, Gab-Jin Hwang^b, Chu-Sik Park^b, Hae-Jin Kim^c, and Ki-Kwang Bae^b

^aDept. of Chemical Engineering, Kyungil University, Gyeongsan-si, 712-701, Korea

^bHydrogen Prod. Res. Center, Korea Institute of Energy Research(KIER), Daejeon, 305-343, Korea

^cEnergy Nano Material Team, Korea Basic Science Institute(KBSI), 305-333, Korea

E-Mail : choihs@kiu.ac.kr

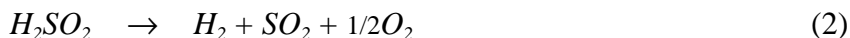
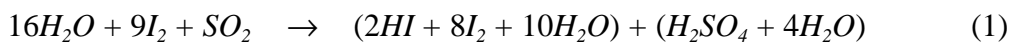
Abstract

The thermochemical splitting of water has been proposed as a clean method for hydrogen production. The IS process is one of the thermochemical water splitting processes using iodine and sulfur as reaction agents. The silica membrane to apply for the HI decomposition membrane reactor of the IS process was prepared by sol-gel and thermal CVD methods. In the preparation of membrane through sol-gel method, the permeation characteristics of hydrogen and nitrogen belong to the Knudsen flow pattern, but water is different. The hydrogen permeation was dominated by the activated diffusion, then the activation energy of hydrogen was ca. 5 kJ/mol. In the preparation through thermal CVD method, the size of deposited silica particle was obtained less than 11 nm, and the thickness of deposited layer was about 2 μm . Then, the selectivity of H_2 on N_2 was 26.3 at 450, and the permeance of H_2 was 6×10^{-8} mol/Pa.m².s.

Introduction

Hydrogen is the most abundant element on earth, and an attractive fuel for the secondary energy carrier system of future, because it is renewable as the energy resources and also it has the potential to be storable, transportable, and environmentally prior. Currently, hydrogen is produced primarily by steam reforming of fossil fuel, but there is little generation of carbon dioxide in an operation. The important interest is in hydrogen production from renewable clean resources, and the technology using water is significant as well.

The thermochemical splitting of water has been proposed as a clean method for hydrogen production. The IS(Iodine-Sulfur) process is one of the thermochemical water splitting process using the nuclear heat of 1 000°C from the high temperature gas-cooled reactor (HTGR). The IS process consisted of the following reactions[1,2], and Figure 1 shows a schematic diagram of the IS process,



The reaction(1) is the Bunsen reaction. Water reacts with I₂ and SO₂ into the two kinds of acids (HI, H₂SO₄). These acids are separated due to their immiscible properties at excess I₂ condition. H₂SO₄ decomposition reaction(2) is an endothermic reaction, which proceeds in two stages: gaseous H₂SO₄ decomposes spontaneously into H₂O and SO₃ at 400~500°C, and then SO₃ decomposes into SO₂ and O₂ at 800°C in the presence of a solid catalyst. HI decomposition reaction(3) can be carried out in the gas phase or in the liquid phase.

The Iodine-Sulfur (IS) process has such attractive characteristics that all chemicals circulate in the process as fluid, H₂SO₄ decomposition proceeds stoichiometrically with a high conversion ratio, and this reaction is a large entropy change, the temperature range of which is suitable for utilising the nuclear heat energy supplied by the high temperature gas-cooled reactor (HTGR). Kasahara *et al.* [3,4] evaluated the effects of process parameters on the total thermal energy for IS process, and hydrogen production on IS process reported by JAERI research group[5]. Finally, HI decomposition procedure to obtain hydrogen is one of the core operations in the IS process, as the equilibrium conversion is comparatively low. Recently, Nomura *et al.* [6] analysed and estimated on a hydrogen permselective membrane reactor using silica membrane. Chemical vapor deposition(CVD) has become one of the most important methods of the active layer of an inorganic membrane. The CVD technique is also used in the wide area for improving and modifying the membranes or the chemical catalysts[7-9].

In this study, the silica membranes to apply for HI decomposition reaction was investigated, and prepared by the sol-gel and the thermal chemical vapor deposition (CVD) methods. The objective of this work is to study the characteristics of the silica membrane preparation and the hydrogen permselectivity of the membrane reactor used for HI decomposition in the thermochemical water splitting IS process.

Experimentals

The silica membrane was prepared through sol-gel deposition and chemical vapor deposition methods. The porous α -alumina tube (O.D., 5.0 mm; I.D., 3.5 mm; length, 300 mm), supplied by Nano Pore Materials Co. Ltd., Korea, was used as a support. The mean pore size and porosity of the support tube were 0.1 μm and 35%, respectively. The effective length of membrane was 100~150 mm at the middle of the tube, and both edges were glazed with a SiO_2 -BaO-CaO sealant (Nippon Electric Glass, GA-13), and then calcined at 1200°C.

The preparation of silica membrane through sol-gel method was followed as Figure 1. The chemicals used for combination of metal alkoxide solution in sol-gel coating were tetraethylorthosilicate [TEOS, $\text{Si}(\text{OC}_2\text{H}_5)_4$], tetrapropylzirconate [$\text{Zr}(\text{OC}_3\text{H}_7)_4$], and yttrium-acetatehydrate [$\text{Y}(\text{CH}_3\text{COO})_3 \cdot 4\text{H}_2\text{O}$], obtained from Aldrich. The metal alkoxide content in sol-gel solution was 72.7 wt%.

The preparation of silica membrane by the thermal chemical vapor deposition was performed through the apparatus of Figure 2. the silica deposition in the absence of oxygen (by TEOS pyrolysis) was carried out. TEOS(obtained from Aldrich) carried by nitrogen flowing through the bubbles was introduced to the quartz CVD reactor tube at 6.5 NL/min. The reactor tube was 42 mmID and 300 mm length. The reactor tube was designed able to treat the alumina tube bundle as the multi-preparation type at once. Figure 3 is shown the expected structure of both silica composite membranes.

Figure 1. Procedure for a silica membrane preparation by sol-gel method.

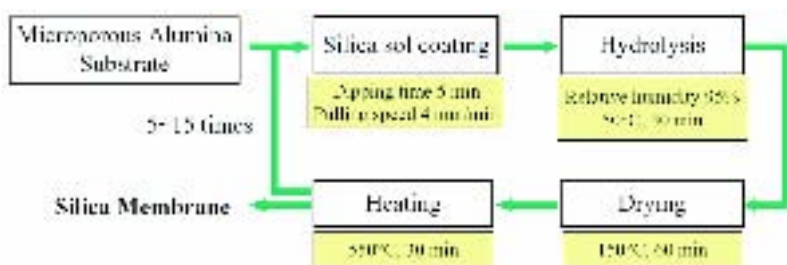


Figure 2. The schematics drawings for CVD apparatus of silica membrane preparation.

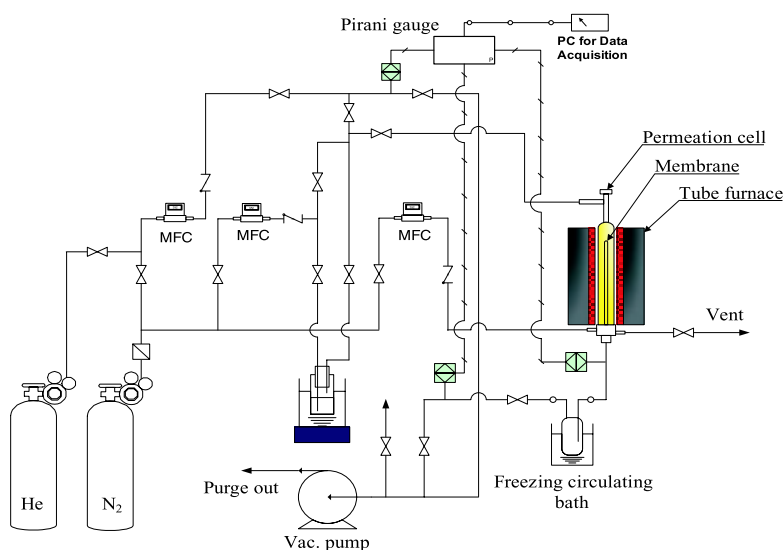
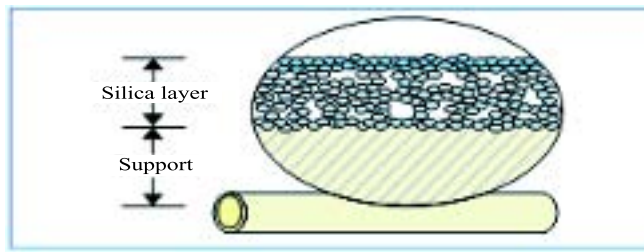


Figure 3. The expected structure of a silica membrane



Gas permeation experiments were carried out at 303~773K by using single or binary gas systems of hydrogen and nitrogen, etc. The membrane was fixed in a stainless steel(SS316) reactor placed in an electrical furnace.

Results and Discussions

Membrane characteristics through sol-gel coating

First of all, the permeation test has been performed by using pure gas. The total mass flow in the membrane is composed of surface flow and Knudsen flow [7]. The change of total flow has affected with surface flow and Knudsen flow.

If the permeation mechanism of composite membrane was affected by only Knudsen flow, the permeability was decreased with increasing operation temperature. But this phenomenon is different from the kind of gas. Even if it is considerable to the surface diffusion flow, the results are such as Figure 7. As shown in Figure 4, hydrogen and nitrogen are following with Knudsen flow, but water is different. Therefore, the former was not affected with changing temperature, the latter was not in accordance. In case of hydrogen, the hydrogen permeation was dominated by the activated diffusion. The nitrogen permeability was smaller than the hydrogen permeability in the range over about 450K. This may be thought that the kinetic diameter of nitrogen(3.64 Å) is larger than that of hydrogen (2.86 Å) and nitrogen cannot penetrate through the non-porous layer of the membrane. The nitrogen gas would permeate through pores much larger than the molecular diffusion.

Figure 4. Examination of surface and Knudsen flow

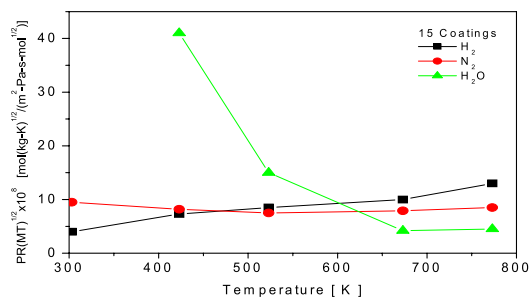


Figure 5 shows the effect of the operating temperature on the permeability of composite membrane. With increasing temperature, the permeability increased linearly all together. The activation energies of hydrogen in the operating temperature range were ca. 5 kJ/mol, which was in the range of the other data reported for silica-modified membrane. A linear relationship is observed between the permeability and the inverse of the absolute temperature. This suggests that the silica membrane

structure did not change even if temperature changes. Figure 6 shows the permeation flux of nitrogen as a function of the operating pressure gradient in the silica composite membrane system.

Figure 5. The relationship of permeability on operating temperature by sol-gel preparation

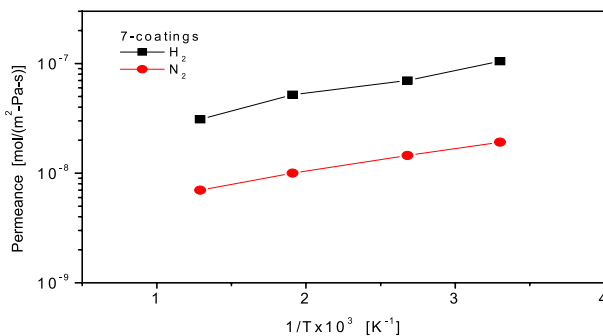
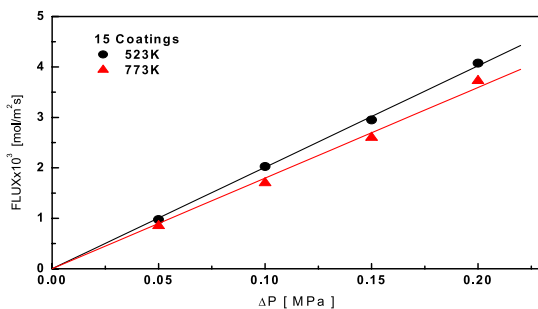


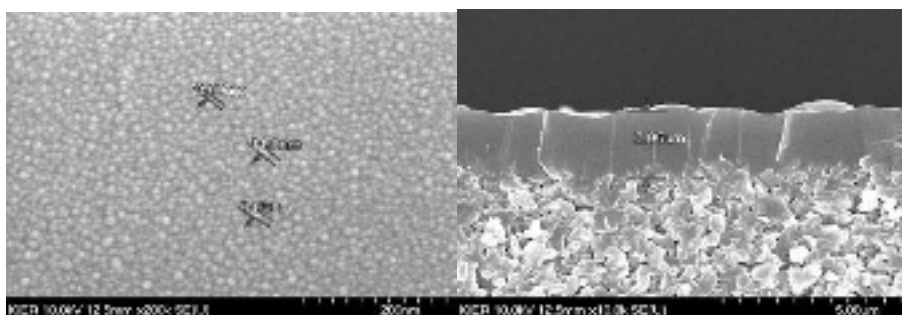
Figure 6. The pressure difference vs. permeation flux on N₂ gas by sol-gel preparation



Membrane characteristics through thermal CVD

Figure 7 shows the morphology of the thermal CVD prepared membrane. The size of deposited silica particles was mostly not exceeding 11 nm, and the thickness of deposited layer was about 2 μm . Figure 8 shows an EDX analysis of the interface between the support and CVD deposited layer. A silica layer was uniformly formed on the top of the support with or without evacuation through the porous support. It is supposed that the growth of the deposited silica occurred towards the horizontal and the vertical directions in the pore.

Figure 7. The scanning electron micrograph of the prepared membrane through CVD



(a) top surface of silica zone

(b) cross section

Figure 8. The EDX analysis of the interface between the support and CVD deposited

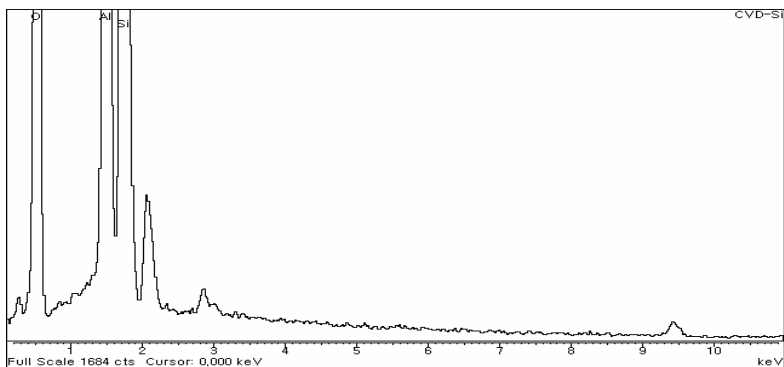


Figure 9 shows the change of CVD pressure and permeance of He and N₂ with the elapsed time. At the treatment of multi-tube bundle, the initial evacuated pressure was high compared with a single tube treatment generally, but the total average permeance of single gas was obtained the similar results. The selectivity of He on N₂ in CVD treatment was 2.48 at starting point, about 6 after 8 hrs, and 8.3 after 15 hrs. In CVD treatment, the calcination time serve an important role for the fixation of deposited silica layer. It was controlled by the change of an evacuated pressure.

Figure 10 shows the effect of permeation temperature on permeance of membrane through CVD of single component gas. With increasing temperature, the permeance was not changed more than a little. In the whole range of operating temperature, the selectivity of H₂ on N₂ was 21.8 at 300°C, 26.3 at 450°C, and 30.8 at 600°C, and the permeance of hydrogen was obtained 6x10⁻⁸ mol/Pa.m².s.

Figure 9. The change of CVD pressure and permeance of He and N₂ with the elapsed time

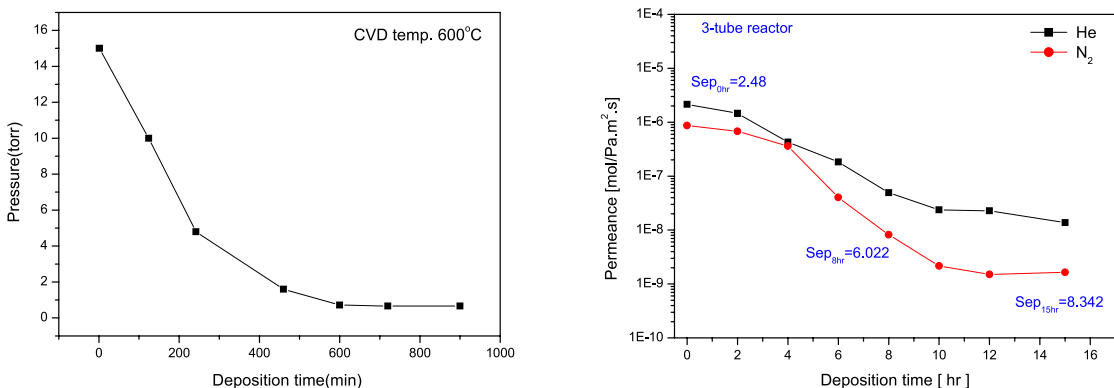
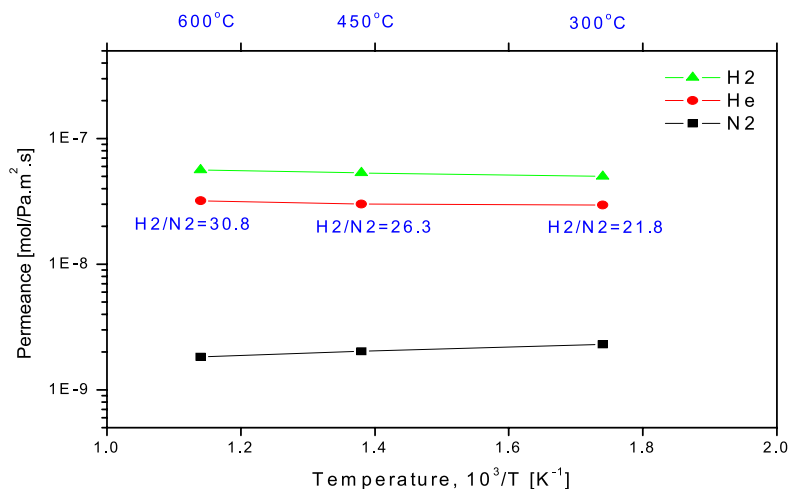


Figure 10. The effect of permeation temperature on permeance of membrane through CVD



Conclusions

The silica membrane to apply to the HI decomposition membrane reactor of the IS process was prepared by sol-gel and thermal CVD methods.

In the preparation of membrane through sol-gel method, the permeation characteristics of hydrogen and nitrogen belong to the Knudsen flow pattern, but water is different. The hydrogen permeation was dominated by the activated diffusion, and the activation energy of hydrogen was ca. 5 kJ/mol.

In the preparation through thermal CVD method, the size of deposited silica particle was obtained less than 11 nm, and the thickness of deposited layer was about 2 μm. Then, the selectivity of H₂ on N₂ was 26.3 at 450, and the permeance of H₂ was 6x10⁻⁸ mol/Pa.m².s.

Acknowledgements

This work has been done under “Nuclear Hydrogen Production Technology Development and Demonstration (NHDD) Project” and we are grateful for financial support to the Ministry of Science and Technology (MOST), Korea.

REFERENCES

- [1] J.H. Norman, G.E. Besenbruch and D.R. O'Keefe, "Thermochemical water-splitting for hydrogen production," GRI-80/0105, (1981).
- [2] J.H. Norman, G.E. Besenbruch, L.C. Brown, D.R. O'Keefe and C.L. Allen, "Thermochemical Water-Splitting Cycle, Bench-Scale Investigations, and Process Engineering," GA-A161713 (1982).
- [3] S. Kasahara, Gab-Jin Hwang, Ho-Sang Choi, K. Onuki, and M. Nomura, "Effects of the process parameters of the IS process on total thermal efficiency to produce hydrogen from water," J. Chem. Eng. Jpn, 36(7), 887-899 (2003).
- [4] S. Kasahara, S. Kubo, K. Onuki, and M. Nomura, "Thermal efficiency evaluation HI synthesis/concentration procedures in the thermochemical water splitting IS process," Int. J. Hydrogen Energy, 29, 579-587 (2003).
- [5] H. Nakajima, K. Ikenoya, K. Onuki, and S. Shimizu, "Closed cycle continuous hydrogen production test by thermochemical IS process," Kagaku Kogaku Ronbunshu, 24(2), 352-358 (1998).
- [6] M. Nomura, K. Ikenoya, S. Kasahara, S. Kubo, K. Onuki, Gab-Jin Hwang, Ho-Sang Choi, and Shin-ichi Nakao, "Development of a hydrogen permselective membrane reactor using a silica membrane for the IS process," Proceeding of WHEC15-Yokohama, 242 (2004).
- [7] S. Yan, H. Maeda, K. Kusakabe, S. Morooka, and Y. Akiyama, "Hydrogen permselective SiO₂ membrane formed in pores of alumina support tube by chemical vapor deposition with tetraethyl orthosilicate", Ind. Eng. Chem. Res., 33, 2096-2101 (1994).
- [8] M. Tsapatsis, S.J. Kim, S.W. Nam, and G. Gavalas, "Synthesis of hydrogen permselective SiO₂, TiO₂, Al₂O₃, and B₂O₃ membranes from the chloride precursors", Ind. Eng. Chem. Res., 30, 2152-2159 (1991).
- [9] S. Sato, M. Toita, T. Sodesawa, and F. Nozaki, "Catalytic and acidic properties of silica-alumina prepared by chemical vapor deposition", Applied Catal. A, 62, 73-84 (1990).
- [10] Gab-Jin Hwang and K. Onuki, "Simulation study on the catalytic decomposition of hydrogen iodide in a membrane reactor with a silica membrane for the thermochemical water-splitting IS process," J. Membr. Sci., 194, 207-215 (2001).
- [11] C. Berndhaeuser and K.F. Knoche, "Experimental Investigations of Thermal HI Decomposition from H₂O-HI-I₂ Solution," Int. J. Hydrogen Energy, 19, 239-244 (1994).

THERMAL DECOMPOSITION OF SO₃

Hidetoshi Karasawa¹⁾, Akira Sasahira¹⁾, and Kuniyoshi Hoshino²⁾

¹⁾ Power & Industrial Systems R&D Laboratory, Hitachi, Ltd.

²⁾ Hitachi Works, Hitachi, Ltd.

Abstract

The iodine-sulfur and the Westinghouse method are recognised as thermochemical methods for producing hydrogen from water. Thermal decomposition of SO₃ is an important process in both methods. This study evaluated the decomposition rate of SO₃ using a flow type apparatus. The decomposition rate of SO₃ was evaluated by the temperature dependence of oxygen concentration using a chemical kinetic model. The decomposition of SO₃ was assumed to be homogeneous reaction of first order. The decomposition rate without catalyst was estimated to be $3.99 \times 10^{11} \exp(-33,096/T) \text{ s}^{-1}$. When hematite was used as the catalyst, the decomposition rate constant increased drastically to $1.31 \times 10^{15} \exp(-36,299/T) \text{ s}^{-1}$. The decomposition ratio for cases with the catalyst was found to approach 1.0 within 2 seconds at 1173K by the chemical dynamics calculation. This indicated that the decomposition of SO₃ was efficient at 1173K.

Introduction

Hydrogen is a promising fuel for the next-generation energy systems. Nuclear energy can provide heat and electricity to produce hydrogen. Thermochemical decomposition of water using nuclear heat has been studied for hydrogen production. Iodine-sulfur (IS) and Westinghouse (WH) method are recognised as high efficient thermochemical methods of producing hydrogen from water [1]. Thermal decomposition of sulfur trioxide (SO_3) is an important process in both the IS and WH method. Although thermochemical data of SO_3 is available, the decomposition rate of SO_3 is not established.

This study evaluated the decomposition rate of SO_3 using a flow type experimental apparatus. Using the obtained decomposition rate, time dependence of the SO_3 concentration was calculated by the chemical kinetic model to find a suitable temperature for the decomposition of SO_3 .

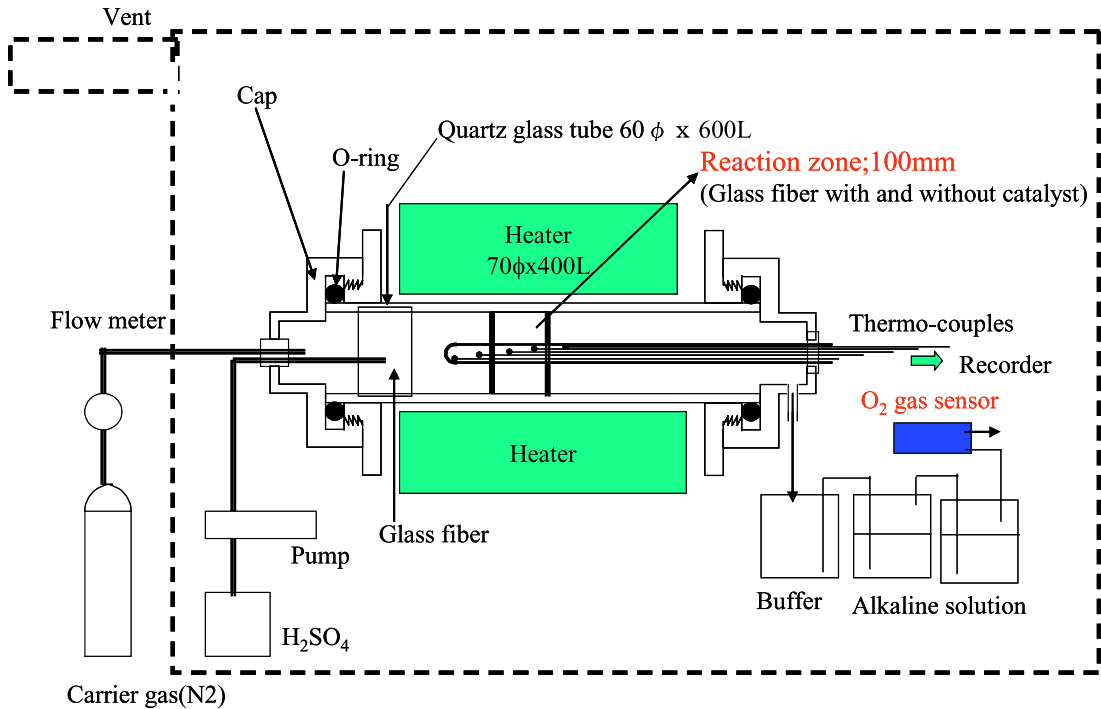
Experimental

The experimental apparatus consisted of an electric heater, a glass tube and gas bubblers as shown in Figure 1. The apparatus was set in a ventilator due to high toxicity of sulfur dioxide (SO_2). The glass tube was set inside the heater. Nitrogen was used as a carrier gas. Sulfuric acid (H_2SO_4) decomposed into SO_3 and water in the inlet part of the glass tube. Then SO_3 decomposed into SO_2 and oxygen in near the center of the glass tube, where a temperature was the highest in the glass tube. After the gases were passing through water in the gas bubblers, the concentration of oxygen was measured.

The flow rate of nitrogen was changed from 0.2 to 0.4 L/min. H_2SO_4 was fed to the glass tube at a rate of about 0.05 cc/min. The temperature inside the glass tube was heated up to 1323K. Temperature distribution in the glass tube was measured by 5 thermocouples. The temperature increase rate was changed from 5 to 20 K/min. The decomposition rate of SO_3 was estimated by the temperature dependence of oxygen concentration using a chemical kinetic model.

Glass fiber with and without a catalyst was used to examine effect of the catalyst on the decomposition of SO_3 . Although a suitable catalyst for the SO_3 decomposition is not known well, a catalyst such as the salts of vanadium and silver, ferric oxide, chromium oxide, and some of rare earths is used by industry for production of H_2SO_4 . The catalyst used for the decomposition of SO_3 was ferric oxide or hematite due to its availability.

Figure 1. Experimental apparatus



Decomposition Rate of SO_3

Chemical Kinetic Model

H_2SO_4 decomposes thermally as follows;



The first reaction occurs at a temperature of around 773K. So H_2SO_4 was expected to decompose at the inlet of the glass tube. The decomposition rate constant of the reaction 2, k , can express in an Arrhenius' formula,

$$k = A \exp (-B/T) \quad (3)$$

where A is pre-exponential factor, B is constant equals E/R , E is activation energy, R is gas constant, and T is temperature. The decomposition ratio, X , was defined as follows,

$$\begin{aligned} X &= [\text{SO}_2] / [\text{SO}_3]_0 \\ &= 2 [\text{O}_2] / [\text{H}_2\text{SO}_4] \end{aligned} \quad (4)$$

where [A] represented molar concentration of A species and 0 showed the initial state. Here the initial concentration of SO₃ was equal to the feeding concentration of H₂SO₄ assuming complete decomposition of H₂SO₄. The oxygen concentration corresponded to half of SO₂ concentration according to the reaction 2. When the decomposition of SO₃ was assumed to be homogeneous reaction of first order, the thermal decomposition rate was expressed as follows,

$$\begin{aligned} d[\text{SO}_2] / dt &= k [\text{SO}_3] \\ d([\text{SO}_2]/[\text{SO}_3]_0) / dt &= k ([\text{SO}_3]_0 - [\text{SO}_2]) / [\text{SO}_3]_0 \\ dX / dt &= k (1 - X) \end{aligned} \quad (5)$$

The following equation could be obtained by integrating the equation 5 [2].

$$\ln\{-\ln(1 - X) / T^2\} = \ln(A / \phi B) - B / T \quad (6)$$

where ϕ is temperature increase rate. If the term of $\ln\{-\ln(1 - X) / T^2\}$ was plotted against $1/T$, the decomposition rate constant could be obtained from the slop and intercept.

Determination of Decomposition Rate Constant

Figure 2 shows plots of $\ln\{-\ln(1 - X) / T^2\}$ as a function of $1/T$ for cases without the catalyst. The slops should be the same for the cases with different temperature increase rates. The temperature increase rates were 5, 10, and 20 K/min. After the experiment, there was yellowish residual near the outlet of the glass tube. If it was sulfur, further decomposition of SO₃ might occur. In that case, the slops were not the same for the three cases since the decomposition mechanism was differ from the above reactions.

If the decomposition of SO₃ assumed to follow the reaction 2, the average decomposition rate constant without the catalyst was evaluated to be $3.99 \times 10^{11} \exp(-33,096/T) \text{ s}^{-1}$ from the slops and intercepts shown in Figure 2.

Figure 3 shows plots of $\ln\{-\ln(1 - X) / T^2\}$ as a function of $1/T$ for cases with the catalyst. The slops were the same for cases with different temperature increase rates. The temperature increase rates were 5, 10, and 20 K/min. The average decomposition rate constant with the catalyst was evaluated to be $1.31 \times 10^{15} \exp(-36,299/T) \text{ s}^{-1}$. The decomposition rate constant increased drastically when the catalyst was used.

Figure 2. Decomposition rate without the catalyst

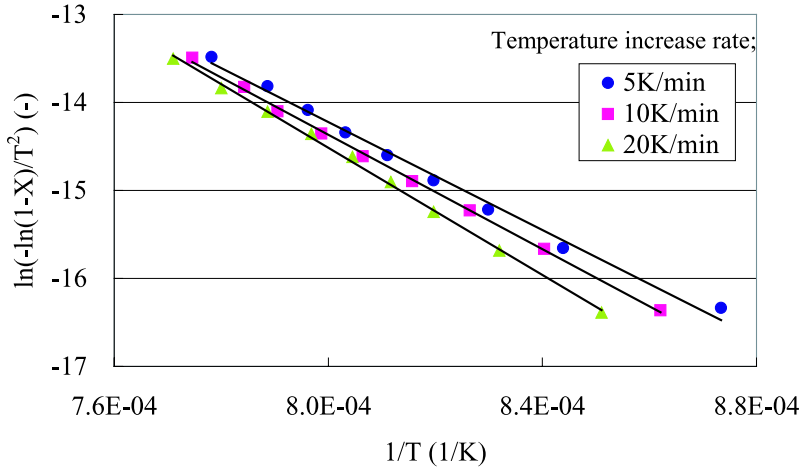
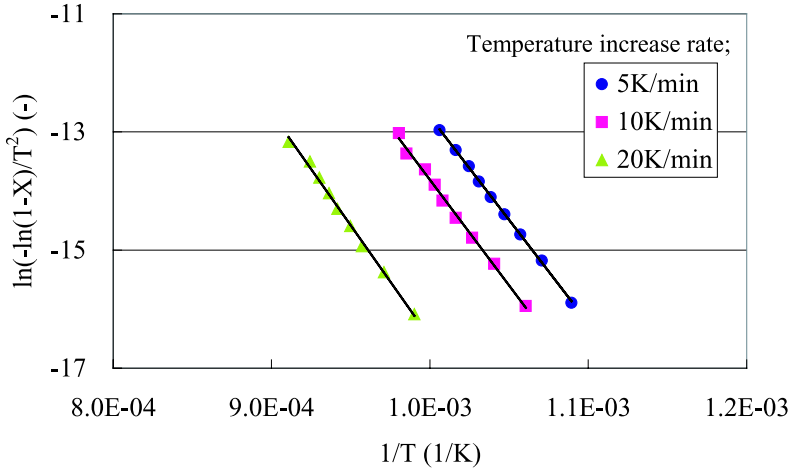


Figure 3. Decomposition rate with the catalyst



Temperature Dependence of Decomposition Ratio

Although the reaction 2 was assumed to be the decomposition reaction, the actual decomposition mechanism of SO_3 was written as follows,

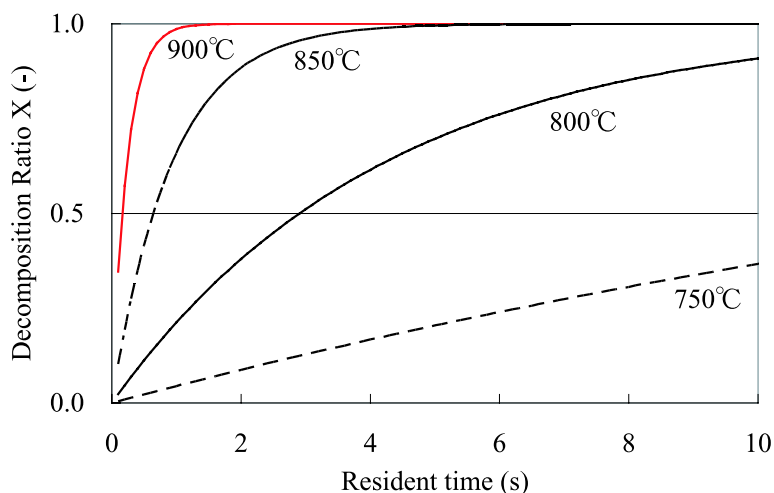


where k is rate constant and M is third species such as water and nitrogen gas in this case. The concentrations of species were calculated by the chemical dynamics calculation. In the calculation, the rate constants were assumed based on the above data and the references [3, 4]. Figure 4 shows the time

dependence of the decomposition ratio for cases with the catalyst. The time needed to reach the decomposition ratio of 1.0 corresponded to resident time in a decomposer of SO_3 . The resident time decreased with increase of a temperature. This indicated that the thermal efficiency was improved with increase of a temperature. The resident time was about 2 seconds at 1 173K. At this temperature, the size of the decomposer could be reduced with the high thermal efficiency.

The decomposition ratio was approaching 1.0 as shown in Figure 4. The decomposition ratio calculated by a thermal equilibrium calculation was about 0.9 at 1 173K. This indicated that the back reaction rate was slower than that expected by the equilibrium calculation. The rate constant of the reaction 9 corresponding to the back reaction was smaller by a factor of 3 than that of the reaction 8 corresponding to the forward reaction. Therefore, the decomposition ratio became nearly 1.0.

Figure 4. Time dependence of decomposition ratio



Summary

The iodine-sulfur (IS) and the Westinghouse (WH) method are recognized as thermochemical methods for producing hydrogen from water. Thermal decomposition of SO_3 is an important process in both the IS and WH method. This study evaluated the decomposition rate of SO_3 using a flow type apparatus. The time dependence of oxygen concentration was measured with a constant temperature increase rate. The decomposition rate of SO_3 was estimated by the temperature dependence of oxygen concentration using a chemical kinetic model. The followings were clarified.

(1) The decomposition of SO_3 was assumed to be homogeneous reaction of first order. The decomposition rate without catalyst was estimated to be $3.99 \times 10^{11} \exp(-33,096/T) \text{ s}^{-1}$. When hematite was used as the catalyst, the decomposition rate constant increased drastically to $1.31 \times 10^{15} \exp(-36,299/T) \text{ s}^{-1}$.

(2) The concentration of chemical species was evaluated by the chemical dynamics calculation. The decomposition ratio for cases with the catalyst approached 1.0 within 2 seconds at 1 173K.

(3) The size of the decomposer of SO_3 could be reduced if the decomposition temperature increased to 1 173K. The thermal efficiency of the decomposition was evaluated to be almost 1.0 at 1 173K.

REFERENCE

- [1] L.C. Brown *et al.*, “Initial screening of thermochemical water-splitting cycles for high efficiency generation of hydrogen”, General Atomics Report, GA-A23373 (2000).
- [2] A.W. Coats and J.P. Redfern, *Nature*, 201, 68(1964).
- [3] K.J. De Wiff, “Sulfur Oxidation and Contrail Precursor Chemistry”, NASA, NASA/CR-2003-212293(2003).
- [4] T.A. Chubb, “Analysis of Gas Dissociation Solar Thermal Power System”, *Solar Energy*, 17, 129(1975).

This page intentionally left blank

DIRECT ENERGY CONVERSION BY PROTON-CONDUCTING CERAMIC FUEL CELL SUPPLIED WITH CH₄ AND H₂O AT 600-800°C

Satoshi Fukada*, Shigenori Suemori, Ken Onoda

Department of Applied Quantum Physics and Nuclear Engineering, Kyushu University

*Corresponding author: 6-10-1 Hakozaki, Higashi-ku, Fukuoka 812-8581, Japan

Tel +81-92-642-4140, Fax +81-92-642-3800, Email sfukada@nucl.kyushu-u.ac.jp

Abstract

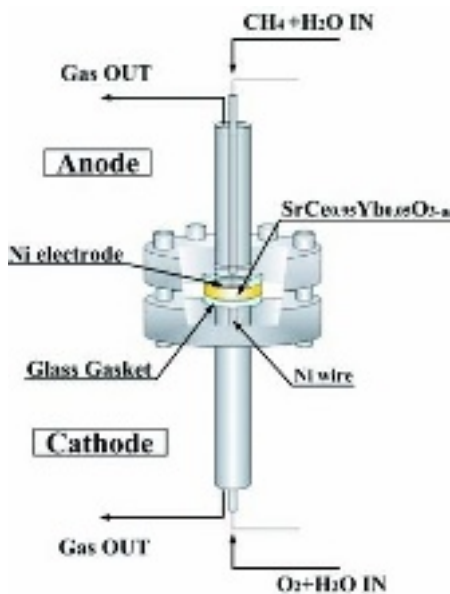
Relations between current density and terminal voltage (I-V curves) of the proton-conducting ceramic of SrCe_{0.95}Yb_{0.05}O_{3-a} were determined for application to a fuel cell working at 600 - 800°C. In a similar way to the introduction of a H₂ + H₂O mixture, its anode supplied with a CH₄ + H₂O mixture worked as a fuel cell efficiently without any external CH₄-to-H₂ reformer. The overall electric resistance for the CH₄ + H₂O supply was larger than that for the H₂ + H₂O supply, because of activation over-potential of the anode electrode. Although a small amount of carbon deposited at a narrow interface between the ceramic and the Ni/SiO₂ electrode, it did not affect cell performance. The overall conductivity was smaller than other fuel-cell systems such as PEM-FC. Application to the recovery of tritium from process streams of a fusion reactor was discussed in terms of the protonic conductivity.

Keywords: proton-conducting ceramic, Sr-Ce-Yb oxide, fuel cell, high temperature, CH₄ steam reforming, internal reform.

1. Introduction

Some doped perovskite-type oxides exhibit proton conduction at higher temperatures. SrCeO₃- or CaZrO₃-based ceramics demonstrated higher proton-conducting performance at 600°C to 1 000°C [1]. Therefore, application to a hydrogen pump, a hydrogen sensor and a hydrogen (or tritium) purifier operated at 600-800°C is expected in the nuclear engineering field, especially in the tritium recovery process of fusion reactors [2-4]. In order to apply proton-conducting ceramics to produce H₂ and electricity for the effective use of nuclear heat as well as to recover tritium from gas streams in fusion reactors, combining steam-reforming reaction of CH₄ on a Ni catalyst with a proton-conducting ceramic fuel cell was studied experimentally. Especially we focused on mass and charge transfer in a SrCeO₃-based proton-conducting ceramic with internal reformation on a Ni electrode under the supply of CH₄ + H₂O. The oxide used in the present experiment was SrCe_{0.95}Yb_{0.05}O_{3-a}, and the electrodes were composed of a Ni wire mesh and Ni-SiO₂ paste comprising Ni and SiO₂ fine particles and a vaporable paste. The cell system was described by CH₄+H₂O|Ni|SrCe_{0.95}Yb_{0.05}O_{3-a}|NiO|O₂+H₂O. Several I-V characteristic curves (i.e., electric current density, I, versus cell potential, V) were determined for different H₂O/CH₄ concentration ratios in the temperature range of 600 to 800°C. A thermodynamic electromotive force, E₀, and an overall electric conductivity, σ, were determined from the interrupt on the y-axis of an I-V curve and its slope, respectively. These results were compared with our previous results of the direct and alternating current methods [4,5]. They were determined under the condition where a similar cell system composed of SrCe_{0.95}Yb_{0.05}O_{3-a} and porous Ni/SiO₂ electrodes was supplied with a mixture of H₂ + H₂O in the anode and with a mixture of O₂ + H₂O in the cathode. We observed surfaces in/on the porous anode electrode using a SEM (Scanning Electron Microscope) and an EDX (Energy Dispersive X-ray spectroscopy), and we investigated whether or not carbon deposited in/on the porous Ni/SiO₂ electrode.

Figure 1. Experimental apparatus of a fuel



2. Experimental

Figure 1 shows a schematic illustration of the fuel-cell system used in the present study. Ni-SiO₂ paste (Aremco Corp. Pyro-Duct 598) was painted on both surfaces of a SrCe_{0.95}Yb_{0.05}O_{3-a} ceramic pellet with Ni wire mesh. The surface area and thickness of the ceramic pellet was 1.77 cm² and 3.5 mm. The ceramic was calcinated in an electric heater at 1 000°C for several hours.

Figure 2. SEM photo of NiO/SiO₂ electrode

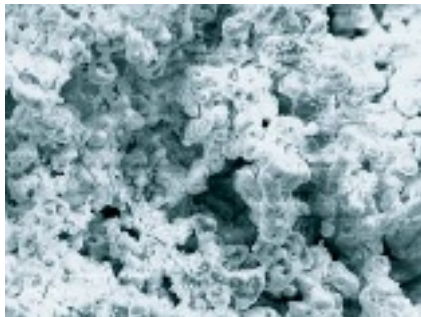
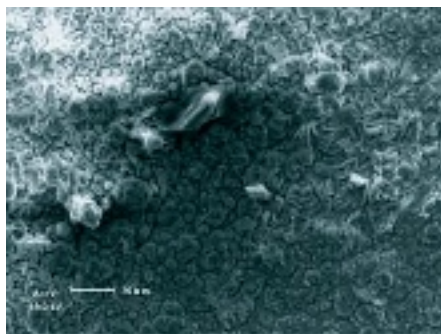


Figure 2 shows a SEM photo of a porous NiO/SiO₂ electrode. The Ni/SiO₂ electrode in the anode was reduced under H₂ atmosphere at 800°C for several hours. Figure 3 shows a SEM photo of the SrCe_{0.95}Yb_{0.05}O_{3-a} electrolyte. A structure of multi-crystal ceramic was observed in this photo.

Figure 3. SEM photo of SrCe_{0.95}Yb_{0.05}O_{3-a}



The ceramic pellet with the porous Ni/SiO₂ electrodes was placed in a 316 stainless-steel holder. A glass gasket was used in order to eliminate gas leak through interfaces between the anode and cathode. The anode was supplied with a gas mixture of H₂ + H₂O or CH₄ + H₂O. The H₂ concentration was 20%. The CH₄ concentration was 10%. Results for other H₂ or CH₄ concentrations were reported elsewhere [4,5]. H₂O was added to the CH₄ or H₂ gas flow by a bubbler immersed in a constant temperature bath. The cathode was supplied with a mixture of O₂ and H₂O. The H₂O concentration in the cathode was 20%. The concentrations of H₂, O₂, CH₄, CO, CO₂ and other hydrocarbons at the outlets of the anode and cathode were detected by gas chromatography. The H₂O concentration was measured by a dew-point meter. The gas flow rate was controlled to a constant flow rate by mass-flow regulators. The fuel-cell holder was placed in an electric furnace controlled to a constant temperature. Temperature was measured by C-A thermocouples. I-V curves were determined by a two-terminal direct-current method.

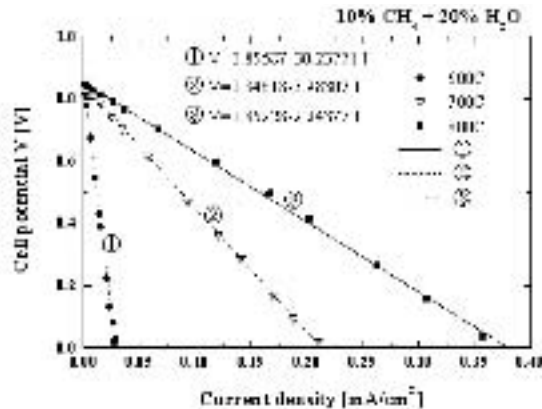
3. Results and Discussion

(1) I-V curves

Figures 4 and 5 show typical I-V curves for the Sr-Ce-Yb fuel-cell system. The former figure shows results for different temperatures and the latter does those for different input $\text{CH}_4/\text{H}_2\text{O}$ ratios. As seen in the two figures, the whole I-V curves were correlated to the following relation:

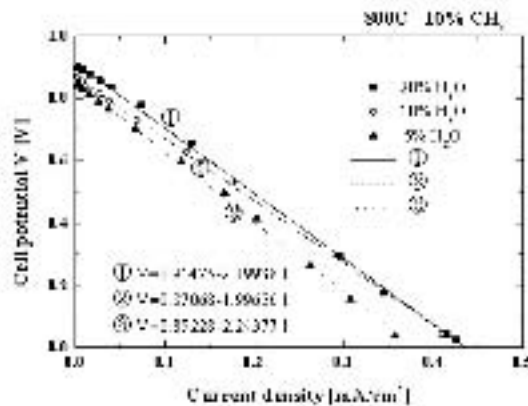
$$V = E_0 - Id/\sigma \quad (1)$$

Figure 4. I-V curves for $\text{CH}_4+\text{H}_2\text{O}|\text{Ni}|\text{SrCe}_{0.95}\text{YbO}_{3-\alpha}|\text{NiO}|\text{O}_2+\text{H}_2\text{O}$ cell



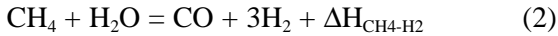
Here, V and E_0 are cell potentials or terminal voltage at arbitral current density I and $I = 0$. Usually, E_0 is called a thermodynamic electromotive force, EMF. The notations of A and δ are a surface area and thickness of the ceramic electrolyte, and s is an electric conductivity. Since measurement was carried out by a direct current method, the s value corresponded to an overall one including the contributions of anode and cathode polarities as well as the protonic conductivity of ceramic electrolyte. The dependence of E_0 on temperature was very small and almost independent of it. On the other hand, the E_0 values slightly depended on the input $\text{CH}_4/\text{H}_2\text{O}$ ratio.

Figure 5. I-V curves for $\text{CH}_4+\text{H}_2\text{O}|\text{Ni}|\text{SrCe}_{0.95}\text{YbO}_{3-\alpha}|\text{NiO}|\text{O}_2+\text{H}_2\text{O}$ cell



(2) Correlations of E_0 and σ

It was found that the system could work well even without any external CH_4 -to- H_2 reformer. Figure 6 shows a relation of E_0 and the partial pressure of H_2O , $p_{\text{H}_2\text{O}}$, supplied to the anode. As seen in the figure, E_0 (on the left-hand-side axis) slightly increased with an increase in $p_{\text{H}_2\text{O}}$. This is because the steam-reforming reaction proceeded more with elevating temperature. This increase was attributable to a difference in the H_2 partial pressure, p_{H_2} , on the anode electrode. When a CH_4 and H_2O mixture was introduced into the anode, the following CH_4 steam-reforming reaction occurred as well as other by-product reactions [6,7].



The E_0 values determined were compared with the following Nernst equation [8].

$$E_0 = -\frac{\Delta G_{\text{H}_2\text{O}}}{2F} - \frac{R_g T}{2F} \ln \left(\frac{P_{\text{H}_2\text{O}, \text{cathode}}}{P_{\text{H}_2, \text{anode}} P_{\text{O}_2, \text{cathode}}^{0.5}} \right) \quad (3)$$

Here, $\Delta G_{\text{H}_2\text{O}}$ is a Gibbs free-energy change of the reaction of $\text{H}_2 + (1/2)\text{O}_2 = \text{H}_2\text{O} + \Delta H_{\text{H}_2\text{O}}$, and its value was given in the reference [9]. The $p_{\text{H}_2, \text{anode}}$ values determined using Eq. (3) were plotted on the right-hand-side axis of Figure 6. Since the residence time of the $\text{CH}_4 + \text{H}_2\text{O}$ gas in the anode was around one second, the exhaust gas was not under equilibrium condition. Since the order of reaction was the first on $p_{\text{H}_2\text{O}}$ [10,11], the partial pressure of H_2 produced in the anode should be in proportion to $p_{\text{H}_2\text{O}}$. The experimental results also showed a proportional relation between $p_{\text{H}_2\text{O}}$ supplied and p_{H_2} produced. Therefore, $p_{\text{H}_2, \text{anode}}$ was deeply related with the rate of the steam-reforming reaction of Eq. (2). This will be investigated also in the following discussion on σ .

Figure 6. Relation of EMF and p_{H_2} versus $p_{\text{H}_2\text{O}}$

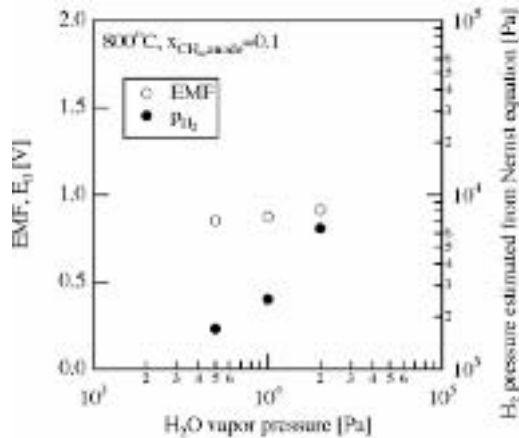


Figure 7 shows a comparison of σ between the $\text{CH}_4 + \text{H}_2\text{O}$ and $\text{H}_2 + \text{H}_2\text{O}$ supplies. As seen in the figure, σ for the $\text{CH}_4 + \text{H}_2\text{O}$ supply was much smaller than that for the $\text{H}_2 + \text{H}_2\text{O}$ one. The ratio became over one-tenth, and the σ values for the $\text{CH}_4 + \text{H}_2\text{O}$ supply were independent of $p_{\text{H}_2\text{O}}$. Referring to the discussion in our previous paper [4], where complex impedance plots were obtained in the system of a $\text{SrCe}_{0.95}\text{Yb}_{0.05}\text{O}_{3-a}$ fuel cell supplied with $\text{H}_2 + \text{H}_2\text{O}$ mixtures, the rate-determining step of the overall charge transfer was H^+ diffusion in the ceramic electrolyte. Therefore, a decrease in σ for the $\text{CH}_4 + \text{H}_2\text{O}$ supply was not caused by the H^+ conduction in the ceramic electrolyte. This is because the cathode was under the same condition between the $\text{H}_2 + \text{H}_2\text{O}$ and $\text{CH}_4 + \text{H}_2\text{O}$ supplies. The second contribution

was the oxidation reaction of H_2 in/on the cathode. However, it could not be also explained by the same reason. Therefore, the rate-determining step of the charge transfer for the $CH_4 + H_2O$ supply should be related to the steam-reforming reaction of CH_4 on the anode electrode.

Figure 7. Comparison of conductivity between CH_4+H_2O and H_2-H_2O supplies

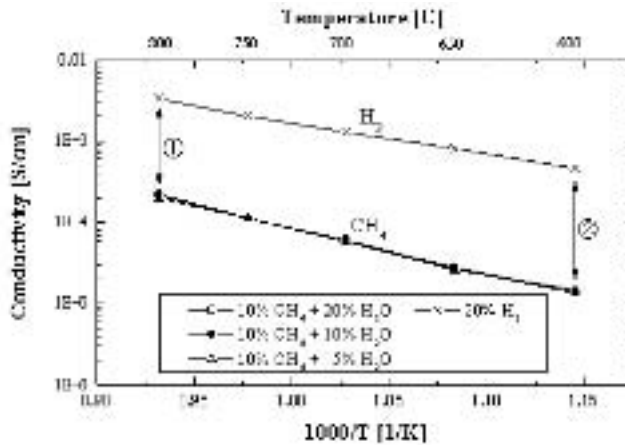


Figure 8. Mass and charge transfer on proton-conducting ceramics fuel cell

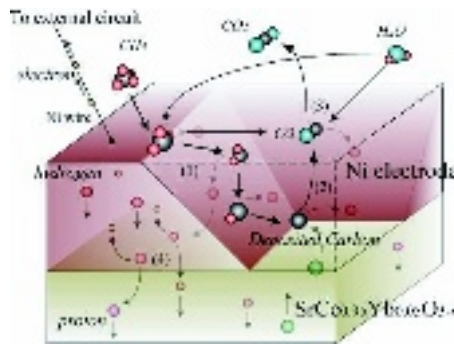


Figure 8 shows a schematic illustration of the anode reaction in the present proton-conducting ceramic fuel-cell system. In the anode, the following reactions may occur simultaneously:

- (i) convection of CH_4 and H_2O in the anode,
- (ii) CH_4 and H_2O reaction on/in the porous Ni/SiO₂ electrode,
- (iii) CH_4 and H_2O diffusing through the porous Ni/SiO₂ electrode,
- (iv) reaction product of CO, CO₂ and so on diffusing in a counter-current way,
- (v) decomposition to H atom,
- (vi) H_2 or H diffusion in the porous Ni/SiO₂ electrode,
- (vii) H⁺ diffusion through the ceramic electrolyte.

The activation energy of σ was 106 kJ/mol for the $\text{CH}_4 + \text{H}_2\text{O}$ supply and 75.6 kJ/mol for the $\text{H}_2 + \text{H}_2\text{O}$ supply. Difference between the two energies was 30 kJ/mol. The value was in close agreement with the activation energy of the reaction-rate constant of Eq. (2) [10]. Therefore, the largest contribution to σ , in other words the rate-determining step, was considered the intrinsic rate of Eq. (2). It was clear that the steam-reforming reaction contributed heavily to the overall conductivity.

(3) Carbon deposition

Figure 9. Profiles of carbon deposition in/on porous Ni electrode

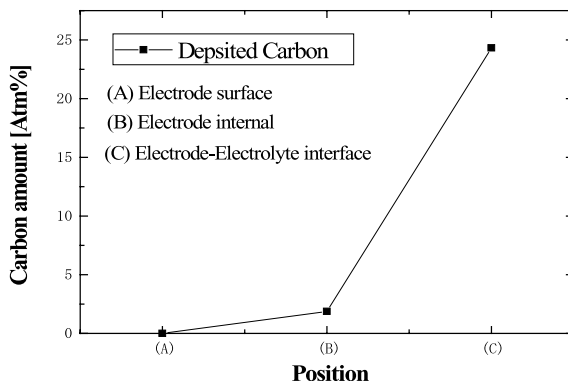


Figure 9 shows the profile of carbon deposition in the porous Ni/SiO₂ electrode determined using SEM-EDX. There was no carbon deposition on its surface. There were also very few carbon depositions in the porous electrode. This was because the following direct decomposition reaction did not occur in/on the porous electrode.



The ratio of the CH_4 -to- H_2 direct decomposition rate to that of the CH_4 steam-reforming reaction one was not found to be different from location to location in the porous electrode. Therefore, it was considered that the supply of H_2O was sufficient in the present experiment. It was probable that a sufficient amount of CH_4 and H_2O diffused through the porous electrode and arrived at an electrode-electrolyte interface. The direct decomposition reaction as well as the steam-reforming reaction simultaneously occurred at a narrow interface under the condition of the sufficient supply of electric charge to the cathode electrode. As seen in Figure 9, some carbon deposited at the narrow interface between the electrolyte and electrode. This may be because the steam-reforming reaction was slower than the protonic conductivity of electrolyte and, consequently, the direct decomposition of CH_4 provided electron and H^+ ion to the interface. Since the carbon deposition was localized at the interface. Therefore, there was no effect on the mass and charge transfer in the present cell system.

The Sr-Ce oxides were stable at 600-800°C when H_2O was added in the streams of anode and cathode. The addition of H_2O was necessary in order to maintain protonic conduction through the ceramic electrolyte [4]. However, it is known that Sr-Ce oxides decomposed to SrCO_3 and CeO_2 at high CO_2 atmosphere [12]. Therefore, the use of the Sr-Ce oxide is not proper under the condition of CO_2 atmosphere. In the present study, gas composition detected in the exhaust from the anode was CH_4 , H_2 , H_2O , and CO . No CO_2 was observed throughout the present study. This may be because the reaction temperature was higher than 600°C, and a sufficient amount of H_2O was supplied to the anode and cathode. There was high possibility of production of CO_2 at lower temperatures of 300-500°C [7]. The use of a compact Ni electrode in place of the porous Ni/SiO₂ electrode may be proper if CO_2 is

generated in the anode. The ceramic electrode with a compact Ni electrode that was electrically deposited will not contact with CO₂ directly. Therefore, there may be no possibility of the decomposition to SrCO₃ and CeO₂.

(4) Application of Sr-Ce-Yb oxide to high-temperature system

There are several advantages and disadvantages for the present Sr-Ce-Yb oxide fuel-cell system. The largest advantage is that it can work at 600-800°C, at which the steam-reforming reaction simultaneously occurred. The internal reformation became possible at these temperatures. Therefore, its structure became very simple. Heat to maintain the steam-reforming reaction can be converted to electricity directly because of endothermic reaction of Eq. (2). This thing makes it possible to convert the chemical energy of CH₄ to electricity with a higher efficiency. The Carnot-cycle efficiency can be raised by operation at higher temperatures. Its working temperature is near that of a high-temperature nuclear reactor. Therefore, it may be possible to provide measures to utilise nuclear heat with high efficiency. This thinking is taken into consideration in other countries in different ways. There are applications of some ceramics to high-temperature steam electrolysis with use of nuclear heat, such as Generation IV nuclear energy system [13].

On the other hand, the largest disadvantage is that the protonic resistance of the Sr-Ce-Yb oxide was comparatively larger than that of a polymer-electrolyte-membrane fuel cell (PEM-FC) and was comparable with O²⁻ ion conductivity of an yttria-stabilised zirconia (YSZ). Consequently, as seen in Figs. 4 and 5, the current density through the Sr-Ce-Yb oxide fuel cell was order of mA/cm² and was much smaller than that of PEM-FC. This is because a thin ceramic is very difficult to manufacture. The protonic conductivity of the Sr-Ce-Yb oxide itself was around one-tenth smaller than that of PEM. Moreover, the conductivity was order of 10⁻⁴ S/cm when a CH₄ and H₂O mixture was supplied directly to the cell without external reformer. The overall conductivity became around 10⁻²-fold less than that of PEM, because the rate-controlling step was in the steam-reforming reaction.

Judging from the data available in the present study, it is difficult to apply the Sr-Ce-Yb oxide (as it is) to the effective use of nuclear reactor heat, where a large amount heat should be converted to electricity. Considering H₂ production rate, the current density of 1 mA/cm² corresponds to the H₂ production rate of 1.2x10⁻⁶ Nm³/m²s. Therefore, the surface area of 8.6x10⁵ m² is necessary for the H₂ production rate of 1 Nm³/s. This is an unrealistic scale. On the other hand, it is desirable to utilise the proton-conducting ceramic under special or severe conditions, such as hydrogen or tritium pump at higher temperatures. Converting to tritium activity, the current density of 1 mA/cm² corresponds to 11 MBq/cm²s. Since the tritium generation rate in a blanket to maintain 1 GW commercial fusion power reactor is 0.63 TBq/s, the surface area of the Sr-Ce-Yb oxide necessary to extract tritium from CH₄ – H₂O or H₂ – H₂O streams as a tritium pump amounts to 5.7 m². It is expected that the tritium pump will be operated at 600-800°C in a blanket tritium recovery system or a tritium purification system in a fusion fuel cycle. This is a realistic scale.

4. Conclusions

The I-V curves for the fuel-cell system composed of a SrCe_{0.95}Yb_{0.05}O_{3-a} ceramic electrolyte and Ni/SiO₂ porous electrodes were determined under the conditions of CH₄ + H₂O and H₂ + H₂O supplies, and the values of E₀ and σ were correlated to a function of temperature and the anode H₂O partial pressure. The E₀ values were consistent with the Nernst equation. It was found that E₀ was a good indication of p_{H2} generated on the anode electrode when the CH₄ and H₂O mixture was introduced into the anode. The σ values determined included the two contributions of the protonic conductivity of the

Sr-Ce-Yb oxide electrolyte and the activation polarity of the steam-reforming reaction on the Ni/SiO₂ porous electrode. Because of stable operation of the Sr-Ce-Yb oxide as a fuel cell at 600-800°C, it is expected to utilise the ceramic for tritium pump. The profile of carbon depositions were determined by SEM-EDX, and it was found that carbon depositions by the direct decomposition of CH₄ were localised at a narrow interface between the electrode and electrolyte.

REFERENCES

- [1] H. Iwahara, *Solid State Ionics*, 77 (1995) 289-298.
- [2] Y. Kawamura, S. Konishi, M. Nishi, *Fus. Sci. Technol.*, 45 (2004) 33-40.
- [3] M. Tanaka, K. Katahira, Y. Asakura, T. Uda, H. Iwahara, I. Yamamoto, *J. Nucl. Sci. Technol.*, 41 (2004) 61-67.
- [4] S. Fukada, K. Onoda, S. Suemori, *J. Nucl. Sci. Technol.*, 41 (2005) 1-7.
- [5] S. Fukada, S. Suemori, K. Onoda, *J. Nucl. Mater.*, in printing.
- [6] S. Fukada, N. Nakamura, J. Monden, M. Nishikawa, *J. Nucl. Mater.*, 329-333 (2004) 1365-1369.
- [7] S. Fukada, N. Nakamura, J. Monden, *Int. J. Hydrogen Energy*, 29 (2004) 619-625.
- [8] P. W. Atkins, "Physical chemistry", Oxford University Press, England, (1990).
- [9] O. Kubaschewski, C. E. Alcock, "Metallurgical Thermochemistry, 5th ed.", New York, Pergamon Press, (1979).
- [10] W. Jin, X. Gu, S. Li, P. Huang, N. Xu, J. Shi, *Chem. Eng. Sci.*, 55 (2000) 2671-2625.
- [11] I. Alstrup, *J. Catalyst*, 151 (1995) 216-225.
- [12] T. Scherban, A. S. Nowick, *Solid State Ionics*, 35 (1989) 189-194.
- [13] For examples, <http://www.futurepundit.com/archives/002495.html>

This page intentionally left blank

SEPARATION AND UTILISATION OF RARE METAL FISSION PRODUCTS IN NUCLEAR FUEL CYCLE AS FOR HYDROGEN PRODUCTION CATALYSTS?

Masaki Ozawa^{*1,3}, Reiko Fujita^{*2}, Tatsuya Suzuki^{*3} and Yasuhiko Fujii^{*3}

^{*1}Japan Atomic Energy Agency

^{*2}Toshiba Corporation

^{*3}Tokyo Institute of Technology

Abstract

A novel reprocessing system with recovery of actinides, long-lived fission products (LLFP) and valuable rare metal fission products (RMFP) has been proposed. This process is based on ion exchange (IX) and catalytic electrolytic extraction (CEE). The pre-filtration step using tertiary pyridine-type anion-exchange resin is set prior to the main actinide recovery steps in this system. The perfect isolation of platinum group elements (Pt-G) such as ¹⁰⁶Ru from fuel dissolver solution was successfully demonstrated for irradiated mixed oxide (MOX) fuel. The CEE method, being set as a post-pre-filtration process, was applicable to separation of RMFP including TcO_4^- and ReO_4^- by selective and accelerative deposition with Pd^{2+} as a catalyst. Quaternary Pd-Ru-Rh-Re deposited Pt electrodes showed the highest cathodic current. The catalytic ability is about twice superior to that of the base Pt electrode when used for artificial sea water as well as alkaline solution.

The recovery and separation of actinides and RMFP by a multi-functional reprocessing system consisting of IX and CEE will minimise the quantity and improve the quality of high level liquid waste (HLLW). The recovered RMFP will be used as a “FP-catalyst” for hydrogen production in water electrolysis.

Introduction

In order to optimise the radioactive waste treatment in the nuclear fuel cycle, partitioning and transmutation (i.e., P&T) of actinides (An) and fission products (FP) have been considered. Actinides are α radioactive, and their half-lives are long; e.g., 2.4×10^4 , 4.3×10^2 and 2.1×10^6 years for ^{239}Pu , ^{241}Am and ^{237}Np , respectively. Among FPs concerned, Tc, Pd, Se and Te are long-lived fission products (LLFP), and Ru, Rh, Pd, Tc, Se and Te are precious and rare metal fission products (RMFP). The half-life of ^{99}Tc is as long as 2.1×10^5 years. By considering its fate, utilization with and without transmutation ($^{99}\text{Tc} (n, \gamma) ^{100}\text{Tc} \rightarrow \beta^- \rightarrow ^{100}\text{Ru}(\text{stable})$) are pictured in the future. Typical amounts of FP estimated by calculations with the ORIGEN-II code are shown in Table 1. Amounts of RMFP generated are proportional to burnup of the fuel, and spent mixed oxide (MOX) fuel, highly irradiated in fast reactor (burnup: 150 GWd/t, cooling time: 4 years), will contain more than 30 kg of RMFP per metric ton.

It is, therefore, indispensable to establish effective separation methods and a way of utilisation as the concept of P&T,U (Partitioning, Transmutation and Utilisation) by using innovative technologies [1,2]. Thereby, the HLLW containing non- α , non-LLFP and non-RMFP nuclides would be preferably produced for a non-deep disposal.

The current fuel reprocessing system cannot respond to such delicate processes as recovery and separation of LLFP and RMFP. We propose a new reprocessing system based on ion exchange (IX) and catalytic electrolytic extraction (CEE) methods. The state of the arts of separation technology on RMFP and minor actinides (MA) from spent fuel by the IX method and utilization technology of RMFP (including Tc) and Re (as hydrogen generation catalysts) by the CEE method are described.

Novel Reprocessing System Provided with Separation Function of LLFP and RMFP

An innovative reprocessing system is newly proposed. A schematic diagram of the process is shown in Figure 1. The process is based on IX chromatography using pyridine resin. Tertiary pyridine resin has functions of a weakly basic anion exchanger and a soft donor extractant. As shown in Figure 1, the reprocessing system mainly consists of three processes; the first step (Step I-A) consists of a pre-filtration process prior to main reprocessing of Step II and a recovery process of RMFP by CEE (Step I-B). Step II is the main process for separation of spent fuel, i.e., spent fuel is separated into 3 groups such as FPs with Ln (III), MA (III), and Pu with U, Np. The fraction of FPs with Ln(III) will be HLLW. The third step (Step III) is a mutual separation process of MA(III) to Am and Cm products.

On Step I-A, technetium and Pt-G elements are expected to adsorb on the gelled tertiary pyridine resin in the diluted hydrochloric acid medium referring to the basic adsorption property on anion exchange resin. The adsorbed elements are rinsed out by alkaline elution from the resin. Technetium and Pt-G elements in this effluent are recovered again on an electrode by CEE.

On Step II, the column packed with a high-porous type of tertiary pyridine resin embedded in silica beads is used for hydrochloric acid-based reprocessing. The resin was produced by Research Laboratory for Nuclear Reactors, Tokyo Institute of Technology [3,4,5]. The chemical structure of this resin is presented in Figure 2. The resin has high radiation resistance in hydrochloric acid solution. The average diameter of the resin is 60 μm . The total exchange capacity is 1.94 meq/g (dry) in Cl^- form and the cross-linkage is 20 %. While multivalent U(VI), Np(VI) and Pu(IV) are strongly adsorbed on anion exchange resin in highly concentrated hydrochloric acid solution[6], the distribution of trivalent MA(III) and Ln(III) are lower than the multivalent Ans in such a medium. Moreover, the distribution coefficient of Ce(III) was about 4 times lower than those of Am(III) in a pure hydrochloric acid. Therefore, groups of Ln(III) with other FPs like Cs and Sr, trivalent MA(III) and multivalent U(VI),

Np(VI) and Pu(IV) are individually separated in this order.

The mutual separation of Am and Cm at Step III is already confirmed by trace experiments [4]. In this process, the same resin as on Step II was used, while nitric acid solution was used instead of hydrochloric acid solution.

Separation and Recovery of RMFP

Separation of RMFP by tertiary pyridine resin (Step I-A)

Mixed oxide (MOX) fuel, 21.0-wt% Pu in 18.0-wt% enriched uranium, was irradiated from the 16th to 35th cycle at the 3rd row in the experimental fast reactor JOYO. The effective full power days were 1019.33, and the peak burnup was 143.8 GWd/t. A total of 1560 days have passed from the reactor shut down to analysis.

A chopped irradiated fuel pin was transported to Alpha-Gamma Facility (AGF) of the Japan Nuclear Cycle Development Institute. The irradiated fuel was further sliced into pieces of 5 mm in length at AGF.

The sliced specimen was then placed in a flask mounted with reflux condenser, and dissolved in 28 mL of 8 mol/dm³ nitric acid solution by heating for 6 h at boiling temperature. After several drops of concentrated hydrofluoric acid were added, the solution was again heated for 6 h in order to minimize amounts of insoluble residue. The weight of dissolved fuel was estimated to be 1.27 g.

The fundamental flow sheet is based on a concept shown in Figure 1. The separation on Step I-A was employed to remove RMFP (¹⁰⁶Ru, ⁹⁹Tc, etc). On this step, gamma spectrometry was applied to identify gamma nuclides like ¹⁰⁶Ru, ¹²⁵Sb, ¹⁴⁴Ce, ¹⁵⁵Eu, ²⁴¹Am and so on.

A 0.1 ml aliquot of the dissolved spent fuel solution was diluted by adding 50 mL of pure water. The sample solution was heated and dried, and was dissolved again in 3 mL of 0.5 mol/dm³ hydrochloric acid. The resulted hydrochloric dissolver solution was loaded onto resin (8 mL column volume). Tertiary pyridine resin of a non-support type was used as pre-filter anion exchange resin. After sample loading, the column was fed with 4 column volumes of 0.5 mol/dm³ hydrochloric acid solution. The resin was rinsed by pure water of 4 column volumes. Then, 1 mL of resin was taken from the column and rinsed again by pure water. After the rinse, the rinsing water and resin were encapsulated in a plastic vial. Furthermore, 3 column volumes of 1 mol/dm³ sodium hydroxide solution were fed to the resin. After the alkali rinse, the resin and eluted sodium hydroxide solution were analyzed by γ -ray spectrometry to confirm the adsorbed nuclides.

Strong γ -ray peaks of ¹⁰⁶Ru and ¹²⁵Sb were observed in the resin rinsed by pure water after anion-exchange. Other nuclides, such as ²⁴¹Am and ¹³⁷Cs were scarce. Figure 3 shows the material balance of main nuclides before and after the pre-filtration. A weight ratio of nuclide was assumed 100 % at the inlet. Ruthenium-106 and ¹²⁵Sb were not detected in the eluate by elution with 0.5 mol/dm³ hydrochloric acid solution. While other nuclides, ²⁴¹Am, ¹⁵⁵Eu and ¹³⁷Cs, were scarcely detected in the outlet of rinsing water and alkaline solution, the amounts of each nuclide were less than 0.5%. It is concluded that ¹⁰⁶Ru and ¹²⁵Sb can be isolated perfectly from the spent fuel and the α contamination is very small. Noticeable FP (¹⁰⁶Ru and ¹²⁵Sb) – free dissolver solution is preferable to increase the decontamination factor in the whole reprocessing process.

Since the tertiary pyridine is a soft donor ligand and the ions of Pt-G elements are soft acid, they are strongly bonded by coordination. Technetium (^{99}Tc) was not detected by γ -spectrometry. Although absorption of Tc(VII), Ru(IV) and Pd(II) on Dowex 1 resin in hydrochloric acid decreases with increasing acidity, these species have rather high distribution coefficients ($\log D > 1$) in the region $0.1 \text{ mol/dm}^3 < [\text{HCl}] < 12 \text{ mol/dm}^3$ [6]. The $\log D$ values of actinide ions, on the other hand, increase with increasing acidity, but the values are smaller than 0 for $[\text{HCl}] < 1 \text{ mol/dm}^3$. Therefore, anionic TcO_4^- and other Pt-G elements are considered to be well adsorbed on tertiary pyridine resin and thus separated from actinides in the same manner as Dowex 1 resin of a weakly basic anion exchanger.

Recovery of RMFP by catalytic electrolytic extraction (Step I-B)

Details of the CEE method applied here to Step I-B to recover and purify RMFP obtained from Step 1A were discussed elsewhere [7]. In principle, Pd^{2+} (or Fe^{2+}) would accelerate electro-deposition of the other ions as a promoter (i.e., $\text{Pd}_{\text{adatom}}$) at the electrode surface or as a mediator in the bulk solution. As for a typical example of CEE of RMFP from simulated HLLW, the galvanostatic electrolysis resulted in the quantitative deposition, where metal ions with $E^0 > 0.7\text{V}$ tended to deposit on the cathode, and the deposition ratio seemed to be proportional to the order of the redox potential; $\text{Pd} > \text{Te} > \text{Se} > \text{Rh} > \text{Ru} > \text{Re}$. Molybdenum and Zr can be recovered as co-precipitation at $\text{H}^+ < 1.5 \text{ mol/dm}^3$.

An interaction between Pd^{2+} and TcO_4^- during CEE was also confirmed [2]. The working Pt electrode was polarised from noble to base potential side, every 30 min step by step. The amount of deposition was measured by a radiometric method at each polarised potential. While the deposition of Tc was significantly suppressed with an increase of the nitric acid concentration, addition of Pd^{2+} ($\text{Pd} / \text{Tc} = 5$) enhanced its electro-deposition expectedly even though nitric acid concentration was 2 mol/dm^3 . Namely, the Pd^{2+} effect can conquer a negative nitric acid effect causing the redissolution of Tc deposit. The Tc deposit was brownish in color and apparently not dendritic. The deposition ratio was, however, as low as 2% at maximum, and the deposition amount of Tc was larger than that of Ru under almost the same nitric acid concentration. An observed potential region of TcO_4^- for quantitative electro-deposition was 0.4 V-0.05 V (V vs. NHE), agreeing with the hydrogen adsorption-desorption potential region of a Pt electrode. The maximum deposition was observed near the hydrogen evolution potential. Thus, H_{ad} likely participates in the electro-deposition of TcO_4^- in the system



In the extremely negative conditions (i.e., $< -0.3\text{V}$) however, hydrogen evolution occurred simultaneously and disturbed again the Tc deposition reaction. In the case of a carbon electrode which had no H_{ad} region in 3 mol/dm^3 nitric acid solution, reduction of TcO_4^- to TcO^{2+} was the most significant in the potentiostatic electrolysis at $\phi_{\text{E}} = -0.3 \text{ V}$ or -1.0V (V vs. Ag/AgCl) [8].

Utilisation of RMFP

The hydrogen overpotential of metals periodically changes, and specifically Pt-G elements, Re and Tc show lower overpotentials. One can explain those in referring to *d*-hole characteristics based on the band theory. For utilization of RMFP, hydrogen evolution characteristic of the RMFP-deposit on Pt electrodes was investigated for electrolysis in alkaline solution.

RMFP-deposited electrodes were fabricated based on the CEE method. Details of electrolysis conditions are described elsewhere [2,9]. Results of electrochemical reduction are summarised in Table 2, where “Pd-Ru-Rh-Re (3.5:4:1:1)” means the quaternary Pd-Ru-Rh-Re deposited Pt electrode

obtained from electrolyte containing Pd, Ru, Rh and Re (Tc) ions in the ratio of 3.5:4:1:1, which corresponds to the composition of the fast-reactor MOX spent fuel listed in the Table 1. The deposition ratios of RMFP were estimated from the reduction ratios calculated from the balance of ionic concentration during the electrolysis. The highest reduction ratio of 95-99% was obtained for Pd by discharging from Pd²⁺ to metallic Pd, and the deposit tended to form dendrites which were easily detached by simultaneous hydrogen evolution. The reduction manner of Rh was similar to that of Pd; a 1 step reduction of Rh³⁺ to metallic Rh. On the contrary, reduction of Ru might proceed by 2 steps, i.e., RuNO³⁺→Ru²⁺ and Ru²⁺→Ru (metal) which the reduction ratio around 14%. The reduction ratios of ReO₄⁻ and TcO₄⁻ were 16 % and only 1.7 %, respectively. As reported previously [1,2,7], the presence of Pd²⁺ accelerated deposition of Rh as well as Ru, and co-existence of Rh³⁺ also accelerated the reduction of ReO₄⁻ in the present experiment (16%→43.0%). Specifically, in CEE with a low cathode current density, e.g., 2.5 mA/cm², compulsory stirring was necessary to get a minute and stable deposit of Pd layers. This procedure was very essential to obtain larger amounts of co-deposit with other ions. Figure 4 shows an element map of the surface deposit observed with EPMA (electron probe micro analyzer) for the final run (*2) in Table 2. In this run, Pd²⁺ was added to catholyte divided by 5 times to allow Pd to exist constantly in the bulk solution (as Pd²⁺) and at the electrode surface (as Pd_{adatom}). The shape of deposit was not dendritic but rather spherical and homogeneous, likely cohered with fine particles. In the quaternary ionic solution system, an excess and divided addition of Pd²⁺ resulted in the deposit with almost equal atom composition of Pt-G metals (Pd-Ru-Rh). However, the number of Re atoms at the surface of deposit was smaller than those of others despite with rather higher reduction ratios.

The cathodic currents corresponding to hydrogen evolution at the given polarized potential vs. initial hydrogen evolution potential for various RMFP-deposited electrodes are shown in Figure 5. The cathode currents decreased for the Pd, Rh and Re deposited Pt electrodes in 1 mol/dm³ sodium hydroxide solution, but increased only for the Ru deposited Pt electrode. The current of the quaternary Pd-Ru-Rh-Re (3.5:4:1:1) deposited Pt electrode was the highest, exceeding that of the Pt electrode by factor 2 in 1 mol/dm³ sodium hydroxide solution and artificial sea water. Among RMFPs, Ru seems to be responsible for high reactivity on hydrogen evolution. As for the apparent relative reactivity of RMFP estimated from the currents per mg of deposit, however, binary deposits of Ru-Re and Rh-Re showed the highest reactivity. The cathode current of the quaternary Pd-Ru-Rh-Re deposited Pt electrode in artificial sea water decreased about a half to a third of that in 1 mol/dm³ sodium hydroxide solution. The reactivities were still comparable to that of Pt in 1 mol/dm³ sodium hydroxide solution. The roles of Re and Tc in this system are still unclear, and we are planning further parametrical experiments.

Figure 6 shows a FBR cycle concept, where the FBR will transmute An and LLFP with generating primary electricity and heat. The enhanced reprocessing plant will generate less radiotoxic rad. wastes with providing RMFPs as useful catalysts. Therefore, the FBR cycle would be expected to realise environment-friendly, symbiotic nuclear/hydrogen energy system.

Conclusions

A novel reprocessing system for recovery of LLFP and RMFP as well as actinides using IX and CEE methods is proposed. The process can directly separate Pt-G elements with Tc as well as Am and Cm from the spent fuel in the minimum number of reprocessing steps. The perfect isolation of ¹⁰⁶Ru and ¹²⁵Sb from fuel dissolver solution by IX at the pre-filtration step was successfully demonstrated for irradiated MOX fuel. The CEE, being set in the post-IX process, was applicable to recover RMFP including TcO₄⁻ and ReO₄⁻ through unique and accelerative deposition by adding Pd²⁺ as a catalyst. The quaternary Pd-Ru-Rh-Re deposited Pt electrodes showed the highest cathodic current corresponding to

the hydrogen evolution reaction. The current was about twice higher than that of the base Pt electrode in the use for artificial sea water as well as alkaline solution.

The recovery and separation of actinides, LLFP and RMFP by the multi-functional reprocessing system consisting of IX and CEE processes are relevant to minimize the quantity and improve the quality of HLLW. The promising utilisation field of recovered RMFP will be a “FP-catalyst” for hydrogen production in water electrolysis. RMFP (including Tc) and Re will be highly expected to be flow material to bridge nuclear and hydrogen energy systems.?

REFERENCES

- [1] M. Ozawa, Y. Sano and Y. Shinoda, *Progress in Nuclear Energy*, 40, 527 (2002).
- [2] M. Ozawa, T. Suzuki, S. Koyama and Y. Fujii, 1st COE-INES International Symposium, Tokyo, Japan, October 31-November 4 (2004).
- [3] T. Suzuki, M. Aida, Y. Ban and Y. Fujii, *Journal of Radioanal. Nucl. Chem.*, 255, 581 (2003).
- [4] A. Ikeda, T. Suzuki, M. Aida, K. Otake, Y. Fujii, K. Itoh, T. Mitsugashira, M. Hara and M. Ozawa, *J. Nucl. Sci. Technol.* 41, 915 (2004).
- [5] A. Ikeda, T. Suzuki, M. Aida, Y. Fujii, K. Itoh, T. Mitsugashira, M. Hara and M. Ozawa, *J. Chromatog. A.* 1041, 195 (2004).
- [6] K.A. Kraus, F. Nelson, *Proc. Intern. Conf. Peaceful Uses At. Energy*, Geneva, 7, 113 (1995).
- [7] M. Ozawa, M. Ishida and Y. Sano, *Radiochemi.* 45, 225 (2003).
- [8] T. Asakura, S-Y. Kim, Y. Morita, M. Ozawa and T. Ikegami, *JAERI-Conf 20043-011*, 99, July (2004).
- [9] M. Ozawa, K. Mizoguchi, and R. Fujita, 15th World Hydrogen Energy Conference, Yokohama, Japan, June 27-2 July (2004).

Table 1. Typical amount of RMFP per ton of fast-reactor spent fuel

Pure metal	Ru	Rh	Pd	Tc	Te	Se	Note
Amount (kg/HMt)	12.5	3.6	11.1	3.3	2.7	0.2	FBR-SF; 150 GWd/t, Cooled 4 years.

Table 2. Reduction ratios of RMFP by catalytic electrolytic extraction

System	Reduction ratio / %					Composition of Electrode Surface
	Pd	Ru	Rh	Re	Tc	
Pd	>99	-	-	-	-	-
Ru	-	14	-	-	-	-
Rh	-	-	>99	-	-	-
Re	-	-	-	16	-	-
Tc	-	-	-	-	1.7	-
Pd-Ru	99.3	60.9	-	-	-	Pd \approx Ru
Pd-Rh	99.0	-	84.7	-	-	Pd \approx Rh
Pd-Re	99.4	-	-	10.0	-	Pd > Re
Ru-Rh	-	58.2	32.5	-	-	Ru \approx Rh
Ru-Re	-	14.5	-	13.5	-	Ru > Re
Rh-Re	-	-	10.0	43.0	-	Rh > Re
Pd-Ru-Rh-Re(1:1:1:1)	95.7	46.0	14.5	19.0	-	Pd \approx Ru \approx Rh > Re
Pd-Ru-Rh-Re(3.5:4:1:1)*1	99.0	11.8	2.10	33.4	-	Pd \approx Ru \approx Rh > Re
Pd-Ru-Rh-Re(3.5:4:1:1)*2	94.7	16.5	26.6	55.3	-	Pd \approx Ru \approx Rh > Re

*1 : Pd block addition.

*2 : Pd 5 divided addition.

Figure 1. Reprocessing flow sheet provided with multi-functional separation ability

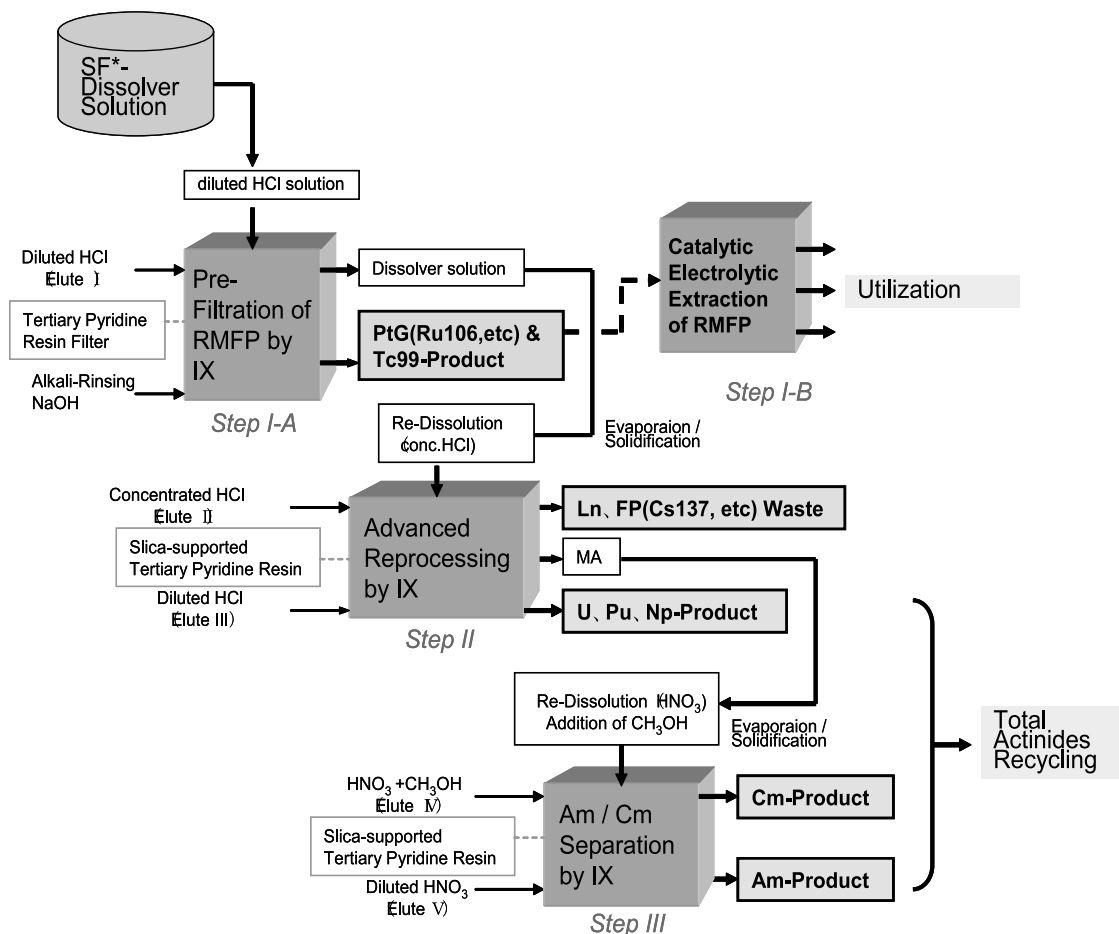


Figure 2. Chemical formula of tertiary pyridine-type anion exchange resin

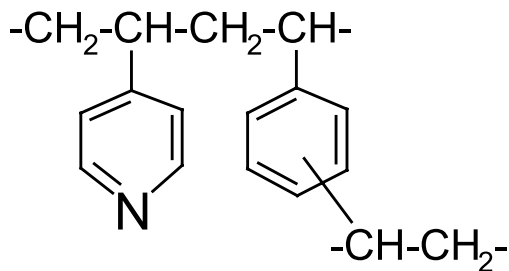


Figure 3. Material balance of ^{106}Ru , other FPs and ^{241}Am on pre-filtration (Step I-A)

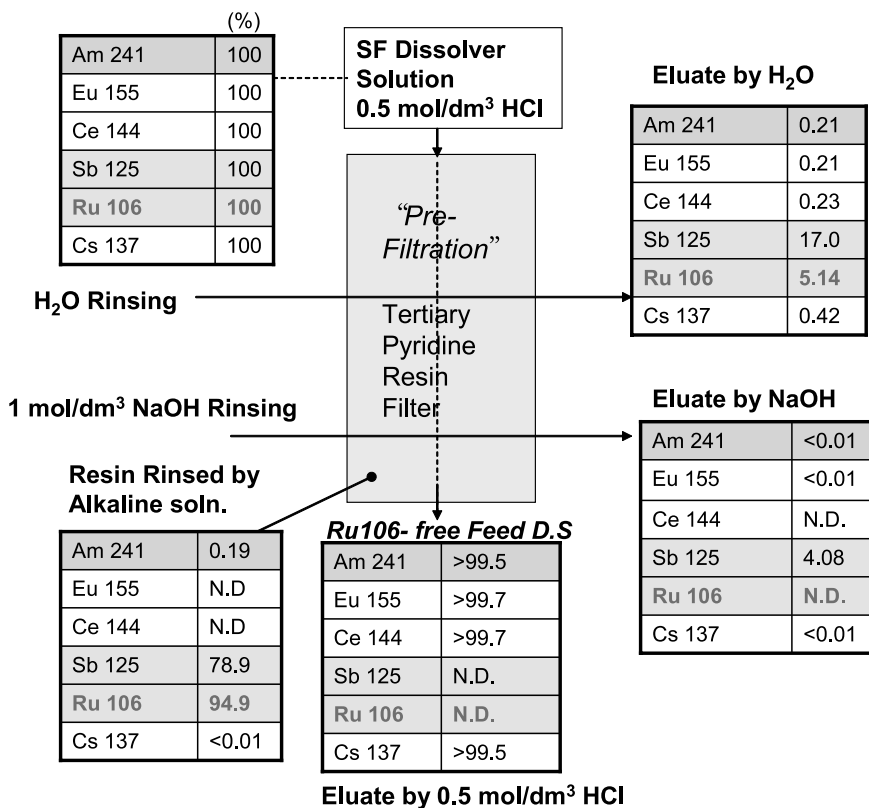


Figure 4. EDS(EPMA) of the deposits on the Pt electrode from nitric acid solution; Solution composition: Pd-Ru-Rh-Re (3.5:4:1:1), divided of Pd²⁺

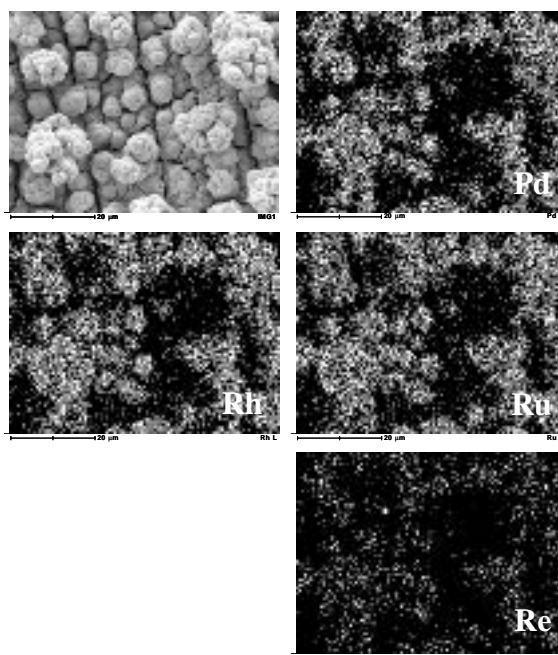


Figure 5. Relation between cathodic current corresponds to hydrogen evolution at -1.25V (vs. Ag/AgCl) and initial hydrogen evolution potential on each deposit electrode in 1mol/dm³ sodium hydroxide solution

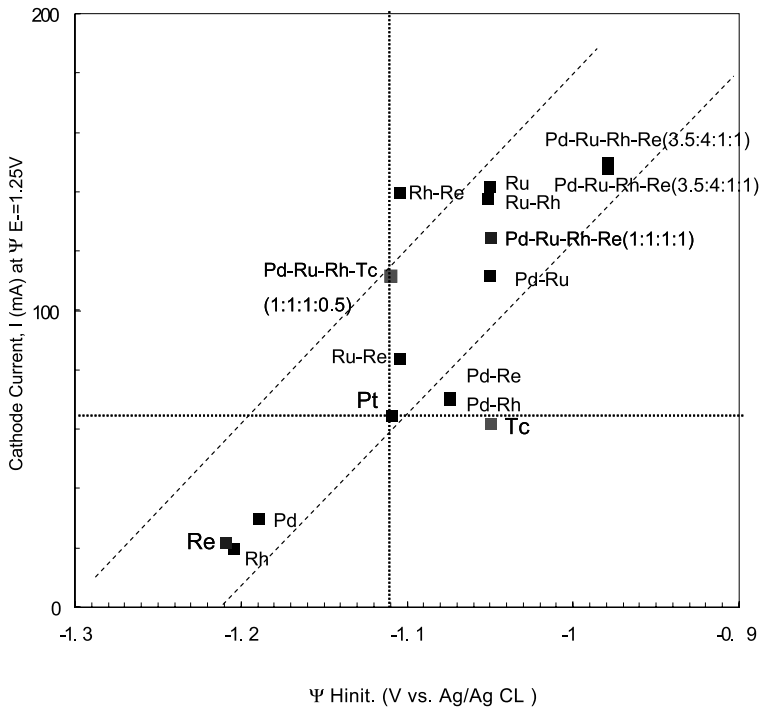
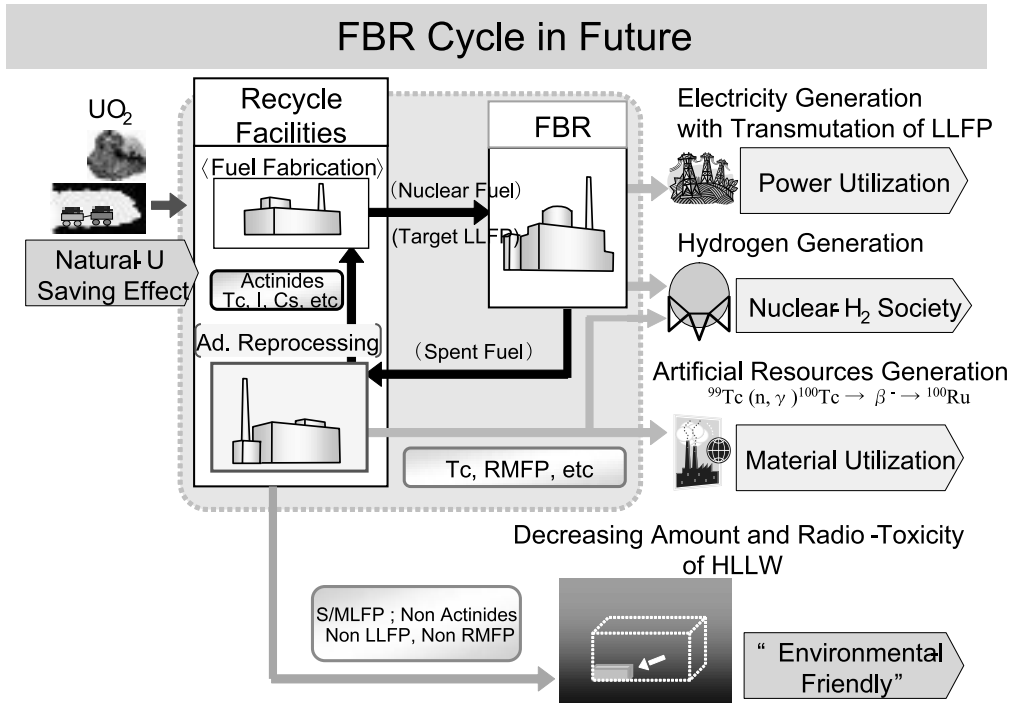


Figure 6. An environment-friendly FBR cycle concept providing fission-energy and fission-material to actualise a symbiotic nuclear/hydrogen energy system



ELECTRICAL CONDUCTIVE PEROVSKITE ANODES IN SULFUR-BASED HYBRID CYCLE

Hiroataka Kawamura, Masashi Mori, Song-Zhu Chu and Masaki Uotani

Central Research Institute of Electric Power Industry (CRIEPI)

2-6-1 Nagasaka, Yokosuka, Kanagawa, 240-0196 JAPAN

E-mail: kawamuh@criepi.denken.or.jp

Abstract

Sulfur-based hybrid cycle (SHC) process has been attracted much attention as a mass production process of hydrogen, which consists of an electrolysis step, $2\text{H}_2\text{O} + \text{SO}_2 \rightarrow \text{H}_2 + \text{H}_2\text{SO}_4$ (353 K), and a thermal decomposition step, $\text{H}_2\text{SO}_4 \rightarrow \text{H}_2\text{O} + \text{SO}_2 + 1/2\text{O}_2$ (1123 K). To achieve high efficiency for hydrogen evolution, exploring and fabricating electrode materials with high corrosion resistance, high electrical conductivity, and low anodic over-potential is a key technology for the electrolysis in H_2SO_4 solutions, and it has not been solved well yet.

In our previous study, we found that Ti-based perovskite oxides, such as SrTiO_3 and CaTiO_3 , showed high corrosion resistance in a 50 wt % solution at 353 K. Since there are no d-electrons (Ti^{4+} : d_0 system) and f-electrons in stoichiometric Ti-based perovskites (chemical formula: $\text{A}^{2+}\text{Ti}^{4+}\text{O}_3$), no electrical conductivity of these materials is anticipated at the operating temperature. To obtain electrical conductivity, the formation of Ti^{3+} in the perovskites is necessary.

In this paper, doping rare earth metal (RE = Nd, Pr, and La) in the Ti-based perovskites and a successive reducing treatment at high temperatures in H_2 gas flow were adopted to achieve electrical conductivity. In the case of SrTiO_3 , RE-doping results in oxygen excesses, such as $\text{Sr}^{2+}_{1-z}\text{RE}^{3+}_z\text{Ti}^{4+}\text{O}_{3+\delta}$. After reducing in the H_2 atmosphere at high temperatures no lower than 1273 K, these materials possessed a stoichiometry of A-site, B-site and O-site, such as $\text{Sr}^{2+}_{1-z}\text{RE}^{3+}_z\text{Ti}^{4+}_{1-z}\text{Ti}^{3+}_z\text{O}_3$. The reduced perovskites showed good electrical conductivity, but exhibited a low corrosion resistance in a 50 wt% H_2SO_4 solution, due to the formation of SrSO_4 in the perovskites.

Doping various elements in SrTiO_3 -based perovskites for A-site deficiency was performed to suppress the reaction of Sr with H_2SO_4 . It was found that Nb- or Ta-doping to B-site formed A-site deficiency in the SrTiO_3 -based perovskite. The doped perovskites, $\text{Sr}_{1-x}\text{Ti}_{1-y}\text{M}_y\text{O}_{3+\delta}$, showed a good electrical conductivity higher than 1S/cm after the reducing treatment. Moreover, the high corrosion resistance of $\text{Sr}_{1-x}\text{Ti}_{1-y}\text{M}_y\text{O}_{3+\delta}$ perovskites was maintained under the electrolysis conditions.

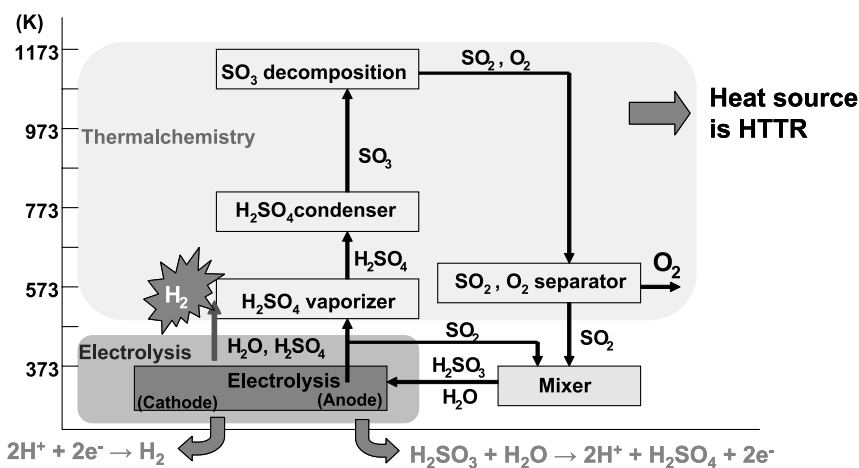
Keywords: Hydrogen production, Sulfur-based hybrid cycle, Electrolysis, Anode material, Electronic conductive ceramics, perovskite

1. Introduction

According to a desiring of hydrogen energy cycle in the near future, such as coming into wide use of fuel cells (FCs) and fuel cell vehicles (FCVs), the establishments of hydrogen production, its transportation and storage technologies are required. The use of hydrogen in FCs and FCVs will reduce Japanese dependence on foreign sources of petroleum and enhance our energy security.

As concerned for hydrogen transportation and storage technologies, a lot of research activities have been conducted and new technologies have been developed. However, a large-scale hydrogen production technology without using fossil fuel has not been established yet. Several kinds of large-scale of hydrogen production process have been proposed. Sulfur-based hybrid cycle (SHC) for hydrogen production using an advanced gas-cooled reactor (HTTR), is one of the hydrogen production processes by nuclear power and has attracted the attention as a large-scale and carbon dioxide (CO₂) free process, because of a high efficiency, simple process and low cost for hydrogen production [1]. The SHC process consists of two main processes, i.e., the electrolysis of $\text{H}_2\text{SO}_3 + \text{H}_2\text{O} \rightarrow \text{H}_2 + \text{H}_2\text{SO}_4$ at ~ 353 K and the thermal decomposition of $\text{H}_2\text{SO}_4 \rightarrow \text{H}_2\text{O} + \text{SO}_2 + 1/2\text{O}_2$ at ~ 1123 K. In order to reduce the material cost and to improve electrolysis efficiency in the SHC process, it is necessary to develop an inexpensive and high quality anode material, which has the high corrosion resistance, high electronic conductivity and low electrode over-potential for the electrochemical reaction, substitute for platinum group materials. Figure 1 shows the schematic flow of SHC.

Figure 1. Schematic flow of SHC



Our research group pointed out that some electronic conductive ceramics might be a candidate as the anode materials [2]. These ceramics are classified into two types by crystal structures. One is pyrochlore (chemical formula: $\text{A}_2\text{B}_2\text{O}_7$) and another is perovskite (chemical formula: ABO_3). We have reported the compatibility of the pyrochlores as the anodes in the SHC process [3], [4]. Also, we have found that Ti-based perovskite oxides, such as SrTiO_3 and CaTiO_3 , showed high corrosion resistance in the 50 weight (wt) % H_2SO_4 solution at 353K, simulated electrolytic condition [2]. Since there are no d-electrons (Ti^{4+} : d_0 system) and f-electrons in stoichiometric Ti-based perovskites (chemical formula: $\text{A}^{2+}\text{Ti}^{4+}\text{O}_3$), no electrical conductivity of these materials is anticipated at the operating temperature. Namely, the existence of Ti^{3+} ions in the perovskites leads to an appearance of electronic conduction. Formation techniques of Ti^{3+} ion in the perovskites are important.

In the previous paper [5], we have found that A-site deficient and rare earth metal (RE = Yb, Y, Sm, Gd, Nd, Pr, La)-doped $\text{RE}_{2-x}\text{Ti}_2\text{O}_7$.

In the present study, we focused rare earth metal (RE = Y, Yb, Gd, Sm, Nd, Pr, La)-doping technique to SrTiO₃, such as Sr²⁺_{1-z}RE³⁺_zTi⁴⁺_{1-z}Ti³⁺_zO₃, which was reduced at the high temperatures in the H₂ atmosphere, and A-site deficient one in the SrTiO₃-based perovskites, a series of Sr_{1-x}TiO_{3-δ}, in order to suppress a chemical reaction of Sr in SrTiO_{3-δ} with H₂SO₄. In addition, to form Ti³⁺ ion in the perovskites, it was thought to synthesise Nb- or Ta-substituted Sr_{1-x}Ti_{1-y}M_yO_{3+δ} (M = Nb, Ta) perovskites. In this paper, the crystallographic property, electrical conductivity and corrosion resistance of Sr_{1-x}Ti_{1-y}M_yO_{3+δ} (M = Nb, Ta) perovskites were investigated.

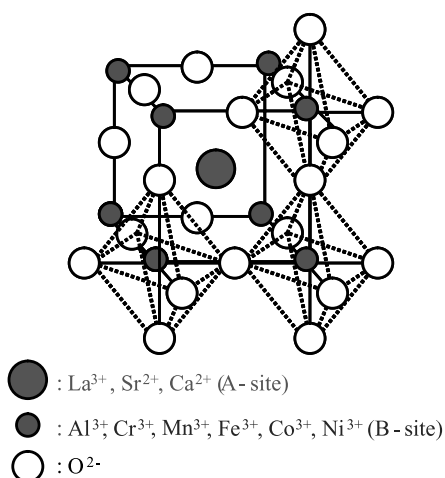
2. EXPERIMENTAL

2.1 Material Preparation

Figure 2 shows a structure of perovskite. In the previous work [2], it is found that some kinds of Ti oxide-based titanium oxide perovskites have high corrosion resistance in the 50 wt % H₂SO₄ solution at 353 K. Since non-doped SrTiO₃ perovskite is not electronic conductive ceramics at the electrolysis temperature, A-site substituents, rare earth metal (RE=Y, Yb, Gd, Sm, Nd, Pr, La)-doping (Sr_{1-z}RE_zTiO_{3+δ}), B-site substituents, metal ions (M = Nb, Ta)-doping, A-site deficient (Sr_{1-x}Ti_{1-y}M_yO_{3+δ} (M = Nb, Ta)) and a reducing treatment at high temperatures were thought in order to give electrical conductivity to SrTiO₃.

Sr_{1-z}RE_zTiO_{3+δ} (RE = Y, Yb, Gd, Sm, Nd, Pr, La) powders were synthesised by a Pechini method and Sr_{1-x}Ti_{1-y}M_yO_{3+δ} powders were synthesized by a solid-state reaction technique. Starting material powders, SrCO₃ (99.9%, High Purity Chem. Co., Japan), RE₂O₃ or Pr₆O₁₁ (pre-heated at 1 773 K for 1 hour, 99.9%, High Purity Chem., Japan), Nb₂O₅ (99.5%, Nacalai Tesque Co., Japan), Ta₂O₅ (99.9%, High Purity Chem. Co., Japan), and TiO₂ (pre-heated at 1 473K for 4 hours, 99.9%, rutile phase, High Purity Chem. Co., Japan) were used without further purification. They were weighed and mixed in a rotary-type Y₂O₃ partially stabilized ZrO₂ ball mill with iso-propyl alcohol. After drying, the mixtures were heated to 1 473K in air and held at this temperature for 10 hours. The powders were uniaxially pressed into a tablet under pressure of 40 MPa, and the tablets were pressed at a pressure of 100 MPa. The tablets were then sintered at 1 773 K for 10 hours in air, at a heating/cooling rate of 200 K/h. After pressing into the tablet again, a reducing treatment was conducted at 1 473 K for 1 hour under 50 ml/min hydrogen gas condition, at a heating rate of 2 K/min and at a cooling rate of 20 K/min.

Figure 2. Structure of perovskite



2.2 XRD Study

Crystallographic study was conducted using X-ray diffraction (XRD) technique. XRD patterns of powdered samples were obtained on a diffractometer (40 kV/40 mA, Mac Science, M18XHF²²) using monochromated Cu K α radiation and a scintillation detector, at a scanning rate of 0.02 $^{\circ}$ /s.

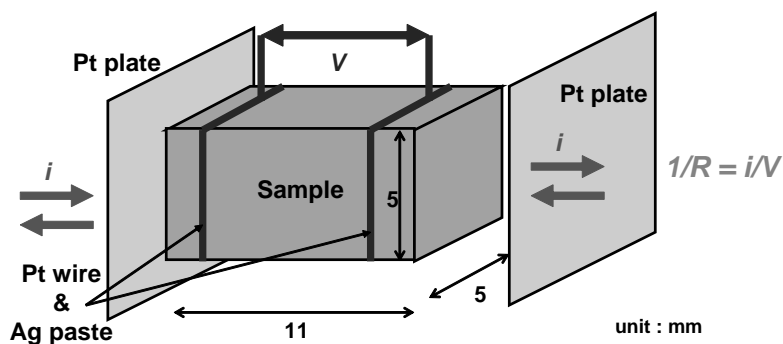
2.3 Oxygen Deficiency Measurement

Oxygen deficiency in a series of doped SrTiO_{3+ δ} perovskites was measured using thermo-gravity measurement (TG, Mac Science, TG-DTA-5000S). A flow rate of 50 ml/min H₂ gas was used in the TG measurements after the gas had been bubbled through pure water at 283K. The partial pressure of oxygen observed was almost the same as that calculated (3.6×10^{-19} atm for the calculated value versus 4.2×10^{-19} atm for the observed value).

2.4 Electrical Conductivity Measurement

Electrical conductivities for a series of sintered Sr_{1-z}RE_zTiO_{3+ δ} (RE = Y, Yb, Gd, Sm, Nd, Pr, La) and Sr_{1-x}Ti_{1-y}M_yO_{3+ δ} (M = Nb, Ta) perovskites were measured as a function of temperature using a D.C. current four-terminal method. The size of specimen used in the measurement was 5mm^t x 5mm^h x 11mm^l. Figure 3 shows the general view of the D.C. current four-terminal measurement. After the Pt-terminals were attached to the perovskite specimens using Ag-paste, electrical conductivity measurements were performed stepwise in air between 298 and 373 K under a vacuum condition.

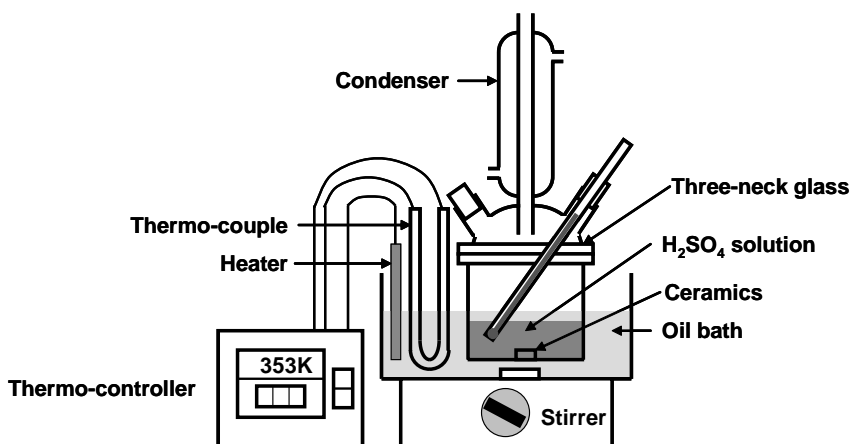
Figure 3. General view of the D.C. current four-terminal measurement



2.5 Corrosion Resistance Measurement

For corrosion resistance of a series of Sr_{1-z}RE_zTiO_{3+ δ} (RE = Y, Yb, Gd, Sm, Nd, Pr, La) and Sr_{1-x}Ti_{1-y}M_yO_{3+ δ} (M = Nb, Ta) perovskites, the sintered specimens and sample powders were evaluated in the 50 wt % H₂SO₄ aqueous solution at 353K. Figure 4 shows the three-neck glass cell used for the corrosion test. After the corrosion test, dissolved A-site and B-site elements in the H₂SO₄ solution were measured using Inductively Coupled Plasma Mass Spectrometry (ICP-MS, Shimazu, ICPM-8500).

Figure 4. Three-neck glass cell used for the corrosion test



3. RESULTS and DISCUSSION

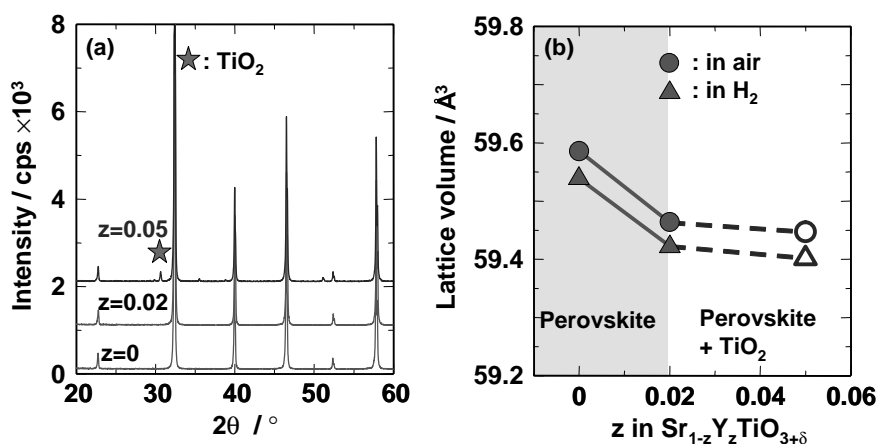
3.1 Crystallographic Study

3.1.1 Crystal structure of $Sr_{1-z}RE_zTiO_{3+\delta}$ ($RE=Y, Yb, Gd, Sm, Nd, Pr, La$)

All of the sintered $Sr_{1-z}RE_zTiO_{3+\delta}$ ($RE=Y, Yb, Gd, Sm, Nd, Pr, La$) were cubic perovskites.

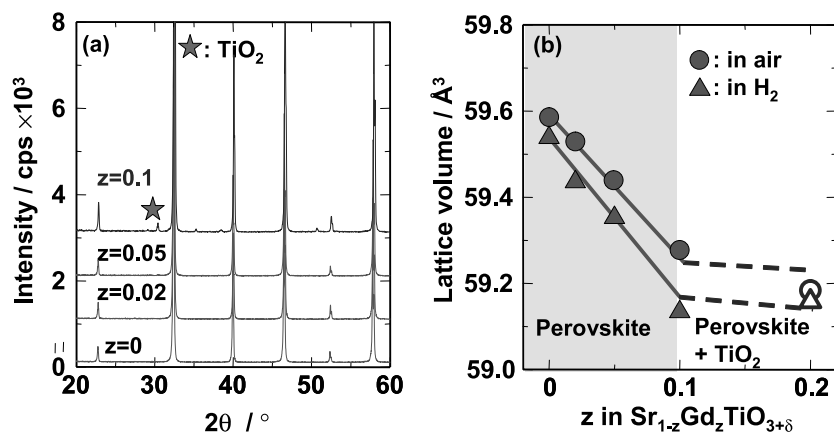
Figure 5(a) shows the XRD patterns of the $Sr_{1-z}Y_zTiO_{3+\delta}$ samples ($0 \leq z \leq 0.05$, $2\theta = 20 - 60^\circ$) after heating at 1873 K for 10 hours in air. The lattice volumes of $Sr_{1-z}Y_zTiO_{3+\delta}$ perovskites after heating at 1873 K for 10 hours in air and after heating at 1473 K for 1 hour in the H_2 atmosphere are summarized in Figure 5(b). In Figs. 5(a) and (b), the symbol represents a peak of TiO_2 . The XRD patterns showed that $Sr_{1-z}Y_zTiO_{3+\delta}$ perovskite contained a very small amount of TiO_2 in addition to the perovskite phase, when z was 0.05. The lattice volumes of the $Sr_{1-z}Y_zTiO_{3+\delta}$ perovskites in the H_2 atmosphere were smaller than those in air, because of the reduction of Ti^{4+} (74.5×10^{-3} nm) into Ti^{3+} (81.0×10^{-3} nm) and the formation of oxygen enrichment. The samples showed a single perovskite phase in the narrow A-site substituent region of $0 \leq z < 0.05$.

Figure 5. (a) The XRD patterns and (b) lattice volumes of the $Sr_{1-z}Y_zTiO_{3+\delta}$ samples



Figures 6(a) and (b) show the XRD patterns and lattice volumes of the $\text{Sr}_{1-z}\text{Gd}_z\text{TiO}_{3+\delta}$ samples ($0 \leq z \leq 0.1$, $2\theta = 20 - 60^\circ$) after heating at 1 873 K for 10 h in air, and after heating at 1 473 K for 1 h in the H_2 atmosphere, respectively. In Figures 6(a) and (b), the symbol represents a peak of TiO_2 . The XRD patterns showed that the samples contained a very small amount of TiO_2 in addition to the perovskite phase, when z was 0.1. The lattice volumes of the $\text{Sr}_{1-z}\text{Gd}_z\text{TiO}_{3+\delta}$ perovskites in the H_2 atmosphere were smaller than those in air, because of the reduction of Ti^{4+} into Ti^{3+} and the formation of oxygen enrichment. The samples showed a single perovskite phase in the narrow A-site substituent region of $0 \leq z < 0.1$.

Figure 6. (a) The XRD patterns and (b) lattice volumes of the $\text{Sr}_{1-z}\text{Gd}_z\text{TiO}_{3+\delta}$ samples



Figures 7(a) and (b) show the XRD patterns and lattice volumes of the $\text{Sr}_{1-z}\text{La}_z\text{TiO}_{3+\delta}$ samples ($0 \leq z \leq 0.3$, $2\theta = 20 - 60^\circ$) after heating at 1 873K for 10 hour in air, and after heating at 1 473 K for 1 h in the H_2 atmosphere, respectively. In Figs. 7(a) and (b), the symbol represents a peak of TiO_2 . The XRD patterns showed that the samples contained a very small amount of TiO_2 in addition to the perovskite phase, when z was 0.3. The lattice volumes of the $\text{Sr}_{1-z}\text{La}_z\text{TiO}_{3+\delta}$ perovskites in the H_2 atmosphere were smaller than those in air, because of the reduction of Ti^{4+} into Ti^{3+} and the formation of oxygen enrichment. The samples showed a single perovskite phase in the wide A-site substituent region of $0 \leq z < 0.3$.

Figure 7. (a) The XRD patterns and (b) lattice volumes of the $\text{Sr}_{1-z}\text{La}_z\text{TiO}_{3+\delta}$ samples

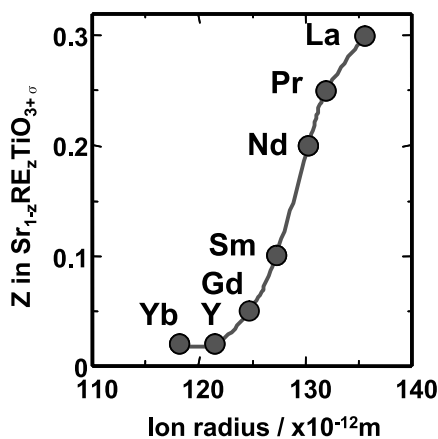
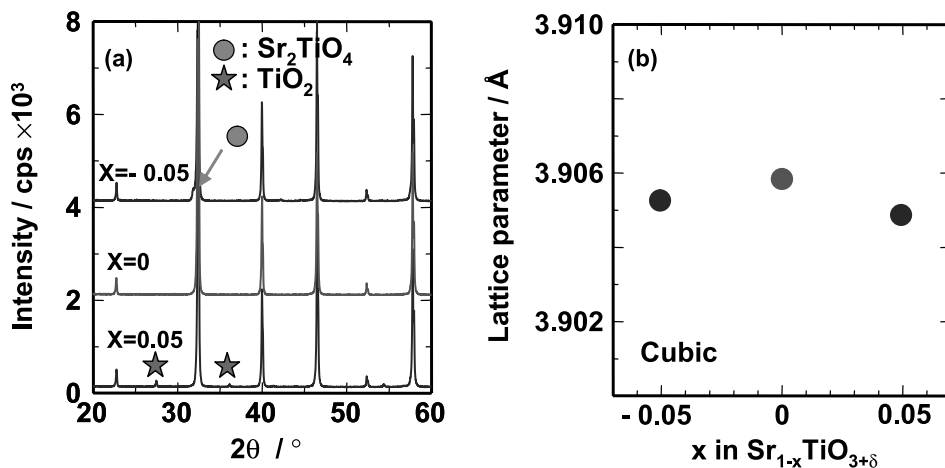


Figure 8 shows the relationship between A-site ionic radius and stable A-site substituents (z) in the $\text{Sr}_{1-z}\text{RE}_z\text{TiO}_{3+\delta}$ ($\text{RE}=\text{Y}, \text{Yb}, \text{Gd}, \text{Sm}, \text{Nd}, \text{Pr}, \text{La}$) structure. A-site substituents in the perovskites increased with increasing ionic radius of RE ion up to approximately $135 \times 10^{-3} \text{ nm}$.

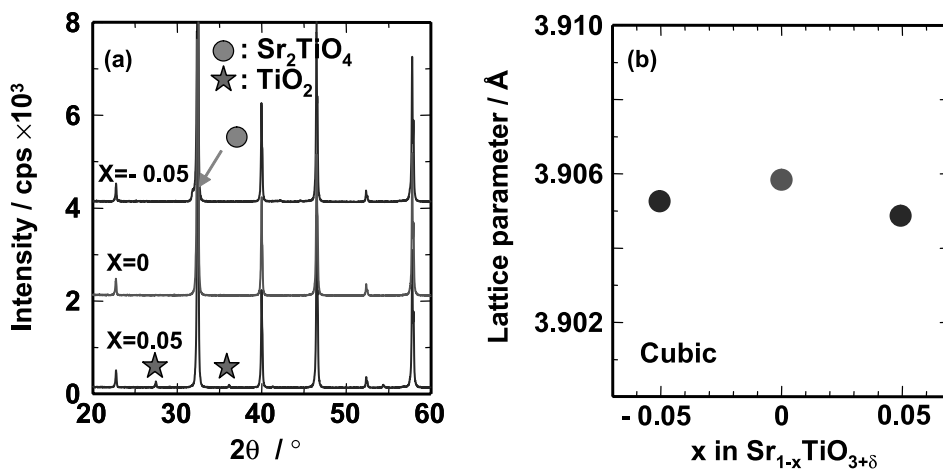
Figure 8. The relationship between A-site ionic radius and stable A-site substituents (z) in the $\text{Sr}_{1-z}\text{RE}_z\text{TiO}_{3+\delta}$ ($\text{RE}=\text{Y}, \text{Yb}, \text{Gd}, \text{Sm}, \text{Nd}, \text{Pr}, \text{La}$) structure



3.1.2 Crystal structure of $\text{Sr}_{1-x}\text{TiO}_{3+d}$

Figures 9(a) and (b) show the XRD patterns and lattice parameters of the $\text{Sr}_{1-x}\text{TiO}_{3+\delta}$ samples ($-0.05 \leq x \leq 0.05$, $2\theta = 20 - 60^\circ$) after heating at 1773 K. After heating at 1773 K, the $\text{SrTiO}_{3+\delta}$ crystallized in a cubic perovskite unit $a = 3.9058(2) \text{ \AA}$, $V = 59.59 \text{ \AA}^3$ and $z = 1$. The value was in good agreement with the previous work [6]. The solubility limit of each oxide into $\text{SrTiO}_{3+\delta}$ was determined by an appearance of peaks of the oxides and reaction products, and a change of lattice parameters of $\text{SrTiO}_{3+\delta}$. The XRD patterns showed that the samples contained very small amounts Sr_2TiO_4 for $\text{Sr}_{0.95}\text{TiO}_{3+\delta}$ and TiO_2 for $\text{Sr}_{1.05}\text{TiO}_{3+\delta}$, as second phases, in addition to the perovskite, respectively.

Figure 9. (a) The XRD patterns and (b) lattice parameters of the $\text{Sr}_{1-x}\text{TiO}_{3+\delta}$ samples



3.1.3 Crystal structure of $\text{SrTi}_{1-y}\text{M}_y\text{O}_{3+\delta}$ ($M=\text{Nb}, \text{Ta}$)

Figure 10(a) shows the XRD patterns of the $\text{SrTi}_{1-y}\text{Nb}_y\text{O}_{3+\delta}$ samples ($0 \leq y \leq 0.3$, $2\theta = 20 - 60^\circ$) after heating at 1 773 K in air. The XRD patterns showed that although the $\text{SrTi}_{0.7}\text{Nb}_{0.3}\text{O}_{3+\delta}$ samples contained very small amounts of $\text{Sr}_6\text{Nb}_{10}\text{O}_{30}$ [7] and SrO as second phases in addition to the perovskite phase, no peaks for second phase was observed for other samples. No significant differences of the patterns between the samples before and after reducing were observed. It is seen in the figure that, the [100] reflection decreased with increasing Nb content. In the perovskite structure, the [100] reflection is appeared by a difference of X-ray amplitude after diffracting. Thus, the decrease of this reflection would relate that the difference of the amplitude would be diminished by B-site doping of heavy element. These results suggest that it can be occupied by Nb^{5+} ion substituted for Ti^{4+} ion at the B-site.

Figure 10(b) summarises the lattice parameters of $\text{SrTi}_{1-y}\text{Nb}_y\text{O}_{3+\delta}$ as a function of dopant content, after heating at 1 773 K in air and at 1 273 K for 1 h in the H_2 atmosphere. With increasing dopant contents, the lattice parameters of the Nb doped perovskites increased up to 20 mol% and then showed the constant value. The increases in lattice parameters can be explained by the fact that ionic radius of Nb^{5+} ($=78 \times 10^{-3} \text{ nm}$) is larger than that of Ti^{4+} ion ($=74.5 \times 10^{-3} \text{ nm}$) in the perovskites structure. It was concluded that the solubility ranges were $0 \leq x \leq 0.2$ for Nb_2O_5 . No significant changes of the lattice parameters in the stoichiometric perovskites after heating in the H_2 atmosphere were observed. This result indicates that it is not an easy task to reduce Ti^{4+} and Nb^{5+} ions in the stoichiometric perovskites.

Figure 10. (a) The XRD patterns and (b) lattice parameters of the $\text{SrTi}_{1-y}\text{Nb}_y\text{O}_{3+\delta}$ samples

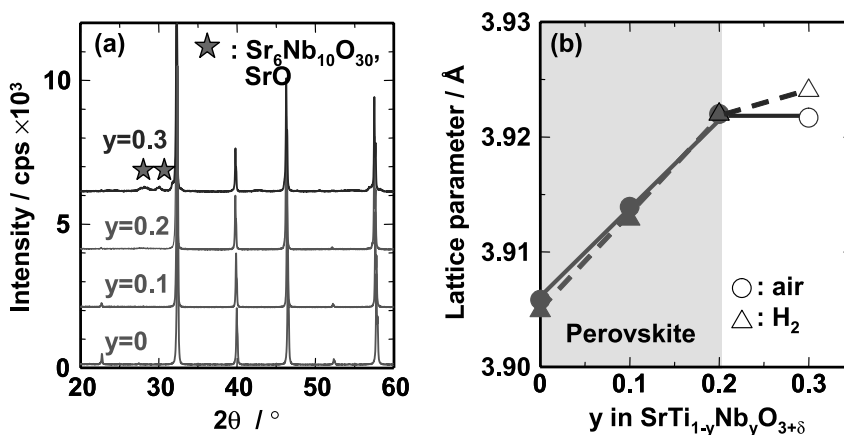


Figure 11(a) shows the XRD patterns of the $\text{SrTi}_{1-y}\text{Ta}_y\text{O}_{3+\delta}$ ($0 \leq y \leq 0.3$, $2\theta = 20 - 60^\circ$) after heating at 1773 K in air. No significant differences of the patterns between the samples before and after reducing were observed. The samples showed a single perovskite phase in the wide B-site substituent region of $0 \leq y \leq 0.3$. In the $\text{SrTi}_{1-x}\text{Ta}_x\text{O}_{3+\delta}$ system, SrO as second phases was observed for $\text{SrTi}_{0.7}\text{Ta}_{0.3}\text{O}_{3+\delta}$ sample. It is also seen in this figure that, the [100] reflection decreased with increasing Ta content.

Figure 11(b) summarises the lattice parameters of $\text{SrTi}_{1-x}\text{Ta}_x\text{O}_{3+\delta}$ as a function of dopant content, after heating at 1,773K in air and at 1,273K for 1 hour in the H_2 atmosphere. The lattice parameters of the Ta- doped perovskites increased monotonically up to 30 mol%. The increases in lattice parameters can be explained by the fact that ionic radius of Ta^{5+} ($=78 \times 10^{-3} \text{ nm}$) is larger than that of Ti^{4+} ion ($=74.5 \times 10^{-3} \text{ nm}$) in the perovskites structure. It was concluded that the solubility range was $0 \leq y < 0.3$ in the system of $\text{SrTi}_{1-x}\text{Ta}_x\text{O}_{3+\delta}$. No significant changes of the lattice parameters in the stoichiometric perovskites after heating in the H_2 atmosphere were observed.

Figure 11. (a) The XRD patterns and (b) lattice parameters of the $\text{SrTi}_{1-y}\text{Ta}_y\text{O}_{3+\delta}$ samples

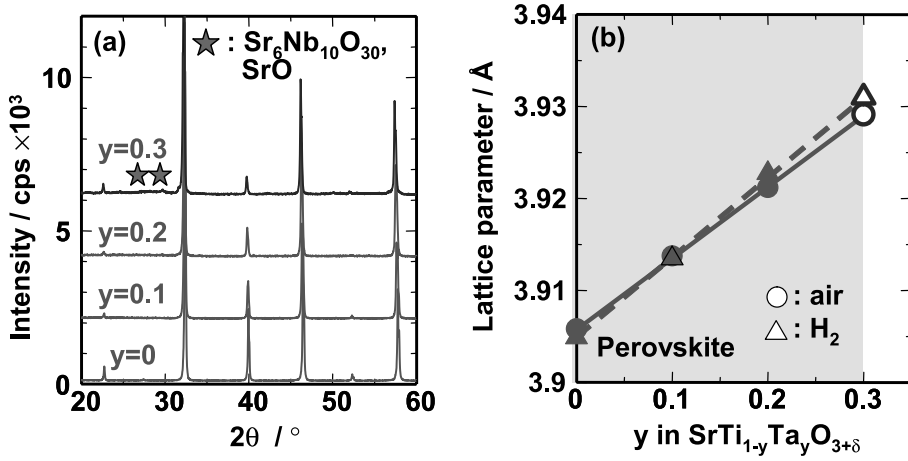
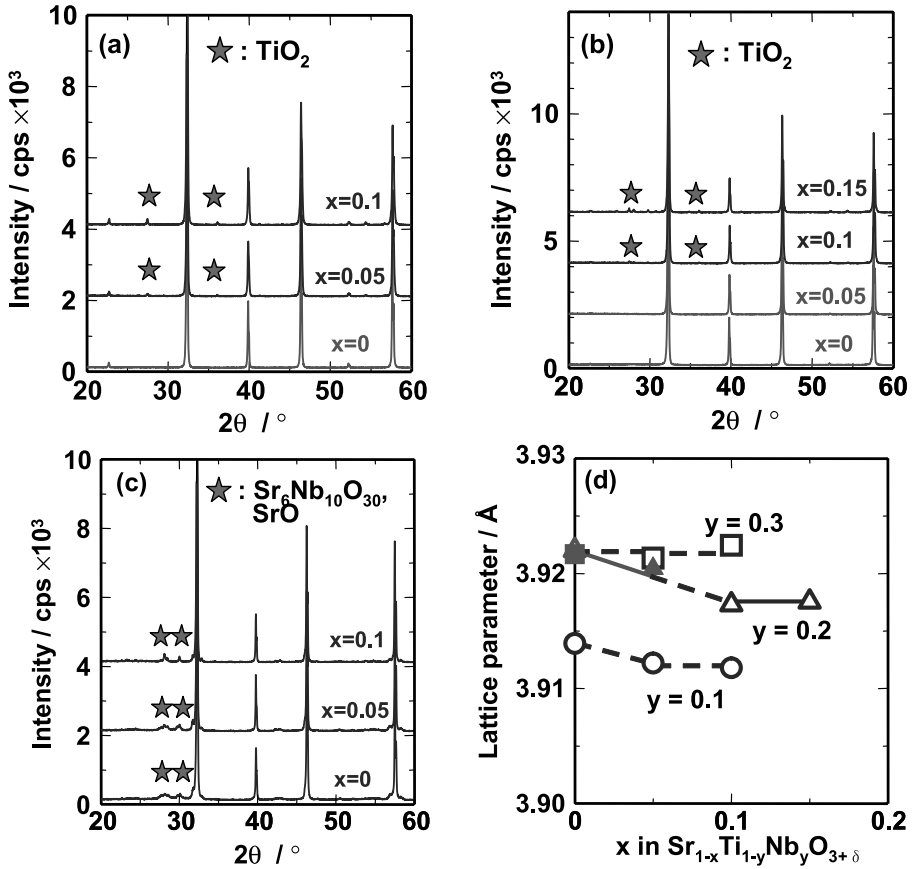


Figure 12. The XRD patterns of (a) $\text{Sr}_{1-x}\text{Ti}_{0.9}\text{Nb}_{0.1}\text{O}_{3+\delta}$, (b) $\text{Sr}_{1-x}\text{Ti}_{0.8}\text{Nb}_{0.2}\text{O}_{3+\delta}$, (c) $\text{Sr}_{1-x}\text{Ti}_{0.7}\text{Nb}_{0.3}\text{O}_{3+\delta}$, and (d) lattice parameters of the $\text{Sr}_{1-x}\text{Ti}_{1-y}\text{Nb}_y\text{O}_{3+\delta}$ samples

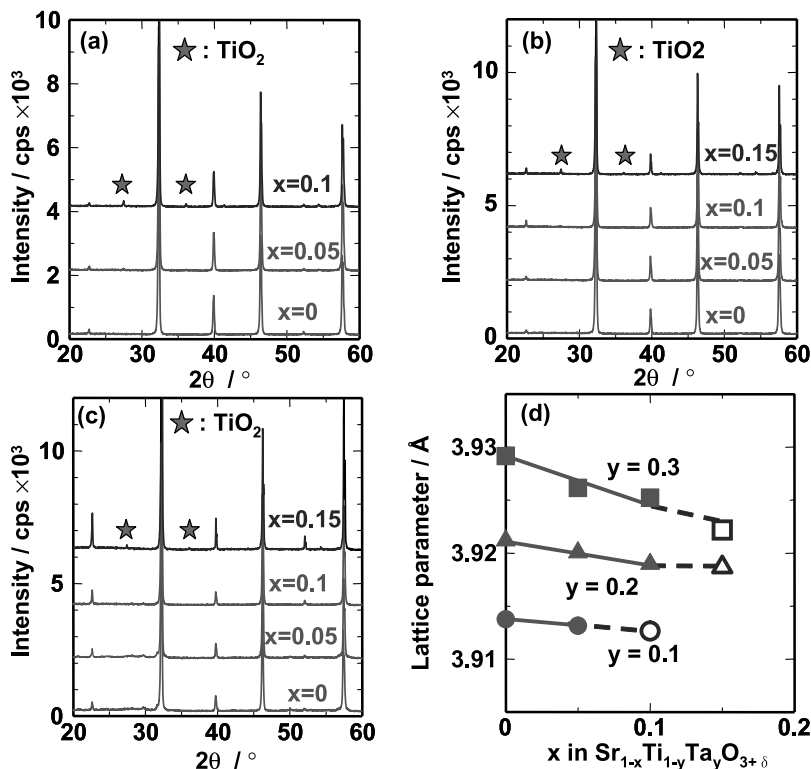


3.1.4 Crystal structure of $Sr_{1-x}Ti_{1-y}M_yO_{3+\delta}$ ($M=Nb, Ta$)

Figures 12(a), (b), and (c) show the XRD patterns of the $Sr_{1-x}Ti_{0.9}Nb_{0.1}O_{3+\delta}$ ($0 \leq x \leq 0.1$, $2\theta = 20 - 60^\circ$), $Sr_{1-x}Ti_{0.8}Nb_{0.2}O_{3+\delta}$ ($0 \leq x \leq 0.15$, $2\theta = 20 - 60^\circ$), and $Sr_{1-x}Ti_{0.7}Nb_{0.3}O_{3+\delta}$ perovskites ($0 \leq x \leq 0.1$, $2\theta = 20 - 60^\circ$) after heating at 1773 K in air. No significant differences of the patterns between the samples before and after reducing were observed. Except for $Sr_{0.95}Ti_{0.8}Nb_{0.2}O_{3+\delta}$ sample, TiO_2 , SrO and $Sr_6Nb_{10}O_{30}$ [7] as second phases were observed in addition to the perovskite phase. The samples showed a single perovskite phase in the B-site substituent region of $0 \leq x \leq 0.05$. Figure 12(d) summarises the lattice parameters of $Sr_{1-x}Ti_{1-y}Nb_yO_{3+\delta}$ as a function of dopant contents with a parameter of A-site deficiency. The closed symbols represent the samples with single perovskite phase. The lattice parameter of $Sr_{1-x}Ti_{1-y}Nb_yO_{3+\delta}$ perovskites has a tendency to decrease with decreasing Sr content. Only $Sr_{0.95}Ti_{0.8}Nb_{0.2}O_{3+\delta}$ sample showed a single perovskite phase.

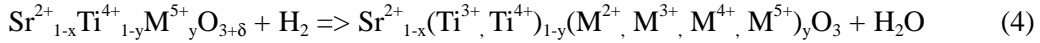
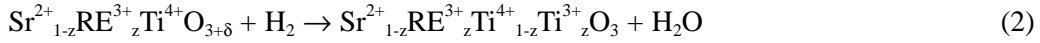
Figures 13(a), (b), and (c) show the XRD patterns of the $Sr_{1-x}Ti_{0.9}Ta_{0.1}O_{3+\delta}$ ($0 \leq x \leq 0.1$, $2\theta = 20 - 60^\circ$), $Sr_{1-x}Ti_{0.8}Ta_{0.2}O_{3+\delta}$ ($0 \leq x \leq 0.15$, $2\theta = 20 - 60^\circ$), and $Sr_{1-x}Ti_{0.7}Ta_{0.3}O_{3+\delta}$ perovskites ($0 \leq x \leq 0.1$, $2\theta = 20 - 60^\circ$) after heating at 1773 K in air. The XRD patterns showed that the samples contained a very small amount of TiO_2 as a second phase in addition to the perovskite. No significant differences of the patterns between the samples before and after reducing were observed. Figures 13(d) summarizes the lattice parameters of $Sr_{1-x}Ti_{1-y}Ta_yO_{3+\delta}$ as a function of dopant contents with a parameter of A-site deficiency. The closed symbols represent the samples with single perovskite phase. In the $Sr_{1-x}Ti_{1-y}Ta_yO_{3+\delta}$ system, the single phase region of A-site deficient perovskites and the A-site deficiency increased with increasing Ta content. When the $Sr_{1-x}Ti_{1-y}Ta_yO_{3+\delta}$ samples were compared with the $Sr_{1-x}Ti_{1-y}Nb_yO_{3+\delta}$ ones, it showed much wider region of a single perovskite phase with A-site deficiency.

Figure 13. The XRD patterns of (a) $Sr_{1-x}Ti_{0.9}Ta_{0.1}O_{3+\delta}$, (b) $Sr_{1-x}Ti_{0.8}Ta_{0.2}O_{3+\delta}$, (c) $Sr_{1-x}Ti_{0.7}Ta_{0.3}O_{3+\delta}$, and (d) lattice parameters of the $Sr_{1-x}Ti_{1-y}Ta_yO_{3+\delta}$ samples



3.2 Oxygen contents in titanium oxide perovskites

In order to add electrical conductivity to non-conductive $\text{Sr}_{1-z}\text{RE}_z\text{TiO}_3$ (RE = Y, Yb, Gd, Sm, Nd, Pr, and La), $\text{SrTi}_{1-y}\text{M}_y\text{O}_3$ and $\text{Sr}_{1-x}\text{Ti}_{1-y}\text{M}_y\text{O}_3$ perovskites, the formation of Ti^{3+} ion has been considered by a hydrogen reducing treatment at high-temperatures. This reaction should be expressed by the following equations.



Since the decrease of excess oxygen, δ , namely the formation of Ti^{3+} ion, in the perovskites is achieved by the hydrogen reducing treatment, oxygen is removed from the structure by the hydrogen reduction.

Figures 14 and 15 show the oxygen vacancy in $\text{Sr}_{1-z}\text{RE}_z\text{TiO}_{3+\delta}$ (RE = Y, Yb, Gd, Sm, Nd, Pr, and La) and $\text{Sr}_{1-x}\text{Ti}_{1-y}\text{M}_y\text{O}_{3+\delta}$ perovskites (M = Nb, Ta) in the H_2 atmosphere as a function of temperature, respectively. In this figure, the oxygen content of the perovskites at approximately 323K in the H_2 atmosphere is assumed to be the value, which is stoichiometrically charge-compensated by the cations. The broken line in Figures 14 and 15 show the stoichiometry of oxygen in the perovskites. Although the oxygen vacancy of the stoichiometric perovskites existed at high-temperatures, it recovered during the cooling process. On the other hand, there remained the oxygen vacancy in the A-site substituted perovskites. Oxygen vacancies value in $\text{Sr}_{0.8}\text{La}_{0.2}\text{TiO}_{3+\delta}$ and $\text{Sr}_{0.9}\text{Ti}_{0.8}\text{Nb}_{0.2}\text{O}_3$ reached at approximately 0.07 and 0.22 at 1473 K and 1673 K, respectively, and these values were kept until room temperature. Therefore, it was tentatively concluded that the A-site substituent and deficiency in the perovskites resulted in the high stability of oxygen vacancy formation in the perovskites.

3.3 Electrical Conductivity

Figure 16 shows the electrical conductivity of the $\text{Sr}_{1-z}\text{RE}_z\text{TiO}_{3+\delta}$ (RE=Y, Yb, Gd, Sm, Nd, Pr, La) and $\text{Sr}_{1-z}\text{Ti}_{1-y}\text{M}_y\text{O}_{3+\delta}$ (M = Nb, Ta) perovskites at 353 K, in comparison with the conductivities of $\text{RE}_{2-x}\text{Ti}_2\text{O}_{7-\delta}$ pyrochlores [3, 4] and the A-site doped $\text{Sr}_{1-z}\text{RE}_z\text{TiO}_{3+\delta}$ (RE = Y, Yb, Gd, Sm, Nd, Pr, La) perovskites. As seen in Figure 16, it was revealed that the electrical conductivities of reduced samples at 353 K were approximately 0.7 to 9 S/cm for $\text{Sr}_{1-z}\text{RE}_z\text{TiO}_{3+\delta}$, 1 to 2 S/cm for $\text{Sr}_{0.95}\text{Ti}_{1-y}\text{M}_y\text{O}_{3+\delta}$ and approximately 10 to 15 S/cm for $\text{Sr}_{0.9}\text{Ti}_{1-y}\text{M}_y\text{O}_{3+\delta}$. These conductivities were higher than those of titanium oxide pyrochlores [3, 4] and the A-site-doped $\text{Sr}_{1-z}\text{RE}_z\text{TiO}_{3+\delta}$ perovskites.

Figure 14. Relationship between oxygen vacancy δ of (a) $\text{Sr}_{1-x}\text{Nd}_x\text{TiO}_{3+\delta}$, (b) $\text{Sr}_{1-x}\text{Pr}_x\text{TiO}_{3+\delta}$, and (c) $\text{Sr}_{1-x}\text{La}_x\text{TiO}_{3+\delta}$ in the H_2 atmosphere and temperature

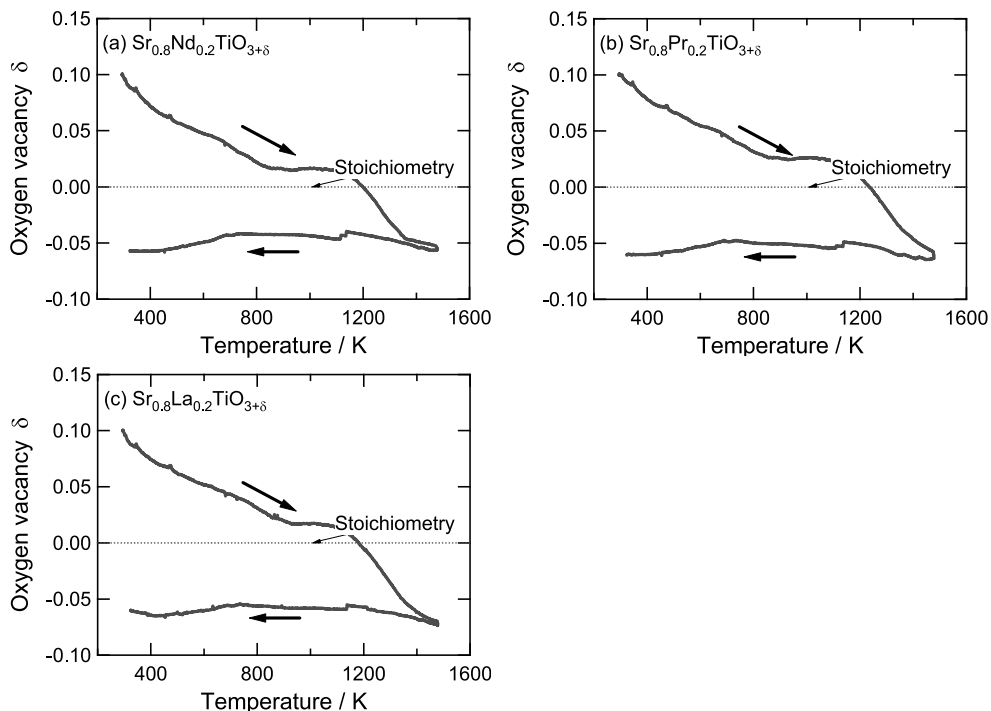


Figure 15. Relationship between oxygen vacancy δ of (a) $\text{Sr}_{0.95}\text{Ti}_{0.8}\text{Nb}_{0.2}\text{O}_3$, (b) $\text{Sr}_{0.95}\text{Ti}_{0.9}\text{Ta}_{0.1}\text{O}_3$, and (c) $\text{Sr}_{0.95}\text{Ti}_{0.8}\text{Ta}_{0.2}\text{O}_3$ in the H_2 atmosphere and temperature

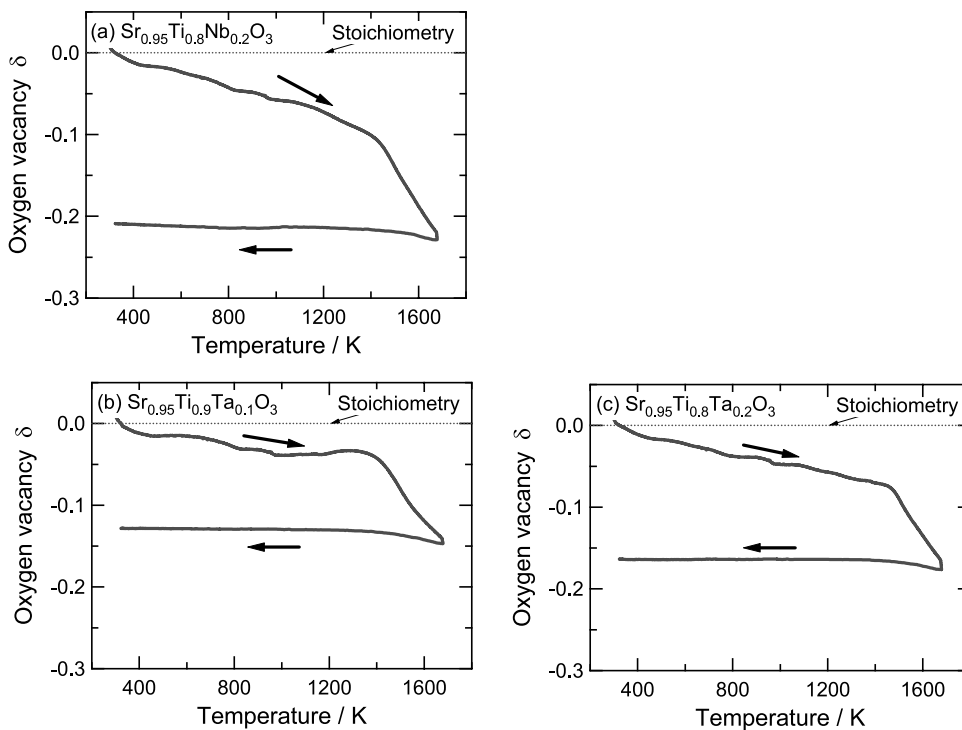
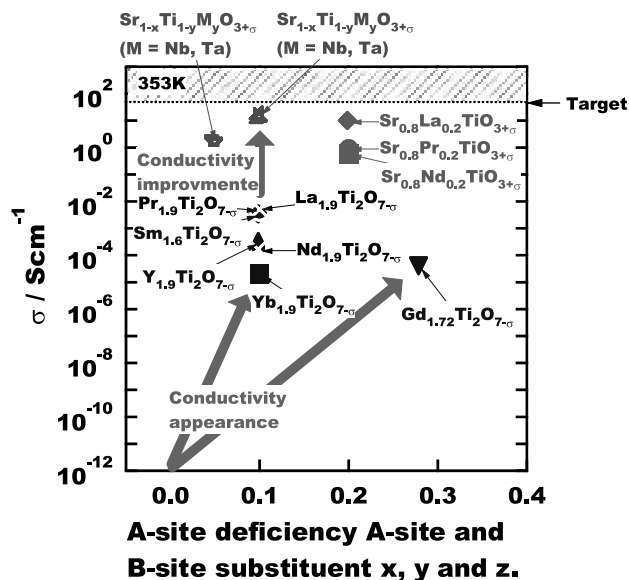


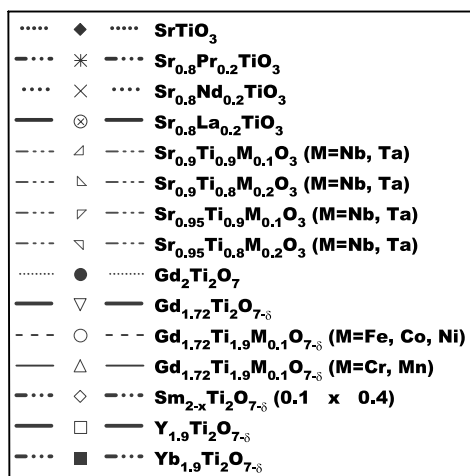
Figure 16. Relationship between electronic conductivity and A-site deficiencies and substituents of perovskites and pyrochlores at 353K

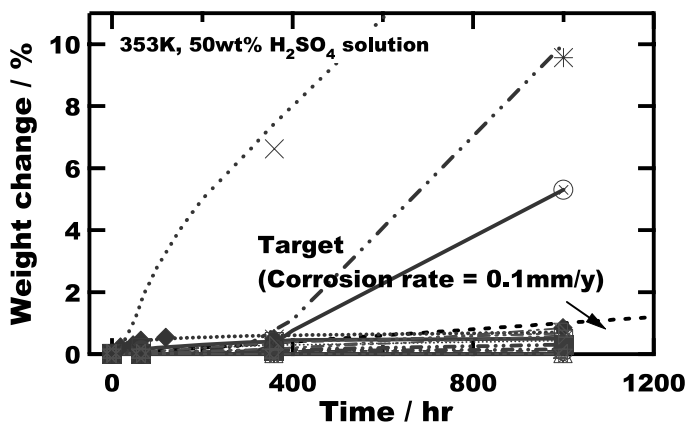


3.4 Corrosion Resistance

Figure 17 shows the relationship between test time and weight change of the titanate perovskites in 50 wt% H_2SO_4 aqueous solution at 353 K, simulated electrolytic condition. The weight changes of titanium oxide pyrochlores [3, 4] are also shown in the Figure. As seen in this Figure, it was revealed that all of the A-site doped $Sr_{1-z}RE_zTiO_{3+\delta}$ ($RE = Y, Yb, Gd, Sm, Nd, Pr,$ and La) perovskites showed low corrosion resistance in the H_2SO_4 , and $SrSO_4$ as a reaction product was formed. On the other hand, $Sr_{1-x}Ti_{1-y}M_yO_{3+\delta}$ ($M = Nb, Ta$) perovskites had high corrosion resistance. From the ICP-MS analysis, the dissolved A-site and B-site elements in the H_2SO_4 solution were several ppb.

Figure 17. Times dependence of weight change of perovskites and pyrochlores in 50w% H_2SO_4 solution at 353K





4. CONCLUSIONS

We reported the preparation and crystallographic characteristics of various perovskites as candidates of the anode materials in sulfur-based hybrid cycle for hydrogen production and proposed some techniques of electrical conductivity appearance for the perovskites.

- (1) Ti^{3+} ions with d_I system can exist stably in the A-site doped $Sr_{1-z}RE_zTiO_{3+\delta}$ ($RE = Y, Yb, Gd, Sm, Nd, Pr,$ and La) perovskites at room temperature. The concentration of Ti^{3+} ions in the perovskites leads to an increase of electrical conductivity. Amounts of A-site doping $Sr_{1-z}RE_zTiO_{3+\delta}$ perovskites with cubic symmetry had a tendency to form a single phase with increasing doping ion radius.
- (2) As possible B-site substituents, $Sr_{1-x}Ti_{1-y}M_yO_{3+\delta}$ ($M = Nb, Ta$) are appropriate with respect to an appearance of electrical conductivity. Ti^{3+} ions with d_I system can be existed stably by the formation of A-site deficiency in the B-site-substituted $Sr_{1-x}Ti_{1-y}M_yO_{3+\delta}$ ($M = Nb, Ta$) perovskites at room temperature. From the results of crystallographic study, it is revealed that the B-site-substituted $Sr_{1-x}Ti_{1-y}M_yO_{3+\delta}$ with cubic symmetry showed a single perovskite phase in the range of $0 \leq y \leq 0.2$ for Nb and $0 \leq y < 0.3$ for Ta.
- (3) A series of corrosion tests, which conducted in a 50 wt% H_2SO_4 solution at 353 K, revealed that all of the $Sr_{1-x}Ti_{1-y}M_yO_{3+\delta}$ ($M = Nb, Ta$) perovskites had high corrosion resistance, indicating that the $Sr_{1-x}Ti_{1-y}M_yO_{3+\delta}$ perovskites with good electrical conductivities (> 1 S/cm) are promising anode materials for SHC process.
- (4) Rare earth metal RE-doped $SrTiO_3$ ($RE = Nd, Pr,$ and La) in forms of $Sr_{1-z}RE_zTi_{1-z}Ti_zO_3$ showed good electrical conductivity after being reduced at high temperatures in the H_2 atmosphere, but exhibited low corrosion resistance in a 50% H_2SO_4 solution at 353 K, due to the formation of $SrSO_4$.

REFERENCES

- [1] The Conceptual Design of an Integrated Nuclear-Hydrogen Production Plant Using the Sulfur Cycle Water Decomposition System, Westinghouse Electric Co., NASA CR-134976, (1976).
- [2] M. Mori, H. Kwamura, D. Kusano and M. Uotani: Electrode for the Sulfur Cycle for Thermochemical Decomposition of Water – $\text{Ln}_{2-x}\text{Ti}_2\text{O}_{7-\delta}$ Based Oxides –, Proceedings of Japan Electrochem. Soc., in Japanese, (2003).
- [3] H. Kawamura, M. Mori D. Kusano and M. Uotani, “Sulfur-based hybrid cycle for hydrogen production (Part 1) – Electrical conductivity and corrosion resistance of reduced $\text{Gd}_{2-x}\text{Ti}_{2-y}\text{M}_y\text{O}_{7-\delta}$ ($\text{M}=\text{Cr}, \text{Mn}, \text{Fe}, \text{Co}, \text{and Ni}$) anode by B-site doping”, Proceedings of 15th World Hydrogen Energy Conference, June (2004).
- [4] M. Mori, H. Kawamura, D. Kusano and M. Uotani, “Sulfur-based hybrid cycle for hydrogen production (Part 2) – Electrical conductivity and corrosion resistance of reduced $\text{Gd}_{2-x}\text{Ti}_{2-y}\text{M}_y\text{O}_{7-\delta}$ ($\text{M}=\text{Cr}, \text{Mn}, \text{Fe}, \text{Co}, \text{and Ni}$) anode by B-site doping”, Proceedings of 15th World Hydrogen Energy Conference, June (2004).
- [5] M. Mori, H. Kawamura, D. Kusano, and M. Uotani, “Hydrogen production for sulfur-based hybrid cycle -Relationship between electrical conductivity and corrosion resistance of reduced $\text{Sr}_{1-x}\text{RE}_x\text{TiO}_{3+\delta}$ anode – ”, Proceedings of Annual ECS Meeting, Hawaii, USA, October 2-7, (2004).
- [6] H. Swanson, Natl. Bur. Stand (U.S), Circ, 539, 3, 44 (1954).
- [7] E. Antipov, O. D'yachenko, Moscow State Unive., Russia. ICDD Grant-in-Aid (1993).

This page intentionally left blank

GENERATION OF H₂ BY DECOMPOSITION OF PULP IN SUPERCRITICAL WATER WITH RUTHENIUM (IV) OXIDE CATALYST

Yukihiro Izumizaki¹, Ki Chul Park², Yuu Tachibana²,

Hiroshi Tomiyasu³ and Yasuhiko Fujii¹)

¹Research Laboratory for Nuclear Reactors, Tokyo Institute of Technology

²Department of Chemistry and Material Engineering,

Faculty of Engineering, Shinshu University

³Nippon TMI Co., Ltd

Abstract

The production of hydrogen from pulp, a kind of biomass, in supercritical water in the presence of ruthenium (IV) dioxide RuO₂ as a catalyst was studied. All experiments were carried out under argon atmosphere to avoid the effect of oxide during reaction. It was observed that RuO₂ enhanced the decomposition ratio for pulp. And reaction time does not so much affect the generated amount of hydrogen. Higher water density enhanced decomposition ratio. Hydrogen distribution was however decreased.

Introduction

In view of an environmental problem concerning the global warming and a depletion of petroleum, interest has been focused on the reduction of carbon dioxide and the use of alternative energy. The use of biomass is one of the possible methods not to increase carbon dioxide, because amount of CO₂ in the atmosphere is balanced during the growth and the combustion of biomass. Furthermore, biomass is an energy source that can be reproduced.

The use of hot compressed water as a reaction medium is one of the methods producing fuel from biomass. Biomass contains moisture. The process using water does not have to carry out drying process as pretreatment. A number of studies have been reported with respect to the gasification of biomass. In many cases, biomass decomposition was conducted with an aid of catalyst. Ni catalyst was one of the major catalysts [1-5]. Alkali catalyst was also used in supercritical water [6-10]. Many researchers have been investigating properties of these catalysts. The exploitation of other catalysts has been continued to be researched [11-15]. In earlier paper, we reported the catalytic decompositions of organic compounds by use of RuO₂ in supercritical water [16]. Organic compounds including aromatic compound (e.g. Naphthalene) were completely decomposed and gasified in supercritical water in the presence of ruthenium (IV) dioxide as a catalyst. Aromatic compound are too stable to be decomposed in supercritical water without catalyst [17]. Produced gasses were mainly methane, hydrogen and carbon dioxide. We utilised this catalyst for decomposition of pulp an example of biomass. RuO₂ catalyst enhanced decomposition ratio for pulp (17.8% without catalyst, 71.3% with catalyst). In this work, we report the effect of two more fundamental factors in this paper.

Experimental

The reactor, whose inner volume was 10.8dm³, made of INCONEL625 as seen in Figure 1 was used in all experiments. Experimental procedure is displayed in Fig 2. Pulp, RuO₂ catalyst (purchased from Kanto chemicals), and distilled water were loaded into the reactor. A valve was attached for the quantitative gas analysis. Inside air was replaced with argon atmosphere. Reactor and inner contents were heated by electric heater. Inside pressure automatically increased with increasing temperature. After reaction and cooling of the reactor, produced gas was analysed based on the previously determined volume of gas-line (Figure 3). The decomposition (gasification) ratio was calculated as follow: (Gasification ratio) = 100 x (carbon in gaseous products)/(carbon in samples loaded)

Figure 1. The Reactor and Valve

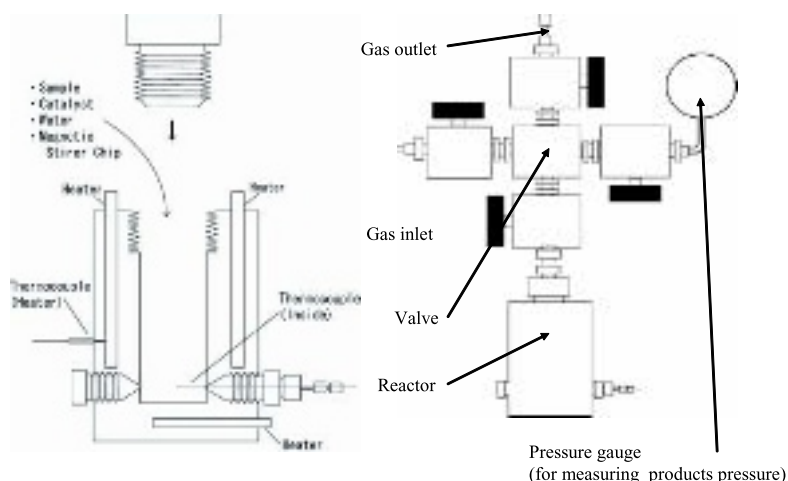


Figure 2. Experimental procedure

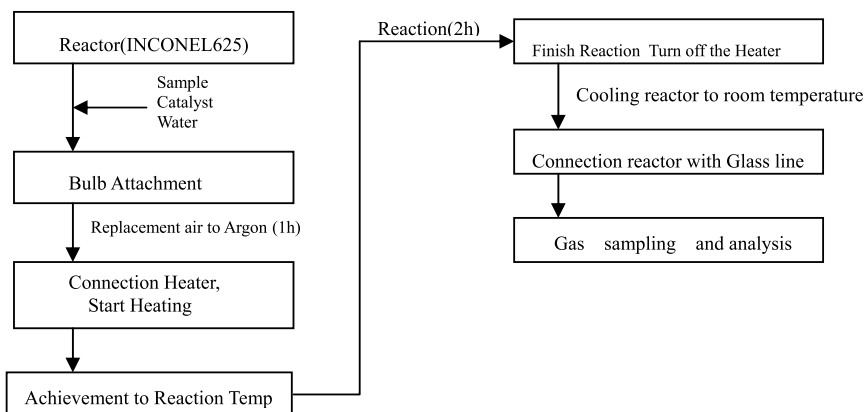
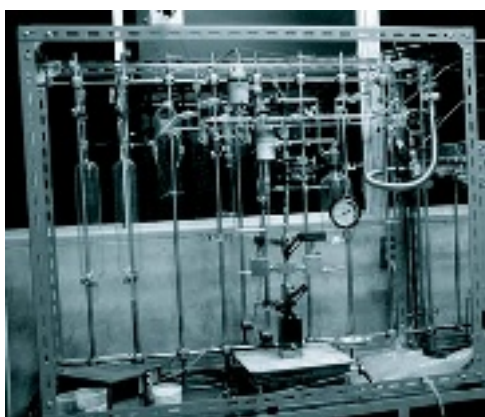
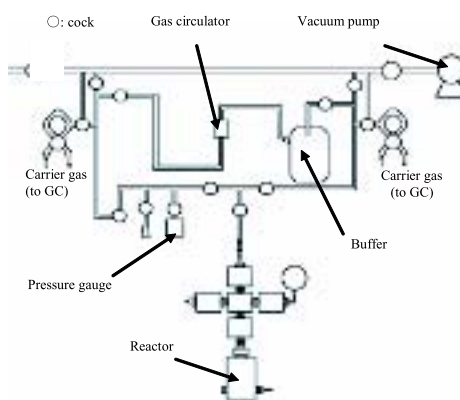


Figure 3. On-line gas chromatography



(a) Actual picture



(b) Layout

Results

Figure 1 shows the effect of reaction time on the productions of gasses from pulp. Decomposition ratio was slightly increased with increasing reaction time. The influence of reaction time on the decomposition of pulp is low compared with Naphthalene [16]. In the case of Naphthalene, half reaction time led to approximately half decomposition ratio. Pulp seems to be easy to decomposition. The volume of produced hydrogen was virtually the same as one among three difference reaction time parameters.

Figure 2 shows comparisons of each decomposition ratio and gas distributions by changing the volume of loaded water. Increasing loaded water enhanced decomposition ratio and methane ratio. Hydrogen ratio was conversely decreased.

Figure 4. Influence of reaction time on biomass decomposition

Common experimental condition: Pulp 100mg, Catalyst 20mg, Water 3ml, Temperature 450°C, Amount of generated gas (left vertical line) indicate volume from 1g of pulp at the standard state [0°C(273K), 1atm(10⁵Pa)]

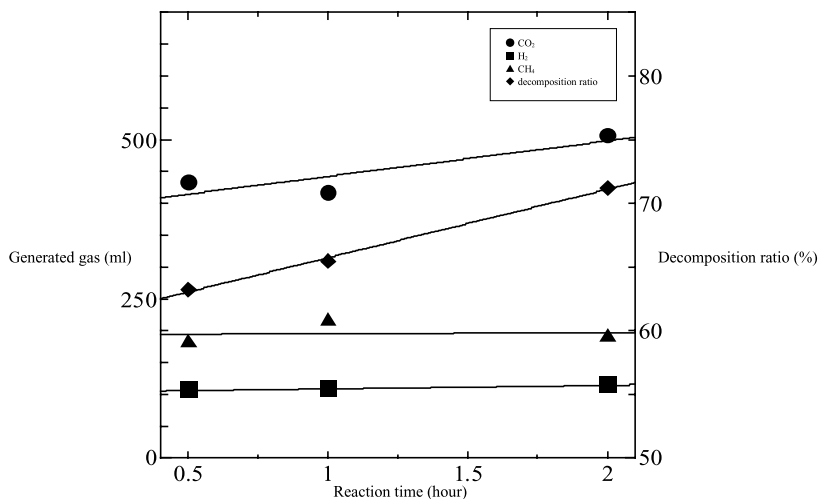
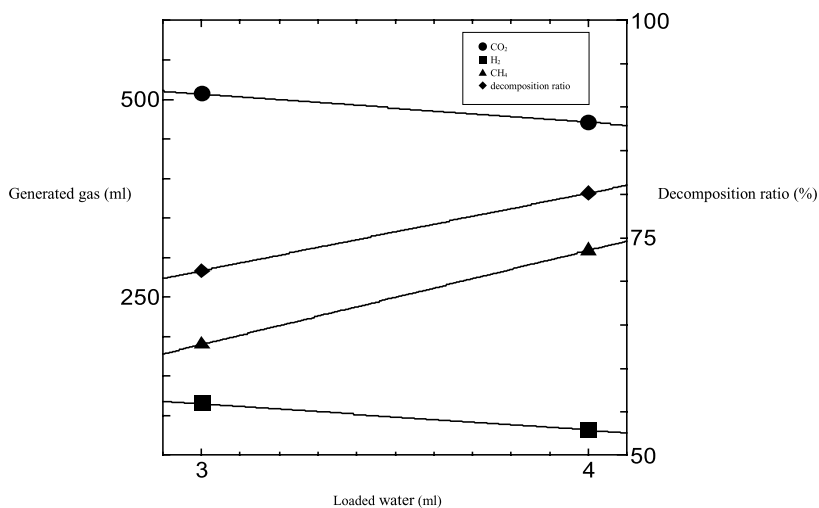
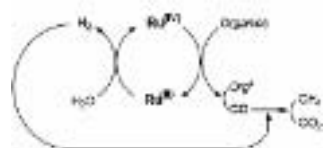
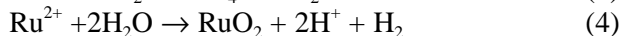


Figure 5. Comparisons of each gas compositions by changing water

Common experimental condition: Pulp 100mg, Catalyst 20mg, Temperature 450°C, Time 2 hours, Amount of generated gas (left vertical line) indicate volume from 1g of pulp at the standard state [0°C(273K), 1atm(10⁵Pa)]



An estimated reaction mechanism is written below [16]:



[Org⁺ refers to an oxidized intermediate of Org (organic compound)]

In this catalytic reaction, hydrogen is produced from water (reaction 4). Methane is synthesised from the reaction of hydrogen and carbon monoxide (reaction 2-3). The production ratios of hydrogen and methane consequently opposite each other. It is seen that the higher methane ratio leads to the lower hydrogen ratio. The reactor used in this experiment is a kind of autoclave. Inner pressure is increased with increasing amount of loaded water. High pressure tends to move equilibrium to right side about reaction 2-3.

CONCLUSIONS

This result indicated the present method using RuO_2 as a catalyst in SCW enables to decompose biomass and to produce fuel gases. In the case of hydrogen production, lower pressure is better condition and even shorter reaction time can produce hydrogen. This tendency is desirable if practical application is considered. We conclude the present method is technically feasible for the production of hydrogen from biomass.

REFERENCES

- [1] Douglas C. Elliot, L. John Sealock, Jr., Eddie G. Baker. (1994), Chemical Processing in High-Pressure Aqueous Environments. 3. Batch Reactor Process Developments for Organics Destruction. *Ind. Eng. Chem. Res.* 33,558-565.
- [2] Tomoaki Minowa, Tomoko Ogi, Shin-ya Yokoyama. (1995), Hydrogen Production from Wet Cellulose by Low Temperature Gasification Using a Reduced Nickel Catalyst. *Chemistry Letters*, 937-938
- [3] Tomoaki Minowa, Tomoko Ogi. (1998), Hydrogen production from cellulose using a reduced nickel catalyst. *Catalysis Today*, 45,411-416.
- [4] Takuya Yoshida, Yukihiko Matsumura (2001), Gasification of Cellulose, Xylan, and Lignin Mixtures in Supercritical. *Ind. Eng. Chem. Res.* 40,5469-5474.
- [5] Takuya Yoshida, Yoshito Oshima, Yukihiko Matsumura. (2004). Gasification of biomass model compounds and real biomass in supercritical water. *Biomass and Bioenergy*. 26, 71-78
- [6] H. Schmieder, J. Abeln, N. Bpukis, E. Dinjus, A. Kruse, M. Kluth, G. Petrich, E. Sadri, M. Schacht. (2000), Hydrothermal gasification of biomass and organic wastes. *Journal of Supercritical Fluids*. 17,145-153.
- [7] Andrea Kruse, Danny Meier, Pia Rimbrecht, Michael Schacht. (2000), Gasification of Pyrochatechol in Supercritical Water in the presence of Potassium Hydroxide. *Ind. Eng. Chem. Res.* 39,4842-4848.
- [8] A. Kruse, T. Henningsen, A. Sinag, J. Pfeiffer. (2003), Biomass Gasification in Supercritical Water: Influence of the Dry Matter Content and the Formation of Phenols. *Ind. Eng. Chem. Res.* 42,3711-3717.
- [9] Masaru Watanabe, Hiroshi Inomata, Kunio Arai. (2002). Catalytic hydrogen generation from biomass (glucose and cellulose) with ZrO₂ in supercritical water. 22, 405-410.
- [10] Masaru Watanabe, Hiroshi Inomata, Mitsumasa Osada, Takafumi Sato, Adschiri, Kunio Arai. (2003), Catalytic effects of NaOH and ZrO₂ for partial oxidative gasification of *n*-hexadecane and lignin in supercritical water. *Fuel*. 82,545-552.
- [11] X. Xu, Yukihiko Matsumura, Jonny Stenberg, Michael Jerry Antal, Jr. (1996), Carbon-Catalyzed Gasification of Organic Feedstocks in Supercritical Water. *Ind. Eng. Chem. Res.* 35,2522-2530.
- [12] X. Xu, Michael Jelly Antal, Jr. (1998), Gasification of Sewage Sludge and Other Biomass for Hydrogen Production in Supercritical Water. *Environmental Progress*. 17,215-220.

- [13] Douglas C. Elliot, L. John Sealock, Jr., Eddie G. Baker. (1993), Chemical Processing in High-Pressure Aqueous Environments. 2. Development of Catalysts for Gasification. *Ind. Eng. Chem. Res.* 32,1542-1548.
- [14] Takafumi Sato, Mitsumas Osada, Masaru Watanabe, Masayuki Shirai, Kunio Arai. (2003). Gasification of Alkylphenols with Supported Noble Metal Catalysts in Supercritical Water. *Ind. Eng. Chem. Res.* 42,4277-4282
- [15] Mitsumasa Osada, Takahumi Sato, Masaru Watanabe, Tadahumi Adschiri, Kunio Arai. (2004) Low temperature Catalytic Gasification of Lignin and Cellulose with a Ruthenium Catalyst in Supercritical Water. *Energy & Fuels.* 18,327-333.
- [16] Ki Chul Park and Hiroshi Tomiyasu. (2003), Gasification reaction of organic compounds catalyzed by RuO₂ in supercritical water. *Chem. Commun*, 694-695.
- [17] Thomas J. Howser, David M. Tiffany, Zhuangjie Li, Michael E. McCarville E. Houghton. (1986). Reactivity of some organic compounds with supercritical water.

This page intentionally left blank

SESSION SUMMARIES

The Third Information Exchange Meeting on the Nuclear Production of Hydrogen was divided into five technical sessions. Results of the sessions are summarised by M.C. Petri below.

Session I

The Prospects for Hydrogen in Future Energy Structures and Nuclear Power's Role

Chairs: M.C. Petri

World energy demand will grow substantially over the next fifty years. With that energy growth will come increasing demands on limited traditional fossil fuels and on a fragile environment already seeing the effects of man-made greenhouse gas emissions. Nuclear power can play an important role in the energy sector as a non-carbon-emitting power source. The use of nuclear heat to assist steam methane reforming or to produce hydrogen through water cracking could provide carbon-free solutions to other sectors of the world economy. The viability of these technologies will depend on the technical success of the ongoing research and development, but also on their economics with respect to the markets they aim to serve. By some measures, the nuclear production of hydrogen through electrolysis or thermochemical processes may already be competitive with steam methane reforming, given rising natural gas prices. The extent of nuclear power's future role may depend on other factors such as the availability of uranium and the development of reprocessing and waste storage options.

Session II

The Status of Nuclear Hydrogen Research and Development Efforts around the Globe

Chairs: M. Methnani, W.A. Summers

Major nuclear hydrogen research and development programs are underway in many parts of the world, including Japan, China, Korea, France, Canada, and the United States. The largest research efforts are directed at the sulfur-iodine thermochemical process coupled to very high temperature gas cooled reactors. Significant work is also being done on high-temperature steam electrolysis and other thermochemical cycles. There are expectations that large-scale demonstration of nuclear hydrogen production will be achieved before 2020. Current test reactors such as the HTTR in Japan and the HTR-10 in China are capable of reaching temperatures to allow testing of some nuclear hydrogen production concepts. Canadian efforts are focused on lower-temperature options that would be compatible with the super-critical water reactor being developed, including water electrolysis. The European Union has separate nuclear research programmes and hydrogen development programmes, but the potential of nuclear-generated hydrogen is recognised.

Session III

Integrated Nuclear Hydrogen Production Systems

Chairs: A. Miller, K. Verfondern

Different reactor concepts are being developed to support hydrogen generation. The Japan Atomic Energy Agency, for example, is considering the Gas Turbine High-Temperature Reactor 300 (GTHTR300) with core outlet temperatures compatible with the sulfur-iodine hydrogen production cycle. Similarly, General Atomics (U.S.) is collaborating on a Modular Helium Reactor suited for the sulfur-iodine process and high-temperature electrolysis. International collaborators are looking at issues surrounding the coupling of the hydrogen-generation processes and the nuclear heat source. Well designed coupling of the heat sources and needs can optimize hydrogen production efficiency.

Session IV

Nuclear hydrogen technologies and design concepts

Chairs: K. Kunitomi, J.S. Herring, Y.J. Shin, T. Takeda

Significant progress has been made since 2003 on the research and development of nuclear hydrogen technologies. For example, a bench-scale demonstration of the sulfur-iodine cycle was made at JAEA in 2004. Plans are in place for larger demonstrations over the next decade. These experiments are leading to better insights into an optimized design of the system and ways to overcome remaining technical issues.

Most countries participating in the meeting are studying high-temperature steam electrolysis. The United States, for instance, has recently demonstrated steam electrolysis hydrogen production at 100 liters/hour.

Several alternatives to the sulfur-iodine process and steam electrolysis are being considered. Thermo-electrochemical cycles at various stages of development are being studied, including two hybrid sulfur-based cycles, the copper-chloride cycle, the magnesium-chloride cycle, the copper ferrite cycle, . Screening tools have been developed to rapidly assess less mature thermo-electrochemical cycles to help decide whether further research is warranted.

The Tokyo Institute of Technology is exploring a novel idea for on-board reforming of methane with carbon dioxide capture to provide hydrogen as a transportation fuel. The reformer cartridges would be regenerated in a 550°C reaction with hydrogen. The heat and hydrogen could be produced through the various nuclear technologies being discussed.

Session V

Basic and Applied Science in Support of Nuclear Hydrogen Production

Chairs: Y. Kato, P. Anzieu, Y. Sun

The technical and commercial viability of the nuclear hydrogen production options being pursued is not assured. Fundamental advances in the materials and processes may be key to their commercial adoption. Advanced membranes and catalysts, for instance, could improve the efficiency of difficult chemical separations in the sulfur-iodine process and the hybrid sulfur processes.

RECOMMENDATIONS

The Third Information Exchange Meeting on the Nuclear Production of Hydrogen ended with an open discussion, led by meeting co-chairs R. Hino and M.C. Petri, on a critique of the meeting and recommendations for future meetings. Dr. Petri provided a summary of the meeting sessions and the conclusions drawn from them.

The participants agreed that this meeting series is the best forum for a focused examination of issues related to nuclear hydrogen production with key researchers from around the world. There was no hesitancy in recommending that the meeting series be continued.

Comments on the organisation of the meeting included the following:

- More time should be allocated for open discussions on topics raised at the meeting. For instance, panel discussions could be scheduled into future meetings.
- Some care should be taken by the organisers and the speakers to consolidate similar talks and to reduce repetition in the background discussions in the presentations.

The closing session allowed an opportunity for a further, open technical discussion among the participants.

A. Miller (AECL) posed to the participants that a hydrogen production facility or any other facility that requires process heat should be located as close to the nuclear heat source as possible to minimise heat transfer losses. This requires a special look at safety issues to ensure that the chemical and nuclear facilities pose no risk to each other.

The open discussion led to some recommendations for the next information exchange meeting:

- Regulatory agencies should be invited so that they become aware early of the technologies being considered.
- Additional topics should be considered:
 - ⇒ The safety of coupling the nuclear and chemical plants.
 - ⇒ The economics of hydrogen production and assessments of potential markets.
 - ⇒ The sustainability of large-scale nuclear hydrogen production.
 - ⇒ The standardisation of thermodynamic efficiency assessments.
 - ⇒ Licensing and regulatory issues.

M. Methnani (IAEA) discussed the International Atomic Energy Agency's plans for a programme in 2006 to fund activities related to high-temperature gas-cooled reactor process heat applications. In addition, an international meeting is being planned for mid 2007 on non-electricity applications for nuclear power. The IAEA meeting would include sessions on nuclear hydrogen production and, indeed, may be a preferred forum for some of the broader topics suggested in the closing session of this meeting. In light of the IAEA's plans, the information exchange meeting participants recommended postponing the next OECD/NEA meeting until 2008.

The information exchange meeting participants strongly endorsed further international cooperation on issues related to nuclear hydrogen production. Extensive collaboration already exists in some research areas, including the sulfur-iodine cycle. Additional areas of cooperation could include:

- Alternative thermo-electrochemical cycles and high-temperature electrolysis.
- Standardisation of thermodynamic efficiency assessments.
- Safety.
- Materials and chemical property measurement and verification.
- Materials development, including structural materials, membranes, and catalysts.
- Advanced fabrication techniques.
- Development and verification of thermochemical database.

In many of these areas the OECD/NEA has programmes that could facilitate expanded cooperation.

Annex A
LIST OF PARTICIPANTS

CANADA

MILLER, Alistair I.
Manager, Heavy Water Technology Branch
Atomic Energy of Canada Ltd
Chalk River Laboratories
Chalk River, Ontario K0J 1J0

Tel: +1 613 584 8811 ext 3207
Fax: +1 613 584 8247
Eml: millera@aecl.ca

SUPPIAH, Sellathurai (Sam)
Atomic Energy of Canada Ltd.
Chalk River Laboratories
Chalk River, Ontario K0J 1J0

Tel: +1 613 584 8811
Fax: +1 613 584 8247
Eml: suppiahs@aecl.ca

FRANCE

ANZIEU, Pascal
Project Manager
CEA Saclay
F-91191 Gif-sur-Yvette cedex

Tel: +33 1 6908 3204
Fax: +33 1 6908 5892
Eml: pascal.anzieu@cea.fr

LE NAOUR, François
CEA GRENOBLE
17 avenue des Martyrs
F-38054 GRENOBLE CEDEX 9

Tel: +33 4 3878 4301
Fax:
Eml: francois.le-naour@cea.fr

GERMANY

VERFONDERN, Kar
Research Center Juelich
Institute for Safety Research
and Reactor Technology ISR-I
D-52425 Juelich

Tel: +49 2461 61 3438
Fax: +49 2461 61 3133
Eml: k.verfondern@fz-juelich.de

ITALY

CAPUTO, Giampaolo
ENEA
Via Anguillarese,301,
I-00159 Rome

Tel: +39 6 30484265
Fax: +39 6 30486779
Eml: giampaolo.caputo@casaccia.enea.it

FAVUZZA, Paolo
ENEA
Via Anguillarese, 301
I-00159 Rome

Tel: +39 6 30486862
Fax: +39 6 30486779
Eml: paolo.favuzza@casaccia.enea.it

JAPAN

ABE, Shinji
Engineering Development Co., Ltd
3-3-1 Minato Mirai, Nishi-ku
Yokohama-shi, Kanagawa-ken

Tel: +81 45 224 9094
Fax:
Eml: aoki@edc.atom.hq.mhi.co.jp

AMAYA, Takayuki
JGC Corporation
2205, Narita-cho, Oarai-machi
Higashi-ibaraki-gun, Ibaraki-ken

Tel: +81 29 267 0165
Fax: +81 29 267 0129
Eml: amaya.takayuki@jgc.co.jp

AOKI, Shigeaki
Engineering Development Co., Ltd
3-3-1 Minato Mirai, Nishi-ku
Yokohama-shi, Kanagawa-ken

Tel: +81 45 224 9094
Fax:
Eml: aoki@edc.atom.hq.mhi.co.jp

BABA, Osamu
Nuclear Safety Commission
Kasumigaseki 3-1-1, Chiyoda-ku
Tokyo

Tel: +81 3 3581 9259
Fax:
Eml: Osamu.baba@cao.go.jp

CAPITINI, Robert
CEA/DEN Japan Office
Teranomom 3 Chome Annex 3F
3-7-12 Teranomom, Minato-ku
Tokyo

Tel: +81 3 5472 1533
Fax: +81 3 5472 2236
Eml: capitini@cea-tokyo.jp

CHITOSE, Keiko
MITSUBISHI HEAVY INDUSTRIES, LTD.
3-3-1 Minato Mirai, Nishi-ku
Yokohama-shi, Kanagawa-ken

Tel: +81 45 224 9678
Fax:
Eml: chitose@atom.hq.mhi.co.jp

CHU, Song-Zhu
Materials Science Research Laboratory
CRIEPI
Nagasaka 2-6-1, Yokosuka
Kanagawa-ken, 240-0196

Tel: +81 46 856 2121
Fax: +81 46 856 5571
Eml: chusongz@criepi.denken.or.jp

FUJIKAWA, Seigou
ATOX
1408, Takada, Kashiwa-shi
Chiba-ken

Tel: +81 4 7145 3330
Fax: +81 4 7145 3649
Eml: seigoh_fujikawa@atox.co.jp

FUJISHIRO, Toshio
Research Organisation for Information
Science and Technology (RIST)
2-4 Shirakata-Shirane, Tokai-mura
Naka-gun, Ibaraki-ken, 319-1106

Tel: +81 29 282 5017
Fax: +81 29 282 0625
Eml: fujisiro@tokai.rist.or.jp

FUKADA, Satoshi
Kyushu University
Hakozaki,Higashi-ku
Fukuoka 812-8581

Tel: +81 92 642 4140
Fax: +81 92 642 3800
Eml: sfukada@nucl.kyushu-u.ac.jp

GUERON, David
Japan Atomic Energy Agency
3607 Narita-cho, Oarai-machi
Higashi-Ibaraki-gun
Ibaraki-ken, 311-1394

Tel: +81 29 266 7713
Fax: +81 29 266 7741
Eml: gueron.david@jaea.go.jp

HANDA, Norihiko
ToshibaCorporation
8 Shinsugita-cho, Isogo-ku
Yokohama-shi 235-8523

Tel: +81 45 770 2401
Fax: +81 45 770 2266
Eml: norihiko.handa@toshiba.co.jp

HARUTA, Daizou
Kyushu Electric Power Co. Inc.
Research Laboratory
2-1-47,Shiobara, Minami-ku
Fukuoka-shi, Fukuoka-ken

Tel: +81 92 541 0769
Fax:
Eml: daizou_haruta@kyuden.co.jp

HASEGAWA, Akira
Div. of Nuclear Data & Reactor Eng.
Japan Atomic Energy Agency
2-4 Shirakata-Shirane, Tokai-mura
Naka-gun, Ibaraki-ken, 319-1195

Tel: +81 29 282 6369
Fax: +81 29 282 6122
Eml: hasegawa.akira@jaea.go.jp

HAYAKAWA, Hitoshi
Fuji Electric Systems
1-1,Tanabeshinden,Kawasaki-ku
Kawasaki-city, 210-9530

Tel: +81 44 329 2191
Fax: +81 44 329 2178
Eml: hayakawa-hitoshi@fujielectric.co.jp

HAYASHI, Kimio
Blanket Irradiation and Analysis Group
Div. of Fusion Energy Technology
Japan Atomic Energy Agency
Oarai-machi, Ibaraki-ken, 311-1393

Tel: +81-29-266-7360
Fax: +81-29-266-7480
Eml: hayashi.kimio@jaea.go.jp

HINO, Ryutaro
Japan Atomic Energy Agency
3607 Narita-cho, Oarai-machi
Higashi-Ibaraki-gun
Ibaraki-ken, 311-1394

Tel: +81 29 266 7716
Fax: +81 29 266 7608
Eml: hino.ryutaro@jaea.go.jp

HIRAO, Kazunori
Japan Atomic Energy Agency
4002 Narita-cho, Oarai-machi
Higashi-Ibaraki-gun
Ibaraki-ken, 311-1393

Tel: +81 29 267 4141 EXT.2261
Fax: +81 29 266 3677
Eml: hirao.kazunori@jaea.go.jp

HIROSAWA, Tomoya
Nuclear Fuel Industries, Ltd.
1-950, Asashiro-Nishi, Kumatori-cho
Sennan-gun, Osaka-fu

Tel: +81 724 52 8111
Fax:
Eml: hirosawatomoya@aol.com

HODOTSUKA, Masatoshi
Japan Atomic Energy Agency
3607 Narita-cho, Oarai-machi
Higashi-Ibaraki-gun
Ibaraki-ken, 311-1394

Tel: +81 29 266 7457
Fax: +81 29 266 7741
Eml: hodotsuka.masatoshi@jaea.go.jp

HORI, Masao
Nuclear Systems Association
1-7-6 Toranomom, Minato-ku
Tokyo, 105-0001

Tel: +81 3 3506 9071
Fax: +81 3 3506 9075
Eml: mhorim@mx.mesh.ne.jp

HOSODA, Masaki
Chief Research Scientist
Taiheiyō cement co., Ltd.
2-4-2, Osaku, Sakura city
Chiba-ken

Tel: +81 43 498 3820
Fax: +81 43 498 3809
Eml: masaki_hosoda@taiheiyō-cement.co.jp

IDE, Shuuichi
Nuclear Fuel Industries, Ltd.
3-12-10, Mita, Minato-ku, Tokyo

Tel: +81 3 5440 1263
Fax: +81 3 5440 1264
Eml: ide@nfi.co.jp

IJICHI, Masanori
Japan Atomic Energy Agency
3607 Narita-cho, Oarai-machi
Higashi-Ibaraki-gun
Ibaraki-ken, 311-1394

Tel: +81 29 266 7570
Fax: +81 29 266 7741
Eml: ijichi.masanori@jaea.go.jp

IMAI, Yoshiyuki
Japan Atomic Energy Agency
3607 Narita-cho, Oarai-machi
Higashi-Ibaraki-gun
Ibaraki-ken, 311-1394

Tel: +81 29 266 7570
Fax: +81 29 266 7741
Eml: imai.yoshiyuki@jaea.go.jp

IWATSUKI, Jin
Japan Atomic Energy Agency
3607 Narita-cho, Oarai-machi
Higashi-Ibaraki-gun
Ibaraki-ken, 311-1394

Tel: +81 29 266 7715
Fax: +81 29 266 7741
Eml: iwatsuki.jin@jaea.go.jp

IYOKU, Tatsuo
Japan Atomic Energy Agency
3607 Narita-cho, Oarai-machi
Higashi-Ibaraki-gun
Ibaraki-ken, 311-1394

Tel: +81 29 266 7530
Fax: +81 29 266 7486
Eml: iyoku.tatsuo@jaea.go.jp

IZUMIZAKI, Yukihiro
Research Lab. for Nuclear Reactors
Tokyo Institute of Technology
1-21-1 OOOKAYAMA MEGURO CITY
TOKYO,152-8550

Tel: +81 3 5734 2378
Fax: +81 3 5734 2958
Eml: 05d19010@nr.titech.ac.jp

KAMEI, Atsushi
IHI
1, Nakahara-cho, Isogo-ku
Shin-Nakahara-cho, Yokohama-shi

Tel: +81 45 759 2563
Fax:
Eml: atsushi_kamei@ihi.co.jp

KAN, Norio
IHI
1, Nakahara-cho, Isogo-ku
Shin-Nakahara-cho, Yokohama-shi

Tel: +81 45 759 2080
Fax: +81 45 759 2601
Eml: norio_kan@ihi.co.jp

KANAGAWA, Akihiro
Japan Atomic Energy Agency
3607 Narita-cho, Oarai-machi
Higashi-Ibaraki-gun,
Ibaraki-ken, 311-1394

Tel: +81 29 266 7715
Fax: +81 29 266 7741
Eml: kanagawa.akihiro@jaea.go.jp

KARASAWA, Hidetoshi
Power & Industrial Systems R&D Lab
Hitachi, Ltd.
7-2-1 Omika, Hitachi
Ibaraki-ken 319-1221

Tel: +81 294 52 914
Fax:
Eml: hidetoshi_karasawa@pis.hitachi.co.jp

KASAHARA, Seiji
Japan Atomic Energy Agency,
3607 Narita-cho, Oarai-machi
Higashi-Ibaraki-gun
Ibaraki-ken, 311-1394

Tel: +81 29 266 7713
Fax: +81 29 266 7741
Eml: kasahara.seiji@jaea.go.jp

KASAI, Shigeo
Toshiba
8 Shinsugita-cho Isogo-ku
Yokohama 235-8523
Tel: +81 45 770 2415
Fax: +81 45 770 2266
Eml: shigeo1a.kasai@glb.toshiba.co.jp

KATANISHI, Shoji
Japan Atomic Energy Agency
3607 Narita-cho, Oarai-machi
Higashi-Ibaraki-gun
Ibaraki-ken, 311-1394
Tel: +81 29 266 7718
Fax: +81 29 266 7608
Eml: katanishi.shoji@jaea.go.jp

KATO, Ryoma
Japan Atomic Energy Agency
3607 Narita-cho, Oarai-machi
Higashi-Ibaraki-gun
Ibaraki-ken, 311-1394
Tel: +81 29 266 7706
Fax: +81 29 266 7710
Eml: kato.ryoma@jaea.go.jp

KATO, Shigeru
Nuclear Fuel Industries, Ltd.
3135-41 Muramatsu, Tokai-mura
Naka-gun, Ibaraki-ken
Tel: +81 29 287 8211
Fax: +81 29 287 8223
Eml: kato@nfi.co.jp

KATO, Yukitaka
Tokyo Institute of Technology
N1-22, 2-12-1 O-okayama, Meguro-ku
Tokyo 152-8550
Tel: +81 3 5734 2967
Fax: +81 3 5734 2967
Eml: yukitaka@nr.titech.ac.jp

KITA, Koichi
Mitsubishi Materials Corporation
476, Shimoishido-shita, Kitahonn-shi
Saitama-ken
Tel: +81 48 591 6555
Fax: +81 48 591 6433
Eml: kita@mmc.co.jp

KOMORI, Yoshihiro
Japan Atomic Energy Agency
3607 Narita-cho, Oarai-machi
Higashi-Ibaraki-gun
Ibaraki-ken, 311-1394
Tel: +81 29 266 7500
Fax: +81 29 266 7484
Eml: komori.yoshihiro@jaea.go.jp

KONDO, Tatsuo
Tohoku University
Aramaki, Aoba-ku, Sendai-shi
Miyagi-ken
Tel: +81 22 217 7517
Fax:
Eml: kondo@rift.mech.tohoku.ac.jp

KUBO, Shinji
Japan Atomic Energy Agency
3607 Narita-cho, Oarai-machi
Higashi-Ibaraki-gun,
Ibaraki-ken, 311-1394
Tel: +81 29 266 7739
Fax: +81 29 264 7741
Eml: kubo.shinji@jaea.go.jp

KUNITOMI , Kazuhiko Japan Atomic Energy Agency 3607 Narita-cho, Oarai-machi Higashi-Ibaraki-gun Ibaraki-ken, 311-1394	Tel: + 81 29 266 7892 Fax: +81 29 264 8608 Eml: kunitomi.kazuhiko@jaea.go.jp
LIEM, Peng Hong NAIS Co., Inc. 416 Muramatsu Tokai-mura, Naka-gun Ibaraki-ken 319-1112	Tel: +81 29 270 5000 Fax: +81 29 270 5001 Eml: liemph@nais.ne.jp
MAEDA, Toshiya CSA of Japan Co., Ltd. Shibadaimon Daiichi Bldg. 3-9, Shibadaimon 1-chome Minato-ku,Tokyo 105-0012	Tel: +81 3 5776 1838 Fax: +81 3 5776 1859 Eml: maeda@csaj.co.jp
MINATSUKI, Isao Mitubischi Heavy Industries, Ltd 3-3-1 Minato Mirai, Nishi-ku Yokohama-shi	Tel: +81 3 6716 4936 Fax: Eml: isao_minatsuki@mhi.co.jp
MITA, Yoshiyuki OBAYASHI Corporation Shinagawa Inter-City B 2-15-2, Konan, Minato-ku Tokyo	Tel: +81 3 5769 2737 Fax: Eml: mita.yoshiyuki@obayashi.co.jp
MIYAKAWA, Shunnichi Wakasawan Energy Center 64-52-1 Nagatani, Tsuruga-shi Fukui-ken	Tel: +81 770 24 2300 Ext.206 Fax: Eml: smiyakawa@werc.or.jp
MOTOOKA, Naoto Mitubischi Heavy Industries, Ltd 2-16-5 Konan, Minato-ku, Tokyo	Tel: +81 3 6716 4964 Fax: Eml: naoto_motooka@mhi.co.jp
MURAKAMI, Tomoyuki Japan Atomic Energy Agency, 3607 Narita-cho, Oarai-machi, Higashi-Ibaraki-gun, Ibaraki-ken, 311-1394	Tel: +81 29 266 7712 Fax: +81 29 266 7710 Eml: murakami.tomoyuki@jaea.go.jp
MURAZUMI, Yasuyuki Taisei Corp. 1-25-1 Nishi-Shinjuku, Shinjuku-ku Tokyo	Tel: +81 3 5381 5196 Fax: +81 3 3345 8330 Eml: murazumi@eng.taisei.co.jp

NABESHIMA, Kunihiko
Japan Atomic Energy Agency
2-4 Shirakata-Shirane, Tokai-mura
Ibaraki-ken 319-1195
Tel: +81 29 282 6198
Fax: +81 29 282 6122
Eml: nabeshima.kunihiko@jaea.go.jp

NAKAGAWA, Shigeaki
Japan Atomic Energy Agency
3607 Narita-cho, Oarai-machi
Higashi-Ibaraki-gun
Ibaraki-ken, 311-1394
Tel: +81 29 266 7534
Fax: +81 29 266 7486
Eml: nakagawa.shigeaki@jaea.go.jp

NAKAGIRI, TOSHIO
Japan Atomic Energy Agency
4002 Narita-cho, O-Arai-machi
Higashi-Ibaraki-gun
Ibaraki-ken 311-1393
Tel: +81 29 267 4141
Fax: +81 29 267 7548
Eml: nakagiri.toshio@jaea.go.jp

NAKAMURA, Hiroo
Japan Atomic Energy Agency
2-4 Shirakata-Shirane, Tokai-mura
Ibaraki-ken 319-1195
Tel: +81 29 284 3791
Fax: +81 29 282 5551
Eml: nakamura.hiroo@jaea.go.jp

NISHIHARA, Tetsuo
Japan Atomic Energy Agency
3607 Narita-cho, Oarai-machi
Higashi-Ibaraki-gun
Ibaraki-ken, 311-1394
Tel: +81 29 266 7711
Fax: +81 29 266 7710
Eml: nishihara.tetsuo@jaea.go.jp

NOGUCHI, Hiroki
Japan Atomic Energy Agency
3607 Narita-cho, Oarai-machi
Higashi-Ibaraki-gun
Ibaraki-ken, 311-1394
Tel: +81 29 266 7572
Fax: +81 29 266 7741
Eml: noguchi.hiroki@jaea.go.jp

NUMATA, Mamoru
JGC Technologies Research Center
2205, Narita-cho, Oaraimachi,
Higashi-Ibaraki-gun,
Ibaraki Pref, 311-1313
Tel: +81 29 266 3315
Fax: +81 29 266 3310
Eml: numata.mamoru@jgc.co.jp

OGAWA, Masuro
Japan Atomic Energy Agency
3607 Narita-cho, Oarai-machi
Higashi-Ibaraki-gun
Ibaraki-ken, 311-1394
Tel: +81 29 266 7603
Fax: +81 29 266 7608
Eml: ogawa.masuro@jaea.go.jp

OHASHI, Hirofumi Japan Atomic Energy Agency 3607 Narita-cho, Oarai-machi Higashi-Ibaraki-gun Ibaraki-ken, 311-1394	Tel: +81 29 266 7606 Fax: +81 29 266 7608 Eml: ohashi.hirohumi@jaea.go.jp
OHASHI, Kazutaka Japan Atomic Energy Agency 3607 Narita-cho, Oarai-machi Higashi-Ibaraki-gun Ibaraki-ken, 311-1394	Tel: +81 29 266 7704 Fax: +81 29 266 7710 Eml: ohashi.kazutaka@jaea.go.jp
OKAMOTO, Futoshi Fuji Electric System Co. Ltd 1-1 Tanabeshinden Kawasaki-ku Kawasaki-shi, Kanagawa-ken	Tel: +81 44 329 2169 Fax: +81 44 329 2178 Eml: okamoto-futoshi@fesys.co.jp
OKUDA, Yasuyuki Japan Atomic Energy Agency 3607 Narita-cho, Oarai-machi Higashi-Ibaraki-gun Ibaraki-ken, 311-1394	Tel: +81 29 266 7746 Fax: +81 29 266 7741 Eml: okuda.yasuyuki@jaea.go.jp
OKUDE, Katsuhiro Southwest Research Institute 1-24-19 Nishiki, Nerima-ku Tokyo	Tel: +81 3 3933 5222 Fax: Eml: katsuhiro.okude@swri.org
ONUKE, Kaoru IS Process Technology Group Nuclear Applied Heat Technology Div. Japan Atomic Energy Agency Narita-cho 4002, Oarai-machi Ibaraki-ken, 311-1393	Tel: +81 29 266 7738 Fax: +81 29 266 7741 Eml: onuki.kaoru@jaea.go.jp
OOHASHI, Junnpei Nuclear Fuel Industries, Ltd. 3-12-10, Mita, Minato-ku Tokyo	Tel: +81 3 5440 1265 Fax: +81 3 5440 1266 Eml: j-ohashi@nfi.co.jp
OONO, Akira IHI 1, Nakahara-cho, Isogo-ku Shin-Nakahara-cho, Yokohama-shi	Tel: +81 45 759 2580 Fax: Eml: akira_oono@ihi.co.jp
OOSHIRO, Shuuji Sumitomo Corporation 1-8-1 Harumi, Chuo-ku Tokyo	Tel: +81 3 5166 4582 Fax: Eml: shuji.oshiro@sumitomocorp.co.jp

OOTA, Hiroyuki
Japan Atomic Energy Agency
3607 Narita-cho, Oarai-machi
Higashi-Ibaraki-gun
Ibaraki-ken, 311-1394

Tel: +81 29 266 7642
Fax: +81 29 266 7741
Eml: ota.hiroyuki@jaea.go.jp

OYAMADA, Osamu
Japan Atomic Energy Agency
2-4 Shirakata-Shirane, Tokai-mura
Ibaraki-ken 319-1195

Tel: +81 29 282 6774
Fax: +81 29 282 6122
Eml: oyamada.osamu@jaea.go.jp

OYAMADA, Sunao
Japan Atomic Energy Agency
3607 Narita-cho, Oarai-machi
Higashi-Ibaraki-gun
Ibaraki-ken, 311-1394

Tel: +81 29 267 0590
Fax:
Eml: oyamada.sunao@jaea.go.jp

OZAWA, Masaki
Japan Atomic Energy Agency
4002 Narita-cho, O-Arai-machi
Higashi-Ibaraki-gun
Ibaraki-ken 311-1393

Tel: +81 29 267 6918
Fax: +81 29 267 5180
Eml: ozawa.masaki@jaea.go.jp

SAIGOU, Masao
Japan Atomic Industrial Forum (JAIF)
Daiichi-Choja-Building
1-2-13 Shiba-Daimon
Minato-ku, Tokyo

Tel: +81 3 5777 0752
Fax: +81 3 5777 0760
Eml: saigo@jaif.or.jp

SAIKUSA, Akio
Japan Atomic Energy Agency
3607 Narita-cho, Oarai-machi
Higashi-Ibaraki-gun
Ibaraki-ken, 311-1394

Tel: +81 29 266 7677
Fax: +81 29 266 7686
Eml: saikusa.akio@jaea.go.jp

SAKABA, Nariaki
Japan Atomic Energy Agency
3607 Narita-cho, Oarai-machi
Higashi-Ibaraki
Ibaraki-ken, 311-1394

Tel: +81 29 266 7720
Fax: +81 29 266 7608
Eml: sakaba.nariaki@jaea.go.jp

SAWA, Kazuhiro
Japan Atomic Energy Agency
3607 Narita-cho, Oarai-machi
Higashi-Ibaraki-gun,
Ibaraki-ken, 311-1394

Tel: +81 29 266 7670
Fax: +81 29 266 7710
Eml: sawa.kazuhiro@jaea.go.jp

SHIBATA, Takemasa
Japan Atomic Energy Agency
3607 Narita-cho, Oarai-machi
Higashi-Ibaraki-gun
Ibaraki-ken, 311-1394

Tel: +81 29 266 7714
Fax: +81 29 266 7741
Eml: shibata.takemasa@jaea.go.jp

SHIINA, Yasuaki
Japan Atomic Energy Agency
3607 Narita-cho, Oarai-machi
Higashi-Ibaraki-gun
Ibaraki-ken, 311-1394

Tel: +81 29 266 7705
Fax: +81 29 266 7710
Eml: shiina.yasuaki@jaea.go.jp

SHIOZAWA, Shusaku
Japan Atomic Energy Agency
3607 Narita-cho, Oarai-machi
Higashi-Ibaraki-gun
Ibaraki-ken, 311-1394

Tel: +81 29 266 7100
Fax: +81 29 266 7608
Eml: shiozawa.shusaku@jaea.go.jp

SOEJIMA, Tsutomu
Kyushu Electric Power
Research Laboratory
2-1-47, Shiobara, Minami-ku
Fukuoka-shi, Fukuoka-ken

Tel: +81 92 541 0769
Fax:
Eml: tsutomu_soejima@lab.kyuden.co.jp

SUMITA, Junya
Japan Atomic Energy Agency
3607 Narita-cho, Oarai-machi
Higashi-Ibaraki-gun
Ibaraki-ken, 311-1394

Tel: +81 29 266 7678
Fax: +81 29 266 7686
Eml: sumita.junya@jaea.go.jp

SUZUKI, Yukinndo
Hitachi Engineering Co. Ltd
832-2, Hitachinaka-shi
Ibaraki-ken

Tel: +81 29 276 4031
Fax: +81 29 276 4033
Eml: yk_suzuki@psg.hitachi-hec.co.jp

TACHIBANA, Yukio
Japan Atomic Energy Agency,
3607 Narita-cho, Oarai-machi,
Higashi-Ibaraki-gun,
Ibaraki-ken, 311-1394

Tel: +81 29 266 7520
Fax: +81 29 266 7486
Eml: tachibana.yukio@jaea.go.jp

TAKADA, Shoji
Japan Atomic Energy Agency,
3607 Narita-cho, Oarai-machi,
Higashi-Ibaraki-gun,
Ibaraki-ken, 311-1394

Tel: +81 29 266 7717
Fax: +81 29 266 7741
Eml: takada.shoji@jaea.go.jp

TAKAHASHI, Masashi
Power and Industrial Systems R&D Center
Toshiba Corp.,
2-4, Uehiro-cho, Tsurumi-ku
Yokohama-shi, Kanagawa-ken

Tel: +81 45 510 6656
Fax: +81 45 510 2542
Eml: masashi1.takahashi@toshiba.co.jp

TAKAHASHI, Toshio
Japan Atomic Energy Agency
3607 Narita-cho, Oarai-machi
Higashi-Ibaraki-gun
Ibaraki-ken, 311-1394

Tel: +81 29 266 7721
Fax: +81 29 266 7608
Eml: takahashi.toshio@jaea.go.jp

TAKEDA, Tetsuaki
Japan Atomic Energy Agency
3607 Narita-cho, Oarai-machi
Higashi-Ibaraki-gun
Ibaraki-ken, 311-1394

Tel: +81 29 266 7707
Fax: +81 29 266 7486
Eml: takeda.tetsuaki@jaea.go.jp

TAKEI, Katsuhito
CRIEPI
2-11-1 Iwato-Kita, Komae-shi
Tokyo

Tel: +81 3 3480 2111
Fax: +81 3 3480 3401
Eml: takei@criepi.denken.or.jp

TAKEISHI, Kaoru
Faculty of Engineering
Shizuoka University
3-5-1, Jouhoku, Hamamatsu-shi
Shizuoka-ken, 432-8561

Tel: +81 53 478 1159
Fax: +81 53 478 1159
Eml: tcktake@ipc.shizuoka.ac.jp

TAKIZUKA, Takakazu
Nuclear Science and Engineering Dir.
Oarai Research and Development Center
Japan Atomic Energy Agency (JAEA)
Oarai-machi, Ibaraki-ken, 311-1393

Tel: +81 29 266 7703
Fax: +81 29 266 7608
Eml: takizuka.takakazu@jaea.go.jp

TANAKA, Nobuyuki
Japan Atomic Energy Agency
3607 Narita-cho, Oarai-machi
Higashi-Ibaraki-gun
Ibaraki-ken, 311-1394

Tel: +81 29 266 7643
Fax: +81 29 266 7741
Eml: tanaka.nobuyuki61@jaea.go.jp

TAZAWA, Yujiro
Fuji Electric Advanced Technology Corp.
1-1 Tanabeshinden Kawasaki-ku
Kawasaki-shi, Kanagawa-ken

Tel: +81 44 329 2169
Fax: +81 44 329 2178
Eml: tazawa-yujiro@fujielectric.co.jp

TERADA, Atsuhiko
Japan Atomic Energy Agency
3607 Narita-cho, Oarai-machi
Higashi-Ibaraki-gun
Ibaraki-ken, 311-1394
Tel: +81 29 266 7643
Fax: +81 29 266 7741
Eml: terada.atsuhiko@jaea.go.jp

TSUCHIE, Yasuo
The Japan Atomic Power Company
Mitoshiro Bldg.
1-1 Kanda Mitoshiro-cho, Chiyoda-ku
Tokyo, 101-0053
Tel: +81 3 4415 6605
Fax: +81 3 4415 6690
Eml: yasuo-tsuchie@japc.co.jp

TSUKADA, Ryuuji
Chiyoda Cooperation
3-13, Moriya-cho, Kanagawa-ku
Yokohama-shi 221-0022
Tel: +81 45 441 1916
Fax: +81 45 441 1902
Eml: rtsukada@ykh.chiyoda.co.jp

UENO, Shuuichi
Ebara Cooperation
11-1, Haneda-Asahi-cho, Ohta-ku
Tokyo 144-8510
Tel: +81 3 3743 7008
Fax: +81 3 3745 7157
Eml: ueno.shuichi@ebara.com

UGAJIN, Hirotoishi
Toyoda
2-14-9 Nihonbashi, Chuo-ku
Tokyo 103-8655
Tel: +81 3 3242 8403
Fax: +81 3 3242 8535
Eml: HIROTOSHI_UGAJIN@gw.toyotsu.co.jp

UMEKI, Katsuhiko
Obayashi Corporation
Shinagawa Intercity Tower B
2-15-2, Konan, Minato-ku
Tokyo 108-8502
Tel: +81 3 5769 2690
Fax: +81 3 5769 1943
Eml: umeki.katsuhiko@obayashi.co.jp

UMENO, Makoto
Japan Atomic Energy Agency
2-4 Shirakata-Shirane Tokai-mura
Ibaraki-ken 319-1195
Tel: +81 29 282 6026
Fax:
Eml: umeno.makoto@jaea.go.jp

WATANABE, Hideaki
Sumitomo Corporation
1-8-1 Harumi, Chuo-ku
Tokyo
Tel: +81 3 5166 4582
Fax: +81 3 5166 9001
Eml: hideaki.watanabe@sumitomocorp.co.jp

WATANABE, Yutaka
Graduate School of Engineering
Tohoku University
6-6-11-906, Aoba, Aramaki, Aoba-ku
Sendai-shi 980-8579
Tel: +81 22 795 6896
Fax:
Eml: yutaka@rift.mech.tohoku.ac.jp

YAGASAKI, Tadashi
IHI
1, Nakahara-cho, Isogo-ku
Shin-Nakahara-cho, Yokohama-shi

Tel: +81 45 759 2563
Fax:
Eml: tadashi_yagasaki@ihi.co.jp

YAMAMOTO, Nagaaki
Kyuki Corporation
4-19-18, Shimizu, Minami-ku
Fukuoka-shi 815-0031

Tel: +81 92 551 1793 EXT.509
Fax:
Eml: nagaaki.yamamoto@kyuki.co.jp

YAN, Xing L.
Japan Atomic Energy Agency
3607 Narita-cho, Oarai-machi
Higashi-Ibaraki-gun
Ibaraki-ken, 311-1394

Tel: +81 29 266 7897
Fax: +81 29 266 7710
Eml: yan.xing@jaea.go.jp

YOSHIDA, Mitsunori
Japan Atomic Energy Agency
3607 Narita-cho, Oarai-machi
Higashi-Ibaraki-gun
Ibaraki-ken, 311-1394

Tel: +81 29 266 7642
Fax: +81 29 266 7741
Eml: yoshida.mitsunori@jaea.go.jp

KOREA

BAE, Ki-Kwang
Hydrogen Production Research Center
Korea Institute of Energy Research
71-2 Jang-dong, Yuseong-gu
Daejeon 305-343

Tel: +82 42 860 3440
Fax: +82 42 860 3428
Eml: kkkbae@kier.re.kr

CHOI, Ho-Sang
Kyungil University
33, Buhori, Hayang, Gyeong-San
Gyeong-Buk, 712-701

Tel: +82 53 850 7332
Fax: +82 53 850 7613
Eml: choihs@kiu.ac.kr

HAN, Sang-Sup
Korea Institute of Energy Research
71-2 Jang-dong
Yuseong-gu
Daejeon 305-343

Tel: +82 42 860 3378
Fax: +82 42 860 3378
Eml: sshan@kier.re.kr

HWANG, Gab-Jing
Korea Institute of Energy Research
71-2 Jang-dong
Yuseong-gu
Daejeon 305-343

Tel: +82 42 860 3227
Fax: +82 42 860 3428
Eml: gjhwang@kier.re.kr

JUNG, Kwang-Deog
Korea Inst. of Science and Technology
Sungbuk-Gu Hawolgok-dong
39-1, Seoul

Tel: +82 2 958 5218
Fax: +82 2 958 5219
Eml: jkdcats@kist.re.kr

KANG, Kyoung-Soo
Korea Institute of Energy Research
71-2 Jang-dong,
Yuseong-gu,
Daejeon 305-343

Tel: +82 42 860 3114
Fax:
Eml: kskang@kier.re.kr

KIM, Chang-Hee
Hydrogen Production Research Center
Korea Institute of Energy Research
71-2 Jang-dong, Yuseong-gu
Daejeon 305-343

Tel: +82 42 860 3609
Fax: +82 42 860 3428
Eml: chk14@kier.re.kr

KIM, Hong-Soo
Korea Institute of Energy Research
71-2 Jang-dong
Yuseong-gu, Daejeon 305-343

Tel: +82 42 860 3141
Fax: +82 42 860 3133
Eml: hskim@kier.re.kr

KIM, Jong-Ho
KAERI
150, Duckjin-dong
Yusong-gu, Daejeon-si

Tel: +82 42 868 8846
Fax: +82 42 868 8086
Eml: jhkim5@kaeri.re.kr

KIM, Tae-Hwan
Korea Institute of Energy Research
71-2 Jang-dong
Yuseong-gu, Daejeon 305-343

Tel: +82 42 860 3115
Fax: +82 42 860 3309
Eml: thkim@kier.re.kr

LEE, Byung-Gwon
Korea Inst. of Science and Technology
Sungbuk-Gu Hawolgok-dong
39-1, Seoul

Tel: +82 2 958 5801
Fax: +82 2 958 5219
Eml: bglee@kist.re.kr

LEE, Dong-Won
Korea Institute of Energy Research
71-2 Jang-dong
Yuseong-gu, Daejeon 305-343

Tel: +82 42 860 3530
Fax: +82 42 860 3538
Eml: dwlee@kier.re.kr

PARK, Jong-Kee
Korea Institute of Energy Research
71-2 Jang-dong
Yuseong-gu, Daejeon 305-343

Tel: +82 42 860 3131
Fax:
Eml: jngkprk@kier.re.kr

SHIN, Young-Joon
Korea Atomic Energy Research Institute
150 Dukjin-dong, Yuseong-gu
Daejeon, 305-600

Tel: +82 42 868 2795
Fax: +82 42 868 2636
Eml: nyjshin@kaeri.re.kr

P.R. OF CHINA

SUN, Yuliang
Nuclear Engineering
Institute of Nuclear Energy Technology
Tsinghua University
Beijing 100084

Tel: ++86 10 6277 9000
Fax: ++86 10 6277 1150
Eml: sunyl@tsinghua.edu.cn

XU, Jingming
Institute of Nuclear Energy Technology
Tsinghua University
Qinghuayuan, Haidian District
Beijing 100084

Tel: ++86 10 6278 3570
Fax:
Eml: xujingming@mail.tsinghua.edu.cn

ZHANG, Ping
P.O.Box 1021, Division 201
Tsinghua University
Beijing 102201

Tel: ++86 10 8172 1705
Fax: ++86 10 6977 1714
Eml: zhangping77@mail.tsinghua.edu.cn

SWEDEN

MÖLLER, Erik J.O.
SwedPower AB
PO Box 527
162 16 Stockholm

Tel: +46 770 24 2300 ext 206
Fax:
Eml: moeller_erik@swedpower.com

UNITED STATES OF AMERICA

BUCKNER, Melvin R.
Savanna River National Laboratory
Aiken, SC 29808

Tel: +1 803 725 0596
Fax: +1 803 725 4704
Eml: mel.buckner@srnl.doe.gov

CHEN, Yitung
University of Nevada
4505 Maryland Parkway
Box 454027
Las Vegas, NV 89154-4027

Tel: +1 702 895 1202
Fax: +1 702 895 1860
Eml: uuchen@nscee.edu

HENDERSON, David
Nuclear Hydrogen Research
Office of Nuclear Energy
Science and Technology
U.S. Department of Energy
Washington, D.C. 20585

Tel: +1 301 903 3097
Fax: +1 301 903 5057
Eml: David.Henderson@nuclear.energy.gov

HERRING, J. Stephen
Idaho National Laboratory
Environmental Laboratory
Bechtel BWXT Idaho, LLC
P.O. Box 1625 MS 3860
Idaho Falls

Tel: +1 208 526 9497
Fax: +1 208 526 2930
Eml: j.herring@inl.gov

PETRI, Mark C.
9700 South Cass Avenue
Building 208
Argonne, Illinois 60439

el: +1 630 252 3719
Fax: +1 630 252 1932
Eml: mcpetri@anl.gov

RICHARDS, Matt
General Atomics
P.O. Box 85608, San Diego
CA 92186-5608

Tel: +1 858 455 2457
Fax: +1 858 455 2599
Eml: matt.richards@gat.com

ROTHWELL, Geoffrey
Dept. of Economics and Public
Policy Program
Stanford University
Stanford, CA 94305-6072

Tel: +1 650 725 3456
Fax: +1 650 725 5702
Eml: rothwell@stanford.edu

SUMMERS, William A.
Hydrogen Technology Center
Savannah River National Laboratory
Building 773-42A
Aiken, SC 29808

Tel: +1 803 725 7766
Fax: +1 803 725 8829
Eml: william.summers@srnl.doe.gov

VENNERI, Francesco
General Atomics
P.O. Box 85608 San Diego
CA, 92186-5608

Tel: +1 858 455 3000
Fax:
Eml: venner@gat.com

INTERNATIONAL ORGANISATIONS

METHNANI, Mabrouk
Unit Head – Gas cooled Reactor
International Atomic Energy Agency
Wagramer Strasse 5
Box 100
A-1400 Vienna, Austria

Tel: +43 1 2600 22810
Fax: +43 1 2600 29598
Eml: M.Methnani@iaea.org

CARON-CHARLES, Marylise

Tel: +33 1 4524 1070
Fax: +33 1 4524 1110
Eml: marylise.caron-charles@oecd.org

DUJARDIN, Thierry
Deputy Director

Tel: +33 145 24 10 06
Fax: +33 145 24 11 06
Eml: thierry.dujardin@oecd.org

YAMAGISHI, Isao

Tel: +33 1 4524 1152
Fax: +33 1 4524 1106
Eml: isao.yamagishi@oecd.org

OECD Nuclear Energy Agency
Le Seine Saint-Germain
12 boulevard des Iles
92130 Issy-les-Moulineaux, France

Annex B
MEETING ORGANISATION

Organising Committee

R. Hino, JAEA, Japan (Co-chair)
M. Petri, ANL, USA (Co-chair)
J.H. Chang, KAERI, Korea
R. Duffey, AECL, Canada
M. Hori, Nuclear Systems Association, Japan

International scientific advisory members

S. Shiozawa, JAEA, Japan (Chair)
Y. Makihara, IAEA
M. Methnani, IAEA
A.I. Miller, AECL, Canada
C. Nordborg, OECD/NEA
Y. Shin, KAERI, Korea
D.C. Wade, ANL, USA

Meeting Secretariat

I. Yamagishi, OECD/NEA
Y. Shiina, JAEA, Japan

This page intentionally left blank

Annex C

ADDITIONAL PRESENTATIONS TO THE SECOND HTTR WORKSHOP

After the NEA Information Exchange Meeting, the JAEA organised a special session in the framework of the second HTTR workshop on 7 October. The session was chaired by T. Iyoku where the following presentations on the recent progress of HTTR technologies were made by JAEA speakers;

- Fuels Researches in the HTTR Project
by K. Sawa, S. Ueta, J. Aihara
- Safety Demonstration Tests Using the HTTR
by S. Nakagawa
- Materials Development for HTGRs in JAERI and JAEA
by Y. Tachibana, T. Shibata, T. Iyoku, K. Sawa
- JAEA's R&D Activities on Gas Turbine
by S. Takada

The session was closed by Y. Komori and followed by the technical tour for the HTTR and hydrogen production apparatus.